DEPOSITIONAL ASPECTS OF POLLUTANT BEHAVIOR IN FOG

Thesis by

Jed Michael Waldman

In Partial Fulfillment of the Requirements

for the Degree of

Doctor of Philosophy

California Institute of Technology

Pasadena, CA

1986

(Submitted 29 August 1985)

ABSTRACT

Droplet deposition during fog is shown to play an important role in the removal of anthropogenic pollutants from the atmosphere. Relevant theoretical principles are reviewed, and a survey of previous investigations is made. Results of extensive field monitoring programs are presented, and characterizations of fog chemistry and deposition in several environments are reported.

The in-cloud scavenging of aerosols and soluble gases coupled with the small size of fog droplets are found to result in higher chemical concentrations in fogwater than in rainwater. In the urban regions of southern California and the southern San Joaquin Valley, fogwater chemistry is dominated by sulfate, nitrate, and ammonium ions, which are measured at millimolar levels. High fog- and cloudwater acidities (pH 2 to 4) are routinely found in the western Los Angeles basin where ammonia emissions are low. San Joaquin Valley fogwater samples are less acidic due to greater ammonia release from local sources.

The formation of fog is shown to accelerate deposition rates for water-scavenged atmospheric constituents. Surrogate-surface measurements made in the San Joaquin Valley indicate that major species were removed at rates 5 to 20 times greater during fogs compared to nonfoggy periods. During stagnation episodes, pollutant removal by ventilation of valley air requires at least 5 days, while the enhancement of deposition by fog formation leads to pollutant lifetimes on the order of 6-12 h. Thus, in an environment characterized by flat, open landscape and low wind speed, droplet sedimentation can be the dominant removal mechanism of pollutants during prolonged stagnation episodes with fog.

THESIS SUMMARY

The formation of fog is shown to accelerate deposition rates for many water-scavenged atmospheric constituents. Sedimentation and impaction are substantially enhanced when haze aerosols ($\lesssim$ 1 μm) grow to larger, droplet (2 to 100 μm) sizes. Wind speed and receptor-surface geometry are the primary factors that govern deposition in fog. Droplet sedimentation is found to be dominant at low wind speed ($\lesssim$ 2 m s^{-1}); turbulent transport becomes important as wind speed increases. Droplet capture by impaction can lead to very high deposition rates for receptors with developed canopy structure such as a pine forest.

In addition to droplet transport, scavenging of soluble gases (e.g., SO_2, HNO_3, and NH_3) and nucleation scavenging of aerosol in fog determine the deposition rates of atmospheric constituents. For major aerosol species such as ammonium sulfate and ammonium nitrate, scavenging generally rises with increasing fog density (i.e., liquid water content) which promotes more complete nucleation scavenging. Other factors, such as the balance of preexisting acids and bases in the atmosphere, also affect the degree to which soluble gases and interstitial aerosol are incorporated into fog droplets.

During initial field monitoring efforts, fogwater collected in urban-impacted coastal regions of southern California was found to have higher acidity and higher concentrations of sulfate, nitrate, and ammonium ions than previously observed in atmospheric water droplets. Condensation and evaporation of water vapor on preexisting aerosols were determined to be dominant processes controlling fogwater chemistry.

Fogwater acidities were in the range of pH 2.2 to 4.0 and were often associated with scavenging of gas-phase nitric acid.

Stratus clouds, which frequently intercepted Pacific coastal mountain slopes, were intensively monitored at a site 25 km northeast of downtown Los Angeles. Highly concentrated, acidic cloudwater was found on a routine basis. Observed pH was in the range of 2.1 to 3.9 and had a median value below pH 3 for measurements made on more than 20 sampling dates in the spring months of 1982 and 1983. Based on a reasonable estimate of cloud-droplet capture, the contribution intercepting clouds make to the annual depositional flux of these species was comparable to those monitored in incident rainfall. In addition, the solute deposition associated with several light, spring rains (1% annual rainfall) contributed 20% or more of annual H^+, NO_3^-, and SO_4^{2-} wet flux totals.

At the same site, cloudwater that had deposited on local pine needles was collected and found to be more concentrated than suspended droplets. Enrichment of K^+ and Ca^{2+} in those samples and in measured throughfall was apparently due to leaching from foliar surfaces. Injury to sensitive plant tissue has been noted in the literature when prolonged exposure to this severe kind of micro-environment has been imposed.

A study of atmospheric pollutant behavior was conducted in the southern San Joaquin Valley of California during periods of stagnation, both with and without dense fog. Measurements of solute deposition were made by surrogate-surface methods. Deposition rates for major species were 5 to 20 times greater during fogs compared to measurements during

nonfoggy periods. The proportions of deposited solute were closely matched to the fogwater composition. In this environment, droplet deposition was close to the sedimentation rate.

Sulfate-ion deposition velocity during fog was 0.5 to 2 cm s^{-1}. Rates measured for nitrate ion were generally 50% below those for sulfate, except for acidic fog (pH < 5) conditions, because nitrate was less effectively scavenged by neutral or alkaline fogs. Higher atmospheric acidity appeared to alter N(V) aerosol formation and N(V) speciation (i.e., favoring gaseous nitric acid) in the pre-fog atmosphere and lead to more efficient nitrate scavenging. In radiation fog, scavenging of ambient aerosol was observed to increase as LWC rose. These measurements showed that the efficiency of nucleation scavenging could be as important in controlling fogwater composition as water vapor exchange processes such as condensation and evaporation at the droplet surface.

In the San Joaquin Valley, 2 to 3 times the initial atmospheric loading of sulfate and N(-III) species were deposited during prolonged fogs, yet their depletion in the atmosphere was not observed. Steady aerosol sulfate concentrations required S(IV) oxidation to proceed rapidly. Lower limits for a pseudo first-order constant for SO_2 oxidation was calculated to be in the range of 2-7% hr^{-1}. In a similar fashion, ammonia emissions, that were required to balance ammonium removal during fog, were calculated to be approximately 1 ppb h^{-1}.

Measurements made in the San Joaquin Valley supported the hypothesis that fog deposition lowered the ambient concentrations of sulfate and nitrate aerosol during stagnation periods, compared to similar periods with no fog. Ammonia release from local sources was

found to be promoted by higher soil temperature and moisture; for periods with these conditions, lower fogwater acidities were observed.

Fog-sampling techniques were evaluated in the field to assess the performance of the Caltech rotating arm collector (RAC). The lower size-cut (i.e., 50% collection efficiency) for the RAC has been reported as 20 μm diameter. A comparison was made with fogwater collectors of different designs which reportedly collected all droplets greater than 5 μm. No significant sampling biases were found among the various designs, despite the difference in calibrated lower size-cuts. A comparison was also made of methods for field determination of liquid water content (LWC) in fog. Theses methods included fogwater collector rates, droplet sizing, infrared extinction, and fog filtration. A considerable scatter and wide range of indicated values were found among various methods. This underscored the uncertainties in present methods to parameterize fog LWC.

ACKNOWLEDGEMENTS

Very special acknowledgements are due my closest colleagues, Daniel Jacob and Bill Munger. It was their help and advice that made much of this research possible. Thanks to the shared interests, attitudes, and respect, "fog squad" endeavors were also a great deal of fun. I am very grateful to my advisor, Michael Hoffmann, who gave me support and freedom in pursuing some novel approaches in my work. Members of my examining committee, Jim Morgan, Glen Cass, Fred Shair, and Yuk Yung, and other members of the faculty, Rick Flagan, John List, Norman Brooks, and John Seinfeld, have provided an enriching environment for research and learning.

At the locations used for field sampling sites, I am grateful to the many individuals who facilitated my efforts and helped cut through otherwise impenetrable bureacracies: special thanks to the Henninger Flats rangers and NWS Bakersfield personnel. My thanks also go to Dr. William Grant at JPL for his help with the laser transmissometer and to Dr. Suzanne Hering and the other participants of the CRC fog sampler study. This research was supported by the California Air Resources Board and, partially, by the Institute President's Fund.

I am thankful to many indivduals who have given their help during this research: Sandy Brooks and Elaine Granger, for their fine clerical skills and pleasant company; librarians, Rayma Harrison and Guinilla Hastrup, who were invaluable in buoying me and my classmates during the more odious portions of the graduate grind; shop personnel, Elton Daly, Joe Fontana, Rich Eastvedt, and Leonard Montenegro, whose diligence and advice were essential to the construction of field instruments; and

Theresa Fall and Nancy Tomer, who tirelessly drafted the drawings.

Lab-mates, office-mates and other colleagues at Caltech have enriched my years here: to Roger Bales, Bob Arnold, David James, Tom DiChristina, and Jenna Zinck, I am grateful for your tolerance, advise, and thoughtfulness. To Dr. Dixon et al., thanks for both the encouragements and the distractions. To Martha Conklin and Costas Synolakis, you have been very special friends, at the pool, dinner and everywhere: thank-you. To my most faithful assistant and friend, Ms. Mai: I'm glad we did it together.

My mother, Claire, has been a truly wonderful and my dearest friend through these years at Caltech. You were always quite helpful in prior years, but, lately, I have appreciated your love and support more than ever.

Finally, I dedicate this thesis to my son, Mischa, who literally popped into my life when I least expected. Mischa, you have taught me so much about loving and caring. You did not make my graduate career easier, but you have given me a greater happiness in pursuing my goals as I helped you to develop and grow.

TABLE OF CONTENTS

page

APPENDICES

LIST OF FIGURES

Figure page

LIST OF TABLES

Chapter 1

INTRODUCTION

1.1 OVERVIEW

The removal of anthropogenic emissions and windblown material to ground-layer surfaces occurs by processes known as wet and dry deposition. While the deposition of airborne pollutants is essential for cleansing the atmosphere, these materials may have the potential for significant environmental impact when they reach the surface. Key deposition pathways are shown schematically in Figure 1.1.

Scavenging and deposition of ambient gases and aerosol by raindrops is more rapid and efficient than removal under dry conditions. However, precipitation is an intermittent event. The dry flux of pollutants may contribute a greater mass of material than rainfall, due to the cumulative effect of long dry periods. Liljestrand (1980) found this to be the case in southern California. A small fraction of total NO_x and SO_2 emissions in the region were accounted by wet deposition monitoring; Liljestrand estimated a ten-fold greater removal by dry versus wet deposition, while the majority of emissions were advected away from the region. On the other hand, the net deposition in the eastern United States has been associated primarily with precipitation. Bischoff et al. (1984) estimated the wet fluxes as a percent of precursor emissions to be 75% for SO_2 and more than 90% for NO_x.

In addition to precipitation and dry deposition, there exists the potential for appreciable deposition during fog occurrences. While its frequency is often low, fog-induced deposition may be important in several specific environments. In coastal regions, fogs often serve as a dominant source of moisture and nutrient input to local ecosystems

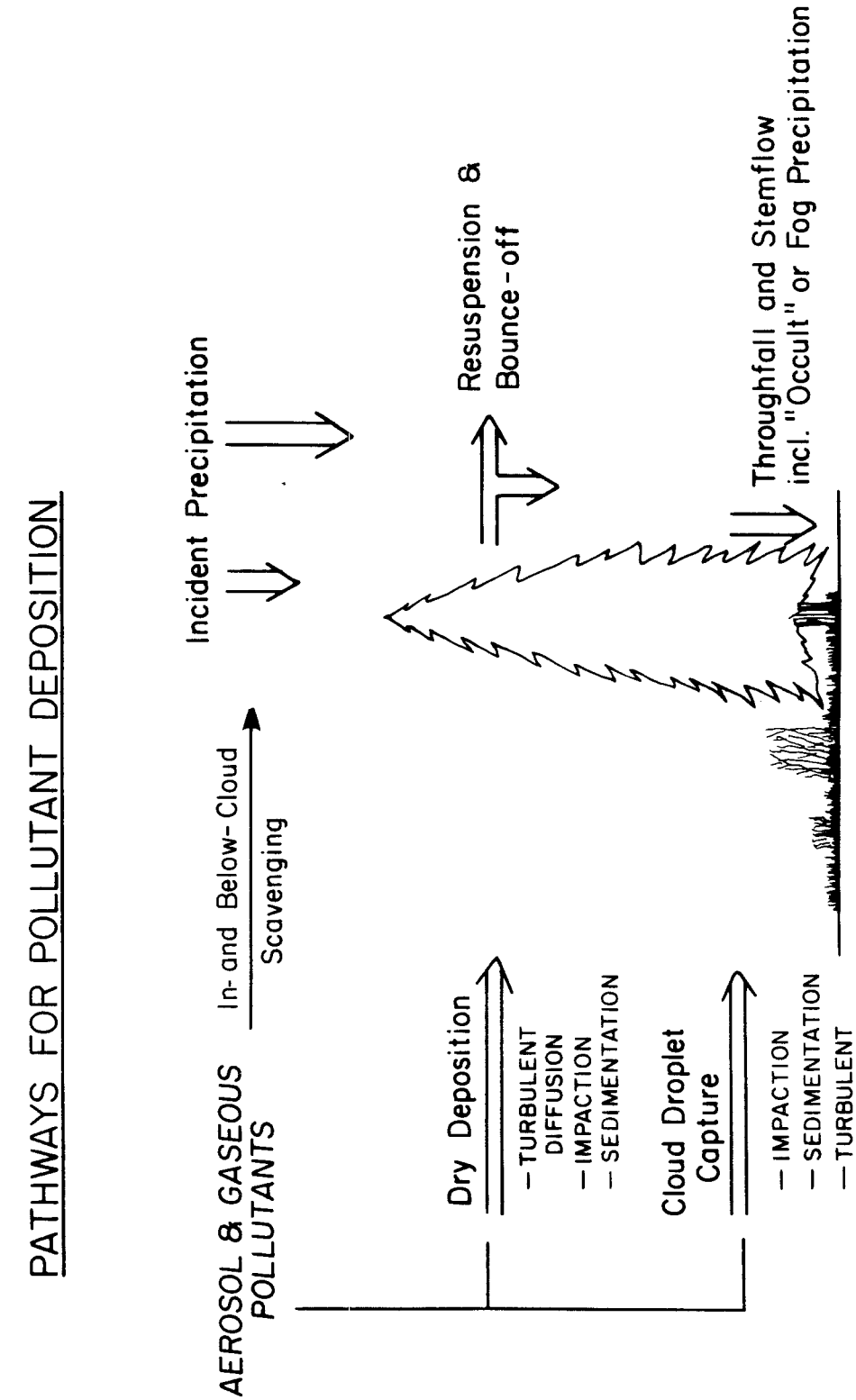
PATHWAYS FOR POLLUTANT DEPOSITION
Incident Precipitation
Resuspension &
Bounce-off
Throughfall and Stemflow
incl. "Occult" or Fog Precipitation
AEROSOL & GASEOUS
POLLUTANTS
In- and Below-Cloud
Scavenging
Dry Deposition
– TURBULENT
DIFFUSION
– IMPACTION
– SEDIMENTATION
Cloud Droplet
Capture
– IMPACTION
– SEDIMENTATION
– TURBULENT
DIFFUSION

Figure 1.1

(e.g., Azevedo and Morgan, 1974). Similarly, many mountainous regions are frequently intercepted by clouds and the accompanying chemical input (e.g., Schlesinger and Reiners, 1974). Urban areas, subject to higher ambient pollutant concentrations, may have substantial fog-induced deposition as well.

In many respects, fog is simply a ground-level cloud in which processes such as nucleation, gas scavenging, and droplet growth are important. At the same time, fogs consist of discrete water droplets, and sedimentation and inertial impaction are dominant transport mechanisms due to the relatively large sizes of these particles. However, since fog droplets may change size continually, their transport behavior may be altered.

Fog may make important contributions to pollutant deposition or its impacts in selected environments for the following reasons:

1) Fog and cloud droplets are important chemical reactors (Peterson and Seinfeld, 1980) that can modify the nature of pollutant material in the atmosphere (Barrett et al., 1979). They act as sinks for many gaseous pollutants that are appreciably soluble in aqueous solutions, such as nitric acid, ammonia, and sulfur dioxide. Fog and cloud droplets are sufficiently small such that gas scavenging is not limited by mass transport in most cases (Schwartz and Freiberg, 1981). Their effect on pollutant speciation, in turn, will have impacts on the chemical balance of depositing components.

2) Under dry conditions, much of the aerosol mass of pollutant species is found in the size range 0.1 to 1.0 μm diameter. Deposition velocities (V_d) of these small particles are extremely low (Slinn, 1982). Scavenging of ambient aerosol by fog droplets leads to the

association of solute mass with larger-sized particles. Hence, when dissolved in fog droplets, solute species are more efficiently deposited by particle impaction and sedimentation.

3) Surface moisture deposited by fog and dew can significantly increase the V_d of aerosols by reducing bounce-off and resuspension (Chamberlain, 1967). In addition, moisture on surfaces also serves as a sink for soluble gases (Brimbelcombe, 1978).

4) The capture of fog droplets by foliar and ground surfaces can be a significant component of the water and nutrient fluxes to an ecosystem (Azevedo and Morgan, 1974; Schlesinger and Reiners, 1974). Lovett (1984) reported water flux at rates of 0.1-0.3 mm hr^{-1} from advected clouds to a subalpine forest canopy. This range agreed with his numerical model, which indicated that sedimentation and inertial impaction -- especially to the upper 3 m of the canopy -- were the dominant deposition mechanisms.

5) The analyses of fog- and cloudwater show at least an order of magnitude greater concentrations for ambient solutes compared to rainwater (see Table 2.2 in next chapter). Therefore, droplets can make a greater contribution to pollutant flux per volume of water depositing.

6) Intercepted fog and drizzle wet surfaces but do not necessarily flush them clean as does rain. By dissolution of previously accumulated material, this can lead to concentrated solutions of acids (Wisniewski, 1982) and metals (Lindberg et al., 1982) at collection surfaces. Waldman et al. (1985) found that droplets, after depositing to pine needles, were in general more concentrated than ambient cloudwater, except when the needles had been previously rinsed by measurable rainfall. The acidity of drops removed from foliar surface

was as high as the ambient cloudwater despite enrichment with calcareous material.

7) Damage to sensitive receptor surfaces has been caused by the exposure to acidic fog droplets (Thomas et al., 1952; Haines et al., 1980; Granett and Musselman, 1984).

Specifically wet or dry deposition pathways have become the subject of intensive research in recent years. Fog deposition is an area that has not been extensively studied. As described above, there are many reasons to expect that fog has an important role in pollutant exchange processes. Because of its impact on material surfaces, its potential for affecting the chemical balance of the atmosphere, and its place as a hybrid in the spectrum of deposition pathways, the fog phenomenon is a fruitful area of research.

1.2. RESEARCH OBJECTIVES AND THESIS OUTLINE

The objectives of this thesis research have been to monitor and to evaluate depositional aspects of the fog phenomenon. Emphasis has been placed on the role it plays in the removal of anthropogenic pollutants from the atmosphere. The primary starting point was a careful characterization of the chemical composition of fogwater. At the onset of this research, there were little field data available describing fog or cloudwater chemistry, especially in highly polluted regions. Our research was conducted largely in a series of field programs, and, in its course, detailed data sets were collected that greatly augmented the current body of measurements. These new data were used to identify key chemical and physical processes under a variety of circumstances.

In Chapter 2, important theoretical principles are outlined which describe the role of fog in enhancing pollutant deposition. The chapter includes a microphysical description of fog and its formation, descriptions of processes affecting pollutant scavenging by fog, a discussion of particle transport specifically applied to fog occurrences, and finally, a survey of previous investigations of fog chemistry and deposition.

In Chapter 3, experimental methods used to monitor fog chemistry, microphysics and deposition are described. In earlier fogwater studies, there was no generally accepted methodology for collection of samples. The performance of the fogwater collector used in this research was evaluated under field conditions (Chapter 5). This included side-by-side operation with several other collectors of different designs. Measurements of liquid water content by various methods were also compared.

Early results of our fogwater sampling in the Los Angeles region are presented in Chapter 4. The dominant processes controlling fogwater chemistry are identified in these field data. Therein, extreme acidities not previously monitored in atmospheric droplets are reported.

The chemical characterization for stratus cloudwater in southern California is presented in Chapter 6. Results are taken from several seasons of monitoring at a site in the San Gabriel Mountains. This chapter focuses on fog occurrence as a vector for pollutant deposition and evaluates the potential effects of acidic fogwater deposition. Along with the program to monitor fog and rainfall deposition, a study of pollutant deposition during drizzle of stratus cloudwater is described. Novel measurements of the composition of droplets that had deposited onto pine needles are also reported.

Regional studies of extended episodes of widespread fog were conducted in the southern San Joaquin Valley of California. In Chapter 7, these field measurements have been applied to characterize the enhancement of pollutant removal accompanying radiation fog in the valley. Deposition to surrogate surfaces was monitored during this study in addition to the chemical composition of fogwater, total aerosol and the gas phase. Simultaneous sample collection in these three phases was used to quantify scavenging efficiencies and, with flux determinations, to calculate removal efficiencies during fog. Finally, recommendations for future research are made in Chapter 8.

Chapter 2

TECHNICAL BACKGROUND AND LITERATURE REVIEW

2.1 MICROPHYSICAL AND CHEMICAL DESCRIPTIONS OF FOG

2.1.1 Microphysical

Fog and cloud droplets are formed by condensation of water vapor in saturated air. They are found having diameters between 2 to 100 μm, although in non-precipitating clouds and fog the majority of droplet mass occurs in the range of 5 to 30 μm. In contrast, raindrops are far larger, mostly in the range of 200 to 2000 μm. The mass of liquid water is typically 0.01 to 0.5 g m^{-3}; the number concentration of droplets is generally 10 to several 100 cm^{-3}. Droplet interactions, such as coagulation or differential settling, have negligible impact on their dynamics, except when intensive convection leads to rain or drizzle (Pruppacher and Klett, 1978).

While vertical motions lead to the formation of most clouds, this is not the case for the majority of fogs. Generally, extensive ground contact suppresses net vertical motion. Fogs are primarily classified as either advection- or radiation-type, based on their mechanism of formation (Myers, 1968). Advection fogs are formed by large-scale, horizontal air movement. For example, in the cases of marine fogs, a warm, moist air mass comes in contact with a cooler surface. Radiation fog forms by radiative cooling near the ground to a clear nighttime sky. This cooling causes an intense thermal gradient within the ground layer which may lead to fog or dew formation. Turbulent eddy transfer of momentum and heat play important roles under these conditions. A high level of turbulence inhibits fog (Tayor, 1917), but some eddy mixing is essential to its formation (Roach et al., 1976). Finally, fogs also

occur on mountain slopes by the interception with a mesoscale cloud deck or fog formed locally by the upslope wind component.

The presence of condensation nuclei, which are composed of both soluble and non-soluble material, is essential to the formation of atmospheric water droplets. The effects of surface tension and the chemical potential of the aquated solutes are important processes; these raise and lower the saturation vapor pressure near the droplet surface, respectively. Accretion or evaporation of water to the condensation nucleus or droplet is forced by the difference between the ambient and local (i.e., surface) humidities. Droplet growth equations have been derived by coupling microscale heat and mass transfer at the aerosol surface (Pruppacher and Klett, 1978). The principal terms depend on: a) atmospheric relative humidity; b) droplet surface tension; c) solute activity. Condensation caused by the radiative cooling of water droplets may also be an important factor in the dynamics of radiation fog (Roach, 1976).

During growth, the droplet temperature differs from the ambient due to latent heat release, which in turn depends upon the instantaneous growth rate. Hence, the complete growth-rate equation takes an implicit form; however, simplifying assumptions can be applied for all but the very smallest nuclei (Pruppacher and Klett, 1978). The equation for rate of change in droplet diameter (D_o) is given in Table 2.1.

Families of curves can be deduced by solving the growth equation for the equilibrium condition (i.e., $dD_o/dt=0$) at various saturation ratios for different dry aerosol masses. An example of these, known as the Köhler curves, is shown in Figure 2.1. The maxima occur at points known as the critical supersaturation, SS_{cr}, and activation size, D_{act}.

Table 2.1 DROPLET GROWTH EQUATION

$$D_o \frac{dD_o}{dt} = \frac{S_v - a_w \exp(B)}{C + E\,(A-1)\,a_w \exp(B)}$$

$$A = \frac{M_w L}{RT} \qquad B = \frac{4 M_w \sigma}{\rho_w D_o RT} \qquad C = \frac{\rho_s RT}{4 \mathcal{D}_m M_w e_s(T)} \qquad E = \frac{\rho_s L}{4kT}$$

$$a_w = \exp\left(-\Phi \frac{n_s}{n_w}\right)$$

Activation point:

$$\frac{dD_o}{dt} = 0; \qquad D_o = D_{act}; \qquad \text{and,} \quad S_v = 1 + SS_{cr}$$

gives:

$$D_{act} = \left(\frac{3\,LNA}{B}\right)^{1/2} \qquad \text{where,} \quad LNA = \frac{M_w \rho_s}{M_s \rho_w} D_{dry}^3$$

$$SS_{cr} = \frac{2}{3\sqrt{3}} \left(\frac{B^3}{LNA}\right)^{1/2}$$

$$= K\, D_{dry}^{-3/2}$$

Solute	K for D_{dry} in μm (10°C)
$(NH_4)_2SO_4$	4.93×10^{-5}
NH_4HSO_4	4.59 "
NH_4NO_3	4.82 "
H_2SO_4	4.21 "
NaCl	3.68 "

Parameters:

D_o, D_{act}	=	droplet diameter, diameter at activation point.
D_{dry}	=	dry diameter for hygroscopic aerosol.
e, $e_s(T)$	=	ambient, saturation water vapor pressure at T.
S_v	=	ambient water vapor saturation ratio, $e/e_s(T)$.
ρ_w, ρ_s	=	density of pure water, solute salt.
R	=	gas constant.
T	=	temperature (K).
L	=	latent heat of evaporation.
$\mathcal{D}_m$	=	molecular diffusivity of water vapor in air.
k	=	heat conductivity of air.
σ	=	surface tension of water.
M_w, M_s	=	molecular weight of water, dissociated solute ions.
n_w, n_s	=	number of moles of water, dissociated solute in droplet.
a_w	=	activity of water in droplet.
Φ	=	osmotic coefficient of water in solution (assumed=1).

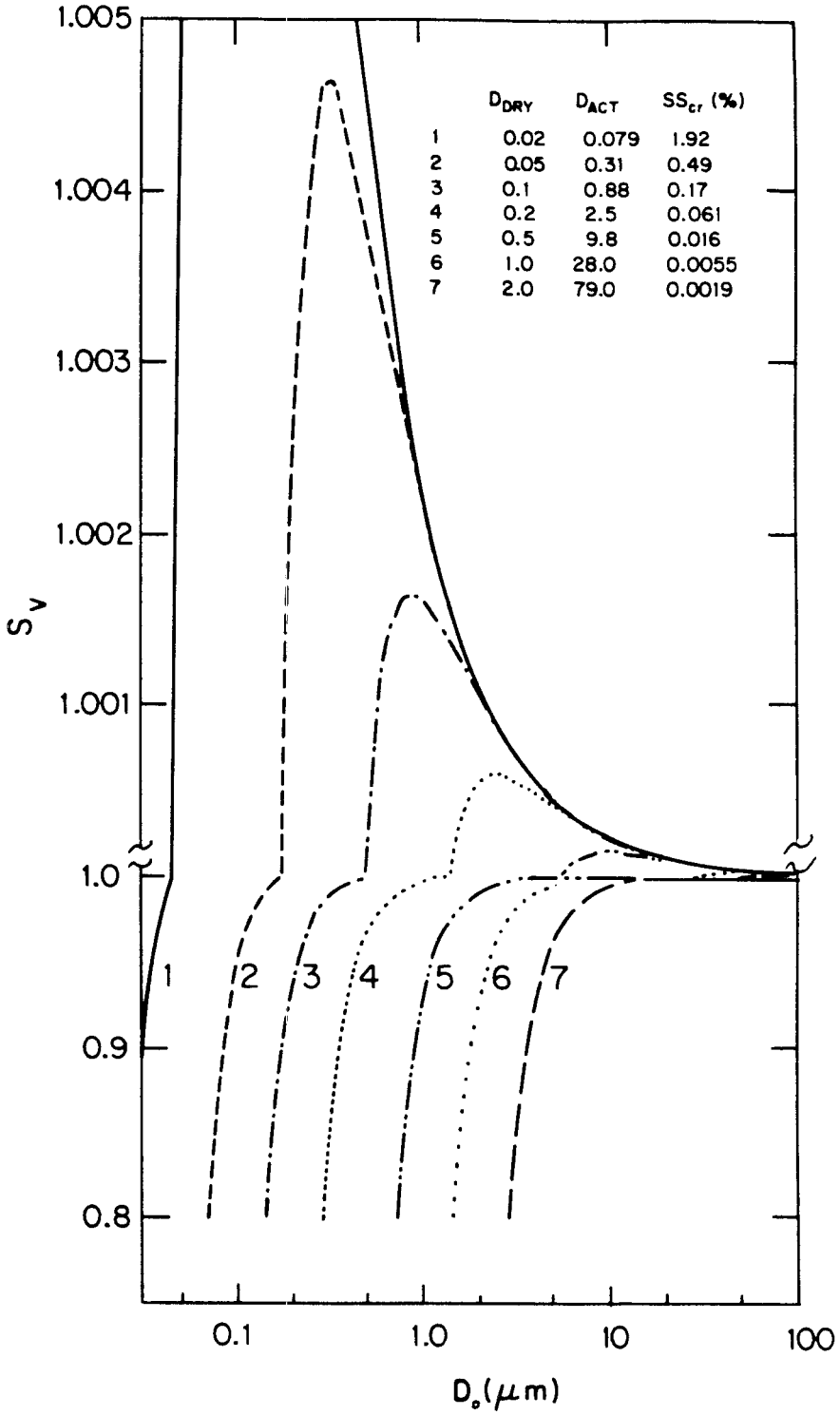

Figure 2.1 Equilibrium vapor pressure (S_v) over aquated ammonium sulfate nuclei as a function of droplet diameter (D_0). Table shows dry diameter, activation diameter, and critical supersaturation.

When the ambient water vapor supersaturation, SS_v, is below SS_{cr}, nuclei achieve stable equilibrium sizes, $D_{eq} < D_{act}$. When the SS_v is sustained at values greater than SS_{cr}, droplets can form and continue to grow.

2.1.2 Chemical

The study of fog has traditionally remained in the domain of atmospheric physicists principally concerned with its effect on visibility or the mechanisms of formation analogous to clouds. Yet, even the data of early investigations of fog indicate that fogwater can be highly concentrated with respect to a variety of chemical components (see Table 2.2). Cloudwater, sampled aloft, has been found to exhibit similar composition, although not with the same extreme values (cf, Oddie, 1962; Hegg and Hobbs, 1982; Daum et al., 1984). On the other hand, rainwater compositions, when compared to fogwater, are found to be far more dilute. Fog droplets are approximately 100 times smaller than raindrops, which form partially by the further condensation of water vapor. They should be more concentrated in solute derived from the condensation nuclei. Furthermore, fog forms in the ground layer where gases and aerosol are most concentrated.

The higher aqueous concentrations and extremes in acidity found in fogwater are reason for concern. Fog-derived inputs have the potential to substantially add to the burden of acid deposition caused by precipitation. Its contribution can be disproportional to the sum of additional moisture, because of its higher concentrations. Perhaps more important, deleterious effects of fog deposition may be associated with the intensity of solution acidity. For instance, appreciable nutrient leaching (e.g., Scherbatskoy and Klein, 1983) and damage to leaf tissue

Table 2.2 SUMMARY OF FOGWATER COMPOSITION MEASUREMENTS

Location	Date	Type[b]	N[c]	pH	Na^+	NH_4^+	Ca^{2+}	Mg^{2+}	Cl^-	NO_3^-	SO_4^{2-}	Ref.
Mt. Washington, NH (1900 m)	1930-1940	I	35*	4.5 3.0-5.9					4 0-34		150 4-1100	I
Coastal MA & ME	"	M	37*	4.7 3.5-6.3					940 0-5800		380 60-2600	"
Germany, Baltic Sea	1955-65	M	42*	3.8	1500	2300	750		700	900	1900	II
nr. Dresden	"	R	12*	4.2		2100	3200		590	450	780	"
Harz Mtn. (1150 m)	"	I	18*	5.1	300	710	220		200			
Japan, Mt. Noribura (3026 m)	July 1963	I	10+	3.9 3.4-4.3	87 45-165	175 115-260			110 75-230	36 25-175	3300 230-1250	III
Mt. Tsukaba (876 m)	Nov. 1963	I	5+	5.9 5.6-6.5	290 180-435	880 110-965			800 295-1290	17 5-37	1600 360-2100	"
Whiteface Mtn., NY (1500 m)	Aug. 1976	I[d]	28*	3.7	11	89	17	6	31	90	140	IV
	Aug. 1980	"	50	3.2-4.0	1-7	1-200			1-14	7-190	32-800	V
Los Angeles foothills (780 m)	Spring 1982 & 83	I	120+	2.9 2.1-3.9	240 135-8700	580 62-7400	140 5-3000	80 1-1800	190 15-9650	1510 160-16300	840 130-9300	VI
Nova Scotia	Aug. 1975	M	14°		1040 600-1530	33 3-94	45 20-69	100 13-130	87 3-450		250 50-500	VII
California, Central Coast	Fall 1976	M	8°		320 80-950	190 0-580	55 9-100	68 23-175	400 95-1240	115 24-235	200 77-490	VIII
Los Angeles area	Fall-Winter 1980-82	M & I	11+	3.3 2.7-7.1	139 30-620	1580 420-4260	168 0-460	54 22-310	223 68-423	110 580-2980	584 354-1875	IX
Los Angeles area	Fall-Winter 1981-82	M	24	2.3-5.8	12-2180	370-7960	190-4350	7-1380	56-1110	130-12000	62-5000	X
Pt. Reyes, CA	Aug. 1982	M	17+	4.5 3.5-5.0	190 21-4700	64 28-330	10 0-240	36 5-1200	215 34-7000	23 2-526	186 36-1281	XI
San Nicholas Is., CA	Aug. 1982	M	7x	3.9	6100	450	450	1500	5300	1580	1080	XII
San Diego Area, CA	Jan. 1983	M	5x	2.9	510	780	49	130		1850	470	"
Albany, NY	Oct. 1982	R	24+	5.8 4.3-6.4	36 10-100	215 70-350	120 65-350	13 6-47	47 18-175	85 11-220	155 21-1360	XIII
Bakersfield, CA	Winter 1983	R	108+	4.2 2.6-7.0	20 1-325	1440 490-1330	47 7-3500	6 1-430	47 1-980	850 200-6800	1160 10-9400	XIV
Italy, Po Valley	Feb. & Nov. 1984	R	5°	3.5-4.3	10-110	580-1620	60-130	10-50	20-120	290-1100	400-990	XV

Table 2.2 (cont.)

NOTES

a. Concentrations in micro-equiv L^{-1}.

b. Fog type: I = intercepted stratiform cloud;
M = marine or coastal fog;
R = radiation fog

c. Number of samples or events: (*) = average, (+) = median,
(x) = volume-weighted mean of n samples;
(o) - average and/or range of n events

d. Non-precipitating stratiform cloud data only.

References:

I. Houghton (1955)
II. Mrose (1966)
III. Okita (1968)
IV. Castillo et al. (1980)
V. Falconer (1981)
VI. Waldman et al. (1985)
VII. Mack and Katz (1976)
VIII. Mack et al. (1977)
IX. Brewer et al. (1983)
X. Munger et al. (1983)
XI. Jacob (1985)
XII. Jacob et al. (1985c)
XIII. Fuzzi et al. (1984)
XIV. Jacob et al. (1984)
XV. Fuzzi (unpubl. data)

(e.g., Haines et al., 1980) have been noted with application of acid fogs or mists. Finally, a historical correlation of fog with the most severe air pollution episodes provides additional cause for concern (Environmental Protection Agency, 1971). Identification of a link between urban fog events and human health injury was made even before detailed measurements of fog composition (Firket, 1936). Understanding health effects has been facilitated by studies of fog chemistry (see Hoffmann, 1984).

2.1.3 Fog Scavenging Processes

Fog droplets are highly effective at scavenging ambient materials present in the air. The overall fraction incorporated into fog droplets depends upon two processes: nucleation scavenging (i.e., activation) of aerosol and gas dissolution. The speciation of pollutant components precursory to fog formation is therefore important. Furthermore, in situ chemical transformations may alter this speciation and the effectiveness of fog scavenging while the droplet phase is present.

The following notation has been adopted: (C) is the total concentration of species C in the atmosphere; $(C)_f$, $(C)_g$, and $(C)_a$ are the concentrations of C in fogwater, gas, and non-activated aerosol phases, respectively, given as mol m^{-3} of air. Aqueous concentrations in fogwater are expressed in units mol L^{-1} with the notation [C]. Multiplication of these concentrations by the liquid water content yields: $(C)_f$ = LWC [C], with LWC expressed as L m^{-3}. For components in the gas-phase, partial pressure (P_C) values may be converted to give the same units. The mass balance may be then written as follows:

$$(C) = LWC\ [C] + P_C\ (RT)^{-1} + (C)_a \qquad (2.1)$$

where R is the gas constant (atm m^3 mol^{-1} K^{-1}) and T is absolute temperature (K). The components for which we are most concerned are sulfur dioxide, sulfuric acid, nitric acid, and ammonia (and their neutralized salts) because of their abundance and effect on acidification in urban-impacted environments. The terms, S(IV), S(VI), N(V), and N(-III), are used to refer to all species of that oxidation state in any phase.

Nucleation Scavenging. The pollutant species of concern are often present as hygroscopic aerosol (e.g., ammonium sulfate and ammonium nitrate). These will deliquesce to form aquated condensation nuclei at high relative humidity (RH), growing to larger equilibrium aizes as RH approaches 100%. The Kohler curves show the range of aerosol which can become activated into droplets. For soluble nuclei, the following proportionalities hold: D_{eq}: $D_{dry}^{1.5}$: SS_{cr}^{-1}. Achievement of higher SS_v can lead progressively to activation of smaller nuclei. The presence of a nonsoluble fraction in particles of a given size can significantly raise their SS_{cr} (Saxena and Fisher, 1984). The chemical composition of nuclei also plays a role, although the differences between aerosol composed of pure solute species are minor (see Table 2.1).

Figure 2.2a shows three hypothetical particle size distributions formed by superimposing the two modes generally observed in the aerosol size spectra of sulfate (Whitby, 1978). The smaller (0.05 μm) mode corresponds to particles formed by condensation of gases; the larger (0.5 μm) is known as the accumulation mode, that is formed primarily by coagulation and combustion. A third, coarser fraction is also routinely observed, although the contribution from anthropogenic sources may vary, especially with regard to nitrate aerosol (cf, Wolfe, 1984; Manane and

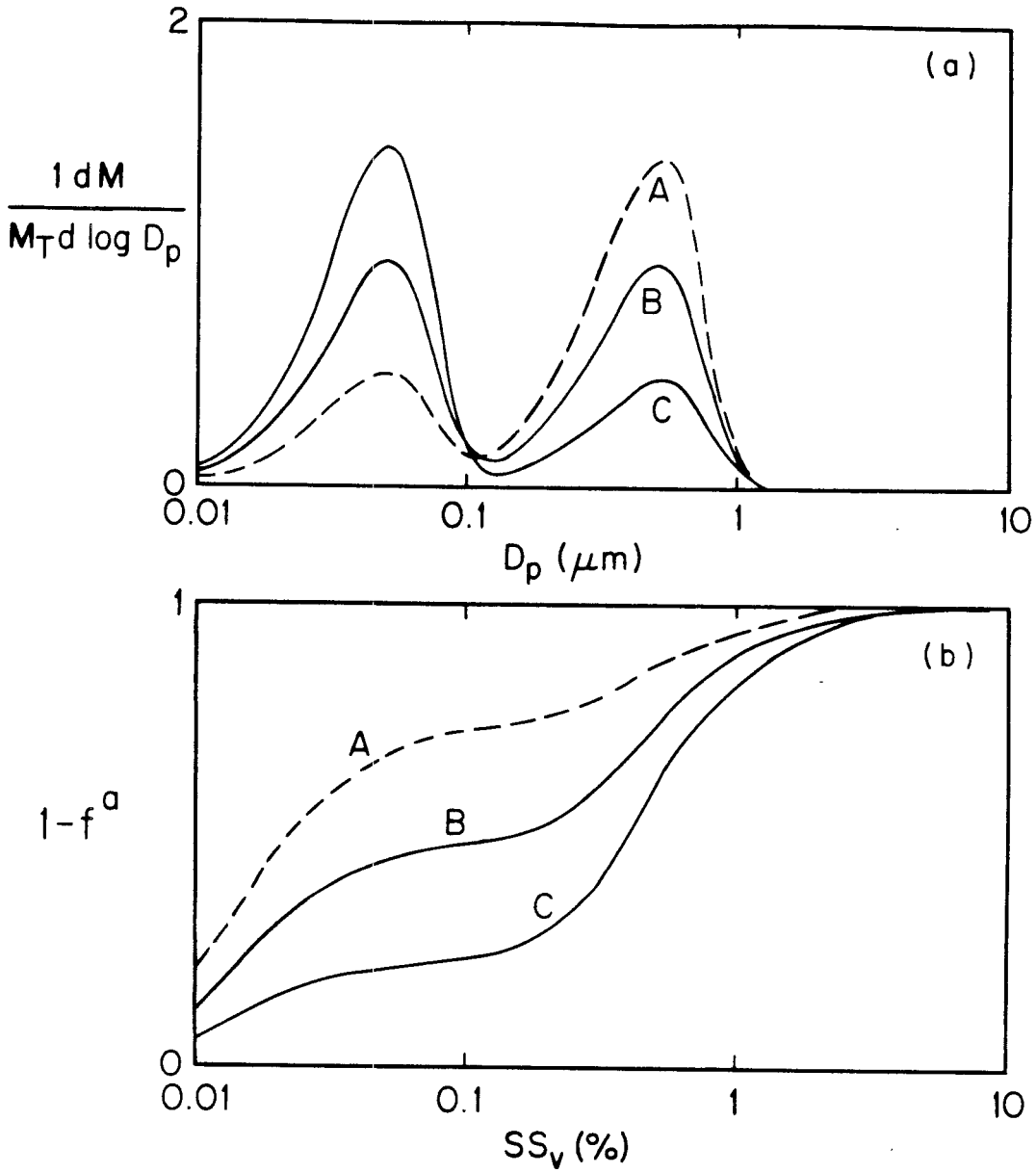

Figure 2.2 (a) Hypothetical fog nuclei size distributions and (b) scavenging efficiency ($1-f^a$) as function of supersaturation (SS_v). Curves A, B, and C for 75 50, and 25% total mass in larger size mode, respectively.

Noll, 1985). The activation of these distributions, corresponding to $(NH_4)_2SO_4$ particles, are shown in Figure 2.2b as functions of SS_v. The nonactivated fraction is expressed as $f^a_C = (C)_a/(C)$, and $1-f^a$ represents the aerosol scavenging efficiency in the fog.

Measurements of SS_v in the atmosphere are not widely available. Gerber (1981) found that rapid oscillations of ambient humidities occurred in radiation fog with excursions about a mean near to RH=100%; SS_v rarely exceeded 0.1-0.2%. Hudson (1984) measured interstitial aerosol in fog and cloud environments; he found a systematic removal (i.e., activation) of larger nuclei. These cutoff values were used to calculate an effective supersaturation for the ambient atmosphere. In fogs and ground-based sampling of stratus clouds, Hudson's measurements indicated SS_v were in the range 0.03 to 0.2%. Comparing these measured or calculated values to Figure 2.2b shows that little of the smaller-size mode is likely to be scavenged in these environments. Conversely, solutes which are associated with a coarser (>1 μm) fraction can be readily activated.

At the same time, it is not known what fraction of these nuclei (i.e., $D_{eq} > D_{act}$) will be activated or what droplet size they will achieve. The relative increase in droplet size is faster for smaller diameters, and modeling has shown it is possible for droplets of any size to grow from nuclei of any mass, depending upon the SS_v history they have experienced, mixing, and the aerosol size spectrum (e.g., Lee and Pruppacher, 1977). There are limited field data that address this controversy. Measurements of solute mass for individual fog droplets have been attempted. On the Japanese coast, Naruse and Maruyama (1971) found correlations between droplet size and nucleus mass, in which the

biggest droplets generally had large sea salt nuclei, and the smaller droplets formed on smaller, ammonium sulfate aerosol. Hudson and Rogers (1984) indirectly measured condensation nuclei within stratus cloud droplet spectra, selectively removing droplets above a certain size. They reported an increasing fraction of low SS_{cr} (i.e., large) nuclei in the larger droplets and a vanishing fraction of these nuclei in the interstitial aerosol spectrum. These relationships are at best qualitative. This area of fog microphysics, the size-composition relationship within droplet spectra, may strongly affect the chemistry and deposition of fog-borne material. It remains an area in need of further research.

Equilibrium Dissolution of Soluble Gases. Dissolution of gaseous species in fogwater is dependent on gas-aqueous equilibria and the quantity of liquid water present. Temperature and pH are the most important parameters which affect phase equilibria (e.g., aqueous, gas-aqueous, etc.). Ionic strength effects are not as important for the aqueous concentrations generally found (see Table 2.2). For highly soluble species, LWC may control the overall partitioning because the droplets can provide a sufficient solution volume to deplete the gas phase. Thermodynamic data for important gas-aqueous equilibria for SO_2, HNO_3, and NH_3 are given in Table 2.3.

Sulfur dioxide is fairly insoluble at low pH. At higher pH (7 and above), dissociation of $SO_2 \cdot H_2O$ (to HSO_3^- and SO_3^{2-}) can lead to much greater S(IV) solubility. With increasing LWC, $(S(IV))_f$ rises and can lead to depletion of the gas phase (Figure 2.3a). The fraction of solute partitioning into the droplet phase is expressed as $f_C = (C)_f/((C)_f+(C)_g)$. Appreciable [S(IV)(aq)] may be supported in the

Table 2.3

THERMODYNAMIC CONSTANTS

		$pK^{(a)}$	$H^{(b)}$	Ref.
H_s:	$SO_2(g) + H_2O = SO_2 \cdot H_2O(aq)$	-0.095	-6.25	I
K_{s1}:	$SO_2 \cdot H_2O(aq) = H^+ + HSO_3^-$	1.89	-4.16	I
K_{s2}:	$HSO_3^- = H^+ + SO_3^{2-}$	7.22	-2.23	I
K_s:	$HSO_4^- = H^+ + SO_4^{2-}$	2.20	-4.91	I
H_N^*:	$HNO_3(g) = H^+ + NO_3^-$	-6.51	-17.3	II
H_A:	$NH_3(g) + H_2O = NH_3 \cdot H_2O(aq)$	-1.77	-8.17	I
K_B:	$NH_3 \cdot H_2O(aq) = NH_4^+ + OH^-$	4.77	0.9	I
H_F:	$CH_2O(g) + H_2O = CH_2O \cdot H_2O(aq)$	-3.8	-12.85	III
K_F:	$HMSA = CH_2O + HSO_3^-$	-5.	na	IV
K_w:	$H_2O = H^+ + OH^-$	14.00	13.35	I

a. K in M or M atm^{-1}.

b. kcal mol^{-1}.

References: (I) Smith and Martell, 1976; (II) Schwartz and White, 1981; (III) Ledbury and Blair, 1925; (IV) Dasgupta et al., 1980.

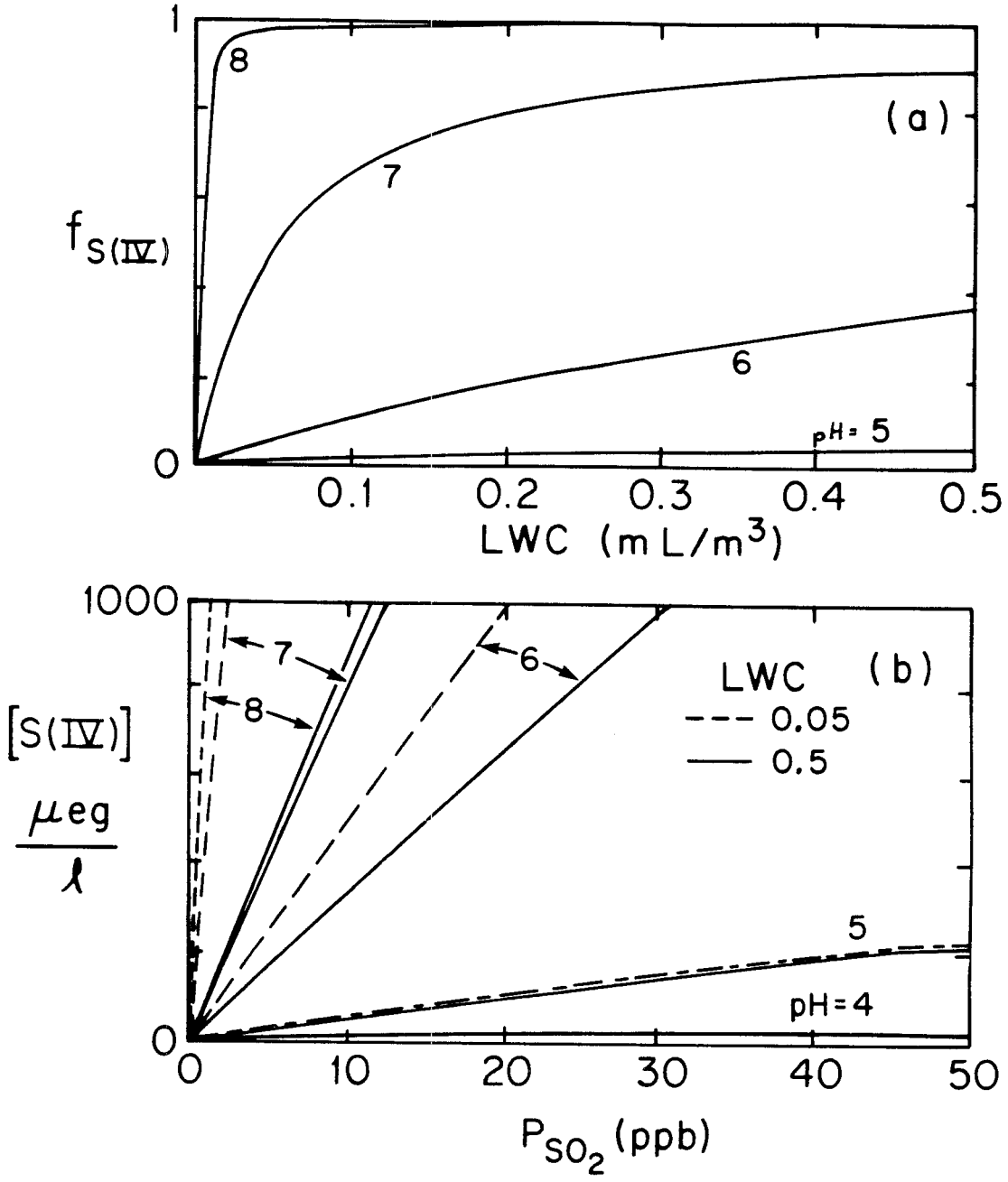

Figure 2.3 SO_2 dissolution in fog: (a) fraction scavenged as function of LWC; (b) fogwater concentration versus P_{SO_2}.

aqueous phase even at low P_{SO2}. Figure 2.3b shows the aqueous concentration as a function of pre-fog P_{SO2} at high and low LWC. Presence of gaseous aldehydes has been shown to substantially increase S(IV) solubility by the formation of stable bisulfite adducts (Munger et al., 1984).

Nitric acid is completely scavenged to droplets for fogs even at minimal LWC because it has such a high Henry's Law coefficient (for $HNO_3(g) + H_2O = HNO_3\ H_2O(aq)$: $H_N=2.1 \times 10^5$ M atm^{-1}; Schwartz and White, 1981). Ammonia scavenging is variable in the ranges of pH and LWC found. Similar to the case of $SO_2(g)$, the atmosphere may exist as a reservoir for $NH_3(g)$ that can be dissolved or released from fogwater as a function of the relative amount of atmospheric acidity and liquid water. Reservoir of N(V) and N(-III) which also exists in the aerosol phase (e.g., ammonium nitrate) are discussed in the next section.

Gas transfer to fog-sized droplets by molecular diffusion is sufficiently rapid for phase equilibria to be achieved on the order of seconds or less under most conditons (Baboolal et al., 1981; Schwartz, 1984). Greater time may be required in the cases where high solubility strongly favors gas-phase partitioning. The characteristic times required to supply the total amount of solute necessary to attain this equilibrium were evaluated by Schwartz and Freiberg (1981). They found that times of the order 10 s were sufficient for gaseous SO_2 to dissolve into droplets even at high pH. Similarly, the absorption of $HNO_3(g)$ by fog droplets is not instantaneous. However, the rate is not limiting to the assumption that phase equilibria are rapidly established.

Overall Fog Scavenging. Nonactivated aerosol fractions of nitrate, sulfate and ammonium coexist with fogwater and gaseous

constituents in the atmosphere. Solutes incorporated within the droplet spectrum are subject to gas-aqueous equilibria; nonactivated aerosol appear to remain inert in this regard. In the case of nonvolatile species such as sulfate, partitioning is exclusively between non-activated aerosol and droplet phases. Applying mass balances for $HNO_3(g)$ and $NH_3(g)$, the overall fractions, $F_C = (C)_f/(C)$, may be calculated as functions of gas-aqueous equilibria and non-activated aerosol fraction (Table 2.4).

Without specific knowledge about solute size-composition relationships, a more general model of fog scavenging is proposed based on solute speciation and the relative abundance of ambient acids and base. Aerosols are generally found as neutral salts in the system dominated by H_2SO_4-HNO_3-NH_3. Nitrate and sulfate are counterbalanced by ammonium ion, while excess acids or bases reside in the gas phase as $HNO_3(g)$ or $NH_3(g)$ (Daum et al., 1984; Jacob et al., 1985b). Only for the cases where sulfate acidity exceeds the ambient ammonia (i.e., (S(VI))>(N(-III))) would an acidic aerosol be thermodynamically stable in the dry atmosphere (Stelson and Seinfeld, 1982; Bassett and Seinfeld, 1983). Consider two examples for these constituents:

i. $(N(V)) + 2\ (S(VI)) = (ACIDS) > (N(-III))$;

and ii. $(N(-III)) > (ACIDS)$.

Nucleation scavenging is assumed to depend on LWC. For example, a linear dependence up to a maximum $F_{S(VI)} = 90\%$ at LWC $= 0.3$ mL m^{-3} is assumed for sulfate in Figure 2.4a. This approximates the progressive activation of a spectrum dominated by the large aerosol fraction. We also assume that scavenging of aerosol N(V) and N(-III) follow this same relationship. Solute-specific size spectra are not addressed at this

Table 2.4 FOG SCAVENGING EFFICIENCIES

A. S(VI)

Mass Balance:

$$(S(VI)) = L\,[S(VI)] + (S(VI))_a$$

Scavenging Efficiency:

$$F_{S(VI)} = (S(VI))_f/(S(IV)) = 1 - f^a_{S(VI)}$$

B. N(V)

Mass Balance:

$$(N(V)) = \frac{P_{HNO_3}}{RT} + L\,[NO_3^-] + (N(V))_a$$

Scavenging Efficiency:

$$F_{N(V)} = (N(V))_f/(N(V))$$

$$= \frac{H_N^* LRT}{H_N^* LRT + [H^+]}\,(1 - f^a_{N(V)})$$

C. N(-III)

Mass Balance:

$$(N(-III)) = \frac{P_{NH_3}}{RT} + L\,([NH_3 \cdot H_2O] + [NH_4^+]) + (N(-III))_a$$

Scavenging Efficiency:

$$F_{N(-III)} = (N(-III))_f/(N(-III))$$

$$= \frac{H_A LRT(1 + K_B[H^+]/K_w)}{1 + H_A LRT(1 + K_B[H^+]/K_w)}\,(1 - f^a_{N(-III)})$$

D. S(IV)

Mass Balance:

$$(S(IV)) = \frac{P_{SO_2}}{RT} + L\,([SO_2 \cdot H_2O] + [HSO_3^-] + [SO_3^-] + [HMSA])$$

Scavenging Efficiency:

$$F_{S(IV)} = (S(IV))_f/(S(IV))$$

$$= 1 - [1 + LH_sRT\,(1 + \frac{K_{s1}}{[H^+]} + \frac{K_{s1}K_{s2}}{[H^+]^2} + \frac{K_{s1}K_F H_F P_{CH_2O}}{[H^+]})]^{-1}$$

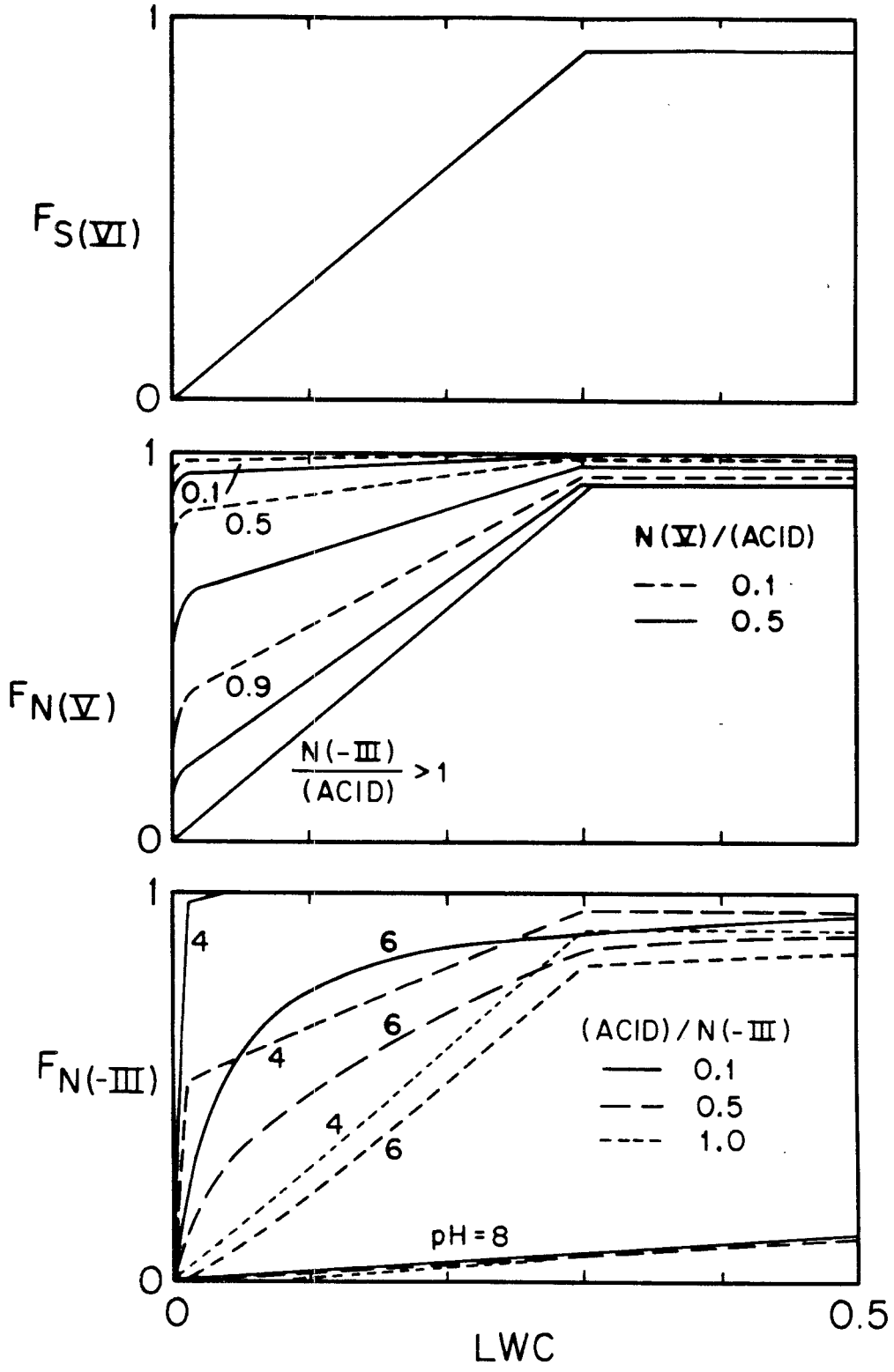

Figure 2.4 Fog scavenging for S(VI), N(V), and N(-III) as function of liquid water content (LWC). Aerosol scavenging for N(V) and N(-III) similar to form shown for S(VI).

point; actual differences in the proportion of fine versus coarse particles would be reflected in the nucleation scavenging efficiencies for each solute.

For case (i), available N(-III) is immediately exhausted in neutralizing acidic sulfate and nitrate. In the atmosphere, the dissocation of ammonium nitrate aerosol ($NH_4NO_3 = NH_3(g) + HNO_3(g)$) is highly dependent upon ambient temperature and RH (Stelson and Seinfeld, 1982). It volatilizes at low RH and high temperature. However, at high RH the formation of aerosol leads to equimolar depletion of the gases until one is present at a negligible level; essentially, the gases do not coexist. Hence, N(V) in excess of N(-III) remains in the gas phase; When a droplet phase forms, $HNO_3(g)$ is 100% scavenged, leaving only nonactivated N(V) aerosol outside the droplet spectrum. Figure 2.4b shows the effect of N(-III)/ACID and N(V)/ACID equivalent ratios based on the assumption that aerosol scavenging for nitrate proceeds similar to sulfate. Overall, ambient N(V) will be more efficiently scavenged when (a) the total acids are in greater excess of N(-III) and other bases; and (b) S(VI) makes a greater contribution to the net acidity in the precursor atmosphere.

In case (ii), we assume $(NH_3(g)) = (N(-III)) - (ACID)$ in the humid atmosphere, while the remaining material forms neutral ammonium aerosol. Furthermore, assuming ammonium aerosol nucleation proceeds as in Figure 2.4a, the total N(-III) scavenging depends on the gas-aqueous equilibrium, fogwater pH, and LWC (Figure 2.4c). In the alkaline regime, the presence of soluble weak acid gases can play an important role in determining the resultant pH of fogwater which forms, and this affects the scavenging of N(-III). Dissolution of formic and acetic

acids (pK_a=3.8 and 4.8; Martell and Smith, 1977), for example, provides base-neutralizing capacity to the droplet. Also, the acidity of the droplet can be increased by the formation of S(IV)-formaldehyde adducts (which increases S(IV) solubility) or in situ S(VI) production. Each process will lead to N(-III) scavenging which can eventually deplete $NH_3(g)$.

It has been found that nitrate and sulfate aerosol may be found within different size fractions. In Southern California, Appel et al. (1978) reported that nitrate is found predominately in a coarser fraction than sulfate. In the San Joaquin Valley, Heisler and Baskett (1981) found a similar relationship except during the wintertime; a substantial increase in the coarse sulfate fraction (>2.5 μm) was observed during wintertime stagnation. Ammonium was found to occur in the same fraction as nitrate. However, the measurements of Heisler and Baskett did not include gaseous ammonia which can be a sizeable portion of total N(-III) in the region (see Chapter 7). Therefore, the true partitioning was not determined. Differences in predominant sizes for these three major constituents can significantly alter results of the simplified model given above. Most significant would be the presence of a coarse particle fraction enriched with N(V) or S(VI) which would be readily scavenged. Simultaneous measurements of these components in the three phases have not been satisfactorily made in fog.

2.2 FOG DEPOSITION

2.2.1 Previous Investigations

Early studies documented the hydrological and chemical importance of intercepted cloud and fogwater inputs to mountainslope and coastal ecosystems (e.g., Kerfoot, 1968). For instance, open collectors placed below trees exposed to fog-laden wind on the San Francisco pennisula measured an average water flux of 50 cm in one, rainless month (Oberlander, 1956). Natural and artificial "fog-drip" collectors exposed for extended periods have shown that these "occult" inputs can have comparable magnitudes to annual precipitation values for water (Nagel, 1956; Vogelmann et al., 1968) and nutrient capture (Azevedo and Morgan, 1974; Schlesinger and Reiner, 1974). However, it was uncertain what true relationship these measurements had to the capture by actual vegetation.

Fog deposition from the ambient atmosphere to ground surfaces can be viewed as a two-step process (Davidson and Friedlander, 1978). First, a droplet in the ambient atmosphere must be transported through an aerodynamic layer toward the ground; next, once within a canopy layer, droplets must be deposited to canopy surfaces. The resistance to mass transport may reside in either layer, primarily depending on the geometry of the canopy and the degree of atmospheric turbulence. Research in the subject area of droplet or large particle deposition has addressed the specific mechanisms that can control their flux.

From measurements of droplet capture by monitored trees, Hori (1953) and co-workers reported deposition rates on the order of 0.5 mm h^{-1} for a forest intercepted by dense coastal fog. Yosida and Kuroiwa (1953) found that momentum and droplet transport coefficients were of

similar order of magnitude, based on measurements of wind force and droplet-capture rate by a small conifer tree. However, while the drag coefficient for the canopy elements decreased with increasing wind speed, the authors found that capture efficiency rose, due to impaction. In the same field area, Ōura (1953) determined that interception near the leading edge of the forest was about three times more effective than for interior locations.

Lovett (1984) adapted a resistance model to the cloud droplet capture by a balsam fir forest canopy. He included turbulent transport and impaction to the canopy elements, conceived as a set of 1-m-thick height strata in a 10 m high forest, and edge effects were not included. The model predicted a nearly linear correspondence between water flux and canopy-top wind speeds above 2 m s^{-1}. Droplet impaction, primarily to the upper 3 m of strata, was the dominant deposition mechanism. Wind speeds between 2 and 10 m s^{-1} gave water fluxes of 0.2 to 1.1 mm h^{-1} (equivalent to V_d = 10 to 70 cm s^{-1} for the simulated conditions). For lesser wind speeds, Lovett found that sedimentation controlled the water capture.

Legg and Price (1980) calculated that the sedimentation flux of large particles to vegetation with a large leaf-area index (i.e., total leaf area per surface area of ground) would also increase with wind speed. This would be caused by wind-driven turbulence bringing particles to the lower leaves where sedimentation there would lead to additional removal. Their model did not account for a vertical profile caused by depletion of particles, especially by impaction to the top of the canopy. Lovett (1984) showed that the depletion reduced the net sedimentation flux nearer to the ground as wind speeds increased;

nonetheless, greater leaf-area index caused sedimentation fluxes slightly higher than by terminal fall velocities alone.

Davidson and Friedlander (1978) identified particle size regimes where different transport mechanisms dominated for a shortgrass canopy. Under moderate wind conditions, the filtration efficiencies in calculations for D_o>10 μm were high enough that deposition was effectively limited by turbulent transport or sedimentation to the canopy from above.

Droplet precipitation measured to flat plates in radiation fog averaged 0.03 mm h^{-1}, which agreed with calculated terminal fall velocities (Wattle et al., 1984). Measured rates for grass-model collectors (<1 m high) indicated approximately a factor of two greater deposition. In another field study of radiation fog, Roach et al. (1976) calculated that sedimentation removed up to 90% of water that condensed to droplets during fog. Brown and Roach (1976) parameterized the fog deposition rate as a linear function of LWC in their companion modeling paper. However, Brown (1980) later determined that the gravitational flux was overestimated by this relationship for higher LWC. Jiusto and Lala (1983) also found a linear fit between sedimentation rate and LWC as measured from droplet size spectra in radiation fog. Corrandini and Tonna (1980) evaluated this parameterization for droplet size spectra given in the literature for different types of fog and found it did not fit well for advection and valley fogs.

Dollard and Unsworth (1983) made direct measurements of turbulent fluxes for wind-driven fog drops above a grass surface. Their technique relied on precise determinations of LWC and wind speed made simultaneously at several heights. From the gradient of these

parameters, the authors calculated turbulent transport for droplets and momentum. Their experimental data gave values of turbulent droplet flux 1.8 ± 0.9 times the sedimentation rate when wind speeds were 3 to 4 m s^{-1}. At wind speeds below 2 m s^{-1}, their measurements showed total fluxes were no more than 50% greater than by sedimentation alone.

2.2.2 Transport Parameters and Processes

The differences between deposition in dry and fog-ladden air are primarily due to the increase in particle size for the latter case. Fog droplets are of the size where inertial impaction and sedimentation dominate their deposition to collection surfaces (e.g., Davidson et al., 1982). In the general case, impaction to surface elements occurs because particles diverge, due to their inertia, from the airflow streamlines where they curve around the obstacle. The efficiency of impaction depends on the radius of curvature of the impaction surface (R) and the particle inertia and is characterized by the Stokes number:

$$St = \frac{\rho_w D_o^2 U_s}{18 \mu R} \qquad (2.2)$$

where, ρ_w is the density of the particle (i.e., water for droplets); D_o is the droplet diameter; μ is the dynamic viscosity of air; and, U_s is the relative velocity between the particle and the obstacle. Fog and cloud droplet sedimentation or terminal fall velocity (V_s) follows the form (Stokes law):

$$V_s = \frac{\rho_w g D_o^2}{18 \mu} \qquad (2.3)$$

where, g is the gravitational acceleration. At larger diameters, such

as raindrops, Stokes law no longer holds due to viscosity and drop deformation effects (Pruppacher and Klett, 1978).

Impaction. The droplet impaction to cylinders can be viewed as an idealized analog of particle capture by grasses or conifer leaves. Impaction efficiencies have been theoretically derived for potential flow as a function of Stokes number (Brun et al., 1955) and extended for higher Reynolds number ($Re = \rho_w U_s D_o / \mu$) (Israel and Rosner, 1983).

Experimental data have also been applied to calculations of particle or droplet flux to receptor surfaces. For example, Davidson and Friedlander (1978) used a least-squares fit to the data of Wong and Johnstone (1953) for impaction to cylinders. The efficiency η represented the fraction of particles which impact compared to the total number of particles passing through the projected area of the obstacle; for a single cylinder, the empirical expression was given:

$$\eta = \frac{St^3}{St^3 + 0.75\ St^2 + 2.80\ St - 0.20} . \qquad (2.4)$$

The flux by impaction to a canopy of cylinders (diameter=d_f) was calculated by integrating over the length of the cylinder and multiplying by the number cylinders per unit area of ground (N):

$$J = - d_f N \int_{z_s}^{H} \eta(z) U(z) C(z) dz \qquad (2.5)$$

where, J is the flux of particles per unit area of ground, z is the vertical scale, U is the horizontal wind speed, C is the concentration of particles, H is the canopy height, and z_s is the particle sink (i.e., the level at which either C or U is assumed to vanish to zero, and

impaction no longer occurs; Davidson and Friedlander, 1978). The convention is that J is positive for upward flux.

Alternatively, Lovett (1984) used the experimental results of Thorne et al. (1982), which were measured specifically for components of the balsam fir canopy that he studied. The efficiency was given as:

$$\eta = \exp\left[-1.84 + 0.90(\ln St) - 0.11(\ln St)^2 - 0.04(\ln St)^3\right]. \quad (2.6)$$

The needles were oriented randomly, and the effect of interferences in airflow caused by neighboring canopy elements was accounted for empirically. The St for 50% efficiency was approximately 4 for the results of Thorne et al. (1982) and 2 in Eqn 2.4. Lovett (1984) calculated the matrix of boundary-layer resistances for droplet capture as a function of horizontal wind speed and canopy structure (e.g., leaf area index) for the different levels within the canopy.

Since the wind speed and droplet concentration profiles are also strongly dependent on the canopy structure, solutions for fog deposition due to impaction are not readily generalized. Davidson et al. (1982) showed that the range of large particle deposition rates was an order of magnitude among five wild grass canopies that were studied. As stated in the previous section, the overall efficiency was found to be limited by turbulence transport to the top of the canopy for large particles (> 10 μm). In the case of the balsam fir canopy studied by Lovett (1984), no such limitations were found to occur, and impaction led to very high deposition rates, also mentioned previously.

In practice, the collection efficiency of particles may be different from impaction efficiency. This largely depends on the surface properties of the collector element. In wind tunnel experiments

(Chamberlain, 1967; Chamberlain and Chadwick, 1972) and field measurements (Davidson, 1977), particle deposition to dry surfaces was far below that to wet ones. As wind speeds increase, so did particle bounce-off. For wet surfaces, collection efficiencies of dry particles were more in accord with impaction theory. Experimental results for droplet collection efficiencies were generally in good agreement with theory (May and Clifford, 1967). The surface tension of water droplets was found to provide adequate adhesion to ensure near perfect retention for $D_o < 50$ μm (Hartley and Brunskill, 1958). Wind-induced shear may cause some droplet removal from foliar elements, observed in wind tunnel tests with glycerol droplets when St>10 (Thorne et al., 1982). Nonetheless, sheared drops will generally fall because of their large size, rather than be resuspended. In the wind tunnel experiments of Merriam (1973), liquid water content was found to be a more important factor in determined total droplet capture than variations in canopy element geometry.

Deposition Velocity. While an overall deposition may be modeled for a specific canopy geometry and elements, wind speed and turbulence profiles, and particle size distribution (Lovett, 1984; Davidson et al., 1982; Bache, 1979), the flux to the canopy can be parameterized by the quantity known as deposition velocity, V_d. In this approach, the depositional flux (J_d) is scaled to the ambient concentration of some component at a reference height (H) above the the canopy:

$$J_d = - V_d C(H). \qquad (2.7)$$

The deposition velocity may be calculated in terms of droplet fluxes or the specific chemical elements contained within the droplets.

Turbulence versus Sedimentation. The flux of droplets through the aerodynamic layer (J_a) can be expressed by:

$$J_a = - K_p(z) \frac{dC}{dz} - V_s C \qquad (2.8)$$

where, K_p is the eddy diffusivity for particles and V_s is the sedimentation velocity. In the steady state, J_a is constant with height, so C and dC/dz are functions of z.

The relative importance of turbulence versus sedimentation transport may be expressed by $E = V_d/V_s$, the ratio of deposition to sedimentation velocities. With substitution ($J_a = J_d$), Eqn 2.8 becomes:

$$K_p(z) \frac{dC}{dz} + V_s C = E V_s C(H) \qquad (2.9)$$

This can be readily solved for C(z) to give the concentration profile:

$$\frac{C(z)/C(H) - E}{1 - E} = \exp\left[- \int_H^z \frac{V_s}{K_p(z)} dz\right] \qquad (2.10)$$

For the momentum exchange between the air and the ground, a logarithmic wind profile can be assumed to hold for thermally neutral conditions (Thom, 1975):

$$U(z) = \frac{U^*}{k} \ln \left(\frac{z}{z_o}\right) \qquad (2.11)$$

where, U* is known as the friction velocity; k is von Karman's constant (0.4); and, z_o is a roughness scale. In cases where an appreciable canopy structure exists, the profile will be displaced some height, d, above the ground surface, and z is replaced by (z-d). Above the canopy, an analogy between turbulent exchange of particles and momentum is often

assumed for neutral atmospheric stability (e.g., Chamberlain, 1967; Thom, 1975; Davidson et al., 1982):

$$K_p(z) = k\ u^*\ z. \qquad (2.12)$$

As above, when displacement of the wind profile is observed, z-d replaces z. The presumption of neutral stability is not always warranted; with daytime heating, vertical motions are enhanced by buoyancy. However, fog occurs during periods of minimal insolation and thermal neutrality or slight stability predominate (Pilié et al., 1975; Roach et al., 1976).

The analogy between momentum and particle transport may sometimes be inappropriate. For example, in the viscous boundary layer, momentum transfer to the canopy elements is augmented by the bluff-body (or normal pressure) forces. There is no analogy in heat or mass transport. Hence, the resistance to momentum exchange is generally less than for the other entities (Chamberlain, 1975). The failure of large particles to follow fluid streamlines will also reduce their effective turbulent diffusivity, although this is only important for $D_0 > 30\ \mu m$, based on the calculations of Csanady (1963). However, for the conditions of fog, the analogy between momentum transfer with turbulent transport of particles has given satisfactory results (Dollard and Unsworth, 1983).

In applying measurements made in radiation fog (Chapter 7), we were interested in identifying the relative importance of sedimentation and turbulent transport for various degrees of turbulence (i.e., U*) and sizes of particles (or V_s). We solved Eqn 2.10 using Eqn 2.12 for eddy diffusivity and the boundary condition of $C \longrightarrow 0$ at $z = z_s$, the particle sink (Davidson and Friedlander, 1978). Figure 2.5 shows the results of

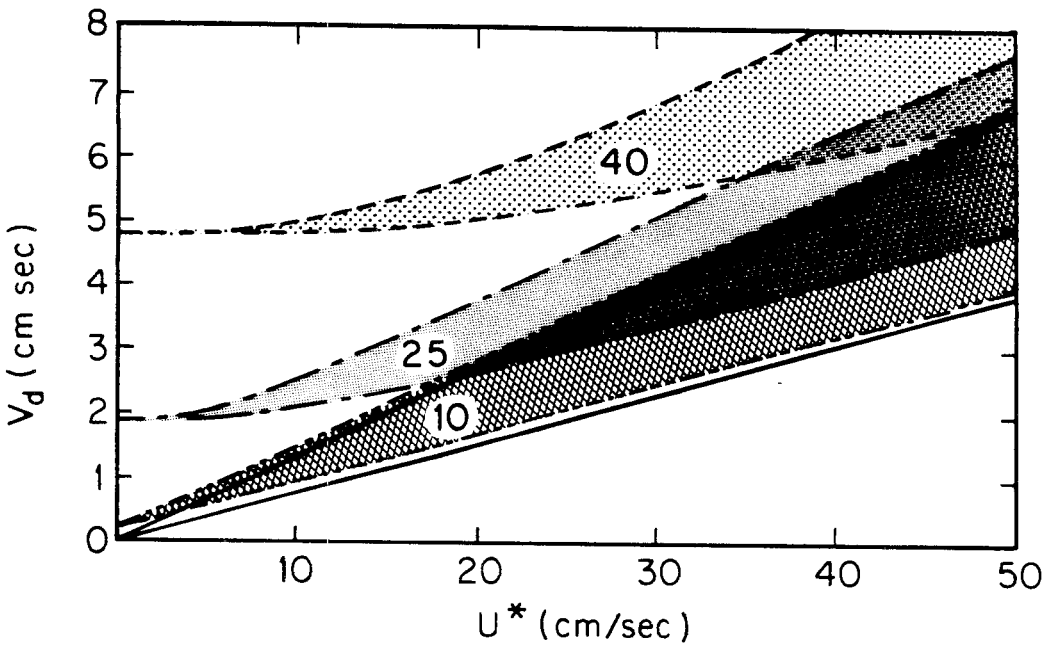

Figure 2.5 Fog deposition curves. Deposition velocitiy (V_d) as a function of friction velocity of wind (U*) for droplet diameters indicated (μm). Range indicated is for z_s/H between 0.05 (upper) and 0.005 (lower), where z_s is the particle sink and H is the reference height for V_d.

calculations for z_s/H between 0.05 and 0.005 (e.g., for H=3 m, particle sink at 15 or 1.5 cm). This corresponds to a shallow canopy where impaction is effective enough that transport is limited by turbulence or sedimentation (Davidson et al., 1982). The enhancement of deposition by turbulent-driven droplet transport is seen to be rather limited for low and moderate wind speeds. The reasons stated for less effective turbulent exchange for particles vis-à-vis momentum would require that the indicated rates could be even lower. These calculations identified the same range of turbulent transport values given by Dollard and Unsworth (1983).

Droplet lifetimes. Changes in particle size will strongly affect depositional processes. The rate at which hygroscopic aerosols achieve equilibrium in the humid region over wet surfaces was recently studied in wind tunnel experiments by Jenkin (1984). If equilibria were attained as particles approached the wet surface, an order of magnitude enhancement in deposition would be expected. Jenkin's experiments indicated that the growth rate was not sufficiently rapid; a two-fold increase was the maximum observed. Hence, the residence of depositing particles within the humid region was not long enough for growth to equilibrium sizes.

An alternative concern is for the converse case in which fog droplets are exposed to lower humidity in the region near warmer-than-air surfaces. A rapid shift of the droplet distribution to smaller sizes would significantly alter both the chemistry and deposition rate. Even under nighttime, radiative conditions, the ground itself may remain warmer than the overlying air during fog, due to its high heat capacity. However, the vertical extent of conductive warming is limited to several

centimeters in fog, until insolation becomes important (Jiusto and Lala, 1983).

The lifetimes for fog droplets instantaneously exposed to drier air were calculated from the growth equation (Table 2.1) as a function of relative humidity (RH) and nucleus mass. These are shown in Figure 2.6 for several initial diameters. Mature fog droplets ($D_o \geq 20$ μm) are very resistant to rapid evaporation until RH drops well below 100%. Solute concentration has little effect on the shrinkage rate for these larger droplets. On the other hand, the rates at which smaller droplets evaporate could be quite rapid; those with greater solute mass change size less rapidly. Since sedimentation alone will transport larger droplets downward at 1-3 cm s^{-1}, droplet evaporation would not be expected to alter size-dependent depositional processes until a drier region extends several meters above the canopy surface. This is what happens when a fog starts to "lift", generally within several hours after sunrise. Even before the fog dissipates, evaporation from wetted surfaces can be important to the net water flux (Lovett, 1984), but until the atmosphere dries sufficiently, the flux of fogwater solutes will continue.

Pollutant Scavenging. An essential facet of fog deposition is the scavenging of ambient aerosol and gaseous constituents into droplets (see Chapter 2.1.3). Partitioning of species between phases determines the relative importance of respective removal pathways. As particulates are incorporated into droplets, their deposition rate will increase with enhanced sedimentation and impaction efficiency. Simple models of fog deposition presume that fog leads to an increase for all particle sizes. However, when only a portion of aerosol mass achieves droplet sizes, the

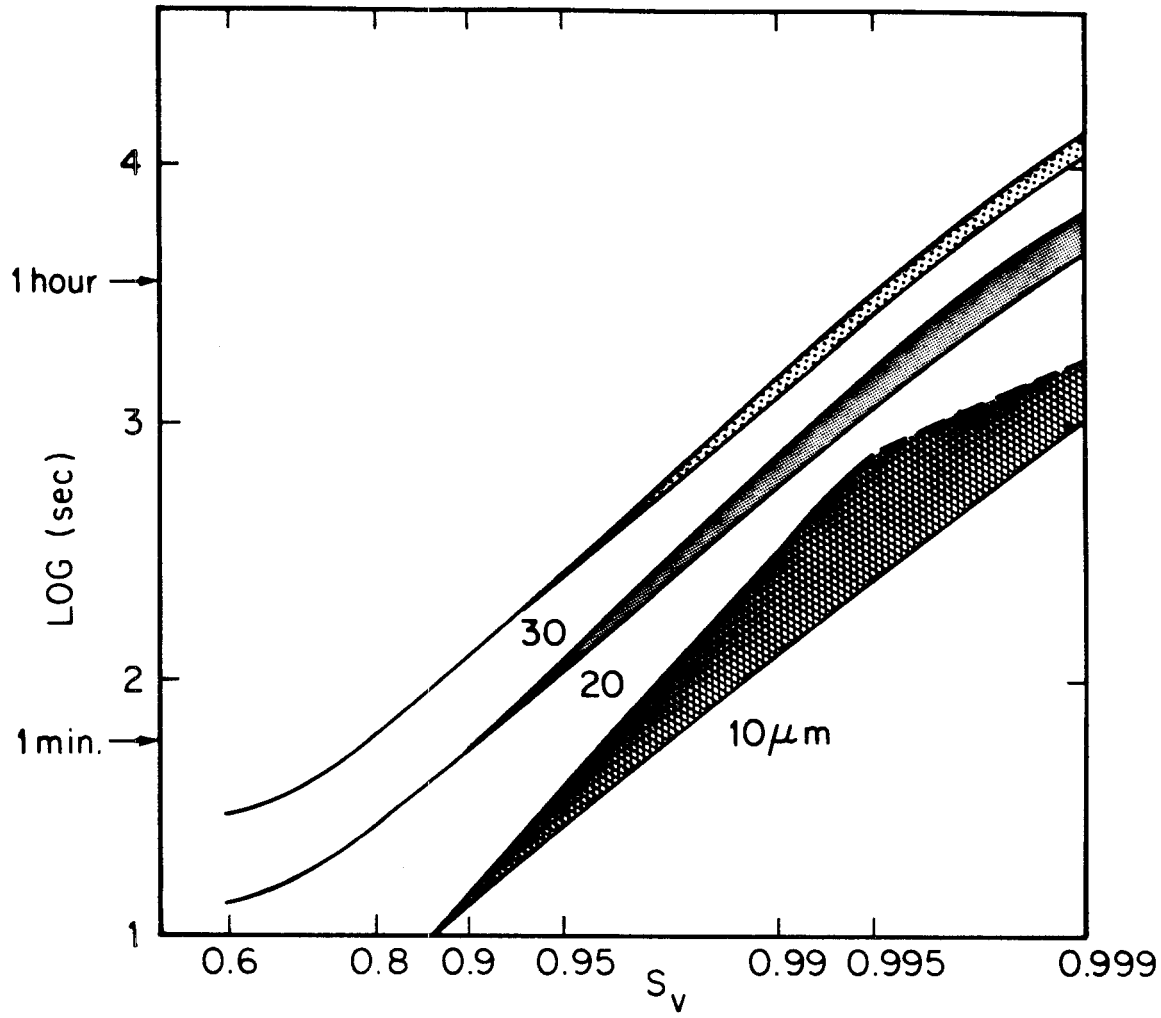

Figure 2.6 Droplet lifetimes. Time required for droplet of initial diameter given to shrink to equilibrium size for indicated humidity (S_v= RH/100); range indicated is for 0.1 (lower) to 1.0 (upper) μm diameter nucleus.

actual increase in deposition would be reflected in this proportionality. Furthermore, fog may effectively scavenge important pollutant gases, such as $SO_2(g)$, $HNO_3(g)$, and $NH_3(g)$. Turbulent diffusional processes are dominantly responsible for deposition of gases, and deposition velocities have been reported about 1 cm s^{-1} for $SO_2(g)$ (Sehmel,1980) and 2 cm s^{-1} for $HNO_3(g)$ (Huebert and Robert, 1985). However, gas scavenging by droplets would cause removal of these species to be dominated by the sedimentation or impaction flux.

2.2.3 Summary.

The deposition associated with fog transport could be divided into three transport-limit regimes: (a) impaction (high wind, efficient canopy filtration); (b) turbulence (high wind, inefficient canopy); and, (c) sedimentation (low wind, efficient or inefficient canopy). A cross-over point seemed to exist for wind speeds of 2 m s^{-1}; at lower wind speeds, transport was generally dominated by sedimentation. The sizes of mature droplets were found to be stable with respect to brief exposure to slightly undersaturated air. Thus, chemical transport associated with fog deposition should not be affected, although evaporation may be important in determining water fluxes by fog droplet capture. Finally, fog scavenging is important in determining deposition rates for pollutant species as they can partition between the phases present in the atmosphere.

Chapter 3

EXPERIMENTAL METHODS

An essential goal of this research has been to obtain detailed information on the chemical and physical properties of fogwater and fog processes from a variety of locations. To satisfy this goal, measurements have been made during extensive field trips over the past several years. Sampling sites are listed in Table 3.1. Descriptions of most of these sites have been provided in the references given in this table. Results from field sampling programs at Henninger Flats and Meadows Field Airport in Bakersfield are discussed in detail in chapters of this thesis. The methods used in acquiring samples in the field and subsequent analyses in the laboratory are given in the following sections.

3.1 Fogwater Collection

Fogwater samples for chemical analysis were collected with a rotating arm collector (RAC). The Caltech RAC, which was based on an earlier design by Mack and Pilié (1975), was modified by application of current aerosol collection design criteria (Jacob et al., 1984a). In essence, the RAC was a rapidly rotating (1700 rpm) narrow rod with slots on the leading edges and collection bottles on both ends (Figure 3.1). Its steel surfaces were coated with Teflon. Prior to each field use, it was acid-soaked and carefully cleaned with distilled, de-ionized water (D_2-H_2O). Calibration of a scale model instrument was performed with chemically tagged solid particles. This calibration indicated a lower size-cut (i.e., diameter for 50% collection efficiency) of 20 μm (Jacob et al., 1984a).

Table 3.1

SUMMARY OF CALTECH FOG SAMPLING PROGRAM

1981 to 1985

	Site Description
Southern California	
1. Pasadena (Keck roof at Caltech)	a
2. Long Beach (downtown Harbor)	b
3. Lennox (SCAQMD air monitoring station)	a
4. Corona del Mar (Kerkoff Marine Laboratory)	b
5. Del Mar (County fire station at fairgrounds)	"
6. San Marcos Pass (County fire station)	"
7. Henninger Flats (Nursery)	c
8. San Nicolas Island (U.S. Navy base)	b
9. Upland (CARB air monitoring station)	a
10. Ontario (CARB air monitoring station)	
San Joaquin Valley	
11. Oildale (CARB monitoring station)	a
12. Bakersfield (CARB air monitoring station)	d
13. Bakersfield (Meadows Field Airport)	e
14. Buttonwillow (Parks and Recreation building)	f
15. McKittrick (WOGA air monitoring station)	"
16. Visalia (CARB monitoring station)	"
Central California coast	
17. Point Reyes (National Monument)	b
18. San Francisco (Mt. Sutro tower)	"
19. Morro Bay	"
20. San Luis Obispo (3 km off-shore aboard RV Acania) and;	
21. Albany, NY (County airport).	g

References: a. Munger et al., 1983; b. Jacob et al., 1985c; c. Waldman et al., 1985 (Chapter 6, this thesis); d. Jacob et al., 1984b; e. Jacob et al., 1985a; f. Chapter 7; g. Jiusto and Lala, 1983.

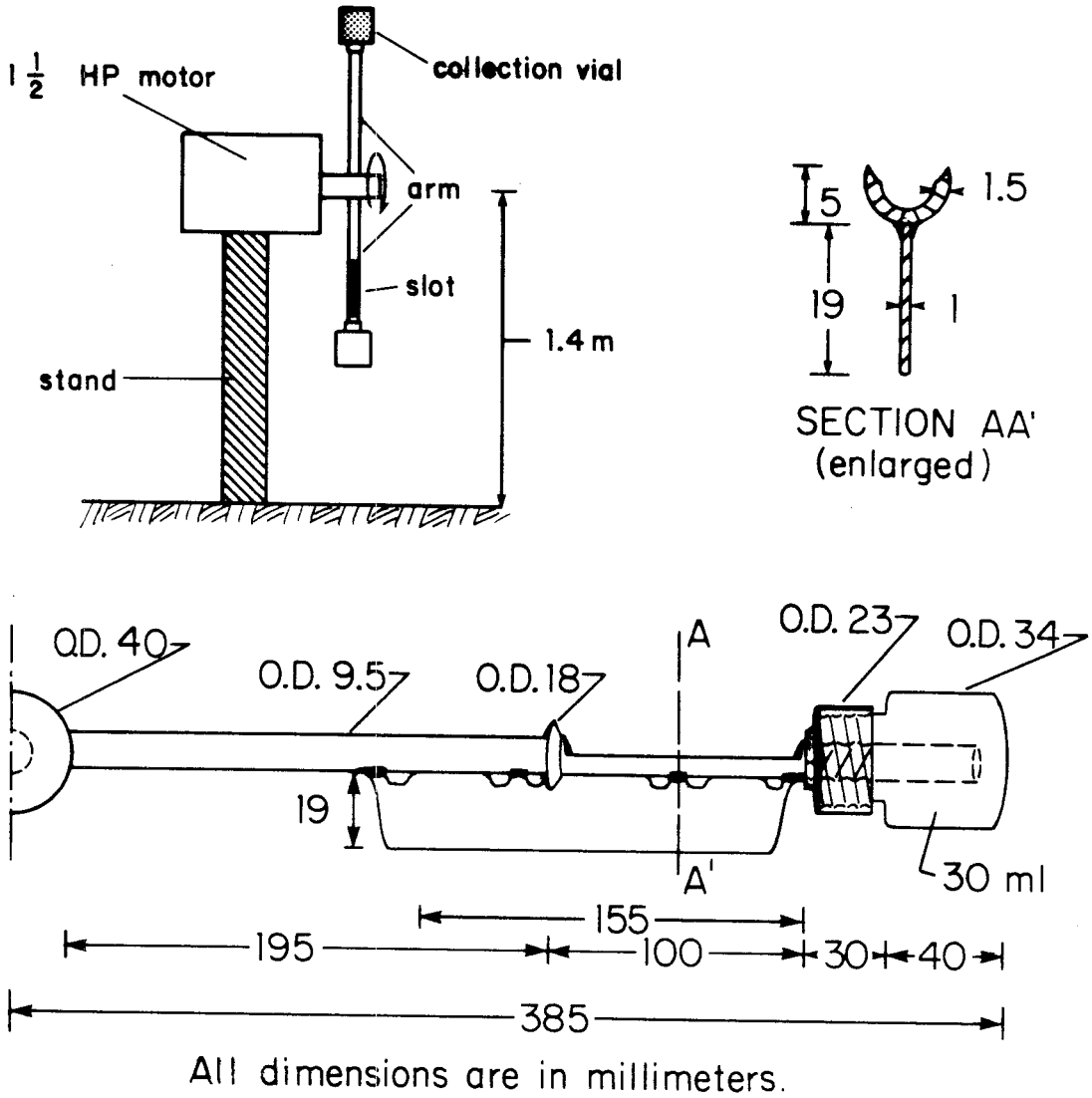

Figure 3.1 Caltech rotating arm collector (RAC).

At most sites, the RAC was placed on top of buildings. At several remote or rural sampling sites, the apparatus was situated on the ground in an open area. During sampling, the collection bottles (Nalgene, pre-soaked in D_2-H_2O) were manually exchanged at the end of each interval. Between 30 to 120 min were generally adequate to provide sample volumes of 10-60 mL, depending on fog density. Samples as small as 1 mL were collected in light fogs and subsequently analyzed. Aliquots for certain analyses (pH, formaldehyde, S(IV), and trace metals) were separated immediately following collection. The remaining volume was stored in the collection bottle and refrigerated.

3.2 Aerosol and Gaseous Nitric Acid & Ammonia Concentrations

Ambient aerosol concentrations were measured on 47 mm Teflon filter medium, using open-faced filter holders. At the flow rate of 10 l min^{-1}, the holder inlet was large enough that anisokinetic bias should not have affected the collection of even large particles or fog droplets. For example, the Stokes number based on the inlet dimension and velocity (St_{inlet}; see Eqn 2.2) for a 50 μm diameter droplet is 0.02; this value is below the point where an inlet bias will be important (Davies and Subari, 1982).

A dual-filter technique was used to measure gaseous HNO_3 and NH_3 in the atmosphere (Appel et al., 1980; Cadle et al., 1980; Russell and Cass, 1984). Nylon (for nitric acid) and oxalic acid-impregnated glass fiber (for ammonia) filters were placed in the backup position of polycarbonate filter holders; each was immediately behind a Teflon filter. On several occasions, simultaneous filter samples were collected behind a cyclone separator to give the aerosol concentrations

in the fine ($\leq$3 μm) fraction (John and Reischl, 1980). Filters were extracted in water with a reciprocating shaker for at least 1 hour. Previously, concern has been raised that aqueous extraction may be insufficient to fully wet the Teflon medium and to dissolve trapped particles (Derrick and Moyers, 1981). This possibility was tested by wetting extracted filters with methanol; less than 5% additional solute was recovered.

3.3 Surrogate-Surface Deposition Measurement Methods

Polyethylene buckets and polystyrene petri dishes were used to measure deposition of water-soluble material in fog environments. Collectors were generally placed at the same level as the aerosol sampler inlets ($\geq$3 m AGL). Deposition rates were measured over 3 h to 7 d intervals. Petri-dish exposures in fog were usually 3 to 4 h. Water extractions were done for both containers, which were rotated or tilted by hand to wet the bottom and sides. This method gave consistently good recovery of water soluble species, i.e., better than 90% when compared to subsequent extractions. Further details of precipitation and surrogate-surface measurements are given in Chapter 6 (Henninger Flats) and Chapter 7 (San Joaquin Valley).

3.4 Sample Analyses

Major ions were determined in fogwater, aerosol and deposition samples using similar techniques. Specific protocols were refined over the course of the research program. Due to the high aqueous concentration in most fogwater samples, detection limitations were rarely a problem. Quantitative dilutions (5 to 50:1) were often

necessary to bring major constituents within analytical range. The methods are summarized below.

Hydrogen Activity (pH) was determined with a Radiometer Model PHM80 or PHM82 with combination electrode (Model GK2401C). Measurements were made in 0.5-1.0 mL without agitation immediately after each fogwater sample was collected. Stable values were found comparing field with laboratory pH measured days later when pH < 4. Neutral and alkaline samples occasionally showed a shift in pH after storage.

Anions (Cl^-,NO_3^-,SO_4^{2-}) concentrations were determined by ion chromatography (IC) (Dionex Model 10 or 2000 with anion columns AS1, AS3, or AS4). We used $Na_2CO_3/NaHCO_3$ eluents for strong-acid anions in accordance with the manufacturer's recommendations (Dionex, 1981). The eluent strength used after 1983 (2.7/2.16 mM) was 10% lower than reported in earlier work (Waldman et al., 1982; Munger et al., 1983) and was found to give better ion separation with the newer columns.

Weak organic acids eluted very quickly during strong anion determinations given above. These interfered in the fluoride peak for fogwater samples which were found to contain appreciable amounts of these acids. The high [F^-] reported in our earlier papers has been now recognized to be due to these interferences. In some samples with relatively high organic acid concentrations, these interfered with the chloride determination as well (see Jacob et al., 1985c).

Although a sulfite peak could be measured by IC, there was no way to be certain that this represented the in situ concentration, since oxidation in storage would cause an increase in measured sulfate. When appreciable S(IV) was found (>5% total S), aliquots were dosed with H_2O_2 to 0.06% prior to IC injection. This was done to determine a total

sulfur value. Complete conversion of reduced sulfur to sulfate was verified with sulfite standards. Using S(IV) values (see below), sulfate was calculated by difference.

Analytical uncertainties were $\leq \pm 5\%$ for nitrate and sulfate and $\pm 10\%$ for chloride; when interference was observed for Cl^-, the value was not reported.

Ammonium ion was determined by the phenol-hypochlorite method of Solorzano (1967) with colorimetric determination of indophenol blue at 640 nm. Oxalic acid filter extracts were analyzed for NH_4^+ with a variation of this method described by Russell (1983). Analytical uncertainty for NH_4^+ determinations was $\leq \pm 10\%$.

Cations (Na^+, K^+, Ca^{2+}, Mg^{2+}) were determined by atomic absorption spectrophotmetry (AAS) using an air/acetylene flame (Varian Model AA5 or AA6). Aliquots were spiked with lanthanum (to 0.025% La^{3+} and 30 mM HCl) to release chelated calcium or magnesium ions. Analytical uncertainties were $\leq \pm 5\%$ for cations by AAS.

Preservation of S(IV) in separated fogwater aliquots was done by the addition of excess formaldehyde at pH 4, and the pararosaniline method and colorimetric detection at 580 nm were used for subsequent S(IV) analyses (Dasgupta et al., 1980). Some samples before 1984 were preserved by addition of EDTA and phosphate buffer at pH 7 and analyzed by the colorimetric method given by Humphrey et al. (1970); see Munger et al. (1984) for details.

Formaldehyde was determined by the formation of 3,5-diacetyl-1,4-dihydrolutidin through the addition of acetyl acetone in the presence of NH_4^+ (Nash, 1953) and detection at 412 nm. High S(IV) concentrations caused interference with the CH_2O determination,

presumably due to formation of hydroxymethanesulfonate (HMSA). Addition of I_2 to aliquots, to oxidize S(IV), eliminated this interference (Smith and Erhardt, 1975). This was verified by comparing CH_2O response in HMSA standards with I_2 added; see Munger et al. (1984).

Trace Metals (Fe, Mn, Pb, Cu, Ni) were determined by flameless AAS with graphite furnace (Perkin-Elmer 360 equipped with a HGA 2100 or Varian AA6 with CRA 90). Aliquots were stabilized with a 1% spike of Ultrex-grade HNO_3 and stored in acid-washed Nalgene containers. Analytical uncertainties depended upon the element and concentration range; $\pm$20% may be taken as an average.

3.5 Liquid Water Content Measurement (LWC) Techniques

Four separate methods were used at field sites during this research; these included: (a) estimation by fogwater collection rate; (b) mass determination with high volume sampler and paper filter; (c) infrared (IR) extinction with a carbon dioxide laser transmissometer; and, (d) droplet sizing with an optical particle counter. Additional details of field measurements have been given in Chapter 5.3.

a. Fogwater Collection Rate (RAC) Method. The RAC ideally sampled air at a rate of 5 m^3 min^{-1}, given its rotational speed and dimensions. The air in the wake of the collection surface would need to be renewed in the time required for each half-rotation. While this was not verified experimentally, the RAC motion caused a fan effect which, along with the turbulence, induced air motion sufficient to satisfy this requirement. Besides incomplete renewal of sampled air, another factor which could decrease the overall water collection efficiency was the omission of smaller droplets. The size-cut indicated for the collector,

20 μm (Jacob et al., 1984a), was comparable to droplet mass-median diameter measured in fog (e.g., Pilié et al., 1975; Roach et al., 1976; Goodman, 1977). Hence, a nontrivial fraction of the droplet spectrum may have been omitted. Taking these factors into consideration, the value calculated from the nominal RAC collection rate represented a lower limit for LWC.

b. High-Volume Sampler (Hi-Vol) Method. A known volume of fog-laden air was drawn through a paper filter, and the amount of water collected was determined by mass-difference. Standard high-volume (Hi-Vol) samplers were used with the flow rate maintained by a flow controller and/or checked with flow orifice. Short (5-20 min) intervals were used. Before each sample, the filter paper was briefly run or "primed" to saturate it with respect to water vapor. For the inlet dimension (20 cm), $St_{inlet}<0.1$ for 50 μm droplets, hence anisokinetic sampling biases were not a problem (Davies and Subari, 1982).

c. Carbon Dioxide Laser Transmissometer (CO_2LT) Method. An infrared transmissometer to operate in fog was designed and built at the Jet Propulsion Laboratory with the assistance of Dr. William Grant. Background theory is given in Appendix A. The instrument was successfully tested at Henninger Flats during June 1983. Similar attempts were made at Albany, NY in October 1982 and in Bakersfield during 1984 and 1985 field studies. Laser power failures prevented successful field operation in these cases.

The instrument design is given in Figure 3.2. A CO_2 waveguide laser (Hughes Model 3820-HGBD) emitted coherent infrared radiation at 9.4 μm wavelength. The laser beam was split into a reference signal and a transmitted signal (1:2.8). The ZnSe beam splitter was constructed

CO_2 LASER TRANSMISSOMETER (CO_2 LT)

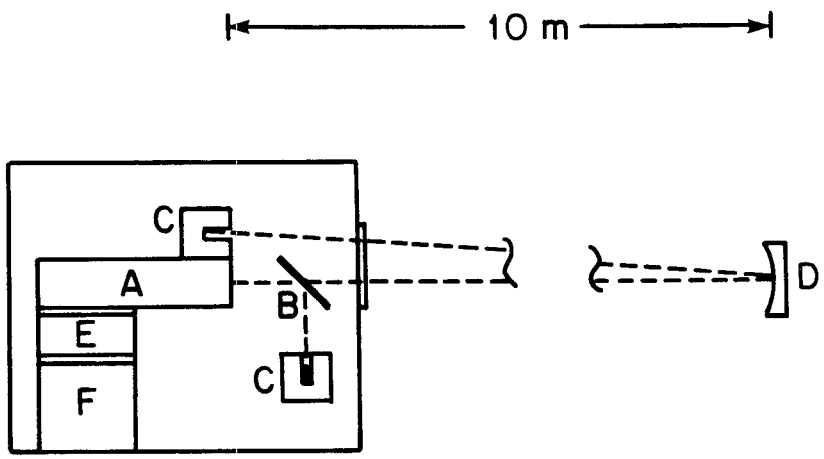

A. LASER
B. BEAM SPLITTER
C. DETECTORS
D. PARABOLIC METER
E. RATIO METER
F. STRIP--CHART RECORDER

Figure 3.2

with a 7^{o} wedge angle. This was done after we found that the fraction of transmitted laser radiation changed with minor wavelength variations, multiply-reflected by the beam splitter surfaces, without this wedge. The optical path was folded with a total length 20 m at 1.5 m above the ground. A mirror (15 cm diameter) with a 10 m radius of curvature focused the transmitted beam back to the instrument. The emitted beam diameter (86% power) was 1.4 mm with 10 mrad divergence; focused by the mirror, the return beam diameter was approximately as small.

Two disk (2.5 cm diameter) calorimeters (Scientech Model 360) were used to thermally sense laser radiation. One was used as a reference for laser output and the other to monitor the return signal. Laser output changed slowly with small amplitude, low frequency oscillation, indicating some instability of the laser emission line. The ratio of signals was formed directly by using an analog ratiometer (Princeton Applied Research, Model 188). Thus, transmission measurements were largely independent of these minor laser power fluctuations. The clear air ratio was stable before and after fog was monitored. For the data reported herein, both the signal ratio and laser output were recorded with a dual-channel strip chart and later digitized.

d. Optical Particle Counter (CSASP) Method. Droplet size spectra were measured in the fog with Classical Scattering Aerosol Spectrometer Probe manufactured by Particle Measuring Systems, Inc. (Model PMS CSASP-100HV). The instrument provided counts of droplets passing through a HeNe laser beam and classified them according to the intensity of light scattered onto photodetectors; further details of the principals of operation have been describe by Knollenberg (1981) and other. Particles can be classified into 15 size intervals for 4

different ranges. In fog, droplet spectra were taken in Range 0 (2-47 μm diameter) which had size intervals of 3 μm. Sizing calibration and acitvity corrections provided by the manufacturer were used.

3.6 Meteorological Measurements

Most fog sampling sites were collocated where meteorological instrumentation was available. At more remote locations, temperature was measured with a glass-bulb thermometer, and wind speeds and directions were periodically assessed by observation. At Henninger Flats, Los Angeles County Fire Department records of precipitation, cloud cover, temperature and relative humidity were used to supplement field measurements. In the spring 1983, supplementary wind data were provided by mechanical weather stations reported in Hering and Blumenthal (1983).

For the San Joaquin Valley 1984-85 study (Chapter 7), wind and temperature data were recorded at the Bakersfield Airport fog sampling site with sensors and data acquisition equipment specifically deployed for this research (Qualimetrics, Inc., Sacramento, CA). Cup anenometers (Model 2005) and temperature sensors (Model 4480-A) were positioned on a 3 m tower. Sensor signals were conditioned with manufacturer-designed modules. Analog outputs were continuously logged with an A/D converter and an IBM personal computer. Additional data from that period were also taken from National Weather Service observations. Relative humidity and ambient temperature were recorded with hygrothermographs located at other valley sites. Parameters aloft (wind speed, direction, temperature, and relative humidity) were measured by a tethersonde at Buttonwillow. Mixing height data for that period were also provided

from acoustic radar located at Kernridge (Westside Producers or Western Oil and Gas Association) and cloud top observations at Bakersfield Airport by Flight Tower personnel (FAA, private communication).

Chapter 4

EARLY RESULTS:

CHEMICAL COMPOSITION OF ACID FOG

by

Jed. M. Waldman, J. William Munger, Daniel J. Jacob,

Richard C. Flagan, James J. Morgan, and Michael R. Hoffmann

Science 218, 677-680 (1982)

COVER

Power plant emissions discharged directly into a marine fog bank along the central California coast at Morro Bay. Fog and cloud droplets appear to provide a propitious environment for the rapid oxidation of sulfur dioxide to sulfate and for the scavenging of gas phase nitric acid and ammonia. Fog water collected in various urban locations in California was found to have higher concentrations of sulfate, nitrate, and ammonium ion than previously observed in acidic precipitation. The *p*H of fog water in Los Angeles was found to be routinely in the range of 2.2 to 4.0. See page 677. [J. William Munger, California Institute of Technology, Pasadena 91125]

Chemical Composition of Acid Fog

Abstract. *Fog water collected at three sites in Los Angeles and Bakersfield, California, was found to have higher acidity and higher concentrations of sulfate, nitrate, and ammonium than previously observed in atmospheric water droplets. The* p*H of the fog water was in the range of 2.2 to 4.0. The dominant processes controlling the fog water chemistry appear to be the condensation and evaporation of water vapor on preexisting aerosol and the scavenging of gas-phase nitric acid.*

In the fall of 1981, a field study was initiated to determine the chemical composition of fog water in the Los Angeles basin. Results show that the fog water is significantly more acidic and concentrated with respect to chemical composition than cloud and rain water collected in southern California. Liljestrand and Morgan (*1*) determined the chemical composition of rain in Los Angeles and reported that light, misting rainfalls had the highest acidity (*2*). Earlier fog water studies (*3–5*) in nonurban environments have reported concentrations of major

0036-8075/82/1112-0677$01.00/0

Table 1. Ranges in concentrations observed during six fog events in the Los Angeles area during 1981 and 1982 (*11*). Representative concentrations for other fog, cloud, and rain samples are presented for comparison. The ranges shown in the values for this study are from

Location	N	Date	pH	Concentration (μeq/liter)					
				H^+	Na^+	K^+	NH_4^+	Ca^{2+}	Mg^{2+}
Pasadena	4	11/15/81	5.25–4.74	5.6–55	12–496	4–39	370	19–360	7–153
Pasadena	4	11/23/81	4.85–2.92	14–1,200	320–500	33–53	1,290–2,380	140–530	89–360
Lennox	8	12/7/81	5.78–2.55	2–2,820	28–480	6–160	1,120–4,060	44–4,350	17–1,380
Lennox	3	12/17/81	2.81–2.52	1,550–3,020	80–166	19–40	950–1,570	73–190	43–99
Bakersfield*	3	1/14/82	3.07–2.90	850–1,260	151–1,220	39–224	5,370–10,520	165–1,326	20–151
Pasadena*	1	1/17/82	2.25	5,625	2,180	500	7,870	2,050	1,190
Los Angeles rain (volume-weighted means at nine sites)		1978–1979	5.4–4.4	4–39	4–37	0.24–4.9	1–36	3.9–17	1.7–11
Coastal California fogs		9–10/76			78–944	8–26	1–578	9–102	17–175
Whiteface Mountain		7–8/80	4.2–3.2	63–630	1–55	1–6	4–310		
Fog and clouds, U.S.S.R.		1961–1964	5.3–4.7	5–20	30–104	15–44	33–100	20–50	17–83

*$[Na^+]$, $[K^+]$, $[Ca^{2+}]$, $[Mg^{2+}]$, and $[NH_4^+]$ for filtered aliquots.

ions comparable to those reported for cloud (*6*, *7*) and rain (*8*) water. However, urban fogs tend to form under more polluted conditions than clouds. Our research program expands upon these earlier studies in an attempt to focus on the chemical and physical processes that occur in the atmospheric aqueous phase before a precipitation event. In the Los Angeles basin, fog and cloud water processes may represent a significant pathway for SO_2 and NO_x oxidation and for the concomitant production of acidity. Furthermore, morning fog and low clouds along the coast have been strongly correlated with high SO_4^{2-} aerosol concentrations during the afternoon in the Los Angeles basin (*9*).

In this study, fog water was collected with a rotating arm collector (*10*). Droplets impact in slots along the ends of the arm and are driven outward by centrifugal force into sample collection bottles which serve effectively to isolate the collected liquid. In cloud chamber tests, the lower particle size cutoff for this collector was estimated to be 8 μm. Two of the collection sites were in the Los Angeles basin (Pasadena and Lennox), and the third was located in the San Joaquin Valley near Bakersfield. The Pasadena site was located in a residential neighborhood 25 km from downtown Los Angeles; the Lennox site, 2 km from the Los Angeles International Airport, was adjacent to a freeway and near two power plants and one oil refinery; and the site in the San Joaquin Valley was located in Oildale, which is surrounded by secondary oil recovery operations.

The concentration ranges of major chemical components observed during six separate fog events are listed in Table 1. These ranges represent the low and high values measured in time-sequenced samples over the duration of the particular fog events (*11*).

The first fog event in Pasadena followed a day with good air quality; the second fog event in Pasadena was preceded by a hazy day. Concentrations of most ions in the second fog event were much higher than in the first. The third and fourth fog events were sampled in Lennox on nights of dense coastal fog. Smog and dense haze had persisted throughout the day preceding the third fog event, accompanied by high ambient NO_x concentrations along the coast. These samples had even higher concentrations than the Pasadena fog samples. In addition, the fog water contained a significant amount of solid material, especially the final sample taken as the fog dissipated. Most of the particles remained suspended in the samples after standing for several days, which suggests that they were too small to have been collected unless incorporated in larger droplets.

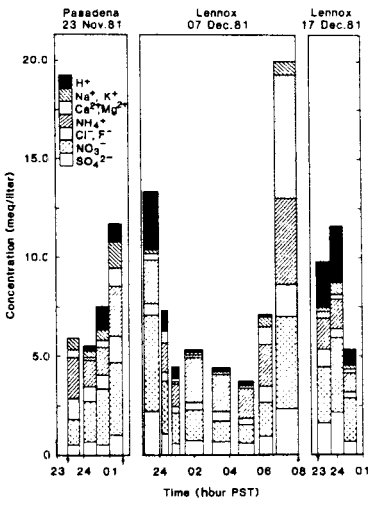

Fig. 1. Ionic composition in serial samples collected during three Los Angeles fog events; *PST*, Pacific standard time. The width of each bar represents the sampling interval. Fog formation and dissipation (that is, the beginning and end of individual fog events) are indicated by arrows. Fog had formed at least 1 hour prior to the taking of the first sample on 7 December 1981; sampling on 17 December 1981 ended before the fog dissipated. The effect of dilution and concentration can be seen in terms of the proportional changes in ionic concentration.

A single fog event at Bakersfield was monitored during a period of extended fog throughout the entire San Joaquin Valley. The southern portion of the valley has a number of oil fields in which steam-injection oil recovery methods are used. Consequently, the sulfur emissions are high for a nonurban, agricultural area. The fog water analyses, which were characterized by low *p*H values (2.9) and high $[SO_4^{2-}]$ (5.0 meq/liter), $[NO_3^-]$ (5.1 meq/liter), and $[NH_4^+]$ (10.5 meq/liter), reflect the dichotomous land use in the San Joaquin Valley.

The last sample, a single fog water sample, was collected on the night of 17 January 1982 in Pasadena. The *p*H of this sample (2.25) was unusually low with corresponding high $[NO_3^-]$ (12 meq/liter), $[SO_4^{2-}]$ (5 meq/liter), and $[NH_4^+]$ (8 meq/liter); however, the duration of this fog event was relatively short (~ 1 hour).

The concentrations of the major components in the California fog samples were significantly higher than in previously reported samples of fog, cloud, and rain water (Table 1). The observed values of $[SO_4^{2-}]$, $[NO_3^-]$, $[NH_4^+]$, and $[H^+]$ were 10 to 100 times higher than the earlier values. Values of $[Na^+]$, $[K^+]$, $[Ca^{2+}]$, $[Mg^{2+}]$, and $[Cl^-]$ were high but more in line with values reported for fog

sequential samples during individual events with the exception of the sixth event. For the comparison data, the ranges represent many events.

Concentration (μeq/liter)				Concentration (mg/liter)		Reference
F^-	Cl^-	NO_3^-	SO_4^{2-}	Fe	CH_2O	
120	56–280	130–930	62–380	0.094–2.1		
180–410	480–730	1,220–3,520	481–944	0.92–1.77	3.1–3.5	
115–395	111–1,110	820–4,560	540–2,090	0.34–24	4.6–12.8	
180–500	90–197	2,070–3,690	610–1,970	1.02–2.08		
126–242	203–592	3,140–5,140	2,250–5,000		6.1–14.4	
637	676	12,000	5,060			
	5–52	11–44	7–56	0.004–0.17		(1)
	96–1,230	23–234	52–490			(5)
11–54	1–15	7–190	40–800			(7)
	59–177	2–13	13–185			(4)

and cloud water in other areas. High values of $[CH_2O]$, [Fe], [Mn], and $[SO_3^{2-}]$ (30 to 260 μeq/liter) were also found. The observed concentrations of S(IV) appear to be in excess of those predicted by Henry's law considerations, although formation of sulfonic acid derivatives and iron sulfito complexes can account for this apparent discrepancy (*12*).

Figure 1 illustrates the changes in total ionic concentration with respect to time for three fog events. A concave trend in the profile of concentration versus time (decreasing at the beginning and rising toward the end) was observed. Changes in the absolute concentration of individual ions that are proportional to the changes in total concentration indicate that water vapor condensation and the evaporation of fog droplets are the dominant processes. Sharp decreases in concentration during the first few hours of the fogs in Lennox were due primarily to initial droplet deliquescence on preexisting aerosol. Similarly, most of the increase in concentration that was observed as the fogs dissipated was due to evaporation and the regeneration of fine aerosol. These physical effects apparently play a dominant role in determining fog chemistry in the Los Angeles basin.

The dominant ions in the fog water were NH_4^+, H^+, NO_3^-, and SO_4^{2-}, and their highest concentrations were observed after days of dense haze. During the early phases of the Lennox fogs, these ions make up ≥ 90 percent of the total ionic concentration. This result suggests that preexisting aerosol is a major determinant of the chemical composition of fog water, since these four species are the major components of the daytime aerosol haze (*13*).

In Los Angeles, the equivalent concentration ratio of NO_3^- to SO_4^{2-} in fog water was about 2.5, which is comparable to the reported emission ratio (*9*). The corresponding ratio in Los Angeles precipitation was close to 1.0 (*1*). In the Bakersfield fog, the same ratio was ~ 1.

The observed changes in fog water composition may have resulted either from chemical changes in the droplets or from the advection of different air masses over the sites. In Pasadena, $[H^+]$ and $[NO_3^-]$ increased simultaneously as a function of time; this result suggests the transport of HNO_3 or N_2O_5 into the droplets (*14*). On 7 December 1981 in Lennox, $[NH_4^+]$ doubled from the third to the fourth sampling period while there was a corresponding decrease in $[H^+]$. Transfer of gaseous NH_3 into the droplets could account for this neutralization. However, the delay in the $[NH_4^+]$ increase after the onset of fog suggests that the advection of fog formed on condensation nuclei with different characteristics was responsible. During the last few hours of that event, an increase in $[Ca^{2+}]$, $[Mg^{2+}]$, and [Fe] was observed. This increase coincides with the morning rush hour traffic on the adjacent freeway and can be attributed to the incorporation of road and soil dust into the fog. The fogs in Lennox initially exhibited a high acidity that was progressively neutralized, whereas the fogs in Pasadena became more acidic during a fog event. This result suggests differences in the composition of the aerosol preceding the fog at each site and differences in the transfer characteristics from gas or solid to liquid.

The results of this study show that the concentrations of major chemical species in fog water collected at three sites in Los Angeles and Bakersfield are significantly higher than previously reported in atmospheric water droplets. The chemistry of fog water in Los Angeles appears to be dominated by the composition of the haze-forming aerosol that precedes it. Subsequent effects of condensation and evaporation control the observed concentrations. Secondary aerosol, which has high $[NH_4^+]$, $[H^+]$, $[NO_3^-]$, and $[SO_4^{2-}]$, deliquesces initially to give a concentrated fog water. Further condensation of water results in dilution. After initial formation, the fog water appears to incorporate additional NH_3, HNO_3, and calcareous dust. As the fog dissipates by evaporation, higher concentrations are again observed.

In light of the inordinately high concentrations of acidic components found in Los Angeles fog, further research is needed to determine the role of aqueous atmospheric droplets in SO_2 and NO_x conversion and acidity transport processes. High $[H^+]$, $[NO_3^-]$, and $[SO_4^{2-}]$ found in fog water may have a significant effect on health and on materials and plants in urban areas such as Los Angeles and in nonurban areas such as Bakersfield.

JED M. WALDMAN
J. WILLIAM MUNGER
DANIEL J. JACOB
RICHARD C. FLAGAN
JAMES J. MORGAN
MICHAEL R. HOFFMANN*
Environmental Engineering Science, W. M. Keck Laboratories, California Institute of Technology, Pasadena 91125

References and Notes

1. H. M. Liljestrand and J. J. Morgan, *Environ. Sci. Technol.* **12**, 1271 (1978); *ibid.* **15**, 333 (1981); H. M. Liljestrand, thesis, California Institute of Technology, Pasadena (1980).
2. J. J. Morgan and H. M. Liljestrand, *Report Ac-2-80* (California Air Resources Board, W. M. Keck Laboratory, California Institute of Technology, Pasadena, 1980).
3. H. Houghton, *J. Meteorol.* **12**, 355 (1955).
4. O. M. Petrenchuk and V. M. Drozdova, *Tellus* **18**, 280 (1966).
5. E. Mack and U. Katz, *Report CJ-6017-M-1* (Calspan Corporation, Buffalo, N.Y., 1977).
6. H. Mrose, *Tellus* **18**, 266 (1966); T. Okita, *J. Meteorol. Soc. Jpn.* **46**, 120 (1968); C. S. Martens and R. C. Harriss, *J. Geophys. Res.* **78**, 94 (1973); R. E. Falconer and P. D. Falconer, *ibid.* **85**, 7465 (1980); R. Castillo, personal communication.
7. P. D. Falconer, Ed., *Publication 806* (Atmospheric Sciences Research Center, State University of New York, Albany, 1981).
8. V. M. Drozdova and E. P. Makhon'ko, *J. Geophys. Res.* **75**, 3610 (1970); L. Granat, *Tellus* **24**, 550 (1972); C. V. Cogbill and G. E. Likens, *Water Res.* **10**, 1133 (1974).
9. G. R. Cass, thesis, California Institute of Technology, Pasadena (1977); *Environ. Qual. Lab. Mem. 5* (California Institute of Technology, Pasadena, 1975).
10. The Caltech rotating arm collector was modified from an original design by E. J. Mack and P. Pilie [U.S. Patent 3885532 (1975)]. The impaction surfaces move at a velocity of approximately 50 m/sec. A sampling velocity that is much greater than the ambient wind speed serves to minimize the bias due to anisokinetic sampling [K. R. May, in *Airborne Microbes*, P. H. Gregory and J. L. Monteith, Eds. (Society for Gene

al Microbiology, Cambridge, England, 1967), p. 60]. Thermodynamic and mass transfer calculations suggest that evaporation of the fog water is insignificant during the time of collection.
11. Immediately after collection, the *p*H of the sample was measured and aliquots were separated for later analyses. Major metal cations were determined by atomic absoption spectrophotometry and major anions by ion chromatography. Both NH_4^+ and CH_2O were determined by standard colorimetric methods. Ultrex grade HNO_3 was added to preserve the trace metals; SO_3^{2-} was stabilized by reaction with CH_2O at *p*H 4.
12. L. D. Hansen, L. Whiting, D. J. Eatough, T. E. Jensen, R. M. Izatt, *Anal. Chem.* **48**, 634 (1976).
13. B. R. Appel, E. L. Kothny, E. M. Hoffer, J. J. Wesolowski, *Adv. Environ. Sci. Technol.* **9**, 315 (1980).
14. J. H. Seinfeld, *Air Pollution* (McGraw-Hill, New York, 1975).
15. Financial support was provided by the California Air Resources Board (grant AO-141-132), and logistical support was provided by the South Coast Air Quality Management District. We thank G. Cass, D. Lawson, and J. H. Seinfeld for assistance.
* To whom correspondence should be addressed.

15 March 1982; revised 10 May 1982

12 November 1982 • Vol. 218 • No. 4573

$2.50

SCIENCE

AMERICAN ASSOCIATION FOR THE ADVANCEMENT OF SCIENCE

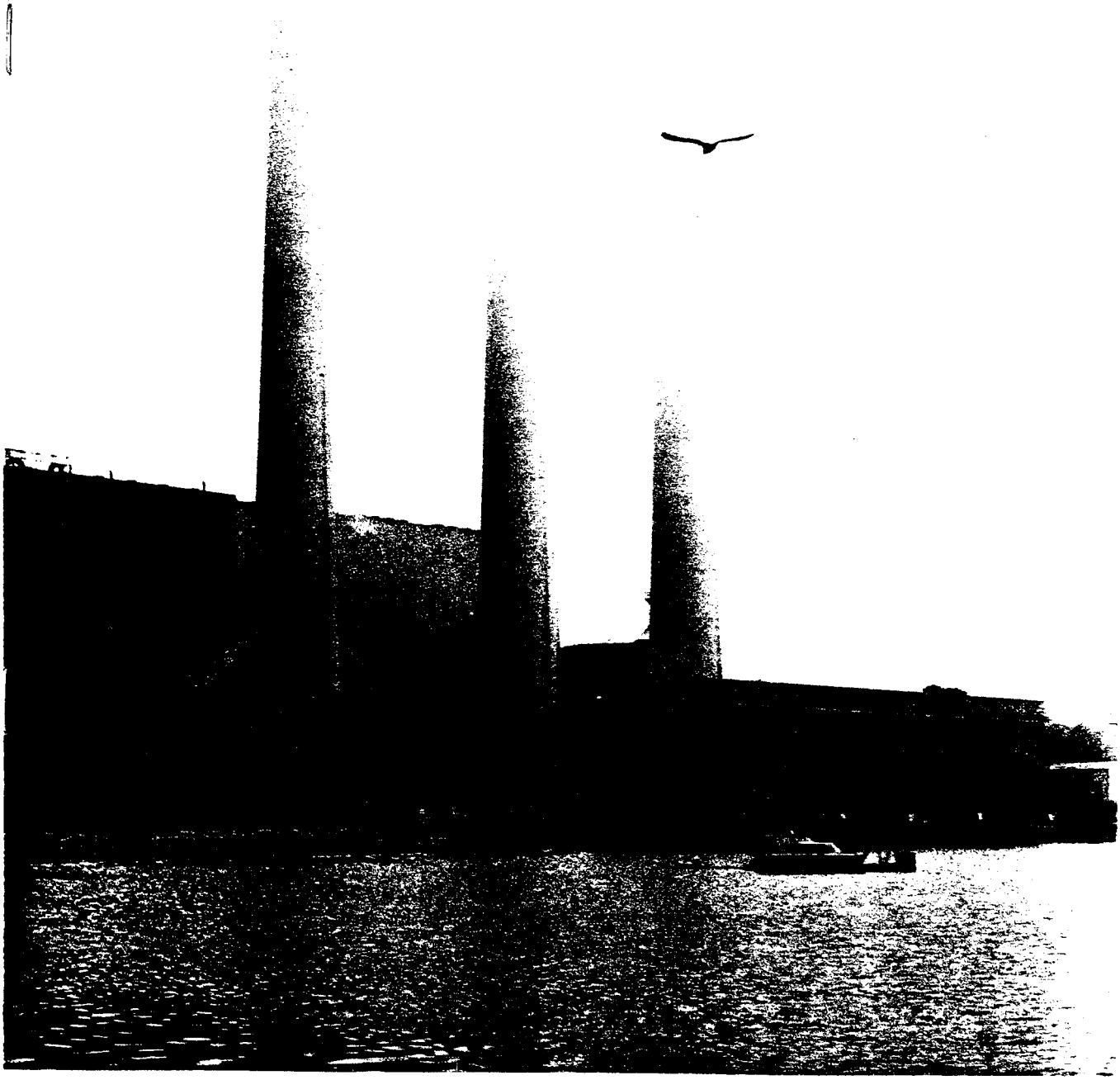

Chapter 5

FIELD INTERCOMPARISON OF FOG COMPOSITION AND LIQUID WATER CONTENT MEASUREMENTS BY VARIOUS METHODS

ABSTRACT

Efforts to evaluate fog sampling techniques in field conditions are described. A primary emphasis was to assess the performance of the Caltech rotating arm collector (RAC) with respect to possible sampling biases based on the lower size-cut of 20 μm droplet diameter (i.e., 50% collection efficiency) determined by Jacob et al. (1984a). Liquid water content (LWC) measurements by various methods were also compared.

Simultaneous operation of two RAC's showed that its measurements of chemical composition were highly reproducible (±10% or less for major ions); fogwater collection rates were only slightly more variable. Comparison was made with two internal-surface collectors (ISC) which reportedly collected all droplets greater than 5 μm. The fundamental characterization of fogwater chemistry measured by all three collectors was similar. For major ions (H^+, NH_4^+, NO_3^-, and SO_4^{2-}), the pooled standard deviation of samples for the three collectors were 15 to 25%.

There were systematic differences in cation concentrations for collector samples, apparently due to differences in collection efficiency for larger droplets and particles. The RAC most effectively captured soil dust particles, while one of the ISC collectors excluded these larger particles by its inlet orientation. The third collector gave spurious cation concentrations because its inlet was located close to the ground.

Field determinations of fog LWC were made by four methods: (a) fogwater collection rates for RAC and ISC's sampler; (b) sampling with paper filters; (c) droplet sizing with an optical particle counter; and, (d) infrared (IR) extinction measurement. A wide range and

considerable scatter between compared methods highlighted the large uncertainties in determining fog LWC. Operational difficulties for several methods were identified in light and patchy fogs. In some cases, fair correlations between methods were found, generally better in more stable, dense fog conditions. The use of fogwater collection rates for the determination of LWC was found to have several advantages in field studies, although a large uncertainty in the absolute values was acknowledged.

The collection efficiencies were somewhat lower for the RAC compared to the two ISC's. However, the factor that distinguished collector designs was not as great as would be predicted for their nominal lower size-cuts and the droplet size distributions in fog. The magnitude of LWC indicated by IR extinction and filtration methods was roughly 50% higher than by any other the fog collectors; the higher values were more consistent with fog densities previously reported for similar conditions. This indicated that none of the collectors was 100% efficient and the presumption of total droplet collection by ISC's was not substantiated. Because the differences in solute concentrations for the dominant species was very similar for samples in dense fog, it is possible that the lower size-cut of the RAC and ISC designs may be far closer than given by their respectively calibrations.

The LWC values calculated from measured droplet spectra were unrealistically high but correlated well with other methods. A linear correlation between IR extinction and LWC was verified for most fog conditions encountered. The IR extinction technique showed promise for accurate LWC measurements with rapid response.

Chapter 5

FIELD INTERCOMPARISON OF FOG COMPOSITION AND LIQUID WATER CONTENT MEASUREMENTS BY VARIOUS METHODS

5.1 INTRODUCTION

Sampling techniques for early research of fog and cloudwater chemistry were not widely used or standardized. To our knowledge, the reproducibility of results was never determined by intercomparison of available methods. Since interest in this area has grown in recent years, many fogwater collection devices have been resurrected or newly developed, although few have been evaluated thoroughly.

It is essential for collector performance to be evaluated because droplets in the size range encountered in fogs and clouds are sensitive to anisokinetic sampling biases (May, 1967). The important design considerations for fogwater collectors have been enumerated by Jacob et al. (1984a). These are: (a) a sharp lower size-cut which effectively excludes interstitial aerosol; (b) representative collection of all droplet sizes; and (c) preservation of physical and chemical integrity of sample volumes.

Calibration of a scale model of the Caltech rotating arm collector (RAC) indicated a lower size-cut of 20 μm. That is, at this diameter, 50% collection efficiency is attained while higher efficiencies are achieved for larger sizes (Jacob et al., 1984a). This lower size-cut is approximately twice as large as that determined for impaction to a rod of similar dimension without slots (Israel and Rosner, 1983). Since fog droplet size distributions have mass median diameters close to 20 μm

(Garland, 1971; Pilie et al., 1975; Roach et al., 1976; Goodman, 1977; Juisto and Lala, 1983), field measurements made with the RAC may be subject to an unknown bias due to omission of smaller droplets. In order to properly interpret fog chemistry based on RAC samples, it was essential to determine if a collector bias existed.

In the course of our multiyear program to monitor stratus cloudwater at Henninger Flats, the opportunity was taken to evaluate the performance of several fog collection techniques used in current research. In June 1983, a fog sampler intercomparison, sponsored by the Coordinating Research Council, was performed using the Caltech RAC and four other collectors of various designs (Hering and Blumenthal, 1985). In addition, this provided an opportunity to compare our analytical protocol to that of an independent laboratory.

Interpretation of fogwater chemistry is highly dependent on a knowledge of liquid water content (LWC) in the fog environment. This requires that the total droplet mass within a volume of air be measured. Water droplets are in a tenuous thermodynamic state with air at very low supersaturation and a large reservoir of water vapor. For example, saturated air at $10^{o}C$ contains 12 g-H_2O(g) m^{-3}, which can be compared to $\leq$0.5 g-H_2O(l) m^{-3} in dense fog. As a consequence, evaporation or condensation can easily bias measurements. Furthermore, the relatively large inertia of fog droplets increases the difficulty of representative sampling with an inlet (May, 1967; Davies and Subari, 1982). A comparison of LWC methods was also performed at several sites. The presentation of the data is intended to underscore the uncertainties in LWC measurements made in the field and to assess the reliability of the RAC collection rate to estimate LWC.

5.2 FOGWATER COMPOSITION COMPARISONS

In the following section, various data sets have been compared to determine their statistical relationships. Linear least-squares regressions and correlation coefficients have been determined and are presented with the data sets in Appendix B. However, since neither measurement in data pairs represented an "error-free" independent parameter, least-squares analysis was not strictly applicable (Kennedy and Neville, 1976). As an alternative, we have also calculated standard errors for sets of paired data (X_i, Y_i) based on their relative difference with respect to the mean of the pair:

$$\Delta_i = \frac{2\,(Y_i - X_i)}{X_i + Y_i} \qquad (5.1)$$

Since the values of many of the parameters ranged over several orders of magnitude, this statistical treatment was advantageous because it avoided an overemphasis on data pairs of the highest concentrations. Major constituents were normally present at levels far above the limits of detection. The samples which had greatest analytical error were frequently the most concentrated ones. These had the smallest volumes plus required substantial dilution. The mean and standard deviation of Δ were compared with the t-test to determine whether a non-zero mean had significance (Kennedy and Neville, 1976).

5.2.1 Caltech Fog Collector (RAC) Reproducibility.

Two identical RAC instruments were operated in fogs at Henninger Flats (see Figure 6.1) during seven separate events in June 1983. During one event (11 June), samples were taken while the collectors were

situated adjacent to each other (3 m apart). The remainder of simultaneous samples were taken with the RAC's located 30 m apart at opposite corners of the nursery area. Sample handling and analytical protocols were identical, and sampling intervals were generally 60 minutes.

Comparisons for simultaneous RAC samples are summarized in Table 5.1. Plots and addition statistical parameters are presented in Appendix B.3. Despite wide ranges of ambient concentrations, the agreement between samples was remarkably good. Samples collected apart did not show statistically greater compositional variability than those collected side-by-side. For the dominant ions (H^+, NH_4^+, NO_3^-, and SO_4^{2-}) the standard errors (σ_Δ) were $\leq$10%. With the exception of calcium, the remainder of measured ions had standard errors between 10-15%.

There was a greater difference observed in the collection rates for the separated collectors, although most of the scatter was associated with a few outliers. Part of this may be due to temporal and spatial variability of fog density at the site, although these fluctuations were generally dampened by taking longer sampling intervals. For example, the third column in Table 5.1 shows the improvement in the comparison for a data set with averaging times of 2 to 3 hours intervals (see next section). Nonetheless, the occasional differences in collection rates did not result in greater compositional disparities for those samples.

5.2.2 Comparison of the RAC with Other Collectors.

Five different collectors were operated simultaneously on five

Table 5.1

ROTATING ARM COLLECTOR (RAC)
SAMPLING REPRODUCIBILITY

	Side-by-Side[a]		Separated[a]		Time-Averaged[b]	
Parameter	n[c]	$\sigma(\Delta)$[d]	n	$\sigma(\Delta)$	n	$\sigma(\Delta)$
pH in field[e]	13	0.01	17	0.04	14	0.02
Hydrogen	13	3	17	10	14	4
Sodium	9^{x}	10	16	10	12^{x}	8
Potassium	7^{x}	13	12	16	11^{x}	17
Ammonium	12	10	16	12	14	7
Calcium	12	26	16	14	13	11
Magnesium	11^{+}	8	15	10	13	7
Chloride	6	13	10	9	13^{+}	9
Nitrate	11^{+}	6	14^{+}	9	14	5
Sulfate	11^{+}	4	14^{+}	8	14	5
Collection	13	12	17 (14^{+++}	27 13)	14	8

a. Based on Caltech laboratory results;
RAC's located 3 and 30 m apart, respectively.

b. Based on RI laboratory results; time-averaged samples per H&B.

c. Number of sample pairs; + indicates exclusion of 1 outlier pair;
x indicates exclusion of 1-2 pairs near detection limits.

d. Standard deviation, $\sigma(\Delta)$, of relative difference between pairs (expressed in percent) where:

$$\Delta_i = 2(y_i - x_i)/(x_i + y_i).$$

e. For the pH difference (ΔpH), with $\sigma(\Delta)$ expressed in pH units.

dates in June 1983 at the Henninger Flats nursery. These were (a) the Caltech RAC; (b) the Desert Research Institute jet impactor (DRI); (c) the Global Geochemistry Corp. mesh sampler (GGC); (d) the Atmospheric Science Research Center rotating string collector (ASRC); and, (e) the AeroVironment rotating rod collector (AV). The RAC has been described in Chapter 3. Descriptions of the others are given below.

DRI. The DRI linear-jet impactor was designed for use inside an experimental cloud chamber; a lower size-cut between 2 and 5 μm has been reported (Katz, 1980). Air was drawn through three rectangular jets at a total rate of 1.2 m^3 min^{-1}. The instrument contained internal impaction surfaces that rotated and moved the impacted droplets away from the air jet to minimize evaporative losses. At Henninger Flats, the DRI collector was located inside a 55 gallon drum, elevated 2 m above ground level and open at the bottom. This design feature was intended to eliminate collection of raindrops and to reduce a sampling bias that could be caused by variable wind conditions at the inlet. A fan was used to supplement the upward air flow inside the drum.

GGC. The GGC collector was a V-shaped, Teflon-lined tube (10-cm diameter) with its inlet approximately 0.8 m above ground level. At the inlet of the tube, a 4-cm thick polypropylene mesh of filaments (0.41 mm diameter with 96% void volume) was used to collect fog droplets with an air sampling rate of 1.7 m^3 min^{-1}. The droplet size cut was below 3 μm diameter with nearly 100% efficiency for D_o>5 μm, based on the mesh manufacturer's specifications (Brewer et al., 1983). The collected liquid drained into a bottle at the bottom of the V-tube.

ASRC. Nylon strings (0.41 mm diameter) were mounted at a slight angle from vertical between two plates which were rotated at 100 rpm.

The instrument was located on a mast about 3 m above ground level. Water collected on the lower plate and was manually transferred into collection bottles at the end of each sampling period.

AV. Two fractions of droplets were collected by impaction to a Teflon-coated rod rotated at 3450 rpm. The outer part of the rod was 1.6 mm and the inner part 19 mm in diameter; the nominal size-cuts for each have been given as 2.5 and 10 μm, respectively (D. Wilbur, personal communication, AeroVironment, Inc., Pasadena, CA). The impacted droplets were transferred to stationary polyethylene troughs by centrifugal force and drained by gravity to separate collection bottles.

A detailed report on the collector intercomparison was prepared for the sponsor by Hering and Blumental (1985), along with a comprehensive data volume (Hering and Blumenthal, 1983). In the Hering and Blumenthal study, samples from all collectors were submitted to Rockwell International Corp. (RI) for analysis. In Appendix B.4, the two sets of laboratory results for RAC samples are presented, along with plots, statistical analyses, and discussion. Excellent agreement was found between the Caltech and RI laboratory results for most individual samples.

Because most of the other instruments collected liquid at lower rates than the RAC, they generally required longer sampling intervals. For most of the compared data sets, volume-weighted averages were calculated for 2 or 3 sequential RAC samples in order to match the intervals required by the other collectors. For example, comparison of these combined values for simultaneous RAC samples has been presented in Table 5.1.

A comparison of data sets for the RAC and the DRI and GGC collectors was conducted to ascertain differences in chemical composition due to differences in the reported droplet size-cuts. We used the combined sample results given in Hering and Blumenthal (1985), which have been included in Appendix B.5 along with calculated statistics. Because the ASRC collector was an external impaction design that had not been calibrated, it was excluded from this discussion. Also, the AV sample concentrations were higher by a factor of 2 or more than any of the other collectors for all analytes except pH. Along with the low liquid water collection rates, this indicated that significant evaporative losses were occurring. The AV design relied upon gravity for removal of the impacted droplets from the exposed circular trough. This was not rapid enough and demonstrated the importance of sample preservation immediately following impaction.

The agreement among the RAC, GGC and DRI collectors was reasonably good for the dominant species (Table 5.2), although it was less than for paired RAC (or GGC - see Appendix B.5) collectors. Comparison of relative differences (Δ) identified somewhat lower concentrations for RAC samples than for the other two collectors in several cases. The differences in collector size-cuts may have caused the observed bias, if a greater fraction of smaller droplets collected by DRI and GGC designs was substantially more concentrated. However, the observed differences were primarily from the 2 or 3 samples with higher concentrations that were collected during lower LWC. The remainder of data pairing showed 1:1 correspondence in dense fog. These results suggested that compositional differences were caused by evaporation of samples within the two internal-surface collectors during

Table 5.2

COMPARISON BETWEEN FOGWATER SAMPLES
FROM DIFFERENT COLLECTOR DESIGNS[a]

	DRI vs RAC		GGC vs RAC		DRI vs GGC		POOLED	
Parameter	n	$\sigma(\Delta)$[b]	n	$\sigma(\Delta)$	n	$\sigma(\Delta)$	n	psd[c]
pH in field[d]	16	0.08	15	0.07	15	0.11	16	2
Hydrogen	16	19	15	16	15	25	16	15
Ammonium	16	21*(+13)[e]	16	14*(+20)	15	19	17	24
Nitrate	16	21	16	12*(+12)	15	10*(-10)	17	17
Sulfate	16	20	16	14*(+15)	15	21	17	21
	n	Ratio[f]	n	Ratio	n	Ratio		
Sodium	14	0.4±0.2	13	1.5±1.5	13	0.4±0.2	14	50
Potassium	11	0.8±0.5	13	3.2±3.9	10	0.4±0.2	14	76
Calcium	14	0.4±0.2	13	2.8±0.7	13	0.2±0.1	14	81
Magnesium	14	0.6±0.3	13	1.3±0.7	13	0.6±0.2	14	37
Chloride	16	0.9±0.2	16	1.6±0.7	15	0.7±0.3	17	25
LWC[g]	10	1.2±0.3	10	1.2±0.2	9	1.0±0.3	17	41

a. Data for combined samples as given in Hering and Blumenthal (1985).
RAC = Caltech rotating arm collector (CRC code "C");
DRI = Desert Research Inst. jet impactor;
GGC = Global Geochemistry Corp. mesh collector (CRC code "G").

b. Standard deviation, $\sigma(\Delta)$, of relative difference between pairs (for collector y vs x), expressed in percent. See Table 5.1 note d.

c. Pooled standard deviation (i.e., averaged for n sets) expressed as percent of pooled mean value.

d. For the pH difference (ΔpH), with $\sigma(\Delta)$ expressed in pH units.

e. Non-zero $\bar{\Delta}$ has statistically significant (>95%) based on t-test; $\bar{\Delta}$ (as percent) given in parentheses.

f. Mean and standard deviation for concentration ratio: [y]/[x].

g. Liquid water contents from collection rates; ratios for dense fog samples only; psd for all samples.

light and patchy fogs. This effect was most pronounced in periods when the RAC collected measurable liquid water while GGC and DRI collectors could not. In those cases, impacted droplets had completely evaporated before sufficient volumes were able to drain to the collection bottles.

Concentrations of cation species such as sodium and calcium were routinely greater in RAC and GGC samples than in DRI samples. In Table 5.2, the ratios for cations rather than their relative differences are given. These species are associated with soil dust and expected in the coarse particle fraction. Thus, the observed differences for cation concentrations may be caused by the collector inlets. At low wind speeds, the collection efficiency for droplets of increasing size would decrease because their inertia prevents them from following streamlines entering the inlet (May, 1967; Davies and Subari, 1982). For example, $St_{inlet} \leq 0.25$ assures that the inlet sampling bias remains below 30% (Davies and Subari, 1982), for the Stokes number is based on droplet diameter, inlet velocities, and the inlet radius (see Eqn 2.2).

For the RAC, the upper size-cut (D_u) was estimated to be 200 μm, for the RAC-arm taken as an "inlet" and the fan-induced wind (1.5 m s-1) as an "inlet velocity". For the GGC collector inlet geometry, D_u=45 μm was calculated for the same criterion of St_{inlet}. In the case of the DRI collector, the inlet to the drum was large (60 cm diameter), therefore collection of droplets up to 200 μm should not be biased due to inertial considerations. However, since the inlet faced downward, this would result in an exclusion of larger droplets caused by gravity. The threshold droplet size was calculated to be 70 μm, based on the velocity at the drum inlet (15 cm^3 s^{-1}). Dry particles with greater than unit-density would be excluded at even smaller sizes (e.g., ρ_s=2 g

cm^{-3} gives D_u=35 and 22 μm for DRI and GGC, respectively).

In addition, it appeared that the intense research activity at the field site caused the higher levels of soil dust cations, notably calcium, in RAC and GGC samples. For example, the volume-weighted Ca/Mg equivalent ratio was 1.1 for 31 RAC samples collected at Henninger Flats earlier in 1983, before intercomparison activities had commenced. During the intercomparison, this ratio was raised to 1.9 for RAC samples and >3 for GGC samples. For for DRI samples, this ratio was 1.0. The RAC and GGC collectors apparently captured dust particles along with the fog droplets, while these were generally segregated at the DRI inlet. As opposed to the RAC, the GGC inlet was not more efficient for collection of larger particles. However, the positioning of their inlet too close to ground level allowed soil dust to contaminate the GGC samples, as demonstrated by the frequent disparities in cation concentrations observed for adjacent GGC collectors (see Appendix B.5).

In summary, the essential chemical characterizations of fogwater were the same for each collector. Relatively good agreement among the three designs was found for concentrations of major chemical constituents such as H^+, NH_4^+, NO_3^- and SO_4^{2-} during most sampling periods. Collection of soil dust by RAC and GGC collectors was noted. In spite of sample evaporation or inherent differences in droplet size-cuts (large and small), the collective uncertainties for major ions were between 15 and 25%. In fact, for the majority of samples, far closer agreement was achieved. For major ions, the substantial differences in collector design did not result in systematic bias in chemical composition under conditions of dense fog.

5.3 LIQUID WATER CONTENT MEASUREMENTS

The methods used to determined LWC at Henninger Flats in June 1983 included (a) rates of collection for the various fogwater collectors; (b) droplet sizing by an optical particle counter (OPC); (c) infrared (IR) extinction measurements; and (d) sampling of fog-laden air with filter papers. Measurements obtained by these methods were averaged for the RAC sampling intervals or, for comparison with other other fogwater collectors, the longer sampling interval (see Appendix B.6).

A considerable scatter existed among measurements (Figure 5.1). Several methods indicated entirely different ranges of LWC. It is important to recognize that these techniques did not necessarily measure the absolute quantity of liquid water in the air; rather, they provided an operational parameter based on instrument response. A significant problem in assessing different techniques has been that there is not an accepted standard method for the determination of LWC.

5.3.1 Fogwater Collection Rates

The fogwater collectors inherently provided a gravimetric assay of LWC. In fogwater chemistry studies, this has the advantage that it is uniquely paired with compositional data for each sample. Estimations of LWC were based on the rate of liquid water collection normalized to the specific air sampling rate for each collector. The RAC sampled air at a flow rate of 5 m^3 min^{-1}, given its rotation velocity and dimension. Incomplete renewal of air in the wake of the rotating arm or the omission droplets smaller than the lower size-cut would reduce the efficiency of liquid water collection. The RAC collection rate has been compared to the DRI and GGC collectors for which the air sampling rates

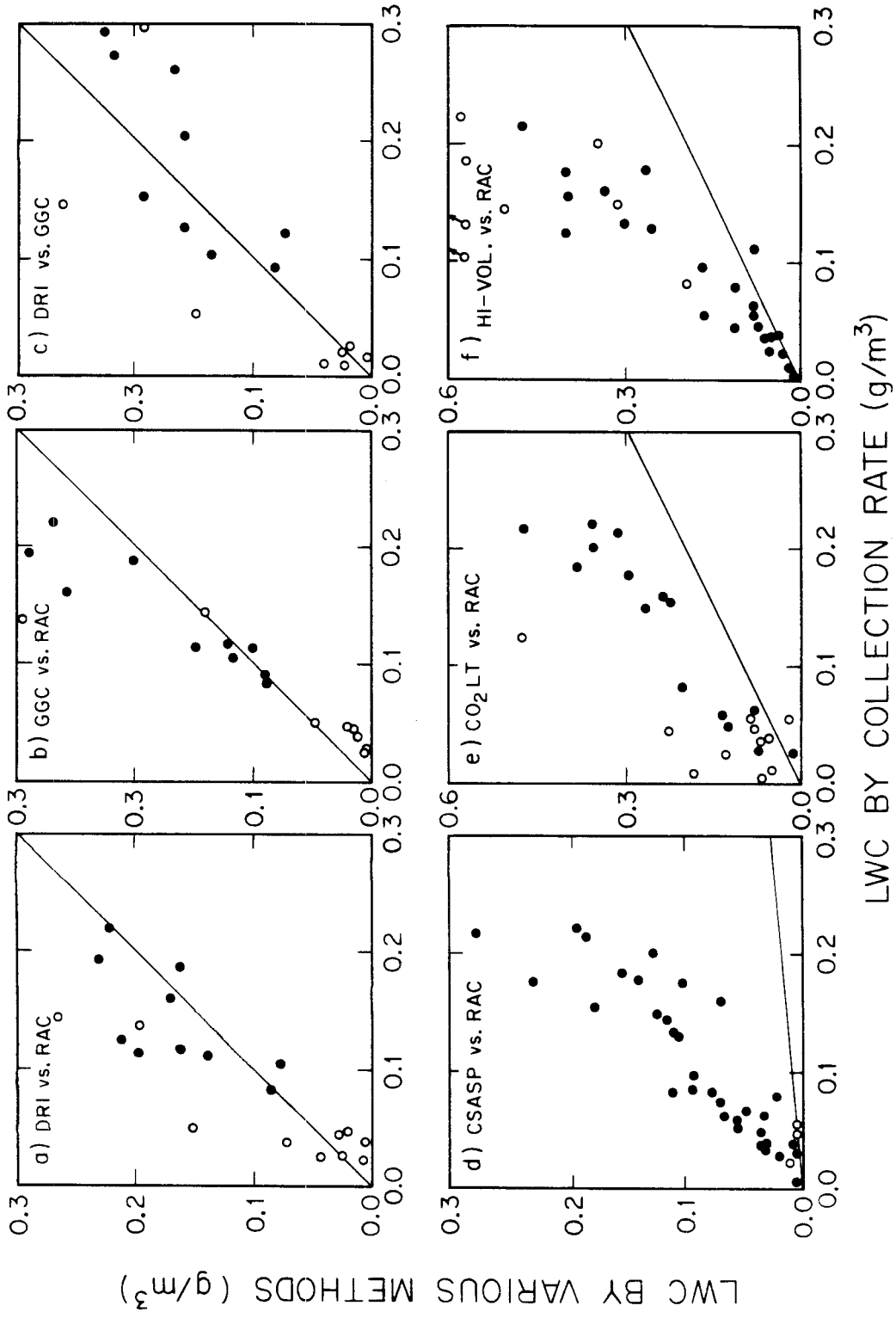

Figure 5.1 Liquid water content comparisons at Henninger Flats during June 1983. Y versus X with 1:1 line given.

could readily be measured: 1.2 and 1.7 m^3 min^{-1}, respectively.

As compared to the compositional correlations, greater deviations from 1:1 agreement existed in the LWC values (Figure 5.1a-c). The density of fog was found to alter the relationship between collector rates. As mentioned previously, the RAC was efficient in collecting samples during periods of light fog while the other collectors were not able to operate. The RAC motion supplied ample centrifugal force for immediate removal of impacted liquid. For DRI and GGC collectors, a sufficient wetting of the internal surfaces was required before water flowed by gravity to the collection vials, and this was sometimes limited by evaporation during light or patchy fog conditions. The data that was obtained during periods of relatively stable and dense fog is indicated by the shaded circles of Figure 5.1a-c.

The scale and sharpness of lower size-cuts are important aspects of quantitative liquid water collection. Droplet size distributions during fog (see next section) showed that >95% of liquid water was in the range of 5 to 35 μm diameter. Given the lower size-cuts for DRI and GGC samplers, these collectors should be close to 100% efficient, except when sample evaporation becomes a problem. In contrast, between 30 and 70% of liquid water was measured in droplets larger than 20 μm, which is the lower size-cut indicated for the RAC (Jacob et al., 1984a). Based on these estimates, the collection efficiencies of DRI and GGC designs should be 0.5 to 3 times higher than the RAC. However, the actual collection efficiencies showed a fairly close agreement (Figure 5.2). On the average, the DRI and GGC values were essentially the same, although each was only about 20% higher than those determined for the RAC during dense fog (see Table 5.2).

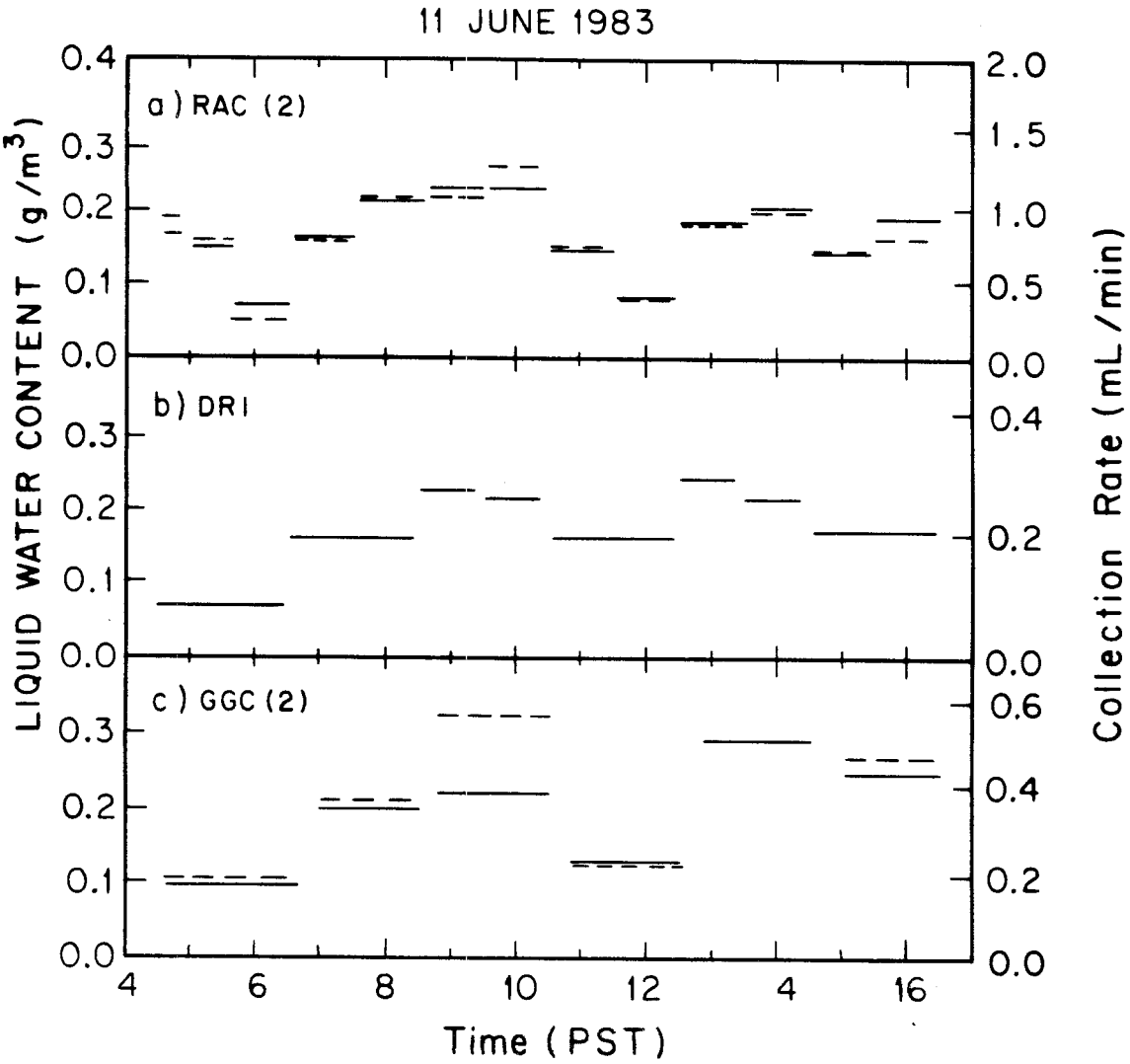

Figure 5.2 Fog collection rates and calculated liquid water content for 11 June 1983.

5.3.2 Droplet Size Spectra (CSASP Method)

The optical particle counter used at Henninger Flats was the Classical Scattering Aerosol Spectrometer Probe (CSASP-100 HV) manufactured by Particle Measuring Systems, Inc. (Boulder, CO). Several droplet size distributions measured in 60-second intervals with the CSASP are shown in Figure 5.3. The measured spectra agreed well with typical droplet size parameters, such as mass median diameter and spectrum shape, that have been reported in the literature for fogs (Garland, 1971; Pilie et al., 1975; Roach et al., 1976; Jiusto and Lala, 1983) and specifically for intercepted stratus (Goodman, 1977). However, the LWC values resulting from integration of the size data were high by a factor of 4 to 10 compared to values determined by the other methods. These high values were unrealistic relative to previously reported LWC and to the basic principles of cloud microphysics. For example, updraft velocities typical of strongly convective clouds are generally the only conditions for which LWC values higher than 1 g m^{-3} are found (Pruppacher and Klett, 1978). Yet, sizing data from the CSASP at Henninger Flats indicated LWC values sometimes higher than 2 g m^{-3}!

Preliminary attempts in our laboratory to calibrate the instrument in the size range of interest, 10-30 μm, were inconclusive except to demonstrate that significant oversizing was not occurring in this range. Based on the reported calibrations of PMS instruments (Pinnick et al., 1981; Cerni, 1983), sizing errors are generally limited to $\pm$3-4 μm. While such errors can cause appreciable errors in LWC, they are not sufficient to cause an upward shift of the magnitude we found. Other investigators have reported somewhat similar experiences in LWC determinations with particle spectrometers in ambient fogs and haze,

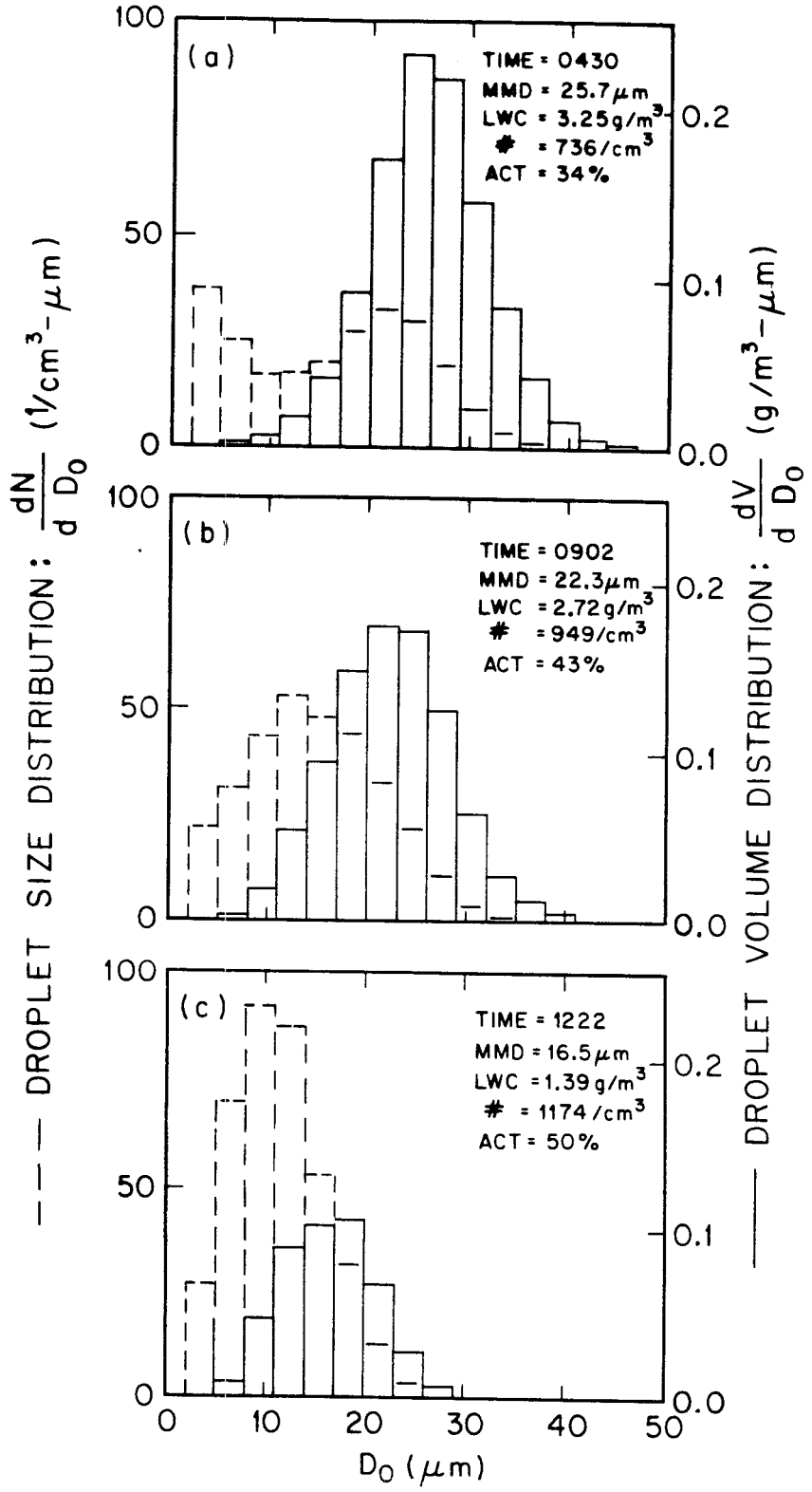

Figure 5.3 Droplet size and volume distributions from CSASP. 11 June 1983.

although not to the same extreme. Biases of two or more in calculated LWC or extinction coefficients, relative to other methods (or for side-by-side OPC's), were not uncommon (Baumgardner, 1983; Richards et al., 1983; Jiusto and Lala, 1983; Jensen et al., 1983).

Nonetheless, the time series of CSASP-derived LWC were consistent with the trends measured by the other methods (compare Figure 5.4a and Figure 5.2). The scaling between values was also fairly consistent (Figure 5.1d) which indicated that errors in sizing, if occurring, did not appreciably change with LWC. The CSASP-measured size distributions showed that variations of LWC were primarily dependent on the droplet number concentrations. For more than ten-fold changes in LWC, the measured median size did not appreciably change (Figure 5.4a-c).

Droplet number concentrations at Henninger Flats were compared to fog condensation nuclei (FCN) monitored during the same period by Hudson and Rogers (1984). They alternately measured the total condensation nuclei in fog-laden air and in air with droplets removed (D_o>2-5 μm). By difference (total minus non-active FCN), this indirectly provided values of droplet number concentrations between 100 and 400 per cm^{-3}. Direct comparison of simultaneous CSASP nad FCN data indicated that the CSASP number concentrations were higher by a factor of 3.8 ± 2.1 for 42 cases in dense fog (J. Hudson, unpublished data).

Since the CSASP data were so strongly correlated with fogwater collector rates and the measured infrared extinction (see next section), we feel that this instrument provided a qualitative measurement of temporal variability in LWC and associated size spectra. These data were useful in understanding the nature of stratus cloud interactions at the mountain slope and the variability found among other methods. The

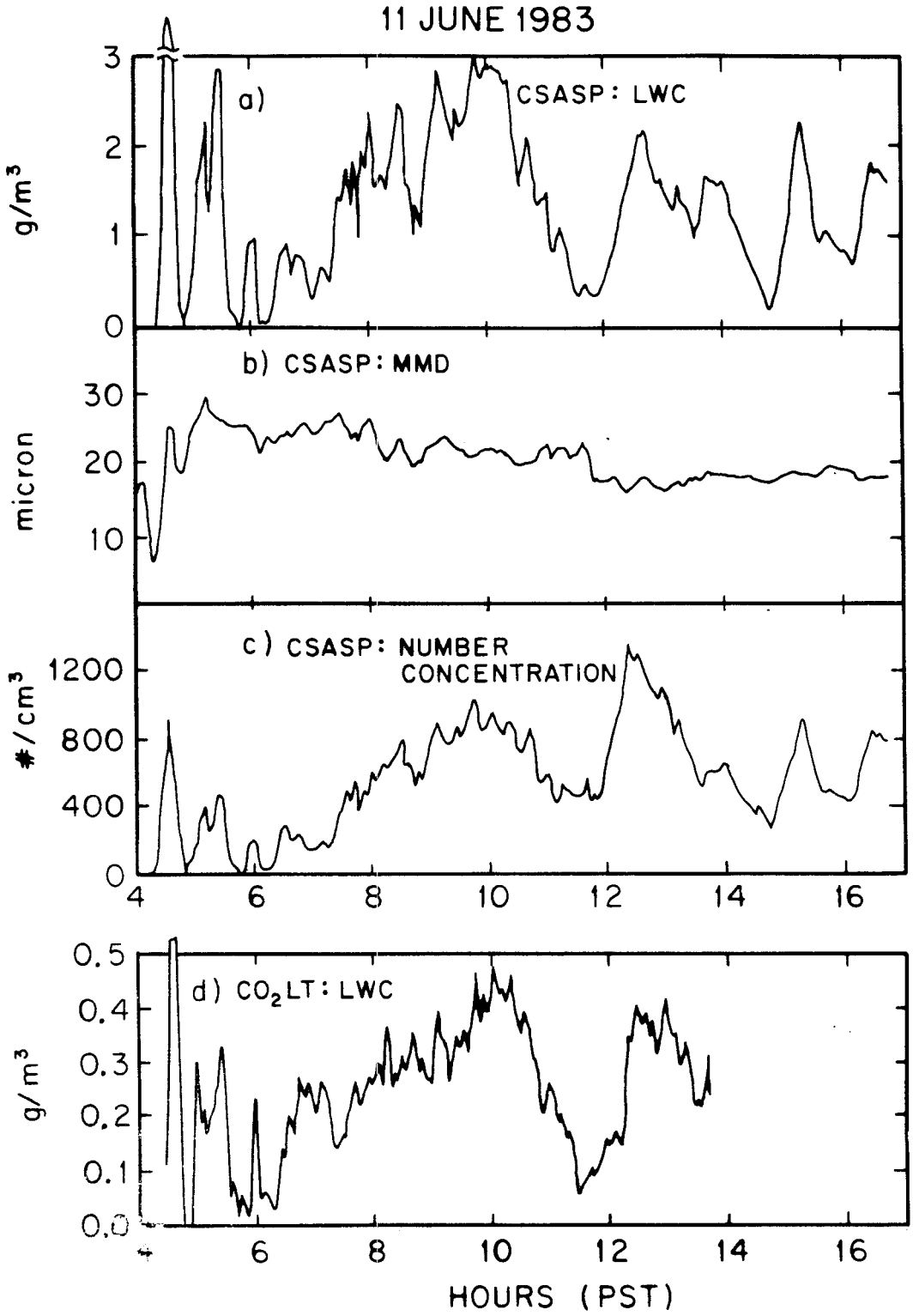

Figure 5.4 CSASP and CO_2LT data for 11 June 1983.

existence of the fine structure of LWC during fog was hidden by the long sampling intervals required by most of the other techniques. The cause of instrument bias has not been identified with certainty, however.

5.3.3 Infrared Extinction (CO_2LT Method)

In the absence of a LWC standard, calibration of the CO_2 laser transmissometer was difficult (see Chapter 3.5 for description of the CO_2LT). However, attenuation measured for the IR laser in fog was strongly correlated with other methods (Figure 5.1e). In fact, the time series for the CO_2LT and CSASP data were nearly identical except for scale (Figures 5.4 and 5.5). The CO_2LT measurements verified the existence of rapid fluctuations in fog density, showing similar frequency and scale.

The extinction coefficient (k_e) for λ=9.4 μm was calculated by the numerical integration of the CSASP-measured size distributions $n(D_o)$:

$$k_e = \frac{\pi}{4} \Sigma\, Q_{ext} D_o^2\, n(D_o)\, \Delta D_o \qquad (5.2)$$

where Q_{ext} is the extinction efficiency for water droplets at wavelength λ. The dependence of Q_{ext} on D_o is illustrated in Figure A.1 in Appendix A. Values for k_e were compared to the calculated LWC from the same distributions. In this way, uncertainties in absolute number concentrations were eliminated. A high degree of linearity was found for most spectra sampled in Henninger Flats fogs. In the earlier sampling hours of 11 June, the droplet size distributions were determined to have mass median diameters (MMD) greater than 25 μm. As shown in Figure 5.6, the observed relationship continued to be linear, but the slope of the line was lower. Taking the form:

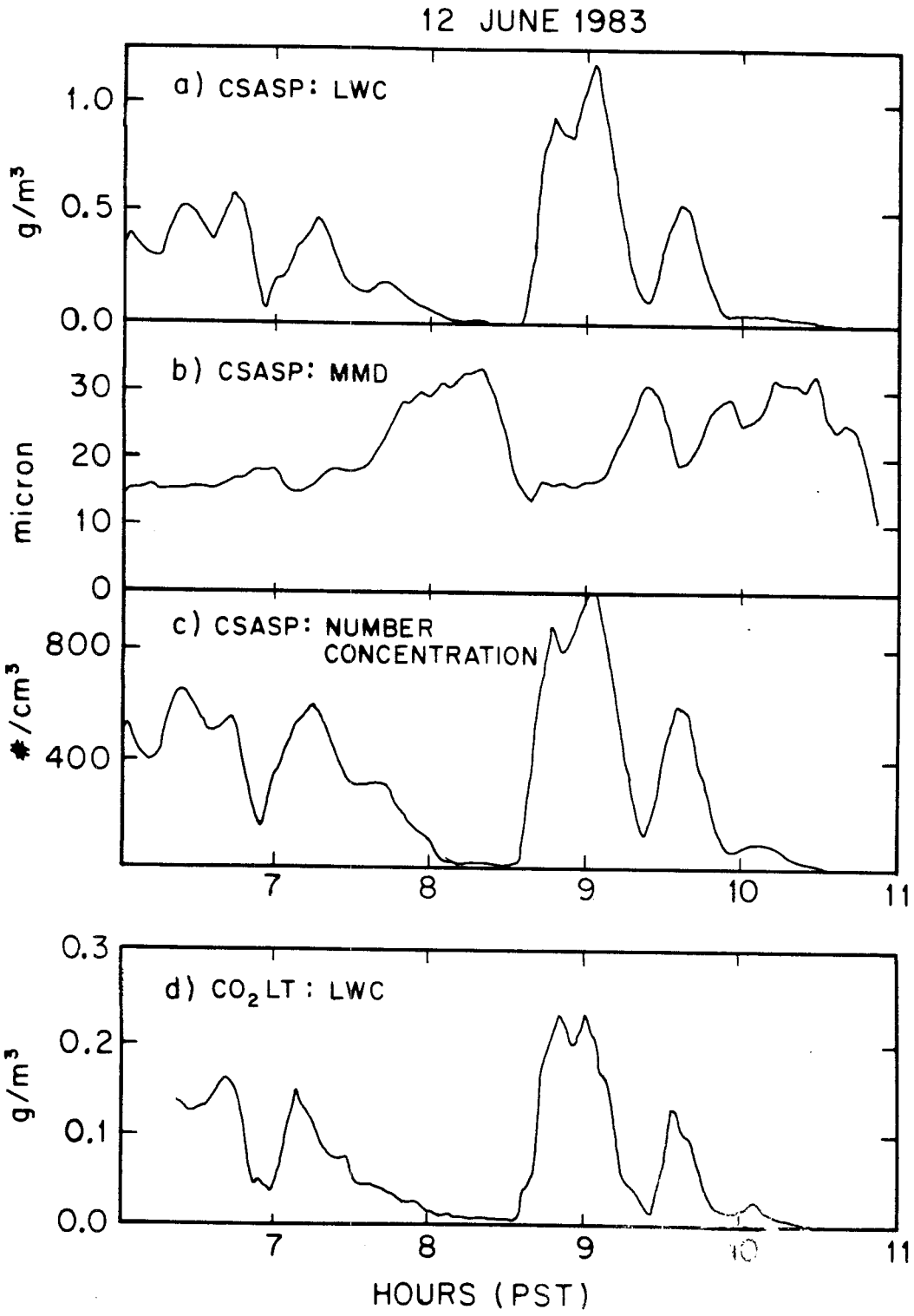

Figure 5.5 CSASP and CO_2LT data for 12 June 1983.

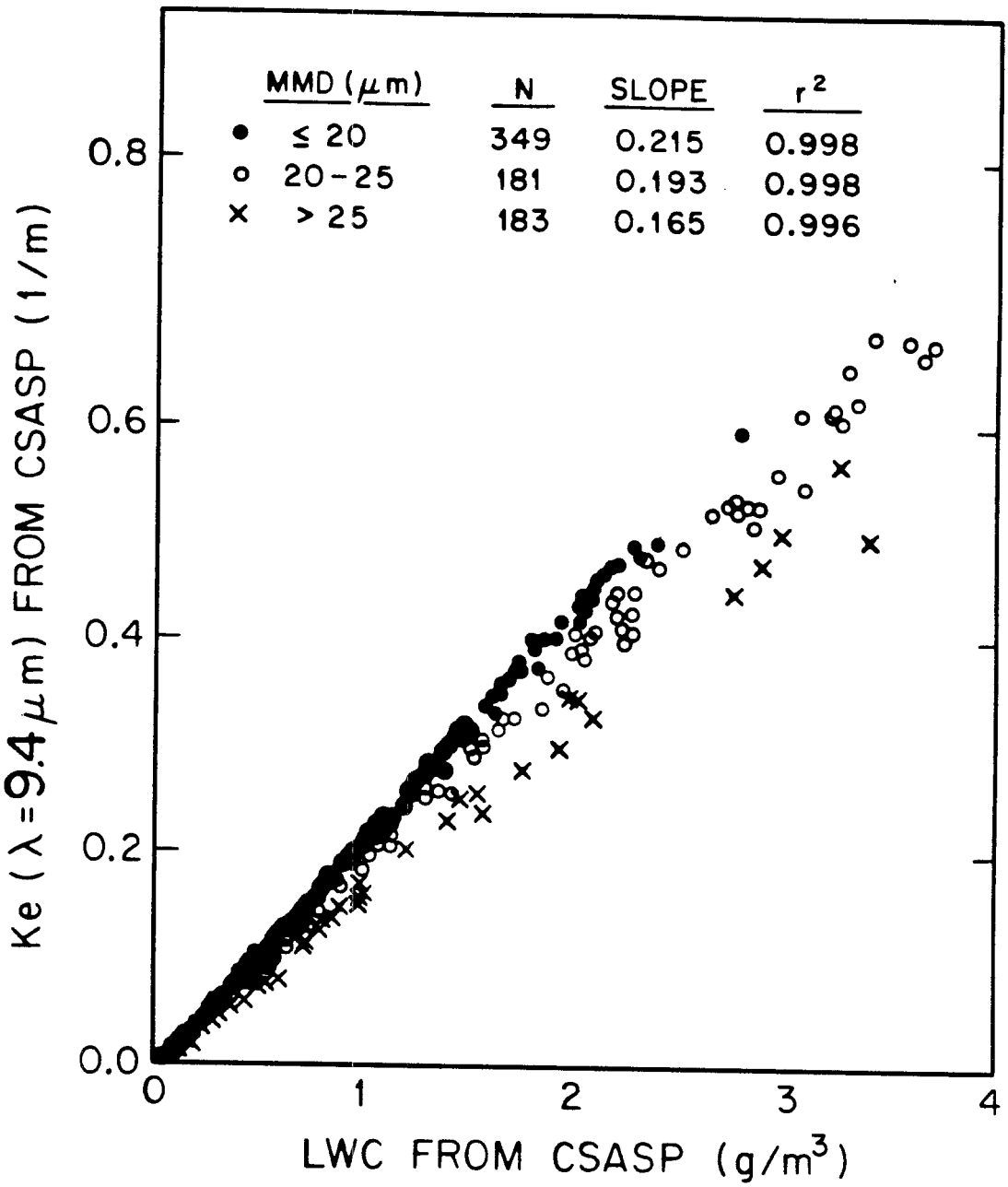

Figure 5.6 Infrared extinction coefficient (k_e) versus liquid water content (LWC), both calculated from CSASP droplet size spectra for all June 1983 fogs.

$$k_e = c' \text{ LWC} \tag{5.3}$$

we calculated the values for c' (units = $m^2\ g^{-1}$) to be 0.22, 0.19, and 0.17 for droplet size spectra with MMD $\leq$20 μm, 20< MMD $\leq$25 μm, and MMD >25 μm, respectively.

A linear approximation for extinction efficiency was proposed in Appendix A for cases in which large droplets (D_o>25 μm) did not contribute substantially to LWC (Chylek, 1978). A simplified k_e versus LWC relationship was derived. A value of $c' \simeq 0.2\ m^2\ g^{-1}$ was calculated from the relationship shown in Figure A.1. Hence, the linear approximation derived in Appendix A was consistent with the relationship found for the measured size distributions. An assumption of overall linearity with c'= 0.2 resulted in agreement within ±5% for most (75%) of the sampling intervals. An underestimation of LWC was less than 20% for k_e determined at higher MMD in all other cases. Furthermore, sizing errors of ±3-4 μm did not seriously degrade the linearity of k_e and LWC.

Field measurements of IR extinction with the CO_2LT were used to calculate LWC, given c' and a pathlength of 20 m:

$$\text{LWC } (g\ m^{-3}) = \frac{1}{4} \ln(I_o/I) \tag{5.4}$$

where I_o and I were the incident and attenuated beam intensities, respectively. The comparison between LWC calculated from IR extinction and CSASP values is shown in Figure 5.7 for measurements taken on 11 and 12 June. The individual readings have been grouped in roughly 10-minute intervals to mitigate errors from spatial variability or clocktime (i.e., CO_2LT output was logged by a strip chart recorder versus computer logging of CSASP data). As previously noted, LWC values calculated from CSASP-measured size distributions were inordinately high. The

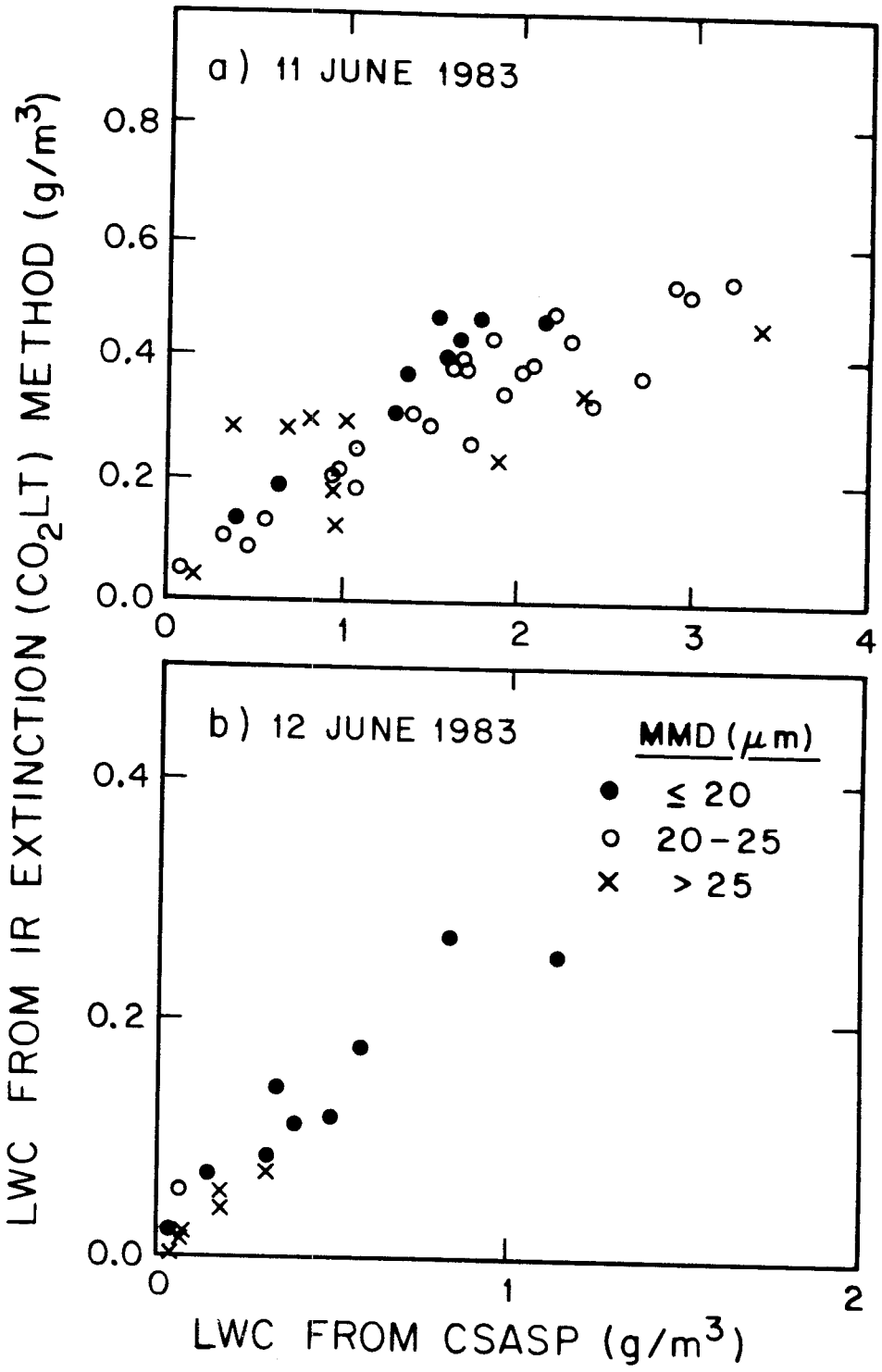

Figure 5.7 Liquid water content from measured IR extinction versus integrated CSASP droplet size spectra.

CSASP/CO_2LT ratio for LWC values was about 4 with good linearity in the measurements on each sampling date.

Normally, fluctuations in laser power were compensated by forming the ratio of the sensor and reference beams, and the value of c' was largely insensitive to small variations in IR wavelength. On 11 and 12 June, the laser power of the CO_2LT was steady ($\pm$10%), but during the following week, the power output started to decay. Due to anomalies of the system we could not identify, the clear air baseline changed on the later dates. In the future, better control over laser output needs to be attained. Further refinement of the present instrument would be necessary to allow transportable and fully reliable determination of IR transmission in the field.

Nonetheless, the CO_2LT showed promise as an accurate and fast-response technique for LWC measurements. The instrument operation proved that the approximation used to derive Eqn 5.4 was applicable to field conditons. We feel that the determinations made by the CO2LT were accurate indications of ambient LWC values, at least on 11 and 12 June (indicated as shaded circles in Figure 5.1e). For the CO_2LT method, there were not problems due to inlet bias, droplet size-cuts, or sample handling, and variations in droplet parameters were shown to have limited impact on the LWC determinations. Given the visual range observed on those dates (<100 m at times), the LWC values determined by fogwater collection rates appeared to be too low. The LWC of fog which has been monitored in mountain-top clouds were generally as high as 0.5 g m^{-3} (Houghton and Radford, 1938; Goodman, 1977; Lovett, 1984). A value of this magnitude is more consistent with the peak hourly values given by the CO_2LT. The factor of approximately four between CSASP and

CO_2LT values was also consistent with the bias in droplet number concentrations indicated by Hudson and Roger's FCN measurements.

5.3.4 Filter Results (Hi-Vol Method)

Three standard high volume (Hi-Vol) samplers with paper filters were operated at Henninger Flats, generally two at a time. The average for these are shown in Figure 5.1. There were operational difficulties associated with measurements at the site. The accumulated moisture on filters was subject to evaporation in the fogs of low density and short duration. In addition, the Hi-Vol samplers were oriented with the axis of the inlet facing upward. A positive bias was suspected from the direct collection of drizzle during periods of fog sampling on 11 June. On dates thereafter, rain shields were deployed over the inlets.

In spite of problems associated with patchy fogs or drizzle, the Hi-Vol method appears to be the most direct method available for ground-based measurements of LWC. All droplets are collected on the filter, and there is no dependence on impaction efficiency or droplet size-cut, as for fogwater collector designs. The St_{inlet} criterion given previously indicates no inlet bias for D_0<100 μm. In stable fogs, this technique has been reported to have good precision (Pilié et al., 1975), although reproducibility between samplers at Henninger Flats was only fair (σ_Δ=30%).

From the limited number of intervals with reliable Hi-Vol samples, measurements indicated that LWC was in the range of 0.1 to 0.4 g m^{-3}. This was consistent with the range of LWC determined with the CO_2LT. Together, these two methods demonstrated that the efficiencies of the fogwater collectors were below 100% in dense fog at the mountain site

(Figure 5.1f; non-drizzle data have been indicated with shaded circles).

Bakersfield Results. Measurements of LWC were performed by Hi-Vol method during two studies in Bakersfield (1983 and 1985). In 1983 sampling, the instrument inlet was faced upward, similar to those at Henninger Flats; in 1985, the inlet axis was instead faced horizontally. The Bakersfield sites were more open and less disturbed by nearby canopy than the Henninger Flats site (see Jacob et al., 1984b and this thesis, Chapter 7, for descriptions of sites). Fog densities appeared to be more uniform during these radiation fog episodes than during stratus cloud events; in additon, drizzle was not observed during those sampling periods. The uncertainties associated with the Hi-Vol method were not as great under the more stable fog conditions. For example, sampling invervals were limited to 3-5 minutes in 1985, and sequential samples usually agreed within 20% (see Appendix C.6).

Hi-Vol data for the two years have been compared with RAC-determined LWC in Figure 5.8a. Despite the obvious scatter, the collector efficiency was below 100% relative to the Hi-Vol method. The range for relative efficiencies can be identified in Figure 5.8b, in which the ratio of the two measurements has been plotted against the RAC value. Evaporation from filters was apparent at low fog density. Above a certain LWC of fog, the ratio averaged 60% but ranged between 40 and 80%. Sampling handling errors in the Hi-Vol measurement may have contributed to this wide range of uncertainty. However, the collector efficiency would be expected to exhibit real changes with shifts within the droplet size distributions. Thus, the greater scatter between filter and fogwater collector methods (versus that among RAC, DRI, and GGC collectors) may be inherent to operational differences in their

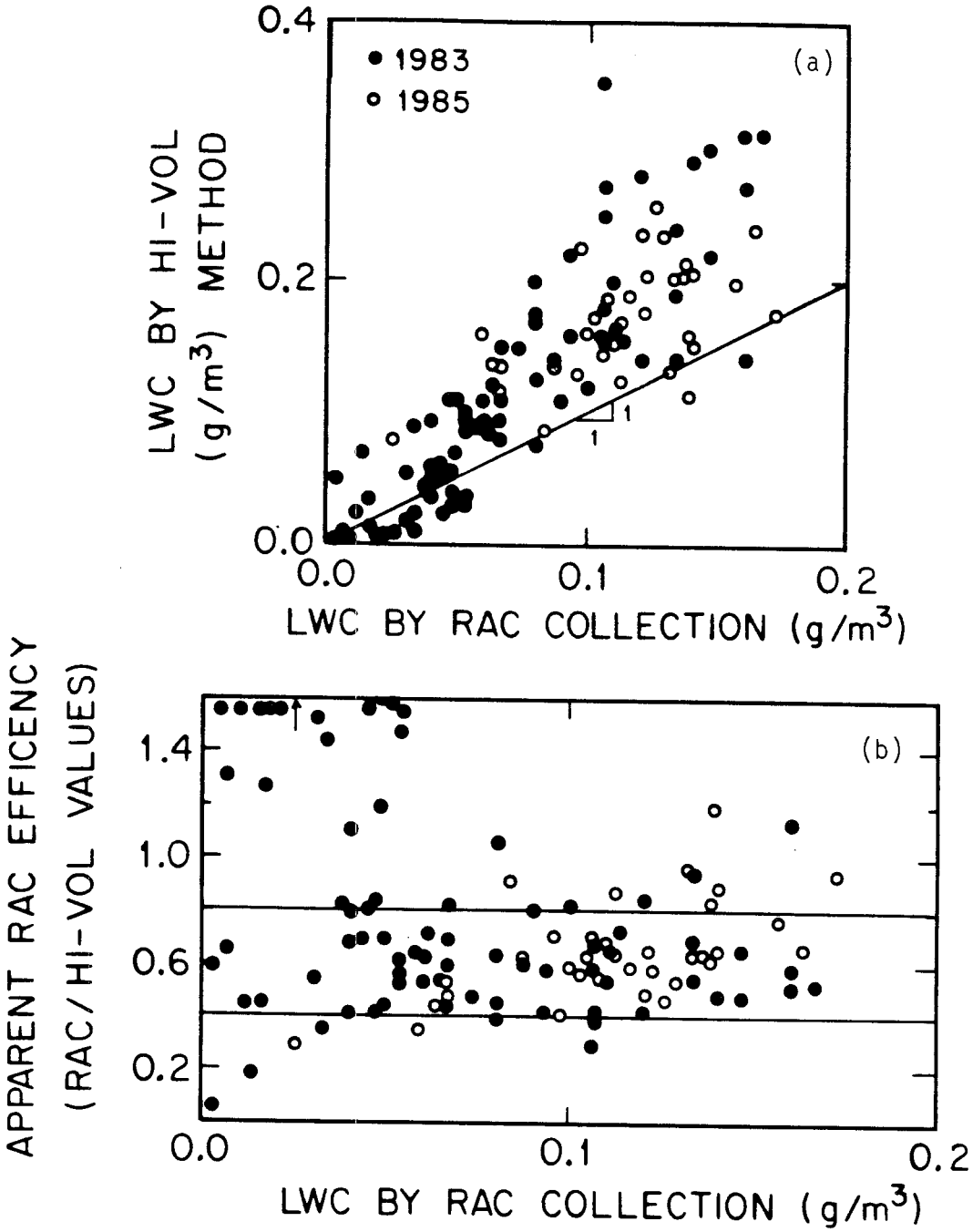

Figure 5.8 Liquid water content comparison between Hi-Vol measurements and RAC collection rates in Bakersfield fogs. (a) Comparison of values; (b) ratio of values versus LWC calculated from RAC collection rate.

determinations and the omission of a changing fraction of the droplet size spectra by fogwater collectors.

5.3.5 Conclusions

Large uncertainites in measurements of LWC during fogwater sampling were underscored by the wide range and considerable scatter between the methods compared. In some cases, fair correlations between methods were found. A bias at low LWC was noted for several fogwater collectors and for the Hi-Vol filter method. Correlations improved for dense fog conditions. The best precision was found for adjacent operation of identical fog collectors.

Collection efficiencies in dense fog were somewhat lower for the RAC compared to DRI and GGC collectors. However, the factors that distinguished the collectors were not commensurate with the differences that were predicted on the basis of their nominal size-cuts and droplet size distributions in fog. The magnitude of LWC indicated by IR extinction and filtration methods were roughly 50% higher than indicated from fogwater collection rates. Furthermore, the higher range of LWC determined by the CO_2LT and Hi-Vol was more consistent with the densities previously reported for intercepted clouds and fogs.

It appeared that each of the fogwater collectors was less than 100% efficient. Thus, the presumption of total droplet collection by GGC or DRI collectors was not substantiated. The disparity between expected and actual collection was apparently not caused by segregation of larger droplets at the collector inlets. No substantial differences in solute concentrations were found for the dominant species. These results suggest that the actual collection characteristics of the three

distinctly different designs are more closely aligned than indicated by their design specifications and respective calibrations.

A factor that contributed to the scatter observed among alternative methods was the systematic variations in instrument responses with rapidly changing fog conditions, displayed by CSASP and CO_2LT data. The uncertainty among LWC measurements was $\pm$30 to 50%. At this time, the techniques available to us precluded greater accuracy in the absolute determination of LWC.

We have estimated an average efficiency for the RAC collector to be approximately 60%. Because the chief interest of our research has been in the fogwater chemistry, the RAC collection rates with this factor applied have been used to determined LWC in the field. We feel that the RAC-derived values were the most appropriate because: (a) they were highly reproducible; (b) they correlated reasonably well with the other fog collector values and other LWC measurement methods; (c) the comparison of fog collectors provided no conclusive information about the composition of the fogwater fraction omitted by the collectors; (d) the validity of droplet size distributions measured by the CSASP was vitiated by an unresolved bias in LWC; and, (e) RAC-derived values were available at all field sites and for all sampling intervals.

Chapter 6

CHEMICAL CHARACTERIZATION OF STRATUS CLOUDWATER AND ITS ROLE AS A VECTOR FOR POLLUTANT DEPOSITION IN A LOS ANGELES PINE FOREST

Jed. M. Waldman, J. William Munger, Daniel J. Jacob,
and Michael R. Hoffmann

Tellus 37B, 91-108 (1985)

Tellus (1985), *37B*, 91–108

Chemical characterization of stratus cloudwater and its role as a vector for pollutant deposition in a Los Angeles pine forest

By JED M. WALDMAN, J. WILLIAM MUNGER, DANIEL J. JACOB, and MICHAEL R. HOFFMANN, *Department of Environmental Engineering Science, W. M. Keck Engineering Laboratories (138-78), California Institute of Technology, Pasadena, CA 91125, USA*

(Manuscript received June 25; in final form December 4, 1984)

ABSTRACT

Highly concentrated, acidic stratus cloudwater was monitored as it intercepted a pine forest (Henninger Flats) 25 km northeast of Los Angeles. Observed pH values ranged from 2.06 to 3.87 for over 100 samples collected in 1982 and 1983 with a median value below pH 3. The ratio of nitrate/sulfate in cloudwater samples was between 1.5 and 2; rainwater at the same site had a ratio of approximately 1. The solute deposition accompanying several light, spring rains (summing to ~1% of annual rainfall) was a disproportionate fraction of the annual total: H^+, NO_3^- and SO_4^{2-} were ~20% or more. Based on a reasonable estimate of fog precipitation, deposition of sulfate, nitrate and free acidity due to intercepting stratus clouds may be of comparable magnitude as that due to the incident rainfall at Henninger Flats.

Cloudwater that had deposited on local pine needles was collected. It was in general more concentrated than ambient cloudwater but with comparable acidity. Enrichment of K^+ and Ca^{2+} in those samples and in throughfall is believed to be due to leaching from foliar surfaces. Injury to sensitive plant tissue has been noted in the literature when prolonged exposure to this severe kind of micro-environment has been imposed.

1. Introduction

In addition to the orographic enhancement of precipitation at mountain sites, cloud droplet capture can lead to greater pollutant deposition relative to the surrounding lowlands. Fog-derived (sometimes called *mist* or "*occult*") precipitation has been determined to be an important hydrological input to some ecosystems (Kerfoot, 1968). Also, measurements of cloudwater composition have shown it to have higher aqueous-phase concentrations compared to precipitation at the same locale (Mrose, 1966; Okita, 1968; Munger et al., 1983b). These two factors combine to suggest the potential for significant pollutant deposition in mountain forests impacted by frequent cloud interception. Often omitted from mass-balance calculations or regional monitoring, this pathway may represent an important component of the total deposition. By accelerating removal of local emissions, this may be especially significant in urban-impacted environments.

Enhanced precipitation in coastal and mountain forests has been reported for collectors located beneath trees exposed to fog-laden wind. Topography, leaf shape and total area, and canopy structure are important parameters (Kerfoot, 1968). In an early study of fog interception in Japan (Yosida, 1953), an average fogwater deposition rate of 0.5 mm h^{-1} was reported for a coastal forest. Oberlander (1956) measured between 45 and 1500 mm of fog-derived precipitation in less than 6 weeks on the San Francisco peninsula with collectors beneath 5 trees. Although it did not include the frequency or duration of fog,

that study underscored the magnitude of water flux and emphasized the importance of location in addition to the height of the trees in affecting fog-derived precipitation. A number of investigators have employed artificial foliar collectors (Schlesinger and Reiners, 1974) or screen "fog-catchers" (Nagel, 1956; Ekern, 1964; Vogelmann et al., 1968; Vogelmann, 1973; Azevedo and Morgan, 1974) to measure the enhancement of water catchment by horizontal interception. Because of their relatively small interception cross-sections, these collectors may underestimate the flux of fog precipitation induced by the actual forest canopy. The fog-derived precipitation in these studies represented a significant fraction of the total water flux—up to several times the measured incident rainfall.

Following the incorporation of aerosol and gaseous species into cloud and fog droplets, dissolved pollutant species may be brought into contact with vegetative surfaces. The chief mechanisms for deposition are impaction, sedimentation—both strongly enhanced by increased particle inertia—and turbulent transport. Damage to sensitive plant tissue and other elements of the biota caused by direct exposure to aqueous acids has been the subject of field and laboratory research (e.g. Tukey, 1970; Evans, 1982). Cases of specific injury and growth retardation have been reported for several plant and tree species in exposure studies (Wood and Bormann, 1974; Haines et al., 1980; Scherbatskoy and Klein, 1983) with threshold for effects generally noted in the range of pH = 2 to 3.

Our objectives were to characterize the chemical composition of stratus cloudwater and to address the potential that droplet capture may play as a vector for pollutant deposition. In this paper, we report the composition of rainwater, cloudwater, aerosol, bulk deposition, and throughfall samples collected in a Los Angeles pine forest. These are used to compare the relative contributions by these various deposition pathways. Interception of stratus clouds on the mountain slope is evaluated for its role in enhancing pollutant deposition. Our findings are presented as a measure of regional pollution not generally monitored. We also report the composition of deposited cloudwater collected from pine needles. These data are discussed in terms of chemical interactions occurring at the vegetative surfaces.

2. Experimental

Our monitoring site was located at Henninger Flats, a campground and tree nursery located at approximately 780 m MSL on the southern slope of Mount Wilson, 25 km northeast of Los Angeles Civic Center. The site is shown in elevation and plan views in Fig. 1. During the spring and early summer, stratus clouds are common along coastal California, associated with the persistent marine layer (Keith, 1980). An inversion base forms the top of the stratus deck. When drawn inland by an onshore pressure gradient, these low-lying clouds can intercept coastal mountain slopes, leading to frequent, dense fog at elevated sites from late evening through morning hours.

Cloudwater was collected on 8 days in June 1982 and 15 days in May and June 1983. On two of the sampling dates in May 1983, the cloud top was below Henninger Flats, and cloudwater was collected 100–200 m downslope. On most dates sampling proceeded from the time cloud had intercepted the site to the time the fog had dissipated. When fog occurred at the site, it was usually preceded by a relatively strong onshore breeze. The local, nighttime drainage flows inherent to the topography also affected the fog characteristics. Note: we refer to the phenomenon as fog at the site; however on the regional scale, the mountain slope was intercepted by stratus clouds. Hence, we refer to our samples as cloud-, rather than fogwater.

A Caltech rotating arm collector (RAC) was used to collect cloudwater (Jacob et al., 1984b). In essence, the RAC is a rapidly rotating (1700 rpm) propeller with slots and collection bottles located on both ends. The axis of the rotating arm was 1.4 m above ground level. The collector was situated approximately 200 m back from the ridge in a gently sloped, open area, surrounded by dense and tall (30 m) vegetation (Fig. 1). The external collection surfaces of the RAC minimize collection losses for large droplet sizes. Because of the collector design and the rapidity in which impacted droplets are removed from the slots to the bottles, evaporation of collected cloudwater is not a problem. Model-scale calibration of the collector design using solid particles has indicated the lower size-cut (50% collection efficiency) to be approximately 20 μm diameter (Jacob et al., 1984b). Little research has been conducted to determine size-

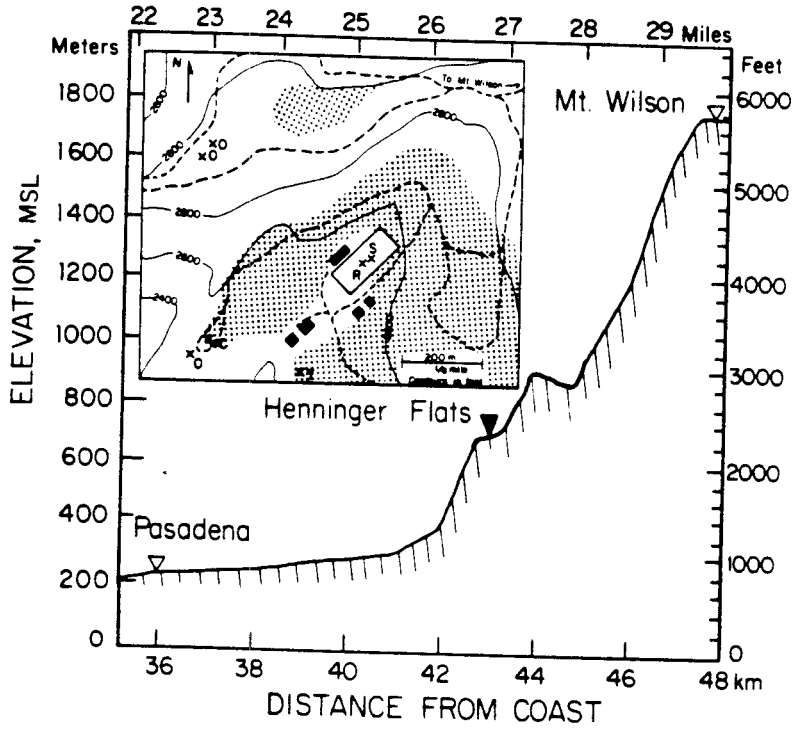

Fig. 1. Profile of southwestern Mount Wilson slope showing location of sampling site. Los Angeles Civic Center is located at 24 km from Pacific Ocean along same profile. On site plan (insert), S is cloudwater sampling site in nursery; R is rainwater collector location; O and C are open (bulk) and canopy (throughfall) bucket collectors; and T is location of tree drop samples. Shading indicates dense pine forest vegetation; dashed lines are dirt roads.

composition relationships of the cloud droplet spectrum experimentally. However, during an intercomparison of fogwater collectors at Henninger Flats (Hering and Blumenthal, 1984), the RAC samples gave consistently very good agreement with those of a jet-impactor having a lower size-cut measured between 2 and 5 μm diameter (Katz, 1980). Hence, the concentrations of the smaller droplets was not sufficiently different to alter the overall composition of simultaneously collected samples.

Sampling intervals generally ranged from 30 to 60 minutes; sample volumes were usually 10–30 ml, although some as small as 1 ml were analyzed. The RAC water collection rate has been found to correlate well with several independent methods (Hering and Blumenthal, 1984). Jacob et al. (1984b) reported that the theoretical RAC collection rate (5 m^3 min^{-1}) gave liquid water content (LWC) which was approximately 60% the value determined by total filter measurements made in radiation fog. For this study, RAC-derived LWC values were calculated with this empirical correction factor:

$$\text{LWC} = \frac{\text{Sample volume}}{\text{Sample interval} \times \text{theoretical air volume sampling rate} \times 0.6}$$

In an environment where LWC greatly varies, temporally and spatially, the RAC-derived measurements have the advantage that they are collocated with each of the chemical samples and similarly time-averaged. This relationship gave good agreement with the other methods, except for patchy and dissipating fogs (Waldman, 1985).

Immediately after each sample was collected, pH was measured using a Radiometer PHM 82 meter and combination electrode; standard calibration of the electrode was performed at pH 7, 4 and 1.68. Within 30 minutes, aliquots were preserved from each sample for analysis of formaldehyde, S(IV)

and trace metals. For major ion determinations, aliquots were necessarily diluted from 5 to 50:1. Further details of fogwater sample handling and analytical protocols are presented elsewhere (Munger et al., 1983a).

In addition to cloudwater collection as in 1982, ambient aerosol measurents were made during the spring of 1983. Total and fine-fraction aerosol loadings were determined using 47 mm Teflon (Zefluor—1 μm pore size) filters sampling at 10 lpm. Samples—in dry and fog-laden air—were collected simultaneously on an open-faced filter (total) and behind a cyclone separator (fine <3 μm). The concentrations of water soluble ions were determined following aqueous extraction with a reciprocating shaker for 1 hour. Subsequent extractions of the filters produced satisfactory blanks.

Rainwater was monitored at the nursery from November 1982 to June 1983 using a wet-only collector (Liljestrand, 1980). Bulk deposition samples were collected between May and July 1983 in open, plastic buckets. On several occasions droplets that had accumulated on pine needles by cloud droplet capture were collected. This was done by manual, drop-by-drop removal. Selected trees were repeatedly sampled. Further details of these deposition measurements are given in separate sections.

3. Results and discussion

The objective of this field study was to determine the relative contributions of various pathways to the overall pollutant deposition. For clarity, a summary of cloudwater data is first presented and discussed. Several specific fog episodes are described. Wet and bulk deposition data sets are then presented. This is followed by calculations of the magnitude of fog-derived precipitation and the associated pollutant deposition based on the cloudwater composition reported. With these, a comparison of the pollutant fluxes associated with precipitation (incident and occult) and dry deposition pathways is given. Finally, the composition of intercepted cloudwater is presented with a discussion of its potential interactions with foliar surfaces.

3.1 *Cloudwater composition*

Summaries of 1982 and 1983 results for cloudwater and rainwater chemical analyses are presented in Table 1. For comparison, values are also given for the 1978–79 volume-weighted mean rainwater concentrations at Pasadena and Mount Wilson (225 and 1800 m MSL, respectively). For most species, the median values for Henninger Flats cloudwater concentrations are 20 or more times those for local rainwater. The ionic balances for cloudwater data are presented in Fig. 2. In general, the results for both years are satisfactory with 1983 data giving very consistent balance. Ionic balance was calculated as a check on both the analytical precision and the completeness of the ion determinations. We are confident that all the major ionic species have been measured. There were a few cases in the 1982 data set which gave poor ionic balance, these for samples with the highest acidities and concentrations (and the smallest sample volumes). For those samples, much of the worse imbalances could be explained by a small analytical error at low pH: e.g. at pH ~ 2, d(pH) = ±0·1 gives d[H^+] of ±2500 μeq^{-1}. The better agreement for 1983 data was also due to our experience working with samples of such high concentrations. The protocol for the latter year included a single, quantitative dilution of each sample (5 to 50:1) rather than separate ones for the individual ion determinations, as for the 1982 samples.

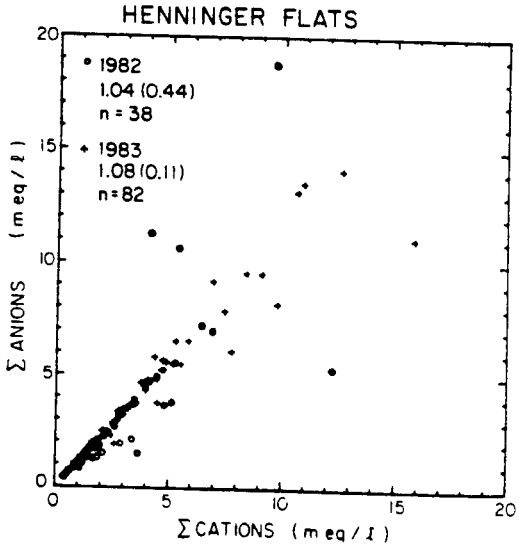

Fig. 2. Total anion versus cation concentrations for cloudwater samples of 1982 and 1983 with mean (std. dev.) of ion balances for n samples.

Table 1. *Median and range of concentrations for cloudwater samples-Henninger Flats: 1982 and 1983*

		Cloudwater		Rainwater		
		1982[a]	1983[b]	Site[c]	Pasadena[d]	Mt. Wilson[d]
pH		2.86	2.96	4.6	4.4	5.0
		2.06–3.65	2.07–3.87			
H^+	$\mu eq\ l^{-1}$	1365	1100	24	39	10
		224–8710	135–8510			
Na^+		146	285	14	24	26
		5–2465	3–6320			
K^+		18	22	0.9	1.7	1.7
		1–161	3–197			
NH_4^+		576	582	9.2	21	36
		128–3130	62–7420			
Ca^{2+}		132	142	4.1	6.7	9.3
		5–975	3–3020			
Mg^{2+}		54	106	5.2	7.2	6.6
		2–762	1–1735			
Cl^-		125	220	18	28	28
		21–1965	15–9650			
NO_3^-		1435	1510	17	31	23
		191–9500	161–16,300			
SO_4^{2-}		617	971	19	39	40
		128–7310	133–9300			
S(IV)	$\mu mol/l^{-1}$	15	7	na	na	na
		7–85	0.4–94			
CH_2O		66	50	na	na	na
		34–920	12–173			
Fe	$\mu g\ l^{-1}$	1055	455	na	223	28
		200–6880	20–4800			
Pb		346	212	na	na	na
		80–2780	38–2500			

[a] Median and range for 38 samples (42 for pH) on 8 days.
[b] Median and range for 82 samples (86 for pH) on 15 days.
[c] Volume-weighted mean values for October 1982 to July 1983 (see Table 3).
[d] Volume-weighted mean values for 1978–79 (Liljestrand and Morgan, 1981).
na = not analyzed.

Hydrogen, ammonium, nitrate, and sulfate dominated the ionic composition in most samples; this is consistent with previous observations for Los Angeles aerosol (Appel et al., 1978). For most samples, non-sea salt sulfate was greater than 90% of measured sulfate, assuming as an upper limit that sodium was solely of marine origin. The nitrate-to-sulfate equivalent ratio for these samples was between 1.5 and 2 (Fig. 3). This ratio is similar to fogwater samples collected in the Los Angeles basin (cf. Munger et al., 1983a) but markedly different from local rainwater with ratios less than 1 (Table 1). The basinwide nitrate-to-sulfate equivalent ratio for precursor emissions has been reported between 2 and 3 (California Air Resources Board, 1979; 1982).

The low pH values in the cloudwater occurred in a rather narrow range: pH = 2 to 4 (Fig. 4). The degree to which ambient acids have been neutralized in the atmosphere following their formation is indicated by the equivalent ratio of $[H^+]$ versus $[NO_3^-]$ plus $[SO_4^{2-}]$. The ratio for Los Angeles stratus cloudwater was generally ~0.5 (Fig. 5). That is, in the cloudwater about half of the acidic anions were not neutralized.

Even for the cases with low aqueous concentrations, sufficient ambient bases were either not available or scavenged to fully neutralize the acid.

Gaseous ammonia should be completely scavenged by acidic cloud droplets (Jacob and Hoffmann, 1983). Basinwide, ammonia emissions are one-third of the SO_2 and NO_x sum on an equivalent basis; however, major source areas are located in San Bernadino and eastern Los Angeles counties (Russell et al., 1983). The degree of fractional acidity reported herein is similar to coastal fogs collected in southern California (Munger et al., 1983a). However, for sites with very high ammonia emissions (cf. Jacob et al., 1984a), fogwater with similarly high ionic concentrations of acidic anions were largely neutralized. For some of the highly concentrated cloudwater samples, $[Ca^{2+}]$ and $[Mg^{2+}]$ were 10–50% lower for filtered (0.2 μm pore size) compared to non-filtered aliquots. Na^+, K^+ and NH_4^+ showed little difference between aliquots. This suggests that some of these ions in the condensation nuclei do not rapidly or completely dissolve. That is, there may be a kinetic limitation to the neutralization of cloudwater by the dissolution of an alkaline fraction.

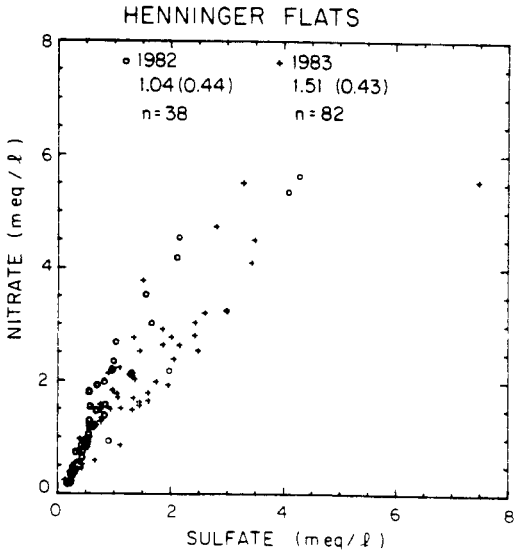

Fig. 3. Concentrations of nitrate versus sulfate in cloudwater samples of 1982 and 1983 with mean (std. dev.) of equivalent nitrate/sulfate ratios.

The median values of trace metals (Fe, Pb, Mn, Ni and Cu) concentrations for approximately 100 cloudwater samples collected both years were 520, 260, 46, 36, and 20 ppb, respectively. For iron and lead, the values range from ~100 ppb to several ppm. The occurrences of stratus clouds intercepting inland slopes were linked to on-shore pressure gradients. As a whole, the trace metal concentrations and loadings in the cloud samples reflect the transport of anthropogenic pollutants to elevated sites downwind from their sources.

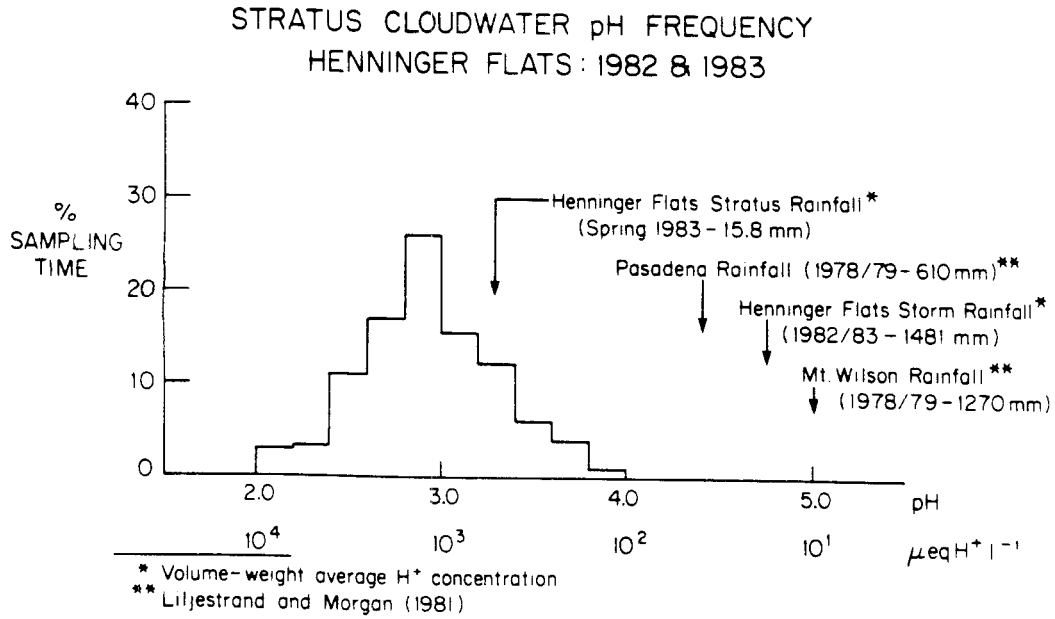

Fig. 4. Frequency histogram of pH for 1982 and 1983 Henninger Flats cloudwater samples.

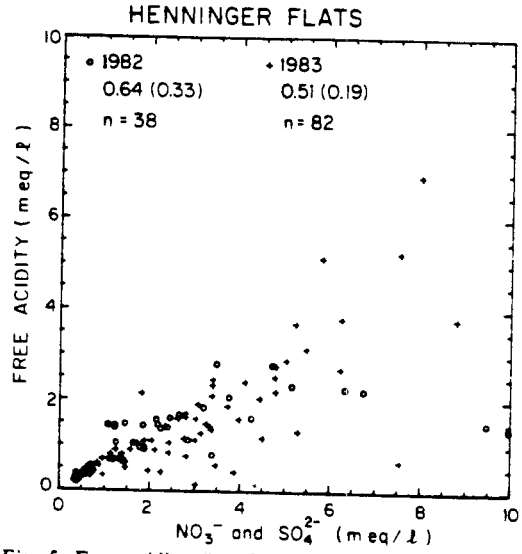

Fig. 5. Free acidity (i.e., $[H^+]$) versus sum of nitrate and sulfate concentrations in cloudwater samples for 1982 and 1983 with mean (std. dev.) of equivalent ratios.

The concentration of S(IV) in cloudwater samples ranged between 1 and 100 μmol l^{-1}, with a two-season median value of 10. Formaldehyde was measured at concentrations 4 to 10 times greater than for S(IV) (median value = 56 μml l^{-1}). These data are given in Munger et al., (1984). Gaseous SO_2 levels at Henninger Flats were measured to be generally 10 ppb or below (Hering and Blumenthal, 1984). Similarly low levels are typical in nearby Pasadena during the spring. The formations of S(IV)-aldehyde adducts in solution led to total aqueous S(IV) concentrations which exceeded the Henry's law solubility for gaseous SO_2 at low pH (Munger et al., 1984), although these were yet a small fraction of aqueous sulfur.

3.2. *Examples of specific events*

Ambient aerosol was sampled prior, during and following several fog episodes in 1983 (Table 2). Aerosol concentrations (μeq m^{-3} of air) measured on Teflon filters were comparable to those of cloudwater samples (Fig. 6). During fog, these samples included droplets as well. Values for aerosol $[H^+]$ concentration were calculated from the ionic charge deficiency. This procedure is justified by the large excess of anions observed and the resulting low aerosol pH predicted. Several points are suggested from these data. First, the acidities of the precursor aerosol were somewhat lower than those measured for cloudwater. Filter samples collected wholly during fog were generally more acidic. Daum et al. (1984) found clear-air aerosol to contain much less acidity than the cloudwater in the eastern United States for samples collected aloft, although they make the caveat that the samples they compare were from different days. Our calculations indicate that much of the cloudwater solute was derived from ambient aerosol scavenged by cloud formation; some but not all of the resultant aqueous acidity is measured in the precursor aerosol. Second, the nitrate-to-sulfate ratios of the afternoon and late evening (non-fog) intervals were usually less than one, while the concentrations of nitrate generally showed a large increase immediately following the onset of fog, wherein the ratio was between 1.5 and 2. Shown in Fig. 6, the aerosol nitrate measured after fog formed increased (June 11) while all the other measured species remained unchanged.

A likely source of additional nitrate is the scavenging of nitric acid vapor by the droplets. Compared to levels measured in non-fog aerosol, the increase in nitrate was around 0.1 to 0.2 μmol m^{-3}, similar to nitric acid values reported for the Los Angeles atmosphere (Spicer et al., 1982). Nitric acid was measured in clear air at Henninger Flats during June 1984 between 0.01 and 0.4 μmol m^{-3} (Waldman, 1985). In all aerosol and cloudwater samples, there was unneutralized acidity. Under these conditions, gaseous ammonia would be completely scavenged by acidic sulfate aerosol. Nitric acid would remain unneutralized and, in clear air, in the gas phase. The increase in suspended liquid water upon fog formation results in 100% scavenging of nitric acid (Jacob and Hoffmann, 1983). Conversely, for dissipating fog conditions, nitric acid would be driven back into the gas phase.

The lower pre-fog concentrations measured could have also been caused by particulate nitrate loss due to ammonium nitrate volatilization from the Teflon filter medium (Appel et al., 1979). For cool, humid conditions at Henninger Flats (e.g. T = 10 °C and R.H. $\geq$ 90%), the equilibrium dissociation constant (K_1) for NH_4NO_3 is below 0.1 ppb^2 or 1.8×10^{-4} (μmol m^{-3})^2 (Stelson and Seinfeld, 1982). Therefore, during most sample intervals, K_1 would be too low for this to be a significant artifact. It appears that some nitric acid

Table 2. *Ambient aerosol chemical concentrations—Henninger Flats: June 1983*

Date & Time	Size[a]	Fog[b]	μeq m^{-3} NH_4^+	NO_3^-	SO_4^{2-}	"pH"[c]	NO_3^-/SO_4^{2-}	cloudwater[d] pH	NO_3^-/SO_4^{2-}
June 8									
	T	post	0.196	0.067	0.312	"3.11"	0.22		
0000–0600	F		0.189	0.018	0.273			2.71	1.11
	(C)		(0.007)	(0.049)	(0.039)	"3.47"	1.26		
2145–0215	T	fog	0.101	0.294	0.213	"2.74"	1.38		
	F		0.009	0.042	0.086			3.00	1.68
	(C)		(0.092)	(0.252)	(0.127)	"2.86"	1.98		
June 10									
1200–1800	T	pre	0.154	0.070	0.284	"3.25"	0.25		
	F		0.159	0.012	0.265				
	(C)		(0.005)	(0.058)	(0.019)	"3.98"	3.05		
2230–0230	T	pre	0.136	0.073	0.195	"3.39"	0.37		
	F		0.188	0.044	0.190				
	(C)		(0.052)	(0.029)	(0.005)	"3.51"	5.80		
June 11									
0630–1030	T	fog	0.154	0.265	0.185	"2.87"	1.43		
	F		0.050	0.010	0.069			3.01	1.85
	(C)		(0.104)	(0.255)	(0.116)	"2.92"	2.20		
1040–1430	T	fog	0.057	0.105	0.109	"3.22"	0.96		
	F		0.034	0.004	0.045			3.26	1.36
	(C)		(0.023)	(0.101)	(0.064)	"3.27"	1.58		
June 12									
0800–1200	T	fog/post	0.200	0.201	0.197	"3.40"	1.02		
	F		0.041	0.044	0.082			3.57	1.43
	(C)		(0.159)	(0.151)	(0.115)	"3.82"	1.31		
June 19									
0045–0600	T	patchy fog	0.027	0.068	0.100	"3.33"	0.68	2.87	1.65
June 21									
0835–1045	T	patchy fog	0.257	0.269	0.480	"2.95"	0.56		
	F		0.242	0.057	0.267			2.67	na
	(C)		(0.015)	(0.212)	(0.213)	"3.05"	1.00		
June 22									
0430–0830	T	fog/post	0.243	0.141	0.262	"3.46"	0.54		
	F		0.213	0.098	0.229			3.09	2.50
	(C)		(0.030)	(0.043)	(0.033)	"4.52"	1.30		

[a] T, total particulate (open-faced filter); F, fine particulate ($d_p < 3\ \mu$m); (C), coarse: T minus F.
[b] Conditions during sampling relative to fog episode.
[c] "pH" calculated assuming H^+ balanced charge deficiency of major ions and LWC = 0.2 g m^{-3}.
[d] LWC and time-weighted average values for cloudwater samples relative to b; nitrate/sulfate ratios are on equivalent basis.

loss from the filters during patchy and dissipating fogs (e.g., June 21 and 22) led to NO_3^-/SO_4^{2-} values below cloudwater ratios. A third possibility exists by which the noted increase in nitrate concentrations were due to its advection to the site. However, there was no increase in measured gaseous pollutants (SO_2, NO_x and O_3) following the onset of the fog (Hering and Blumenthal, 1984).

Prior to the fog, most of the particulate solute, especially sulfate, was measured in the fine (<3 μm) size class. In dense fog, very little of the particulate solute remained in the fine-size class. However, the proportion of sulfate found in the

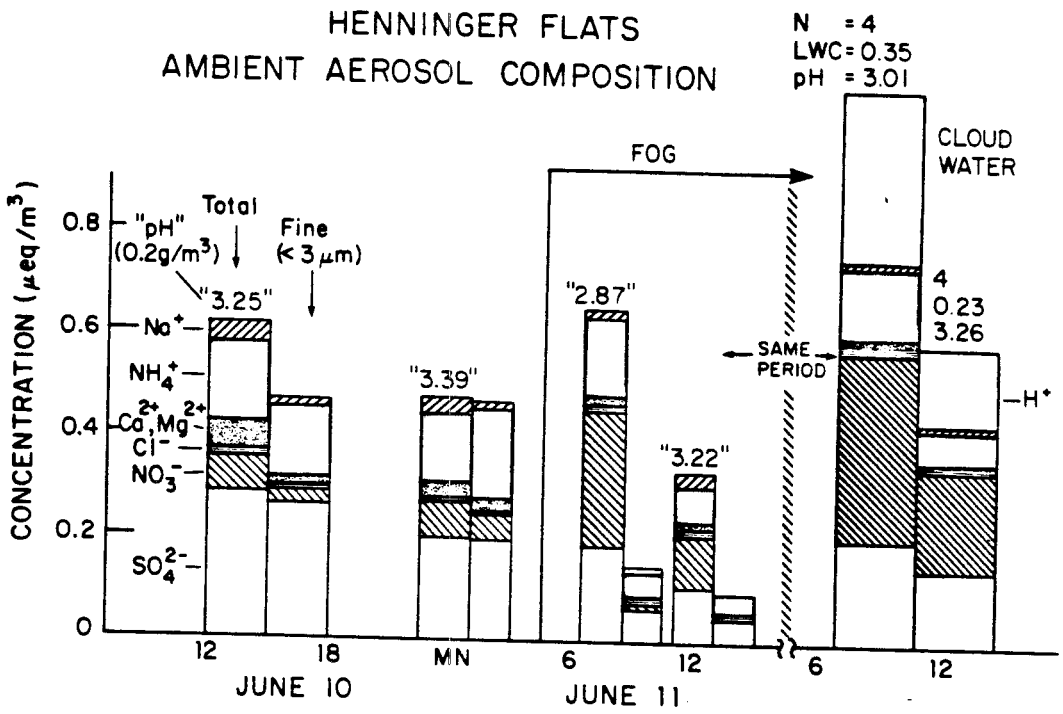

Fig. 6. Ambient aerosol composition for June 10–11, 1983. Total and fine (d_p < 3 μm) particulate concentrations given are for each sample interval. Time-weighted solute concentrations for cloudwater samples are shown for the latter two intervals.

fine-size fraction of the filter samples (1/3 to 1/2) was greater than for nitrate. This difference is primarily due to the presence of precursor nitrate in the air as nitric acid which is subsequently absorbed into fog droplets. Also, as nitrate and sulfate salts are highly hygroscopic, the difference in the portion which was activated into droplets would be a function of particle size. The model of Bassett and Seinfeld (1984) predicts that nitric acid will be more favorably absorbed by larger aerosol, due to the Kelvin effect. Previous findings that nitrate is associated with larger-sized aerosol (Appel et al., 1978) would support an interpretation that particulate nitrate was more completely scavenged by droplet activation. Cloudwater samples collected during post-precipitation intervals generally had the lowest nitrate-to-sulfate ratios. As suggested above, this could be caused by mechanisms which scavenge (and deposit) nitrate more effectively than sulfate.

Concentration, LWC, and solute mass loading profiles for cloudwater samples from June 11 and 12, 1983 are shown in Fig. 7. During the first several hours of sampling, as the marine air permeated the forest, the fog was patchy, and the LWC fluctuated dramatically. In addition, there were brief periods of complete dissipation at the onset of this fog episode when deactivation of cloud droplets would remove cloudwater solute mass to the haze-size range, below the collector size-cut. For these first few intervals, the RAC-derived value (estimated from the entire sampling period) underestimated LWC for the fog actually collected. Thus, a representative indication of the cloudwater solute loading is difficult to determine for time-averaged samples in locally patchy fogs.

After 0700, fog became more stable at the site (Fig. 7b), and the solute loading remained fairly constant for the next 4 to 5 hours (Fig. 7c). A slight drizzle began at 0800, intensifying to a measurable rate in the mid-afternoon. Often, drizzle-size drops do not fall far below the cloud base before they evaporate. During the afternoon (June 11), 5.8 mm of rainfall was measured at the site, which was

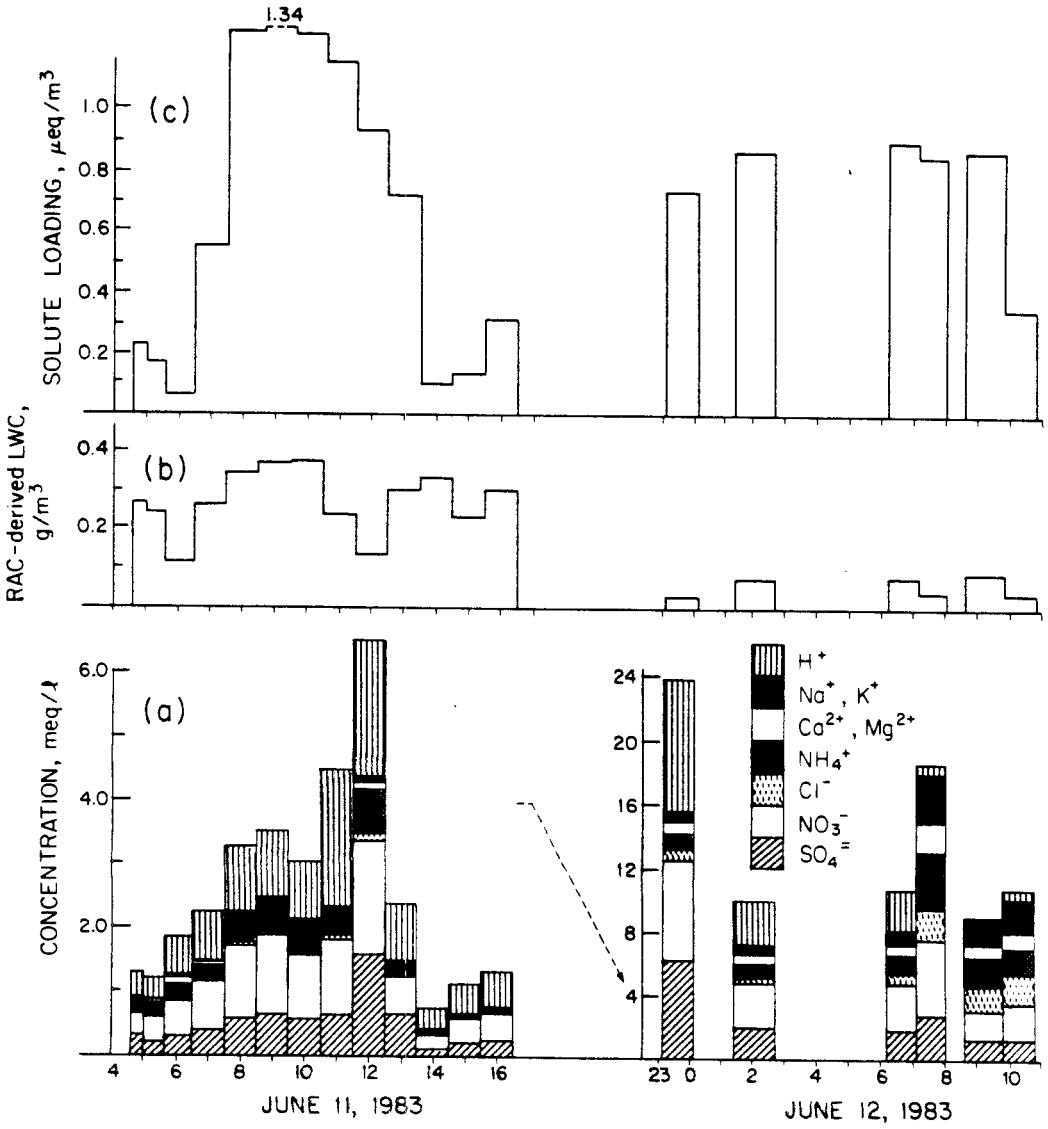

Fig. 7. (a) Concentration, (b) LWC, and (c) ambient solute loading for sequential cloudwater samples on June 11 and 12, 1982. Note the change in scale (a). A slight drizzle began 0800 on June 11, intensifying after 1200 and ending by early evening.

above the cloud base, compared to the trace (<0.25 mm) measured ~500 m below the base in Pasadena. Coincident with afternoon drizzle was a drop in ambient solute concentrations (see Fig. 6 and 7c). The total solute deposited in the drizzle (see subsequent section) was several times the product of aerosol concentration and cloud height, which indicates a continuing source of solutes. Advection of pollutant-laden cloud air to the mountain slope adds to the amount deposited in the rainfall there, while upwind over the lower basin no precipitation was occurring. Also following the onset of rainfall, the mass median diameter for measured cloud droplet spectra became lower. The collection efficiencies of cloud droplets by drizzle-size drops falling to the ground increases for larger droplets (Pruppacher and Klett, 1978). Hudson and Rogers (1984) have shown that a significant fraction of

the larger nuclei are found in the larger droplets. The depletion of larger, cloud droplets, taken with the magnitude of solute deposition measured in the drizzle, lends further support to the interpretation that the drop in cloudwater solute loading was caused by its depletion by precipitation scavenging.

The fog continued with fairly uniform LWC through that day—drizzle ceasing in the late afternoon—and into the following morning. Cloudwater sampling was discontinued until 2300. Two intermittent samples were collected before continuous sampling was resumed at 0600 on June 12. For June 12 samples, the ambient solute loading was elevated to the pre-drizzle level—aqueous concentrations were much higher with fluctuations mirrored by commensurately lower LWC. Similarly, the solute measured in fog on filters was greater (Table 2). The large-scale eddy circulation which had deepened the marine layer in the previous afternoon had weakened. The increase in pollutant levels in the cloud was partially a reflection of this decrease in the mixing depth. Also, as the drizzle had ceased, advected pollutants in the cloud air would not be locally depleted. In the morning, the cloudwater samples became progressively less acidic, and equimolar Na^+ and Cl^- increases occurred. This latter point suggests that air of greater marine character was advected to the site. The roles of vertical mixing and ventilation within stratus clouds and fogs are major uncertainties. Until we can better quantify the transport component of cloud/fog dynamics at a given sampling site, our explanations remain speculative. Finally, the drop in solute loading for the last sample accompanied evaporation of fog droplets.

3.3 *Deposition: measurements and calculations*

3.3.1. Storm and stratus rain. Rainfall at Henninger Flats was collected and analyzed from November 1982 to June 1983. In Table 3, the wet deposition is split between storm (A) and (B) spring stratus events. The 1982–83 season (October 1 to September 30) was above average rainfall—the wettest on record at Henninger Flats: 1660 mm compared to an average of 670 mm. Pasadena and Mt. Wilson deposition (from 1978–79 data) are presented for comparison. Because of the high frequency and water flux per storm event, the

Table 3. *Wet deposition—Henninger Flats: October 1982 to July 1983*

			meq m^{-2}								
Month	#	mm	H^+	Na^+	K^+	NH_4^+	Ca^{2+}	Mg^{2+}	Cl^-	NO_3^-	SO_4^{2-}
A. Storms[a]											
Sum (mean[d])	34	1480	27.8 (18.8)	20.6 (13.9)	1.2 (0.8)	12.1 (8.2)	4.9 (3.3)	7.2 (4.8)	25.2 (17.0)	18.4 (12.4)	23.4 (15.8)
B. Stratus[b]											
Sum (mean[d])	6	15.8	8.33 (526)	0.87 (55)	0.13 (8)	1.68 (106)	1.24 (78)	0.64 (41)	1.30 (82)	7.40 (467)	5.45 (344)
$\frac{B}{A+B} \times 100$		1.1	23.1	4.1	9.7	12.2	20.2	8.2	4.9	28.7	18.9
1978/1979[c]											
Pasadena (mean[d])		610	23.8 (39)	14.6 (24)	1.0 (1.7)	12.8 (21)	4.1 (6.7)	4.4 (7.3)	17.1 (28)	18.9 (31)	23.8 (39)
Mt. Wilson (mean[d])		1270	12.7 (10)	33.0 (26)	2.2 (1.7)	45.7 (36)	11.8 (9.3)	8.4 (6.6)	35.6 (28)	29.2 (23)	30.8 (40)

[a] Five major storms (total = 250 mm) and several light rains (< 10 mm) between Oct. and Apr. were missed. Standard rainfall gauge values were used to calculate individual storm deposition when portion of rainfall was missed by collector. The volume-weighted concentrations were used to determine total storm deposition.

[b] Actually, two stratus events (total = 13.3 mm) were collected; four additional trace events (total = 2.5 mm) were assumed to have similar concentrations to calculate total stratus deposition.

[c] Liljestrand and Morgan (1981).

[d] Volume-weighted mean concentration (μeq l^{-1}).

volume-weighted mean concentrations (A) were lower than in the earlier year. Stratus events (i.e., drizzle or light rainfall) occurred within a developed marine layer, similar to that which led to stratus cloudiness and fog on mountain slopes but with more intense deepening. The ionic concentrations of these light rains were dramatically higher than for the storm events, but in a range somewhat less concentrated and acidic than the cloudwater samples. Morgan and Liljestrand (1980) noted similarly higher concentrations in sparser rains they measured in Pasadena. Brewer et al. (1983) reported a similar relationship between fog and "mist" (i.e. drizzle) samples at several Los Angeles locations.

The meteorology is an important factor to consider in comparing the precipitation types. Most wintertime storms are associated with weather systems which advect moist, unstable oceanic air with fairly intense convective activity extending up to >5000 m (Keith, 1980). On the other hand, drizzle and fog events usually occur within a developed marine layer constrained by a strong temperature inversion aloft. This limits the vertical extent of mixing; thus, stratus cloud droplets form and can have longer residence times in the polluted atmosphere. The mean pH values for stratus and storm rainwater are compared to cloudwater samples in Fig. 4. The fog → drizzle → rain hierarchy of solute concentration also reflects the relationship between droplet size and dilution. The growth of non-freezing cloud droplets to a size with appreciable sedimentation velocity occurs solely by condensation of water vapor for sizes below 50 μm diameter; subsequently both coalescence and condensation lead to drizzle (0.2 to 0.5 mm) and raindrop (>0.05 mm) sizes, depending upon the intensity of vertical motion (Pruppacher and Klett, 1978).

Stratus events led to solute deposition which was disproportionate to the water flux. While accounting for ~1% of measured rainfall, nearly 20% or more of H^+, NO_3^- and SO_4^{2-} were deposited in less than 16 mm precipitation. Na^+ and Cl^- were much less enhanced in stratus rainfall. The winter storms responsible for most of the precipitation form over the eastern Pacific Ocean. They are more effective at generating and transporting sea salt aerosol due to their greater convective activity. For stratus events, the enhancement of H^+ and NO_3^- was greatest and, for NH_4^+ and SO_4^{2-}, it was somewhat less. The difference in nitrate/sulfate ratios for stratus (1.4) versus storm (0.8) events is a further indication of the meterological and seasonal variation in SO_2 and NO_x oxidation and transport.

3.3.2. *Bulk deposition and throughfall.* For our program, bulk deposition was collected with open buckets. These provided large collection areas, minimized resuspension (relative to flat surfaces) and were convenient to use and rinse. Standard 4-gallon, polyethylene buckets (open area = 566 cm^2) were placed with the rim at least 1 meter above the ground in the vicinity of the nursery (see Fig. 1). One bucket was placed beneath a dense stand of Coulter pine (*Pinus coulteri*). The containers were extracted with 0 to 500 ml of H_2O, depending on the exposure duration and precipitation amount.

Surrogate surface methods, such as flat plates and open containers, remain controversial due to the variability of their results and the uncertainty in extrapolation of specific results to a regional value. From intercomparison of surrogate surfaces (Dolske and Gatz, 1984; Dasch, 1983), buckets were shown to give flux values which were sensitive to ambient aerosol sulfate levels. Dry deposition of SO_2 and NO_x has been reported to be inconsequential for the plastic buckets (Dasch, 1983); however, gaseous nitric acid might be expected to contribute to the measured deposition because of its reactivity.

There are uncertainties in interpreting these data: for example, atmospheric conditions for the sampling intervals were not well known with respect to aerosol size spectra, pollutant fractionation, or micrometeorology. For simple topography, a very detailed data set sould be required; for complex terrain, the problem is almost intractable. Rather, the bulk deposition measurements are presented to provide a relative measure of solute deposition under varying, ambient conditions.

Overall, bulk deposition for most intervals with precipitation was significantly greater than for intervals with none (Table 4). For example, the deposition rates for H^+, NH_4^+, NO_3^- and SO_4^{2-}, averaged for the two intervals with measurable rainfall (May 26–June 3 and June 9–13), were 10 or more times that of the other intervals listed. The dry-only deposition (i.e., with the measured wet-only values subtracted) was also greater for those intervals. These coincided with stratus clouds and fog. This indicated to us, as noted in the previous section, that trace precipitation (not measured in

Table 4. *Bulk deposition and throughfall—Henninger Flats: May–July 1983*

Interval	Location[a]	meq m^{-2} (std. dev.)									
		"H$^+$"[b]	Na^+	K^+	NH_4^+		Ca^{2+}	Mg^{2+}	Cl^-	NO_3^-	SO_4^{2-}
May 12–19											
(168 h)	O (3)	0.0 (0.0)	0.52 (0.08)	0.35 (0.13)	0.39	(0.37)	0.30 (0.11)	0.40 (0.24)	0.16 (0.08)	0.78 (0.10)	0.59 (0.26)
	C (1)	0.0	0.16	0.09	0.07		0.31	0.19	0.14	0.43	0.17
May 19–26											
(162 h)	O (2)	0.10 (0.10)	0.05 (0.01)	0.10 (0.08)	0.20	(0.23)	0.21 (0.02)	0.09 (0.04)	0.10 (0.10)	0.47 (0.08)	0.10 (0.03)
	C (1)	0.18	0.05	0.07	0.05		0.21	0.07	0.04	0.45	0.17
May 26–June 3											
(191 h)	O (3)	4.69 (0.87)	2.04 (0.25)	0.30 (0.17)	2.28	(0.69)	0.81 (0.02)	0.91 (0.27)	1.87 (0.04)	5.49 (0.06)	4.42 (0.35)
	C (1)	4.41	3.71	5.71	3.48		4.35	3.93	2.96	14.5	5.50
Wet only—15 mm		3.83	0.56	0.09	0.89		0.74	0.42	0.63	3.60	2.80
June 3–9											
(156 h)	O (3)	0.55 (0.60)	0.28 (0.03)	0.19 (0.10)	0.21	(0.17)	0.66 (0.04)	0.34 (0.10)	0.20 (0.03)	1.05 (0.40)	0.73 (0.34)
	C (1)	0.47	0.16	0.07	0.24		0.36	0.13	0.10	0.80	0.37
Wet only—0.5 mm[c]		0.26	0.03	0.00	0.05		0.04	0.02	0.04	0.23	0.17
June 9–13											
(94 h)	O (3)	3.34 (0.64)	0.41 (0.15)	0.12 (0.10)	1.28	(0.21)	0.54 (0.20)	0.26 (0.13)	0.33 (0.16)	4.07 (0.99)	2.64 (0.56)
	C (1)	4.59	1.34	1.65	1.59		2.06	1.44	0.90	8.55	4.04
Wet only—5.8 mm		3.38	0.18	0.02	0.56		0.42	0.21	0.46	2.76	1.85
June 13–19											
(135 h)	O (1)	0.0	0.09	0.14	0.08		0.20	0.14	0.12	0.22	0.11
June 19–July 11											
(531 h)	O (2)	0.15 (0.08)	1.08 (0.01)	0.15 (0.05)	0.81	(0.02)	0.92 (0.08)	0.85 (0.09)	0.11 (0.0)	1.57 (0.11)	1.55 (0.13)
Wet only—2.0 mm[c]		1.05	0.11	0.02	0.21		0.16	0.08	0.16	0.93	0.69
July 11–25											
(342 h)	O (2)	0.05 (0.01)	0.26 (0.0)	0.07 (0.01)	0.16	(0.11)	0.24 (0.18)	0.16 (0.0)	0.13 (0.16)	0.65 (0.05)	0.19 (0.08)

[a] O = Open; C = Under Canopy; (# replicates).
[b] "H^+" deposition from pH of bucket extraction or precipitation sample.
[c] Wet only deposition calculated from measured trace rainfall × mean stratus (B) concentration (see Table 3).

standard rainfall gages) accompanying these low clouds had enhanced solute flux associated with it.

During dry periods, the below-canopy sample had generally lower pollutant deposition compared to open collectors. This reduction may be due to the interception of material to the canopy alone, or the suppression of turbulent transport below the canopy as well. It also appeared that some of this material eventually was deposited as throughfall when appreciable rainfall occurred (cf. June 3–9 to June 9–13). However, some of the additional cations had likely leached from the pine needles.

3.3.3. *Calculation of fog precipitation.* Fog droplet capture by the forest canopy has been recognized as an important hydrologic input. Hori (1953) and co-workers conducted extensive research on the mechanisms and efficiency of droplet capture. Lovett (1984) modeled the transfer of liquid water to the forest canopy in fog-laden winds. Compared to the deposition of dry aerosol (Sehmel, 1974), the capture of fog droplets is significantly more efficient. The parameters that control the rate of deposition are the wind speed and turbulence, canopy and leaf geometries, and fog LWC and droplet size distribution. Lovett calculated water deposition rates, chiefly by impaction to the upper 3 m of the canopy, which varied linearly from 0.2 to 1.2 mm h^{-1} for canopy-top wind speeds of 2 to 10 m s^{-1}. From collection on natural and surrogate surfaces, Yosida (1953) reported an overall average rate of 0.5 mm h^{-1} for fogwater capture by the forest canopy. Fog-induced water flux deposition can vary greatly, even tree-to-tree (e.g. Oberlander, 1956). For sparsely forested areas and chaparral, the average would be expected to be lower. Dollard et al. (1983) estimated a mean cloud drop flux of 0.07 mm h^{-1} to shortgrass by eddy turbulence and sedimentation in fog, based on micrometeorological techniques.

Direct measurement of this deposition was not made during this study. Instead, we assumed a water deposition rate of 0.2 mm h^{-1} to calculate

approximate values of fog-induced fluxes for cloudwater with the measured composition. Henninger Flats has a relatively dense, tall canopy. Canopy-top data were not measured. The LWC at canopy-top would be somewhat higher than at the ground (Lovett, 1984); aqueous concentrations would be commensurately lower at elevated locations. In the nursery, winds were generally <1 m s^{-1}; wind speeds measured just downslope of the site were $\sim$1–2 m s^{-1}, hence a conservative water deposition rate was used. Using the above rate (0.2 mm h^{-1}) with the median [H$^+$] of 1150 μeq l^{-1} gave an average rate equal to 230 μeq m^{-2} h^{-1}. Also using the median values for 1982 and 1983 data, nitrate and sulfate deposition rates were calculated to be 300 and 170 μeq m^{-2} h^{-1}, respectively.

3.3.4. *Comparison of pollutant wet deposition pathways.* It is difficult to generalize about the frequency and duration of cloud interception within the Los Angeles basin. It is subject to spatial and temporal variability as well as year-to-year fluctuation. The presence of marine layer clouds and fog are persistent phenomena in coastal southern California, especially during spring and summer (Keith, 1980). From a daily record kept by rangers at Henninger Flats (Los Angeles County Fire Department, Forestry Bureau, unpublished meteorological records, 1983), the median number of times dense fog was observed at 8 a.m. was 30 per year (range = 8 to 55) and 12 during the May/June period for 1970–83. However, clouds are as often observed to intercept the mountain slope less than several hundred meters above or below the site. Further, clearing prior to the morning observation often occurs. Hence, at an inland location, the Henninger Flats observations are likely a conservative estimate of the frequency that low-lying clouds intercept coastal mountain slopes in the Los Angeles area. Both 1982 and 1983 were above normal for fog, with 31 and 18 morning observations of fog during each May/June period, respectively. During our two years of monitoring, over 120 fog-hours were sampled on 23 days or approximately 5 hours per event.

Assuming deposition rates as in the previous section with 150 hours of cloud interception per year (i.e., 30 events times an average of 5 hours per event), the product gave an annual total of 35 meq H$^+$ m^{-2}. Similar calculations for NH_4^+, NO_3^-, and SO_4^{2-} yield 17, 45, and 24 meq m^{-2}, respectively; for lead, 8 mg m^{-2} deposition annually is calculated. Though the preceding calculations are based on limited data and rough estimates, they are intended to demonstrate the order of magnitude that cloud droplet processes may contribute to the acidic deposition in this urban-impacted mountain environment. Comparing these with measured precipitation (Table 3), cloud interception could deliver up to half the total wet deposition. At coastal sites with less rainfall and greater fog frequency, the effect could be greater.

4. Cloudwater interactions with foliar surfaces

Part of our motivation to sample cloudwater at Henninger Flats was the observation in the spring 1982 of an unseasonably high number of pine trees, especially Monterey-Knobcone (*Pinus radiata* × *attenuata* hybrid) which exhibited necrotic needles (M. Gubrud, Senior Deputy Ranger, Los Angeles Fire Department, Forestry Bureau, private communication, 1982). Normally, needle necrosis is observed in the late summer and early autumn, due to the high oxidant levels in the Los Angeles basin (Richards et al., 1968).

4.1. *Measurements*

To better understand the nature of its interaction with plant tissue, cloudwater was removed from pine needles where it had naturally deposited during several fog events. These samples were aggregated from several hundreds of individual drops (d = 1 to 2 mm) taken from the lower reaches ($\sim$1.5 m) of a variety of individual pine trees. All the pine needles from which samples were removed showed some degree of browning at the tips where the cloudwater had collected, but were otherwise green and healthy. In general, these samples were found to be as acidic though often more concentrated than the suspended cloudwater. In Fig. 8, the equivalent ratio of major ions to sulfate are presented for tree drop samples and for cloudwater samples collected simultaneously. The measured concentrations can be derived from comparing the ratio with the [SO_4^{2-}] given in the figure. Nitrate was 2 or more times greater than sulfate for these samples. The highest ionic con-

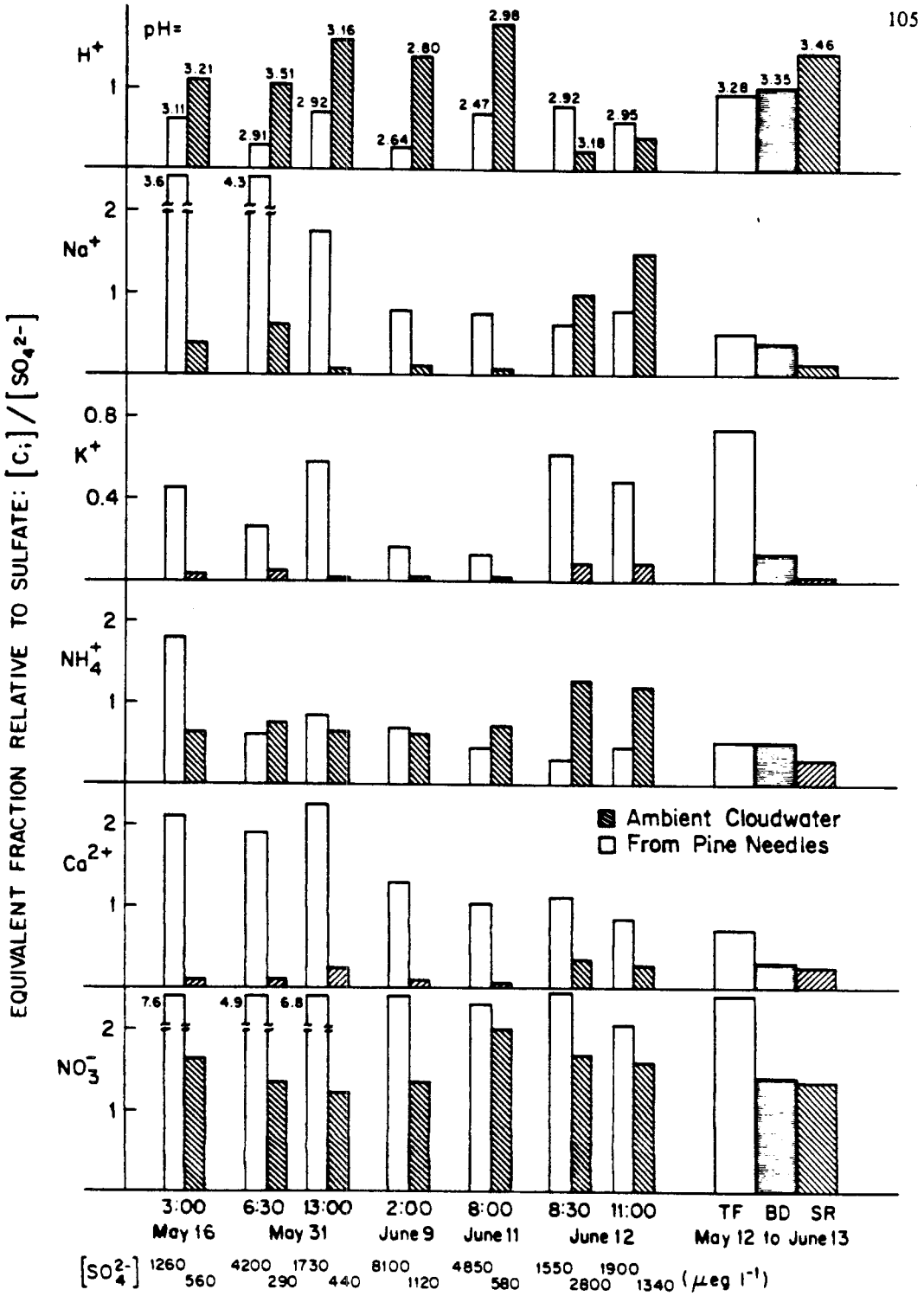

Fig. 8. Equivalent fractions of ionic species relative to sulfate in cloudwater removed from pine needles (open) and ambient cloudwater (shaded) collected simultaneously in 1983. TF is throughfall; BD is bulk deposition; and SR is stratus rainwater (see Table 4).

centrations were found for intervals preceeded by dry periods (e.g., May 16 and May 31). Samples for intervals following rainfall or a long duration of fog had concentrations generally lower compared to the earlier samples. The fractions of Na^+, K^+, Ca^{2+}, and Mg^{2+} in the fog drops were much higher than in any of the fogwater samples.

4.2. *Discussion*

Leaching of internal leaf tissue cations, especially K^+, by aqueous proton could explain their enhanced ratios. Scherbatskoy and Klein (1983) reported leaching of K^+, Ca^{2+}, and amino acids for birch and spruce foliage exposed to acidic (pH = 4.3 and 2.8) mists. They also suggested that the increase in leachate pH compared to the applied mists involved cation exchange process. Hoffman et al. (1980) indicated that proton exchange with cations was negligible as rain (pH ~4) penetrated chestnut canopies, for the total acidity of rainwater was conserved during throughfall, with weak acids exchanging for strong acids. This may be the case for moderate acidity, but at higher $[H^+]$ specific leaf injury could occur, accompanied or, more likely, caused by proton exchange. Cronan and Reiner (1983) also reported enhancement of basic cations in coniferous and hardwood throughfall with concurrent neutralization of precipitation (pH = 4.1). They proposed both proton exchange and Bronsted base leaching in the canopy as important processes. Throughfall measured during stratus rainfall (see Fig. 8) demonstrated similar enhancement of basic cations, however, with nitrate and acidity enhanced as well. The release of accumulated dry-deposited acidic aerosol and nitric acid was likely important.

Without further research, it is not possible to confirm a direct relationship between acidic cloudwater and needle symptoms observed at Henninger Flats. However, similar damage to leaf surfaces has been reported in exposure studies. In simulated acid rain experiments, Haines et al. (1980) found a threshold of leaf damage for most species tested in a pH range 2.5 to 2.0 and for *Pinus strobus* needles at pH 1.0 to 0.5. Wood and Bormann (1974) observed foliar tissue damage at pH 3 for misting of yellow birch seedlings; significant growth decreases occurred when acidic exposure (pH 2.3) was initiated during the germination stage. Thomas et al. (1952) reported cases in which plant injury was not initially caused by concentrated H_2SO_4 aerosol—apparently due to its high surface tension—but followed surface wetting by fog.

Cloudwater capture may represent a more severe threat to plant tissue than deposition accompanying rainfall or by dry particle deposition alone, because it subjects plant surfaces to much higher aqueous concentrations and acidities. Dry deposition of pollutant gases (e.g., SO_2) can also lead to acidic solutions, however, these affecting internal tissue (Hallgren, 1978). Leaf surface wetting may be a critical component of the interaction between foliar membranes and deposited pollutants. This potential has been raised by Lindburg et al. (1982) with respect to the wetting of metal particles they monitored on dry leaf surfaces. Furthermore, surface wetting greatly reduces particle rebound (Chamberlain, 1967) and enhances SO_2 uptake by pine needles (Garland and Branson, 1977).

5. Summary

Highly concentrated, acidic stratus cloudwater was monitored as it intercepted a Los Angeles pine forest. Observed pH values ranged from 2.06 to 3.87 for samples (n = 128) collected on 8 days in June 1982 and 15 days in May/June 1983. The median value was below pH 3 for both seasons' data. The ratio of nitrate/sulfate in cloudwater samples was between 1.5 and 2; rainwater at the same site had a ratio of approximately 1. About half of the nitrate and sulfate measured in the cloudwater was not neutralized. The solute mass per cubic meter of air in the cloudwater was of the same magnitude as for aerosol samples collected before, during and after fog episodes. The nitrate/sulfate ratio of the dry aerosol was lower than in the cloudwater; the additional nitrate is believed to be derived from dissolution of gaseous nitric acid by cloud droplets. Overall, a higher fraction of precursor nitrate (aerosol and gaseous) than sulfate aerosol appears to be scavenged by the cloud droplets.

Wet deposition at Henninger Flats in 1982–83 was comparable to the value for Pasadena in 1978–79, even though the water flux was more than twice as great. The greater frequency and rainfall amount per storm in the recent year is believed to have led to the lower volume-weighted

mean concentrations in the Henninger Flats precipitation. The solute deposition with several light, spring rains (summing to ~1% of annual rainfall) was a disproportionate fraction of the annual total: H^+, NO_3^-, and SO_4^{2-} were ~20% or more.

Based on a reasonable estimate of fog precipitation, deposition of sulfate, nitrate and free acidity due to intercepted stratus clouds may be of comparable magnitude as that due to the incident rainfall at Henninger Flats. Fog and stratus precipitation, though not previously considered on the regional scale, appears to be a seasonally important vector for pollutant deposition in the Los Angeles basin.

Cloudwater that had deposited on local pine needles was collected and found to be in general more concentrated and with acidity comparable to suspended cloudwater. Enhancement of cations, especially K^+, is believed to be due to leaching from foliar surfaces. Enhancement was also found in throughfall samples collected during stratus rainfall. Injury to sensitive plant tissue has been reported in the literature by exposure to similarly acidic solutions.

6. Acknowledgements

We are grateful to the Los Angeles Fire Department Forestry Bureau for allowing us to conduct our field monitoring at Henninger Flats and to the Rangers at the site for their assistance. This research has been supported by a contract with the California Air Resources Board (Contract No. A2-048-32), with additional support from the Coordinating Research Council.

REFERENCES

Appel, B. R., Kothny, E. L., Hoffer, E. M., Hidy, G. M. and Wesolowski, J. J. 1978. Sulfate and nitrate data from the California Aerosol Characterization Experiment (ACHEX). *Environ. Sci. Tech. 12*, 418–425.

Appel, B. R., Wall, S. M., Tokiwa, Y. and Haik, M. 1979. Interference effects in sampling particulate nitrate in ambient air. *Atmos. Environ. 13*, 319–325.

Azevedo, J. and Morgan, D. L. 1974. Fog precipitation in coastal California forests. *Ecology 55*, 1135–1141.

Bassett, M. E. and Seinfeld, J. H. 1984. Atmospheric equilibrium model for sulfate and nitrate aerosols—II. Particle size analysis. *Atmos. Environ. 18*, 1163–1170.

Brewer, R. L., Ellis, E. C., Gordon, R. J. and Shepard, L. S. 1983. Chemistry of mist and fog from the Los Angeles urban area. *Atmos. Environ. 17*, 2267–2271.

California Air Resources Board 1982. *Emission Inventory: 1979*. Emission Inventory Branch, Sacramento, CA.

California Air Resources Board 1979. *Emission Inventory: 1974*. Emission Inventory Branch, Sacramento, CA.

Chamberlain, A. C. 1967. Transport of *Lycopodium* spores and other small particles to rough surfaces. *Proc. Roy. Soc. 296A*, 45–70.

Cronan, C. S. and Reiners, W. A. 1983. Canopy processing of acidic precipitation by coniferous and hardwood forests in New England. *Oecologia 59*, 261–223.

Dasch, J. M. 1983. A comparison of surrogate surfaces for dry deposition collection. In *Precipitation scavenging, dry deposition, and resuspension* (ed. H. R. Pruppacher et al.). Amsterdam: Elsevier Science, 883–902.

Daum, P. H., Schwartz, S. E. and Newman, L. 1984. Acidic and related constituents in liquid water stratiform clouds. *J. Geophys. Res. 89D*, 1447–1458.

Dollard, G. J., Unsworth, M. H. and Harve, M. J. 1983. Pollutant transfer in upland regions by occult precipitation. *Nature 302*, 241–243.

Dolske, D. A. and Gatz, D. F. 1984. A field intercomparison of sulfate dry deposition monitoring and measurement methods. In *Deposition both wet and dry* (ed. B. B. Hicks). Boston: Buttonworth Publisher, 121–132.

Ekern, P. C. 1964. Direct interception of cloud water on Lanaihale, Hawaii. *Soil Sci. Soc. Am. Proc. 28*, 419–421.

Evans, L. S. 1982. Biological effects of acidity in precipitation on vegetation: a review. *Environ. Exp. Bot. 22*, 155–169.

Garland, J. A. and Branson, J. R. 1977. The deposition of sulfur dioxide to pine forest assessed by a radioactive tracer method. *Tellus 28*, 445–454.

Haines, B., Stefani, M. and Hendrix, F. 1980. Acid rain: threshold of leaf damage in eight plant species from a southern Appalachian forest succession. *Water, Air and Soil Pollut. 14*, 403–407.

Hallgren, J. 1978. Physiological and biochemical effects of sulfur dioxide on plant. In *Sulfur in the environment Part II* (ed. J. O. Nriagu). New York: J. Wiley & Sons, 163–209.

Hering, S. V. and Blumenthal, D. L. 1984. Fog Sampler Intercomparison Study Final Report (Draft). Project No. STI 11 90063. Available from Coordinating Research Council, 219 Perimeter Center Pkwy, Atlanta, GA.

Hoffman, Jr., W. A., Lindberg, S. E. and Turner, R. R. 1980. Precipitation acidity: the role of forest canopy in acid exchange. *J. Environ. Qual. 9*, 95–100.

Hori, T. (ed.) 1953. *Studies on fog in relation to fog-preventing forest.* Sapporo/Japan: Tanne Trading Co., 399 pp.

Hudson, J. G. and Rogers, C. F. 1984. Interstitial CCN measurements related to mixing in clouds. Proceedings of 9th Intern. Cloud Physics Conference August 21–28, Tallinn, USSR.

Jacob, D. J. and Hoffmann, M. R. 1983. A dynamic model for the production of H^+, NO_3^-, and SO_4^{2-} in urban fog. *J. Geophys Res. 88C*, 6611–6621.

Jacob, D. J., Waldman, J. M., Munger, J. W. and Hoffmann, M. R. 1984a. A field investigation of physical and chemical mechanisms affecting pollutant concentrations in fog droplets. *Tellus 36B*, 272–285.

Jacob, D. J., Wang, R.-F. T and Flagan, R. C. 1984b. Fogwater collector design and characterization. *Environ. Sci. & Technol. 18*, 827–833.

Katz, U. 1980. A droplet impactor to collect liquid water from laboratory clouds for chemical analysis. In *Communications a la VIII conference internationale sur la physique des nuages* (July 15–19), Clermont-Ferrand/France, 697–700.

Keith, R. W. 1980. *A climatological/air quality profile: California south coast air basin.* South Coast Air Quality Management District, El Monte, CA.

Kerfoot, O. 1968. Mist precipitation on vegetation. *For Abst.* 29, 8–20.

Liljestrand, H. M. 1980. *Atmospheric Transport of Acidity in Southern California by Wet and Dry Mechanisms.* Ph.D. Thesis, California Institute of Technology, Pasadena, CA.

Liljestrand, H. M. and Morgan, J. J. 1981. Spatial variations of acid precipitation in Southern California. *Environ. Sci. & Technol. 15*, 333–338.

Lindberg, S. E., Harriss, R. C. and Turner, R. R. 1982. Atmospheric deposition of metals to forest vegetation. *Science 215*, 1609–1611.

Lovett, G. M. 1984. Rates and mechanisms of cloud water deposition to a subalpine balsam fir forest. *Atmos. Environ. 18*, 361–371.

Morgan, J. J. and Liljestrand, H. M. 1980. *Measurement and Interpretation of Acid Rainfall in the Los Angeles Basin.* W. M. Keck Laboratory Report AC-2-80. California Institute of Technology, Pasadena, CA.

Mrose, H. 1966. Measurements of pH, and chemical analyses of rain-, snow- and fog-water. *Tellus 18*, 266–270.

Munger, J. W., Jacob, D. J., Waldman, J. M. and Hoffmann, M. R. 1983a Fogwater chemistry in an urban atmosphere. *J. Geophys. Res. 88C*, 5109–5121.

Munger, J. W., Waldman, J. M., Jacob, D. J. and Hoffmann, M. R. 1983b. Vertical variability and short-term temporal trends in precipitation chemistry. In *Precipitation scavenging, dry deposition, and resuspension* (ed. H. R. Pruppacher et al.). Amsterdam: Elsevier Science, 275–282.

Munger, J. W., Jacob, D. J. and Hoffmann, M. R. 1984. The occurrence of bisulfite-aldehyde addition products in fog- and cloudwater. *J. Atmos. Chem. 2*, 335–350.

Nagel, J. F. 1956. Fog precipitation on Table Mountain. *Q. J. R. Meteorol. Soc. 82*, 452–460.

Oberlander, G. T. 1956. Summer fog precipitation on the San Francisco penninsula. *Ecology 37*, 851–852.

Okita, T. 1968. Concentration of sulfate and other inorganic materials in fog and cloud water and in aerosol. *J. Meteorol. Soc. Japan 46*, 120–126.

Pruppacher, H. R. and Klett, J. D. 1978. *Microphysics of clouds and precipitation.* Amsterdam: D. Reidel, 714 pp.

Richards, Sr., B. L., Taylor, O. C. and Edmunds, Jr., G. F. 1968. Ozone needle mottle of pine in southern California. *J. Air Pollut. Control Assoc. 18*, 73–77.

Russell, A. G., McRae, G. J. and Cass, G. R. 1983. Mathematical modeling of the formation and transport of ammonium nitrate aerosol. *Atmos. Environ. 17* 949–964.

Scherbatskoy, T. and Klein, R. M. 1983. Response of spruce and birch foliage to leaching by acidic mists. *J. Environ. Qual 12*, 189–195.

Schlesinger, W. H. and Reiners, W. A. 1974. Deposition of water and cations on artificial foliar collectors in fir krummholz of New England mountains. *Ecology 55*, 378–386.

Sehmel, G. A. 1980. Particle and gas dry deposition: a review. *Atmos. Environ. 14*, 983–1011.

Spicer, C. W., Howes, J. E., Bishop, T. A. and Arnold, L. H. 1982. Nitric acid measurement methods: an intercomparison. *Atmos. Environ. 16*, 1487–1500.

Stelson, A. W. and Seinfeld, J. H. 1982. Relative humidity and temperature dependence of the ammonium nitrate dissociation constant. *Atmos. Environ, 16*. 983–992.

Thomas, M. D., Hendricks, R. H. and Hill, G. R. 1952. Some impurities in the air and their effects on plants. In *Air Pollution: Proc. of US Tech. Conf.* (ed. L. McCabe). New York: McGraw-Hill, 41–47.

Tukey, Jr., H. B. 1970. The leaching of substances from plants. *Ann. Rev. Plant. Physiol. 71*, 305–324.

Waldman, J. M. 1985. *Contributions of Fog and Dew to the Depositional Flux of Acidity.* Ph.D. Thesis, California Institute of Technology, Pasadena, CA.

Vogelmann, H. W. 1973. Fog precipitation in the cloud forests of eastern Mexico. *Bioscience 23*, 96–100.

Vogelmann, H. W., Siccama, T., Leedy, D. and Ovitt, D. C. 1968. Precipitation from fog moisture in the Green Mountains of Vermont. *Ecology 49*, 1205–1207.

Wood, T. and Bormann, F. H. 1974. The effects of an artificial acid mist upon the growth of *Betula alleghaniensis Britt. Environ. Pollut. 7*, 259–267.

Yoshida, Z. 1953. General survey of the studies on fog-preventing forest. In *Studies on fog in relation to fog-preventing forest* (ed. T. Hori). Sapporo Japan: Tanne Trading Co., 1–23.

Chapter 7

DEPOSITION IN RADIATION FOG:

FIELD STUDY IN THE SOUTHERN SAN JOAQUIN VALLEY OF CALIFORNIA

ABSTRACT

A study of atmospheric pollutant behavior was conducted in the southern San Joaquin Valley of California during periods of dense fog and stagnation. Fluxes to the ground of water soluble species were determined by surrogate-surface collectors, and simultaneous fogwater and aerosol composition measurements were made. Repetitive, widespread fogs were observed only when the base of the temperature inversion was 150 to 400 m above the valley floor. Dense fogs (visual range <200 m) lasted 10-17 h at sampling locations. Atmospheric loadings of water soluble species in the aerosol and droplet phases were composed almost entirely of NH_4^+, NO_3^-, and SO_4^{2-}. On occasion, free acidity (H^+) and S(IV) species were also measured at substantial concentrations in fogwater samples. Appreciable gaseous ammonia was often present, but only when atmospheric acidity was absent. Deposition samples were similarly dominated by these major ions, although higher contributions were made by soil dust species.

Deposition rates for major species were 5 to 20 times greater during fogs than during non-foggy periods. Deposition velocities, V_d and $V_{d,fog}$, were calculated by normalizing deposition rates with respect to the measured total and droplet-phase atmospheric loadings in each case. The proportions of deposited solute were closely matched to the fogwater composition (i.e., $V_{d,fog}$ were in close agreement). Fogwater solute deposition was close to the values for droplet sedimentation.

Sulfate deposition rates (V_d) during fog were generally 0.5 to 2 cm s^{-1} with a median value about 1 cm s^{-1}; nitrate rates were often 50% below those for sulfate. The fraction of sulfate scavenged by fog rose

with increasing LWC, while nitrate scavenging was low in non-acidic fogs. For pH < 5, the fraction of fogwater nitrate was increased. Higher atmospheric acidity is believed to have altered N(V) partitioning before fog formation. Nitric acid in the pre-fog air was one factor, but this did not fully account for the observed enhancement of N(V) scavenging. Depletion of gaseous ammonia accompanied higher atmospheric acidity and low pH fog, and this is believed to have caused a reduction in the formation of smaller NH_4NO_3 aerosol. In the absence of detectable $NH_3(g)$, newly-formed N(V), presumably incorporated into a coarser aerosol fraction, was more readily scavenged in fog.

A comparison was made between the mass deposited and the overburden of pollutants (i.e., mixing height x ambient loading). For S(VI) and N(-III) species, 2-3 times the apparent overburden was deposited during prolonged fogs, yet their depletion was not observed. Steady aerosol sulfate concentrations required S(IV) oxidation to proceed rapidly. A pseudo first-order constant for SO_2 oxidation was calculated to be in the range of 2-7% hr^{-1}. The actual rate may be somewhat higher, based on the assumptions of analysis. In similar fashion, ammonia emissions to balance solute removal in fog were calculated to be approximately 1 ppb h^{-1}.

Measurements made during three wintertime fog/aerosol studies were summarized to consider the overall mass balances during stagnation episodes. This data set supported the hypothesis that fog deposition lowered the ambient concentrations of aerosol sulfate and nitrate during stagnation periods, compared to similar periods with no fog. Finally, general observations concerning ammonia release from sources were found to apply to the conditions for which fogwater acidity was observed.

Chapter 7

DEPOSITION IN RADIATION FOG: FIELD STUDY IN THE SOUTHERN SAN JOAQUIN VALLEY

7.1 INTRODUCTION

Deposition during fog episodes can make a significant contribution to the overall flux of pollutants in certain ecosystems. This will be particularly important when high pollutant concentrations are present during fog. Enhancement over dry-only pathways can contribute inordinately to the deposition when, for example, atmospheric stagnation prevents normal ventilation in a region and fog deposition becomes the main route of pollutant removal. Consequently, fogs can exert dominant control over pollutant levels in certain atmospheres. In the past, fogs have been a unifying meteorological feature of the worst stagnation episodes in air pollution history (Environmental Protection Agency, 1971) and may have contributed to observed health effects by its presence (Hoffmann, 1984). Yet, fogs may also mitigate the severity of atmospheric contamination by enhancing removal rates while other pathways are ineffective.

The southern San Joaquin Valley (SJV) of California is a region prone to wintertime episodes of atmospheric stagnation leading to elevated pollutant concentrations and dense, widespread fogs. Major oil-recovery operations (by steam-injection) plus widespread agricultural and livestock feeding activites are important sources of SO_2, NO_x, and NH_3 in the valley. Stagnation in the SJV is caused by a persistent high pressure system which produces subsidence over the valley (Holets and Swanson, 1981). This, in turn, causes a strong

temperature inversion aloft. Mountains east, south, and west of the valley floor rise above the inversion base and suppress transport over the ridges. Advection over the mountains is normally the dominant pathway for pollutant transport out of the basin that results in ventilation of the valley air in 1 to 2 days during nonstagnant conditions (Reible, 1982). The stagnant wintertime condition limits direct exchange of air from aloft or to the neighboring Mohave Desert air basin. Surface wind data show that ventilation from the SJV during stagnation is chiefly due to a flow north, away from the source region (Jacob et al., 1985a). This flow is very weak, and consequently it leads to a marked increase of residence times for pollutant species in the basin. Reible (1982) concluded from a series of tracer studies that the residence time of air parcels in the southern of the valley is 4-12 days under stagnant conditions. Ventilation times of about 5 days were found to be consistent with the temporal trends of pollutant concentrations observed during the 1983-84 winter study (Jacob et al., 1985a).

Both impaction and sedimentation rates rise markedly with particle diameter, and fog formation can thus be expected to increase particle deposition rates considerably. The terminal fall velocity of a 20-25 μm water droplet (typical fog droplet diameter) is 1-2 cm s^{-1}. Sedimentation alone can decrease the characteristic residence time to less than 1 day for fog-scavenged material within the shallow (200 to 400 m) mixed layer.

Fog droplets provide a favorable environment for atmospheric oxidation process because a number of electron-transfer reactions are made possible by the presence of an aqueous phase (Hoffmann and Jacob,

1984). An important mechanism for the atmospheric production of SO_4^{2-} is absorption of $SO_2(g)$ by droplets, followed by the rapid oxidation of S(IV) by aqueous-phase oxidants such as H_2O_2, O_3, and O_2 (catalyzed by certain transition metal ions). These reactions lead to production of strong acidity, e.g.:

$$HSO_3^- + 1/2\ O_2(aq) \xrightarrow{Fe^{3+}\ or\ Mn^{2+}} H^+ + SO_4^{2-}. \qquad (7.1)$$

In addition to causing rapid SO_4^{2-} production, droplet-phase oxidation can lead to an accumulation of sulfate within large aerosol particles (following droplet evaporation) compared to the smaller size fraction produced by gas-phase reactions at low humidites (Hidy et al., 1980).

A multifaceted program of field monitoring in the southern San Joaquin Valley spanned three winters and focused on aspects of pollutant fates and S(IV) oxidation. The emphasis of this chapter is to evaluate the effectiveness of fog in enhancing pollutant removal during the winter 1984-85 study. For discussions of the two previous studies (1982-83 and 1983-84), the reader is referred to the analyses of Jacob et al. (1984 and 1985a). In these earlier field programs, pollutant concentrations were measured in the gas, dry aerosol, and fogwater phases. It was found that aerosol concentrations during stagnation episodes were highest in the absence of fogs and decreased markedly following widespread fogs. This was strong indication for the significance of fog deposition. During the winter of 1984-85, methods to monitor depositional fluxes and pollutant scavenging efficiencies in fog were added to the program. These measurements were designed to directly assess depositional enhancement by fog.

7.2 MEASUREMENT METHODS

Aerosol concentrations were monitored at six sites in the southern SJV (Figure 7.1) from 28 December 1984 to 7 January 1985. At two sites, fogwater and deposition measurements were also made: Bakersfield's Meadows Field Airport and Buttonwillow. Most of the results presented in this chapter are from these locations. Air quality data at the other sites were monitored to determine spatial patterns in the region. After 7 January, measurements were continued at Bakersfield Airport only.

At the Bakersfield Airport, the study instrumentation was located in an open field adjacent to the National Weather Service (NWS) station. This will be referred to as the NW site (Figure 7.2). The airport tower and NWS office are the only nearby buildings. Surrounding area is primarily open cropland. Major oil fields are located 3 km north and east of the NW site (see Figure 7.1b). At the time of the field study, the nearby field had been recently tilled. Buttonwillow sampling was conducted atop the one-story Parks and Recreation Department building in a residential neighborhood (hereafter the BW site). Oil fields on the west side of the valley are 15-20 km upslope (west) of Buttonwillow, and Interstate 5 runs 5 km to the east. The surrounding region is virtually all cropland, unplanted at that time.

Fogwater Composition. Fogwater was sampled by event using rotating-arm-collectors (RAC) with sampling intervals of 1 to 2 hours. Analytical procedures commenced at the sampling sites after each interval with determination of sample pH and preservation of aliquots for later analyses of S(IV), formaldehyde, and trace metals (Fe, Mn, Pb, and Cu). In the laboratory, cations were analyzed by atomic absorption; ammonium ion was determined by indo-phenol blue method; anions were

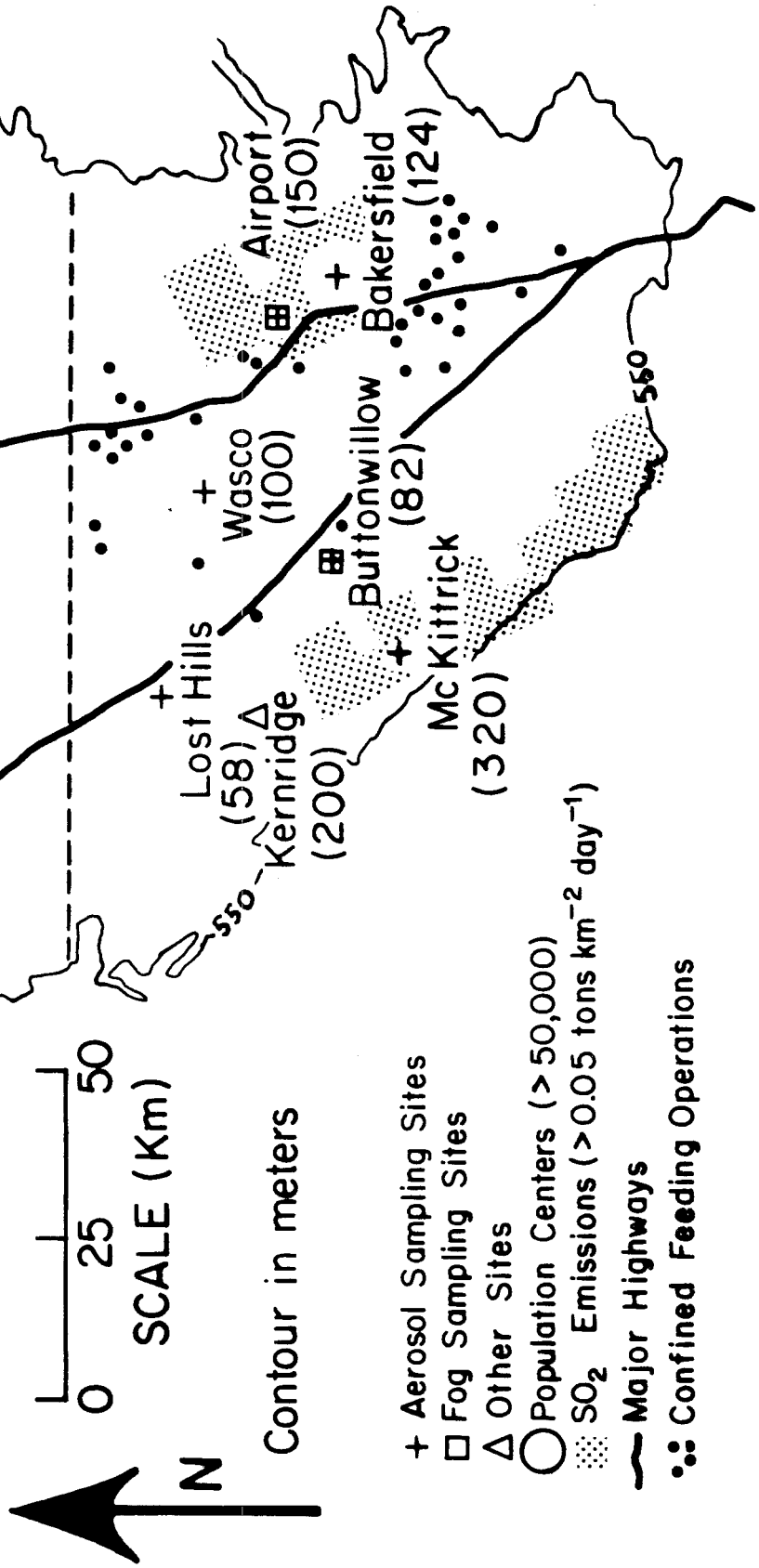

Figure 7.1a Sampling sites in the southern San Joaquin Valley.

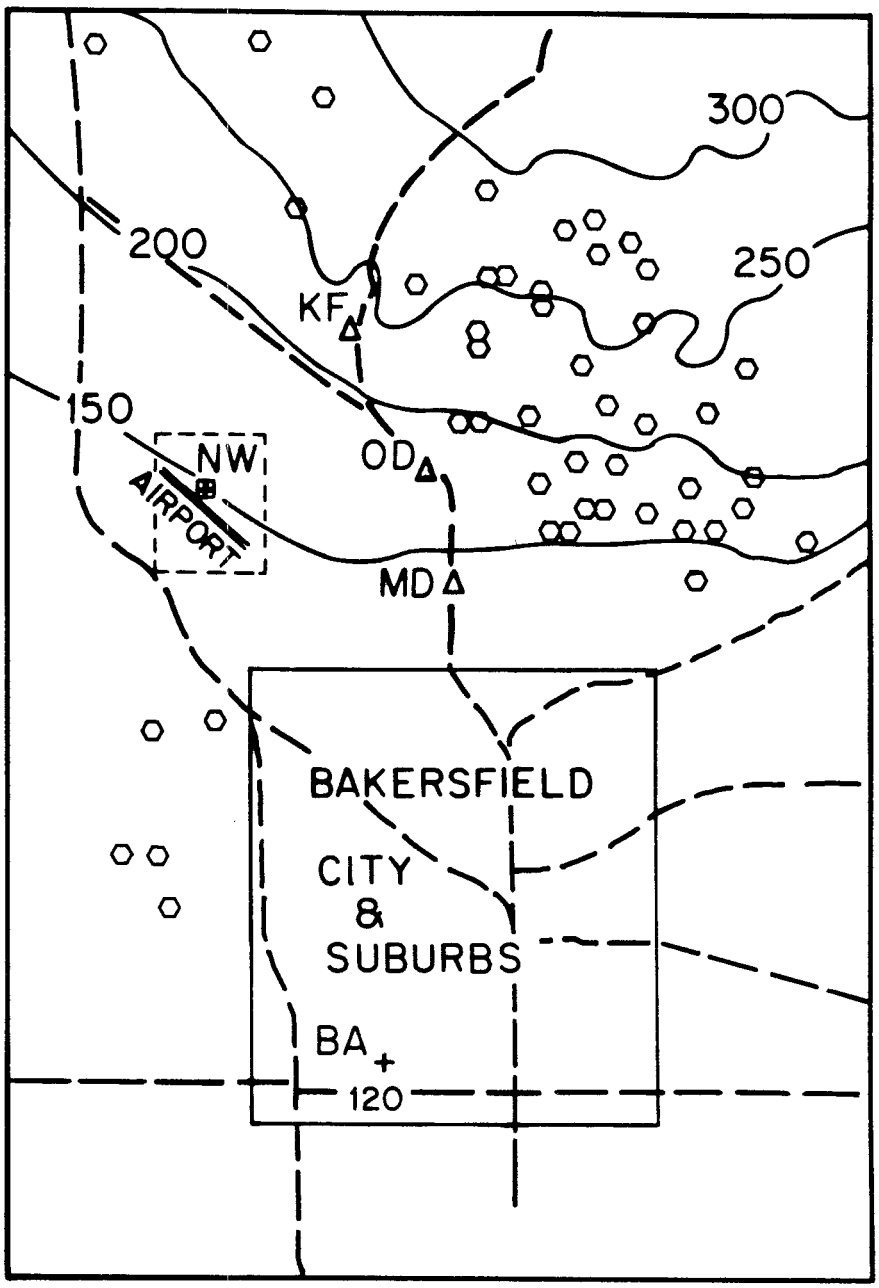

Figure 7.1b Sites in Bakersfield and environs.

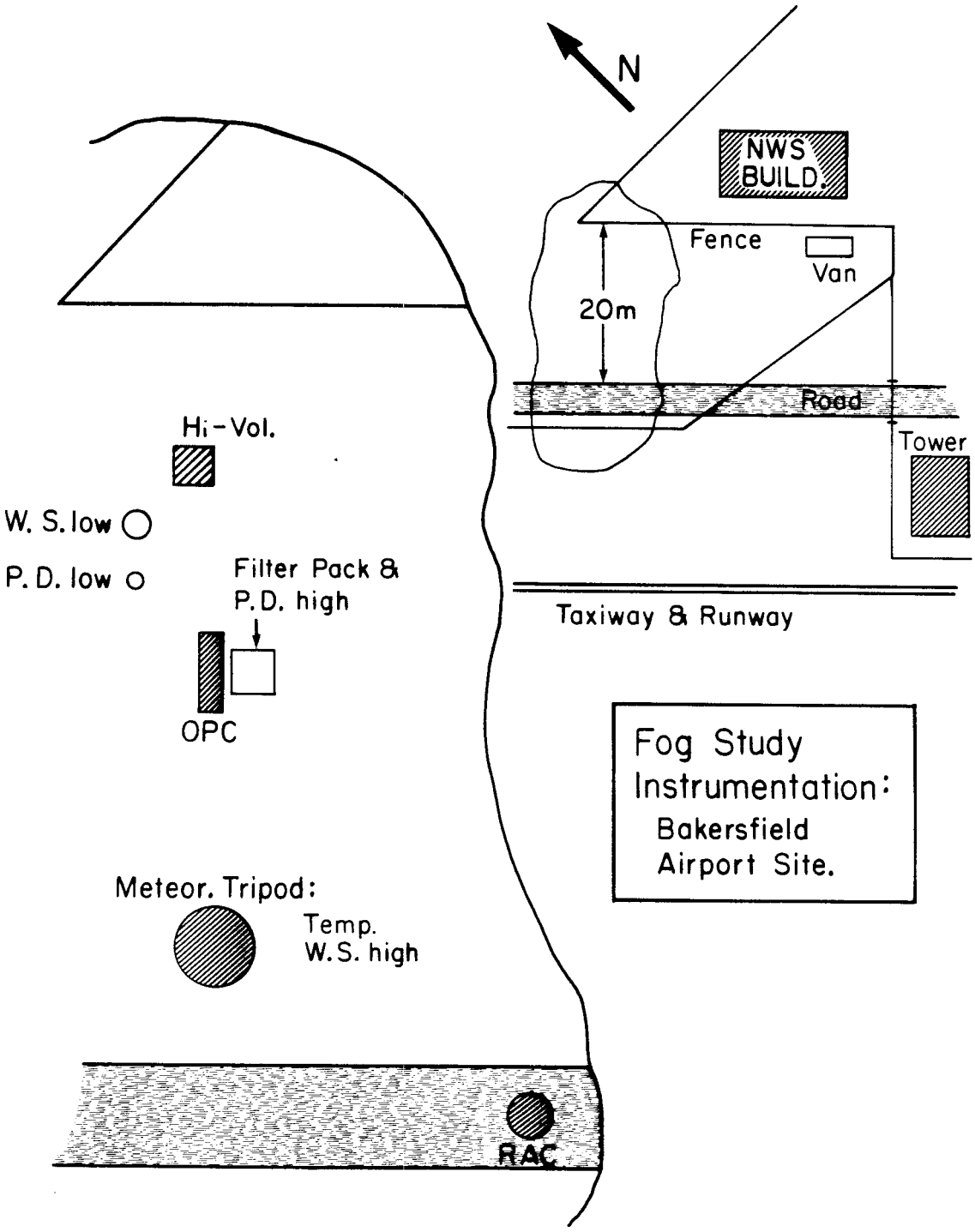

Figure 7.2 Bakersfield Airport (NW) sampling site layout and instrumentation.

measured by ion chromatography (IC). Further details of fog collection and analytical protocols have been described in Chapter 3.

When substantial S(IV) was present in fogwater, its eventual oxidation led to interference with measured sulfate. For this reason, aliquots were spiked with hydrogen peroxide (to 0.05% at pH 8) prior to IC analysis to completely oxidize S(IV) in the sample. This was verified with sulfite and sulfonate standards which gave quantitative recovery of sulfate. The IC analyses therefore gave total soluble sulfur, i.e., S(VI) plus S(IV). Fogwater concentrations of S(IV) in preserved aliquots were then used to calculate in situ concentrations of S(VI).

Liquid water content (LWC) values averaged over the fogwater sampling intervals were calculated from the rate of RAC collection. This method was found to have good reproducibility and gave reasonable agreement with an independent gravimetric method that was also operated at the NW site (see Chapter 5).

Aerosol and Gaseous Concentrations. The atmospheric concentrations of aerosol, nitric acid and ammonia were monitored using dual-filter methods (Russell and Cass, 1984; Jacob et al., 1985a). The filter inlets were $\geq$3 m above the ground at all sites. Total aerosol samples were collected on open-faced Teflon filters (T1 and T2) operated side-by-side (Figure 7.3). Nylon filters (N) and glass-fiber filters impregnated with oxalic acid (OX) collected $HNO_3(g)$ and $NH_3(g)$, respectively. Aerosol samplers were used during fog as well as during dry intervals. The inlet Stokes number was 0.05 for particles with a 50 μm aerodynamic diameter; thus, even very large droplets were collected effectively (Davies and Subari, 1982). Samples at network sites were

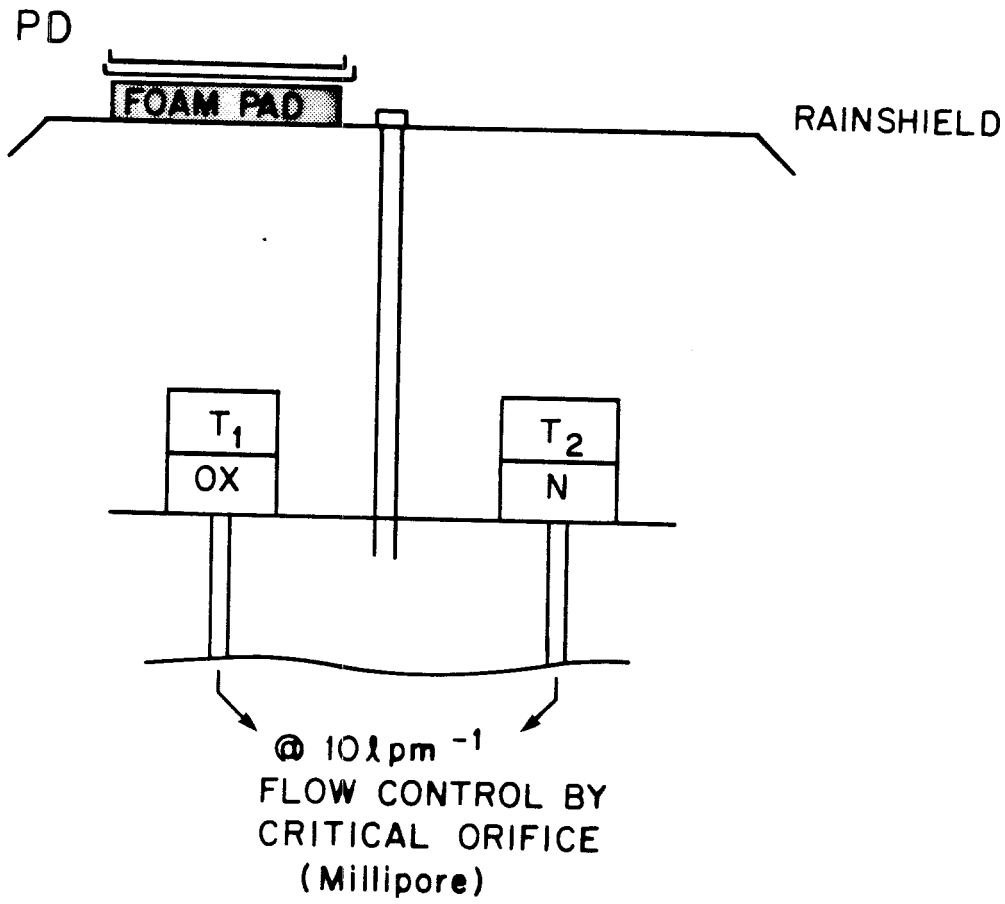

Figure 7.3 Filter pack configuration. Teflon (T_1 and T_2), nylon (N), and oxalic acid impregnated (OX) glass-fiber filters. Petri dish (PD) located on an insulated foam pad.

collected twice daily (0000 to 0400 and 1200 to 1600 PST). At NW and BW sites, samples were collected continuously for 2 to 4 hour periods through fog episodes.

Dry Teflon filters and backup filters were sealed in petri dishes immediately upon collection, put directly into ice chests, and stored for laboratory extraction and analysis. Fog-wetted filters were extracted immediately following the exposure period. This was done to assure that there was no loss of aqueous-phase ammonium or nitrate ions. In the past, when fog-wetted filters were allowed to dry, volatile loss of solute species, such as $NH_3(g)$ or $HNO_3(g)$, were a problem (Jacob et al., 1985b). Filter extractions were done in screw-top polypropylene beakers with 10 mL deionized-distilled water. The solutions were refrigerated and stored in the beakers until laboratory analyses.

Water soluble ions were analyzed in filter extracts in a similar fashion to the fogwater samples. The ammonium determinations for oxalic acid filter extractions were done with a modification of the indo-phenol method (Russell, 1983). As stated above, it was not possible to unambiguously determine the oxidation state of sulfur in an unpreserved sample. The fraction of S(IV) in dry aerosol samples was minor; however, since they can be present in fog droplets, those filter samples collected in fog could also contain appreciable S(IV). Immediate preservation of S(IV) for filter extractions in the field environment was not done. Therefore, we report total soluble S as SO_4^{2-} for all samples.

The uncertainties in determinations were calculated at 15% for NO_3^- and SO_4^{2-} and 22% for NH_4^+ aerosol concentrations, based on the side-by-side filter results for over 100 sets. These results are

comparable to those reported by Russell and Cass (1984) and Jacob et al. (1985a) for similar measurements. For filter samples collected in the 1983-84 SJV field study, Jacob et al. (1985a) showed that approximately 75% of this error was due to uncertainties in the amount of analyte collected and recovered for individual filters (e.g., differences in air flow through the filter or extraction efficiency). Hence, errors in species concentrations were strongly correlated for individual samples.

Gaseous SO_2 and NO_x monitors were operated at NW and BW sites by the California Air Resources Board (CARB) during the 1984/1985 study period. These data were supplemented by monitors operated at nearby CARB stations in the Bakersfield area (downtown [BA] and Oildale [OD]), Texaco-Bakersfield District sites near the airport (Kern Front [KF] and Manor [MD]), and Kern County Westside Operators stations (Kernridge, Lost Hills, and McKittrick). Detection limits were given at 10 and 5 ppb for CARB and oil producers' monitors, respectively. See Figure 7.1 for locations.

Deposition to Surrogate Surfaces. Two different collector surfaces were deployed to monitor fog and dry particle deposition: (i) petri dishes (154 cm^2 x 1.2 cm) made of polystyrene with the lip upwards, and (ii) polyethylene buckets (556 cm^2 x 32 cm). Petri dishes (PD) were placed on top of insulating foam to mitigate the thermal effects of its placement (see Figure 7.3). Deposition samples were collected continuously at BW and NW sites over the study interval. During a period of rainfall (6-8 January), wet fluxes were also monitored at Lost Hills and McKittrick. One bucket and two PD collectors (3.0 m and 0.2 m above ground) were continuously exposed at the NW site. At BW, one of each collector type was placed at the same

level as the filter sampler. Buckets were exchanged once per day, and PD were exchanged twice per day during nonfoggy periods. During fog collection, PD samples were collected for shorter intervals (2-4 hr duration), concurrent to filter sampling intervals.

Both collectors were extracted with distilled, de-ionized water immediately following the end of ambient exposure. This was done with premeasured volumes of 140 mL for buckets and 10 mL for PD's. In cases of fog and dew, the extractions were performed while the surfaces were still wet with accumulated liquid. The inside walls of the buckets were rinsed by carefully rotating the bucket. The PD were extracted with lids in place, using gentle motion to rinse the entire inside surface. Subsequent extractions indicated that complete recovery (i.e., >90%) was achieved. Rinsed buckets were put back outside after extraction; new PD's used for each interval. Replicate PD samples were in good agreement (see results section). The same issue regarding in situ sulfur oxidation states holds for deposition collector extracts. Deposition of total S is reported as SO_4^{2-}.

The use of open containers, flat plates, petri dishes, and other surrogate surfaces remains controversial due to the uncertainty in extrapolating these results to natural surfaces, especially regarding deposition of gases or submicron aerosol (Dolske and Gatz, 1985). Significant variability between different surrogate surfaces has been found in side-by-side comparison under dry conditions (Dolske and Gatz, 1985; Vanderberg and Knoerr, 1985).

The conditions in the SJV fog/aerosol study allowed us to make simplifying assumptions regarding the dominant deposition processes. The relative contributions of sedimentation, impaction, and turbulent

transport in fog depend on the nature of deposition surfaces and on the canopy-level winds. Winds in the SJV under stagnant conditions are usually quite light. Furthermore, the valley is uniformly flat, and over 85% of the surface cover is open cropland or rangeland (Jacob, 1985). There is minimal canopy structure, especially during wintertime. On a regional scale, the terrain is relatively sparse and rather inefficient for impaction. We therefore expect that sedimentation would be the main pathway for fog droplet deposition (see Chapter 2.3), and an open collector would reliably monitor that rate.

The concern that dry deposition of reactive gases may bias measurements of particle fluxes must also be addressed. The direct fumigation of plastic collector materials with SO_2 and NO_x has been found to result in negligible sulfate or nitrate deposition (Dasch, 1983). However, gases can react with particulate materials that have accumulated at the inert surface. Vanderberg and Knoerr (1985) measured deposition to various surfaces including polystyrene petri dishes, polyethylene buckets, cellulose-glass fiber filters. The exposure intervals ranged from 1 to 6 days and allowed substantial material accumulation. An enhancement was found for SO_4^{2-} deposition rates measured to the cellulose-glass surface which had significant correlation with $SO_2(g)$ concentrations measured at the site. It can be reasoned that extrinsic sulfate formation was promoted at alkaline glass fiber reaction sites (Axelrod et al., 1971). Sulfate deposition to petri dish and bucket surfaces showed no such correlated enhancement.

Nitric acid deposition velocities of 1-4 cm s^{-1} have been measured over tall grass, and turbulent transport (vis-à-vis resistance within the surface layer) was determined to control its removal rate (Huebert

and Robert, 1985). However, the level of turbulence measured at Huebert and Robert's site was far greater than for SJV sites. Furthermore, concentrations for $HNO_3(g)$ were extremely low during the SJV study (<0.2 ppb), so its potential contribution to measured N(V) deposition was of minor importance. Also, deposition of nitrogen species from NO_x fluxes to wetted surfaces would be negligible because of the low solubility and slow aqueous-oxidation kinetics leading to NO_3^- (Lee and Schwartz, 1981; Jacob and Hoffmann, 1983).

Appreciable $NH_3(g)$ was measured at sampling sites, and ammonia can react readily with acidic surfaces. During dry intervals, we found N(-III) deposition rates were low, even during periods of high ambient $NH_3(g)$ concentrations, and we believe that these were due to particle flux alone. However, water films from fog and dew on the collector surfaces can provide sinks for the dissolution of NH_3 and SO_2. Solution composition (e.g., pH and alkalinity) are important factors in determining gas-aqueous equilibrium (see Chapter 2.2). Further discussion of this issue is presented in the results section of this chapter.

Meteorological Parameters. Profiles for temperature, relative humidity (RH) and winds aloft were measured with a tethersonde operated at Buttonwillow on 28-30 December and 3-6 January. Continuous measurements of mixing heights were available from an acoustic radar operated at Kernridge after 11 January (Kern County Westside Operators). Pilot observations of cloud tops near Bakersfield airport were recorded to verify that mixing heights were similar on both sides of the valley. Instrumentation deployed at the Bakersfield Airport site continuously recorded temperature and wind speeds near the ground layer (Figure 7.2).

Hourly observations were also available from NWS sensors (10 m AGL) adjacent to the site.

The entire area was open except for the nearby fences and two buildings. The wind fetches were over homogeneous surfaces for >1 km in almost all compass directions. Wind speeds at two heights (3.65 and 0.85 m) were measured with cup anemometers during the sampling program. These data were used to determine the scale of wind turbulence and to observe changes in this scale accompanying fog. Wind profiles closer to the ground were checked with a pair of flow-through wind meters (Air Meter Model 2411, Weathertronics, Inc. Sacramento, CA). One meter was positioned at 0.85 m, and the other was lowered incrementally. The wind profiles were calculated using wind speed ratios between similar instruments.

As a simple model for momentum exchange between the air and the ground, a logarithmic wind profile can be assumed to hold for thermally neutral conditions (Thom, 1975):

$$U(z) = \frac{U^*}{k} \ln\left(\frac{z}{z_o}\right) \qquad (6.2)$$

where U(z) is the wind speed at height z; k is von Karman's constant (0.4); U* and z_o are the friction velocity and roughness height, respectively, which serve to parameterize momentum transfer near the ground. In cases where an appreciable canopy structure exists, a displacement height, d, is necessary to scale the profile above the canopy layer, and z is replaced by (z-d). An unobstructed upwind fetch is required for representative wind measurements.

Figure 7.4 shows the wind profiles measured on two occasions for

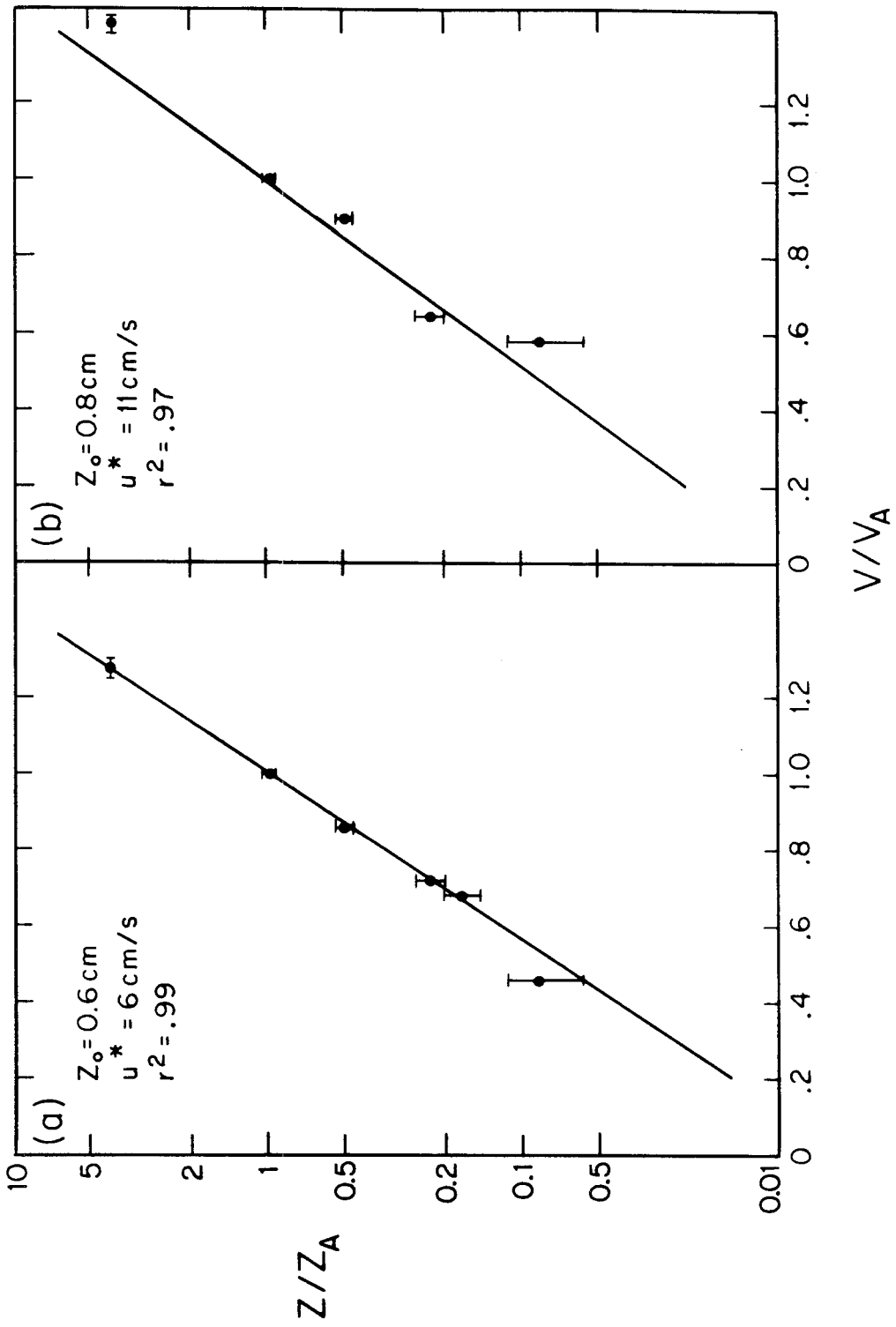

Figure 7.4 Wind profiles at NW site for two wind directions: (a) across open field (north); (b) across runway (southwest).

different wind directions: (a) north -- across the open field; and, (b) southwest -- across the runway, a fence, and roadway berm. Although an unobstructed fetch was not observed in the latter case, only a slight disturbance of the wind profile by the physical barriers can be seen. The roughness heights calculated in Figure 7.4 were <1 cm. Wind speeds (2.85 m level) were mostly below 2 m s^{-1}, and friction velocities were indeed consistently low (U*<20 cm s^{-1}).

7.3 RESULTS

7.3.1 Meteorological Summaries

The winter 1984-85 was characterized by restricted ventilation in the southern SJV. A cap on mixing heights was effectively maintained by a temperature inversion aloft which persisted for virtually the entire months of December 1984 and January 1985. The inversion-layer base was generally located between 200 and 800 m above the valley floor; dense and widespread fog was observed only when it was no more than 400 m above ground level (AGL). Although afternoon clearing was occasionally observed, there was no concurrent breakup of the temperature inversion throughout the intervals when repetitive, nighttime fog occurred. Weather patterns during the study are summarized in Table 7.1.

Locally dense fog was monitored at Bakersfield Airport on the morning 28 December when the temperature-inversion base was 200 m AGL. Thereafter in December, the mixed layer started to deepen, and fog was absent. Figure 7.5a-d shows temperature and RH aloft measured at Buttonwillow for late December soundings. By 29 December, the inversion base was $\geq$500 m AGL indicated by cloud tops observed within the valley perimeter. From noon 30 December through 1 January, cloud tops were 1000 m AGL or greater.

From 2 to 5 January, dense fog was widespread, starting each evening shortly after sunset and lasting until approximately 1000 local time. Soundings made from 3-6 January (Figure 7.5e-l) documented a pronounced temperature-inversion layer and the presence of warm, dry air overriding the cool, moist air. The shallow mixed layer was essentially isothermal and uniform RH. When fog formed, RH $\cong$ 100% was observed from the ground to the base of the inversion layer (e,g,h). The

Table 7.1

METEOROLOGICAL SUMMARY
SAN JOAQUIN VALLEY AEROSOL/FOG STUDY

December 1984 - January 1985

Dates	Observations	Mixing Heights (m @ NWS)
	***** NETWORK SAMPLING INTERVALS *****	
28 December	- FOG after MN, lifted to low clouds before sunrise; brief ground FOG after sunrise.	200
28-31 December	- Heavy overcast with no afternoon clearing. - Ceilings 700-800 m AGL after 28th. - Average T 8°C; daily max/min ±1-2 C. - Wind speeds 1-3 m/s; RH 70-90%.	500 to >1000
1-5 January	- Clearing in the afternoons with unlimited ceilings. - Dense, widespread FOG forming 2000 PST at NW and 1700 at BW (1-4th) then lasting until 1000. - Max T 10-13°C; min T -1-3°C. - Wind speeds: day 4-5 m/s; night <2 m/s. - High cloudiness starting on the afternoon of the 5th.	200 to 300
6-8 January	- Continuing high clouds leading to light rain and drizzle.	cloud tops >3000
	***** BAKERSFIELD (NW) SAMPLING ONLY *****	
8-12 January	- Patchy ground FOG after sunrise (8th, 10th, 11h) - Partial afternoon clearing. - Average T 8°C; daily max/min ±1-2°C. RH 70-90%.	500 to 800
13 January	- Low clouds and haze.	150
14 January	- Ground FOG after MN, lifting before sunrise.	500
17-20 January	- Dense FOG forming early evenings (17th, 18th) or after MN (20th) and lasting to 1000. - Afternoon clearing with max/min T 12/2°C (17th) or heavy overcast with T 5°C, max/min ±1-2°C.	150 to 400
21 January	- Heavy overcast and low clouds.	>500

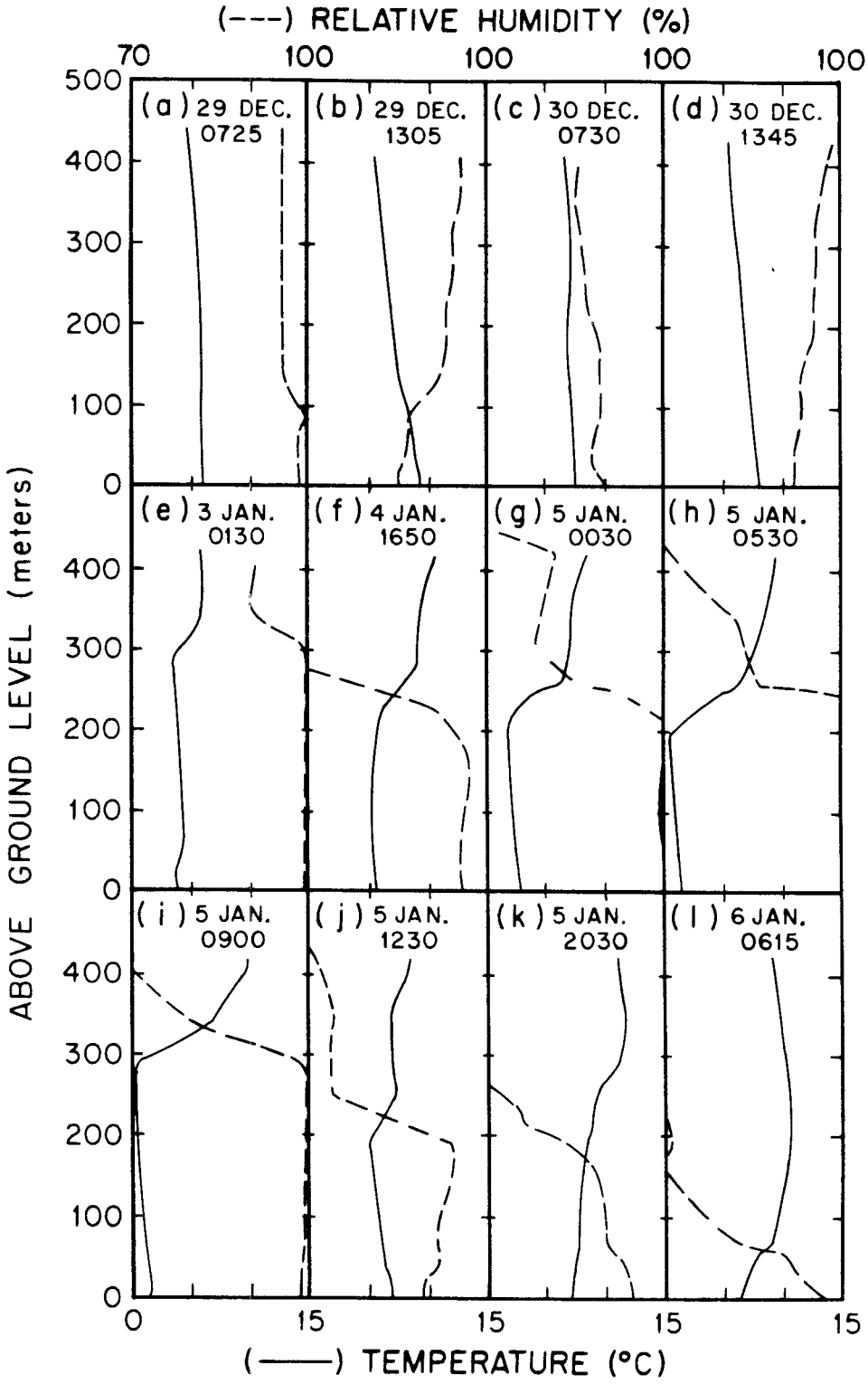

Figure 7.5 Temperature and relative humidity profiles at Buttonwillow measured by tethersonde: winter 1984-85.

temperature was very strong with the gradient as sharp as 0.1^{o} C m^{-1} during that period. This gradient persisted through the afternoons, despite partial clearing and heating at the ground (f,i). The vertical uniformity of RH during afternoon warming attested to the effectiveness with which air was mixed up to the inversion base but that exchange through the layer was sharply limited. Fog was absent after the morning of 5 January. Soundings indicate that the inversion rapidly eroded downward, leading to a ground-based inversion on the night of 5-6 January (k,l). A storm front moved across the valley during the next several days causing light rain and drizzle on 6-8 January. High cloudiness (tops 800 to 1000 m MSL) was observed for most of the next week, when several brief intervals of local ground fog were monitored shortly after sunrise.

The continuous record of mixing heights for 12 to 21 January shows the persistence of the temperature inversion for all days (Figure 7.6). The inversion base heights at Kernridge agreed closely with cloud-top altitudes at Bakersfield recorded from pilot obervations, also shown in Figure 7.6. Low clouds were observed at NWS on 12-13 January when the inversion base rapidly decreased to 300 m MSL. A short period of ground fog followed in the early morning hours of the next day (14th). A more gradual decrease in mixing height began several days later, and dense and widespread fogs were again observed on 17 through 20 January.

It is interesting to note the stepwise progression of mixing heights during those following days (given AGL at NWS Bakersfield). The lowering of the mixing height (16-17th January) accompanied the building of high pressure over the basin. In the general case, this leads to subsidence and causes concurrent warming of the inversion layer. This

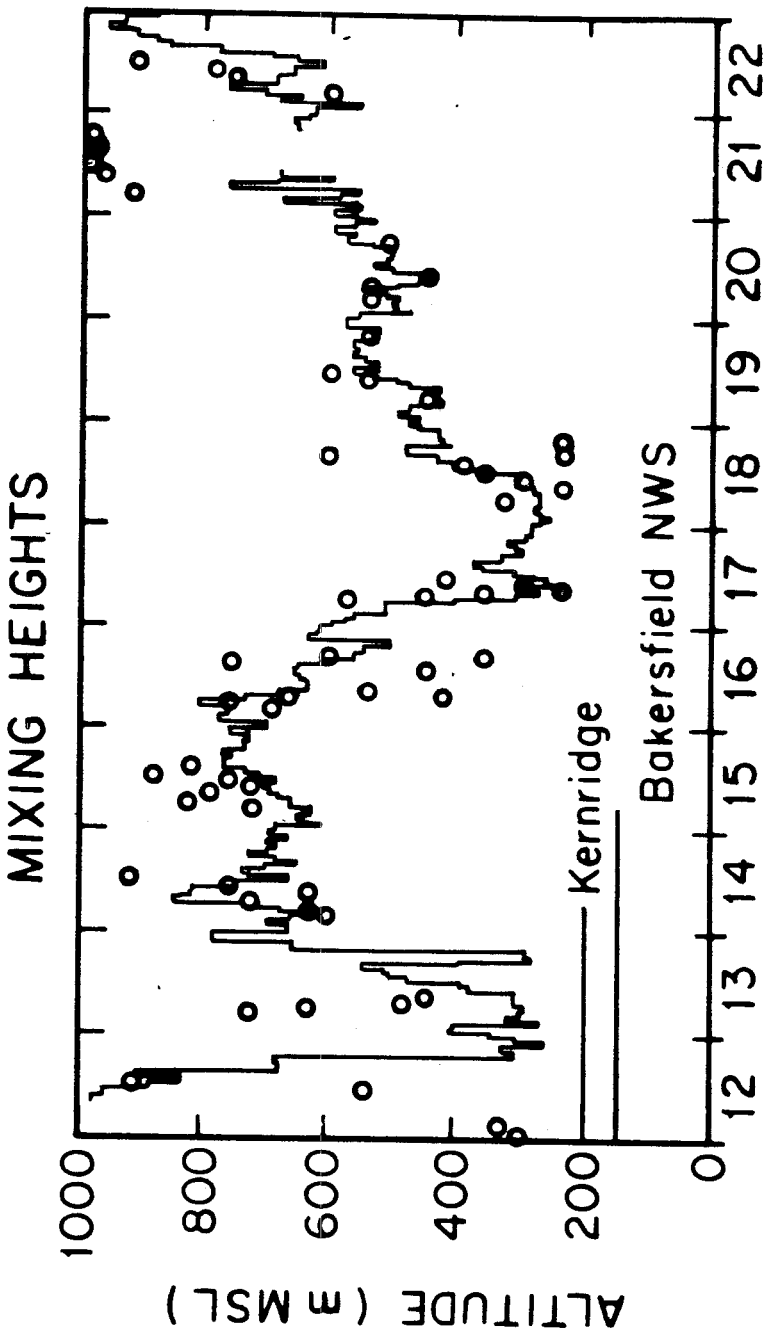

Figure 7.6 Mixing height data for 12 to 22 January 1985. Solid line indicates acoustic radar values obtained at Kernridge; circles represent pilot observations of cloud tops in vicinity of Bakersfield Airport.

effect propagates downward, heating the upper levels of the mixed layer, causing the temperature inversion to occur at progressively lower altitudes, and cutting off upper level air from the mixed layer. On the 17th, when the mixing height was at its lowest, dense fog formed immediately following local sunset (1700) and lasted until 1200 on the 18th. The inversion base rose to 300 m during an the afternoon of haze and partial clearing. On the following evening, fog formation began at 1800 and became dense at 2000; it dissipated at 0900 (19th). On both nights, mixing heights were stable; the greater longevity of the fog in the former case was apparently linked to the lower mixing height. The mixing height rose after fog dissipation on 19 January to 400 m during a day of heavy overcast. Dense fog formation was delayed until 0200 on the next night (20th), concurrent with a slight drop in the inversion base to 350 m. Dissipation at 0930 on the morning of the 20th was followed by heavy overcast. Mixing height remained above 400 m for the following days, and no dense fog was observed.

7.3.2 Concentration of Aerosol and Gaseous Species

The ambient concentrations of major aerosol components, $NH_3(g)$, and $HNO_3(g)$ at all six SJV network sites during the network study intervals are shown in Figure 7.7. As stated previously, the experimental errors in determinations were $\pm$15-20% (from paired filter data), chiefly due to uncertainties in pump flow and filter extraction. Excellent ionic balances were found, however. Differences in measured cation and anion equivalent sums (mean$\pm$s.d., expressed as percent of total; # in paratheses) were as follows : NW -2.2$\pm$7.3 (43); BW 1.2$\pm$7.6 (24); BA -3.6$\pm$7.5 (14); WA 1.6$\pm$4.2 (9); LH 1.2$\pm$6.8 (10); MK 2.7$\pm$7.5

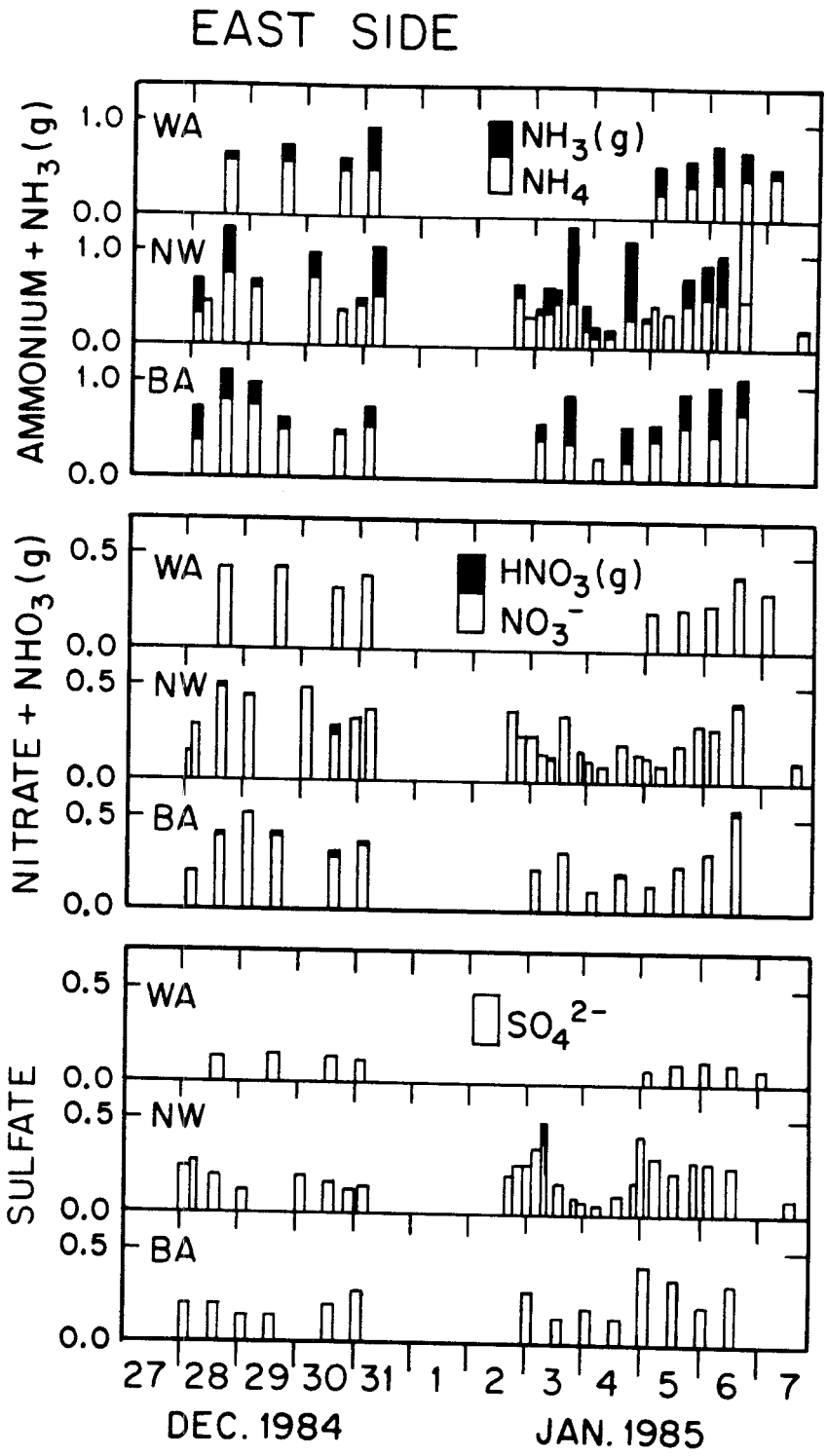

Figure 7.7a Concentration of N(-III), N(V), and sulfate from filter samples (μ eq m^{-3}) at Wasco (WA), Bakersfield Airport (NW), and downtown Bakersfield (BA) sites.

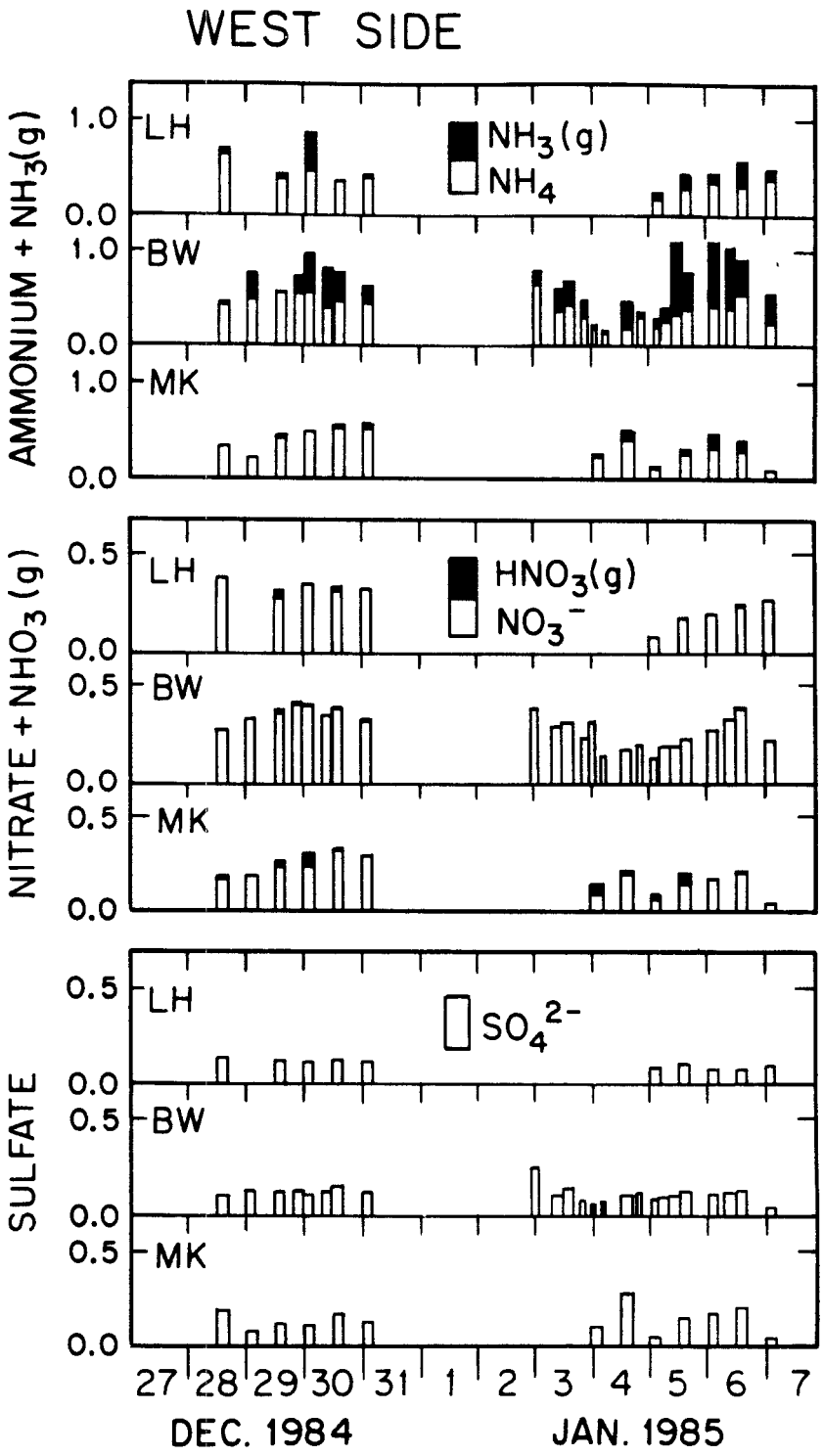

Figure 7.7b Concentrations of N(-III), N(V), and sulfate from filter samples (μeq m^{-3}) at Lost Hills (LH), Buttonwillow (BW), and McKittrick (MK) sites.

(13). Complete data sets are presented in Appendix C.

As in our previous SJV studies, atmospheric aerosol was found to be dominated by NH_4^+, NO_3^- and SO_4^{2-}. This is consistent with the dominant land use of the region: agriculture and livestock feeding (NH_3) and oil recovery (SO_2 and NO_x). Because the other constituents were measured at concentrations so far below the major species ($\leq$5%), the equivalent ratio $(NO_3^- + SO_4^{2-}):NH_4^+$ was essentially always 1:1.

Nitric acid concentrations were low for the majority of samples collected. Only at McKittrick (MK) was $HNO_3(g)$ found in appreciable quantities. Measurable levels were found in occasional afternoon samples at other sites before 1 January. High RH and the abundance of N(-III) (except at MK) precluded measurable levels of gaseous nitric acid during nighttime sampling (Jacob et al., 1985b). For the period of widespread fogs (2-5 January), nitric acid was essentially below detection at the valley sites. The inversion layer was situated downslope of MK; in that clear air region, $HNO_3(g)$ was measured.

Substantial ammonia concentrations were measured on most dates. Afternoon intervals had the highest concentrations (up to 20 ppb), and N(-III) in the the gas phase frequently exceeded the aerosol amount. There was measurable $NH_3(g)$ concurrent to each of the fogs except when fogwater pH$\leq$5 (5, 19, and 20 January NW samples). In higher pH fogs, $NH_3(g)$ was often 20-50% of total N(-III) measured in the atmosphere, although this was much lower than previous afternoon peak values.

Although the aerosol samples were neutral, the widespread abundance of ammonia over nitric acid (except 5 and 18-20 January samples) denoted an atmospheric reservoir of alkalinity (Jacob et al., 1985a; Stumm and Morgan, 1981). That is, at almost all times sufficient

gaseous base was available to fully neutralize strong acids such as H_2SO_4 and HNO_3. This represents a situation wherein *in situ* acid production would not have an observable effect on fogwater pH. Only following the relative depletion of ammonia (i.e., at a rate greater than its local emission) would acidification of fogwater solutions be possible.

Gas monitors in or near oil fields at Kern River (east side) and Kernridge (west side) showed elevated gas-phase concentrations during 2-5 and 17-20 January stagnation periods. There was generally a sharp falloff in measured peak concentrations in the Bakersfield area moving away from the oil fields. For example, the hourly peak SO_2 values monitored mid-morning on 5 January were 140 ppb at Oildale (OD), 60 ppb at Kern Front (KF), 35 ppb at Manor (MD), 30 ppb at the Airport (NW) and 20 ppb at downtown (BA) monitoring stations (see Figure 7.1 for locations). Except during occasional plumes, the average SO_2 concentrations were not very high (<20 ppb) at the sampling sites for the network monitoring periods.

Instruments at Buttonwillow recorded values near detection limits for both SO_2 and NO_x for most of the sampling program. Except for a few sporadic peaks, low concentrations for SO_2 were also measured at the Airport (NW) and downtown (BA) sites (10 ppb or less for >90% of the hourly data). Greater diurnal variations of NO_x were observed at the BA site (daily averages 80-100 ppb), while the NW monitor consistently measured below 50 ppb. The reliability of measurements at NW and BW has been called into question due to failure to meet EPA site-location requirements at these two temporary installations (D. Seacord, California Air Resources Board, personal communication, 1985). Based on

the data measured at nearby sites for similar intervals, we feel the assessment of low gas-phase pollutant concentrations at NW and BW was valid. See Appendix C for presentations of SO_2 and NO_x gas-phase data at valley monitoring sites.

7.3.3 Fogwater Composition

Fogwater composition was dominated by NH_4^+, NO_3^- and SO_4^{2-}, plus, for several samples, H^+ and S(IV). Overall, these ions accounted for >95% of all the measured solute equivalents. Total ion concentrations in fogwater were routinely measured in the 1-3 meq L^{-1} range, similar to those during previous winters' monitoring (Jacob et al., 1984; 1985a). Fogwater acidities were low (pH 5 to 7) with the exception of the NW fogs on 19 and 20 January and several samples on 5 January with pH 3 to 4. Fogwater concentrations and LWC averaged for each event are given in Table 7.2. Ion balances were calculated assuming S(IV) was present in a monovalent form (Munger et al., 1984). Median concentrations of Fe, Mn, and Pb at the NW site were about 100, 20, and 50 mg L^{-1}, respectively. The iron content in BW fogwater was slightly lower, and Mn and Pb were about one-third of the typical NW values. Detailed data sets are given in Appendix C. In discussions of fog measurements, dates correspond to the morning in which collection ended.

Aqueous S(IV) concentrations measured in Buttonwillow fogwater were generally low: <0.05 mmol L^{-1}. At Bakersfield, the majority of samples contained between 0.05 to 0.15 mmol L^{-1}, and S(IV) represented 10-20% of the total moles of sulfur measured in most fogwater samples. However, this fraction exceeded 30% in many 3 and 5 January fog samples. In higher pH fogs, the gas-aqueous equilibrium (Henry's Law) is

Table 7.2 Fogwater Composition Summary

	Date & Time[a]	N	LWC[b]	pH	micro-equiv. L^{-1} Na^+	K^+	NH_4^+	Ca^{2+}	Mg^{2+}	Cl^-	NO_3^-	SO_4^{2-}	micro-mol L^{-1} S(IV)	CH_2O	-/+[c]	Δ (%)
A.	BAKERSFIELD AIRPORT															
	28 December 84 00:35 to 08:35	6	0.149	5.81	14	4	2100	46	9	41	505	1064	153	98	0.81	+410 (10)
	2-3 January 85 20:15 to 10:15	10	0.202	5.09	10	3	1260	25	3	13	335	764	128	78	0.95	+69 (3)
	3-4 January 85 20:00 to 01:55	5	0.176	6.89	5	3	530	171	11	6	96	442	18	32	0.78	+156 (12)
	4-5 January 85 20:10 to 09:15	13	0.191	4.72	21	4	1350	33	4	19	190	889	231[d]	105	0.93	+102 (4)
	8 January 85 09:00 to 10:00	1	0.070	7.37	57	8	1380	109	24	6	570	501	16	27	0.69	+483 (18)
	10 January 85 07:15 to 08:50	2	0.035	6.06	25	9	2600	54	5	50	830	1619	180	na	0.99	+18 (0)
	11 January 85 06:35 to 07:30	1	0.016	6.67	58	24	4920	248	9	20	2115	2920	na	na	0.96	+206 (2)
	14 January 85 01:30 to 04:30	1	0.249	5.92	26	3	2350	37	5	na	630	1400	145	123	0.90	+246 (5)
	18-19 January 85 20:05 to 09:00	10	0.182	4.08	7	7	1780	21	4	32	870	650	89	147	0.86	+263 (7)
	20 January 85 07:15 to 09:30	3	0.040	3.03	26	17	3280	64	10	183	2900	1610	84	165	1.10	-461 (5)
B.	BUTTONWILLOW															
	2-3 January 85 20:20 to 06:50	6	0.174	5.10	7	3	120	38	4	17	640	440	36	55	0.89	+135 (6)
	3-4 January 85 17:25 to 10:30	7	0.173	6.17	5	2	600	27	3	40	225	195	9	28	0.73	+172 (15)
	4-5 January 85 19:30 to 09:00	11	0.133	6.08	3	2	670	19	3	14	190	245	22	33	0.68	+224 (19)

a. Volume-weighted mean values for N individual fogwater samples collected for indicated time periods; see Appendix C for complete data set and observed episode duration; "na" - not analyzed
b. LWC from RAC collection rate.
c. Equivalent balances: "-/+"= Σanion / Σcation; "Δ(%)" = Σanion- Σcation (% Σall ions); assumes S(IV) in monovalent form; does not include correction for bicarbonate.
d. [S(IV)] for 6 samples were >300 μmol/l (upper limit for colorimetric method).

sufficient to explain observed S(IV), even at low $SO_2(g)$ partial pressure (see Figure 2.3 in Chapter 2). For low pH, $SO_2(g)$ is fairly insoluble, and measured S(IV) in these samples was often in excess of the equilibrium. Formaldehyde was also measured in fogwater with concentrations comparable to S(IV). The formation of sulfur-aldehyde adducts has been shown to increase the total S(IV) equilibrium solubility (Munger et al., 1984). Recently, the S(IV)-formaldehyde adduct, hydroxymethanesulfonate (HMSA), has been positively identified in SJV fogwater samples (Munger et al., 1985).

Satisfactory ionic balances were obtained for samples on most days. However, significant anion deficiencies were noted in the more alkaline fogwater samples (Table 7.2). For example, during the several dense fog intervals with pH > 6 (e.g., BW: 4 and 5 and NW: 4 January), total anion equivalents were 20-30% below the sum for cations; the differences amounted to 0.1-0.2 meq L^{-1}. All or part of the anion deficiency measured at high pH may be accounted for by the presence of conjugate bases of weak acids, such as formate, acetate, and carbonate. Formate and acetate, analyzed in alkaline fogwater samples collected during the 1983-84 fog/aerosol study, were both in the range of 0.05 to 0.15 meq L^{-1} (Jacob et al., 1985a). These weak acids would be fully dissociated at pH>6; the pK_a's are 3.8 and 4.9 at 5°C, respectively (Martell and Smith, 1977). Equilibrium HCO_3^- concentrations can also be important at higher pH. For example, $[HCO_3^-]$ = 0.07 meq L^{-1} would be supported by atmospheric CO_2 (340 ppm) in fogwater at pH=7 and 5°C. Although not measured for these samples, expected values of these species were generally sufficient to satisfy the ionic balance.

The lighter, patchy fogs were the most concentrated (Figure 7.8).

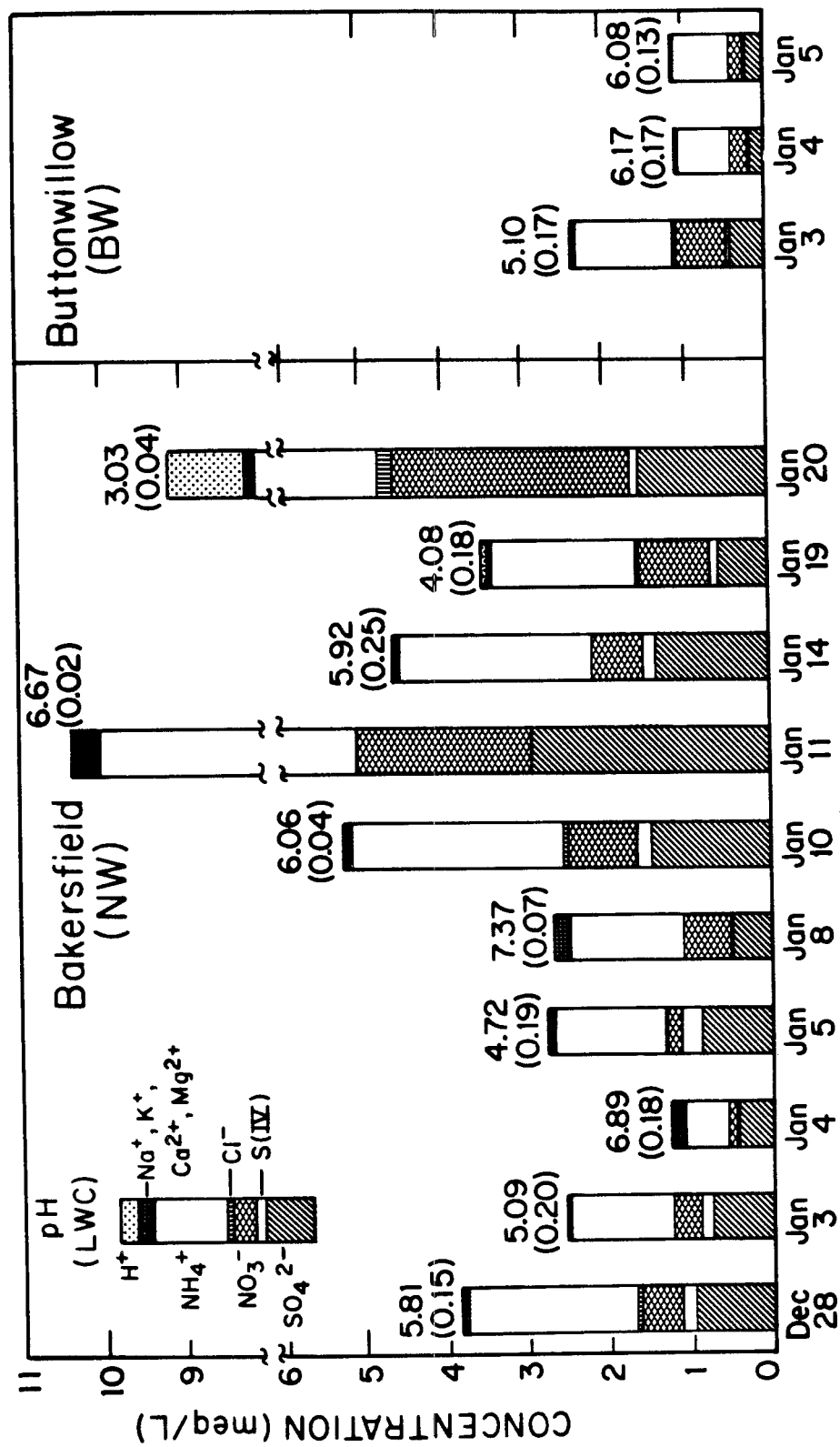

Figure 7.8 Summary of fogwater compositions at San Joaquin Valley sites from winter 1984-85. Volume-weighted concentrations, pH, and liquid water content ($g\ m^{-3}$) for measurements ending on morning of date given

Conversely, the denser fogs were generally the most dilute, although the observed effect was also a function of differences in the ambient pollutant levels. For example, total aerosol concentrations during the 4 January event at both sites were substantially lower than the prior night. With comparable LWC, the fogwater concentrations were also somewhat lower for the latter event. This depended on the relative proportion of material taken up by droplets. Details of fog scavenging are discussed in a subsequent section.

7.3.4 Deposition Measurements

As might be expected to accompany changing ambient conditions, material fluxes to ground surfaces varied greatly during the study periods. The composition of deposition sample extracts was dominated by the same major ion species measured in aerosol and fogwater samples, NH_4^+, NO_3^-, and SO_4^{2-}. These deposition rates for PD surfaces are shown in Figure 7.9 for the important sampling intervals. Fluxes measured to surrogate-surface collectors were generally small for dry periods. A sharp increase in the deposition of all ions accompanied fog in every case. For major ions in fog, the enhancement was 5 to 20 times the rates during dry intervals. This was due to the increases in particle size (triggered by aerosol activation and formation of a droplet phase) plus the replenishment of pollutant species in the fog-ladden atmosphere to match the accelerated removal rate.

Cation fluxes did not show the same systematic increase with fog. These ions (Na^+, K^+, Ca^{2+}, and Mg^{2+}) were always found at low aerosol and fogwater concentrations, and their deposition in fog and non-fog periods was disproportionately high compared to the major species.

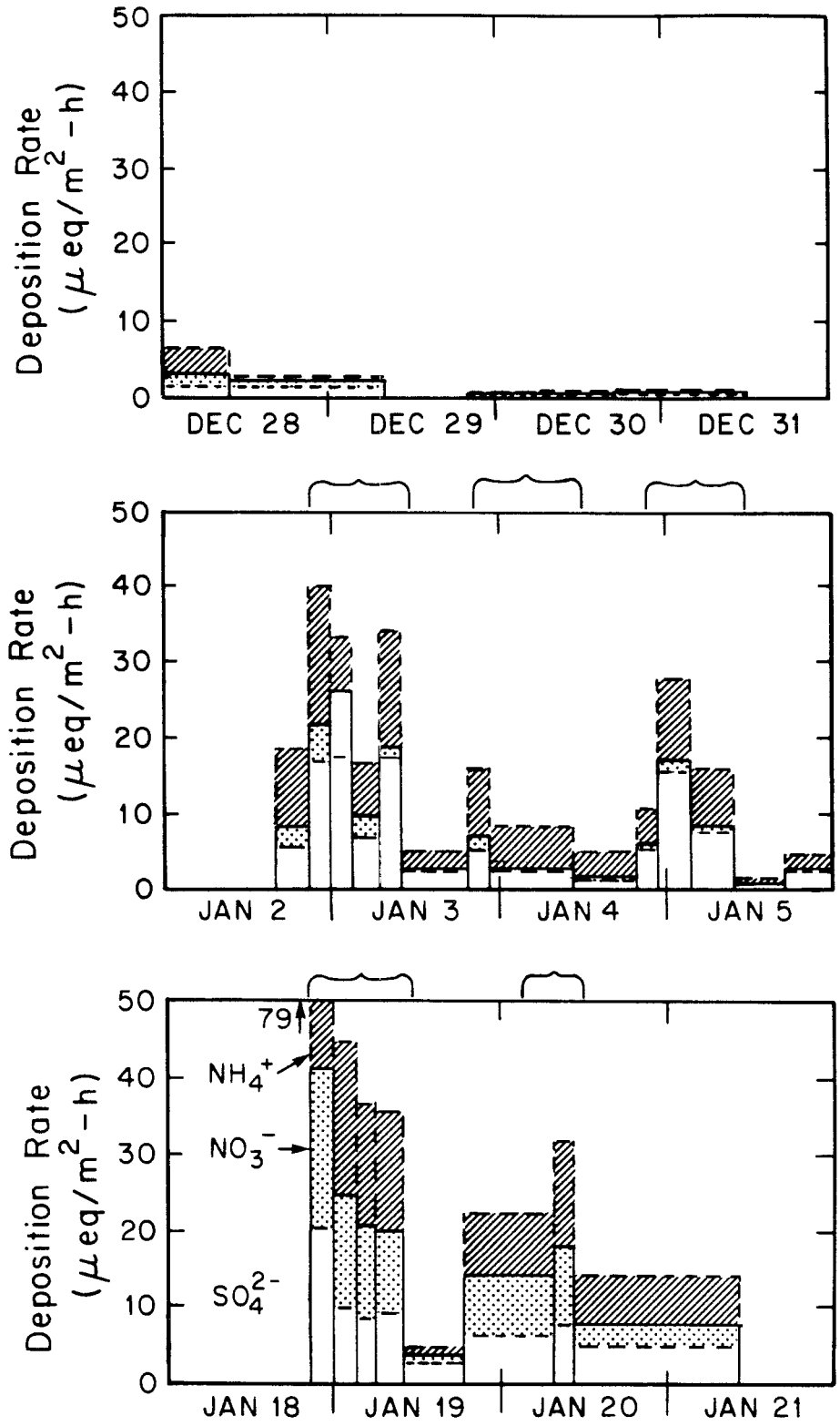

Figure 7.9 Deposition rates of major ions to petri-dish collectors (PD-high) at Bakersfield Airport (NW) site. Braces above figures indicate periods of fog.

However, their contributions to total ion deposition were nonetheless low relative to the major conponents. Since nearby soil was the likely source of this alkaline material, it is difficult to interpret their fluxes to surrogate surfaces as a net deposition. It appears that fallout of nonwetted, windblown soil dust led to these sporadic deposition rates. Yet, this pathway may be important to the resultant acidity of materials that accumulate at vegetative or other sensitive surfaces. Retention of coarse dust may provide additional buffering against acidic deposition, especially at when surfaces become wetted.

The measured deposition rates were normalized to the ambient concentrations of total aerosol loading to give deposition velocities, V_d. Calculations were also made using fogwater loading (aqueous concentration x estimated LWC). We use the notation (C) and $(C)_f$ for total and fogwater loadings of species C in the atmosphere, so V_d= Flux/(C) and $V_{d,fog}$= Flux/$(C)_f$. The fog deposition velocities ($V_{d,fog}$) and the global values (V_d) are shown in Figure 7.10 for major ions. For sulfate measurements in deposition, filter, and fogwater samples, values of total soluble sulfur as SO_4^{2-} were compared.

In this presentation, clear episodes of higher rates can be seen specifically for the episodes of fog. For 2 to 5 January fogs, greater fractions of S(VI) than N(V) were scavenged by droplets during most events, and this led to higher deposition rates for sulfate compared to nitrate (V_d - solid lines in Figure 7.10) . At the same time, the $V_{d,fog}$ values showed strong correlation between the two species (Figure 7.11a), indicating that differences in overall removal rates were determined by their respective scavenging efficiencies (see next section). This also verified that droplets made the overwhelming

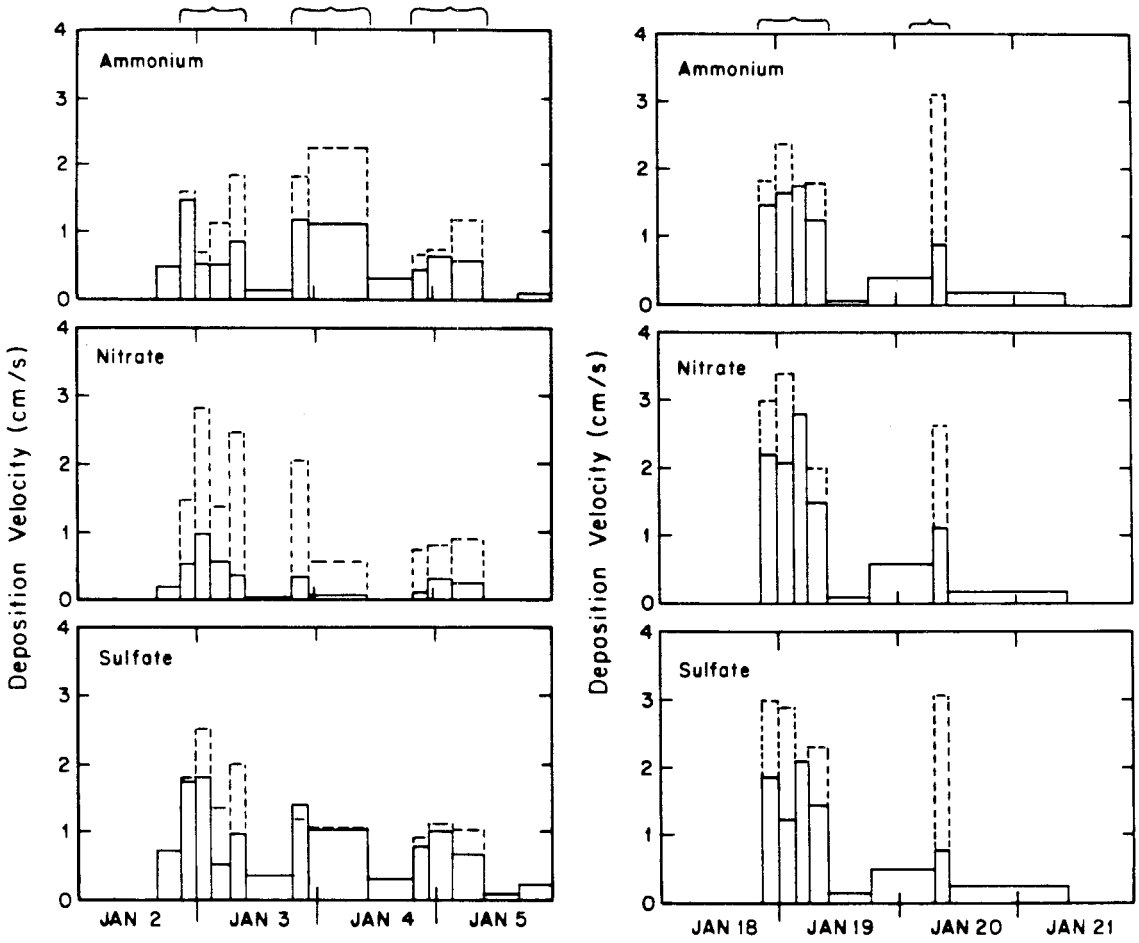

Figure 7.10 Deposition velocities for major ions measured to PD-high collectors at NW site. Concurrent values of V_d and $V_{d,fog}$ are shown as solid and dashed lines, respectively. Braces over figures indicate periods of fog.

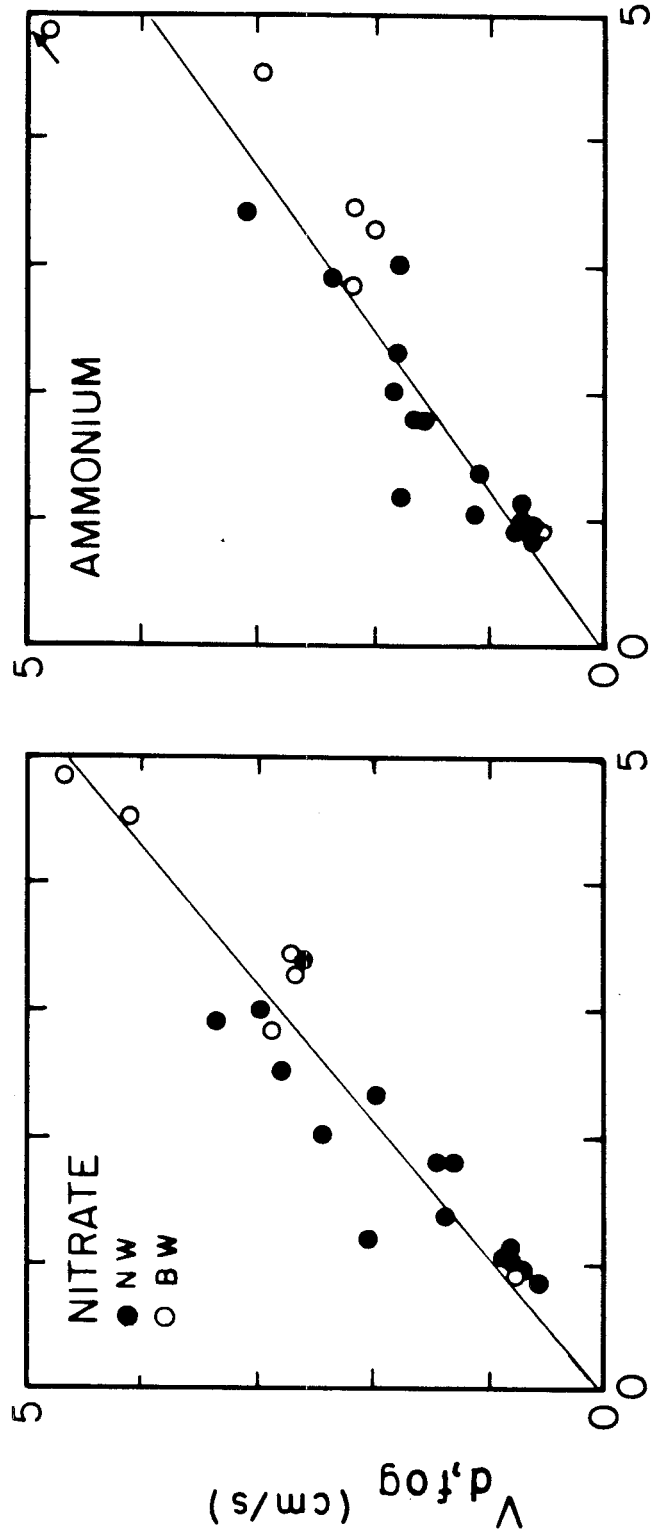

Figure 7.11 Fog deposition velocities ($V_{d,fog}$) to PD-high collectors at NW site: (a) nitrate and (b) ammonium versus sulfate. Shown with lines of best fit.

contribution to measured fog fluxes and that the composition in the fogwater was the principal factor affecting the proportion of solutes removed.

Ammonium Loss. In the case of ammonium ion, the fog deposition velocities were approximately 25% below measured rates for sulfate for the same periods (Figure 7.11b). A similar relationship for V_d was also found. Interstitial aerosol fluxes could not have accounted for the magnitude of these differences, given the low rates measured in the absence of fog. Gaseous exchange at the collector surface must have caused either enhancement for sulfur or loss of NH_3. The parity of nitrate and sulfate rates due to fog is circumstantial evidence that SO_2 absorption was not substantial. Additional fog fluxes of N(V) from HNO_3 or NO_x would not have matched the difference observed between sulfur and ammonium species. It appeared that ammonia loss may have been promoted by alkaline conditions on wetted collection surfaces.

The addition of calcareous material to fogwater can alter N(-III) gas-aqueous equilibria. This promotes a substantial rise in $[NH_3(aq)]$ and, hence, its volatility (see Chapter 2.1). The relative disparity measured for NH_4^+ fluxes (20-30%) was similar to the greater fraction of cation species, mostly calcium, in deposition relative to fogwater and aerosol samples. As a consequence, the N(-III) balance for deposited fog droplets is less certain because of NH_3 volatility. However, this effect may be more important at hydrophobic (e.g., plastic collector) surfaces because they serve to maintain the integrity of a droplike phase while natural surfaces often adsorb liquid water and provide organic ligands to reduce NH_3 loss.

Turbulence versus Sedimentation. As discussed previously,

particle deposition at SJV sites was expected to be dominated by sedimentation of fog droplets due to minimal surface features and predominantly light winds. A dependence of droplet fluxes on atmospheric turbulence was not obvious because wind speeds and U* were always very low. Wind profile data at NW showed U*=5 to 10 cm s^{-1} at all times of dense fog (see Table 7.3). The NWS sensor (10 m AGL) recorded wind speeds of 2-3 m s^{-1}, but nearer to the surface (3.65 and 0.85 m), wind velocities in fog rarely exceeded 2 m s^{-1}. Turbulent transport is slow in such an environment, and its contribution to the measured deposition rates is therefore rather limited. Dollard and Unsworth (1983) have made direct measurements of turbulent fluxes for wind-driven fog drops above a grass surface. For wind speeds of 3 to 4 m s^{-1} (measured at 0.5 m above the zero plane of displacement), the authors reported droplet fluxes about 3 times greater than the sedimentation rate alone, and $V_{d,fog}$ of 3 to 6 cm s^{-1}. However, measurements made at wind speed less than 2 m s^{-1} showed much lower droplet flux by turbulence; total rates were less than 50% over the sedimentation rate. From our measurements in dense fog at SJV sites, most of the $V_{d,fog}$ values were found in a relatively narrow range, 1 to 3 cm s-1, consistent with terminal settling rates for fog droplets.

No correlation was apparent between fog LWC and $V_{d,fog}$ of depositing solutes. The estimation of LWC values and relatively long averaging intervals possibly obscured such a relationship. Droplet size spectra measured by an optical particle counter (OPC) indicated that LWC variations were principally a function of droplet number concentration (see Chapter 5). The measured mass median diameters remained in a relatively narrow range throughout each event. Strictly speaking,

Table 7.3

DEPOSITION VELOCITIES IN FOG[a]

A. Bakersfield Airport (NW) Site

Date & Time	Hr	T[b]	U[b]	LWC[c]	$V_{d,fog}$ (cm s^{-1})			V_d (cm s^{-1})			
					NH_4^+	NO_3^-	SO_4^{2-}	NH_4^+	$+NH_3(g)$	NO_3^-	SO_4^{2-}
28 Dec 84											
00:00-02:40	2.7	3.0	na	0.21	0.67	0.60	0.83	1.28	0.62	0.49	1.23
02:40-04:30	1.9	4.0	na	0.06	1.65	1.34	1.79	na	na	na	na
2-3 Jan 85											
21:00-00:00	3.0	3.6	1.1	0.23	1.60	1.49	1.79	1.45	1.37	0.53	1.74
00:00-03:00	3.0	4.0	0.7	0.21	--	2.81	2.52	--	--	0.98	1.80
03:00-07:00	4.0	2.8	1.5	0.21	1.10'	1.40	1.36	0.50'	0.30'	0.56	0.53
07:00-10:00	3.0	0.8	1.0	0.12	1.83	2.46	2.01	0.84	0.68	0.36	0.97
3-4 Jan 85											
19:30-22:50	3.3	1.0	0.8	0.17	1.79	2.07	1.18	1.16	0.53	0.35	1.41
22:50-10:50	12.	-1.3	0.8	na	--	--	--	1.11	0.72	0.07	1.02
4-5 Jan 85											
23:00-02:00	3.0	3.0	2.0	0.17	0.65'	0.75	0.95'	0.44'	0.39'	0.12	0.79'
23:00-03:45	4.8	3.3	1.3	0.23	0.74'	0.83	1.13'	0.64'	"	0.37	1.01'
03:45-10:00	6.2	2.2	1.1	0.17	1.15'	0.90	1.04'	0.57'	"	0.30	0.67'
14 Jan 85											
01:30-04:30	3.0	3.4	1.0	0.25	0.76'	0.84	1.00	1.18'	"	0.63	2.13
18-19 Jan 85											
20:40-00:00	3.3	3.0	0.8	0.24	1.81	3.00	3.00	1.45	"	2.19	1.86
00:00-03:25	3.4	3.0	1.1	0.16	2.38	3.39	2.90	1.65	"	2.08	1.24
03:25-06:00	2.6	3.0	1.4	na	--	--	--	1.75	"	2.79	2.10
06:00-10:00	4.0	3.3	0.9	0.12	1.81	2.01	2.31	1.25	"	1.50	1.43
20 Jan 85											
07:40:10:30	2.8	2.8	1.0	0.04	3.11	2.63'	3.41	0.90	"	1.12'	0.80

Table 7.3 (cont.)

DEPOSITION VELOCITIES IN FOG[a]

B. Buttonwillow (BW) Site

Date & Time	Hr	LWC[c]	$V_{d,fog}$ (NH_4^+)	$V_{d,fog}$ (NO_3^-)	$V_{d,fog}$ (SO_4^{2-})	V_d (NH_4^+)	V_d (+NH_3(g))	V_d (NO_3^-)	V_d (SO_4^{2-})
			----- (cm s^{-1}) -----			----------			
3 Jan 85									
02:30-07:00	4.5	0.13	5.36	5.24	5.38	1.20	0.96	1.25	1.32
4 Jan 85									
00:00-04:30	4.5	0.18	2.21	2.76	3.45	1.20	0.98	0.84	1.38
04:30-09:00	5.0	0.15	0.82	0.81	0.90	0.57	0.45	0.15	0.44
4-5 Jan 85									
17:30-02:45	9.3	0.14	2.24	2.93	2.83	0.83	0.62	0.44	0.95
03:00-06:15	3.3	0.14	3.00	4.15	4.52	0.94	0.66	0.59	1.45
06:30-10:30	4.0	0.11	2.04	2.72	3.28	0.41	0.11	0.26	0.61

a. Deposition velocities calculated from PD fluxes (high location at NW).
$V_{d,fog}$= (Deposition rate) / (LWC x Fogwater aqueous concentration);
' denotes when low PD flux was >30 % greater than reported values;
V_d= (Deposition rate) / (Aerosol concentration);
V_d for "+NH_3(g)" = (Deposition rate) / (Aerosol + NH_3(g));
" denotes NH3(g) was below detection.

b. Temperature (^oC) and wind speed (m s^{-1} @ 2.65 m AGL) at NW site only; friction velocity (U*) was generally U/10 as measured by profile method.

c. LWC from RAC collection rate (g m^{-3}).

solute depostion will depend on the manner in which solute mass is distributed within the droplet size distibution, not just on the droplet size spectrum itself. Such size-composition relationships in fog have not been adequately studied, although they may be an important aspect of pollutant deposition in fog. On the other hand, the increases in V_d with LWC were related to the effect of LWC on fog-scavenging efficiency; this is discussed in more detail in Chapter 7.4.1.

Comparison of Collector Surfaces. Rates measured for deposition to the surrogate-surface collector pairs at the NW site are shown in Figure 7.12. Comparisons have been made for measured fluxes to (a) side-by-side PD replicates, (b) high and low PD locations, and (c) nearby bucket and PD collectors. Collocated PD surfaces measured major ion fluxes with good agreement over a wide range of values (Figure 7.12a). Differences between paired data (σ_Δ) are $\leq$20% for ammonium, nitrate, and sulfate fluxes. Less agreement was found for cation species (e.g., calcium). This variability was largely due to lower analytical sensitivity at the low concentrations in PD extracts plus the small number of coarse particles that apparently led to measured cation deposition (and contamination).

Fluxes to PD in high (3.0 m) and low (0.2 m) positions also showed fair to good agreement (Figure 7.12b). Nitrate fluxes showed the closest agreement while ammonium and sulfate fluxes showed greater variability. For nonfoggy conditions, there was no statistical significance for differences between positions. During fog, PD surfaces closer to the ground showed greater rates for NH_4^+ and SO_4^{2-}.

Rates for deposition to buckets were compared with PD (high) measurements averaged for the same intervals (Figure 7.12c). The PD

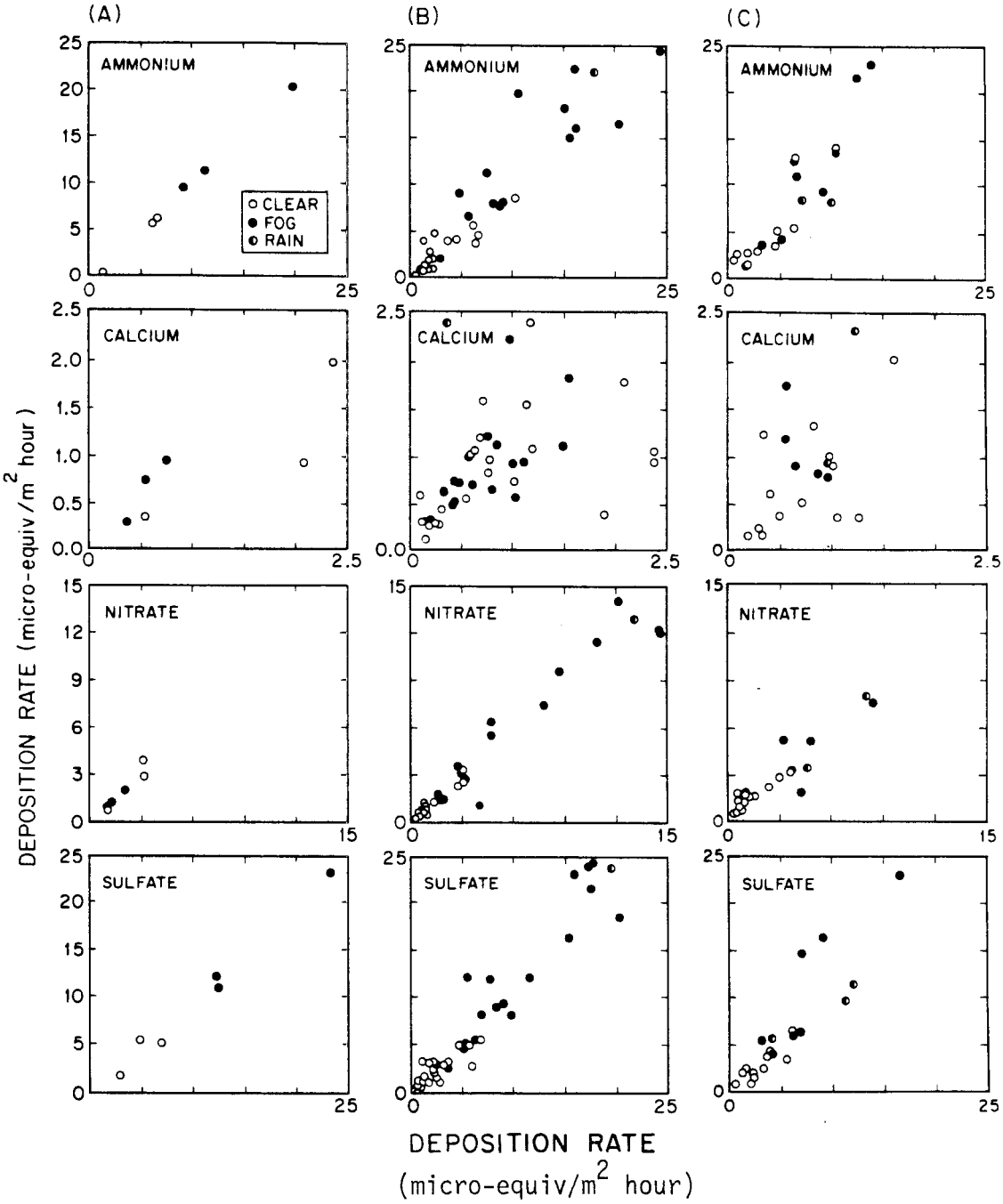

Figure 7.12 Comparisons of solute deposition rates to surrogate-surface collectors. (a) PD replicates; (b) low (0.2 m) versus high (3.0 m) PD positions (y vs. x); (c) Bucket versus PD (high) collectors.

values calculated for bucket periods incorporated up to 6 sequential PD samples. Also, with much different geometries, comparison of surface areas is somewhat ambiguous. Nonetheless, despite these differences in their shape and exposure intervals, the two types of collectors gave similar results. Once again, nitrate rates were generally in good agreement; the dry-period ammonium and sulfate fluxes were also in general agreement. Buckets exposed through fog episodes measured greater NH_4^+ and SO_4^{2-} deposition rates than the PD located at the same height; i.e., bucket data were closer to low PD values.

Higher fog fluxes of ammonium and sulfate to the low PD and bucket collectors (compared to the high PD) were correlated, and several mechanisms could lead to this. Lower NH_3 losses for the bucket and low PD position were possible, but this was not consistent with the pattern for cation fluxes -- also higher to low PD and buckets. The possibility of direct deposition of NH_3 and SO_2 must also be considered. The surface wetting by fog may have provided a sink for gaseous species to deposit. However, on many nights the PD surfaces were also wetted by dew. These non-fog fluxes were indistiguishable from other periods, and the high/low PD bias was not seen in these samples. Release of ammonia from the soil wetted by fog could have been important (Dawson, 1977). This would result in NH_3 profiles with higher surface concentrations than measured aloft. A gradient of $NH_3(g)$ could possibly alter the speciation and concentration of N(-III) aerosol in the layer nearest the ground. Furthermore, ammonia dissolution into accumulated moisture near the ground may have promoted SO_2 absorption. Alternatively, it is possible that quiescent zones, both within the bucket and at ground adjacent to the the low PD surface, promoted more favorable retention of

fog droplets. However, this effect was not noted for nitrate. While the deposition gradient was seen for the earlier fogs, when ambient $NH_3(g)$ was depleted on 18-20 January, the high/low bias was not observed.

Unfortunately, the data are not extensive enough to support conclusions about these observed differences. Despite these trends, the disparities between collection surfaces found at the NW site were minor in light of recent comparisons of collectors reported elsewhere (Dolske and Gatz, 1985; Vanderberg and Knoerr, 1985). They represented an experimental uncertainty in a range similar to the other measurements.

7.3.5 Precipitation Scavenging

A precipitation event followed the 2 to 6 January period of fog and stagnation. Moderate rain and drizzle (4-10 cm) were observed from late evening of the 6th through the early morning hours of 8 January, and wet deposition was monitored at several valley sites over the 36 h period. The total solute fluxes to the ground for major ions are shown in Figure 7.13. Aerosol and $NH_3(g)$ concentrations at each site immediately prior to the rainfall are also given. Rainfall amount strongly influenced the solute deposition, while the ranges of rainwater concentrations were fairly similar at each site. Long range transport from other pollutant source regions was not indicated from wind trajectories of that period. Local air quality was reflected in the relative proportion of major ions in the rainwater (e.g., low NH_4^+ on the west side, high SO_4^{2-} on the east side). However, at all locations, the deposition of sulfate was substantially greater than nitrate, despite relatively higher concentrations of N(V) in the air mass leading

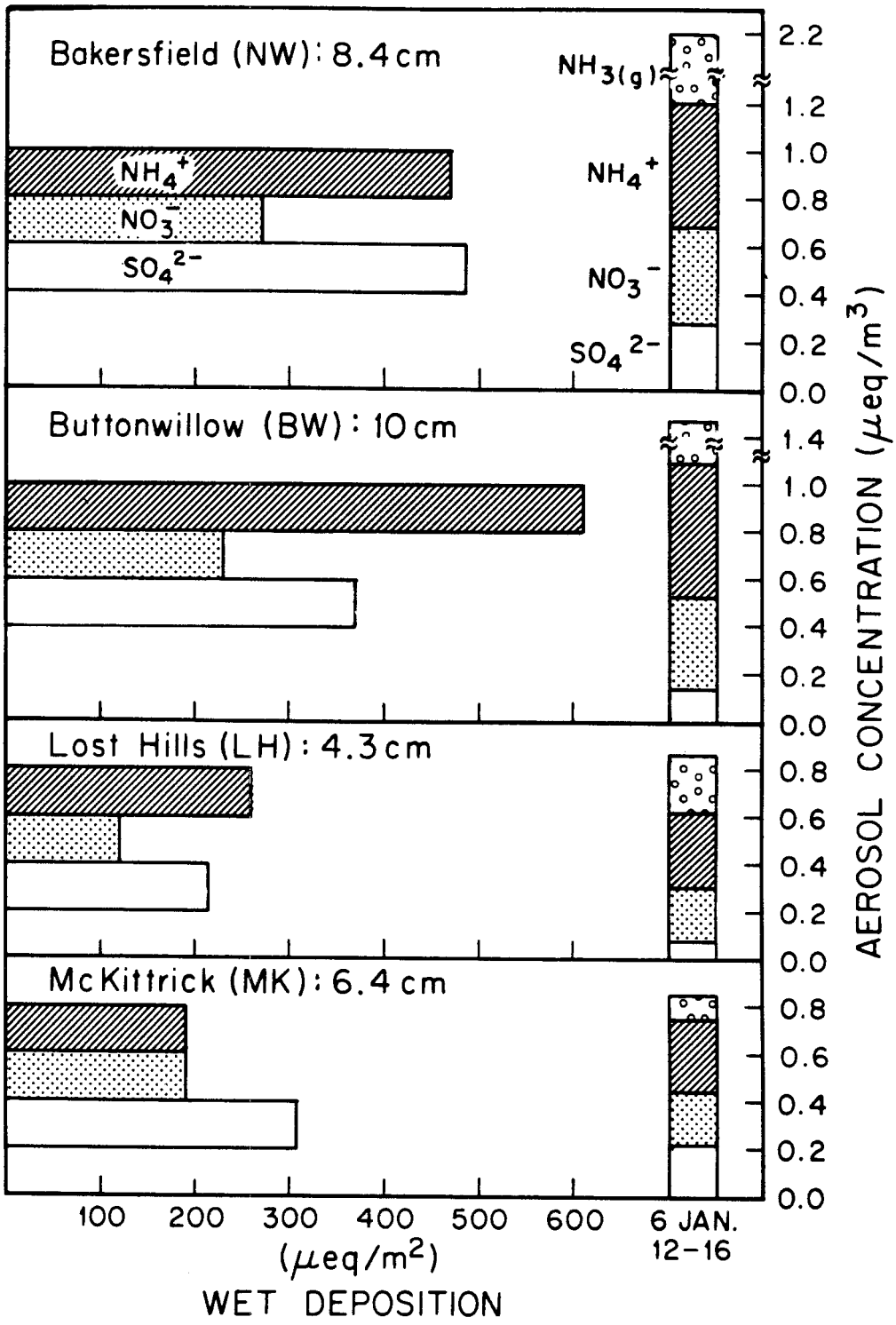

Figure 7.13 Wet deposition of major ions for 4 San Joaquin Valley sites measured 6-8 January 1985. Filter data for sampling interval immediately preceding rainfall also shown.

up to the storm passage. That is, the sulfate-to-nitrate ratios of rainwater fluxes were 2 and 4 times higher than the proportion of these solutes measured in the atmosphere before the rain. Ammonium deposition was also far below the relative atmospheric abundance of N(-III) before the storm passage. Finally, it is interesting to note that the wet deposition rates of major ions averaged for the sampling period (36 h) were comparable to the rates measured in dense fog. Since rainfall was not continuous for the entire 36 h period (e.g., NWS records indicated 12 h of precipitation over the two days at Bakersfield Airport), instantaneous rates were significantly higher. However, rainfall and, to a lesser extent, fog deposition produced fairly complete removal of the pollutants emitted into the SJV atmosphere.

7.4 DISCUSSION

7.4.1 Comparing Fog and Total Solute in the SJV Atmosphere

Solute material in the droplet phase, $(C)_f$, is a subset of the total (aerosol + gas + fog) loading, (C), measured by the filter methods. Ambient atmospheric constituents of varying physical and chemical characteristics will be incorporated into the droplets with different efficiencies. Ion ratios for concurrent SJV fogwater and filter samples reflected the extent of varying conditions in the environment and showed considerable scatter. Data taken during individual fog events tended to cluster, although there were cases showing dramatic changes in the fogwater or filter sample chemistry in sequential intervals.

For example, the nitrate-to-sulfate ratios in total aerosol samples were distinctly different than found in fogwater. The ratio in NW fogwater was near 2 and approximately unity in BW samples. However, the actual proportion of N(V) to S(VI) in the atmosphere was much greater than indicated in fogwater samples (Figure 7.14). During most sampling intervals, N(V) scavenging was from 20 to 80% less efficient than for S(VI). In acid fogs, however, N(V) scavenging was more efficient. All the points above the 1:1 line in Figure 7.14 correspond to intervals with fogwater pH < 5.

Partitioning of species between phases can be calculated by conversion of measured fogwater concentrations (meq L^{-1} of water) to units of meq m^{-3} of air. The conversion factor (LWC) was determined from the collection rate of the rotating arm collector. The error in determining a "true" LWC value might be as high as 50%, but the relative uncertainty for RAC measurements in stable fog is closer to 20% (see

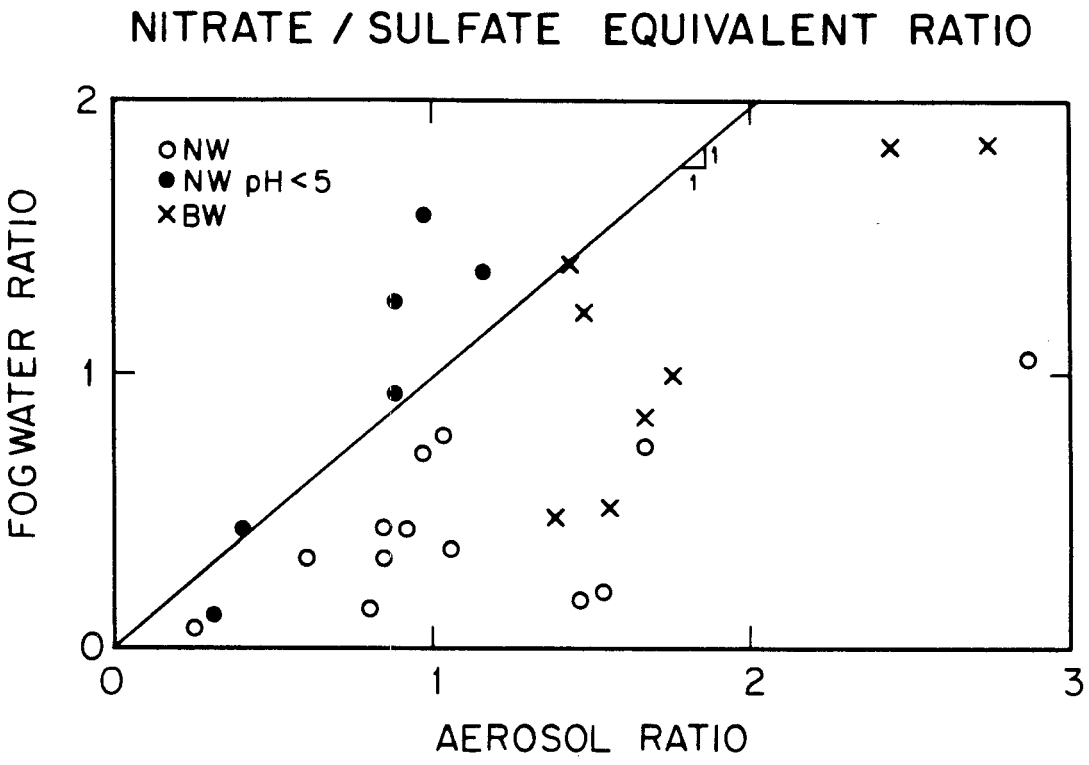

Figure 7.14 Comparison of nitrate-to sulfate equivalent ratios for simultaneous fogwater and filter samples. 1:1 line shown.

Chapter 5). Detailed profiles for three fog sampling dates are shown in Figure 7.15. Droplet-phase values are superimposed onto total atmospheric loading, and N(-III), N(V), and sulfur concentrations are given in separate plots. Values for LWC are also shown. The uncertainty in absolute LWC means that $(C)_f$ may be somewhat higher or lower than indicated. Upper bounds for $(C)_f$, hence for LWC, are obviously set by total nongaseous solute C measured at the same time.

The relative proportion of fog-scavenged fractions are independent of LWC uncertainty in individual determinations since the same scaling is applied to each species. Values for scavenging efficiency, $F_C=(C)_f/(C)$, were calculated for filter and fogwater samples collected simultaneously. Despite uncertainties with regard to the magnitude, the hierarchy for each sample is well represented (Figure 7.16). The F_C for major ions of the same sample are indicated as such (a & b). Error bars are not shown for the sake of clear presentation. As the LWC is plotted against a function of itself (F_C= LWC [C]/(C)), the uncertainty in plotted values lie on a diagonal on which all three points would be adjusted similarly. Since analytical errors in chemical compositions were small and the RAC gave a self-consistent estimation of LWC, the basic relationships in these plots should be left intact.

Acidity and N(V) Scavenging. The samples in which calculated $F_{N(V)}$ are highest were from low pH fogs, indicated in Figure 7.16a,b. Thus, not only had the N(V)/S(VI) ratios increased, but ambient N(V) had more efficiently scavenged in these cases. Under acidic prefog conditions, nitric acid will volatilize from nonactivated aerosol, and N(V) can partially reside in the gas phase. Since $HNO_3(g)$ is completely scavenged by even low pH fog, the greater the precursor atmospheric

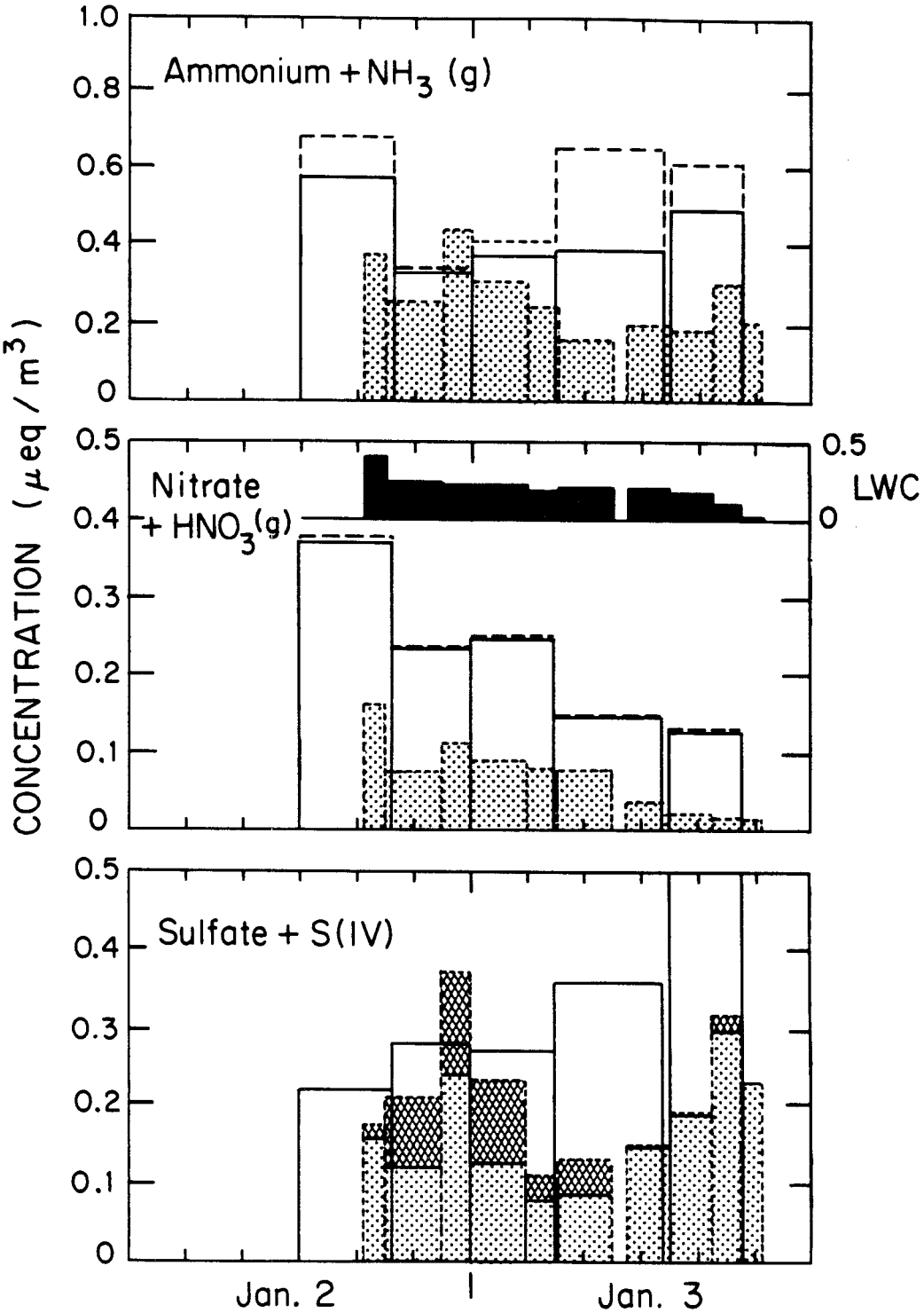

Figure 7.15a Total (line) and fogwater (shaded) concentrations of N(-III), N(V), and sulfur species at Bakersfield Airport site. Gaseous species (dashed line) and liquid water content (black) also shown. Fogwater S(IV) indicated with heavy shading.

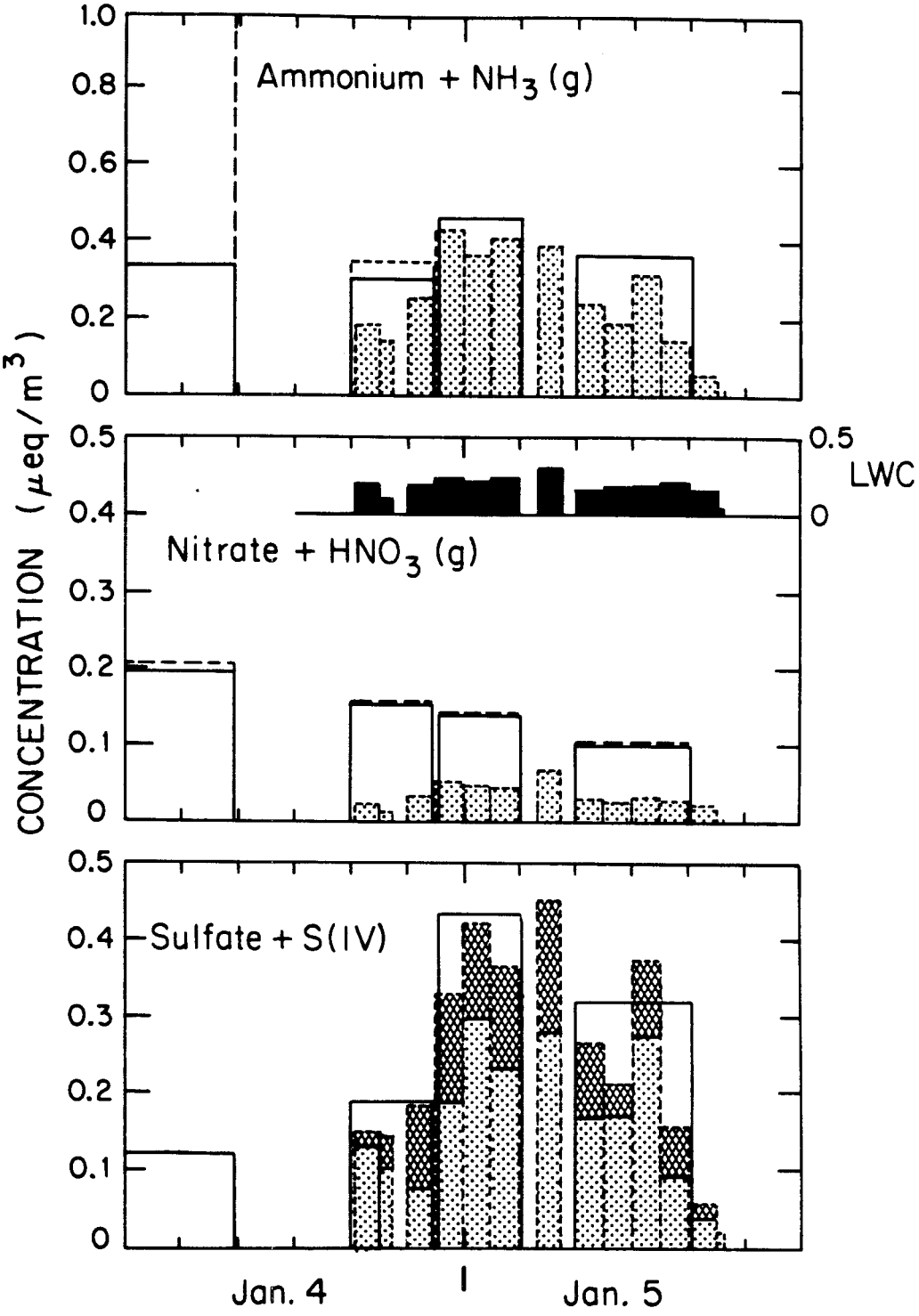

Figure 7.15b Same as 7.15a.

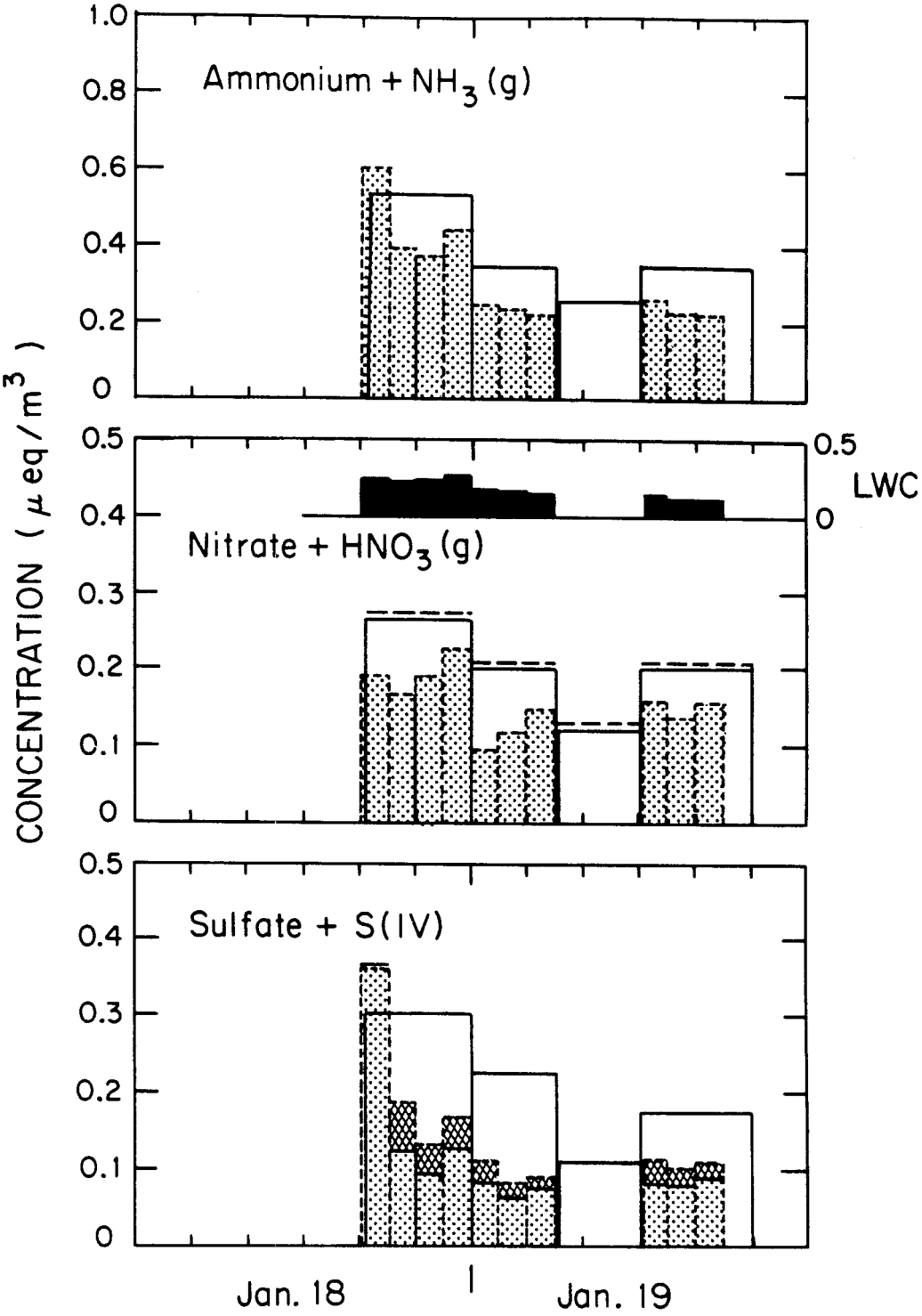

Figure 7.15c Same as 7.15a. Fog during each episode was continuous; omissions in fog parameter were due to breaks in sampling.

Figure 7.16 (following page)

Fog scavenging efficiency (or fraction) for major ions versus liquid water content (LWC) at San Joaquin Valley sites.

Fraction is calculated as $(C)_f$ / (C), with solute in fog, $(C)_f = [C]_f$ x LWC, and total solute, (C), measured by filter.

(a,b,c) Fog scavenging for each ion shown; values for individual samples are shown grouped with shading. Low pH (< 5) samples are indicated with an asterisk. San Joaquin Valley 1984 data taken from Jacob et al. (1985a); low pH samples for McKittrick fogs.

(d) Aggregated solute scavenging fraction, calculated as $(\Sigma C)_f$ / (Σ C), versus LWC for all sampling sites.

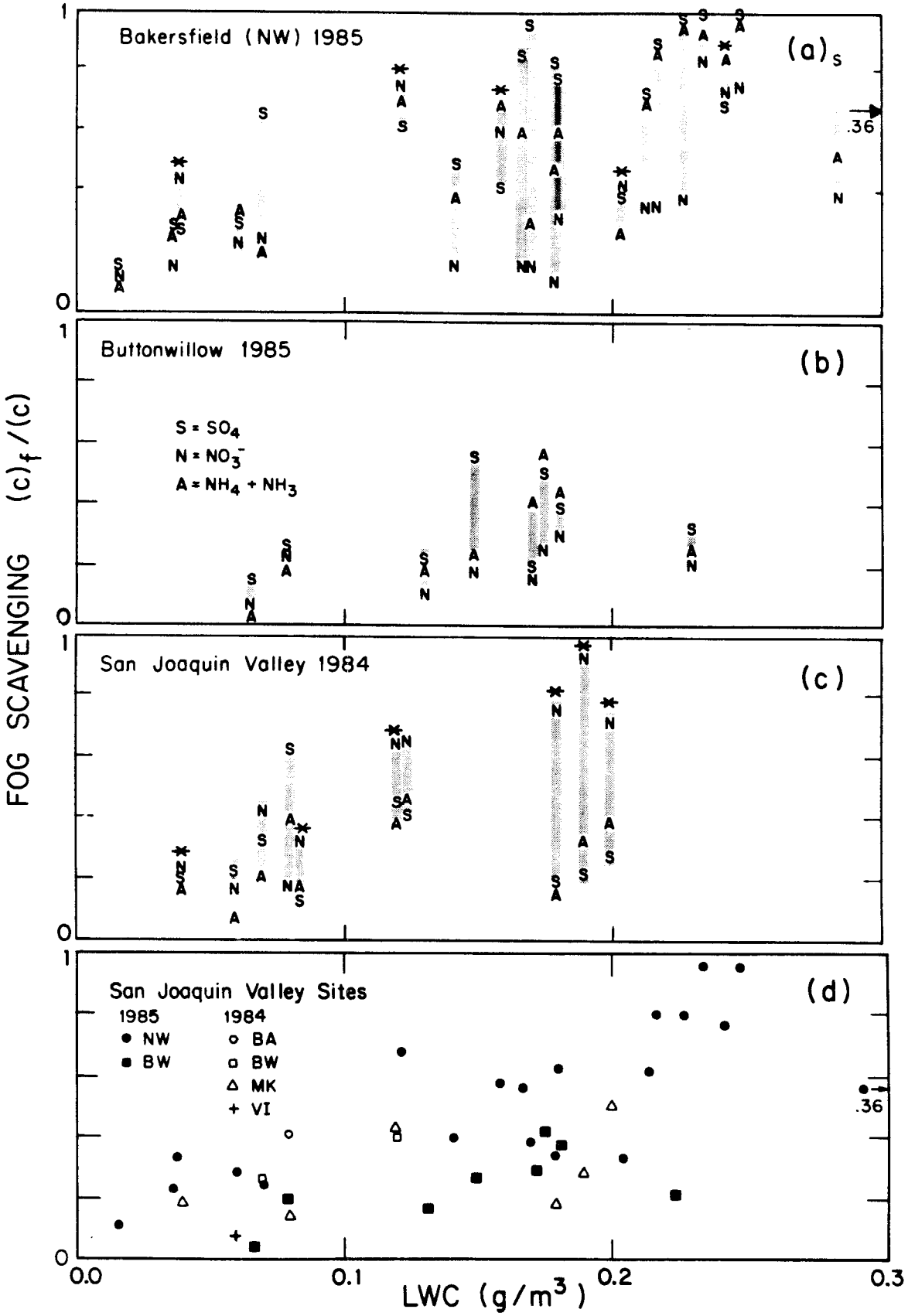
Bakersfield (NW) 1985
(a)s
.36
Buttonwillow 1985
(b)
S = SO4
N = NO3-
A = NH4 + NH3
San Joaquin Valley 1984
(c)
San Joaquin Valley Sites
(d)
1985
NW
BW
1984
BA
BW
MK
VI
.36
FOG SCAVENGING (c)f/(c)
LWC (g/m3)
0.0
0.1
0.2
0.3
0
1

acidity, the higher the fraction of N(V) that will be readily incorporated into the droplet phase (see Chapter 2.2). This in part describes the processes that produced higher N(V) fog scavenging at low pH on 19 and 20 January and in 1984 data for acidic fogs at McKittrick (shown in Figure 7.16c). However, HNO_3 monitored on the afternoons of 19 and 20 January was only 10% of total N(V), while the observed increase in N(V) scavenging was generally greater. This suggests that, in addition to partitioning into the gas phase, for acidic fogs N(V) was not as much associated with the smaller interstitial aerosol fraction as it was for the high pH regime. Following depletion of ammonia gas, scavenging of ambient nitric acid by alkaline dust particles would lead to a coarse aerosol nitrate (Wolfe, 1984).

Importance of LWC. The effect of rising LWC on solute scavenging will depend primarily on the size distribution of fog condensation nuclei (FCN) (i.e., the fraction of hygroscopic aerosol of sizes that can be activated under ambient conditions; see Chapter 2.2). Simple dilution has been noted to effect changes in the aqueous concentrations in coastal southern California fogwater (Waldman et al., 1982; Munger et al., 1983). This was attributed to the accretion of water vapor on existing droplets and indicated that fairly thorough scavenging of FCN had preceeded.

In general, lower supersaturations (SS_v) are achieved in radiation fog compared to coastal fogs (Gerber, 1981; Hudson, 1984; also see Roach et al., 1976). This can result in a lower fraction of activated FCN. When a large portion of the FCN spectrum is unactivated, the formation of new droplets causes a sharp increase in droplet surface area for water vapor accretion. Relative changes in size are most rapid for

smaller droplets, and appreciable liquid water will be added concurrent to the incorporation of FCN solutes into the droplet spectrum.

In a few cases, $(C)_f$ was observed to remain conservative for moderated changes of LWC (see Figure 7.15); however, changes in $(C)_f$ followed LWC excursions in the majority of samples. For the limited data from previous radiation fog studies, nonconservative solute contents were also observed in fogwater loading time-series (Fuzzi et al., 1984; Jacob et al., 1984b). Simultaneous measurements of total solute loadings were not made in those studies.

The scavenging of S(VI) and N(-III) was strongly affected by LWC. For N(-III), ammonia gas absorption was an important factor in fogs between pH 5 and 7. The uptake of sulfur species appeared to depend the availability of large, readily activated sulfate aerosol. In addition, S(IV) in fogwater samples constituted an important fraction of fog-scavenged sulfur in high pH samples. The absorption of $SO_2(g)$ by droplets and subsequent oxidation to sulfate or chemical stabilization (for example, by aldehydes; Munger et al., 1984) will enhance this fraction.

In the acidic regime, N(V) scavenging increased for denser fogs. The data for nonacidic fogs showed a flat response to LWC for $F_{N(V)}$ indicating that, once the easily activated nitrate aerosols were scavenged, little additional solute was incorporated in fog. The residual nitrate apparently remained in the interstitial aerosol, not activated by SS_v reached in these SJV fogs. It is unlikely that size alone was the factor causing these nitrate-containing nuclei not to become activated. For a pure nitrate aerosol, this would have indicated $D_{dry} < 0.1$ μm (see Chapter 2.1.1), and nitrate mass is not generally

found at such small sizes (Appel et al., 1978; Wolfe, 1984). Instead, the explanation must be related to the reduction in nuclei activity caused by insoluble fractions (Saxena and Fischer, 1984). However, data were not available to determine the size distributions of solutes or insoluble fractions in the two cases.

Calculation of an aggregated solute scavenging fraction, $F_T = \Sigma(C)_f/\Sigma(C)$, demonstrates the dependence on LWC (Figure 7.16d). A monotonic rise in F_T with increasing LWC was found for SJV fogs overall. Other factors, such as atmospheric loading and proximity to sources contribute to scavenging efficiency. Theoretical considerations aside, scatter in the data and the many undetermined factors precluded identifying more than a qualitative relationship from these field measurements.

Effect of Droplet-Phase SO_2(g) Oxidation. Distinct contrasts can be seen in the concentration versus time series of 3, 5, and 19 January events in Figure 7.15. Substantial $(S(IV))_f$ was found in fogwater on the former two dates with pH 5 to 7 (a & b). Within hours of fog formation in both events, the total loading of sulfur started to rise sharply. At the same time, N(V) and N(-III) atmospheric loadings were declining or remained constant. Fogwater pH remained high throughout the 2-3 January event, and most of the morning samples remained above pH 6. Early morning filter samples showed a substantial influx of S(VI) that was not matched by N(V) or N(-III). This increase was due to in situ production of sulfate in the fog, since preexisting sulfate aerosol had been depleted rapidly by deposition. Although the observed increase at the site could have been due to advection from the nearby oil fields, any emissions of SO_2 in the area had been discharged directly into an

environment of widespread fog as well. Therefore, regardless of the mode of transport, S(VI) that was measured in the 3 January samples must have been newly formed.

The fogwater pH steadily decreased on the morning of the 5 January, and samples with pH < 4 were measured in dense fog, prior to the dissipation period. The S(IV) concentration remaining in solution was supersaturated with respect to SO_2 gas-aqueous equilibrium. High [S(IV)] may be due to a slow dissociation of HMSA in acid solution (Kok et al., 1985; Munger et al., 1985).

A systematic decline in pollutant loading was observed on 18-19 January (Figure 7.15c). After the first several hours of sampling, fogwater pH dropped below 4. Ammonia gas had been depleted earlier, and local emission rates were insufficient to neutralize the droplet acidity. On 20 January, pH < 3 was measured. In fogwater monitored on 18-19 January, the concentrations of CH_2O were in excess of those for S(IV); the opposite was the case for samples measured on 2-3 and 4-5 January (see Appendix C.1). These data were consistent with more rapid sulfate production for fogwater with free S(IV), given the slow kinetics of HMSA dissociation (Kok et al., 1985; Munger et al., 1985).

Sulfate and nitrate aerosol are hygroscopic, and their activation in fog will largely depend on their size (Pruppacher and Klett, 1978). Thus, the degree of aerosol scavenging is an indirect measure of FCN size; with more solute in the larger (i.e., more easily activated) size fractions, a greater proportion will be nucleated into droplets. Even though NO_x and SO_2 emissions come largely from the same sources in the SJV, their conversion to aerosol nitrate and sulfate follow different mechanisms.

Heisler and Baskett (1981) measured a significant increase in coarse (>2.5 μm) sulfate fraction during wintertime sampling versus other seasonal data for the SJV. For fogs in the neutral to basic regime, we observed that S(VI) scavenging was greater than N(V). This difference may be attributed to differences in predominant sizes of the hygroscopic aerosol. As a proposed mechanism, S(IV) oxidation that occurred in fog added S(VI) directly to droplet spectra. Higher pH fogwater promoted greater SO_2 solubility and S(IV) stability than for acidic fogs. At the same time, fog deposition led to the depletion of the largest droplets (Lovett, 1984) and their associated solute content. The fog scavenging of sulfur was not matched by similar N(V) replenishment in the droplet phase; production of N(V) in the fog environments has been determined to be very limited (Jacob and Hoffmann, 1983). When the remaining droplets evaporated, the result was a net increase in the aerosol sulfate associated with FCN (i.e., the larger size fraction). With greatly diminished particle deposition after the fog ended, subsequent fog formation occurred on a FCN spectrum enriched with sulfates.

7.4.2 Mass Balance Analysis

When widespread stagnation suppresses convective transport out of the basin, the accumulation of pollutants may proceed. The processes which control the fates of primary emissions in the atmosphere are varied and complex (e.g., McRae, 1981). Nonetheless, profiles of concentrations versus time have been reasonably interpreted based on continuous-flow stirred-tank considerations of pollutant inputs and removal pathways (Jacob et al., 1985a). This accumulation of atmospheric constituents will be governed by (a) primary emissions; (b) in situ transformations (production or loss terms); (c) intrabasin circulation; (d) ventilation; and, (e) removal by deposition to ground surfaces. The mixing height, H, controls the volume in which these processes occur. For example, mass balances for S(IV) and S(VI) may be described as follows:

$$\frac{d(S(IV))}{dt} = \frac{E_{SO_2}}{H} - k_s(SO_2) - \nabla\cdot((SO_2)\vec{V}) - \frac{(SO_2)}{v\,\tau} - V_d' \frac{(SO_2)}{H} \qquad (7.3)$$

(a) (b) (c) (d) (e)

$$\frac{d(S(VI))}{dt} = + k_s(SO_2) - \nabla\cdot((SO_4^{2-})\vec{V}) - \frac{(SO_4^{2-})}{v^{\tau}} - V_d\frac{(SO_4^{2-})}{H} \qquad (7.4)$$

where E is an areal emission rate (e.g., mol $m^{-2}h^{-1}$); k_s is a pseudo first-order rate constant for S(IV) oxidation (h^{-1}); $\vec{V}$ is the horizontal transport vector (m h^{-1}); and τ_v (h) is the characteristic time for vertical ventilation. Deposition velocities (m h^{-1}) will depend on the species and the phase: gas, aerosol, or droplet. Similar expressions may be formulated for nitrogen species, although the chemical

transformations involving NO_x species are far more complex.

Under wintertime stagnation conditions in the southern SJV, τ_v is 3-5 days or more (Reible, 1982). Tracer releases during the winter of 1984-85 verified that ventilation times were $\geq$3 days for the period of widespread fog in early January (Shair, unpublished data, 1985).

Time scales characteristic of emission and deposition rates are strongly dependent on mixing height. Mixing heights during stagnation episodes are generally 200 to 800 m above the valley floor. In the years we have conducted studies, widespread fog occurred when the mixing height was $\leq$400 m (cf, Jacob et al., 1984, 1985a). For low wind speeds, deposition velocities can range from $\sim$0.05 cm s^{-1} for submicron aerosol to $\sim$2 cm s^{-1} for fog droplets or reactive gases. Hence, τ_d, given as H/V_d, can range from >3 d to <3 h. For sulfate aerosol, this is largely dependent on the presence or absense of fog.

A characteristic time for S(IV) oxidation may be given as k_s^{-1}. In reality, in situ transformations are rarely simple first-order processes dependent on reactant concentration alone. These rates will depend on the nature and concentration of oxidants, metals and other catalytic components, in addition to pH and LWC (Hoffmann and Jacob, 1984). The pseudo first-order rate constant is a convenient means to parameterize the observed atmospheric kinetics. The oxidation reactions are thought to proceed more rapidly in fog, although interpretations of our prior SJV field measurements have not statistically verified this assertion (Jacob et al., 1984; 1985a). Using values in a range given by Jacob et al. ($1 < k_s < 10$ % h^{-1}), the time for 1/e reduction of (S(IV)) is estimated between 2 and 24 hours.

Emission inventories for SO_2, NO_x, and NH_3 have been determined by

Jacob et al. (1985a) for the southern San Joaquin valley as 192, 190, and 79 ton d^{-1}, respectively. These translate to 29, 20, and 22 μeq $m^{-2}h^{-1}$ when expressed as areawide averages. These units correspond to the secondary products, hence SO_2 yields 2 equivalents per mole. A characteristic time, taken here as the time required for emissions to replace a given atmospheric loading of pollutant C, would be expressed as $\tau_E = (C)H/E$. Given $(SO_2) \sim 10$ ppb and $H \sim 400$ m, the calculated τ_E for SO_2 is on the order of 12 h; for $H \sim 200$ m, it is only half of this value. This term is useful to assess whether a balance of sources and sinks has been achieved. For example, when the time scales for loss terms are longer than τ_E, atmospheric concentrations will increase. Higher concentrations of NO_x are clear indication that its loss rates are slower than either SO_2 or NH_3, since sources are comparable.

During dense fog, deposition becomes the predominant loss term for secondary aerosol species. Flux measurements to surrogate surfaces demonstrated that removal from the atmosphere can be very rapid. In Table 7.4, characteristic times have been calculated for deposition during dense fog. These values were determined from the total solute fluxes, mixing heights, and average aerosol concentrations measured during the individual events. The characteristic removal times were calculated to be 6 to 12 hours for these periods with the exception of N(V). As discussed previously, during the sampling periods of acidic atmospheric condition (19 and 20 January), there was a distinct increase in the relative scavenging efficiency for nitrate species into fogwater. The deposition rate for N(V) also increased for these events, and this can be seen in much lower τ_d for nitrate, compared to the earlier fog events when $pH \geq 5$. Between the occurrences of fog, aerosol deposition

Table 7.4

CHARACTERISTIC REMOVAL TIMES[a]
AND PRODUCTION RATES[b]
IN SAN JOAQUIN VALLEY FOGS

	Duration[c] (hr)	H[d] (m AGL)	τ_d (hr) NH_4^+	τ_d (hr) NO_3^-	τ_d (hr) SO_4^{2-}	Rate (ppb hr^{-1}) E_A	Rate (ppb hr^{-1}) E_N	Rate (ppb hr^{-1}) E_S
Bakersfield (NW)								
28 Dec 84	4	200	6	15	6	1.5	0.3	0.5
2-3 Jan 85	14	240	6	10	6	1.5	0.4	0.7
3-4 Jan 85	12	210	6	42	6	0.6	0.1	0.2
4-5 Jan 85	12	230	11	27	7	0.8	0.1	0.5
14 Jan 85	3	500	12	22	7	0.7	0.2	0.4
18-19 Jan 85	14	300	6	4	5	1.5	1.1	0.5
20 Jan 85	7	350	11	9	12	0.9	0.7	0.3
Buttonwillow (BW)								
2-3 Jan 85	17	290	7	6	7	2.3	1.4	0.3
3-4 Jan 85	17	260	10	17	9	0.5	0.2	0.1
4-5 Jan 85	15	230	7	18	6	0.9	0.2	0.2

a. Characteristic time for pollutant removal:

$\tau_d = H/V_d$, where V_d = Flux/(Ambient Concentration).

b. Production or emission rate to balance deposition rates:

E_C = Deposition/(H x Duration) expressed as NH_3, NO_x and SO_2.

c. Duration of dense fog event.

d. Mixing height at site.

was substantially reduced. Deposition velocities were generally an order of magnitude below in-fog values. Fogs persisted more than 50% of the time during the 2-5 January period. In the absence of production terms, aerosol components would be >90% depleted during protracted fog episodes. However, such a net depletion was not observed; by inference, in situ production rates must have at least equaled the deposition rates.

Advection in this environment is difficult to assess. Wind directions are found to be erratic at valley stations during stagnation episodes (Aerovironment, Inc., 1982). Resultant winds for the early January period were <1 m s^{-1} at all stations; therefore, net cross-valley transport would require ~1 d. Before 1 January, the concentrations of sulfate were uniformly low on both sides of the valley, while after 1 January, higher sulfate values were monitored in Bakersfield than to the west or north (see Figure 7.7). The spatial gradient for sulfate across the valley indicated that advection of sulfate aerosol was a less prominent term for 2-5 January. Clearly, deposition of sulfate was more rapid than its transport away from the source region.

However, nitrate aerosol concentrations were uniform throughout the sampling network at that same time. Similar temporal variations were also observed at all valley sites, except McKittrick, which was above the inversion base throughout that period. Because the deposition rates measured for nitrate were much lower than for sulfate during that period, it was possible for more complete mixing to occur. This uniformity was probably aided by more widely dispersed emissions of NO_x.

For the two sites in the Bakersfield (NW and BA) area,

concurrently measured aerosol concentrations agreed within 20% in most cases (12 for NO_3^- and 10 for SO_4^{2-} of 13 sampling periods), even though temporal variations spanned a factor of 5. Simultaneous peaks in NH_3 concentrations were further indication of the spatial homogeneity at the two sites. However, it is impossible to state unequivocally that short-term changes at a particular site were due to in situ transportation rather than localized transport. Without a network of higher spatial resolution, the interpretion of sequential S(VI) or N(V) concentrations in terms of a generalized continuity-equation analysis would be moot. Nonetheless, advection of pollutant species away from this source region must represent a sink over longer time scales.

As a lower limit, we calculated production rates necessary to balance removal rates of aerosol species measured during fog (i.e., production rate ≈ deposition flux/H). Essentially, this equates terms (b) and (e) in Eqn. (7.b) and neglects the rest. Production rates have been calculated in units of the primary emissions, NH_3, NO_x, and SO_2 (Table 7.4). Sulfur dioxide values measured at the fog-study sites were mostly $\leq$10 ppb, although spatial variability of SO_2, especially near the oil fields make the calculation of an areal average concentration questionable. Assuming 10 ppb for the gaseous concentration, the pseudo first-order S(IV) oxidation rates were calculated to be 2-7% hr^{-1}. Considering that advection represented a loss term for the Bakersfield area, the total sinks were likely to have been even greater than measured by deposition alone. The calculated S(IV) oxidation rates at Buttonwillow were not as high; assuming that SO_2 concentrations were a factor of 2 lower at the BW site compared to Bakersfield, the rates of S(IV) oxidation at the two locations in dense fog were similar. The

S(VI) production and deposition rates should have been comparable at these sites, since the meteorological conditions were similar (i.e., widespread nighttime fog and afternoon haze).

Caveat. Fog deposition as measured to flat surfaces or buckets represented a lower limit to rates occurring in the southern San Joaquin. The Bakersfield Airport site was chosen for its open and featureless terrain. In many ways, it was characteristic of wintertime land use in this region. The majority of the southern SJV is cropland (43%) or rangeland (44%), while the remaining portions of the valley are orchard (8%), residential/commercial (4%) or forest (1%) (Jacob, 1985). In areas of tall (dense or sparse) canopy or buildings, wind profiles would be more turbulent, and canopy-top wind speeds would be closer to the NWS sensor (10 m AGL) values rather than to the low values measured close to the open field. Simply the presence of bare trees will substantially increase the surface area for pollutant deposition. Droplet impaction becomes important under these circumstances (Lovett, 1984). In such cases, $V_{d,fog}$ (hence V_d) would be adjusted upwards. Fog deposition may therefore lead to even higher pollutant influx to these areas. While this may be of significance for certain receptor areas, we believe the effect is relatively unimportant to the conclusion regarding the dominance of sedimentation and the range of deposition values we have reported.

Finally, these measurements were specific to particles and droplets. While we are convinced that dry deposition of SO_2, for example, did not significantly contribute to our measurements, this sink for S(IV) may be substantial in its own right. Moreover, scavenging of SO_2 by droplets aided in its deposition during fog. In addition to the

chemical transformations of S(IV), the removal of SO_2 to surfaces, though not studied herein, is an important term in the overall sulfur budget. Also, HNO_3 deposition may have an important role in N(V) removal under certain circumstances.

Precipitation Scavenging. In the case of the rainfall event, the total amount of material brought to the ground was 2-5 times greater than the overburden of pollutants in the air (i.e., ambient concentration x mixing height) prior to the rain. After the initial loading of accumulated pollutants was washed (or ventilated) out of the air mass, additional nitrate and sulfate must come from the transformation of primary emissions. Low SO_2 concentrations were measured during the rainfall period; simultaneously, sulfate deposition was large. This clearly indicated a period in which rapid S(IV) oxidation must have occurred in the presence of an aqueous phase. The smaller fluxes of nitrate suggested either a lower rate of N(V) formation for the same period or less efficient precipitation scavenging of secondary nitrate. However, without a detailed knowledge of atmospheric mixing and below-cloud processes, in situ oxidation rates cannot be determined from these rainfall measurements.

Comparison with the Prior SJV Studies (1982-83 and 1983-84). The efficacy of fog in scavenging gaseous and aerosol species and in enhancing their removal can cause it to be the dominant factor controlling ambient levels reached by pollutants during wintertime stagnation episodes. The measurements of depositional flux during winter 1985 stagnation periods illustrated the differences between episodes with dense fog and those when fog was absent. Detailed fogwater and air quality data were also collected for the winters of

1983 and 1984 as part of our field programs. These former studies included periods with and without dense, widespread fog. Concentrations of the major species in the fogwater, aerosol, and gas phases are compared in Table 7.5. The comparison is limited to parameters measured in the Bakersfield area. The values presented were for periods of stagnation, conditions, when mixing heights were low and concentrations in the air had achieved apparent steady state levels. Given the characteristic time for fog deposition and the emissions rates of sulfur species, a steady state for sulfate could be attained in less than one day. For nonfoggy intervals, this requires much longer, and true steady-state levels may not have been fully reached before a change in meteorological conditions occurred. It is readily acknowledged that this type of comparison is far from conclusive since other factors have not been evaluated, e.g., daytime insolation, oxidant concentrations, wind trajectories, etc. We use it primarily to point out relationships that these unique data sets have provided.

Mixing heights were comparible during the six episodes. A disparity between two regimes is readily apparent with respect to aerosol nitrate and sulfate concentrations. The highest values were associated with the periods, 2-6 January 1983 and 2-6 January 1984. These were periods of low clouds when fog was absent. Average concentrations of particulate sulfate exceeding California state air quality standards (25 $\mu g\ m^{-3}$ or 520 $neq\ m^{-3}$) were monitored during both these episodes. Periods of dense fog led to lower concentrations of particulate loading -- air of better quality despite lesser visiblity.

The 2-5 January 1985 samples complemented a data set of predominantly acidic fogs measured in January 1983. Simultaneous

Table 7.5

FOGWATER AND AIR QUALITY DURING WINTER STAGNATION EPISODES
CALTECH FOG STUDIES: 1983-1985

		Fogwater[a]						Aerosol[b]			Gas[c]				
	H[d]	pH	NH_4^+	NO_3^-	SO_4^{2-}	%	NH_4^+	NO_3^-	SO_4^{2-}	NH_3	NO_x	SO_2	DENSE FOG	Ref.
December 1982[e]														
30-31	200	4.1	1600	850	800	62	600	280	280	na	100	20	Yes	I
January 1983[e]														
2-6	400	--	--	--	--		900	300	900	na	100	25	No	I
6-8	350	3.9	2600	900	1600	38	600	150	450	na	150	20	Yes	"
11-15	300	3.6	1400	700	900	57	300	40	200	na	200	40	Yes	"
January 1984[e]														
2-6	350	--	--	--	--		1000	400	700	1	100	20	No	II
January 1985[f]														
2-5	200	4.9	1200	250	800	32	350	190	210	9	25	10	Yes	III
							(380)	(210)	(270)	(6)	(100)	(10)		
18-20	300	3.9	1900	1000	600	22	510	280	320	<0.5	(50)	(10)	Yes	"

a. Volume-weighted aqueous concentration: meqiv L^{-1}; % percent S(IV)/Total S in fogwater.
b. Unit: nano-equiv m^{-3}. c. Unit: ppb (= 44 nano-mol m^{-3} at 1^oC).
d. Mixing height (m) AGL Bakersfield Aiport.
e. 1982, 1983, and 1984 measurements at downtown Bakersfield (BA) site.
f. 1985 measurements at Bakersfield Airport (NW) site; ( ) give BA values for same period.
Ref. I. Jacob et al., 1984; II. Jacob et al., 1985a; III. This study.

fogwater and aerosol measurements were not made during the 1982-83 study, but the ionic ratios indicate that N(V) scavenging was as high or higher than for sulfate during these low pH fogs. Both N(V) and S(VI) production were important sources of atmospheric acidity. Emission inventories for all producers during the selected periods are not available, but data on the east side suport an assumption that year-to-year differences in primary emitter operations was not a factor (D. Anderson, Texaco, Inc., private communication). There was no obvious effect of acidity on SO_2 levels; gaseous concentrations were uniformly low for both years. It is interesting to note that dissolution of S(IV) in fogwater was not reduced in the acidic regime of the earlier year (Table 7.5), as might be expected from gas-aqueous equilibria.

The primary determinant for acidity is most likely the relative N(-III) abundance, as discussed in Jacob et al. (1985a) with respect to spatial patterns in the region. In an ammonia source region, there are factors which can suppress or accelerate NH_3 release. Temperature, moisture, and land cover may be primary factors. Dawson (1977) showed that there are strong dependencies for soil release of ammonia; it increases with temperature and with soil moisture up to 20% saturation, then decreases. Uptake by vegetation can drastically reduce the net release of ammonia (Denmead et al., 1976). Hutchinson et al. (1982) measured ammonia release from a large cattle feedlot and found lower fluxes when the surface was wet from rain. However, this was offset by greater-than-average rates while the surface dried.

The 2-5 January 1985 episode distinquished itself in one important regard. During other episodes, no daytime clearing occurred. Heavy overcast generally continued after the fog lifted. On the afternoons of

the early January 1985 episode, there were periods of hazy sunshine and appreciable warming (see Table 6.1). This warming would promote ammonia release, especially from feedlots and agricultural soils. Despite the cooling, the ground would maintain higher temperature at nighttime as well. On the other hand, the acidification of the SJV atmosphere would be promoted by cooler and steady overcast conditions. Ammonia release also may be reduced in post-rainfall periods. At the same time, this moisture is often important in sustaining widespread fog.

7.5 SUMMARY

Atmospheric pollutant behavior was studied in the southern San Joaquin Valley of California during periods of dense fog and stagnation. Fluxes to the ground of water soluble species were determined by surrogate-surface collectors, while simultaneous fogwater and aerosol composition measurements were made. Repetitive, widespread fogs were observed only when the base of the temperature inversion was 150 to 400 m above the valley floor. Dense fogs (visual range <200 m) lasted 10-17 h at sampling locations. Atmospheric loadings of water soluble species in the aerosol and droplet phases were composed almost entirely of NH_4^+, NO_3^-, and SO_4^{2-}. Substantial concentrations of free acidity (H^+) and S(IV) species were occasionally measured in fogwater samples. Appreciable gaseous ammonia was often present, but only when atmospheric acidity was absent. Deposition samples were similarly dominated by these same major ions, although relative higher contributions were made by soil dust species (still far below the major species).

Substantially higher deposition rates for aerosol species occurred during fogs compared to measurements during nonfoggy periods. Rates for major ions were enhanced by factors of 5 to 20. Deposition velocities, V_d and $V_{d,fog}$, were calculated by normalizing measured deposition rates by the total and droplet-phase atmospheric loadings, respectively. The proportions of deposited solute for major ions were closely matched to the fogwater composition. The median value of $V_{d,fog}$ was approximately 2 cm s^{-1} with measurements in the range of 1 to 5 cm s^{-1}. Calculations of $V_{d,fog}$ were sensitive to liquid water content (LWC) data which have large uncertainties ($\pm$50%) for absolute values. An operationally-defined LWC was used for which the relative error was

smaller (±20%). For the data, no correlation with LWC was found for droplet solute deposition. The rates were comparable to the terminal settling velocities of typical fog droplets.

Volatile loss of ammonium ion from the fog-wetted deposition surfaces was indicated. This loss may have been enhanced by the fallout of calcareous dust onto the hydrophobic collector surface. However, under normal conditions, NH_3 loss via volatilization of fog-deposited ammonium aerosol can also be expected to some degree.

There were substantially greater deposition rates (V_d) for sulfate than nitrate in nonacidic fogs. This has been attributed to more efficient scavenging of soluble sulfur species by fog droplets. Sulfate deposition (V_d) during fog was in the range of 0.5 to 2 cm s^{-1} with a median value about 1 cm s^{-1}; the nitrate rate was generally 50% below that for sulfate. In nonacidic fogs, nitrate scavenging was uniformly low, while the fraction of sulfate incorporated into the droplet-phase rose with increasing LWC. For pH < 5, the fraction of fogwater nitrate also increased. Higher atmospheric acidity is believed to have altered N(V) partitioning prior to fog formation, allowing higher $HNO_3(g)$ concentration in the pre-fog air. Nitric acid was subsequently scavenged in the presence of fog. However, the measured $HNO_3(g)$ was not as high as the observed enhancement of N(V) scavenging. Depletion of gaseous ammonia accompanied the period of higher atmospheric acidity and low pH fog, and this is believed to have caused a reduction in the formation of smaller NH_4NO_3 aerosol. In the absence of detectable $NH_3(g)$, newly formed N(V), that was apparently incorporated into a coarser aerosol fraction, was more readily scavenged in fog.

The shallow and poorly ventilated mixed layer of the SJV under the

intense temperature inversion represented a reactor of limited volume. A comparison was made between the mass deposited and the overburden of pollutants (i.e., mixing height x ambient loading). For S(VI) and N(-III) species, 2-3 times the apparent overburden were deposited during prolonged fogs. This should have caused substantial depletion of atmospheric concentrations; however, this was not observed. Steady aerosol sulfate concentrations required S(IV) oxidation to proceed rapidly. A pseudo first-order constant for SO_2 oxidation was calculated to be in the range of 2-7% hr^{-1}. The true rate may be several times higher, since, (a) the reactant concentrations were frequently below the value (10 ppb) used to make the calculation, (b) the depositional flux measurements tacitly neglected the sink due to droplet impaction, and (c) advective loss terms in the mass balance were neglected in the source region. In similar fashion, ammonia emissions were calculated to be approximately 1 ppb h^{-1} in order to balance solute removal in fog.

The two processes important for the determination of ambient sulfate concentration were removal by deposition and production by S(IV) oxidation. Measurements made during three wintertime fog/aerosol studies were summarized to consider the overall mass balances during stagnation episodes. This data set supported the hypothesis that fog deposition lowered the ambient concentrations of aerosol sulfate and nitrate during stagnation periods, compared to periods with no fog. However, the importance of dry deposition of SO_2, sulfate production in haze aerosol, and the contribution of impaction to droplet fluxes needs to be more fully investigated. Finally, the conditions under which fogwater acidity was high were related to factors favoring ammonia release from sources (e.g., higher soil moisture and temperatures).

RECOMMENDATIONS FOR FUTURE RESEARCH

In this thesis, important aspects of fog-related pollutant deposition have been addressed. The work described herein characterized fogwater compositions, identified the range of deposition rates, and outlined the important processes that affect fog deposition. Still, more research is needed to fully assess the "acid fog" problem and to understand the full extent and effect of material fluxes associated with it. The following areas may be fruitful for further investigation.

Droplet size-compositional relationships: The treatment of fog deposition as a flux of large particles is limited because of the uncertainty in droplet size-composition relationships. Improvement in size-resolved fogwater sampling techniques must be made. For examples, this might be attempted by bulk collection of fractionated fogwater samples or by filtration of size-segregated droplets. Attention should also be focused on the total loading of materials in the fog-impacted atmosphere, its partitioning into the various phases, and the processes that lead to scavenging by droplets.

Interactions and reactions of fogwater at deposition surfaces: By careful characterization of ambient fogwater composition, we have provided needed exposure data for the assessment of environmental effects. An area that should be studied further is the interactions of various deposited material at vegetative and material surfaces. For example, suspension and fallout of alkaline particles may be important to the chemical balance at fog-wetted surfaces. Furthermore, material

cycles in the soil also need to be investigated with respect to pollutant fluxes in the fog environment.

Better techniques for liquid water content (LWC) measurement and understanding the effect of LWC on fog processes: We tested a number of alternative methods and, like other investigators, found a great deal of uncertainty in the determination of LWC (Chapter 5). We observed significant temporal and spatial variability in fog density in the field that contributed to the monitoring difficulties. Better time-resolved and more accurate measurements of LWC, especially in the vicinity of receptor surfaces, are needed. The dynamics of droplet behavior near the ground also should be studied because bulk-phase properties may not adequately describe the conditions most relevant to deposition.

More extensive monitoring of fog composition and deposition: In certain environments, deposition to surrogate-surface collectors may adequately quantify the magnitude of fog-derived inputs. This was utilized in the case of San Joaquin Valley radiation fogs (Chapter 7). However, more complex terrains, canopies, and micrometeorologies, such as coastal mountains or developed regions, would require application of deposition models (e.g., Lovett, 1984; Davidson et al., 1982; Slinn, 1982) to generalize measurements as those from early studies described in Chapter 2.

Relationships of fog composition and deposition with precursor air quality parameters that are routinely monitored: Because the fog-phase loading of pollutants is a subset of the total concentration, fogwater

composition is dependent on the precursor air quality and the efficiency of scavenging processes. Attempts to correlate fogwater and air quality parameters may be useful in developing predictive relationships. In similar fashion, attempts should be made to relate pollutant fluxes in fog environments with other records of deposition, for example, dry-side deposition collectors used in precipitation studies.

Investigation of small volume precipitation events in urban regions such as Los Angeles: The present research (Chapter 6) identified a disproportionate contribution to pollutant deposition caused by light, spring rains in the Los Angeles basin. More detailed monitoring during stratus cloud events would provide useful insights concerning their chemistry, physics, and meteorology. A mass balance for emissions within the Los Angeles basin should be made under these conditions.

REFERENCES

(except Chapters 4 and 6)

Aerovironment, Inc., 1982, Development, validation, and application of the AVKERN model, Report AV-FR-80/603R , Aerovironment, Inc., Pasadena, CA.

Appel, B. R., Kothny, E. L., Hoffer, E. M., Hidy, G. M., and Wesolowski, J. J., 1978, Sulfate and nitrate data from the California Aerosol Characterization Experiment (ACHEX), Environ. Sci. Tech. 12, 418-425.

Appel, B. R., Wall, S. M., Tokiwa, Y., and Haik, M., 1980, Simultaneous nitric acid, particulate nitrate, and acidity measurements in ambient air, Atmos. Environ. 14, 549-554.

Axelrod, H. D., Teck, R. J., and Lodge, J. P., Jr., 1971. Further study on prefilter interference for sulfur dioxide measurements, J. Air. Pollut. Control Ass. 21, 218.

Azevedo, J. and Morgan, D. L., 1974, Fog precipitation in coastal California forests, Ecology 55, 1135-1141.

Baboolal, B., Pruppacher, H. R., and Topalian, J. H., 1981, A sensitivity study of a theoretical model of SO_2 scavenging by water drops in air, J. Atmos. Sci. 38, 856-870.

Bache, D. H., 1979, Particulate transport within plant canopies: II. Prediction of deposition velocities, Atmos. Environ. 13, 1681-1687.

Barrett, E., Parungo, F. P., and Pueschl, R. F., 1979, Cloud modification by urban pollution: A physical demonstration, Meteorol. Resch. 32, 136-149.

Bassett, M. E. and Seinfeld, J. H., 1983, Atmospheric equilibrium model of sulfate and nitrate aerosols, Atmos. Environ. 17, 2237-2252.

Baumgardner, D., 1983, An analysis and comparison of five water droplet measuring instruments, J. Clim. Appl. Meteor. 22, 891-910.

Bischoff, W. D. Paterson, V. L., and Mackenzie, F. T., 1984, Geochemical mass balance for sulfur- and nitrogen-bearing acid components: Eastern United States, in Geological Aspects of Acid Deposition (Acid Precipitation Series - Vol. 7, ed. O. P. Bricker), Boston: Butterworth Publishers, 1-21.

Brewer, R. L., Ellis, E. C., Gordon, R. J., and Shepard, L. S., 1983, Chemistry of mist and fog from the Los Angeles urban area, Atmos. Environ. 17, 2267-2271.

Brimblecombe, P., 1978, "Dew" as a sink for SO_2, Tellus 30, 151-157.

Brown, R. and Roach, W. T., 1976, The physics of radiation fog: II. A numerical study, Quart. J. R. Meteor. Soc. 102, 335-354.

Brown, R., 1980, A numerical study of radiation fog with an explicit formulation of the microphysics, Quart. J. R. Meteor. Soc. 106, 781-802.

Bruce, D., Bruce, C. W., Yee, Y. P., Cahenzli, L., and Burket, H., 1980, Experimentally determined relationship between extraction coefficient and liquid water content, Appl. Optics 19, 3355-3360.

Brun, R. J., Lewis, W., Perkins, P. J., and Serafini, J. S., 1955, Impingement of cloud droplets on a cylinder and procedure for measuring liquid water content and droplet sizes in supercooled clouds by rotating multicylinder method, NACA Report 1215.

Cadle, S. H., Countess, R. J., and Kelly, N. A., 1980, Nitric acid and ammonia concentrations in urban and rural locations, Atmos. Environ. 16, 2501-2506.

Castillo, R. A., Jiuso, J. E., and McLaren, E., 1983, The pH and ionic composition of stratiform cloud water, Atmos. Environ. 17, 1497-1505.

Cerni, T. A., 1983, Determination of the size and concentration of cloud drops with an FSSP, J. Clim. Appl. Meteor. 22, 1346-1355.

Chamberlain, A. C., 1967, Transport of Lycopodium spores and other small particles to rough surfaces, Proc. R. Soc. 296, 45-70.

Chamberlain, A. C. and Chadwick, R. C., 1972, Deposition of spores and other particles on vegetation, Ann. Appl. Biol. 71, 141-158.

Chamberlain, A. C., 1975, The movement of particles in plant communities, in Vegetation and the Atmosphere. (ed. J. L. Monteith), London: Academic Press, 155-203.

Chylek, P., 1978, Extinction and liquid water content of fogs and clouds, J. Atmos. Sci. 35, 296-300.

Corrandini, C. and Tonna, G., 1980, The parameterization of the gravitational water flux in fog models, J. Atmos. Sci. 37, 2535-2539.

Csanady, G. T., 1963, Turbulent diffusion of heavy particles in the atmosphere, J. Atmos. Sci. 20, 201-208.

Dasch, J. M., 1983, A comparison of surrogate surfaces for dry deposition collection, in Precipitation Scavenging, Dry Deposition, and Resuspension. (ed. H. R. Pruppacher et al.), Amsterdam: Elsevier Science, 883-902.

Dasgupta, P. K., De Cesare, K., and Ullrey, J. C., 1980, Determination of atmospheric sulfur dioxide without tetrachloromercurate(III) and the mechanism of the Schiff reaction, Anal. Chem. 52, 1912-1922.

Daum, P. H., Schwartz, S. E., and Newman, L., 1984, Acidic and related constituents in liquid water stratiform clouds, J. Geophys. Res. 89, 1447-1458.

Davidson, C. I., 1977, Deposition of trace metal-containing aerosol on smooth surfaces and on Avena fatua (wild oat grass), Ph.D. thesis, California Institute of Technology, Pasadena, CA.

Davidson, C. I. and Friedlander, S. K., 1978, A filtration model for aerosol dry deposition: Application to trace metal deposition from the atmosphere, J. Geophys. Res. 83, 2342-2352.

Davidson, C. I., Miller, J. M., and Pleskow, M. A., 1982, The influence of surface structure on predicted particle dry deposition to natural grass canopies, Water, Air and Soil Pollut. 18, 25-43.

Davies, C. N. and Subari, M., 1982, Aspiration above wind velocity of aerosols with thin-walled nozzles facing and at right angles to the wind direction, J. Aerosol Sci. 13, 59-71.

Dawson, G. A., 1977, Atmospheric ammonia from undisturbed land, J. Geophys. Res. 82, 3125-3133.

Denmead, O. T., Freney, J. R., and Simpson, J. R., 1976, A closed ammonia cycle within a plant canopy, Socl. Biol. Biochem. 8, 161-164.

Derrick, M. and Moyers, J., 1981, Precise and sensitive water soluble ion extraction method for aerosol samples collected on polytetrafluoroethylene filters, Anal. Lett. 14A, 1637-1642.

Dionex Corporation, 1981, Determination of anions in acid rain, Application note 31, Dionex Corp., Sunnyvale, CA.

Dollard, G. J. and Unsworth, M. H., 1983, Field measurements of turbulent fluxes of wind-driven fog drops to a grass surface, Atmos. Environ. 17, 775-780.

Dolske, D. A. and Gatz, D. F., 1985, A field intercomparison of methods for the measurement of particle and gas dry deposition, J. Geophys. Res. 90, 2076-2084.

Environmental Protection Agency, 1971, Guide for Air Pollution Avoidance, Appendix B, History of Episodes, Rep. PH-22-78-32, Washington, D.C., 123-135.

Falconer, P. D. (ed.), 1981, Cloud chemistry and meteorological research at Whiteface Mountain: Summer 1980, Publ. No. 806, Atmospheric Sciences Research Center, State University of New York, Albany.

Firket, J., 1936, Fog along the Meuse Valley, Trans. Faraday Soc. 32, 1192-1197.

Fortune, C. R. and Dellinger, B., 1982, Stabilization and analysis of S(IV) aerosols in environmental samples, Environ. Sci. Tech. 16, 62-66.

Fuzzi, S., Castillo, R. A., Jiusto, J. E., and Lala, G. G., 1984, Chemical composition of radiation fog water at Albany, New York, and its relationship to fog microphysics, J. Geophys. Res. 89D, 7159-7164.

Garland, J. A., 1971, Some fog droplet size distributions obtained by an impactor method, Quart. J. R. Meteor. Soc. 97, 483-494.

Garland, J. A., Bronson, J. R., and Cox, L. C., 1973, A study of the contribution of air pollution to visibility in a radiation fogk Atmos. Environ. 7, 1079-1092.

Gerber, H. E., 1981, Microstructure of a radiation fog, J. Atmos. Sci. 38, 454-458.

Gertler, A. W. and Steele, R. L., 1980, Experimental verification of the linear relationship between IR extinction and liquid water content of clouds, J. Appl. Meteor. 19, 1314-1317.

Goodman, J., 1977, The microstructure of California coastal fog and stratus, J. Appl. Meteorol. 16, 1056-1067.

Granett, A. L. and Musselman, R. C., 1984, Simulated acid fog injures lettuce, Atmos. Environ. 18, 887-891.

Haines, B., Stefani, M., and Hendrix, F., 1980, Acid rain: threshold of leaf damage in eight plant species from a southern Appalachian forest succession, Water, Air and Soil Pollut. 14, 403-407.

Hale, G. M. and Querry, M. R., 1973, Optical constants of water in the 200-nm to 200-micron wavelength region, Appl. Opt. 12, 555-563.

Hartley, G. S. and Brunskill, R. T., 1958, Reflection of water drops from surfaces, in Surface Phenomena in Chemistry and Biology (ed. S. F. Danielli et al.). Oxford: Pergamon Press.

Hegg, D. A. and Hobbs, P. V., 1982, Measurements of sulfate production in natural clouds, Atmos. Environ. 16, 2663-2668.

Heisler, S. and Baskett, R., 1981, Particle sampling and analysis in the California San Joaquin Valley, Report CARB-RR-81-14, California Air Resources Board, Sacramento, CA.

Hering, S. V. and Blumenthal, D. L., 1983, Fog sampler intercomparison study: Data volume, Prepared for Coordinating Research Council, 219 Perimeter Center Pkwy., Atlanta, GA.

Hering, S. V. and Blumenthal, D. L., 1985, Fog sampler intercomparison study: Final report, Prepared for Coordinating Research Council, 219 Perimeter Center Pkwy., Atlanta, GA.

Hidy, G. M. et al. (ed.), 1980, The Character and Origins of Smog Aerosols (Adv. Environ. Sci. Tech. Vol. 9), New York: John Wiley & Sons, 776pp.

Hoffmann, M. R. and Jacob, D. J., 1984, Kinetics and mechanisms of the catalytic oxidation of dissolved sulfur dioxide in aqueous solution: An application to nighttime fog-water chemistry, in SO_2, NO and NO_2 Oxidation Mechanisms: Atmospheric Consideration (Acid Precipitation Series - Vol. 3, ed. J. G. Calvert), Boston: Butterworth Publishers, 101-172.

Hoffmann, M. R., 1984, Comment on acid fog, Environ. Sci. Technol. 18, 61-64.

Holets, S. and Swanson, R. N., 1981, High-inversion fog episodes in central California, J. Appl. Meteorol. 20, 890-899.

Hori, T. (ed.), 1953, Studies on Fog in Relation to Fog-Preventing Forest, Sapporo/Japan: Tanne Trading Co., 399 pp.

Houghton, H. G. and Radford, W. H., 1938, On the measurement of drop size and liquid water content of fogs and clouds, Papers in Phys. Oceano. and Meteor. Vol. VI, No 4, Cambridge: Massachusetts Institute of Technology, 31 pp.

Houghton, H. G., 1955, On the chemical composition of fog and cloud water, J. Meteorol. 12, 355-357.

Hudson, J. G. and Rogers, C. F., 1984, Interstital CCN measurements related to mixing in clouds. Presented at 9th Intern. Cloud Physics Conference, August 21-28, Tallinn, USSR.

Hudson, J. G., 1984, CCN measurements within clouds, J. Climat. Appl. Meteor. 23, 42-51.

Huebert, B. J. and Robert, C. H., 1985, The dry deposition of nitric acid to grass, J. Geophys. Res. 90D, 2085-2090.

Humphrey, R. E., Ward, M. H., and Hinze, W., 1970, Spectrophotometric determination of sulfite with 4,4-dithiopyridine and 5,5-dithiobis(2-nitrobenzoic acid), Anal. Chem. 42, 698-702.

Hutchinson, G. L., Mosier, A. R., and Andre, C. E., 1982, Ammonia and amine emissions from a large cattle feedlot, J. Environ. Qual. 11, 288-293.

Israel, R. and Rosner, D. E., 1983, Use of a generalized Stokes number to determine the aerodynamic capture efficiency of Non-Stokesian particles from a compressible gas flow, Aerosol Sci. Tech. 2, 45-51.

Jacob, D. J. and Hoffmann, M. R., 1983, A dynamic model for the production of H^+, NO_3^-, and SO_4^{2-} in urban fog, J. Geophys. Res. 88C, 6611-6621.

Jacob, D. J., 1985, The origins of inorganic acidity in fogs, Ph.D. thesis, California Institute of Technology, Pasadena, CA.

Jacob, D. J., Wang, R-F. T., and Flagan, R. C., 1984a, Fogwater collector design and characterization, Environ. Sci. & Technol. 18, 827-833.

Jacob, D. J., Waldman, J. M., Munger, J. W., and Hoffmann, M. R., 1984b, A field investigation of physical and chemical mechanisms affecting pollutant concentrations in fog droplets, Tellus 36B, 272-285.

Jacob, D. J., Munger, J. W., Waldman, J. M., and Hoffmann, M. R., 1985a, The H_2SO_4-HNO_3-NH_3 system at high humidities and in fogs: I. Spatial and temporal patterns in the San Joaquin Valley of California, J. Geophys. Res. (in press).

Jacob, D. J., Waldman, J. M., Munger, J. W., and Hoffmann, M. R., 1985b, The H_2SO_4-HNO_3-NH_3 system at high humidities and in fogs: II. Comparison of field data with thermodynamic calculations, J.

Geophys. Res. (in press).

Jacob, D. J., Waldman, J. M., Munger, J. W., and Hoffmann, M. R., 1985c, Chemical composition of fogwater collected along the California coast, Environ. Sci. Technol. 19, 730-735.

Jacob. D.J., Waldman, J.M., Haghi, M., Hoffmann, M.R., and Flagan R.C., 1985d, Instrument to collect fogwater for chemical analysis, Rev. Sci. Inst. 56, 1291-1293.

Jenkin, M. E., 1984, An investigation into the enhancement of deposition of hygroscopic aerosols to wet surfaces in a wind tunnel, Atmos. Environ. 18, 1017-1024.

Jensen, D. R., Jeck, R., Trusty, G. and Schacher, G., 1983, Intercomparison of Particle Measuring Systems, Inc.'s particle-size spectrometers, Opt. Engin. 22, 746-752.

Jiusto, J. E., 1974, Remarks on visibility in fog, J. Appl. Meteor. 13, 608-610.

Jiusto, J. E. and Lala, G. G., 1983, Radiation fog field programs - recent studies, Publ. No. 869, Atmospheric Sciences Research Center, State University of New York, Albany.

John, W. and Reischl, G., 1980, A cyclone for size-selective sampling of ambient air, J. Air Poll. Control Assoc. 30, 872-876.

Katz, U., 1980, A droplet impactor to collect liquid water from laboratory clouds for chemical analysis, in Communications à la VII Conference Internationale sur la Physique des Nuages, Laboratoire Associe de Meteorologie Physique, Aubiere, France, 697-700.

Kennedy, J. B. and Neville, A. M., 1976, Basic Statistical Methods for Engineers and Scientists, 2nd edition, New York: Harper and Row, Publ., 198-220.

Kerfoot, O., 1968, Mist precipitation on vegetation, For. Abst. 29, 8-20.

Knollenberg, R. G., 1981, Techniques for probing cloud microstructure, in Clouds, Their Formation, Optical Properties, and Effects, (eds. Hobbs, P. V. and Deepak, A.), London: Academic Press, 495pp.

Kok, G. L. Gitlin, S. N., and Lazrus, A. L., 1985, Kinetics of the formation and decomposition of hydroxymethanesulfonate, submitted to J. Geophys. Res.

Ledbury, W. and Blair, E. W., 1925, The partial formaldehyde vapour pressure of aqueous solutions of formaldehyde. Part II., J. Am. Chem. Soc. 127, 2832-2839.

Lee, I-Y. and Pruppacher, H. R., 1977, A comparative study on the growth of cloud drops by condensation using an air parcel model with and without entrainment, Pageoph. 115, 523-545.

Lee, Y.-N. and Schwartz, S. E., 1981, Evaluation of the rate of uptake of nitrogen dioxide by atmospheric and surface liquid water, J. Geophys Res. 86C, 11971-11983.

Legg, B. J. and Price, R. I., 1980, The contribution of sedimentation to aerosol deposition to vegetation with a large leaf index, Atmos. Environ. 14, 305-309.

Liljestrand, H. M., 1980, Atmospheric transport of acidity in Southern California by wet and dry mechanisms, Ph.D. thesis, California Institute of Technology, Pasadena, CA.

Liljestrand, H. M. and Morgan, J. J., 1981, Spatial variations of acid precipitation in Southern California, Environ. Sci. & Technol. 15, 333-338.

Lindberg, S. E., Harriss, R. C., and Turner, R. R., 1982, Atmospheric deposition of metals to forest vegetation, Science 215, 1609-1611.

Lovett, G. M., 1984, Rates and mechanisms of cloud water deposition to a subalpine balsam fir forest, Atmos. Environ. 18, 361-371.

Mack, E. J. and Pilié, R. J., 1975, "Fog Water Collector," U.S. Patent No. 3889532.

Mack, E. J. and Katz, U., 1976, The characteristics of marine fog occurring off the coast of Nova Scotia, Report CJ-5756-M-1, Calspan Corp., Buffalo, NY.

Mack, E. J. Katz, U., Rogers, C. W., et al., 1977, An investigation of the meteorology, physics, and chemistry of marine boundary layer processes, Report CJ-6017-M-1, Calspan Corp., Buffalo, NY.

Manane, Y. and Noll, K. E., 1985, Characterization of large particles at a rural site in the eastern United States: Mass distribution and individual particle analysis, Atmos. Environ. 19, 611-622.

Martell, A. E. and Smith, R. M., 1977, Critical Stability Constants, Vol 3, New York: Plenum.

May, K. R. and Clifford, R., 1967, The impaction of aerosol particles on cylinders, spheres, ribbons and discs, Ann. Occup. Hyg. 10, 83-95.

May, K. R. , 1967, Physical aspects of sampling airborne microbes, in Airborne Microbes (eds. P. H. Gregory and J. L. Monteith), 60-80.

McRae, G. J., 1981, Mathematical modeling of photochemical air pollution, Ph.D. thesis, California Institute of Technology, Pasadena, CA. ,

Merriam, R. A., 1973, Fog drip from artificial leaves in a fog wind tunnel, Water Res. Res. 9, 1591-1598.

Mrose, H., 1966, Measurements of pH, and chemical analyses of rain-, snow-, and fog-water, Tellus 18, 266-270.

Munger, J. W., Jacob, D. J., Waldman, J. W., and Hoffmann, M. R., 1983, Fogwater chemistry in an urban atmosphere, J. Geophys. Res. 88C, 5109-5121.

Munger, J. W., Jacob, D. J., and Hoffmann, M. R., 1984, The occurrence of bisulfite-aldehyde addition products in fog- and cloudwater, J. Atmos. Chem. 1, 335-350.

Munger, J. W., Tiller, C., and Hoffmann, M. R., 1985, Identification of hydroxymethanesulfonate in fogwater, submitted to Science.

Myers, J. N., 1968, Fog, Sci. Amer. 219, 75-82.

Nagel, J. F., 1956, Fog precipitation on Table Mountain, Quart. J. R. Meteor. Soc. 82, 452-460.

Naruse, H. and Maruyama, H., 1971, On the hygroscopic nuclei in cloud droplets, Papers in Meteor. and Geophys. 22, 1-21.

Nash, T., 1953, The colorimetric estimation of formaldehyde by means of the Hantzsch reaction, Biochem. J. 55, 426-421.

Oberlander, G. T., 1956, Summer fog precipitation on the San Francisco penninsula, Ecology 37, 851-852.

Oddie, B. C. V., 1962, The chemical composition of precipitation at cloud levels, Quart. J. R. Meteor. Soc. 88, 535-538.

Okita, T. , 1968, Concentrations of sulfate and other inorganic materials in fog and cloud water and in aerosol, J. Meteor. Soc. Japan 46, 120-126.

Oura, H. , 1953, On the capture of fog particles by a forest, in Studies on Fog in Relation to Fog-Preventing Forest (ed. T. Hori), Sapporo/Japan: Tanne Trading Company, 239-252.

Peterson, T. W. and Seinfeld, J. H., 1980, Heterogeneous condensation and chemical reaction in droplets -- Application to the heterogeneous atmosphere oxidation of SO_2, in Advances in Environmental Science and Technology - Vol. 10, (eds. Pitts, J. N. and Metcalf, R. L.), New York: John Wiley and Sons, 125-180.

Pilié, R. J., Mack, E. J., Kolmund, W. C., Eadie, W. J., and Rogers, C. W., 1975, The life cycle of valley fog. Part II: Fog microphysics, J. Appl. Meteor. 14, 364-374.

Pinnick, R. G., Jennings, S. G., Chylek, P., and Auvermann, H. J., 1979, Verification of a linear relation between IR extinction, absorption and liquid water content of fogs, J. Atmos. Sci. 36, 1577-1586.

Pinnick, R. G., Garvey, D. M., and Duncan, L. D., 1981, Calibration of Krollenberg FSSP light-scattering counters for measurements of cloud droplets, J. Appl. Meteor. 20, 1049-1057.

Pruppacher, H. R. and Klett, J. D., 1978, Microphysics of Clouds and Precipitation. Amsterdam: Reidel, pp 9-27, 136-148, and 412-421.

Reible, D. D., 1982, Investigations of transport in complex atmospheric flow systems, Ph.D. thesis, California Institute of Technology, Pasadena, CA.

Reible, D. D., Shair, F. H., Smith, T. B., and Lehrman, D. E., 1984, The origin and fates of air pollutants in California's San Joaquin Valley. I. Winter., Atmos. Environ. (in press).

Richards, L. W., Anderson, J. A., Blumenthal, D. L., Duckhorn, S. C., and McDonald, J. A., 1983, Characteristics of reactants, reaction mechanisms, and reaction products leading to extreme acid rain and acid aerosol conditions in Southern California, Report RR-83-6, California Air Resources Board , Sacramento, CA.

Ridder, T. B., Buisherd, T. A., Reijnders, H. F. R., Hart, J. J., and Slanina, J., 1985, Effects of storage on the composition of noncomponents in rainwater samples, Atmos. Environ. 19, 759-762.

Roach, W. T., 1976, On the effect of radiative exchange on the growth by condensation of a cloud or fog droplet, Quart. J. R. Meteor. Soc. 102, 361-372.

Roach, W. T., Brown, R., Caughey, S. J., Garland, J. A., and Readiness, C. J., 1976, The physics of radiation fog: I - A field study, Quart. J. R. Meteor. Soc. 102, 313-333.

Russell, A. G. , 1983, Analysis of oxalic acid impregnated filters for ammonia determination, Open file Report 83-1, Environmental Quality Laboratory, California Institute of Technology, Pasadena, CA.

Russell, A. G. and Cass, G. R., 1984, Acquisition of regional air quality data model validation for nitrate, sulfate, ammonium ion and their precursors, Atmos. Environ. 18, 1815-1827.

Russell, A. G., McRae, G. J. and Cass, G. R., 1983, Mathematical modeling of the formation and transport of ammonium nitrate aerosol, Atmos. Environ. 17, 949-964.

Saxena, V. K. and Fisher, G. F., 1984, Water solubility of cloud-active aerosols, Aerosol Sci. Tech. 3, 335-344.

Scherbatskoy, T. and Klein, R. M., 1983, Response of spruce and birch foliage to leaching by acidic mists, J. Environ. Qual. 12, 189-195.

Schlesinger, W. H. and Reiners, W. A., 1974, Deposition of water and cations on artificial foliar collectors in fir krummholz of New England mountains, Ecology 55, 378-386.

Schwartz, S. E., 1984, Gas-aqueous reactions of sulfur and nitrogen oxides in liquid-water clouds, in SO_2, NO and NO_2 Oxidation Mechanisms: Atmospheric Considerations (Acid Precipitation Series - Vol. 3, ed., Calvert, J. G.), Boston: Butterworth, 173-208.

Schwartz, S. E. and Freiberg, J. E., 1981, Mass-transport limitation to the rate of reaction of gases in liquid droplets: Application to oxidation of SO_2 in aqueous solutions, Atmos. Environ. 15, 1129-1144.

Schwartz, S. E. and White, W. H., 1981, Solubility equilibria of the nitrogen oxides and oxyacids in dilute aqueous solution, in Advances in Environmental Science and Engineering, Vol. 4 (eds. Pfafflin, J. R. and Ziegler, E. N.), New York: Wiley-Interscience, 1-45.

Sehmel, G. A., 1980, Particle and gas dry deposition: A review, Atmos. Environ. 14, 883-1011.

Slinn, W. G. N., 1982, Predictions for particle deposition on vegetative canopies, Atmos. Environ. 16, 1785-1794.

Smith, R. M. and Martell, A. E., 1976, Critical Stability Constants Vol. 4, New York: Plenum.

Smith, R. V. and Erhardt, P. W., 1975, Nash determination for formaldehyde in the presence of bisulfite, Anal. Chem. 47, 2454-2462.

Solorzano, L., 1967, Determination of ammonia in natural waters by the phenol hypochlorite method, Limnol. Oceanogr. 14, 799-801.

Stelson, A. W. and Seinfeld, J. H., 1982, Relative humidity and temperature dependence of the ammonium nitrate dissociation constant, Atmos. Environ. 16, 983-992.

Stumm, W. and Morgan, J. J., 1981, Aquatic Chemistry, 2nd edition, New York: John Wiley & Sons, 121-221.

Taylor, G. I., 1917, The formation of fog and mist, Quart. J. R. Meteor. Soc. 43, 241-268.

Thom, A. S., 1975, Momentum, mass and heat exchange of plant communities, in Vegetation and the Atmosphere (ed. J. L. Monteith). London: Academic Press, 57-110.

Thomas, M. D., Hendricks, R. H., and Hill, G. R., 1952, Some impurities in the air and their effects on plants, in Air Pollution: Proc. of U.S. Tech. Conf. (ed. L. McCabe). New York: McGraw-Hill, 41-47.

Thorne, P. G., Lovett, G. M., and Reiners, W. A., 1982, Experimental determination of droplet impaction on canopy components of balsam fir, J. Appl. Meteor. 21, 1413-1416.

van de Hurst, 1957, Light scattering by small particles, New York: John Wiley & Sons, 470 pp.

Vanderberg, J. J. and Knoerr, K. R., 1985, Comparison of surrogate surface techniques for estimation of sulfite dry deposition, Atmos. Environ. 19, 627-635.

Vogelmann, H. W., Siccama, T., Leedy, D., and Ovitt, D. C., 1968, Precipitation from fog moisture in the Green Mountains of Vermont, Ecology 49, 1205-1207.

Waldman, J. M., Munger, J. W., Jacob, D. J., Flagan, R. C., Morgan, J. J., and Hoffmann, M. R., 1982, Chemical composition of acid fog, Science 218, 677-680.

Waldman, J. M., Munger, J. W., Jacob, D. J., and Hoffmann, M. R., 1985, Chemical characterization of stratus cloudwater and its role as a vector for pollutant deposition in a Los Angeles pine forest, Tellus 37B, 91-108.

Wattle, B. J., Mack, E. J., Pilie, R. J., and Harley, J. T., 1984, The role of vegetation in the low-level water budget in fog, Report 7096-M-1, Arvin/Calspan Adv. Tech. Center, Buffalo, NY.

Whitby, K. T., 1978, The physical characteristics of sulfur aerosols, J. Aerosol Sci. 12, 135-159.

Whitby, K. T. and Sverdrup, G. M., 1980, California aerosols: Their physical and chemical characteristics, in The Character and Origin of Smog Aerosols. (Adv. Environ. Sci. Tech. Vol. 9, eds. Hidy, G. M. et al.), New York: John Wiley & Sons, 477-518.

Wisniewski, J., 1982, The potential acidity associated with dews, frosts and fogs, Water, Air and Soil Pollut. 17, 361-377.

Wolfe, G. T., 1984, On the nature of nitrate in coarse continental aerosols, Atmos. Environ. 18, 977-981.

Yosida, Z. and Kuroiwa, D., 1953, Wind force on a conifer tree and the quantity of fog water thereby captured, in Studies on Fog in Relation to Fog-Preventing Forest (ed. Hori, T.), Sapporo/Japan: Tanne Trading Company, 261-278.

Yosida, Z., 1953, General survey of the studies on fog-preventing fores, in Studies on Fog in Relation to Fog-Preventing Forest (ed. Hori, T.), Sapporo/Japan: Tanne Trading Company, 1-23.

APPENDIX A
THEORETICAL BACKGROUND: INFRARED EXTINCTION METHOD FOR LIQUID WATER CONTENT MEASUREMENTS

The liquid water content (LWC) in fogs and clouds has been measured or calculated by a number of direct and indirect techniques. These techniques attempt to characterize the mass of condensed atmospheric water within a sample volume. As in Equation A.1, droplets are assumed to be spherical and are sufficiently dilute to have density identical to pure water (ρ_w):

$$LWC = \rho_w \frac{\pi}{6} \int n(D_o)\, D_o^3\, dD_o \qquad (A.1)$$

where, $n(D_o)$ is the droplet size distribution (e.g., $cm^{-3}\mu m^{-1}$).

Attempts for simple correlations of LWC with visiblity have been made for decades (see Jiusto, 1974). However, visible light attenuation is strongly dependent upon droplet spectra and especially sensitive to the smaller sizes. Particles with dimensions similar to the wavelength of light are the most effective with respect to scattering, but they do not contribute as greatly to LWC. Indeed, Garland et al. (1973) determined that roughly half the extinction coefficient (λ=0.55 μm) measured in fog was due to unactivated haze aerosol.

Correlation between LWC and attenuation of light at longer, e.g., infrared, wavelengths has greater potential because it is less sensitive to the smaller, interstitial aerosol. Infrared (IR) transmission is related to a wavelength dependent extinction parameter as indicated:

$$\frac{I(\lambda)}{I_o(\lambda)} = \exp\left[-k_e(m,\lambda)\, L\right] \qquad (A.2)$$

or,

$$k_e = \frac{1}{L} \ln \frac{I_o}{I} \qquad (A.3)$$

where,

I, I_o are the attenuated and incident beam intensities;

k_e is the volume extinction coefficient;

m is the complex refractive index of water for wavelength λ;

and, L is the optical path length.

From single particle scattering (van de Hurst, 1957), k_e can be expressed as a function of $n(D_o)$ and the normalized extinction cross section or efficiency, $Q_{ext}(m,\lambda,D_o)$:

$$k_e(m,\lambda) = \frac{\pi}{4} \int Q_{ext}(m,\lambda,D_o)\, n(D_o)\, D_o^2\, dD_o \qquad (A.4)$$

Q_{ext} is a unique function of m and the wave number, x ($= \pi D_o/\lambda$), shown in Figure A.1 for λ=0.55 and 9.4 μm. Chlyek (1978) suggested that k_e can be related to LWC by applying a linear fit to Q_{ext}, where c is the slope of Q_{ext} versus x. Approximating $Q_{ext} \simeq cx$ in Eqn A.4 gives k_e as a function of D_o^3. By comparison with the integral form for LWC (Eqn A.1), the extinction coefficient can be expressed:

$$k_e = \frac{3\,\pi\,c\,LWC}{2\,\rho\,\lambda} \qquad (A.5)$$

and finally,

$$LWC = \frac{2\,\rho\,\lambda}{3\,\pi\,c\,L} \ln \frac{I_o}{I} \qquad (A.6)$$

The derivation of Eqn A.6 shows it to be fairly insensitive to changes in droplet spectra. The limitations of the linear fit ($Q_{ext} \simeq cx$) occur for larger droplets. The maximum in Q_{ext} occurs at $D_o \simeq 25$ μm. The extinction due to larger sizes would be overestimated, hence, LWC

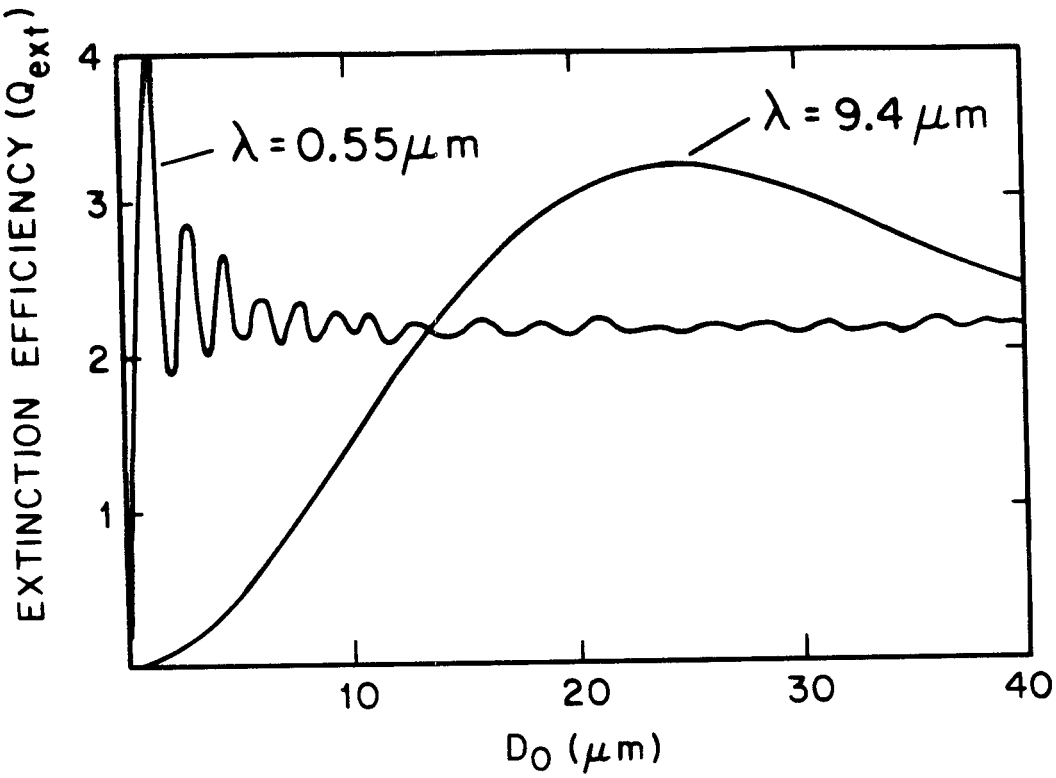

Figure A.1. Light extinction cross section or efficiency, Q_{ext}, as a function of droplet diameter and the complex refractive index for water: m=1.333-0i (0.55 μm) and m=1.247-0.0433i (9.4 μm) (Hale and Querry, 1973).

contributed from such droplets would be underestimated. Within that range, the LWC can be calculated from measurements of IR extinction over a known path length and the value of c taken from Figure A.1. A fit to the curve up to D_o 25 μm gave c=0.42 (r^2=0.96). For λ=9.4 μm, the scaling factor in Eqn A.6 was calculated to be 5/L.

Pinnick et al. (1979) showed that fog droplet spectra reported in the literature gave the linear relationship between LWC and IR extinction predicted by Eqn A.6. They found very close agreement for data taken under a variety of conditions. Radiation fog droplet spectra showed slightly better accord because they generally contain smaller droplets. Verifications have also been made in laboratory experiments (Gertler and Steele, 1980; Bruce et al., 1980) and in field studies in radiation fog (Jiusto and Lala, 1983) where comparison was made with filtration determinations or measured droplet size distributions. Again, good agreement was reported over a wide range of LWC. Not only was the linear relationship found to hold, but the empirical proportionality coefficients were very close to the theoretical fit given above.

APPENDIX B.

HENNINGER FLATS FOGWATER DATA

1. Spring 1982 - RAC Samples:

Caltech Laboratory Results

*** HENNINGER FLATS FOG DATA - JUNE 1982 ***

Henninger Flats Fog - 11 June 1982 — Checked: 3/20/83 Jed

	Start	Stop	min	mL	pH	H	Na	K	NH4	Ca	Mg	Cl	NO3	SO4	S(IV)	CH2O	-/+
						micro-equivalents/liter									micro-mol/l		
1	7:30	8: 0	30	25.0	3.21	617.	186.	32.	297.	109.	53.	118.	781.	350.	10.0	600.	0.966
2	8: 0	8:30	30	10.0	3.06	871.	310.	40.	467.	132.	55.	132.	1311.	539.	-0.1	920.	1.057
3	8:40	8:52	12	1.0	2.97	1072.	-1.	-1.	689.	-1.	-1.	485.	1986.	804.	-0.1	-0.	1.860
Vol-Wt Mean (LWC=0.167)					3.15	700.	221.	34.	355.	116.	53.	132.	962.	415.	10.0	691.	1.020

Henninger Flats Fog - 12 June 1982 — Checked: 3/20/83 Jed

	Start	Stop	min	mL	pH	H	Na	K	NH4	Ca	Mg	Cl	NO3	SO4	S(IV)	CH2O	-/+
						micro-equivalents/liter									micro-mol/l		
1	2:10	3: 0	50	16.0	2.79	1622.	200.	16.	537.	196.	60.	101.	1918.	657.	16.5	99.	1.017
2	3: 0	3:55	55	14.0	2.69	2042.	368.	27.	641.	224.	107.	123.	2685.	958.	22.5	111.	1.105
3	3:55	4:55	60	20.0	2.81	1549.	254.	19.	576.	132.	74.	230.	1589.	790.	17.0	103.	1.002
4	4:55	5:45	50	20.0	2.85	1413.	143.	10.	517.	76.	43.	112.	1479.	637.	13.0	132.	1.012
5	5:45	6:55	70	26.0	2.87	1349.	104.	10.	457.	138.	34.	83.	1809.	530.	13.0	111.	1.158
6	6:55	7:50	55	18.0	2.82	1514.	82.	8.	430.	77.	26.	94.	1562.	527.	13.0	109.	1.021
7	7:50	8:50	60	30.0	2.75	1778.	143.	12.	734.	79.	42.	126.	2192.	912.	16.0	105.	1.158
8	8:50	10: 0	70	20.0	2.56	2754.	325.	32.	1033.	148.	95.	190.	3021.	1512.	24.0	119.	1.077
Vol-Wt Mean (LWC=0.116)					2.76	1735.	191.	16.	620.	127.	57.	132.	2018.	813.	16.5	111.	1.079

Henninger Flats Fog - 13 June 1982 — Checked: 3/20/83 Jed

	Start	Stop	min	mL	pH	H	Na	K	NH4	Ca	Mg	Cl	NO3	SO4	S(IV)	CH2O	-/+
						micro-equivalents/liter									micro-mol/l		
1	5:45	6:15	30	6.0	3.13	741.	1950.	159.	740.	959.	523.	396.	2355.	982.	35.5	77.	0.736
2	7:50	9: 0	70	16.0	2.66	2188.	1673.	102.	1480.	528.	419.	648.	4540.	2010.	45.0	65.	1.127
3	9: 8	9:45	37	12.0	2.65	2239.	1776.	94.	1900.	400.	437.	660.	4175.	1964.	33.0	69.	0.993
4	9:45	10:15	30	8.0	2.64	2291.	1287.	94.	899.	298.	350.	428.	3535.	1450.	42.0	81.	1.037
Vol-Wt Mean (LWC=0.084)					2.70	2015.	1668.	106.	1384.	509.	426.	574.	3932.	1743.	39.6	71.	1.023

*** HENNINGER FLATS FOG DATA - JUNE 1982 ***

Henninger Flats Fog - 14 June 1982 — Checked: 3/20/83 Jed

	Start	Stop	min	mL	pH	H	Na	micro-equivalents/liter K	NH4	Ca	Mg	Cl	NO3	SO4	micro-mol/l S(IV)	CH2O	-/+
1	6:35	7:15	40	20.0	3.00	1000.	594.	39.	1672.	138.	155.	236.	844.	377.	13.0	99.	0.405
2	7:20	8:10	50	20.0	3.01	977.	290.	16.	522.	61.	77.	215.	1063.	537.	10.5	48.	0.934
3	8:15	9: 0	45	30.0	3.04	912.	367.	65.	1621.	218.	140.	323.	1224.	541.	12.0	58.	0.628
4	9: 0	10: 0	60	15.0	2.86	1380.	121.	78.	1810.	397.	318.	1318.	5607.	4108.	39.0	64.	2.688
5	10: 0	11: 0	60	20.0	2.82	1514.	1220.	67.	1820.	380.	330.	1166.	5336.	3888.	29.0	66.	1.949
6	11: 0	12: 0	60	20.0	2.68	2089.	2465.	161.	3130.	975.	762.	1966.	9500.	6770.	59.5	60.	1.903
Vol-Wt Mean (LWC=0.132)					2.89	1277.	834.	70.	1749.	349.	284.	809.	3645.	2474.	25.5	65.	1.519

Henninger Flats Fog - 15 June 1982 — Checked: 3/20/83 Jed

	Start	Stop	min	mL	pH	H	Na	micro-equivalents/liter K	NH4	Ca	Mg	Cl	NO3	SO4	micro-mol/l S(IV)	CH2O	-/+
1	5:45	7: 0	75	30.0	3.42	380.	52.	11.	546.	39.	19.	54.	493.	249.	10.0	46.	0.761
2	8: 8	8:38	30	0.5	3.22	603.	-1.	-1.	-1.	-1.	-1.	-1.	-1.	-1.	-0.1	-0.	0.000
Vol-Wt Mean (LWC=0.097)					3.42	384.	52.	11.	546.	39.	19.	54.	493.	249.	10.0	46.	0.758

Henninger Flats Fog - 17 June 1982 — Checked: 3/20/83 Jed

	Start	Stop	min	mL	pH	H	Na	micro-equivalents/liter K	NH4	Ca	Mg	Cl	NO3	SO4	micro-mol/l S(IV)	CH2O	-/+
1	9:30	10: 0	30	33.0	3.65	224.	12.	4.	145.	18.	4.	21.	191.	127.	7.0	34.	0.836
2	10: 0	10:35	35	32.0	3.58	263.	6.	3.	165.	10.	2.	35.	219.	139.	7.5	35.	0.876
3	10:35	11:10	35	32.0	3.63	234.	5.	1.	139.	5.	2.	24.	209.	150.	75.0	38.	0.990
4	11:10	11:45	35	50.0	3.54	288.	7.	2.	128.	10.	2.	31.	209.	149.	8.0	39.	0.890
5	12: 8	12:19	11	13.0	3.63	234.	-1.	-1.	-1.	-1.	-1.	-1.	-1.	-1.	8.0	-0.	0.000
Vol-Wt Mean (LWC=0.364)					3.59	255.	7.	3.	142.	11.	2.	28.	207.	142.	21.1	37.	0.899

*** HENNINGER FLATS FOG DATA - JUNE 1982 ***

Henninger Flats Fog - 21 June 1982

Checked: 3/20/83 Jed

	Start	Stop	min	mL	pH	H	Na	K	NH4	Ca	Mg	Cl	NO3	SO4	S(IV)	CH2O	-/+
							micro-equivalents/liter								micro-mol/l		
1	4:25	5:25	60	24.0	2.86	1380.	-1.	-1.	334.	-1.	-1.	85.	749.	284.	10.0	51.	0.652
2	5:25	6:25	60	56.0	2.86	1380.	15.	4.	426.	14.	6.	61.	770.	406.	8.0	56.	0.671
3	6:25	7:10	45	50.0	2.88	1318.	8.	3.	298.	7.	3.	59.	764.	410.	11.0	49.	0.753
4	7:10	7:55	45	40.0	2.85	1413.	11.	4.	590.	11.	3.	40.	931.	477.	8.5	53.	0.713
Vol-Wt Mean (LWC=0.270)					2.86	1370.	12.	4.	414.	11.	4.	59.	803.	406.	9.3	52.	0.700

Henninger Flats Fog - 21-22 June 1982

Checked: 3/20/83 Jed

	Start	Stop	min	mL	pH	H	Na	K	NH4	Ca	Mg	Cl	NO3	SO4	S(IV)	CH2O	-/+
							micro-equivalents/liter								micro-mol/l		
1	20:20	20:50	30	22.0	2.80	1585.	343.	97.	1250.	518.	141.	229.	2243.	1865.	51.5	87.	1.103
2	21:30	22:10	40	32.0	2.86	1380.	116.	32.	1030.	203.	57.	70.	936.	848.	40.0	69.	0.658
3	5:35	6: 5	30	60.0	3.40	398.	19.	9.	226.	13.	6.	46.	411.	221.	7.5	35.	1.011
4	6:35	7: 0	25	44.0	3.32	479.	12.	9.	270.	11.	3.	33.	466.	261.	8.5	36.	0.969
5	7:50	8:20	30	56.0	3.30	501.	8.	5.	296.	11.	2.	-1.	-1.	-1.	85.0	39.	0.000
6	9: 8	9:28	20	30.0	3.20	631.	9.	4.	407.	11.	3.	132.	664.	417.	11.0	56.	1.140
7	10:55	11:15	20	40.0	2.88	1318.	19.	8.	880.	81.	12.	106.	1393.	784.	18.5	69.	0.985
8	12:40	13:10	30	30.0	2.56	2754.	79.	34.	1610.	239.	45.	170.	2143.	1179.	36.0	115.	0.733
9	14: 0	14:30	30	1.5	2.06	8710.	242.	105.	2410.	544.	175.	634.	2857.	1402.	-0.1	-0.	0.402
Vol-Wt Mean (LWC=0.411)					2.99	1012.	54.	19.	640.	99.	24.	99.	1035.	672.	32.3	57.	0.977

HENNINGER FLATS FOGWATER DATA - JUNE 1982

METAL CONCENTRATIONS

			microgram/liter				
Date	#	pH	Fe	Mn	Pb	Cu	Ni
11 June	1	3.21	2040.	121.	230.	-1	128.
	2	3.06	6300.	435.	529.	-1	85.
	3	2.97	-1	-1	-1	-1	-1
12 June	1	2.79	3065.	79.	434.	175.	101.
	2	2.69	1197.	68.	738.	70.	48.
	3	2.81	2271.	61.	788.	81.	111.
	4	2.85	2066.	36.	565.	89.	38.
	5	2.87	3246.	58.	388.	36.	35.
	6	2.82	1057.	41.	365.	44.	185.
	7	7.83	525.	33.	504.	53.	26.
	8	8.83	654.	61.	950.	79.	34.
	9	2.40	2230.	178.	1867.	125.	72.
13 June	1	3.13	-1	-1	-1	-1	-1
	2	2.66	6880.	107.	622.	131.	117.
	3	2.65	2630.	64.	583.	157.	61.
	4	2.64	3990.	63	586	102.	65.
14 June	1	3.00	2350.	66.	271.	160.	49.
	2	3.01	1220.	-1	221.	131.	31.
	3	3.04	802.	-1	373.	561.	64.
	4	2.86	251.	-1	-1	261.	74.
	5	2.82	-1	-1	-1	-1	-1
	6	2.68	-1	-1	-1	-1	-1
15 June	1	3.42	2350.	66.	271	160.	49.
	2	3.22	1220.	-1	221.	131.	31.
17 June	1	3.65	362.	14.	146.	20.	15.
	2	3.58	225.	5.	201.	30.	12.
	3	3.63	200.	5.	172.	16.	7.
	4	3.54	201.	6.	201.	16.	8.
	5	3.63	-1	-1	-1	-1	-1
21 June	1	2.86	3240.	57.	243.	44.	248.
	2	2.86	281.	7.	235.	18.	14.
	3	2.88	306.	4.	176.	7.5	9.
	4	2.85	960.	7.	240.	35.	7.
22 June	1	2.80	3240.	115.	1948.	282.	98.
	2	2.86	2240.	76.	2778.	191.	43.
	3	3.40	365.	10.	428.	40.	29.
	4	3.32	314.	4.	222.	62.	37.
	5	3.30	347.	6.	300.	64.	31.
	6	3.20	281.	5.	326.	39.	15.
	7	2.88	441.	19.	126.	37.	11.
	8	2.56	1350.	30.	110.	107.	66.
	9	2.06	-1	-1	-1	-1	-1

APPENDIX B.

HENNINGER FLATS FOGWATER DATA

2. Spring 1983 - RAC Samples:

Caltech Laboratory Results

*** HENNINGER FLATS FOGWATER DATA - MAY/JUNE 1983

Henninger Flats - 16 May 1983

Checked: 7/11/83

	Start	Stop	min	mL	pH	H	Na	micro-equivalents/liter K	NH4	Ca	Mg	Cl	NO3	SO4	micro-mol/l S(IV)	CH2O	-/+
1	1:18	1:40	22	20.8	3.48	331.	158.	14.	276.	56.	48.	72.	587.	379.	5.0	46.	1.175
2	1:42	2:31	49	29.0	3.21	617.	235.	15.	369.	66.	71.	95.	920.	542.	6.0	70.	1.135
3	2:33	3:30	57	28.1	3.14	724.	165.	10.	315.	44.	45.	87.	822.	517.	-0.1	-0.	1.094
4	3:31	4:22	51	3.9	2.85	1413.	616.	41.	817.	225.	173.	230.	2230.	1044.	-0.1	-0.	1.067
Vol-Wt Mean (LWC=0.152)					3.21	619.	210.	14.	348.	63.	61.	93.	864.	516.	5.6	60.	1.120

Henninger Flats - 26 May 1983

Checked: 7/11/83

	Start	Stop	min	mL	pH	H	Na	micro-equivalents/liter K	NH4	Ca	Mg	Cl	NO3	SO4	micro-mol/l S(IV)	CH2O	-/+
1	0:40	2:10	90	20.0	2.16	6918.	555.	75.	1700.	289.	191.	206.	4500.	2852.	19.0	94.	0.777
2	2:10	3:42	92	18.0	2.28	5248.	372.	35.	1426.	207.	134.	316.	4100.	2913.	18.0	98.	0.987
3	3:45	5:55	130	40.0	2.43	3715.	287.	26.	1267.	154.	98.	241.	2800.	2143.	14.0	-0.	0.934
4	5:55	7:20	85	23.0	2.42	3802.	271.	46.	1457.	171.	104.	266.	3260.	2630.	15.0	100.	1.052
5	7:20	8:40	80	9.0	2.29	5129.	333.	132.	1472.	450.	239.	266.	3200.	2219.	66.0	132.	0.733
Vol-Wt Mean (LWC=0.077)					2.33	4682.	350.	49.	1428.	215.	134.	254.	3451.	2506.	20.0	102.	0.906

*** HENNINGER FLATS FOGWATER DATA - MAY/JUNE 1983

Henninger Flats - 27 May 1983

Checked: 7/11/83

	Start	Stop	min	mL	pH	H	Na	micro-equivalents/liter K	NH4	Ca	Mg	Cl	NO3	SO4	micro-mol/l S(IV)	CH2O	-/+
1	0:30	1:50	80	36.0	2.50	3162.	354.	31.	921.	178.	112.	176.	3030.	2186.	10.0	34.	1.133
2	1:50	2:30	40	25.0	2.64	2291.	157.	15.	638.	82.	51.	241.	2020.	1260.	13.0	43.	1.089
3	2:30	3: 0	30	8.0	2.61	2455.	118.	57.	649.	116.	62.	258.	2090.	1199.	7.0	43.	1.026
Vol-Wt Mean (LWC=0.153)					2.56	2765.	255.	28.	787.	136.	84.	209.	2555.	1736.	10.7	38.	1.110

Henninger Flats - 30-31 May 1983

Checked: 7/11/83

	Start	Stop	min	mL	pH	H	Na	micro-equivalents/liter K	NH4	Ca	Mg	Cl	NO3	SO4	micro-mol/l S(IV)	CH2O	-/+
1	23: 0	0:30	90	26.5	3.31	490.	468.	27.	409.	139.	140.	350.	981.	477.	5.6	40.	1.081
2	0:30	1:35	65	26.0	3.21	617.	364.	17.	373.	110.	104.	220.	930.	475.	5.6	44.	1.026
3	1:35	3:35	120	52.7	3.05	891.	496.	22.	420.	104.	143.	368.	1340.	755.	6.9	43.	1.186
4	3:35	4:30	55	41.8	3.04	912.	430.	19.	451.	84.	123.	258.	1210.	659.	5.6	18.	1.053
5	4:30	6: 0	90	63.0	3.16	692.	372.	18.	370.	56.	101.	246.	879.	521.	3.4	23.	1.023
6	6: 0	6:30	30	28.0	3.51	309.	182.	10.	221.	27.	48.	157.	396.	286.	2.1	16.	1.053
7	6:30	7:15	45	41.5	3.63	234.	101.	6.	167.	15.	27.	119.	243.	214.	0.4	13.	1.046
8	7:20	8: 0	40	44.2	3.72	191.	44.	3.	128.	13.	10.	68.	192.	174.	1.3	16.	1.115
9	8: 0	8:40	40	41.0	3.71	195.	46.	21.	110.	16.	11.	59.	160.	177.	11.7	16.	0.991
10	8:40	9:20	40	48.0	3.75	178.	43.	10.	102.	20.	10.	66.	172.	233.	2.8	18.	1.298
11	9:20	10:10	50	45.0	3.60	251.	42.	5.	140.	24.	10.	54.	223.	255.	0.5	19.	1.128
12	10:10	11: 0	50	35.0	3.48	331.	27.	8.	167.	32.	6.	48.	287.	258.	1.0	31.	1.039
13	11: 0	12: 0	60	45.0	3.27	537.	50.	6.	235.	35.	16.	78.	452.	419.	3.1	36.	1.080
14	12: 0	12:30	30	15.5	3.16	692.	41.	5.	289.	103.	15.	81.	523.	426.	-0.1	50.	0.900
Vol-Wt Mean (LWC=0.229)					3.33	468.	199.	13.	253.	51.	56.	158.	578.	387.	3.8	26.	1.080

Henninger Flats - 31 May-1 June 1983

Checked: 7/11/83

	Start	Stop	min	mL	pH	H	Na	micro-equivalents/liter K	NH4	Ca	Mg	Cl	NO3	SO4	micro-mol/l S(IV)	CH2O	-/+
1	21:40	22:35	55	60.0	3.38	417.	57.	12.	284.	29.	18.	58.	430.	349.	2.0	20.	1.025
2	22:35	23:55	80	60.0	3.38	417.	23.	7.	165.	12.	7.	34.	325.	227.	1.0	16.	0.930
3	5:10	5:55	45	9.0	2.95	1122.	1622.	74.	973.	259.	432.	750.	1560.	1388.	10.0	43.	0.825
4	8:10	8:50	40	16.0	3.37	427.	1790.	56.	786.	242.	474.	2670.	863.	1091.	2.0	45.	1.225
5	8:50	10: 0	70	5.0	3.38	417.	6320.	197.	1291.	920.	1735.	9650.	1920.	1927.	-0.1	-0.	1.241
Vol-Wt Mean (LWC=0.173)					3.34	460.	531.	25.	365.	88.	144.	688.	552.	494.	2.1	23.	1.075

*** HENNINGER FLATS FOGWATER DATA - MAY/JUNE 1983

Indicated samples also included in CRC Intercomparison Study data set

Henninger Flats - 7-8 June 1983

Checked: 7/11/83

	Start	Stop	min	mL	pH	H	Na	micro-equivalents/liter K	NH4	Ca	Mg	Cl	NO3	SO4	micro-mol/l S(IV)	CH2O	-/+	CRC CODE
1	20:34	21: 3	29	11.8	2.57	2692.	382.	60.	1169.	770.	223.	266.	3230.	2725.	41.0	103.	1.175	
2	21: 4	22: 2	58	38.1	2.69	2042.	253.	28.	1148.	410.	128.	137.	2380.	1910.	29.0	88.	1.104	607B01
3	22: 3	22:58	55	27.4	2.73	1862.	234.	23.	1008.	333.	112.	-1.	1980.	1632.	24.0	88.	1.011	607B02
4	23: 0	0: 2	62	22.5	2.83	1479.	202.	19.	994.	145.	68.	-1.	1640.	1522.	17.0	74.	1.088	607B03
5	4:33	6: 0	87	1.5	2.66	2188.	362.	-1.	1531.	269.	113.	-1.	2630.	1993.	-0.1	-0.	1.036	
Vol-Wt Mean (LWC=0.116)					2.71	1946.	253.	28.	1084.	370.	121.	168.	2210.	1845.	26.3	87.	1.110	

Henninger Flats - 8-9 June 1983

Checked: 7/11/83

	Start	Stop	min	mL	pH	H	Na	micro-equivalents/liter K	NH4	Ca	Mg	Cl	NO3	SO4	micro-mol/l S(IV)	CH2O	-/+	CRC CODE
1	20:37	21:33	56	10.2	2.94	1148.	847.	-1.	796.	462.	316.	-1.	-1.	-1.	28.0	173.	0.000	608C01
2	21:35	23:30	115	34.9	2.94	1148.	526.	39.	584.	316.	172.	276.	1700.	1023.	14.0	76.	1.077	608C02
3	23:35	0:30	55	26.1	2.96	1096.	359.	23.	425.	140.	108.	166.	1280.	738.	11.0	50.	1.015	608C03
4	0:30	1:30	60	52.3	3.10	794.	155.	8.	263.	57.	45.	96.	860.	506.	4.0	41.	1.105	608C04
5	1:30	3: 0	90	16.0	3.00	1000.	226.	79.	404.	21.	81.	200.	1240.	596.	9.0	55.	1.124	608C05
6	3:25	3:55	30	4.2	2.77	1698.	232.	28.	505.	164.	77.	106.	1830.	911.	-0.1	-0.	1.053	
7	7: 5	8: 0	55	23.0	2.80	1585.	140.	11.	695.	103.	44.	116.	1510.	1055.	9.0	53.	1.040	
8	8: 5	9:10	65	26.4	2.79	1622.	138.	8.	806.	77.	43.	108.	1480.	1241.	14.0	64.	1.050	
9	9:10	10: 5	55	18.3	2.72	1905.	164.	10.	779.	87.	50.	126.	1620.	1351.	11.0	80.	1.034	
10	10: 5	11:30	85	14.0	2.54	2884.	283.	22.	1222.	144.	106.	196.	2530.	2249.	20.0	108.	1.067	
11	11:30	12: 0	30	0.4	2.32	4786.	1435.	85.	3763.	1921.	600.	1070.	5550.	6414.	-0.1	-0.	1.035	
Vol-Wt Mean (LWC=0.108)					2.87	1335.	281.	22.	585.	143.	92.	156.	1421.	977.	11.2	66.	1.039	

*** HENNINGER FLATS FOGWATER DATA - MAY/JUNE 1983

Indicated samples also included in CRC Intercomparison Study data set

Henninger Flats - 11 June 1983

Checked: 7/11/83

	Start	Stop	min	mL	pH	H	Na	micro-equivalents/liter K	NH4	Ca	Mg	Cl	NO3	SO4	micro-mol/l S(IV)	CH2O	-/+	CRC CODE
1	4:35	4:49	14	11.9	3.46	347.	36.	9.	188.	25.	14.	-1.	351.	301.	-0.1	41.	1.053	610B01
2	5: 0	5:37	37	27.6	3.48	331.	26.	-1.	211.	35.	11.	-1.	384.	211.	5.0	37.	0.970	610B02
3	5:39	6:30	51	18.1	3.23	589.	40.	9.	273.	65.	15.	-1.	543.	293.	4.0	56.	0.844	610B03
4	6:35	7:30	55	43.9	3.10	794.	19.	3.	277.	22.	8.	-1.	758.	367.	9.0	64.	1.002	610B04
5	7:35	8:34	59	62.4	2.98	1047.	32.	3.	413.	18.	11.	59.	1140.	552.	6.0	64.	1.150	610B05
6	8:38	9:30	52	59.1	2.96	1096.	41.	3.	445.	18.	14.	59.	1220.	633.	8.0	70.	1.183	610B06
7	9:32	10:26	54	61.2	3.05	891.	41.	3.	453.	18.	14.	40.	1000.	555.	6.0	68.	1.123	610B07
8	10:30	11:28	58	42.0	2.92	1202.	30.	2.	395.	15.	10.	72.	1170.	619.	7.0	74.	1.125	610B08
9	11:34	12:25	51	21.1	2.68	2089.	66.	17.	699.	95.	29.	116.	1780.	1481.	16.0	76.	1.128	610B09
10	12:30	13:32	62	56.5	3.05	891.	14.	3.	201.	27.	8.	15.	592.	638.	6.0	43.	1.089	610B10
11	13:35	14:30	55	55.7	3.55	282.	3.	1.	62.	3.	1.	-1.	249.	131.	2.0	34.	1.082	610B11
12	14:32	15:25	53	37.9	3.33	468.	6.	1.	75.	4.	2.	-1.	376.	215.	3.0	47.	1.064	610B12
13	15:29	16:30	61	57.0	3.26	550.	4.	2.	101.	4.	2.	-1.	427.	250.	3.0	59.	1.024	610B13
Vol-Wt Mean (LWC=0.278)					3.09	817.	25.	3.	288.	20.	9.	53.	784.	469.	5.9	57.	1.123	

Henninger Flats - 12 June 1983

Checked: 7/11/83

	Start	Stop	min	mL	pH	H	Na	micro-equivalents/liter K	NH4	Ca	Mg	Cl	NO3	SO4	micro-mol/l S(IV)	CH2O	-/+
1	23: 4	0: 4	60	5.7	2.09	8128.	552.	65.	1013.	639.	210.	677.	6210.	4996.	-0.1	-0.	1.120
2	0: 6	1: 5	59	1.5	2.07	8511.	-1.	-1.	-1.	-1.	-1.	-1.	-1.	-1.	-0.1	-0.	0.000
3	1:25	2:39	74	19.0	2.56	2754.	615.	47.	849.	327.	181.	424.	2770.	1831.	15.0	52.	1.053
4	6:10	7: 3	53	12.6	2.60	2512.	888.	58.	1074.	401.	262.	753.	2910.	1699.	15.0	51.	1.032
5	7: 5	8: 0	55	7.4	3.18	661.	2810.	185.	3580.	1070.	755.	1980.	4740.	2737.	76.0	120.	1.044
6	8:35	9:45	70	20.0	3.87	135.	1497.	75.	1804.	305.	397.	1690.	1690.	1333.	94.0	102.	1.119
7	9:48	10:48	60	7.4	3.25	562.	1982.	88.	1635.	367.	532.	2030.	2130.	1310.	21.0	83.	1.059
Vol-Wt Mean (LWC=0.057)					2.68	2104.	1268.	76.	1527.	439.	352.	1177.	2903.	1959.	46.3	78.	1.047	

Henninger Flats - 18-19 June 1983

Checked: 7/11/83

	Start	Stop	min	mL	pH	H	Na	micro-equivalents/liter K	NH4	Ca	Mg	Cl	NO3	SO4	micro-mol/l S(IV)	CH2O	-/+	CRC CODE
1	23: 2	23:45	43	1.7	3.40	398.	448.	-1.	674.	619.	316.	-1.	1490.	752.	-0.1	-0.	0.913	618B01
2	6:30	7:31	61	17.2	2.87	1349.	303.	-1.	730.	274.	113.	-1.	2100.	1206.	3.0	12.	1.194	
Vol-Wt Mean (LWC=0.060)					2.90	1263.	316.	0.	725.	305.	131.	0.	2045.	1165.	3.0	12.	1.171	

*** HENNINGER FLATS FOGWATER DATA - MAY/JUNE 1983

Indicated samples also included in CRC Intercomparison Study data set

Henninger Flats - 21 June 1983

Checked: 7/11/83

	Start	Stop	min	mL	pH	H	Na	micro-equivalents/liter K	NH4	Ca	Mg	Cl	NO3	SO4	micro-mol/l S(IV)	CH2O	-/+	CRC CODE
1	7:30	9:30	120	12.5	2.73	1862.	3133.	-1.	2422.	928.	954.	890.	7060.	2332.	-0.1	-0.	1.106	621B01
2	9:35	10:30	55	0.6	2.50	3162.	-1.	-1.	-1.	-1.	-1.	-1.	-1.	-1.	-0.1	-0.	0.000	

Henninger Flats - 22 June 1983

Checked: 7/11/83

	Start	Stop	min	mL	pH	H	Na	micro-equivalents/liter K	NH4	Ca	Mg	Cl	NO3	SO4	micro-mol/l S(IV)	CH2O	-/+	CRC CODE
1	4:30	5:30	60	22.6	3.19	646.	192.	24.	394.	143.	61.	-1.	975.	381.	7.0	32.	0.929	622C01
2	5:31	7:30	119	7.3	2.88	1318.	329.	116.	1475.	652.	466.	503.	3780.	1435.	-0.1	-0.	1.313	
Vol-Wt Mean (LWC=0.056)					3.09	810.	225.	46.	658.	267.	160.	503.	1660.	638.	7.0	32.	1.293	

Henninger Flats - 25 June 1983

Checked: 7/11/83

	Start	Stop	min	mL	pH	H	Na	micro-equivalents/liter K	NH4	Ca	Mg	Cl	NO3	SO4	micro-mol/l S(IV)	CH2O	-/+	CRC CODE
1	6: 6	7: 5	59	38.6	2.85	1413.	239.	11.	475.	103.	60.	133.	1580.	719.	8.0	88.	1.057	624B01
2	7: 6	8: 2	56	15.1	2.62	2399.	471.	20.	776.	159.	124.	193.	2760.	1238.	13.0	132.	1.061	624B02
3	8:13	10: 0	107	12.7	2.42	3802.	823.	53.	1585.	389.	260.	372.	5510.	2894.	25.0	126.	1.270	624B03
4	10:30	11:30	60	3.3	2.25	5623.	5320.	350.	7420.	3020.	1624.	1110	16300	7816.	-1	-1	1.080	
5	11:30	11:44	14	1.5	7.00	0.	3135.	572.	6500.	1644.	857.	-1	11100	6270.	-1	-1	1.367	
Vol-Wt Mean (LWC=0.080)					2.65	2213.	689.	48.	1186.	334.	199.	236.	3414.	1663.	12.4	105.	1.138	

*** HENNINGER FLATS FOGWATER DATA - MAY/JUNE 1983

Indicated samples also included in CRC Intercomparison Study data set

Henninger Flats - 26 June 1983

Checked: 7/11/83

	Start	Stop	min	mL	pH	H	Na	micro-equivalents/liter K	NH4	Ca	Mg	Cl	NO3	SO4	micro-mol/l S(IV)	CH2O	-/+	CRC CODE
1	3:19	5:30	131	29.8	2.80	1585.	601.	25.	369.	153.	156.	231.	2125.	848.	2.0	84.	1.109	625B01
2	5:36	6:35	59	9.9	2.90	1259.	840.	54.	466.	315.	254.	335.	2165.	928.	-0.1	-0.	1.075	625B02
3	6:37	7:30	53	32.8	3.12	759.	1085.	42.	613.	215.	276.	529.	1770.	1019.	3.0	27.	1.110	625B03
4	7:32	8:30	58	37.7	3.08	832.	856.	31.	481.	145.	207.	410.	1495.	907.	1.0	25.	1.102	625B04
5	8:32	9:30	58	22.6	2.98	1047.	778.	30.	377.	116.	186.	410.	1495.	899.	0.0	31.	1.107	625B05
6	9:32	11: 0	88	16.1	2.80	1585.	1302.	47.	580.	210.	323.	768.	2520.	1375.	-0.1	-0.	1.152	625B06
Vol-Wt Mean (LWC=0.111)					2.96	1109.	891.	35.	482.	176.	224.	434.	1837.	970.	2.0	41.	1.111	

Henninger Flats - 27 June 1983

Checked: 7/11/83

	Start	Stop	min	mL	pH	H	Na	micro-equivalent /liter K	NH4	Ca	Mg	Cl	NO3	SO4	micro-mol/l S(IV)	CH2O	-/+
1	11:47	12:30	43	14.0	2.93	1175.	1732.	101.	589.	784.	491.	1080.	2635.	1787.	22.0	89.	1.129

HENNINGER FLATS FOGWATER DATA - MAY/JUNE 1983

METAL CONCENTRATIONS

			microgram/liter				
Date	#	pH	Fe	Mn	Pb	Cu	Ni
16 May	1	3.48	2860.	19.	143.	11.5	14.2
	2	3.21	-1	-1	-1	-1	-1
	3	3.14	384.	22.	267.	36.2	11.4
	4	2.85	-1	-1	-1	-1	-1
27 May	1	2.50	836.	74.	581.	63.8	28.1
	2	2.64	384.	38.	352.	41.6	16.5
	3	2.61	406.	73.	318.	37.8	19.3
31 May	1	3.31	645.	65.6	133.	49.6	23.3
	2	3.21	531.	91.	179.	36.3	20.1
	3	3.05	232.	89.	172.	17.9	11.9
	4	3.04	573.	82.	179.	27.6	11.4
	5	3.16	573.	67.3	128.	18.5	9.9
	6	3.51	90.	34.8	57.	11.1	12.5
	7	3.63	42.	5.6	41.	1.8	3.0
	8	3.72	49.	4.2	38.	5.8	12.1
	9	3.71	67.	4.6	54.	3.9	8.2
	10	3.75	39.	4.4	62.	13.7	12.8
	11	3.60	54.	10.2	95.	5.4	6.6
	12	3.48	100.	9.	132.	38.2	5.7
	13	3.27	659.	17.8	201.	14.1	80.1
	14	3.16	1077.	-1	190.	1-	-1
1 June	1	3.38	206.	14.3	149.	13.2	5.6
	2	3.38	89.	4.5	72.	2.9	1.
	3	2.95	673.	48.	185.	15.6	8.
	4	3,37	575.	58.	144.	20.2	40.6
	5	3.38	-1	-1	-1	-1	-1
7-8 June	1	2.57	2365.	354.	1031.	456.	141.
	2	2.69	1539.	150.	976.	144.	33.1
	3	2.73	1236.	144.	737.	107.	34.9
	4	2.83	1039.	77.	756.	-1	-1
	5	2.66	-1	-1	69.3	20.2	-1
8-9 June	1	2.94	499.	250.	490.	97.	56.8
	2	2.94	433.	110.	431.	40.1	13.8
	3	2.96	402.	46.4	375.	36.3	20.2
	4	3.10	310.	30.	222.	9.9	6.2
	5	3.00	380.	64.	326.	24.7	13.2
	6	2.77	-1	-1	-1	-1	-1
	7	2.80	473.	43.5	283.	34.4	19.7
	8	2.79	455.	30.4	308.	11.1	6.2
	9	2.72	-1	-1	-1	-1	-1
	10	2.54	765.	74.2	761.	38.	18.5
	11	2.32	-1	-1	-1	-1	-1

HENNINGER FLATS FOGWATER DATA - MAY/JUNE 1983

METAL CONCENTRATIONS
(cont.)

			microgram/liter				
Date	#	pH	Fe	Mn	Pb	Cu	Ni
11 June	1	3.46	641.	68.8	158.	66.6	42.8
	2	3.48	167.	26.5	108.	24.9	9.7
	3	3.23	340.	43.4	168.	23.	4.2
	4	3.10	470.	25.7	211.	30.3	6.8
	5	2.98	97.	12.7	293.	6.1	5.6
	6	2.96	206.	30.9	346.	146.	57.1
	7	3.05	86.	14.8	330.	5.6	3.3
	8	2.67	163.	11.1	332.	8.1	3.9
	9	2.68	615.	60.4	577.	25.2	8.8
	10	3.05	141.	17.7	251.	7.	3.9
	11	3.55	68.	1.6	78.	3.3	4.4
	12	3.33	27.	1.9	96.	4.9	1.5
	13	3.26	20.	1.2	106.	1.	3.9
12 June	1	2.09	-1	-1	-1	-1	-1
	2	2.07	-1	-1	-1	-1	-1
	3	2.56	683.	-1	270.	73.4	34.2
	4	2.60	817.	-1	186.	74.5	35.5
	5	3.18	4828.	-1	78.	125.	52.4
	6	3.87	785.	-1	286.	75.6	22.
	7	3.25	1264.	-1	969.	59.5	24.3
19 June	1	3.40	442.	-1	-1	-1	-1
	2	2.87	799.	189.	194.	35.6	56.8
22 June	1	3.19	-1	97.	100.	14.4	12.4
	2	2.88	-1	-1	-1	-1	-1
25 June	1	2.85	28.	65.9	213.	22.4	59.4
	2	2.62	456.	84.7	392.	67.5	-1
	3	2.42	1231.	287.	2487.	126.	-1
	4	2.25	-1	-1	-1	-1	-1
	5	7.00	-1	-1	-1	-1	-1
26 June	1	2.80	301.	63.2	290.	21.8	27.6
	2	2.90	-1	-1	-1	-1	-1
	3	3.12	218.	64.9	157.	41.6	12.1
	4	3.08	182.	38.9	155.	8.8	6.8
	5	2.98	511.	36.4	156.	11.2	6.6
	6	2.80	-1	-1	-1	-1	-1

*** HENNINGER FLATS FOGWATER DATA - MAY/JUNE 1983

REPLICATE SAMPLES for CRC Intercomparison Study only - NOT included in Waldman et al. (1985)

Henninger Flats Fog: 7-8B June 1983 — Checked: 5/1/85

	Start	Stop	min	mL	pH	H	Na	micro-equivalents/liter K	NH4	Ca	Mg	Cl	NO3	SO4	micro-mol/l S(IV)	CH2O	-/+	CRC CODE
1	20:30	21: 4	34	11.1	2.65	2239.	366.	58.	1132.	825.	248.	-1.	-1.	-1.	46.0	-0.	0.000	
2	21: 5	22: 4	59	28.8	2.70	1995.	240.	28.	968.	414.	110.	-1.	1340.	1207.	-0.1	-0.	0.678	607C01
3	22: 5	23: 2	57	34.3	2.73	1862.	234.	22.	912.	306.	93.	-1.	2100.	1726.	-0.1	-0.	1.116	607C02
4	23: 4	0: 4	60	20.8	2.84	1445.	198.	25.	922.	167.	72.	-1.	1640.	1523.	-0.1	-0.	1.118	607C02
Vol-Wt Mean (LWC=0.150)					2.73	1855.	243.	29.	957.	369.	112.	0.	1725.	1498.	46.0	0.	0.904	

Henninger Flats Fog: 8-9B June 1983 (** AERODYNAMIC RAC ARM **) — Checked: 5/1/85

	Start	Stop	min	mL	pH	H	Na	mic o-equivalents/liter K	NH4	Ca	Mg	Cl	NO3	SO4	mic o-mol/l S(IV)	CH2O	-/+	CRC CODE
1	20:37	21:35	58	2.4	3.14	724.	1390.	200.	683.	-1.	368.	849.	2340.	1341.	-0.1	-0.	1.346	608J01
2	21:45	23:35	110	12.6	3.16	692.	937.	-1.	667.	447.	427.	467.	2170.	1148.	-0.1	-0.	1.194	608J02
3	23:45	0:35	50	12.6	2.96	1096.	571.	49.	549.	-1.	174.	283.	1660.	958.	-0.1	-0.	1.189	608J03
4	0:45	1:35	50	12.8	3.11	776.	188.	16.	233.	66.	57.	116.	782.	458.	-0.1	-0.	1.015	608J04
5	1:45	3: 0	75	6.0	3.10	794.	341.	179.	452.	41.	102.	208.	1300.	693.	-0.1	-0.	1.153	608J05
Vol-Wt Mean (LWC=0.045)					3.08	840.	577.	70.	488.	214.	211.	306.	1545.	857.	0.0	0.	1.128	

*** HENNINGER FLATS FOGWATER DATA - MAY/JUNE 1983

REPLICATE SAMPLES for CRC Intercomparison Study only - NOT included in Waldman et al. (1985)

Henninger Flats Fog: 11B June 1983 (** SIDE-BY-SIDE CONFIGURATION **) Checked: 5/1/85

	Start	Stop	min	mL	pH	H	micro-equivalents/liter Na	K	NH4	Ca	Mg	Cl	NO3	SO4	micro-mol/l S(IV)	CH2O	-/+	CRC CODE
1	4:35	4:49	14	13.6	3.46	347.	-1.	-1.	-1.	-1.	-1.	-1.	-1.	-1.	-0.1	-0.	0.000	610C01
2	5: 0	5:35	35	27.6	3.48	331.	28.	3.	196.	43.	9.	-1.	351.	208.	-0.1	-0.	0.917	610C02
3	5:37	6:30	53	13.3	3.19	646.	62.	-1.	333.	104.	24.	-1.	767.	443.	-0.1	-0.	1.036	610C03
4	6:35	7:30	55	44.0	3.10	794.	21.	3.	280.	29.	9.	47.	720.	355.	-0.1	-0.	0.987	610C04
5	7:35	8:34	59	64.2	2.98	1047.	36.	3.	450.	18.	10.	59.	1130.	552.	-0.1	-0.	1.113	610C05
6	8:37	9:30	53	56.6	2.96	1096.	47.	4.	521.	22.	15.	66.	1230.	645.	-0.1	-0.	1.138	610C06
7	9:32	10:26	54	69.1	3.05	891.	41.	3.	401.	13.	14.	40.	974.	544.	-0.1	-0.	1.143	610C07
8	10:30	11:28	58	44.0	2.93	1175.	29.	2.	401.	15.	10.	85.	1180.	632.	-0.1	-0.	1.162	610C08
9	11:32	12:25	53	21.2	2.66	2188.	67.	15.	729.	100.	33.	123.	1970.	1620.	-0.1	-0.	1.186	610C09
10	12:30	13:32	62	56.5	3.04	912.	14.	3.	221.	24.	8.	21.	618.	673.	-0.1	-0.	1.110	610C10
11	13:35	14:30	55	54.0	3.55	282.	5.	1.	59.	2.	1.	-1.	243.	141.	-0.1	-0.	1.097	610C11
12	14:32	15:24	52	37.5	3.33	468.	5.	3.	72.	4.	2.	-1.	421.	212.	-0.1	-0.	1.144	610C12
13	15:29	16:30	61	49.6	3.25	562.	5.	1.	89.	3.	2.	-1.	440.	250.	-0.1	-0.	1.043	610C13
Vol-Wt Mean (LWC=0.276)					3.08	832.	27.	3.	305.	22.	10.	56.	819.	493.	0.0	0.	1.141	

Henninger Flats Fog: 19B June 1983 Checked: 5/1/85

	Start	Stop	min	mL	pH	H	micro-equivalents/liter Na	K	NH4	Ca	Mg	Cl	NO3	SO4	micro-mol/l S(IV)	CH2O	-/+	CRC CODE
1	6:31	7:35	64	9.4	2.81	1549.	381.	-1.	968.	196.	119.	0.	2240.	1254.	-0.1	-0.	1.088	618C01
2	7:37	8: 7	30	0.3	-1.00	0.	2303.	39.	2610.	1005.	574.	-1.	-1.	-1.	-0.1	-0.	0.000	
Vol-Wt Mean (LWC=0.034)					2.81	1549.	431.	39.	1011.	217.	131.	0.	2240.	1254.	0.0	0.	1.035	

*** HENNINGER FLATS FOGWATER DATA - MAY/JUNE 1983

REPLICATE SAMPLES for CRC Intercomparison Study only - NOT included in Waldman et al. (1985)

Henninger Flats Fog: 21B June 1983 — Checked: 5/1/85

	Start	Stop	min	mL	pH	H	Na	micro-equivalents/liter K	NH4	Ca	Mg	Cl	NO3	SO4	micro-mol/l S(IV)	CH2O	-/+	CRC CODE
1	7:30	9:32	122	12.1	2.67	2138.	3458.	-1.	2676.	1122.	-1.	1050.	8600.	2801.	-1.0	-1.	1.325	621C01

Henninger Flats Fog: 22B June 1983 — Checked: 5/1/85

	Start	Stop	min	mL	pH	H	Na	micro-equivalents/liter K	NH4	Ca	Mg	Cl	NO3	SO4	micro-mol/l S(IV)	CH2O	-/+	CRC CODE
1	4:30	5:32	62	10.2	3.15	708.	193.	39.	343.	162.	54.	892.	1250.	457.	-0.1	-0.	1.734	622C01
2	5:35	7:32	117	4.0	2.93	1175.	-1.	-1.	-1.	-1.	-1.	-1.	-1.	-1.	-0.1	-0.	0.000	

Henninger Flats Fog: 25B June 1983 — Checked: 5/1/85

	Start	Stop	min	mL	pH	H	Na	micro-equivalents/liter K	NH4	Ca	Mg	Cl	NO3	SO4	micro-mol/l S(IV)	CH2O	-/+	CRC CODE
1	6: 1	7: 2	61	34.9	2.87	1349.	229.	11.	425.	98.	57.	133.	1540.	721.	7.0	90.	1.104	624C01
2	7: 3	8: 5	62	16.3	2.66	2188.	393.	21.	770.	154.	112.	178.	2680.	1181.	-0.1	-0.	1.110	624C02
3	8:17	10: 2	105	12.4	2.41	3890.	890.	-1.	1765.	451.	284.	402.	5750.	3080.	-0.1	-0.	1.268	624C03
Vol-Wt Mean (LWC=0.093)					2.69	2059.	400.	14.	775.	181.	115.	197.	2653.	1299.	7.0	90.	1.170	

Henninger Flats Fog: 26B June 1983 — Checked: 5/1/85

	Start	Stop	min	mL	pH	H	Na	micro-equivalents/liter K	NH4	Ca	Mg	Cl	NO3	SO4	micro-mol/l S(IV)	CH2O	-/+	CRC CODE
1	3:19	5:30	131	28.4	2.75	1778.	644.	29.	407.	133.	166.	246.	2360.	911.	-0.1	-0.	1.114	625C01
2	5:36	6:38	62	11.3	2.82	1514.	944.	-1.	482.	265.	255.	365.	2480.	1057.	-0.1	-0.	1.128	625C02
3	6:40	7:33	53	37.0	3.13	741.	992.	38.	517.	194.	244.	469.	1655.	946.	-0.1	-0.	1.126	625C03
4	7:35	8:33	58	36.6	3.06	871.	857.	30.	510.	144.	192.	395.	1535.	905.	-0.1	-0.	1.089	625C04
5	8:35	9:32	57	22.6	2.97	1072.	787.	31.	382.	110.	176.	380.	1495.	863.	-0.1	-0.	1.071	625C05
6	9:34	11: 0	86	15.9	2.77	1698.	1453.	52.	578.	227.	350.	813.	2750.	1435.	-0.1	-0.	1.147	625C06
Vol-Wt Mean (LWC=0.113)					2.93	1173.	909.	35.	478.	167.	219.	424.	1910.	977.	0.0	0.	1.111	

APPENDIX B.

HENNINGER FLATS FOGWATER DATA

3. Spring 1983 - RAC Collector Pair Comparisons

RAC-"B"(y) vs. "C"(x): *** All samples ***
[Caltech Lab Results]

Y = b0 + b1 * X b0 & b1 given with (90% confidence)
RD = 2(Y-X)/(X+Y) given as "mean/s.d."

Field pH	mean x,y= 2.97, 2.96	psd=0.023 (0.8%)
n= 30	r2 = 0.9860	b0= 0.01 (0.11)
		b1= 0.987 (0.038)
	y-x= -0.01 /0.03	
Hydrogen	mean x,y =1283., 1298.	psd= 94. (7.3%)
n= 30	r2 = 0.9703	b0= 50.20 (81.88)
		b1= 0.973 (0.055)
	RD= 0.017 / 0.075	only<0.33: 0.017/ 0.075 (30)
Sodium	mean x,y = 429., 451.	psd= 55. (12.4%)
n= 28	r2 = 0.9952	b0= -16.56 (19.38)
		b1= 1.089 (0.025)
	RD= 0.067 / 0.165	only<0.33: 0.021/ 0.097 (25)
Potassium	mean x,y = 18., 19.	psd= 3. (14.8%)
n= 22	r2 = 0.9515	b0= 1.00 (2.11)
		b1= 1.006 (0.086)
	RD= 0.089 / 0.315	only<0.33: 0.034/ 0.114 (18)
Ammonium	mean x,y = 614., 625.	psd= 64. (10.4%)
n= 28	r2 = 0.9752	b0= -28.98 (44.72)
		b1= 1.066 (0.057)
	RD= 0.003 / 0.113	only<0.33: 0.003/ 0.113 (28)
Calcium	mean x,y = 183., 191.	psd= 32. (17.1%)
n= 28	r2 = 0.9796	b0= -14.70 (15.49)
		b1= 1.122 (0.054)
	RD= -0.006 / 0.198	only<0.33: 0.007/ 0.146 (25)
Magnesium	mean x,y = 99., 99.	psd= 9. (9.1%)
n= 27	r2 = 0.9845	b0= -1.69 (6.07)
		b1= 1.014 (0.043)
	RD= 0.002 / 0.128	only<0.33: -0.015/ 0.091 (26)
Chloride	mean x,y = 290., 302.	psd= 33. (11.2%)
n= 16	r2 = 0.9811	b0= -14.28 (28.12)
		b1= 1.091 (0.073)
	RD= 0.050 / 0.112	only<0.33: 0.031/ 0.086 (15)
Nitrate	mean x,y =1724., 1851.	psd=234. (13.1%)
n= 26	r2 = 0.9869	b0=-141.19 (105.13)
		b1= 1.156 (0.046)
	RD= 0.049 / 0.099	only<0.33: 0.038/ 0.080 (25)
Sulfate	mean x,y = 977., 1033.	psd= 92. (9.2%)
n= 26	r2 = 0.9862	b0= -39.78 (54.61)
		b1= 1.098 (0.045)
	RD= 0.047 / 0.099	only<0.33: 0.032/ 0.068 (25)
Collection rate	mean x,y= 0.6, 0.5	psd= 0.1 (10.4%)
n= 30	r2 = 0.9485	b0= -0.05 (0.05)
		b1= 1.051 (0.079)
	RD= -0.087 / 0.228	only<0.33: -0.012/ 0.109 (2

RAC-"B"(y) vs. "C"(x): *** Side-by-side samples, only ***
[Caltech Lab Results]

Y = b0 + b1 * X b0 & b1 given with (90% confidence)
RD = 2(Y-X)/(X+Y) given as "mean/s.d."

Field pH	mean x,y= 3.16, 3.15	psd=0.009	(0.3%)	
n= 13	r2 = 0.9979	b0= -0.02	(0.08)	
		b1= 1.009	(0.025)	
	y-x= -0.01 /0.01			
Hydrogen	mean x,y = 812., 826.	psd= 23.	(2.8%)	
n= 13	r2 = 0.9979	b0= -16.90	(24.08)	
		b1= 1.039	(0.026)	
	RD= 0.014 / 0.027	only<0.33:	0.014/ 0.027	(13)
Sodium	mean x,y = 27., 30.	psd= 5.	(16.8%)	
n= 12	r2 = 0.9213	b0= 0.90	(5.80)	
		b1= 1.086	(0.181)	
	RD= 0.133 / 0.215	only<0.33:	0.027/ 0.104	(9)
Potassium	mean x,y = 4., 4.	psd= 1.	(18.7%)	
n= 10	r2 = 0.9679	b0= 0.72	(0.57)	
		b1= 0.837	(0.097)	
	RD= 0.115 / 0.444	only<0.33:	0.037/ 0.133	(7)
Ammonium	mean x,y = 300., 313.	psd= 25.	(8.2%)	
n= 12	r2 = 0.9726	b0= -4.00	(35.27)	
		b1= 1.054	(0.100)	
	RD= 0.016 / 0.104	only<0.33:	0.016/ 0.104	(12)
Calcium	mean x,y = 27., 31.	psd= 8.	(28.9%)	
n= 12	r2 = 0.9243	b0= -1.78	(7.53)	
		b1= 1.233	(0.201)	
	RD= 0.004 / 0.265	only<0.33:	0.006/ 0.193	(10)
Magnesium	mean x,y = 10., 11.	psd= 2.	(19.2%)	
n= 12	r2 = 0.9281	b0= -0.89	(2.37)	
		b1= 1.184	(0.187)	
	RD= 0.040 / 0.155	only<0.33:	0.001/ 0.084	(11)
Chloride	mean x,y = 60., 66.	psd= 5.	(8.0%)	
n= 6	r2 = 0.9828	b0= 2.70	(8.39)	
		b1= 1.047	(0.124)	
	RD= 0.112 / 0.126	only<0.33:	0.067/ 0.072	(5)
Nitrate	mean x,y = 803., 837.	psd= 62.	(7.6%)	
n= 12	r2 = 0.9723	b0= -6.11	(92.20)	
		b1= 1.050	(0.101)	
	RD= 0.037 / 0.112	only<0.33:	0.009/ 0.061	(11)
Sulfate	mean x,y = 519., 548.	psd= 46.	(8.6%)	
n= 12	r2 = 0.9861	b0= -13.94	(46.94)	
		b1= 1.083	(0.073)	
	RD= 0.049 / 0.121	only<0.33:	0.016/ 0.041	(11)
Collection rate	mean x,y= 0.8, 0.8	psd= 0.1	(6.3%)	
n= 13	r2 = 0.9288	b0= -0.07	(0.14)	
		b1= 1.086	(0.163)	
	RD= -0.015 / 0.122	only<0.33:	0.012/ 0.076	(12)

RAC-"B"(y) vs. "C"(x): *** Separated samples, only ***
[Caltech Lab Results]

Y = b0 + b1 * X b0 & b1 given with (90% confidence)
RD = 2(Y-X)/(X+Y) given as "mean/s.d."

Field pH	mean x,y= 2.83, 2.82	psd=0.030	(1.1%)
n= 17	r2 = 0.9540	b0= 0.05 (0.27)	
		b1= 0.934 (0.095)	
	y-x= -0.01 /0.04		
Hydrogen	mean x,y =1643., 1660.	psd=124.	(7.5%)
n= 17	r2 = 0.9472	b0= 117.57 (186.09)	
		b1= 0.939 (0.103)	
	RD= 0.019 / 0.098	only<0.33: 0.019/ 0.098 (17)	
Sodium	mean x,y = 731., 766.	psd= 72.	(9.6%)
n= 16	r2 = 0.9943	b0= -43.12 (40.89)	
		b1= 1.107 (0.040)	
	RD= 0.018 / 0.097	only<0.33: 0.018/ 0.097 (16)	
Potassium	mean x,y = 30., 32.	psd= 4.	(11.9%)
n= 12	r2 = 0.8628	b0= 4.86 (6.70)	
		b1= 0.903 (0.205)	
	RD= 0.069 / 0.164	only<0.33: 0.032/ 0.107 (11)	
Ammonium	mean x,y = 849., 860.	psd= 83.	(9.7%)
n= 16	r2 = 0.9689	b0= -72.79 (94.70)	
		b1= 1.098 (0.095)	
	RD= -0.007 / 0.121	only<0.33: -0.007/ 0.121 (16)	
Calcium	mean x,y = 301., 311.	psd= 42.	(13.7%)
n= 16	r2 = 0.9782	b0= -45.02 (32.00)	
		b1= 1.183 (0.085)	
	RD= -0.013 / 0.138	only<0.33: 0.008/ 0.112 (15)	
Magnesium	mean x,y = 170., 169.	psd= 12.	(7.1%)
n= 15	r2 = 0.9663	b0= -11.90 (18.66)	
		b1= 1.063 (0.099)	
	RD= -0.028 / 0.097	only<0.33: -0.028/ 0.097 (15)	
Chloride	mean x,y = 427., 443.	psd= 42.	(9.6%)
n= 10	r2 = 0.9725	b0= -48.31 (59.59)	
		b1= 1.151 (0.123)	
	RD= 0.013 / 0.090	only<0.33: 0.013/ 0.090 (10)	
Nitrate	mean x,y =2513., 2720.	psd=314.	(12.0%)
n= 14	r2 = 0.9844	b0=-270.14 (232.19)	
		b1= 1.190 (0.078)	
	RD= 0.060 / 0.088	only<0.33: 0.060/ 0.088 (14)	
Sulfate	mean x,y =1370., 1448.	psd=118.	(8.4%)
n= 14	r2 = 0.9802	b0= -94.85 (128.80)	
		b1= 1.126 (0.083)	
	RD= 0.046 / 0.082	only<0.33: 0.046/ 0.082 (14)	
Collection rate	mean x,y= 0.4, 0.3	psd= 0.1	(18.0%)
n= 17	r2 = 0.8476	b0= -0.01 (0.08)	
		b1= 0.941 (0.185)	
	RD= -0.142 / 0.274	only<0.33: -0.032/ 0.129 (14)	

HF 1983:

RAC-"B"(y) vs. "C"(x)
[CIT Lab results]

Field pH

n = 30

y = B1*x + B0
R2 = 0.9860
B1 = 0.999 (0.038)
B0 = 0.0091 (0.1139)
(+/-90%)

mean x,y: 2.96,2.97
psd=0.023 (0.8%)

For pH(y)-pH(x)

mean/sd: 0.007/ 0.033

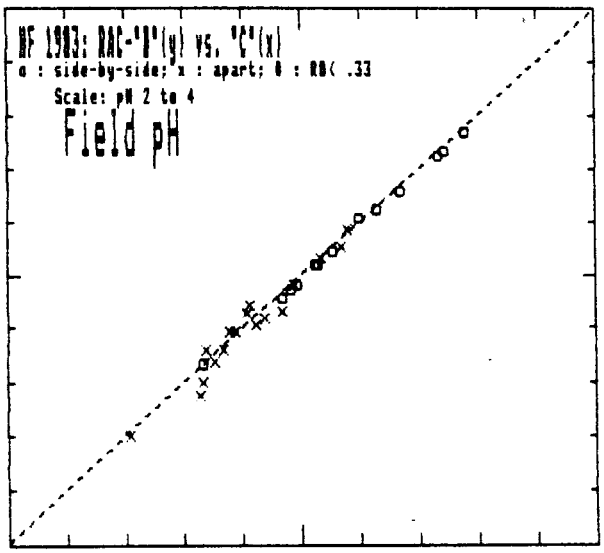

HF 1983:

RAC-"B"(y) vs. "C"(x)
[CIT Lab results]

Collection rate

n = 30

y = B1*x + B0
R2 = 0.9485
B1 = 0.903 (0.068)
B0 = 0.0697 (0.0433)
(+/-90%)

mean x,y: 0.5, 0.6
psd=0.057 (10.4%)

For RD = 2*(Y-X)/(Y+X)

mean/sd: 0.087/ 0.228
RD<0.33 0.012/ 0.109
(26)

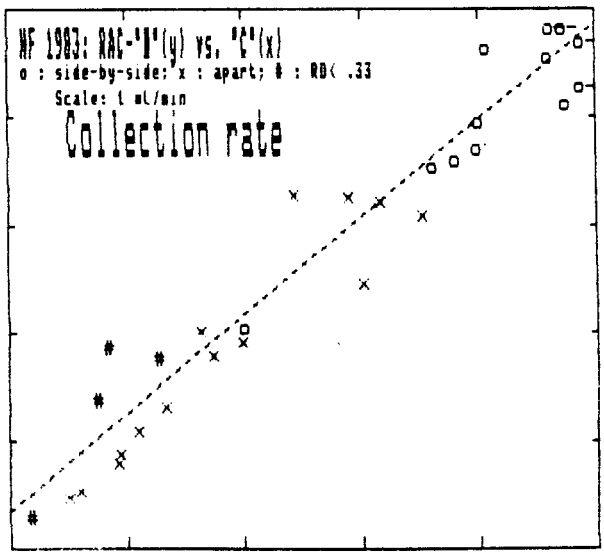

HF 1983:

RAC-"B"(y) vs. "C"(x)
[CIT Lab results]

Hydrogen

n = 30

y = B1*x + B0
R2 = 0.9703
B1 = 0.997 (0.056)
B0 = -11.9 (84.4)
(+/-90%)

mean x,y: 1298., 1283.
psd= 94. (7.3%)

For RD = 2*(Y-X)/(Y+X)

mean/sd: -0.017/ 0.075
RD<0.33 -0.017/ 0.075
(30)

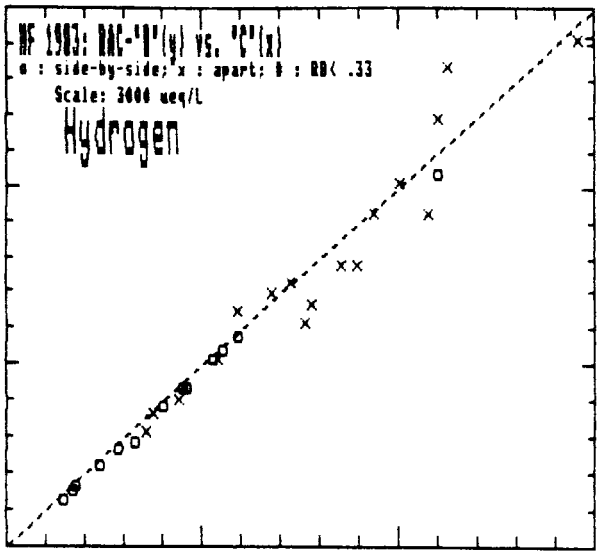

HF 1983:

RAC-"B"(y) vs. "C"(x)
[CIT Lab results]

Sodium

n = 28

y = B1*x + B0
R2 = 0.9952
B1 = 0.914 (0.021)
B0 = 17.2 (17.5)
(+/-90%)

mean x,y: 451., 429.
psd= 55. (12.4%)

For RD = 2*(Y-X)/(Y+X)

mean/sd: -0.067/ 0.165
RD<0.33 -0.021/ 0.097
(25)

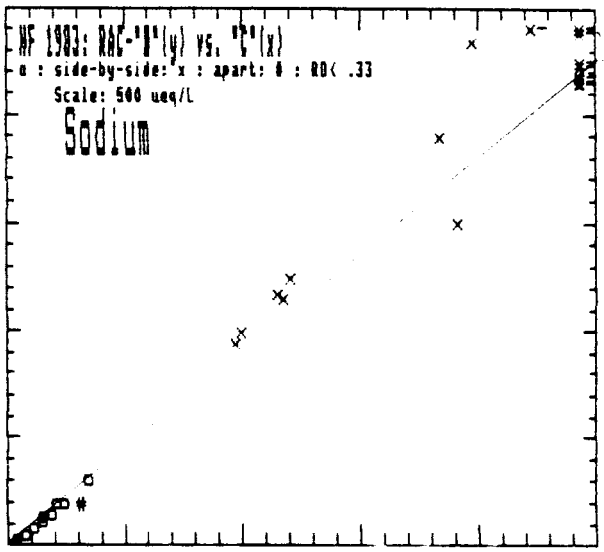

HF 1983:

RAC-"B"(y) vs. "C"(x)
[CIT Lab results]

Potassium

n = 22

y = B1*x + B0
R2 = 0.9515
B1 = 0.946 (0.081)
B0 = -0.1 (2.1)
(+/-90%)

mean x,y: 19., 18.
psd= 3. (14.8%)

For RD = 2*(Y-X)/(Y+X)

mean/sd: -0.089/ 0.315
RD<0.33 -0.034/ 0.114
(18)

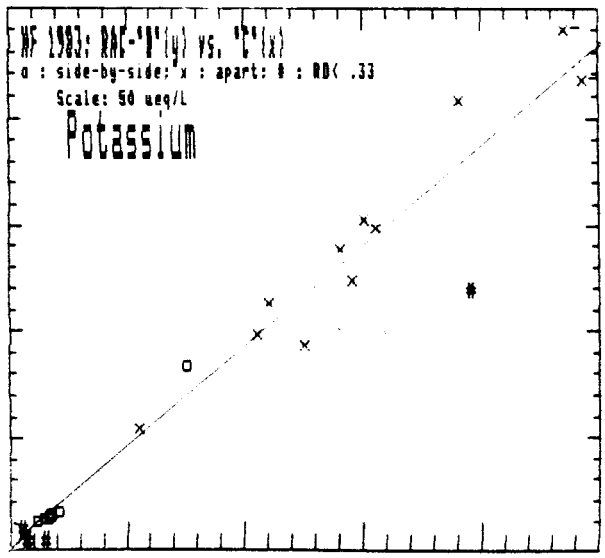

HF 1983:

RAC-"B"(y) vs. "C"(x)
[CIT Lab results]

Ammonium

n = 28

y = B1*x + B0
R2 = 0.9752
B1 = 0.915 (0.049)
B0 = 41.7 (40.1)
(+/-90%)

mean x,y: 625., 614.
psd= 64. (10.4%)

For RD = 2*(Y-X)/(Y+X)

mean/sd: -0.003/ 0.113
RD<0.33 -0.003/ 0.113
(28)

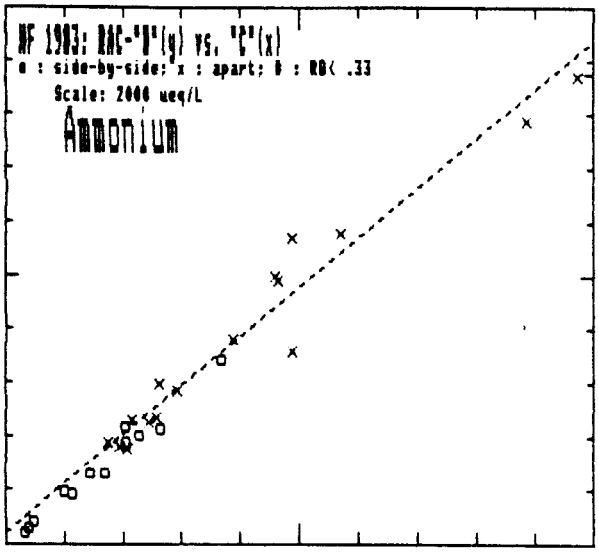

HF 1983:

RAC-"B"(y) vs. "C"(x)
[CIT Lab results]

Calcium

n = 28

y = B1*x + B0
R2 = 0.9796
B1 = 0.873 (0.042)
B0 = 16.6 (13.2)
(+/-90%)

mean x,y: 191., 183.
psd= 32. (17.1%)

For RD = 2*(Y-X)/(Y+X)

mean/sd: 0.006/ 0.198
RD<0.33 -0.007/ 0.146
(25)

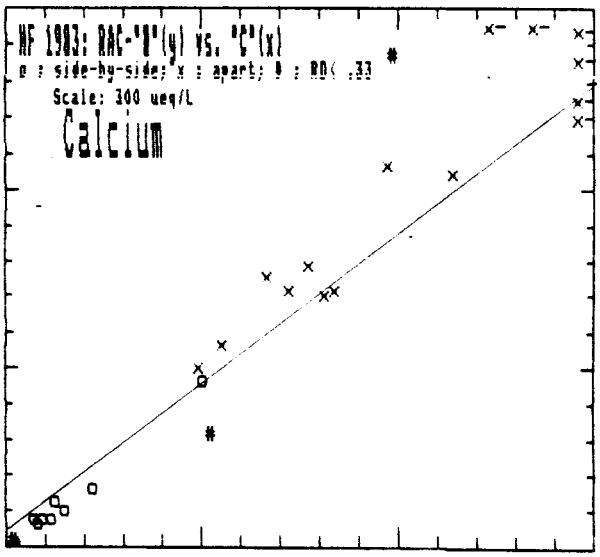

HF 1983:

RAC-"B"(y) vs. "C"(x)
[CIT Lab results]

Magnesium

n = 27

y = B1*x + B0
R2 = 0.9845
B1 = 0.971 (0.041)
B0 = 3.2 (5.9)
(+/-90%)

mean x,y: 99., 99.
psd= 9. (9.1%)

For RD = 2*(Y-X)/(Y+X)

mean/sd: -0.002/ 0.128
RD<0.33 0.015/ 0.091
(26)

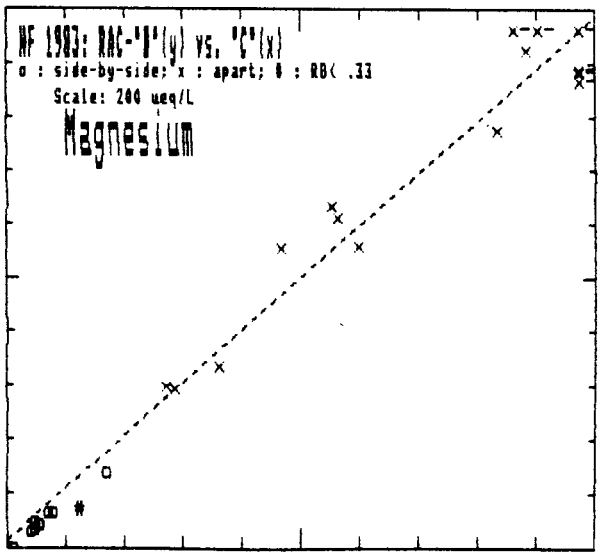

HF 1983:

RAC-"B"(y) vs. "C"(x)
[CIT Lab results]

Chloride

n = 16

y = B1*x + B0
R2 = 0.9811
B1 = 0.899 (0.060)
B0 = 18.3 (24.7)
(+/-90%)

mean x,y: 302., 290.
psd= 33. (11.2%)

For RD = 2*(Y-X)/(Y+X)

mean/sd: -0.050/ 0.112
RD<0.33 -0.031/ 0.086
(15)

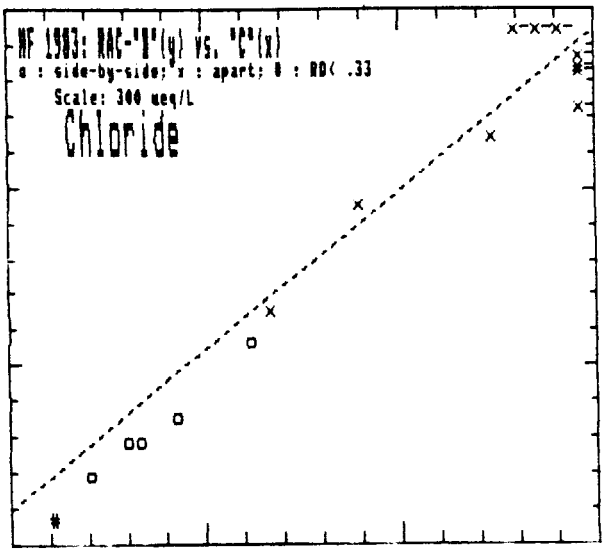

HF 1983:

RAC-"B"(y) vs. "C"(x)
[CIT Lab results]

Nitrate

n = 26

y = B1*x + B0
R2 = 0.9869
B1 = 0.854 (0.034)
B0 = 143.1 (86.5)
(+/-90%)

mean x,y: 1851., 1724.
psd= 234. (13.1%)

For RD = 2*(Y-X)/(Y+X)

mean/sd: -0.049/ 0.095
RD<0.33 -0.038/ 0.080
(25)

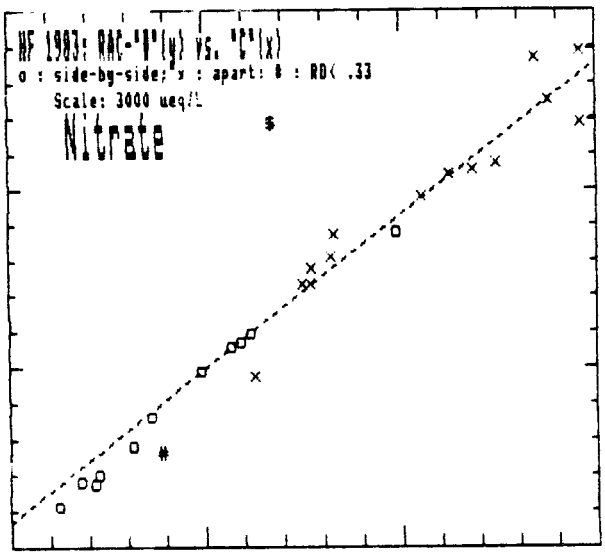

HF 1983:

RAC-"B"(y) vs. "C"(x)
[CIT Lab results]

Sulfate

n = 26

y = B1*x + B0
R2 = 0.9862
B1 = 0.890 (0.037)
B0 = 49.2 (48.2)
(+/-90%)

mean x,y: 1033., 977.
psd= 92. (9.2%)

For RD = 2*(Y-X)/(Y+X)

mean/sd: -0.047/ 0.099
RD<0.33 -0.032/ 0.068
(25)

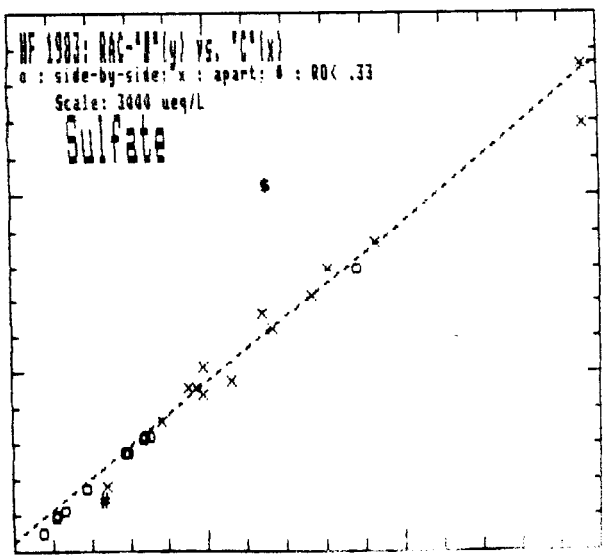

APPENDIX B.

HENNINGER FLATS FOGWATER DATA

4. Spring 1983 - RAC Samples:

Rockwell Laboratory Results and Interlaboratory Comparison

Appendix B.4

INTERLABORATORY COMPARISON
OF CHEMICAL ANALYSES FOR FOGWATER SAMPLES

As part of the CRC Fog Sampler Intercomparison Study (Hering and Blumental, 1985), replicate aliquots from RAC-collected fogwater samples were submitted to Rockwell International Corp. (RI) for analysis of the major chemical constituents. Caltech analytical methods are described in Chapter 3; RI methods are given by Hering and Blumenthal (1985). Protocols used by both laboratories were essentially identical: ion chromotagraphy for anions; atomic absorption spectroscopy for cations; and, colorometric (indophenol blue reaction) procedure for ammonium. Field-measured pH values were taken with the Caltech-owned Radiometer pH meter and electrode. The laboratory pH was measured on replicates with an Orion Research pH meter and electrode.

The concentrations of H^+, NH_4^+, NO_3^- and SO_4^{2-} dominated the ionic composition in most samples. Their total accounted for 90% or more of the measured equivalents in most samples. For NO_3^- and SO_4^{2-}, agreement between laboratories was very good. The standard errors from relative differences (, see Chapter 5) measured between pairs were about 10%, least-squares regression correlation between paired results was very strong ($r^2>0.99$), and slopes were indistinguishable from unity. The pH values in the field were 0.05 ± 0.04 units lower than measured in the laboratory several days later, statistically significant at the >99% confidence level. The pH meters were compared at the beginning of the study, while discrepencies between pH values increased toward the end of the study, suggesting that a calibration drift had occurred (Hering and Blumental, 1985). The possibility also exists that some aging of the

samples occurred in storage (Ridder et al., 1985).

A systematic difference between laboratory results was found for NH_4^+: RI values were about 25% higher than from Caltech determinations. Although the same reaction method was used in both laboratories, RI analyses were performed with a Technicon autoanalyzer, compared to batch mode for Caltech work. In the determination, the final color and rate of color development are both pH dependent (Harwood and Huyser, 1970). It is possible that millimolar fogwater acidities contributed to the noted bias by causing a systematic difference in the end-point pH. The correlation between determinations had little scatter, however. It was more probable that two laboratory NH4+ stock solutions were not in agreement and responsible for the noted disparity. This was not checked at the time, unfortunately. Nonetheless, there was not a notable difference in the overall ionic balances for the two sets of results. Anion-to-cation equivalent ratios, corrected for sulfate speciation at low pH (pK=1.92), were 1.09$\pm$0.10 for RI (lab pH) and 1.10$\pm$0.08 for Caltech (field pH) analyses for this data set.

Ions at relatively lower concentrations (Na^+, Ca^{2+}, Mg^{2+}, and Cl^-) were found with good agreement between the two sets of laboratory results. Greater scatter was noted for K^+ values. As part of the analytical protocols, quantitative dilution (5 to 50:1) were necessary for most samples to bring major constituents down to analytical range. Sample volumes were often limiting. As the ion of lowest concentration, K^+ was often measured close to the detection limit. Despite the poor agreement for interlaboratory K+ data, individual laboratories gave values for quasi-replicate data sets (i.e., side-by-side RAC samples) with a much higher reproducibility.

Lab results: RI(y) vs. CIT(x): *** All samples ***

Y = b0 + b1 * X b0 & b1 given with (90% confidence)
RD = 2(Y-X)/(X+Y) given as "mean/s.d."

Lab vs. Field pH	mean x,y= 3.03, 3.08	psd=0.047 (1.5%)
n= 53	r2 = 0.9761	b0= -0.01 (0.12)
		b1= 1.060 (0.039)
	y-x= 0.05 /0.04	
Hydrogen	mean x,y =1066., 963.	psd=101. (9.9%)
n= 53	r2 = 0.9661	b0= -27.16 (49.27)
		b1= 0.929 (0.041)
	RD= -0.119 / 0.097	only<0.33: -0.119/ 0.097 (53)
Sodium	mean x,y = 434., 455.	psd= 52. (11.8%)
n= 57	r2 = 0.9905	b0= -13.63 (16.66)
		b1= 1.080 (0.024)
	RD= 0.084 / 0.259	only<0.33: 0.052/ 0.103 (56)
Potassium	mean x,y = 28., 25.	psd= 17. (63.0%)
n= 50	r2 = 0.6466	b0= 12.16 (3.96)
		b1= 0.468 (0.085)
	RD= 0.138 / 0.428	only<0.33: 0.075/ 0.135 (34)
Ammonium	mean x,y = 579., 744.	psd=174. (26.3%)
n= 65	r2 = 0.9350	b0= 41.81 (51.45)
		b1= 1.212 (0.068)
	RD= 0.275 / 0.166	only<0.33: 0.163/ 0.131 (36)
Calcium	mean x,y = 153., 159.	psd= 27. (17.5%)
n= 58	r2 = 0.9471	b0= 6.62 (11.90)
		b1= 0.997 (0.053)
	RD= 0.126 / 0.337	only<0.33: 0.024/ 0.145 (48)
Magnesium	mean x,y = 119., 127.	psd= 12. (9.7%)
n= 58	r2 = 0.9923	b0= 4.94 (3.95)
		b1= 1.031 (0.021)
	RD= 0.115 / 0.181	only<0.33: 0.077/ 0.098 (54)
Chloride	mean x,y = 300., 267.	psd= 86. (30.2%)
n= 44	r2 = 0.8125	b0= 21.50 (41.50)
		b1= 0.820 (0.103)
	RD= -0.094 / 0.297	only<0.33: -0.017/ 0.130 (37)
Nitrate	mean x,y =1724., 1727.	psd=100. (5.8%)
n= 64	r2 = 0.9915	b0= 55.55 (44.20)
		b1= 0.969 (0.019)
	RD= 0.023 / 0.098	only<0.33: 0.010/ 0.070 (62)
Sulfate	mean x,y = 994., 957.	psd= 92. (9.4%)
n= 64	r2 = 0.9731	b0= 39.84 (40.66)
		b1= 0.922 (0.033)
	RD= -0.030 / 0.129	only<0.33: -0.024/ 0.104 (61)

HF 1983: RI(y) vs. CIT(x)

Lab Results Comparison

Lab vs. Field pH

n = 53

y = B1*x + B0
R2 = 0.9761
B1 = 1.060 (0.039)
B0 = %-.131179 (0.1199)
(+/-90%)

mean x,y: 3.03,3.08
psd=0.047 (1.5%)

For pH(y)-pH(x)

mean/sd: 0.052/ 0.042

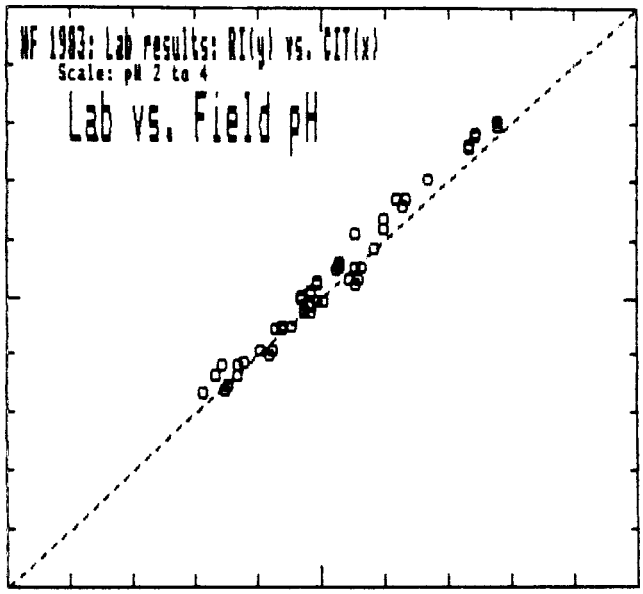

HF 1983: RI(y) vs. CIT(x)

Lab Results Comparison

Hydrogen

n = 53

y = B1*x + B0
R2 = 0.9661
B1 = 0.929 (0.041)
B0 = -27.2 (49.3)
(+/-90%)

mean x,y: 1066., 963.
psd= 101. (9.9%)

For RD = 2*(Y-X)/(Y+X)

mean/sd: -0.119/ 0.097
RD<0.50 -0.119/ 0.097
(53)

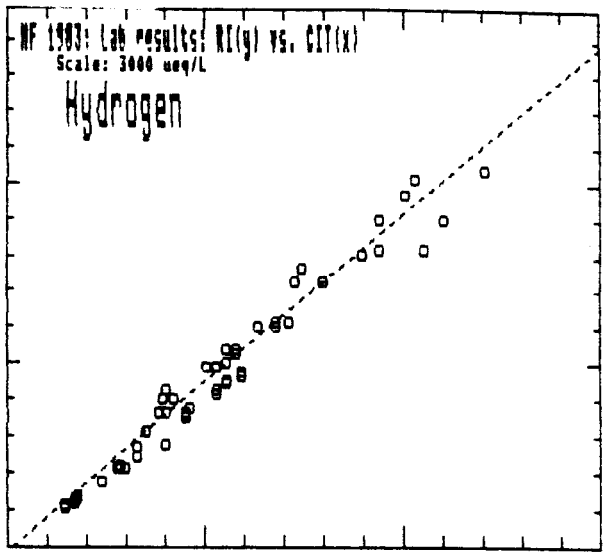

HF 1983: RI(y) vs. CIT(x)

Lab Results Comparison

Sodium

n = 57

y = B1*x + B0
R2 = 0.9905
B1 = 1.080 (0.024)
B0 = -13.6 (16.7)
(+/-90%)

mean x,y: 434., 455.
psd= 52. (11.8%)

For RD = 2*(Y-X)/(Y+X)

mean/sd: 0.084/ 0.259
RD<0.50 0.052/ 0.103
(56)

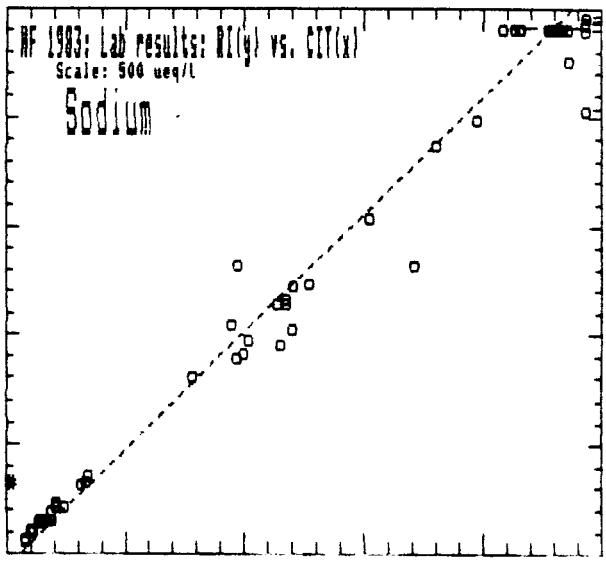

HF 1983: RI(y) vs. CIT(x)

Lab Results Comparison

Potassium

n = 50

y = B1*x + B0
R2 = 0.6466
B1 = 0.468 (0.085)
B0 = 12.2 (4.0)
(+/-90%)

mean x,y: 28., 25.
psd= 17. (63.0%)

For RD = 2*(Y-X)/(Y+X)

mean/sd: 0.138/ 0.428
RD<0.50 0.095/ 0.187
(39)

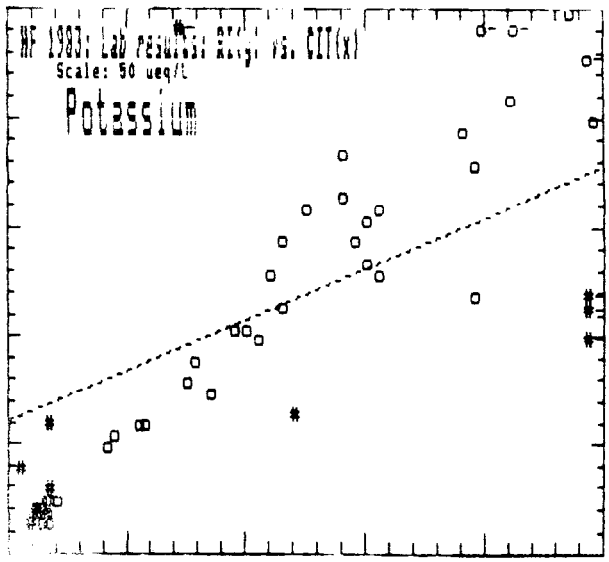

HF 1983: RI(y) vs. CIT(x)

Lab Results Comparison

Ammonium

n = 65

y = B1*x + B0
R2 = 0.9350
B1 = 1.212 (0.068)
B0 = 41.8 (51.5)
(+/-90%)

mean x,y: 579., 744.
psd= 174. (26.3%)

For RD = 2*(Y-X)/(Y+X)

mean/sd: 0.275/ 0.166
RD<0.50 0.259/ 0.153
(62)

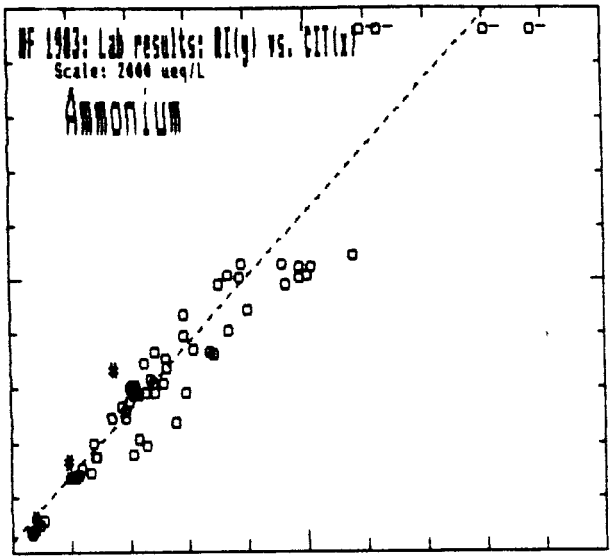

HF 1983: RI(y) vs. CIT(x)

Lab Results Comparison

Calcium

n = 58

y = B1*x + B0
R2 = 0.9471
B1 = 0.997 (0.053)
B0 = 6.6 (11.9)
(+/-90%)

mean x,y: 153., 159.
psd= 27. (17.5%)

For RD = 2*(Y-X)/(Y+X)

mean/sd: 0.126/ 0.337
RD<0.50 0.043/ 0.176
(53)

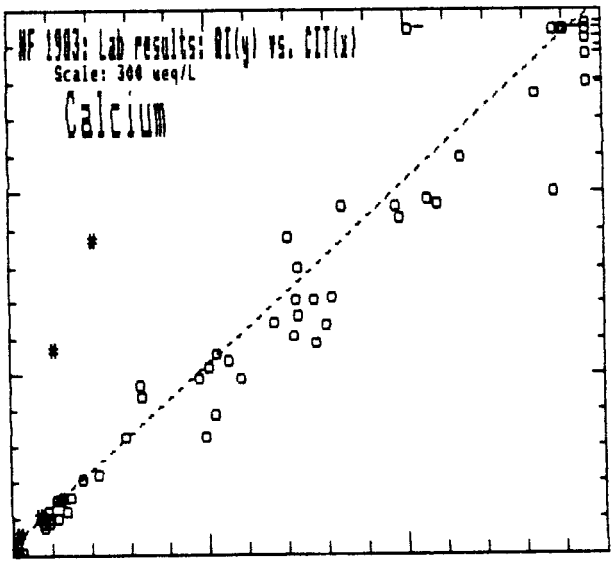

HF 1983: RI(y) vs. CIT(x)

Lab Results Comparison

Magnesium

n = 58

y = B1*x + B0
R2 = 0.9923
B1 = 1.031 (0.021)
B0 = 4.9 (4.0)
(+/-90%)

mean x,y: 119., 127.
psd= 12. (9.7%)

For RD = 2*(Y-X)/(Y+X)

mean/sd: 0.115/ 0.181
RD<0.50 0.082/ 0.104
(55)

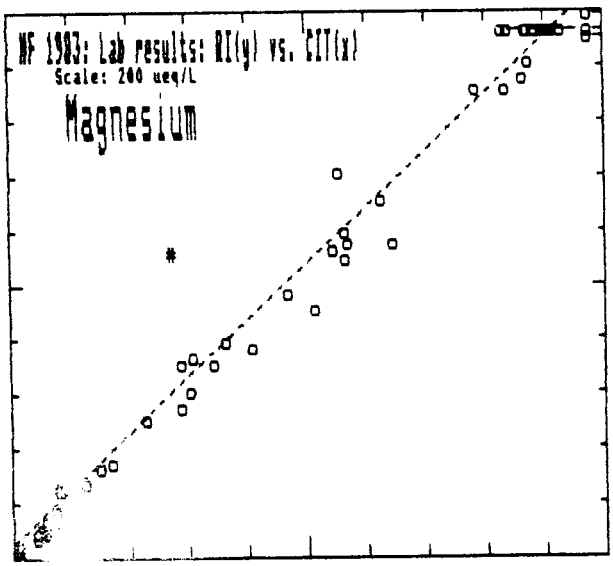

HF 1983: RI(y) vs. CIT(x)

Lab Results Comparison

Chloride

n = 44

y = B1*x + B0
R2 = 0.8125
B1 = 0.820 (0.103)
B0 = 21.5 (41.5)
(+/-90%)

mean x,y: 300., 267.
psd= 86. (30.2%)

For RD = 2*(Y-X)/(Y+X)

mean/sd: -0.094/ 0.297
RD<0.50 -0.035/ 0.186
(41)

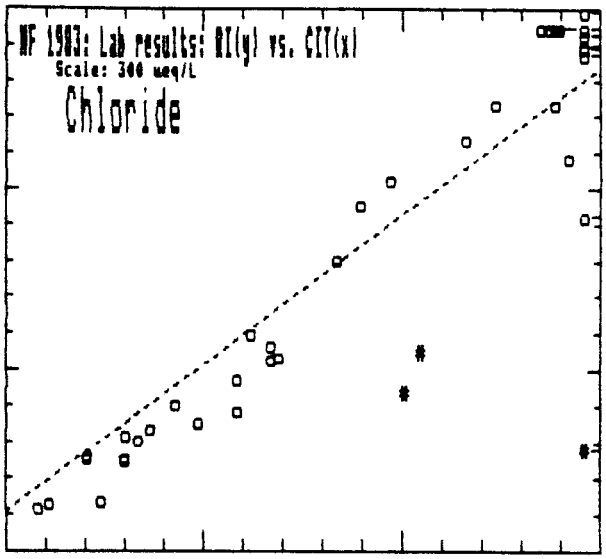

HF 1983: RI(y) vs. CIT(x)

Lab Results Comparison

Nitrate

n = 64

y = B1*x + B0
R2 = 0.9915
B1 = 0.969 (0.019)
B0 = 55.6 (44.2)
(+/-90%)

mean x,y: 1724., 1727.
psd= 100. (5.8%)

For RD = 2*(Y-X)/(Y+X)

mean/sd: 0.023/ 0.098
RD<0.50 0.023/ 0.098
(64)

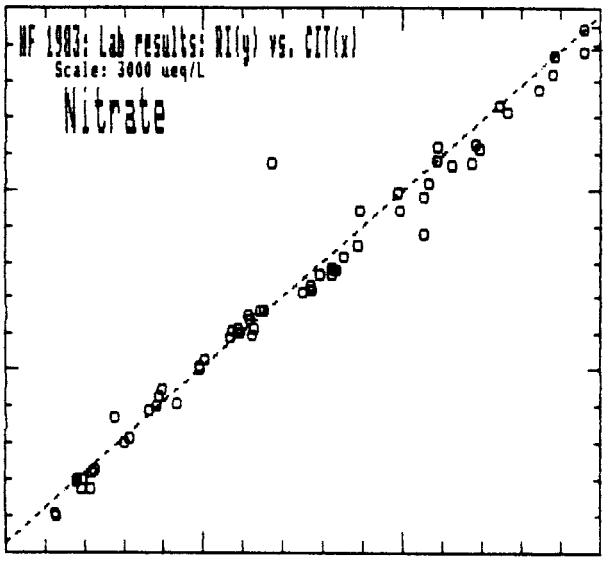

HF 1983: RI(y) vs. CIT(x)

Lab Results Comparison

Sulfate

n = 64

y = B1*x + B0
R2 = 0.9731
B1 = 0.922 (0.033)
B0 = 39.8 (40.7)
(+/-90%)

mean x,y: 994., 957.
psd= 92. (9.4%)

For RD = 2*(Y-X)/(Y+X)

mean/sd: -0.030/ 0.129
RD<0.50 -0.030/ 0.129
(64)

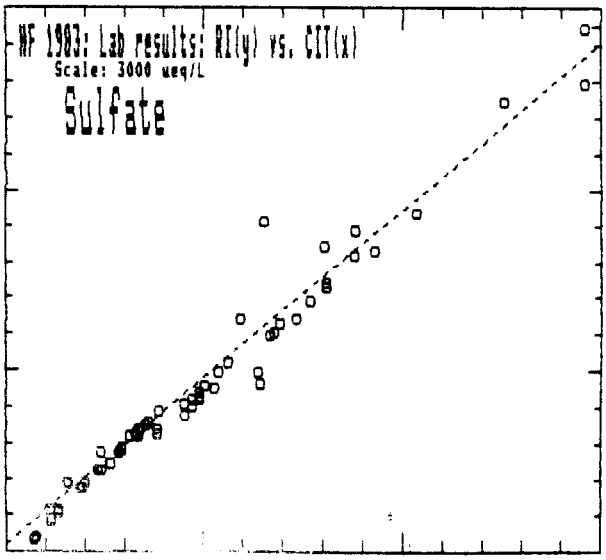

*** ROCKWELL LABORATORY RESULTS FOR HENNINGER FLATS FOGWATER SAMPLES - JUNE 1983 ***
source: Hering & Blumenthal (1984)

CRC code	Start	Stop	mL	-----pH---- (lab)	field	micro-equivalents/liter H	Na	K	NH4	Ca	Mg	Cl	NO3	SO4	-/+	CRC Code
608C01	20:37	21:33	10.2	(2.97)	2.94	1148.	-1.	-1.	904.	-1.	-1.	457.	2290.	1366.	1.975	608C01
608C02	21:35	23:30	34.9	(2.96)	2.94	1148.	550.	36.	606.	320.	176.	248.	1659.	1014.	1.014	608C02
608C03	23:35	0:30	26.1	(2.99)	2.96	1096.	377.	23.	434.	178.	114.	162.	1350.	800.	1.025	608C03
608C04	0:30	1:30	52.3	(3.12)	3.10	794.	165.	10.	309.	68.	52.	72.	839.	512.	1.006	608C04
608C05	1:30	3: 0	16.1	(3.00)	3.00	1000.	232.	39.	379.	116.	78.	89.	1214.	662.	1.052	608C05
610C01	4:35	4:49	13.6	(3.53)	3.46	347.	42.	-1.	325.	44.	22.	18.	424.	344.	1.002	610C01
610C02	5: 0	5:35	21.8	(3.58)	3.48	331.	31.	5.	290.	46.	12.	18.	416.	244.	0.943	610C02
610C03	5:37	6:30	13.3	(3.29)	3.19	646.	68.	14.	512.	114.	28.	39.	883.	480.	1.006	610C03
610C04	6:35	7:30	44.0	(3.24)	3.10	794.	23.	3.	363.	34.	10.	29.	800.	374.	0.971	610C04
610C05	7:35	8:34	64.2	(3.06)	2.98	1047.	33.	3.	600.	20.	10.	51.	1205.	598.	1.068	610C05
610C06	8:37	9:30	56.6	(3.03)	2.96	1096.	45.	5.	692.	22.	14.	63.	1305.	704.	1.090	610C06
610C07	9:32	10:26	69.1	(3.12)	3.05	891.	45.	5.	622.	22.	14.	53.	1041.	574.	1.031	610C07
610C08	10:30	11:28	44.1	(3.01)	2.66	2188.	33.	4.	628.	20.	10.	82.	1230.	662.	0.667	610C08
610C09	11:32	12:25	21.2	(2.74)	2.66	2188.	76.	16.	1028.	106.	36.	122.	2009.	1788.	1.096	610C09
610C10	12:30	13:32	54.2	(3.11)	3.04	912.	16.	6.	300.	32.	10.	27.	659.	720.	1.082	610C10
610C11	13:35	14:30	54.0	(3.60)	3.55	282.	-1.	-1.	92.	4.	2.	12.	243.	96.	0.921	610C11
610C12	14:32	15:25	37.9	(3.42)	3.33	468.	-1.	-1.	102.	-1.	-1.	17.	380.	190.	1.024	610C12
610C13	15:29	16:30	49.6	(3.33)	3.25	562.	-1.	-1.	122.	-1.	-1.	11.	470.	242.	1.049	610C13
618C01	6:31	7:35	9.4	(%-1)	2.81	1549.	-1.	-1.	1023.	188.	-1.	119.	2148.	1218.	1.238	618C01
621C01	7:30	9:30	12.1	(%-1)	2.67	2138.	-1.	-1.	3245.	-1.	-1.	1051.	8602.	3030.	2.314	621C01
622C01	4:30	5:32	10.2	(%-1)	3.15	708.	268.	24.	675.	146.	112.	176.	1249.	470.	0.974	622C01
624C01	6: 1	7: 2	34.9 *	(2.91)	2.87 *	1349.	194.	12.	591.	68.	56.	108.	1461.	670.	0.971	624C01
624C02	7: 3	8: 5	16.3 *	(%-1)	2.66 *	2188.	402.	20.	1015.	120.	120.	192.	2569.	956.	0.943	624C02
624C03	8:12	10: 2	12.4	(%-1)	2.41	3890.	944.	58.	2766.	406.	284.	414.	5482.	3150.	1.037	624C03
625C01	3:19	5:30	28.4	(2.79)	2.75	1778.	689.	29.	595.	132.	172.	248.	2265.	862.	0.978	625C01
625C02	5:36	6:38	11.3	(%-1)	2.82	1514.	1005.	48.	751.	256.	272.	384.	2474.	1062.	1.004	625C02
625C03	6:40	7:33	37.0	(%-1)	3.13	741.	1033.	39.	726.	194.	256.	453.	1573.	878.	0.963	625C03
625C04	7:35	8:33	36.6	(%-1)	3.06	871.	896.	31.	632.	144.	226.	413.	1489.	868.	0.979	625C04
625C05	8:35	9:32	22.6	(%-1)	2.97	1072.	783.	26.	538.	110.	194.	411.	1449.	840.	0.979	625C05
625C06	9:34	11: 0	15.9	(%-1)	2.77	1698.	1520.	49.	887.	220.	378.	801.	2659.	1408.	1.006	625C06
608J01	20:37	21:35	2.6	(%-1)	3.14	724.	1175.	94.	742.	-1.	-1.	539.	2167.	1274.	1.442	608J01
608J02	21:45	23:35	12.6	(3.19)	3.15	708.	1070.	266.	756.	648.	496.	460.	2252.	1302.	1.009	608J02
608J03	23:45	0:35	12.1	(2.96)	2.96	1096.	574.	40.	492.	256.	182.	218.	1580.	942.	1.023	608J03
608J04	0:45	1:35	12.8	(3.08)	3.11	776.	213.	18.	327.	90.	72.	79.	918.	574.	1.038	608J04
608J05	1:45	3: 0	6.0	(3.06)	3.10	794.	268.	74.	408.	176.	92.	111.	1353.	744.	1.206	608J05

*H&B data volume in error fog these values.

*** ROCKWELL LABORATORY RESULTS FOR HENNINGER FLATS FOGWATER SAMPLES - JUNE 1983 ***
source: Hering & Blumenthal (1984)

CRC code	Start	Stop	mL	-----pH---- (lab)	field	micro-equivalents/liter H	Na	K	NH4	Ca	Mg	Cl	NO3	SO4	-/+	CRC Code
607B01	21: 4	22: 2	38.1	(2.69)	2.69	2042.	251.	33.	100.	410.	116.	109.	2244.	1892.	1.039	607B01
607B02	22: 4	22:58	27.4	(2.78)	2.73	1862.	236.	29.	1059.	346.	110.	91.	1900.	1656.	0.971	607B02
607B03	23: 0	0: 2	22.5	(2.81)	2.83	1479.	199.	21.	1026.	162.	72.	91.	1591.	1496.	1.046	607B03
610B01	4:35	4:49	11.9	(3.54)	3.46	347.	43.	-1.	345.	34.	18.	24.	421.	394.	1.059	610B01
610B02	5: 0	5:35	27.6	(3.57)	3.48	331.	33.	-1.	295.	44.	14.	17.	425.	244.	0.952	610B02
610B03	5:37	6:30	18.1	(3.35)	3.23	589.	51.	11.	418.	96.	26.	31.	761.	408.	1.000	610B03
610B04	6:35	7:30	43.9	(3.24)	3.10	794.	24.	4.	371.	32.	10.	31.	823.	380.	0.989	610B04
610B05	7:35	8:34	62.4	(3.07)	2.98	1047.	33.	4.	628.	20.	10.	53.	1243.	606.	1.078	610B05
610B06	8:38	9:30	59.1	(3.04)	2.96	1096.	47.	12.	712.	26.	14.	65.	1323.	700.	1.079	610B06
610B07	9:32	10:26	61.2	(3.13)	3.05	891.	47.	4.	603.	22.	14.	54.	1084.	592.	1.081	610B07
610B08	10:30	11:28	42.1	(3.02)	2.67	2138.	32.	4.	614.	18.	10.	69.	1250.	674.	0.690	610B08
610B09	11:34	12:25	21.1	(2.78)	2.68	2089.	69.	15.	994.	100.	34.	96.	1905.	1700.	1.083	610B09
610B10	12:30	13:32	56.5	(3.14)	3.05	891.	14.	4.	291.	26.	8.	25.	630.	694.	1.074	610B10
610B11	13:35	14:30	55.7	(3.62)	3.55	282.	68.	8.	87.	12.	4.	11.	223.	90.	0.701	610B11
610B12	14:32	15:25	37.5	(3.42)	3.33	468.	-1.	-1.	133.	-1.	-1.	-1.	381.	194.	0.951	610B12
610B13	15:29	16:30	57.0	(3.35)	3.26	550.	-1.	3.	131.	4.	2.	9.	463.	246.	1.033	610B13
618B01	6:30	7:32	17.2	(2.90)	2.87	1349.	311.	18.	825.	202.	116.	99.	1773.	1018.	1.006	618B01
621B01	7:30	9:30	12.5	(%-1)	2.73	1862.	3532.	139.	2675.	928.	954.	887.	7059.	2498.	1.018	621B01
622B01	4:30	5:30	22.6	(3.25)	3.19	646.	182.	13.	571.	124.	74.	106.	1031.	402.	0.950	622B01
624B01	6: 6	7: 5	38.6	(2.90)	2.85	1413.	210.	12.	639.	80.	62.	115.	1551.	704.	0.966	624B01
624B02	7: 6	8: 2	15.1*	(2.68)	2.62*	2399.	455.	21.	1066.	130.	132.	206.	2756.	1228.	0.973	624B02
624B03	8:13	10: 0	12.7*	(%-1)	2.42*	3802.	831.	65.	2597.	370.	256.	396.	5266.	2938.	1.041	624B03
625B01	3:19	5:30	29.8	(2.83)	2.80	1585.	626.	32.	547.	144.	172.	228.	2055.	776.	0.970	625B01
625B02	5:36	6:35	9.9	(2.91)	2.90	1259.	981.	62.	653.	334.	284.	345.	2185.	900.	0.948	625B02
625B03	6:37	7:30	32.8	(3.12)	3.12	759.	1140.	42.	759.	196.	284.	508.	1717.	926.	0.982	625B03
625B04	7:32	8:30	37.7	(3.08)	3.08	832.	883.	32.	604.	136.	222.	409.	1454.	834.	0.986	625B04
625B05	8:32	9:30	22.6	(3.00)	2.98	1047.	796.	27.	508.	100.	202.	410.	1451.	828.	0.991	625B05
625B06	9:32	11: 0	16.1	(2.83)	2.80	1585.	1472.	50.	809.	198.	362.	729.	2445.	1304.	0.983	625B06
607C01	21: 5	22: 4	28.8	(2.71)	2.70	1995.	249.	37.	1059.	432.	142.	98.	2171.	1844.	1.017	607C01
607C02	22: 6	23: 2	34.3	(2.74)	2.73	1862.	231.	26.	1073.	300.	98.	91.	1985.	1682.	1.015	607C02
607C03	23: 4	0: 4	20.8	(2.83)	2.84	1445.	185.	85.	991.	194.	80.	85.	1558.	1478.	1.021	607C03

APPENDIX B.

HENNINGER FLATS FOGWATER DATA

5. Spring 1983

Fog Collector Intercomparison (CRC) Data:

Rockwell Laboratory Results for Combined Samples

and Collector Pair Comparisons

CIT83b(y) vs.CIT83c(x): [RI Lab results]

Y = b0 + b1 * X b0 & b1 given with (90% confidence)
RD = 2(Y-X)/(X+Y) given as "mean/s.d."

Field pH
n= 14
mean x,y= 2.92, 2.93 psd=0.013 (0.5%)
r2 = 0.9962 b0= 0.02 (0.09)
b1= 0.991 (0.032)
y-x= 0.01 /0.02

Hydrogen
n= 14
mean x,y =1419., 1383. psd= 50. (3.6%)
r2 = 0.9956 b0= 1.16 (55.54)
b1= 0.973 (0.033)
RD= -0.025 / 0.038 only<0.50: -0.025/ 0.038 (14)

Sodium
n= 13
mean x,y = 455., 450. psd= 33. (7.3%)
r2 = 0.9913 b0= 11.66 (32.30)
b1= 0.965 (0.049)
RD= 0.111 / 0.420 only<0.50: -0.004/ 0.078 (12)

Potassium
n= 12
mean x,y = 30., 27. psd= 13. (47.0%)
r2 = 0.4335 b0= 11.17 (12.82)
b1= 0.514 (0.334)
RD= 0.029 / 0.420 only<0.50: 0.141/ 0.167 (11)

Ammonium
n= 14
mean x,y = 785., 771. psd= 40. (5.2%)
r2 = 0.9950 b0= 33.14 (34.25)
b1= 0.939 (0.034)
RD= -0.008 / 0.071 only<0.50: -0.008/ 0.071 (14)

Calcium
n= 13
mean x,y = 148., 145. psd= 13. (8.8%)
r2 = 0.9783 b0= 2.24 (14.90)
b1= 0.966 (0.078)
RD= -0.008 / 0.106 only<0.50: -0.008/ 0.106 (13)

Magnesium
n= 13
mean x,y = 128., 126. psd= 8. (6.6%)
r2 = 0.9905 b0= 1.85 (9.00)
b1= 0.972 (0.052)
RD= -0.013 / 0.070 only<0.50: -0.013/ 0.070 (13)

Chloride
n= 14
mean x,y = 206., 201. psd= 16. (8.1%)
r2 = 0.9918 b0= 5.70 (13.56)
b1= 0.945 (0.045)
RD= -0.107 / 0.351 only<0.50: -0.016/ 0.087 (13)

Nitrate
n= 14
mean x,y =1739., 1714. psd= 79. (4.6%)
r2 = 0.9941 b0= 61.80 (80.82)
b1= 0.950 (0.038)
RD= -0.008 / 0.049 only<0.50: -0.008/ 0.049 (14)

Sulfate
n= 14
mean x,y =1032., 1009. psd= 51. (5.0%)
r2 = 0.9942 b0= 38.20 (47.21)
b1= 0.941 (0.037)
RD= -0.014 / 0.048 only<0.50: -0.014/ 0.048 (14)

Collection rate
n= 14
mean x,y= 0.5, 0.6 psd= 0.0 (5.6%)
r2 = 0.9838 b0= 0.03 (0.04)
b1= 0.993 (0.066)
RD= 0.053 / 0.079
only<0.50: 0.053/ 0.079 (14)

GGC83h(y) vs.GGC83g(x): [RI Lab results]

Y = b0 + b1 * X b0 & b1 given with (90% confidence)
RD = 2(Y-X)/(X+Y) given as "mean/s.d."

Field pH	mean x,y= 2.95, 2.94	psd=0.033 (1.1%)
n= 13	r2 = 0.9741	b0= -0.02 (0.26)
		b1= 1.011 (0.089)
	y-x= -0.01 /0.05	
Hydrogen	mean x,y =1361., 1421.	psd=134. (9.6%)
n= 13	r2 = 0.9771	b0=-100.50 (149.65)
		b1= 1.118 (0.093)
	RD= 0.028 / 0.107	only<0.50: 0.028/ 0.107 (13)
Sodium	mean x,y = 273., 336.	psd=185. (60.8%)
n= 12	r2 = 0.5448	b0= 59.32 (204.16)
		b1= 1.014 (0.526)
	RD= -0.073 / 0.527	only<0.50: -0.093/ 0.215 (10)
Potassium	mean x,y = 34., 27.	psd= 11. (37.3%)
n= 12	r2 = 0.6411	b0= 6.08 (11.17)
		b1= 0.628 (0.267)
	RD= -0.209 / 0.485	only<0.50: -0.029/ 0.307 (7)
Ammonium	mean x,y = 959., 919.	psd=144. (15.3%)
n= 14	r2 = 0.9678	b0= 154.57 (94.15)
		b1= 0.797 (0.075)
	RD= -0.026 / 0.157	only<0.50: -0.026/ 0.157 (14)
Calcium	mean x,y = 232., 362.	psd=212. (71.3%)
n= 12	r2 = 0.2586	b0= 87.77 (304.79)
		b1= 1.181 (1.136)
	RD= 0.271 / 0.447	only<0.50: 0.076/ 0.246 (9)
Magnesium	mean x,y = 82., 108.	psd= 61. (64.2%)
n= 12	r2 = 0.4702	b0= 18.60 (71.28)
		b1= 1.088 (0.656)
	RD= 0.038 / 0.442	only<0.50: -0.003/ 0.209 (10)
Chloride	mean x,y = 264., 249.	psd= 37. (14.2%)
n= 14	r2 = 0.9825	b0= 24.97 (21.75)
		b1= 0.847 (0.059)
	RD= -0.010 / 0.202	only<0.50: -0.010/ 0.202 (14)
Nitrate	mean x,y =1979., 1979.	psd=336. (17.0%)
n= 14	r2 = 0.9148	b0= 381.07 (319.41)
		b1= 0.808 (0.128)
	RD= 0.024 / 0.173	only<0.50: -0.013/ 0.108 (13)
Sulfate	mean x,y =1204., 1175.	psd=183. (15.4%)
n= 14	r2 = 0.9430	b0= 213.77 (154.09)
		b1= 0.798 (0.102)
	RD= 0.004 / 0.150	only<0.50: 0.004/ 0.150 (14)
Collection rate	mean x,y= 0.2, 0.2	psd= 0.0 (17.7%)
n= 14	r2 = 0.9299	b0= -0.02 (0.04)
		b1= 1.143 (0.163)
	RD= 0.010 / 0.262	only<0.50: 0.068/ 0.153 (13)

HF 1983:

GGC83g(y) vs.GGC83h(x)
[Combined RI data]

Field pH

n = 13

y = B1*x + B0
R2 = 0.9741
B1 = 0.964 (0.085)
B0 = 0.1194 (0.2516)
(+/-90%)

mean x,y: 2.94,2.95
psd=0.033 (1.1%)

For pH(y)-pH(x)

mean/sd: 0.012/ 0.047

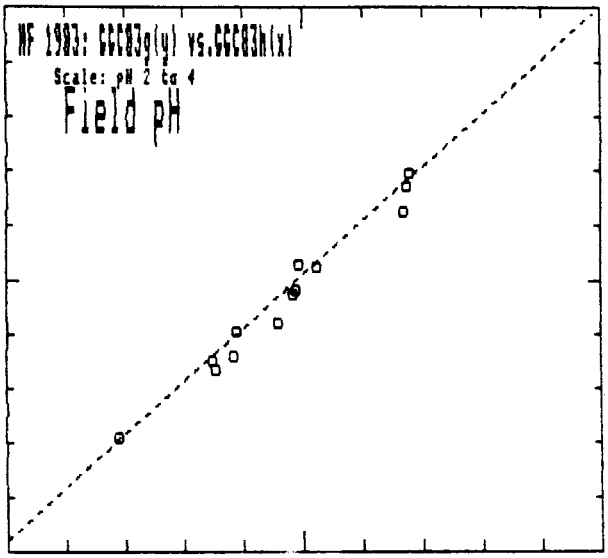

HF 1983:

GGC83g(y) vs.GGC83h(x)
[Combined RI data]

Collection rate

n = 14

y = B1*x + B0
R2 = 0.9299
B1 = 0.814 (0.116)
B0 = 0.0291 (0.0321)
(+/-90%)

mean x,y: 0.2, 0.2
psd=0.037 (17.7%)

For RD = 2*(Y-X)/(Y+X)

mean/sd: -0.010/ 0.262
RD<0.50 -0.068/ 0.153
(13)

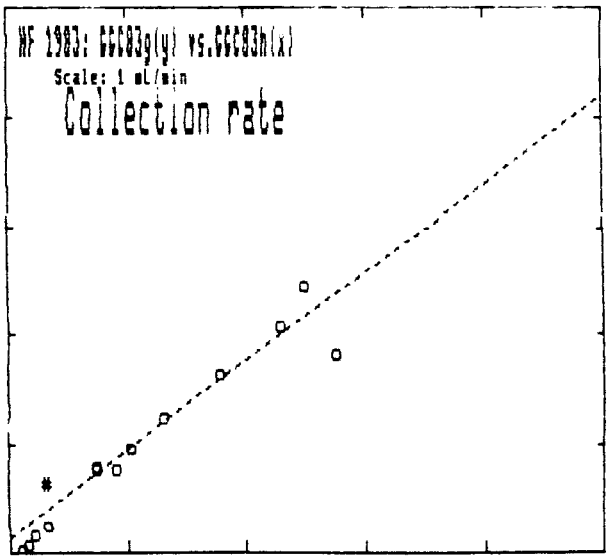

HF 1983:

GGC83g(y) vs.GGC83h(x)
[Combined RI data]

Hydrogen

n = 13

y = B1*x + B0
R2 = 0.9771
B1 = 0.874 (0.073)
B0 = 119.1 (125.1)
(+/-90%)

mean x,y: 1421., 1361.
psd= 134. (9.6%)

For RD = 2*(Y-X)/(Y+X)

mean/sd: -0.028/ 0.107
RD<0.50 -0.028/ 0.107
(13)

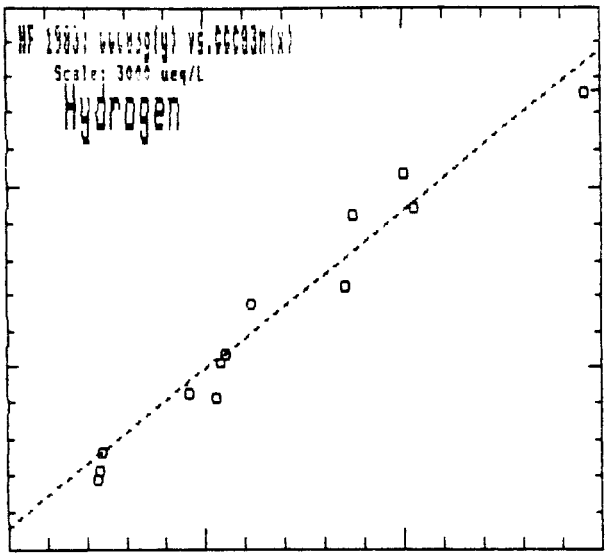

HF 1983:

GGC83g(y) vs.GGC83h(x)
[Combined RI data]

Sodium

n = 12

y = B1*x + B0
R2 = 0.5448
B1 = 0.537 (0.279)
B0 = 92.4 (141.1)
(+/-90%)

mean x,y: 336., 273.
psd= 185. (60.8%)

For RD = 2*(Y-X)/(Y+X)

mean/sd: 0.073/ 0.527
RD<0.50 0.093/ 0.215
(10)

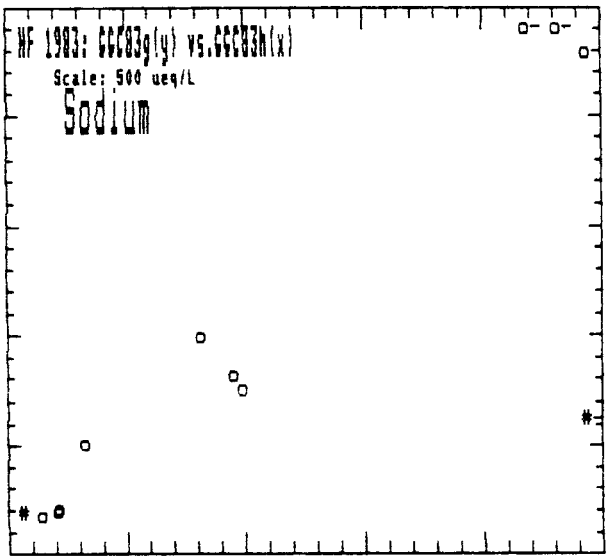

HF 1983:

GGC83g(y) vs.GGC83h(x)
[Combined RI data]

Potassium

n = 12

y = B1*x + B0
R2 = 0.6411
B1 = 1.021 (0.434)
B0 = 5.9 (14.5)
(+/-90%)

mean x,y: 27., 34.
psd= 11. (37.3%)

For RD = 2*(Y-X)/(Y+X)

mean/sd: 0.209/ 0.485
RD<0.50 0.029/ 0.307
(7)

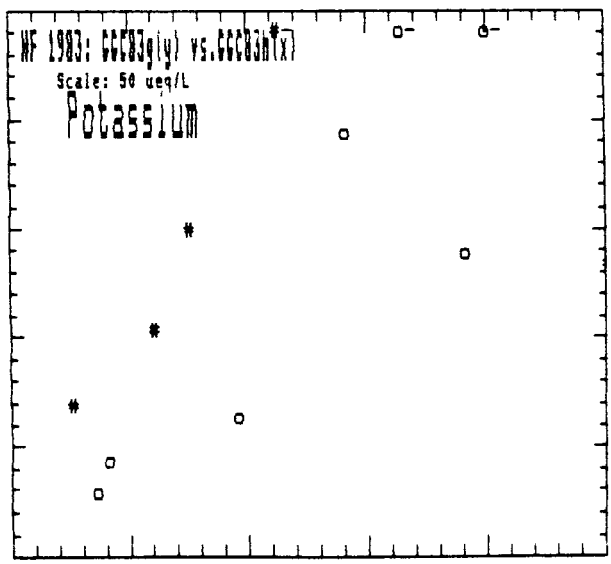

HF 1983:

GGC83g(y) vs.GGC83h(x)
[Combined RI data]

Ammonium

n = 14

y = B1*x + B0
R2 = 0.9678
B1 = 1.215 (0.115)
B0 = -156.9 (129.2)
(+/-90%)

mean x,y: 919., 969.
psd= 144. (15.3%)

For RD = 2*(Y-X)/(Y+X)

mean/sd: 0.026/ 0.157
RD<0.50 0.026/ 0.157
(14)

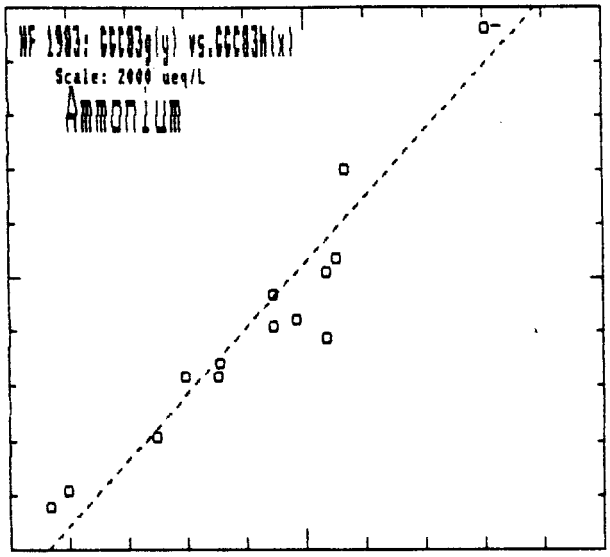

HF 1983:

GGC83g(y) vs.GGC83h(x)
[Combined RI data]

Calcium

n = 12

y = B1*x + B0
R2 = 0.2686
B1 = 0.219 (0.211)
B0 = 152.7 (100.8)
(+/-90%)

mean x,y: 362., 232.
psd= 212. (71.3%)

For RD = 2*(Y-X)/(Y+X)

mean/sd: -0.271/ 0.447
RD<0.50 -0.076/ 0.246
(9)

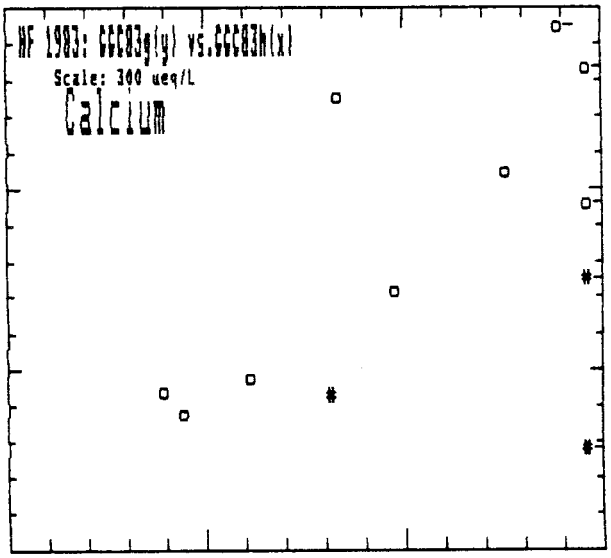

HF 1983:

GGC83g(y) vs.GGC83h(x)
[Combined RI data]

Magnesium

n = 12

y = B1*x + B0
R2 = 0.4702
B1 = 0.432 (0.261)
B0 = 35.4 (40.6)
(+/-90%)

mean x,y: 108., 82.
psd= 61. (64.2%)

For RD = 2*(Y-X)/(Y+X)

mean/sd: -0.038/ 0.442
RD<0.50 0.003/ 0.209
(10)

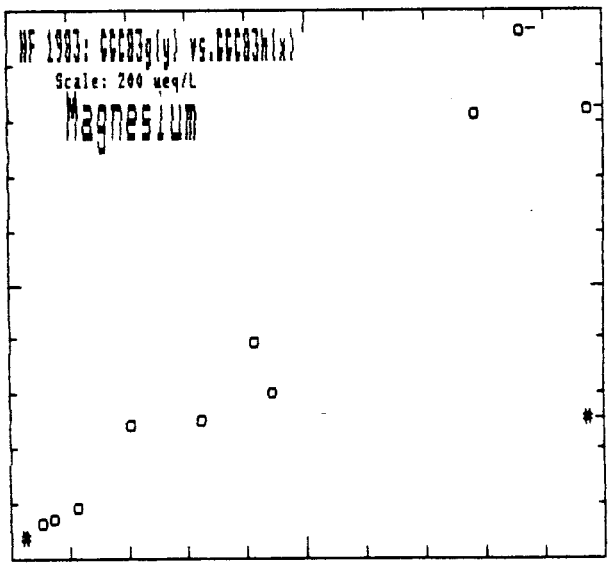

HF 1983:

GGC83g(y) vs.GGC83h(x)
[Combined RI data]

Chloride

n = 14

y = B1*x + B0
R2 = 0.9825
B1 = 1.160 (0.080)
B0 = -24.3 (26.8)
(+/-90%)

mean x,y: 249., 264.
psd= 37. (14.2%)

For RD = 2*(Y-X)/(Y+X)

mean/sd: 0.010/ 0.202
RD<0.50 0.010/ 0.202
(14)

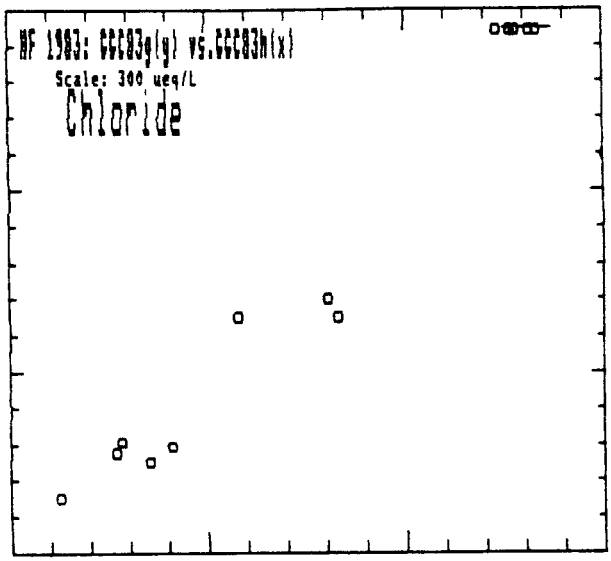

HF 1983:

GGC83g(y) vs.GGC83h(x)
[Combined RI data]

Nitrate

n = 14

y = B1*x + B0
R2 = 0.9148
B1 = 1.133 (0.180)
B0 = -263.0 (423.3)
(+/-90%)

mean x,y: 1979., 1979.
psd= 336. (17.0%)

For RD = 2*(Y-X)/(Y+X)

mean/sd: -0.024/ 0.173
RD<0.50 0.013/ 0.108
(13)

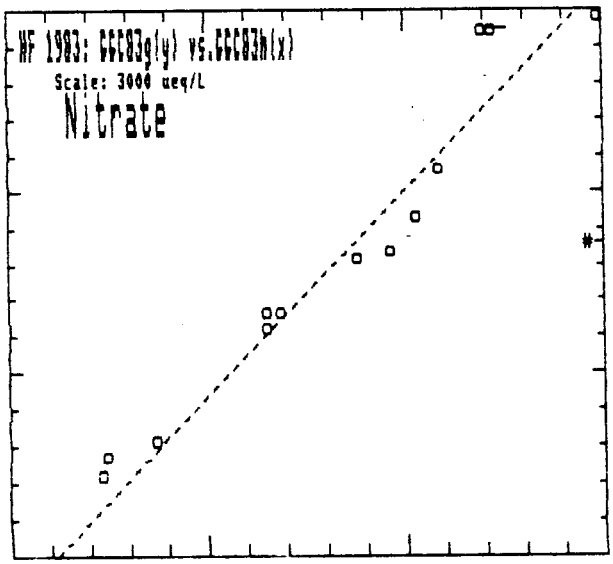

HF 1983:

GGC83g(y) vs.GGC83h(x)
[Combined RI data]

Sulfate

n = 14

y = B1*x + B0
R2 = 0.9430
B1 = 1.181 (0.151)
B0 = -183.9 (210.7)
(+/-90%)

mean x,y: 1175., 1204.
psd= 183. (15.4%)

For RD = 2*(Y-X)/(Y+X)

mean/sd: -0.004/ 0.150
RD<0.50 -0.004/ 0.150
(14)

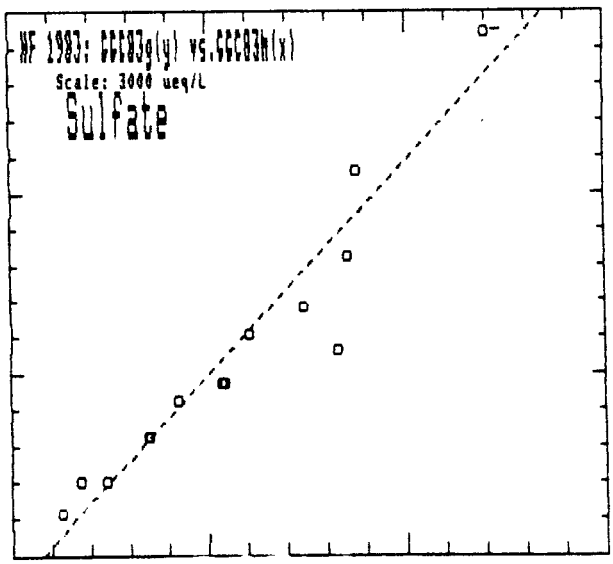

DRI83(y) vs.CIT83c(x): [RI Lab results]

Y = b0 + b1 * X b0 & b1 given with (90% confidence)
RD = 2(Y-X)/(X+Y) given as "mean/s.d."

Field pH
n= 16
mean x,y= 2.95, 2.90 psd=0.063 (2.2%)
r2 = 0.8946 b0= -0.02 (0.48)
b1= 0.977 (0.161)
y-x= -0.04 /0.08

Hydrogen
n= 16
mean x,y =1326., 1459. psd=235. (16.9%)
r2 = 0.8754 b0= 159.29 (276.99)
b1= 0.980 (0.177)
RD= 0.094 / 0.189 only<0.50: 0.094/ 0.189 (16)

Sodium
n= 14
mean x,y = 370., 172. psd=190. (70.1%)
r2 = 0.9098 b0= -17.90 (43.05)
b1= 0.514 (0.084)
RD= -0.820 / 0.327 only<0.50: -0.332/ 0.017 (2)

Potassium
n= 11
mean x,y = 25., 15. psd= 10. (48.5%)
r2 = 0.6516 b0= 2.87 (6.52)
b1= 0.505 (0.221)
RD= -0.398 / 0.475 only<0.50: -0.223/ 0.210 (5)

Ammonium
n= 16
mean x,y = 720., 778. psd=139. (18.6%)
r2 = 0.9033 b0= 185.60 (120.05)
b1= 0.823 (0.129)
RD= 0.129 / 0.210 only<0.50: 0.101/ 0.184 (15)

Calcium
n= 14
mean x,y = 152., 58. psd= 93. (88.2%)
r2 = 0.5981 b0= 12.64 (25.14)
b1= 0.301 (0.128)
RD= -0.873 / 0.411 only<0.50: -0.162/ 0.140 (2)

Magnesium
n= 14
mean x,y = 109., 63. psd= 44. (51.5%)
r2 = 0.8455 b0= -5.05 (19.92)
b1= 0.626 (0.139)
RD= -0.490 / 0.372 only<0.50: -0.239/ 0.262 (8)

Chloride
n= 16
mean x,y = 158., 145. psd= 34. (22.3%)
r2 = 0.9006 b0= -7.04 (32.70)
b1= 0.962 (0.153)
RD= -0.119 / 0.254 only<0.50: -0.075/ 0.191 (15)

Nitrate
n= 16
mean x,y =1598., 1634. psd=252. (15.6%)
r2 = 0.9033 b0= 157.79 (285.11)
b1= 0.923 (0.145)
RD= 0.030 / 0.207 only<0.50: 0.030/ 0.207 (16)

Sulfate
n= 16
mean x,y = 958., 955. psd=150. (15.7%)
r2 = 0.9122 b0= 165.30 (144.72)
b1= 0.825 (0.123)
RD= 0.018 / 0.203 only<0.50: 0.018/ 0.203 (16)

Collection rate
n= 16
mean x,y= 0.5, 0.2 psd= 0.3 (82.7%)
r2 = 0.3903 b0= 0.07 (0.08)
b1= 0.213 (0.128)
Rate(y/x)= 0.383 /0.209

HF 1983:

DRI83(y) vs.CIT83c(x)
[Combined RI data]

Field pH

n = 16

y = B1*x + B0
R2 = 0.8946
B1 = 0.977 (0.161)
B0 = 0.0264 (0.4756)
(+/-90%)

mean x,y: 2.95,2.90
psd=0.063 (2.2%)

For pH(y)-pH(x)

mean/sd: -0.041/ 0.082

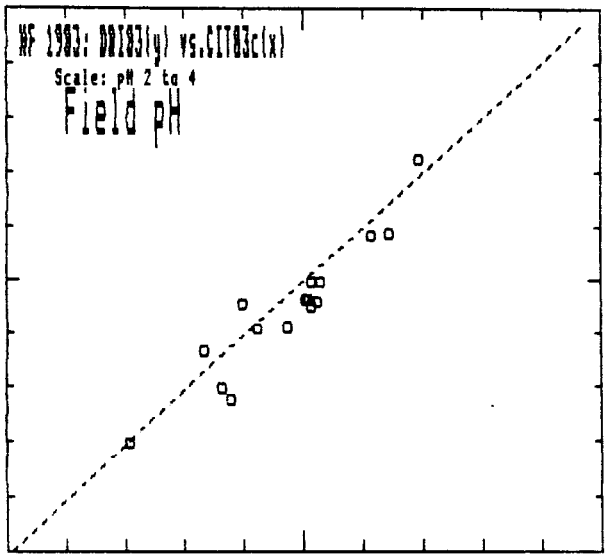

HF 1983:

DRI83(y) vs.CIT83c(x)
[Combined RI data]

Collection rate

n = 16

y = B1*x + B0
R2 = 0.3903
B1 = 0.213 (0.128)
B0 = 0.0700 (0.0770)
(+/-90%)

mean x,y: 0.5, 0.2
psd=0.296 (82.7%)

For rate(y)/rate(x)

mean/sd: 0.383/ 0.209

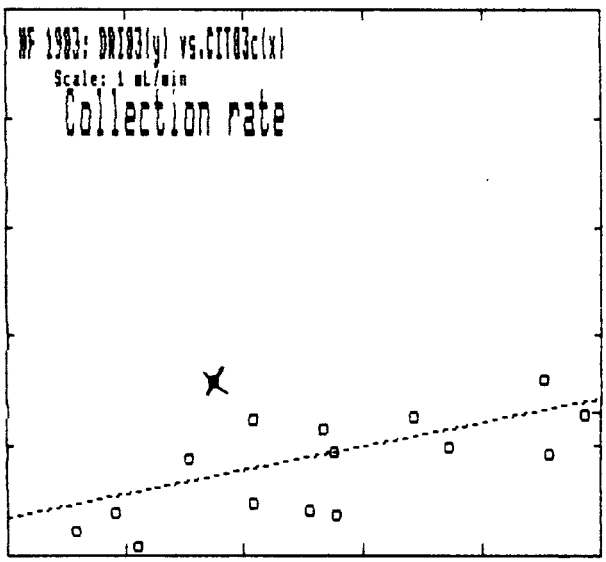

HF 1983:

DRI83(y) vs.CIT83c(x)
[Combined RI data]

Hydrogen

n = 16

y = B1*x + B0
R2 = 0.8754
B1 = 0.980 (0.177)
B0 = 159.3 (277.0)
(+/-90%)

mean x,y: 1326., 1459.
psd= 235. (16.9%)

For RD = 2*(Y-X)/(Y+X)

mean/sd: 0.094/ 0.189
RD<0.50 0.094/ 0.189
(16)

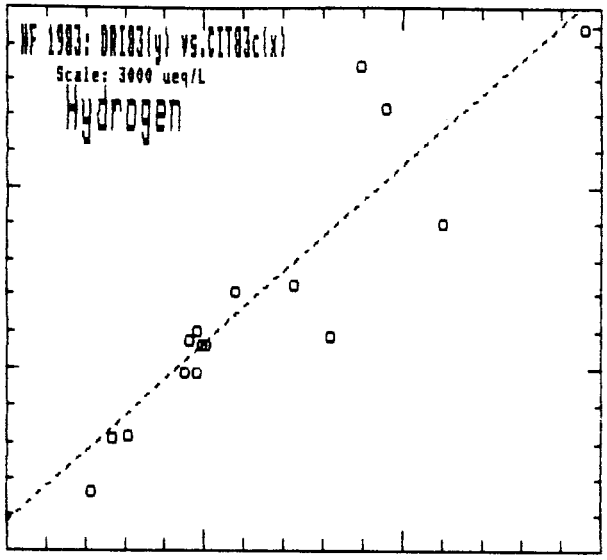

HF 1983:

DRI83(y) vs.CIT83c(x)
[Combined RI data]

Sodium

n = 14

y = B1*x + B0
R2 = 0.9098
B1 = 0.514 (0.084)
B0 = -17.9 (43.0)
(+/-90%)

mean x,y: 370., 172.
psd= 190. (70.1%)

For [y]/[x]

mean/sd: 0.436/ 0.166

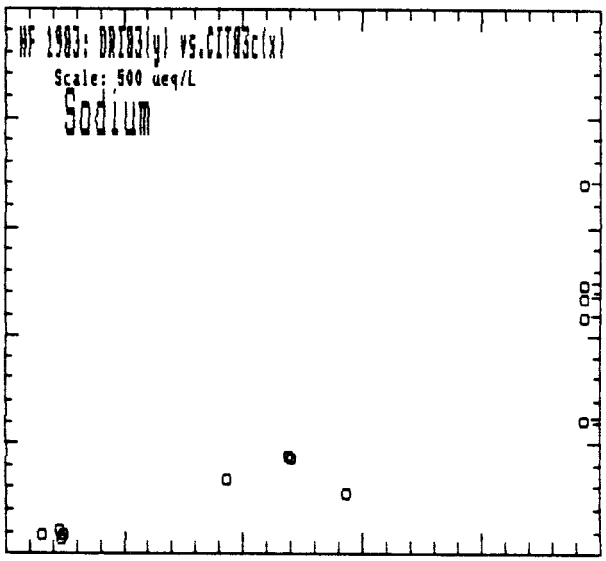

HF 1983:

DRI83(y) vs.CIT83c(x)
[Combined RI data]

Potassium

n = 11

y = B1*x + B0
R2 = 0.6516
B1 = 0.505 (0.221)
B0 = 2.9 (6.5)
(+/-90%)

mean x,y: 25., 15.
psd= 10. (48.5%)

For [y]/[x]

mean/sd: 0.751/ 0.471

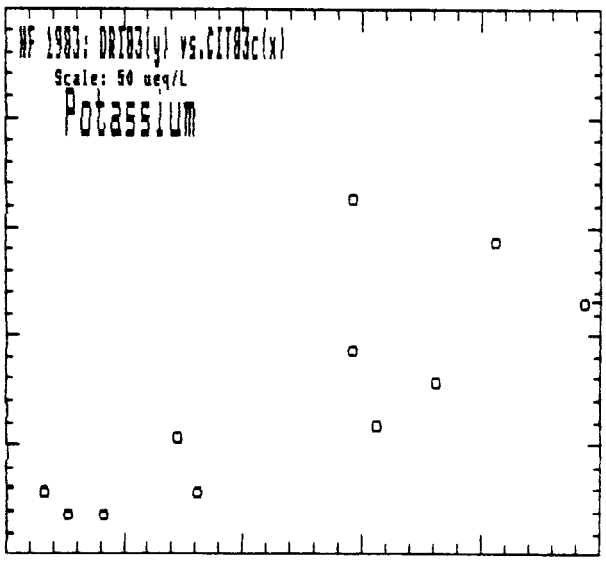

HF 1983:

DRI83(y) vs.CIT83c(x)
[Combined RI data]

Ammonium

n = 16

y = B1*x + B0
R2 = 0.9033
B1 = 0.823 (0.129)
B0 = 185.6 (120.0)
(+/-90%)

mean x,y: 720., 778.
psd= 139. (18.6%)

For RD = 2*(Y-X)/(Y+X)

mean/sd: 0.129/ 0.210
RD<0.50 0.101/ 0.184
(15)

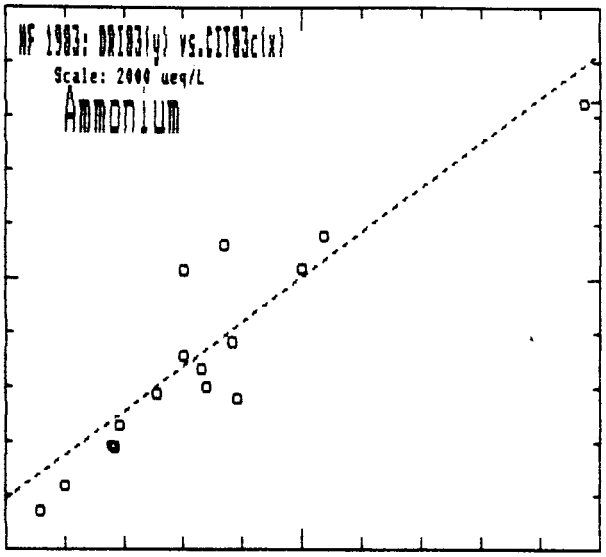

HF 1983:

DRI83(y) vs.CIT83c(x)
[Combined RI data]

Calcium

n = 14

y = B1*x + B0
R2 = 0.5981
B1 = 0.301 (0.128)
B0 = 12.6 (25.1)
(+/-90%)

mean x,y: 152., 58.
psd= 93. (88.2%)

For [y]/[x]

mean/sd: 0.421/ 0.221

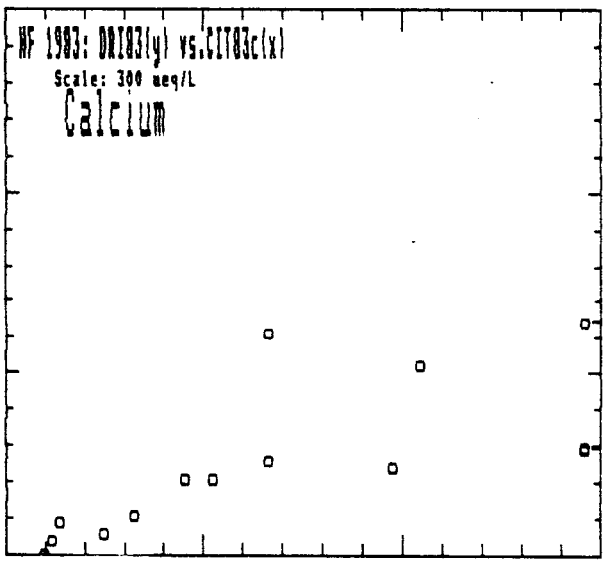

HF 1983:

DRI83(y) vs.CIT83c(x)
[Combined RI data]

Magnesium

n = 14

y = B1*x + B0
R2 = 0.8455
B1 = 0.626 (0.139)
B0 = -5.0 (19.9)
(+/-90%)

mean x,y: 109., 63.
psd= 44. (51.5%)

For [y]/[x]

mean/sd: 0.644/ 0.280

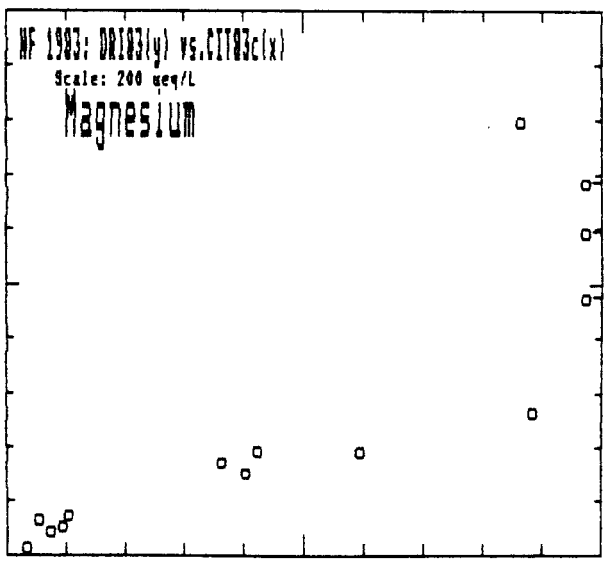

HF 1983:

DRI83(y) vs.CIT83c(x)
[Combined RI data]

Chloride

n = 16

y = B1*x + B0
R2 = 0.9006
B1 = 0.962 (0.153)
B0 = -7.0 (32.7)
(+/-90%)

mean x,y: 158., 145.
psd= 34. (22.3%)

For [y]/[x]

mean/sd: 0.912/ 0.217

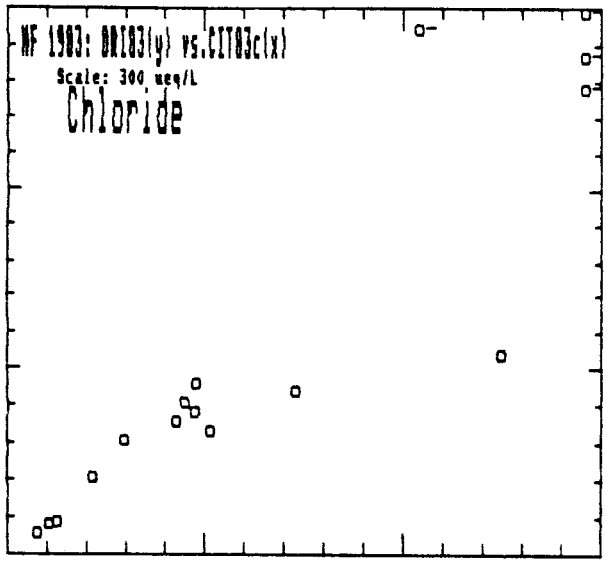

HF 1983:

DRI83(y) vs.CIT83c(x)
[Combined RI data]

Nitrate

n = 16

y = B1*x + B0
R2 = 0.9033
B1 = 0.923 (0.145)
B0 = 157.8 (285.1)
(+/-90%)

mean x,y: 1598., 1634.
psd= 252. (15.6%)

For RD = 2*(Y-X)/(Y+X)

mean/sd: 0.030/ 0.207
RD<0.50 0.030/ 0.207
(16)

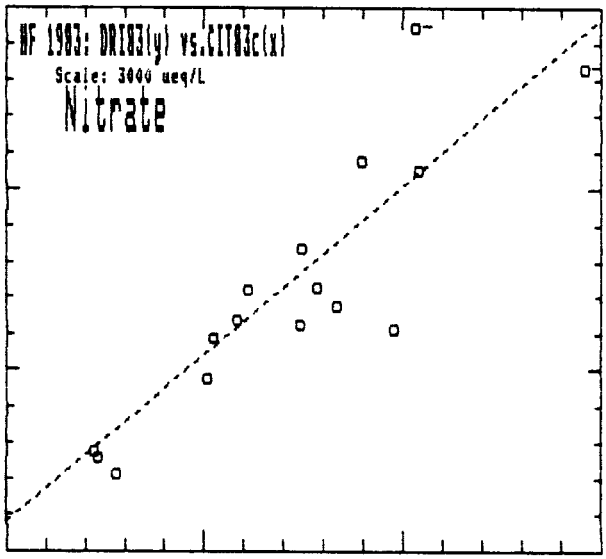

HF 1983:

DRI83(y) vs.CIT83c(x)
[Combined RI data]

Sulfate

n = 16

y = B1*x + B0
R2 = 0.9122
B1 = 0.825 (0.123)
B0 = 165.3 (144.7)
(+/-90%)

mean x,y: 958., 955.
psd= 150. (15.7%)

For RD = 2*(Y-X)/(Y+X)

mean/sd: 0.018/ 0.203
RD<0.50 0.018/ 0.203
(16)

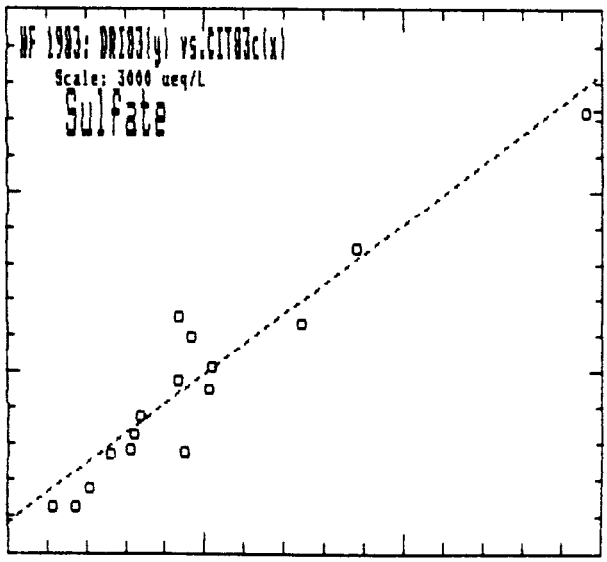

GGC83g(y) vs.CIT83c(x): [RI Lab results]

Y = b0 + b1 * X b0 & b1 given with (90% confidence)
RD = 2(Y-X)/(X+Y) given as "mean/s.d."

Field pH	mean x,y= 2.94, 2.95	psd=0.047 (1.6%)
n= 15	r2 = 0.9448	b0= -0.06 (0.38)
		b1= 1.072 (0.129)
	y-x= 0.01 /0.07	
Hydrogen	mean x,y =1347., 1359.	psd=124. (9.2%)
n= 15	r2 = 0.9579	b0= 34.25 (163.55)
		b1= 0.983 (0.103)
	RD= -0.015 / 0.156	only<0.50: -0.015/ 0.156 (15)
Sodium	mean x,y = 326., 284.	psd= 78. (25.5%)
n= 13	r2 = 0.9352	b0= 34.19 (50.66)
		b1= 0.767 (0.109)
	RD= 0.138 / 0.575	only<0.50: -0.009/ 0.255 (8)
Potassium	mean x,y = 23., 38.	psd= 23. (75.9%)
n= 13	r2 = 0.0804	b0= 29.66 (20.28)
		b1= 0.344 (0.631)
	RD= 0.567 / 0.771	only<0.50: -0.021/ 0.263 (4)
Ammonium	mean x,y = 751., 921.	psd=194. (23.2%)
n= 16	r2 = 0.9678	b0= -47.59 (107.28)
		b1= 1.289 (0.113)
	RD= 0.198 / 0.143	only<0.50: 0.198/ 0.143 (16)
Calcium	mean x,y = 132., 255.	psd=113. (58.6%)
n= 13	r2 = 0.3916	b0= 155.51 (86.10)
		b1= 0.752 (0.508)
	RD= 0.788 / 0.502	only<0.50: 0.170/ 0.337 (4)
Magnesium	mean x,y = 96., 84.	psd= 21. (23.9%)
n= 13	r2 = 0.9060	b0= 11.69 (16.79)
		b1= 0.760 (0.133)
	RD= 0.109 / 0.504	only<0.50: -0.189/ 0.232 (9)
Chloride	mean x,y = 202., 256.	psd= 60. (26.0%)
n= 16	r2 = 0.9440	b0= 26.33 (38.77)
		b1= 1.137 (0.133)
	RD= 0.358 / 0.363	only<0.50: 0.176/ 0.182 (12)
Nitrate	mean x,y =1689., 1932.	psd=299. (16.5%)
n= 16	r2 = 0.9746	b0=-136.51 (194.80)
		b1= 1.225 (0.095)
	RD= 0.120 / 0.123	only<0.50: 0.120/ 0.123 (16)
Sulfate	mean x,y =1004., 1179.	psd=221. (20.3%)
n= 16	r2 = 0.9424	b0= -50.14 (176.95)
		b1= 1.224 (0.145)
	RD= 0.145 / 0.139	only<0.50: 0.145/ 0.139 (16)
Collection rate	mean x,y= 0.5, 0.2	psd= 0.2 (65.0%)
n= 16	r2 = 0.6989	b0= -0.03 (0.09)
		b1= 0.489 (0.154)
	Rate(y/x)= 0.377 /0.182	

HF 1983:

GGCB3g(y) vs.CIT83c(x)
[Combined RI data]

Field pH

n = 15

y = B1*x + B0
R2 = 0.9448
B1 = 1.072 (0.129)
B0 = %-.204917 (0.3815)
(+/-90%)

mean x,y: 2.94,2.95
psd=0.047 (1.6%)

For pH(y)-pH(x)

mean/sd: 0.007/ 0.068

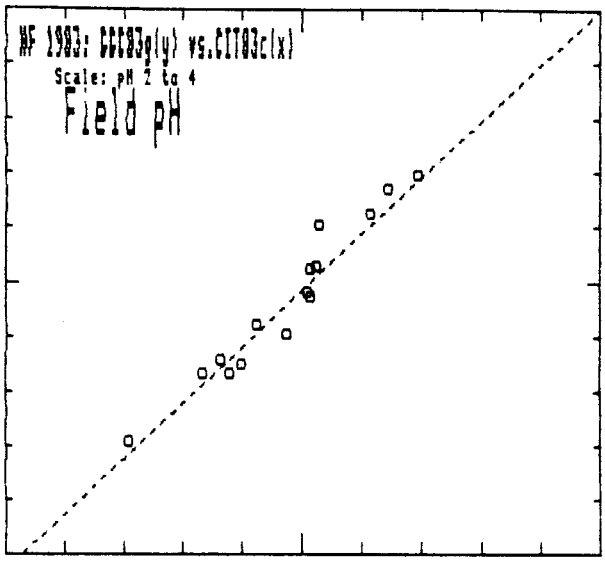

HF 1983:

GGCB3g(y) vs.CIT83c(x)
[Combined RI data]

Collection rate

n = 16

y = B1*x + B0
R2 = 0.6989
B1 = 0.489 (0.154)
B0 = %-.340007E-01 (0.0927)
(+/-90%)

mean x,y: 0.5, 0.2
psd=0.247 (65.0%)

For rate(y)/rate(x)

mean/sd: 0.377/ 0.182

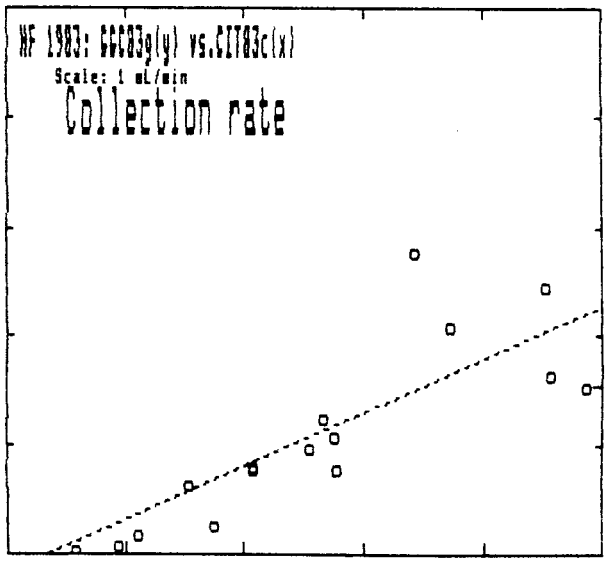

HF 1983:

GGC83g(y) vs.CIT83c(x)
[Combined RI data]

Hydrogen

n = 15

y = B1*x + B0
R2 = 0.9579
B1 = 0.983 (0.103)
B0 = 34.2 (163.6)
(+/-90%)

mean x,y: 1347., 1359.
psd= 124. (9.2%)

For RD = 2*(Y-X)/(Y+X)

mean/sd: -0.015/ 0.156
RD<0.50 -0.015/ 0.156
(15)

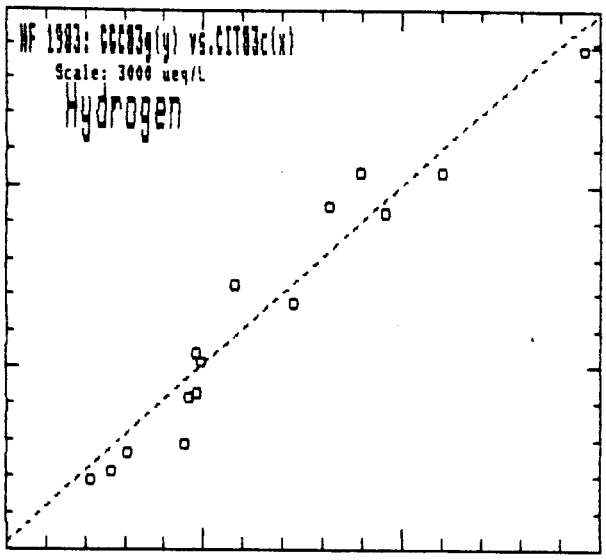

HF 1983:

GGC83g(y) vs.CIT83c(x)
[Combined RI data]

Sodium

n = 13

y = B1*x + B0
R2 = 0.9352
B1 = 0.767 (0.109)
B0 = 34.2 (50.7)
(+/-90%)

mean x,y: 326., 284.
psd= 78. (25.5%)

For [y]/[x]

mean/sd: 1.541/ 1.536

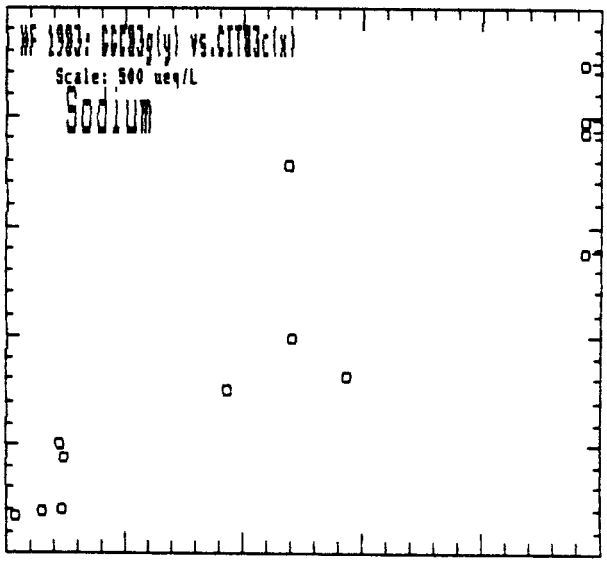

HF 1983:

GGC83g(y) vs.CIT83c(x)
[Combined RI data]

Potassium

n = 13

y = B1*x + B0
R2 = 0.0804
B1 = 0.344 (0.631)
B0 = 29.7 (20.3)
(+/-90%)

mean x,y: 23., 38.
psd= 23. (75.9%)

For [y]/[x]

mean/sd: 3.234/ 3.889

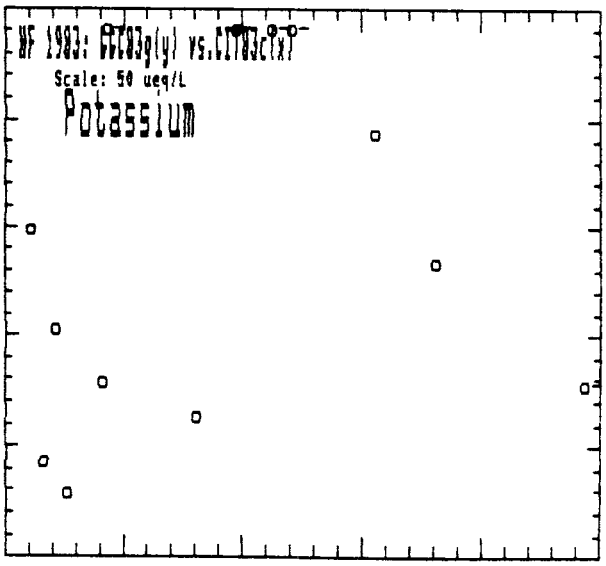

HF 1983:

GGC83g(y) vs.CIT83c(x)
[Combined RI data]

Ammonium

n = 16

y = B1*x + B0
R2 = 0.9678
B1 = 1.289 (0.113)
B0 = -47.6 (107.3)
(+/-90%)

mean x,y: 751., 921.
psd= 194. (23.2%)

For RD = 2*(Y-X)/(Y+X)

mean/sd: 0.198/ 0.143
RD<0.50 0.198/ 0.143
(16)

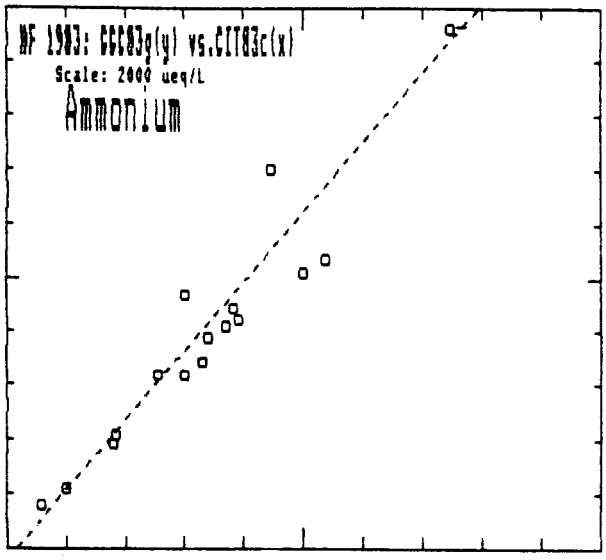

HF 1983:

GGC83g(y) vs.CIT83c(x)
[Combined RI data]

Calcium

n = 13

y = B1*x + B0
R2 = 0.3916
B1 = 0.752 (0.508)
B0 = 155.5 (86.1)
(+/-90%)

mean x,y: 132., 255.
psd= 113. (58.6%)

For [y]/[x]

mean/sd: 2.819/ 1.447

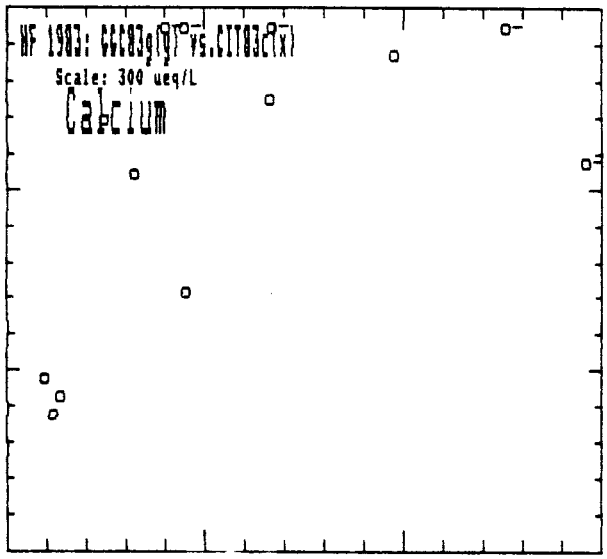

HF 1983:

GGC83g(y) vs.CIT83c(x)
[Combined RI data]

Magnesium

n = 13

y = B1*x + B0
R2 = 0.9060
B1 = 0.760 (0.133)
B0 = 11.7 (16.8)
(+/-90%)

mean x,y: 96., 84.
psd= 21. (23.9%)

For [y]/[x]

mean/sd: 1.291/ 0.721

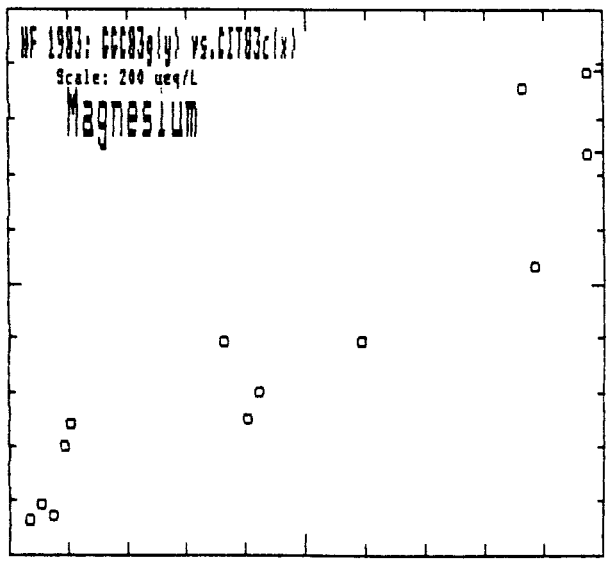

HF 1983:

GGC83g(y) vs.CIT83c(x)
[Combined RI data]

Chloride

n = 16

y = B1*x + B0
R2 = 0.9440
B1 = 1.137 (0.133)
B0 = 26.3 (38.8)
(+/-90%)

mean x,y: 202., 256.
psd= 60. (26.0%)

For [y]/[x]

mean/sd: 1.578/ 0.690

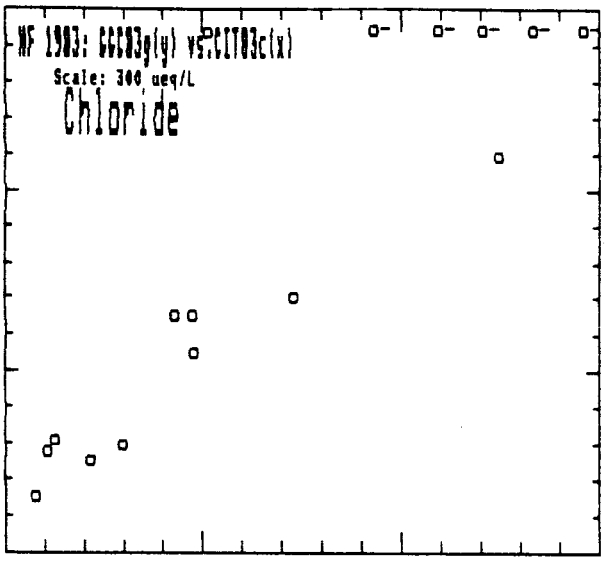

HF 1983:

GGC83g(y) vs.CIT83c(x)
[Combined RI data]

Nitrate

n = 16

y = B1*x + B0
R2 = 0.9746
B1 = 1.225 (0.095)
B0 = -136.5 (194.8)
(+/-90%)

mean x,y: 1689., 1932.
psd= 299. (16.5%)

For RD = 2*(Y-X)/(Y+X)

mean/sd: 0.120/ 0.123
RD<0.50 0.120/ 0.123
(16)

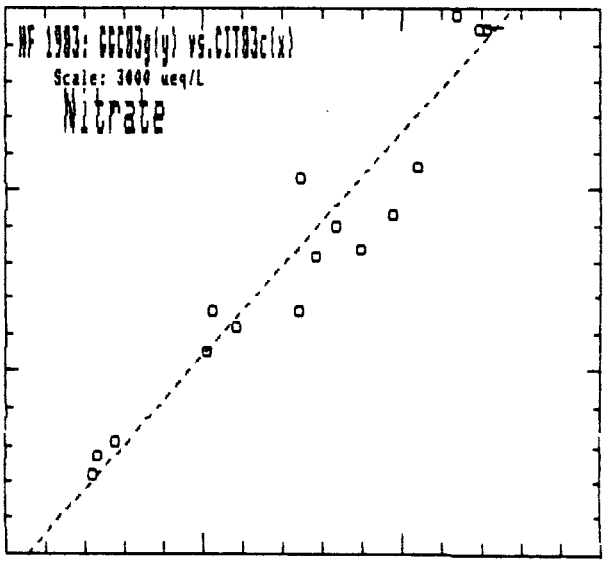

HF 1983:

GGC83g(y) vs.CIT83c(x)
[Combined RI data]

Sulfate

n = 16

y = B1*x + B0
R2 = 0.9424
B1 = 1.224 (0.145)
B0 = -50.1 (177.0)
(+/-90%)

mean x,y: 1004., 1179.
psd= 221. (20.3%)

For RD = 2*(Y-X)/(Y+X)

mean/sd: 0.145/ 0.139
RD<0.50 0.145/ 0.139
(16)

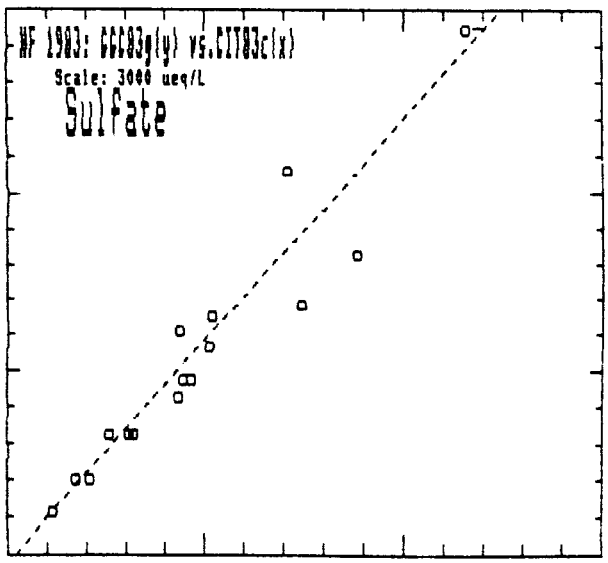

DRI83(y) vs.GGC83g(x): [RI Lab results]

Y = b0 + b1 * X b0 & b1 given with (90% confidence)
RD = 2(Y-X)/(X+Y) given as "mean/s.d."

Field pH	mean x,y= 2.95, 2.90	psd=0.082 (2.8%)
n= 15	r2 = 0.8473	b0= 0.08 (0.54)
		b1= 0.863 (0.183)
	y-x= -0.05 /0.11	
Hydrogen	mean x,y =1359., 1479.	psd=244. (17.2%)
n= 15	r2 = 0.8676	b0= 158.18 (303.43)
		b1= 0.972 (0.189)
	RD= 0.106 / 0.249	only<0.50: 0.106/ 0.249 (15)
Sodium	mean x,y = 284., 152.	psd=114. (52.1%)
n= 13	r2 = 0.9452	b0= -42.25 (34.53)
		b1= 0.685 (0.089)
	RD= -0.885 / 0.428	only<0.50: -0.401/ 0.110 (3)
Potassium	mean x,y = 41., 14.	psd= 25. (90.7%)
n= 10	r2 = 0.6177	b0= 3.36 (6.57)
		b1= 0.259 (0.129)
	RD= -0.863 / 0.368	only<0.50: -0.400/ 0.000 (2)
Ammonium	mean x,y = 888., 798.	psd=243. (28.8%)
n= 15	r2 = 0.8927	b0= 236.69 (128.80)
		b1= 0.632 (0.109)
	RD= -0.057 / 0.193	only<0.50: -0.057/ 0.193 (15)
Calcium	mean x,y = 255., 49.	psd=162. (% 106.679 %)
n= 13	r2 = 0.7024	b0= -10.47 (23.40)
		b1= 0.232 (0.082)
	RD= -1.408 / 9.990	only<0.50: 9.990/ 0.193 (0)
Magnesium	mean x,y = 84., 53.	psd= 27. (39.6%)
n= 13	r2 = 0.9221	b0= -11.75 (12.85)
		b1= 0.762 (0.120)
	RD= -0.612 / 0.318	only<0.50: -0.374/ 0.139 (7)
Chloride	mean x,y = 209., 149.	psd= 59. (33.0%)
n= 15	r2 = 0.8807	b0= -25.47 (40.89)
		b1= 0.835 (0.153)
	RD= -0.481 / 0.398	only<0.50: -0.175/ 0.159 (8)
Nitrate	mean x,y =1847., 1645.	psd=359. (20.6%)
n= 15	r2 = 0.9268	b0= 244.39 (249.42)
		b1= 0.758 (0.106)
	RD= -0.095 / 0.195	only<0.50: -0.095/ 0.195 (15)
Sulfate	mean x,y =1115., 967.	psd=268. (25.7%)
n= 15	r2 = 0.8889	b0= 221.95 (165.44)
		b1= 0.668 (0.118)
	RD= -0.118 / 0.207	only<0.50: -0.090/ 0.185 (14)
Collection rate	mean x,y= 0.2, 0.2	psd= 0.1 (45.9%)
n= 15	r2 = 0.3318	b0= 0.11 (0.07)
		b1= 0.344 (0.244)
	Rate(y/x)= 1.313 /1.474	

HF 1983:

DRI83(y) vs.GGC83g(x)
[Combined RI data]

Field pH

n = 15

y = B1*x + B0
R2 = 0.8473
B1 = 0.863 (0.183)
B0 = 0.3569 (0.5410)
(+/-90%)

mean x,y: 2.95,2.90
psd=0.082 (2.8%)

For pH(y)-pH(x)

mean/sd: -0.047/ 0.109

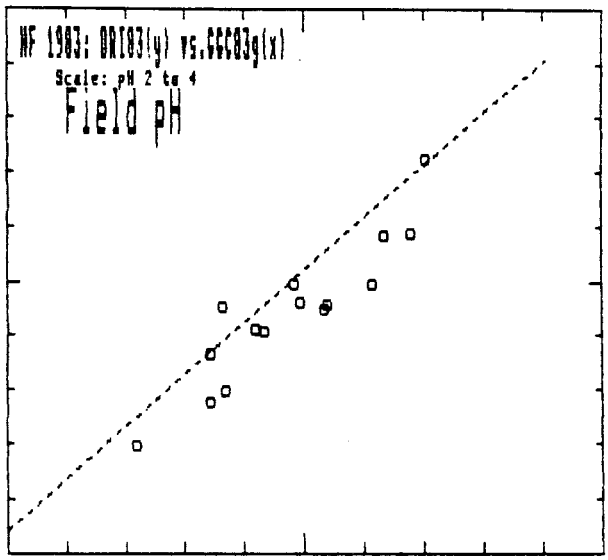

HF 1983:

DRI83(y) vs.GGC83g(x)
[Combined RI data]

Collection rate

n = 15

y = B1*x + B0
R2 = 0.3318
B1 = 0.344 (0.244)
B0 = 0.1072 (0.0701)
(+/-90%)

mean x,y: 0.2, 0.2
psd=0.099 (45.9%)

For rate(y)/rate(x)

mean/sd: 1.313/ 1.474

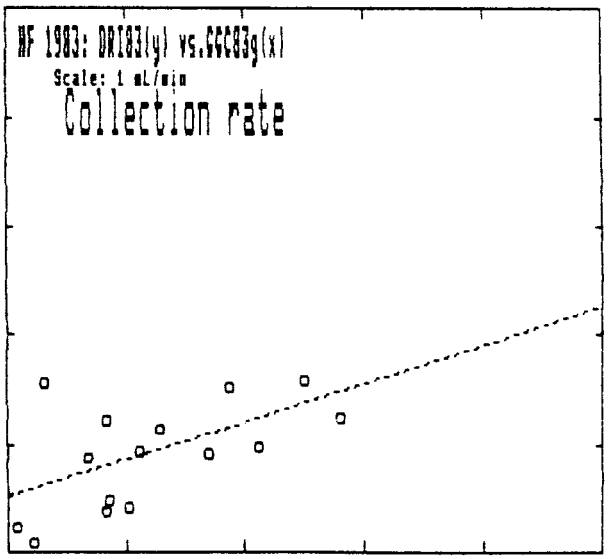

HF 1983:

DRI83(y) vs.GGC83g(x)
[Combined RI data]

Hydrogen

n = 15

y = B1*x + B0
R2 = 0.8676
B1 = 0.972 (0.189)
B0 = 158.2 (303.4)
(+/-90%)

mean x,y: 1359., 1479.
psd= 244. (17.2%)

For RD = 2*(Y-X)/(Y+X)

mean/sd: 0.106/ 0.249
RD<0.50 0.106/ 0.249
(15)

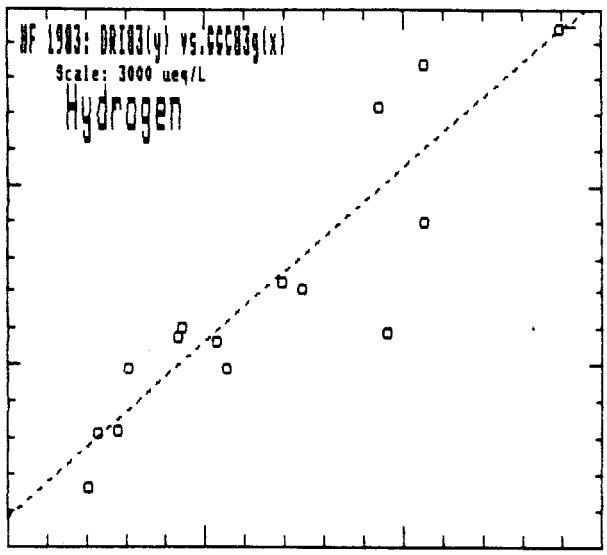

HF 1983:

DRI83(y) vs.GGC83g(x)
[Combined RI data]

Sodium

n = 13

y = B1*x + B0
R2 = 0.9452
B1 = 0.685 (0.089)
B0 = -42.2 (34.5)
(+/-90%)

mean x,y: 284., 152.
psd= 114. (52.1%)

For [y]/[x]

mean/sd: 0.413/ 0.196

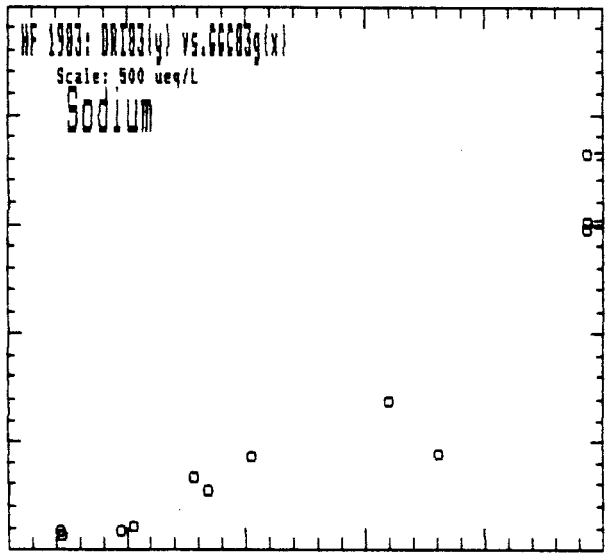

HF 1983:

DRI83(y) vs.GGC83g(x)
[Combined RI data]

Potassium

n = 10

y = B1*x + B0
R2 = 0.6177
B1 = 0.259 (0.129)
B0 = 3.4 (6.6)
(+/-90%)

mean x,y: 41., 14.
psd= 25. (90.7%)

For [y]/[x]

mean/sd: 0.418/ 0.181

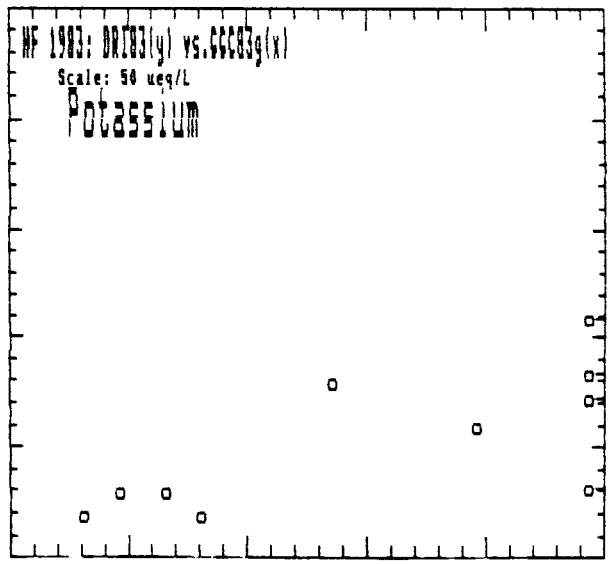

HF 1983:

DRI83(y) vs.GGC83g(x)
[Combined RI data]

Ammonium

n = 15

y = B1*x + B0
R2 = 0.8927
B1 = 0.632 (0.109)
B0 = 236.7 (128.8)
(+/-90%)

mean x,y: 888., 798.
psd= 243. (28.8%)

For RD = 2*(Y-X)/(Y+X)

mean/sd: -0.057/ 0.193
RD<0.50 -0.057/ 0.193
(15)

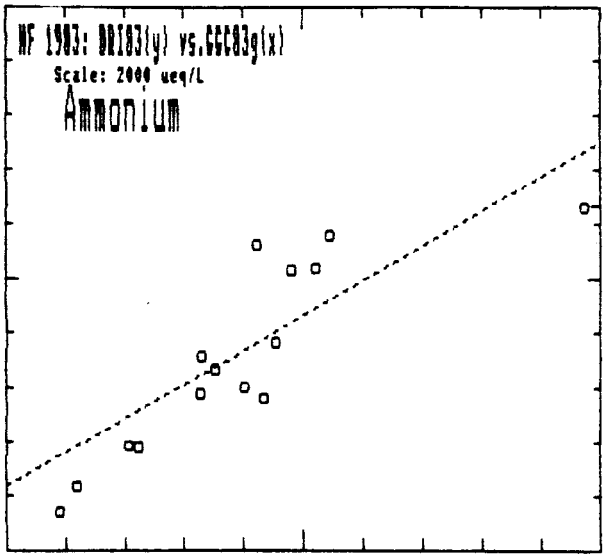

HF 1983:

DRI83(y) vs.GGC83g(x)
[Combined RI data]

Calcium

n = 13

y = B1*x + B0
R2 = 0.7024
B1 = 0.232 (0.082)
B0 = -10.5 (23.4)
(+/-90%)

mean x,y: 255., 49.
psd= 162. (% 106.679 %)

For [y]/[x]

mean/sd: 0.180/ 0.088

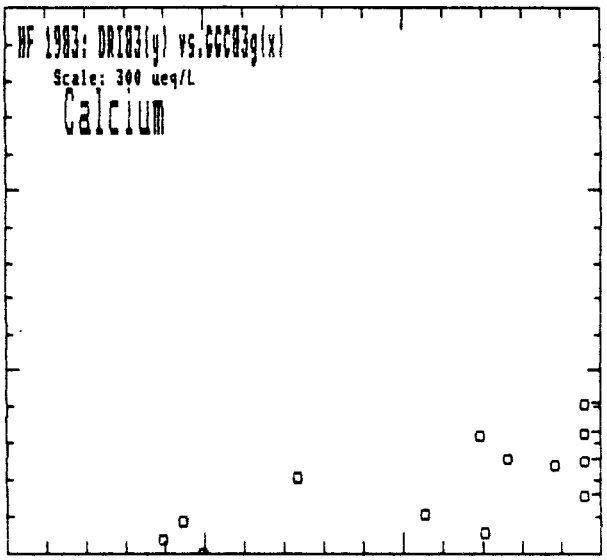

HF 1983:

DRI83(y) vs.GGC83g(x)
[Combined RI data]

Magnesium

n = 13

y = B1*x + B0
R2 = 0.9221
B1 = 0.762 (0.120)
B0 = -11.8 (12.9)
(+/-90%)

mean x,y: 84., 53.
psd= 27. (39.6%)

For [y]/[x]

mean/sd: 0.552/ 0.186

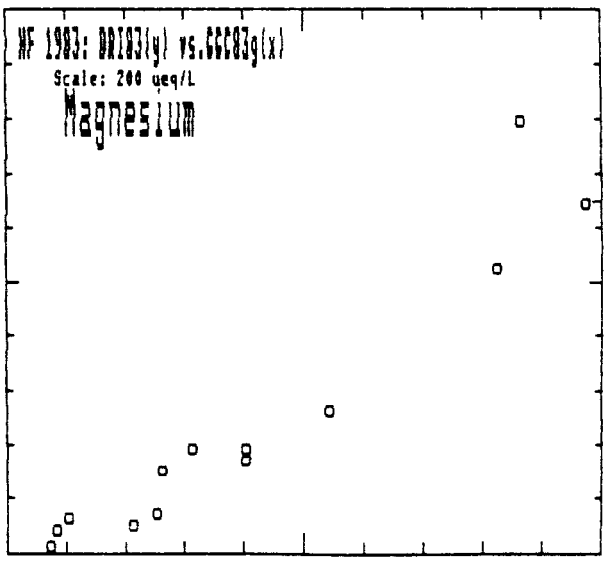

HF 1983:

DRI83(y) vs.GGC83g(x)
[Combined RI data]

Chloride

n = 15

y = B1*x + B0
R2 = 0.8807
B1 = 0.835 (0.153)
B0 = -25.5 (40.9)
(+/-90%)

mean x,y: 209., 149.
psd= 59. (33.0%)

For [y]/[x]

mean/sd: 0.650/ 0.253

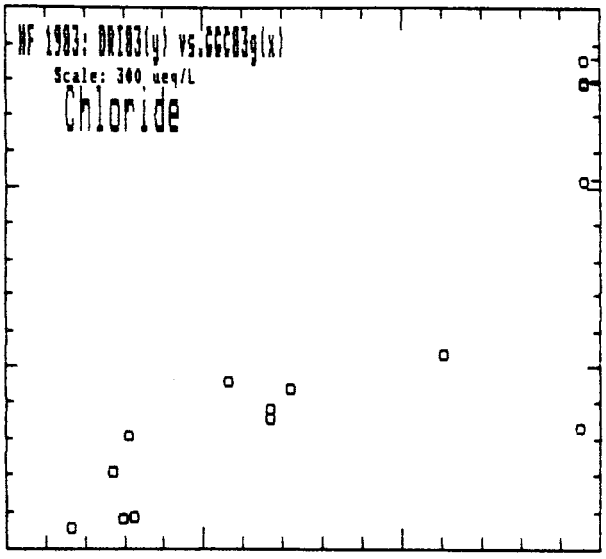

HF 1983:

DRI83(y) vs.GGC83g(x)
[Combined RI data]

Nitrate

n = 15

y = B1*x + B0
R2 = 0.9268
B1 = 0.758 (0.106)
B0 = 244.4 (249.4)
(+/-90%)

mean x,y: 1847., 1645.
psd= 359. (20.6%)

For RD = 2*(Y-X)/(Y+X)

mean/sd: -0.095/ 0.195
RD<0.50 -0.095/ 0.195
(15)

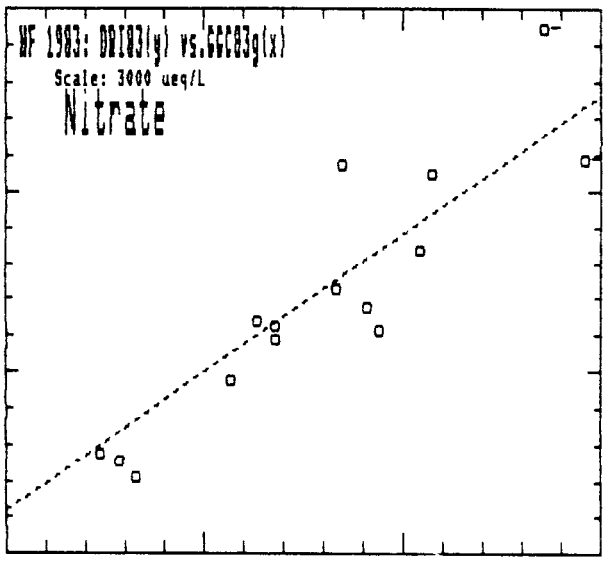

HF 1983:

DRI83(y) vs.GGC83g(x)
[Combined RI data]

Sulfate

n = 15

y = B1*x + B0
R2 = 0.8889
B1 = 0.668 (0.118)
B0 = 221.9 (165.4)
(+/-90%)

mean x,y: 1115., 967.
psd= 268. (25.7%)

For RD = 2*(Y-X)/(Y+X)

mean/sd: -0.118/ 0.207
RD<0.50 -0.090/ 0.185
(14)

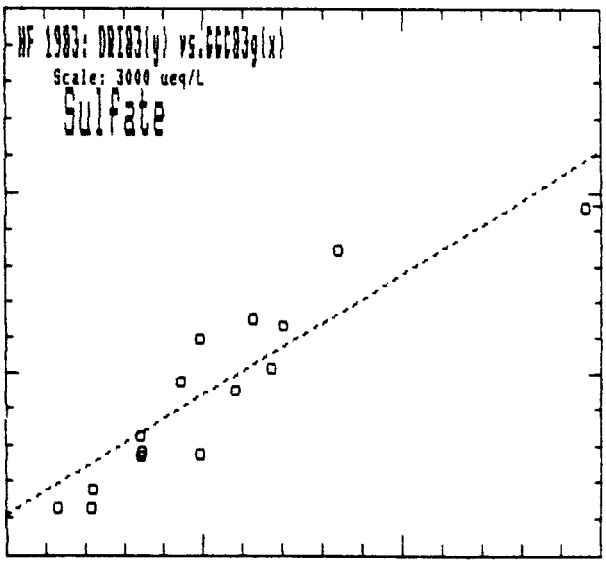

*** HENNINGER FLATS CRC INTERCOMPARISON DATA: Rockwell Laboratory Results - Combined Sample Data ***
source: Hering & Blumenthal (1985)

GGC-G: Global Geochemistry, Corp. - Mesh Collector "G" Data

#	Start	Stop	run	mL	mL/min	----pH---- (lab)	field	micro-equivalents/liter H	Na	K	NH4	Ca	Mg	Cl	NO3	SO4	-/+	CRC Code
1	21:22	22:35	73	18.5	0.253	(2.70)	2.73	1862.	203.	39.	1081.	418.	80.	133.	2141.	1668.	1.040	607G01
2	23: 4	1: 4	120	7.2	0.060	(2.81)	2.86	1380.	155.	28.	1034.	276.	52.	133.	1660.	1392.	1.064	607G03
3	20:30	23:30	180	23.8	0.132	(2.82)	2.83	1479.	318.	27.	794.	238.	108.	220.	1813.	1154.	1.054	608G05
4	23:52	1:30	98	54.6	0.557	(3.12)	3.22	603.	360.	82.	405.	382.	80.	289.	1129.	678.	1.088	608G08
5											no sample							
6	4:40	6:40	120	19.5	0.162	(3.50)	3.40	398.	104.	30.	438.	210.	50.	64.	647.	420.	0.914	610G14
7	7: 0	8:30	90	30.2	0.336	(3.02)	2.96	1096.	42.	9.	650.	88.	20.	53.	1351.	672.	1.075	610G17
8	8:49	10:30	101	37.7	0.373	(3.04)	2.98	1047.	44.	6.	700.	78.	16.	61.	1261.	674.	1.041	610G20
9	10:51	12:31	100	22.0	0.220	(2.74)	2.68	2089.	93.	16.	902.	240.	42.	112.	2077.	1334.	1.012	610G23
10	12:52	14:32	100	49.7	0.497	(3.30)	3.26	550.	38.	21.	230.	98.	14.	58.	561.	426.	1.090	610G97
11	15: 2	16:30	88	37.1	0.422	(3.39)	3.35	447.	39.	14.	176.	90.	8.	32.	463.	254.	0.962	610G25
12	6: 0	8: 0	120	19.6	0.163	(2.81)	2.72	1905.	166.	13.	862.	146.	62.	143.	1874.	974.	0.927	624G38
13	8: 0	10: 0	120	1.5	0.013	(%-1)	2.43	3715.	-1.	-1.	3609.	-2.	-2.	554.	6709.	3986.	1.472	624G41
14	3:15	5:30	135	5.5	0.041	(%-1)	2.68	2089.	642.	73.	954.	432.	172.	390.	2985.	1244.	1.038	625G44
15	5:38	7:30	112	18.8	0.168	(%-1)	3.07	851.	842.	83.	840.	456.	238.	479.	1688.	972.	0.939	625G46
16	7:38	9:30	112	22.4	0.200	(%-1)	3.06	871.	683.	63.	651.	252.	164.	411.	1351.	878.	0.973	625G48
17	9:31	11: 0	89	2.0	0.022	(%-1)	%-1	-1.	-1.	-1.	1410.	-2.	-2.	971.	3196.	2142.	4.474	625G50
Volume-weighted mean values						(3.05)	2.96	1099.	264.	20.	583.	125.	76.	134.	1279.	769.	1.006	

GGC-H: Global Geochemistry, Corp. - Mesh Collector "H" Data

#	Start	Stop	run	mL	mL/min	----pH---- (lab)	field	micro-equivalents/liter H	Na	K	NH4	Ca	Mg	Cl	NO3	SO4	-/+	CRC Code
1	21:22	22:35	73	18.9	0.259	(2.74)	2.76	1738.	161.	28.	1095.	632.	82.	115.	2161.	1692.	1.034	607H02
2	23: 4	1: 4	120	7.5	0.063	(2.86)	2.91	1230.	196.	38.	1062.	530.	64.	165.	1751.	1474.	1.064	607H04
3	20:30	23:30	180	10.9	0.061	(2.76)	2.77	1698.	1218.	50.	1062	1212	402.	300.	3041.	1642.	0.865	608H07
4	23:52	1:30	98	45.7	0.466	(3.10)	3.19	646.	325.	60.	396.	402.	78.	224.	1192.	820.	1.162	608H10
5											no sample							
6	4:37	6:37	120	21.4	0.178	(3.46)	3.35	447.	63.	15.	491.	250.	40.	55.	732.	474.	0.959	610H16
7	7: 0	8:30	90	31.9	0.354	(3.04)	2.96	1096.	40.	8.	698.	162.	22.	70.	1362.	692.	1.034	610H19
8	8:49	10:30	101	55.3	0.548	(3.04)	2.97	1072.	41.	7.	704.	88.	14.	81.	1291.	690.	1.056	610H22
9	10:51	12:31	100	20.1	0.201	(%-1)	2.68	2089.	-1.	-1.	-1.	-1.	-1.	-1.	-1.	-1.	0.000	610I24
10	12:52	14:32	100	49.6	0.496	(3.38)	3.33	468.	27.	12.	193.	122.	10.	52.	476.	342.	1.038	610H99
11	15: 2	16:30	88	40.2	0.457	(3.39)	3.34	457.	11.	5.	132.	78.	4.	24.	459.	248.	1.057	610H27
12	6: 0	8: 0	120	17.4	0.145	(2.78)	2.69	2042.	189.	19.	961.	194.	88.	160.	2042.	1064.	0.913	624H39
13	8: 0	10: 0	120	2.1	0.018	(%-1)	2.37	4266.	-1.	-1.	2976.	-2.	-2.	485.	5602.	3276.	1.234	624H42
14	3:15	5:30	135	5.2	0.039	(%-1)	2.70	1995.	676.	49.	887.	470.	202.	351.	2967.	1196.	1.035	625H45
15	5:38	7:30	112	16.4	0.146	(%-1)	2.98	1047.	800.	68.	887.	434.	210.	437.	1913.	1078.	0.982	625H47
16	7:38	9:30	112	22.7	0.203	(%-1)	3.04	912.	611.	29.	589.	166.	156.	347.	1294.	840.	0.995	625H49
17	9:31	11: 0	89	2.4	0.027	(%-1)	%-1	-1.	1501.	98.	1126.	534.	362.	843.	2614.	1740.	1.435	625H51
Volume-weighted mean val es						(3.05)	2.96	1087.	258.	20.	583.	145.	75.	135.	1279.	770.	1.007	

*** HENNINGER FLATS CRC INTERCOMPARISON DATA: Rockwell Laboratory Results - Combined Sample Data ***
source: Hering & Blumenthal (1985)

CIT RAC-B: California Institute of Technology - Rotating Arm Collector "B" Data

#	Start	Stop	run	mL	mL/min	----pH---- (lab)	field	micro-equivalents/liter H	Na	K	NH4	Ca	Mg	Cl	NO3	SO4	-/+	CRC Code
1	21: 4	22:58	112	65.5	0.585	(2.73)	2.71	1950.	245.	31.	1083.	384.	114.	101.	2100.	1798.	1.017	607B01-02
2	23: 0	0: 2	62	22.5	0.363	(2.81)	2.83	1479.	199.	21.	1026.	162.	72.	91.	1591.	1496.	1.046	607B03
3											no sample							
4											no sample							
5											no sample							
6	4:35	6:30	102	57.6	0.565	(3.48)	3.38	417.	41.	-5.	344.	58.	18.	23.	530.	326.	0.995	610B01-03
7	6:35	8:34	114	116.3	1.020	(3.14)	3.03	933.	29.	4.	522.	24.	10.	44.	1070.	512.	1.056	610B04-05
8	8:38	10:26	106	120.3	1.135	(3.04)	3.00	1000.	47.	8.	657.	24.	14.	59.	1201.	646.	1.075	610B06-07
9	10:30	12:25	102	63.2	0.620	(2.94)	2.67	2138.	44.	8.	741.	46.	18.	78.	1469.	1006.	0.827	610B08-09
10	12:30	14:30	117	112.2	0.959	(3.38)	3.23	589.	41.	6.	180.	20.	6.	18.	429.	394.	0.988	610B10-11
11	14:32	16:30	114	94.5	0.829	(3.38)	3.29	513.	-4.	1.	132.	-4.	-2.	3.	430.	226.	1.013	610B12-13
12	6: 6	8: 2	115	53.7	0.467	(2.80)	2.80	1585.	326.	16.	847.	104.	96.	158.	2123.	952.	1.068	624B01-02
13	8:13	10: 0	107	15.1	0.141	(%-1)	2.42	3802.	831.	65.	2597.	370.	256.	396.	5266.	2938.	1.041	624B03
14	3:19	5:30	131	29.8	0.227	(2.83)	2.80	1585.	626.	32.	547.	144.	172.	228.	2055.	776.	0.970	625B01
15	5:36	7:30	112	42.7	0.381	(3.07)	3.06	871.	1103.	47.	734.	228.	284.	470.	1826.	920.	0.975	625B02-03
16	7:32	9:30	116	60.3	0.520	(3.05)	3.04	912.	850.	30.	568.	122.	214.	412.	1454.	832.	0.990	625B04-05
17	9:32	11: 0	88	16.1	0.183	(2.83)	2.80	1585.	1472.	50.	809.	198.	362.	729.	2445.	1304.	0.983	625B06
Volume-weighted mean values						(3.04)	2.95	1116.	271.	16.	589.	102.	77.	123.	1281.	765.	0.979	

CIT RAC-C: California Institute of Technology - Rotating Arm Collector "C" Data

#	Start	Stop	run	mL	mL/min	----pH---- (lab)	field	micro-equivalents/liter H	Na	K	NH4	Ca	Mg	Cl	NO3	SO4	-/+	CRC Code
1	21: 5	23: 2	115	63.1	0.549	(2.73)	2.72	1905.	239.	31.	1067.	360.	118.	94.	2070.	1756.	1.021	607C01-02
2	23: 4	0: 4	60	20.8	0.347	(2.83)	2.84	1445.	185.	85.	991.	194.	80.	85.	1558.	1478.	1.021	607C03
3	21:35	23:30	115	34.9	0.303	(2.96)	2.94	1148.	550.	36.	673.	320.	176.	248.	1660.	1014.	0.991	608C02
4	23:35	1:30	115	78.4	0.682	(3.08)	3.05	891.	236.	14.	351.	104.	72.	102.	1009.	608.	1.018	608C03-04
5	1:30	3: 0	90	16.1	0.179	(3.00)	3.00	1000.	232.	39.	379.	116.	78.	89.	1214.	662.	1.052	608C05
6	4:35	6:30	102	48.7	0.477	(3.49)	3.38	417.	44.	2.	360.	64.	20.	24.	546.	336.	0.993	610C01-03
7	6:35	8:34	114	108.2	0.949	(3.13)	3.02	955.	29.	3.	504.	26.	10.	42.	1040.	506.	1.028	610C04-05
8	8:37	10:26	107	125.7	1.175	(3.08)	3.01	977.	45.	5.	654.	22.	14.	58.	1160.	632.	1.063	610C06-07
9	10:30	12:25	111	65.3	0.588	(2.92)	2.66	2188.	47.	8.	758.	48.	18.	95.	1483.	1028.	0.824	610C08-09
10	12:30	14:30	117	108.2	0.925	(3.35)	3.22	603.	6.	4.	196.	18.	6.	20.	451.	408.	1.044	610C10-11
11	14:32	16:30	114	87.5	0.768	(3.37)	3.28	525.	-1.	-1.	113.	-8.	-2.	14.	431.	220.	1.035	610C12-13
12	6: 1	8: 5	123	51.2	0.416	(%-1)	2.79	1622.	285.	16.	777.	90.	84.	145.	1946.	882.	1.016	624C01-02
13	8:12	10: 2	110	12.4	0.113	(%-1)	2.41	3890.	944.	58.	2766.	406.	284.	414.	5482.	3150.	1.037	624C03
14	3:19	5:30	131	28.4	0.217	(2.79)	2.75	1778.	689.	29.	595.	132.	172.	248.	2265.	862.	0.978	625C01
15	5:36	7:33	115	48.3	0.420	(%-1)	3.04	912.	1026.	41.	732.	208.	260.	437.	1784.	922.	0.978	625C02-03
16	7:35	9:32	115	59.2	0.515	(%-1)	3.02	955.	853.	29.	596.	132.	214.	412.	1474.	858.	0.976	625C04-05
17	9:34	11: 0	86	15.9	0.185	(%-1)	2.77	1698.	1520.	49.	887.	220.	378.	801.	2659.	1408.	1.006	625C06
Volume-weighted mean values						(3.05)	2.95	1117.	274.	17.	580.	106.	79.	127.	1276.	765.	0.976	

*** HENNINGER FLATS CRC INTERCOMPARISON DATA: Rockwell Laboratory Results - Combined Sample Data ***
source: Hering & Blumenthal (1985)

DRI: Desert Research Institute - Jet Impactor Data

#	Start	Stop	run	mL	mL/min	----pH---- (lab)	field	micro-equivalents/liter H	Na	K	NH4	Ca	Mg	Cl	NO3	SO4	-/+	CRC Code
1	21:12	22:59	107	25.3	0.236	(2.66)	2.61	2455.	90.	12.	1168.	76.	40.	79.	2120.	1702.	0.978	607D01
2	23: 0	23:29	29	9.3	0.321	(2.82)	2.83	1479.	72.	-13.	1056.	50.	32.	74.	1473.	1290.	1.029	607D02
3	22:20	23:30	70	12.9	0.184	(2.87)	2.84	1445.	143.	16.	616.	66.	54.	110.	1371.	926.	1.007	608D03
4	23:38	1:29	110	26.1	0.237	(3.01)	3.00	1000.	93.	11.	400.	44.	36.	69.	982.	588.	1.020	608D05-06
5	1:30	2:35	65	5.8	0.089	(2.87)	2.94	1148.	-1.	-1.	477.	-1.	-1.	84.	1465.	776.	1.410	608D07
6	4:30	6:29	58	9.8	0.169	(3.55)	3.46	347.	26.	-1.	391.	24.	16.	20.	444.	280.	0.921	610D01
7	6:30	8:29	117	22.9	0.196	(3.07)	3.00	1000.	21.	6.	594.	20.	14.	44.	1197.	564.	1.078	610D04
8	8:30	10:29	117	31.1	0.266	(2.99)	2.94	1148.	18.	4.	687.	10.	10.	64.	1302.	678.	1.073	610D07-09
9	10:30	12:30	119	23.4	0.197	(2.80)	2.74	1820.	20.	4.	790.	14.	12.	94.	1695.	1054.	1.043	610D10
10	12:30	14:29	117	32.5	0.278	(3.25)	3.18	661.	1.	0.	249.	2.	4.	19.	540.	382.	1.016	610D12-14
11	14:30	16:30	119	24.6	0.207	(3.23)	3.19	646.	-4.	-1.	156.	-1.	-2.	14.	582.	272.	1.074	610D15
12	6: 0	7: 0	58	15.2	0.262	(2.96)	2.92	1202.	58.	6.	576.	44.	40.	90.	1250.	584.	0.985	624D01
13	8: 3	10: 0	117	6.3	0.054	(%-1)	2.41	3890.	431.	28.	2370.	182.	202.	392.	5056.	2662.	1.096	624D02
14	3:15	5:30	134	3.7	0.028	(%-1)	2.57	2692.	487.	33.	1045.	124.	160.	349.	3212.	1334.	1.051	625D01
15	6:30	7:30	60	6.2	0.103	(%-1)	2.93	1175.	531.	29.	1131.	106.	160.	450.	2166.	1218.	1.207	625D02
16	7:35	9:30	115	10.6	0.092	(%-1)	2.91	1230.	420.	19.	739.	54.	106.	366.	1284.	970.	1.003	625D03
17	9:31	11: 0	89	0.9	0.010	(%-1)	%-1	-1.	3698.	122.	2679.	372.	884.	2079.	6736.	4424.	1.707	625K04
Volume-weighted mean values						(3.04)	2.96	1106.	244.	20.	590.	136.	72.	132.	1285.	775.	1.011	

ASRC: Atmospheric Sciences Research Center (SUNY) - Rotating String Collector Data

#	Start	Stop	run	mL	mL/min	----pH---- (lab)	field	micro-equivalents/liter H	Na	K	NH4	Ca	Mg	Cl	NO3	SO4	-/+	CRC Code
1										no sample								
2										no sample								
3										no sample								
4	23:45	1:35	86	42.0	0.488	(3.13)	3.09	813.	284.	41.	366.	142.	84.	181.	968.	592.	0.996	608A04-05
5	1:43	2:19	36	5.5	0.153	(3.09)	3.12	759.	-1.	-1.	356.	-1.	-1.	124.	1019.	588.	1.537	608A06
6	4:30	6:25	100	35.1	0.351	(4.43)	4.05	89.	478.	45.	343.	134.	52.	60.	488.	336.	0.774	610A01-02
7	6:30	8:21	96	51.7	0.539	(3.26)	3.13	741.	47.	8.	459.	66.	18.	30.	838.	430.	0.960	610A03-04
8	8:26	10:25	103	82.3	0.799	(3.13)	3.03	933.	74.	8.	646.	64.	24.	50.	1061.	566.	0.947	610A05-06
9	10:30	12:35	98	53.8	0.549	(3.03)	2.92	1202.	191.	7.	722.	46.	20.	79.	1347.	816.	1.008	610A07-08
10	12:28	14:28	110	91.7	0.834	(3.32)	3.18	661.	111.	6.	283.	36.	12.	26.	557.	482.	0.949	610A09-10
11	14:31	16:28	109	65.1	0.597	(3.46)	3.37	427.	65.	0.	131.	10.	2.	11.	381.	224.	0.965	610A11-12
12	6: 0	8: 0	107	16.9	0.158	(%-1)	2.81	1549.	-1.	-1.	1303.	-1.	-1.	340.	2587.	1254.	1.441	624A01-02
13	8: 5	10: 0	106	13.5	0.127	(%-1)	2.49	3236.	-1.	-1.	1896.	-1.	-1.	342.	4203.	2118.	1.255	624A03-04
14	3:15	5:30	123	14.1	0.115	(2.69)	2.66	2188.	896.	71.	1476.	392.	246.	378.	3391.	1686.	1.011	625A01
15	5:35	7:30	108	21.3	0.197	(%-1)	2.92	1202.	1053.	77.	905.	278.	266.	445.	2338.	1092.	1.012	625A03-04
16	7:35	9:30	105	46.0	0.438	(3.10)	3.09	813.	790.	41.	599.	166.	200.	374.	1349.	812.	0.962	625A05-06
17	9:35	11: 0	80	12.9	0.161	(%-1)	%-1	-1.	-1.	-1.	777.	-1.	-1.	584.	2004.	1230.	4.914	625A07-08
Volume-weighted mean values						(3.06)	2.97	1070.	248.	20.	584.	128.	70.	132.	1261.	755.	1.014	

APPENDIX B.

HENNINGER FLATS FOGWATER DATA

6. Spring 1983

Liquid Water Content Measurement Data

for Various Methods and Regression Coefficients

Table

LWC MEASUREMENTS BY VARIOUS METHODS[a]
LEAST-SQUARES REGRESSION COEFFICIENTS
(for Figure 5.1 and 5.7)

Least-squares regression[b]	r^2	n	comments
DRI = 1.14 (±0.31) RAC + 0.05 (±0.08)	0.77	20	
GGC = 1.52 (±0.30) RAC - 0.03 (±0.04)	0.85	20	
DRI = 0.64 (±0.22) GGC + 0.05 (±0.04)	0.65	17	
HiVol = 2.24 (±0.34) RAC + 0.02 (±0.08)	0.85	24	except drizzle
CSASP = 9.43 (±1.20) RAC - 0.09 (±0.13)	0.82	41	
CO_2LT = 1.69 (±0.31) RAC - 0.02 (±0.05)	0.88	15	only 6/11 & 12
11 June:			
CO2LT = 0.14 (±0.02) CSASP + 0.12 (±0.04)	0.71	44	all data[c]
= 0.16 (±0.02) CSASP + 0.10 (±0.04)	0.89	34	MMD<25
= 0.22 (±0.05) CSASP + 0.07 (±0.07)	0.91	9	MMD<20
12 June:			
CO2LT = 0.26 (±0.04) CSASP + 0.02 (±0.02)	0.89	17	all data

a. RAC - Caltech rotating arm collector (5.0 m^3 min^{-1});
DRI - Desert Research Institute jet impactor (1.2 m_3^3 min^{-1});
GGC - Global Geochemistry Corp. mesh collector (1.7 m^3 min^{-1});
HiVol - mean of 2 or 3 high volume samplers using paper filters;
CSASP - optical particle counter made by PMS using range 0;
CO2LT - from infrared laser extinction measurements.

b. Slope and intercept with 90% confidence interval indicated.

c. From 10-minute averages; MMD is mass median diameter (micron) measured by CSASP.

Table

RAC COLLECTION RATE AND OTHER DETERMINATIONS OF LWC
AT HENNINGER FLATS: JUNE 1983

Start	Stop	min[a]	LWC ($g\ m^{-3}$) RAC[b]	DRI[b]	GGC[b]	Hi-Vol[c]	CSASP[d]	CO_2LT[e]
7-8 June								
2034	2104	29	0.074	-	-	-	-	-
2104	2204	58	0.115	0.197	0.151	-	-	-
2203	2258	55	0.110	"	"	0.083	-	-
2300	0002	62	0.071	0.267(29)	0.036(120)	-	-	-
8-9 June								
2037	2133	56	0.036	-	0.051	0.053	0.367	-
2135	2330	115	0.061	0.154(70)	"	0.082	0.679	-
2335	0030	55	0.095	0.198	0.299	0.172	0.944	-
0030	0130	60	0.174	"	"	0.405	2.288	-
0130	0300	90	0.036	0.074	-	0.065	0.324	-
0325	0355	30	0.030	-	-	-	0.059	-
0705	0800	55	0.083	-	-	-	0.950	-
0805	0910	65	0.081	-	-	-	1.115	-
0910	1001	51	0.072	-	-	-	0.718	-
1005	1130	85	0.033	-	-	-	0.334	-
1130	1200	30	0.012	-	-	-	0.018	-
11 June								
0435	0449	14	0.177	0.141	0.101	0.273	1.397	0.298
0500	0535	37	0.154	"	"	0.402	1.779	0.227
0539	0630	51	0.061	"	"	0.086	0.335	0.081
0635	0730	55	0.159	0.163	0.203	0.340	0.710	0.242
0735	0834	55	0.213	"	"	0.480[x]	1.857	0.315
0838	0930	52	0.220	0.222	0.271	0.589[x]	1.925	0.359
0932	1026	54	0.215	"	"	0.972[x]	2.780	0.474
1030	1128	58	0.148	0.163	0.124	0.320[x]	1.237	0.268
1134	1225	51	0.081	"	"	0.200[x]	0.792	0.205
1230	1322	62	0.183	0.231	0.292	0.578[x]	1.558	0.383
1335	1430	55	0.199	"	"	0.356[x]	1.273	-
1432	1524	53	0.143	0.171	0.259	0.513[x]	1.166	-
1529	1630	61	0.174	"	"	1.006[x]	1.042	-
11-12 June								
2304	0004	60	0.019	-	-	-	-	-
0006	0105	59	0.005	-	-	-	0.067	-
0125	0239	74	0.050	-	-	-	0.569	-
0610	0703	53	0.047	-	-	-	0.376	0.125
0705	0800	55	0.027	-	-	-	0.210	0.072
0835	0945	70	0.057	-	-	-	0.570	0.136
0948	1048	60	0.025	-	-	-	0.016	0.012
19 June								
0631	0735	64	0.043	0.030	0.019	0.114	-	0.230
0737	0807	30	-	0.002	"	-	-	-
21 June								
0730	0930	120	0.021	0.009	-	0.033	0.141	0.008
0935	1030	55	0.002	-	-	0.012	0.018	-
22 June								
0430	0530	60	0.054	0.028	0.008	0.168	0.072	0.022
0531	0730	119	0.010	"	"	0.020	0.025	0.052
25 June								
0606	0705	59	0.123	0.210	0.091	0.404	-	0.478
0706	0802	56	0.054	-	"	0.083	-	0.090
0813	1000	107	0.024	0.045	0.009	0.055	-	0.133
1030	1130	60	0.004	-	-	-	-	0.071
1130	1144	14	0.007	-	-	-	-	0.188
26 June								
0319	0530	132	0.045	0.023	0.024	0.075	0.078	0.083
0536	0635	59	0.035	-	0.090	-	0.020	0.072
0637	0730	53	0.132	0.086	"	0.305	1.114	1.248
0732	0830	58	0.128	0.077	0.119	0.264	1.068	1.269
0832	0930	58	0.078	"	"	0.114	0.234	-
0932	1100	88	0.037	0.008	0.015	0.042	0.102	0.058
27 June								
1147	1230	43	0.065	-	-	-	0.497	-

Table (cont.)

Notes:

a. RAC collection intervals;
" indicates value averaged with preceeding interval;
- indicates datum not available for interval.

b. Assumed sampling rates:
RAC=5.0, DRI=1.2, and GGC=1.7 cubic meter per min.
RAC and GGC values based on replicate collector pairs, except for RAC values on 8-9, 12, and 27 June intervals.
( ) next to DRI or GGC value gives actual duration (min) when start or stop times did not coincide closely.

c. Hi-Vol LWC time-averaged for several 5 to 20 minute samples per interval from 2 or 3 instruments; superscript x indicates drizzle leading to possible bias in LWC value.

d. From OPC size distributions with activity correction; averaged of Range 0 readings taken 1 min per 4 min cycle.

e. From IR extinction: $LWC=0.25 \times \ln(I_o/I)$; averaged from readings taken every minute.

APPENDIX B.

HENNINGER FLATS FOGWATER DATA

7. Spring 1984 - RAC Samples:

Caltech Laboratory Results

*** HENNINGER FLATS FOGWATER DATA - MAY/JUNE 1984 ***

Henninger Flats - 22 May 1984 — Checked: 7/18/84

	Start	Stop	min	mL	pH	H	Na	micro-equivalents/liter K	NH4	Ca	Mg	Cl	NO3	SO4	micro-mol/l S(IV)	CH2O	-/+
1	7:12	7:33	21	6.6	2.95	1122.	202.	12.	569.	156.	65.	130.	1460.	647.	0.0	31.	1.052

Henninger Flats - 3 June 1984 — Checked: 7/18/84

	Start	Stop	min	mL	pH	H	Na	micro-equivalents/liter K	NH4	Ca	Mg	Cl	NO3	SO4	micro-mol/l S(IV)	CH2O	-/+
1	23: 0	24: 0	60	18.3	2.83	1479.	2760.	54.	1197.	700.	720.	1060.	3900.	2098.	3.0	50.	1.021
2	0: 0	1: 0	60	17.0	2.82	1514.	2900.	54.	1473.	695.	750.	1340.	4080.	2369.	3.0	43.	1.055
3	1: 0	2: 0	60	13.4	2.70	1995.	3890.	72.	1651.	870.	1015.	1260.	5160.	3097.	5.0	66.	1.003
4	2: 0	3: 0	60	8.0	2.68	2089.	3630.	68.	1723.	795.	930.	1265.	4900.	2926.	-0.2	-0.	0.984
5	3: 0	4: 0	60	11.3	2.66	2188.	2760.	55.	1308.	620.	730.	1160.	4110.	2298.	-0.2	-0.	0.988
6	4: 0	5: 0	60	2.8	2.53	2951.	4640.	85.	2016.	1020.	1235.	1640.	7200.	3335.	-0.2	-0.	1.019
Vol-Wt Mean (LWC=0.066)					2.74	1825.	3179.	60.	1458.	741.	828.	1227.	4457.	2526.	3.6	52.	1.015

Henninger Flats - 5 June 1984 — Checked: 7/18/84

	Start	Stop	min	mL	pH	H	Na	micro-equivalents/liter K	NH4	Ca	Mg	Cl	NO3	SO4	micro-mol/l S(IV)	CH2O	-/+
1	4:39	5: 0	21	12.9	3.42	380.	452.	11.	241.	99.	121.	268.	598.	416.	0.0	17.	0.983
2	5: 0	5:22	22	6.1	3.35	447.	814.	15.	428.	158.	209.	467.	1005.	574.	-0.1	19.	0.988
3	7:54	8:38	44	21.9	3.37	427.	185.	4.	254.	60.	50.	166.	392.	379.	4.0	19.	0.957
4	8:38	9: 0	22	6.7	3.31	490.	218.	4.	286.	41.	57.	179.	469.	416.	-0.2	30.	0.971
5	10: 0	11: 0	60	27.2	3.17	676.	404.	7.	343.	73.	110.	330.	670.	670.	0.0	33.	1.035
6	11:14	11:44	30	22.0	3.16	692.	286.	6.	298.	96.	79.	277.	632.	486.	-0.1	-0.	0.958
Vol-Wt Mean (LWC=0.162)					3.25	556.	347.	7.	300.	82.	93.	271.	596.	505.	4.0	25.	0.990

Henninger Flats - 6 June 1984 — Checked: 7/18/84

	Start	Stop	min	mL	pH	H	Na	micro-equivalents/liter K	NH4	Ca	Mg	Cl	NO3	SO4	micro-mol/l S(IV)	CH2O	-/+
1	9:30	10:30	60	51.6	3.63	234.	54.	2.	130.	26.	16.	63.	213.	198.	1.5	29.	1.025
2	10:30	11:30	60	51.2	3.64	229.	54.	2.	127.	31.	17.	54.	225.	214.	0.0	29.	1.072
3	11:30	12:30	60	21.7	3.38	417.	150.	4.	332.	150.	52.	135.	634.	462.	-0.1	39.	1.114
Vol-Wt Mean (LWC=0.231)					3.58	264.	71.	2.	164.	50.	23.	72.	291.	251.	1.5	31.	1.070

*** HENNINGER FLATS FOGWATER DATA - MAY/JUNE 1984 ***

Henninger Flats - 12 June 1984 — Checked: 7/18/84

	Start	Stop	min	mL	pH	H	Na	micro-equivalents/liter K	NH4	Ca	Mg	Cl	NO3	SO4	micro-mol/l S(IV)	CH2O	-/+
1	6: 0	6:30	30	5.5	2.88	1318.	3400.	71.	1680.	1120.	990.	1130.	6330.	1806.	-0.1	-0.	1.080
2	7: 7	7:15	8	0.8	2.75	1778.	4300.	132.	1795.	1320.	1160.	1650.	7250.	2067.	-0.1	-0.	1.046
3	7:48	8:30	42	27.5	3.27	537.	1290.	26.	1090.	390.	360.	495.	2320.	1037.	2.3	14.	1.043
4	8:30	9:30	60	38.0	3.08	832.	1260.	24.	1011.	350.	330.	530.	2330.	1074.	1.9	20.	1.033
5	9:30	10:30	60	30.4	2.92	1202.	1230.	24.	1041.	335.	345.	640.	2540.	1164.	4.0	30.	1.040
6	10:30	10:55	25	6.6	2.85	1413.	1665.	35.	1080.	460.	460.	800.	3550.	1412.	-0.1	-0.	1.127
Vol-Wt Mean (LWC=0.161)					3.03	927.	1413.	28.	1083.	408.	389.	606.	2696.	1154.	2.7	21.	1.049

Henninger Flats - 13 June 1984 — Checked: 7/18/84

	Start	Stop	min	mL	pH	H	Na	micro-equivalents/liter K	NH4	Ca	Mg	Cl	NO3	SO4	micro-mol/l S(IV)	CH2O	-/+
1	8:40	9: 0	20	0.7	2.60	2512.	12500	240.	6440.	4260.	3580.	7960.	16130	7189.	-0.1	-0.	1.059

APPENDIX C.

SAN JOAQUIN VALLEY FIELD SAMPLING DATA: WINTER 1984-85

1. Fogwater Composition Data (NW & BW sites)

Bakersfield Airport (NW) Site - 28 Dec 1984

	TIME		mL	pH	H	Na	K	NH4	Ca	Mg	Cl	NO3	SO4	S(IV)	CH2O	-/+	C-A	(%)	HCO3*
					micro-equivalents/liter									micro-mol/l					
1	0:35	1:15	39.6	6.80	0.2	13.7	5.1	2684.	58.	10.7	-1.	507.	1340.	190.0	135.0	0.735	735	(15)	45*
2	1:30	2:15	26.0	6.20	0.6	14.5	5.0	2777.	50.	9.4	56.	545.	1480.	-1.0	126.0	0.728	776	(16)	11*
3	2:15	3:15	11.0	5.60	2.5	27.7	7.8	2982.	47.	13.9	27.	1480.	1200.	300 #	126.0	0.976	74	(1)	3*
4	3:15	4:15	11.0	5.70	2.0	34.3	5.0	1890.	34.	8.5	18.	753.	1020.	-1.0	-1.0	0.907	183	(5)	4*
5	7: 0	8: 0	33.3	5.45	3.5	5.8	2.9	1080.	36.	6.2	-1.	158.	596.	100.0	47.8	0.753	281	(14)	2*
6	8: 0	8:35	13.3	5.90	1.3	6.0	1.5	1031.	35.	5.3	-1.	275.	526.	53.7	36.6	0.791	226	(12)	6*
Vol-Wt Mean (LWC=0.149)				5.81	1.5	14.0	4.4	2100.	46.	8.9	41.	505.	1064.	153.0	98.1	0.811	412	(10)	17*

Bakersfield Airport (NW) Site - 2-3 Jan 1985

	TIME		mL	pH	H	Na	K	NH4	Ca	Mg	Cl	NO3	SO4	S(IV)	CH2O	-/+	C-A	(%)	HCO3*
					micro-equivalents/liter									micro-mol/l					
1	20:15	21: 0	54.0	6.55	0.3	2.0	2.9	940.	17.	2.5	-1.	400.	393.	23.1	45.3	0.846	149	(8)	25*
2	21: 0	23: 0	84.0	6.20	0.6	3.6	1.8	1097.	25.	3.8	-1.	325.	510.	199.0	93.8	0.914	98	(5)	11*
3	23: 0	24: 0	39.5	5.60	2.5	6.0	3.4	1993.	31.	5.0	16.	515.	1090.	300 #	155.0	0.941	120	(3)	3*
4	0: 0	2: 0	81.7	5.72	1.9	6.1	-1.0	1338.	15.	2.6	13.	394.	554.	238.0	118.0	0.879	165	(6)	4*
5	2: 0	3: 5	36.5	5.66	2.2	4.4	4.2	1291.	10.	1.6	7.	427.	422.	86.0	77.0	0.717	371	(16)	3*
6	3: 5	5: 0	70.0	4.30	50.1	38.0	3.4	781.	17.	2.5	-1.	378.	437.	105.0	47.0	1.031	-28	(2)	0*
7	5:30	7: 0	56.6	6.83	0.1	3.4	-1.0	928.	8.	0.8	-1.	171.	705.	7.6	25.0	0.939	57	(3)	48*
8	7: 0	8:30	46.0	6.82	0.2	2.4	-1.0	1074.	30.	2.7	-1.	126.	1119.	5.7	34.0	1.127	-141	(6)	47*
9	8:30	9:30	19.0	6.51	0.3	14.1	5.7	2897.	131.	9.7	16.	168.	2808.	101.0	139.0	1.011	-35	(1)	23*
10	9:30	10:15	2.4	5.18	6.6	77.3	15.2	11535.	368.	6.4	-1.	880.	12996.	-1.0	-1.0	1.156	-1868	(7)	1*
Vol-Wt Mean (LWC=0.202)				5.09	8.1	9.6	3.2	1261.	25.	3.0	13.	335.	764.	128.0	77.6	0.947	69	(3)	17*

NOTES:
1. Sampling at all times of fog observation unless noted as otherwise.
2. All ion species given as micro-eq/L except S(IV) and CH2O, which are as micro-mol/L.
3. "-1" means not analyzed; "#" after S(IV) value means concentration was >300.
4. SO4 was determined as total sample sulfur: S(VI) + S(IV), then S(IV) from preserved sample aliquot (assumed in monovalent form) was subtracted.
5. "-/+" is equivalent ratio including S(IV) and correction for HSO4 at low pH; "C-A (%)" is cations minus anions (as % of total ions); "HCO3*" is equilibrium value for pH at 278K and 340 ppm CO2.
6. LWC from RAC collection rate, assuming 3.0 m3/min air sampling.

Bakersfield Airport (NW) Site - 3-4 Jan 1985 (Fog Observed: 20:00 to 08:00)

	TIME	mL	pH	micro-equivalents/liter H	Na	K	NH4	Ca	Mg	Cl	NO3	SO4	micro-mol/l S(IV)	CH2O	-/+	C-A (%)	HCO3*
1	20:00 21: 0	34.0	6.62	0.2	4.7	4.5	858.	60.	7.2	6.	160.	687.	36.4	60.4	0.952	45 (2)	30*
2	21: 0 21:10	3.3	6.90	0.1	2.5	9.7	429.	83.	16.0	-1.	105.	247.	-1.0	-1.0	0.651	188 (21)	56*
3	23: 0 24: 0	17.7	7.08	0.1	10.0	-1.0	592.	135.	13.0	-1.	95.	474.	8.7	27.1	0.770	173 (13)	85*
4	0: 0 1: 0	38.7	7.57	0.0	7.2	2.8	379.	371.	14.5	-1.	53.	390.	10.8	20.6	0.586	320 (26)	263*
5	1:24 1:55	24.5	6.76	0.2	0.7	1.4	268.	46.	10.8	-1.	72.	186.	12.3	12.3	0.828	56 (9)	41*
Vol-Wt Mean (LWC=0.176)			6.89	0.1	5.4	3.3	527.	171.	11.5	6.	95.	442.	18.4	31.6	0.782	156 (12)	118*

Bakersfield Airport (NW) Site - 4-5 Jan 1985

	TIME	mL	pH	micro-equivalents/liter H	Na	K	NH4	Ca	Mg	Cl	NO3	SO4	micro-mol/l S(IV)	CH2O	-/+	C-A (%)	HCO3*
1	20:10 21: 0	29.0	6.26	0.5	3.4	-1.0	946.	26.	3.1	-1.	119.	675.	58.8	60.7	0.871	126 (7)	13*
2	21: 0 21:30	9.5	5.16	6.9	48.7	5.7	1341.	72.	9.2	-1.	120.	966.	207.0	61.5	0.871	191 (7)	1*
3	22: 0 23: 0	31.8	5.46	3.5	22.0	3.7	1438.	68.	9.8	21.	195.	440.	300#	74.8	0.619	589 (24)	2*
4	23: 0 24: 0	41.5	5.55	2.8	26.1	3.7	1860.	60.	7.5	18.	238.	820.	300#	198.0	0.702	584 (18)	3*
5	0: 0 1: 0	36.8	5.20	6.3	19.1	5.2	1768.	47.	6.9	16.	234.	1449.	300#	198.0	1.079	-147 (4)	1*
6	1: 0 2: 0	40.0	5.10	7.9	13.0	1.6	1845.	29.	4.0	15.	210.	1039.	300#	155.0	0.823	336 (10)	1*
7	2:40 3:30	43.0	4.81	15.5	63.2	3.2	1354.	21.	3.0	-1.	238.	974.	300#	106.0	1.036	-52 (2)	0*
8	4: 0 5: 0	28.8	4.96	11.0	12.8	2.9	1504.	21.	2.5	-1.	204.	1059.	300#	100.0	1.006	-9 (0)	1*
9	5: 0 6: 0	31.4	5.92	1.2	3.8	2.5	1078.	16.	1.9	2.	156.	982.	119.0	82.3	1.141	-156 (7)	6*
10	6: 0 7: 0	33.8	4.80	15.8	3.3	2.5	1664.	25.	2.5	42.	178.	1461.	264.0	74.0	1.135	-232 (6)	0*
11	7: 0 8: 0	36.2	4.52	30.2	4.9	1.8	716.	14.	1.6	-1.	149.	466.	163.0	47.1	1.012	-10 (1)	0*
12	8: 0 9: 0	29.2	3.90	125.9	38.9	12.7	343.	18.	3.6	17.	151.	249.	53.9	7.2	0.869	71 (7)	0*
13	9: 0 9:15	1.9	3.71	195.0	-1.0	-1.0	412.	-1.	-1.0	-1.	226.	439.	-1.0	-1.0	1.096	-58 (5)	0*
Vol-Wt Mean (LWC=0.191)			4.72	19.2	21.0	3.9	1350.	33.	4.4	19.	191.	889.	231.1	104.5	0.929	102 (4)	2*

Bakersfield Airport (NW) Site - 8 Jan 1985

	TIME	mL	pH	micro-equivalents/liter H	Na	K	NH4	Ca	Mg	Cl	NO3	SO4	micro-mol/L S(IV)	CH2O	-/+	C-A (%)	HCO3*
1	8:57 10: 0	13.2	7.37	0.0	57.0	8.4	1378.	109.	24.0	6.	570.	501.	16.3	26.7	0.694	483 (18)	166*

Bakersfield Airport (NW) Site - 10 Jan 1985

	TIME	mL	pH	micro-equivalents/liter H	Na	K	NH4	Ca	Mg	Cl	NO3	SO4	micro-mol/L S(IV)	CH2O	-/+	C-A (%)	HCO3*
1	7:15 8: 0	6.0	5.89	1.3	29.0	11.0	2690.	59.	5.1	-1.	853.	1550.	180.0	-1.0	0.924	212 (4)	6*
2	8: 0 8:50	4.1	6.57	0.3	19.0	5.0	2478.	46.	3.5	50.	795.	1720.	-1.0	-1.0	1.005	-13 (0)	26*
Vol-Wt Mean (LWC=0.035)			6.06	0.9	24.9	8.6	2604.	54.	4.5	50.	829.	1619.	180.0	0.0	0.993	18 (0)	14*

Bakersfield Airport (NW) Site - 11 Jan 1985

	TIME		mL	pH	H	Na	K	NH4	Ca	Mg	Cl	NO3	SO4	S(IV)	CH2O	-/+	C-A	(%)	HCO3*
					micro-equivalents/liter									micro-mol/L					
1	6:35	7:30	2.7	6.67	0.2	58.0	23.6	4923.	248.	8.5	20.	2115.	2920.	-1.0	-1.0	0.961	206	(2)	33*

Bakersfield Airport (NW) Site - 14 Jan 1985

	TIME		mL	pH	H	Na	K	NH4	Ca	Mg	Cl	NO3	SO4	S(IV)	CH2O	-/+	C-A	(%)	HCO3*
					micro-equivalents/liter									micro-mol/L					
1	1:30	2:30	60.0	6.17	0.7	17.4	2.1	2426.	36.	4.5	-1.	540.	1462.	149.0	121.0	0.865	336	(7)	10*
2	2:30	3:30	41.7	5.56	2.8	40.5	3.0	2393.	40.	5.1	-1.	550.	1784.	253.0	140.0	1.041	-102	(2)	3*
3	3:30	4:30	33.0	6.72	0.2	24.0	3.0	2171.	36.	4.4	-1.	881.	813.	20.3	104.0	0.766	524	(13)	37*
Vol-Wt Mean (LWC=0.249)			5.92	1.2	26.2	2.6	2353.	37.	4.7	0.	627.	1403.	149.7	122.7	0.898	246	(5)	15*	

Bakersfield Airport (NW) Site - 18-19 Jan 1985 (Fog Observed: 18:00 to 09:00)

	TIME		mL	pH	H	Na	K	NH4	Ca	Mg	Cl	NO3	SO4	S(IV)	CH2O	-/+	C-A	(%)	HCO3*
					micro-equivalents/liter									micro-mol/l					
1	20: 5	21: 5	45.0	5.85	1.4	12.5	-1.0	2400.	25.	8.1	34.	770.	1450.	-1.0	211.0	0.921	193	(4)	5*
2	21: 5	22: 0	38.0	4.85	14.1	6.7	-1.0	1712.	31.	4.9	32.	730.	540.	138.0	138.0	0.814	329	(10)	1*
3	22: 0	23: 0	42.0	4.18	66.1	4.3	-1.0	1607.	20.	3.4	17.	811.	402.	78.0	126.0	0.769	392	(13)	0*
4	23: 0	24: 0	47.0	4.04	91.2	5.2	5.7	1692.	15.	3.2	35.	866.	483.	80.7	120.0	0.808	347	(11)	0*
5	0: 0	1: 0	30.8	3.99	102.3	5.4	6.1	1447.	15.	2.9	42.	548.	475.	83.8	128.0	0.727	430	(16)	0*
6	1: 0	2: 0	30.0	3.86	138.0	5.1	-1.0	1446.	28.	3.8	39.	716.	369.	56.7	105.0	0.728	440	(16)	0*
7	2: 0	3: 0	25.0	3.67	213.8	5.4	6.8	1587.	19.	3.1	43.	1050.	524.	62.6	151.0	0.915	155	(4)	0*
8	6:10	7: 0	21.7	4.53	29.5	5.6	6.5	1813.	13.	2.2	-1.	1100.	572.	105.0	148.0	0.950	93	(3)	0*
9	7: 0	8: 0	20.5	4.36	43.7	5.1	6.4	2031.	17.	2.5	10.	1200.	695.	104.0	166.0	0.954	96	(2)	0*
10	8: 0	9: 0	20.0	3.65	223.9	7.5	15.0	2034.	24.	3.9	33.	1420.	805.	88.0	193.0	1.016	-38	(1)	0*
Vol-Wt Mean (LWC=0.182)			4.08	82.2	6.5	7.3	1779.	21.	4.1	32.	871.	647.	88.5	146.9	0.862	263	(7)	1*	

Bakersfield Airport (NW) Site - 20 Jan 1985 (Fog Observed 02:00 to 09:30) Data checked: 2/12/85

	TIME		mL	pH	H	Na	K	NH4	Ca	Mg	Cl	NO3	SO4	S(IV)	CH2O	-/+	C-A	(%)	HCO3*
					micro-equivalents/liter									micro-mol/l					
1	7:15	8: 0	6.9	3.06	871.0	29.4	14.3	3130.	50.	8.6	162.	2750.	1475.	83.6	165.0	1.090	-368	(4)	0*
2	8: 0	8:45	6.5	3.06	871.0	22.0	-1.0	3360.	63.	10.4	189.	2900.	1611.	83.6	164.0	1.106	-457	(5)	0*
3	8:45	9:30	2.6	2.92	1202.3	29.0	19.1	3500.	10 .	14.7	226.	3340.	1976.	-1.0	-1.0	1.138	-674	(6)	0*
Vol-Wt Mean (LWC=0.040)			3.03	924.8	26.3	15.6	3284.	64.	10.3	183.	2907.	1612.	83.6	164.5	1.107	-461	(5)	0*	

Buttonwillow (BW)- 2-3 Jan 1985 (Fog Observed: 17:00 to 10:00)

	TIME		mL	pH	H	Na	K	NH4	Ca	Mg	Cl	NO3	SO4	S(IV)	CH2O	-/+	C-A	(%)	HCO3*
					micro-equivalents/liter									micro-mol/l					
1	20:20	21:20	62.5	5.94	1.1	5.4	-1.0	983.	32.	3.4	12.	391.	311.	51.0	37.8	0.746	260	(15)	6*
2	21:20	22:20	69.2	6.00	1.0	8.3	2.4	1126.	44.	4.3	32.	606.	519.	45.4	53.1	1.014	-17	(1)	7*
3	22:20	24: 0	55.6	6.10	0.8	10.4	2.9	1119.	65.	6.8	22.	505.	519.	50.1	66.7	0.910	109	(5)	9*
4	0: 0	2:15	32.1	5.25	5.6	14.0	4.6	2080.	62.	8.9	14.	1105.	821.	35.8	75.8	0.908	199	(5)	1*
5	2:35	4:30	51.8	4.92	12.0	3.5	2.2	1174.	13.	1.9	3.	781.	301.	7.6	52.8	0.905	114	(5)	1*
6	4:45	6:50	39.4	4.42	38.0	4.0	2.9	1146.	14.	2.5	14.	698.	276.	10.0	54.4	0.826	210	(10)	0*
Vol-Wt Mean (LWC=0.174)				5.10	8.0	7.3	2.8	1205.	38.	4.4	17.	637.	441.	35.6	54.9	0.893	135	(6)	5*

Buttonwillow (BW)- 3-4 Jan 1985 (Fog Observed: 17:15 to 10:30)

	TIME		mL	pH	H	Na	K	NH4	Ca	Mg	Cl	NO3	SO4	S(IV)	CH2O	-/+	C-A	(%)	HCO3*
					micro-equivalents/liter									micro-mol/l					
1	17:25	18:35	50.0	6.53	0.3	6.7	4.1	739.	74.	7.3	15.	325.	249.	5.5	29.8	0.715	237	(17)	24*
2	20:10	22: 0	76.4	6.66	0.2	2.2	1.6	568.	34.	4.1	89.	230.	122.	1.1	23.8	0.724	168	(16)	32*
3	0:15	2:15	65.0	5.73	1.9	1.8	1.1	553.	9.	1.0	27.	274.	137.	5.6	20.7	0.781	124	(12)	4*
4	4:30	6:30	63.0	6.14	0.7	2.1	1.2	519.	10.	1.3	46.	207.	198.	22.3	26.2	0.887	61	(6)	10*
5	6:35	8:25	52.0	6.32	0.5	14.4	1.9	600.	11.	1.6	19.	130.	305.	0.0	32.5	0.721	175	(16)	15*
6	8:30	10:10	29.5	6.79	0.2	6.0	2.5	731.	27.	5.3	9.	153.	222.	15.2	43.2	0.517	373	(32)	44*
7	10:10	10:30	1.5	-1.00	0.0	18.0	7.5	1423.	130.	2.1	-1.	-1.	-1.	-1.0	-1.0	---			
Vol-Wt Mean (LWC=0.173)				6.17	0.7	5.1	2.0	604.	27.	3.2	40.	226.	195.	9.1	27.6	0.733	172	(15)	20*

Buttonwillow (BW)- 4-5 Jan 1985 (Fog Observed: 17:00 to 09:00)

	TIME		mL	pH	H	Na	K	NH4	Ca	Mg	Cl	NO3	SO4	S(IV)	CH2O	-/+	C-A	(%)	HCO3*
					micro-equivalents/liter									micro-mol/l					
1	19:30	20:30	33.5	6.55	0.3	3.8	1.5	968.	50.	6.8	-1.	224.	147.	1.0	21.7	0.361	658	(47)	25*
2	20:30	21:35	30.6	6.76	0.2	1.5	1.9	858.	28.	3.3	-1.	215.	164.	0.0	19.5	0.424	514	(40)	41*
3	21:40	23:50	36.7	6.60	0.3	2.9	2.0	686.	24.	3.3	-1.	191.	287.	16.8	35.4	0.689	223	(18)	28*
4	23:50	2: 2	58.3	5.66	2.2	2.3	1.5	677.	13.	1.6	7.	185.	375.	42.8	36.0	0.875	87	(7)	3*
5	2: 5	3: 0	27.3	5.70	2.0	6.9	2.0	529.	9.	1.4	6.	201.	335.	30.6	32.8	1.040	-22	(2)	4*
6	3: 0	4: 0	25.4	5.87	1.3	1.6	1.0	483.	7.	1.5	23.	158.	318.	21.9	34.1	1.052	-26	(3)	5*
7	4: 0	5: 0	23.4	6.16	0.7	1.6	1.1	456.	9.	1.3	6.	152.	184.	-1.0	-1.0	0.728	128	(16)	10*
8	5: 0	6:15	31.0	6.78	0.2	3.8	1.5	683.	12.	1.6	38.	201.	174.	5.6	26.5	0.596	284	(25)	43*
9	6:15	7: 0	19.9	6.89	0.1	1.9	1.8	582.	14.	2.6	2.	208.	167.	-1.0	-1.0	0.626	225	(23)	55*
10	7: 0	8: 0	22.0	6.87	0.1	1.8	2.1	542.	11.	1.5	14.	156.	143.	17.1	44.6	0.591	229	(26)	53*
11	8: 0	9: 0	11.8	6.97	0.1	6.6	2.5	697.	25.	4.0	15.	157.	232.	34.2	59.7	0.595	297	(25)	66*
Vol-Wt Mean (LWC=0.133)				6.08	0.8	3.0	1.7	668.	19.	2.6	14.	189.	245.	22.3	32.5	0.678	224	(19)	25*

SAN JOAQUIN VALLEY FOGWATER DATA 1984-95

Metals Concentrations

A. Bakersfield Airport (NW) Site

Date	#	pH	microgram/liter Fe	Mn	Pb	Cu
28 Dec 1984	1	6.80	347	51	65	15
	5	5.45	384	29	55	22
	FB(a)		<1		2	2
2-3 Jan 1985	1	6.55	51	15	18	5
			(<1)(b)	(9)	(13)	(13)
	2	6.20	165	19	59	18
	3	5.60	172	20	82	13
	4	5.72	200	16	96	25
	5	5.66	45	17	34	14
	6	4.30	91	31	77	16
	7	6.83	79	10	18	16
	8	6.82	93	8	15	9
			(11)	(5)	(14)	(5)
	9	6.51	286	33	52	15
3-4 Jan 1985	1	6.62	134	29	15	9
	4	7.57	176	17	12	6
	FB		63	8	8	6
4-5 Jan 1985	1	6.26	82	11	6	7
	5	5.20	508	23	139	36
			(63)	(16)	(29)	(17)
	8	4.96	68	14	40	6
	10	4.80	68	12	43	5
	FB		11	<1	1	12
8 Jan 1985	1	7.37	242	95	21	37
14 Jan 1985	1	6.17	164	24	27	69
	2	5.56	114	19	22	9
	3	6.72	90	12	26	7
	FB		7	<1	2	6
18-19 Jan 1985	1	5.85	123	36	25	33
	3	4.18	80	12	126	165
	4	4.04	89	11	139	80
	6	3.86	173	12	134	20
			(178)	(6)	(110)	(9)
	8	4.53	42	11	46	10
	10	3.65	189	13	188	21
	FB		<1	<1	2	2

A. Bakersfield Airport (NW) Site (cont.)

Date	#	pH	microgram/liter Fe	Mn	Pb	Cu
20 Jan 1985	2	3.06	426	53	400	34
	FB		42	<1	1	7

B. Buttonwillow (BW) Site

Date	#	pH	microgram/liter Fe	Mn	Pb	Cu
2-3 Jan 1985	2	6.00	45	6	15	19
			(0)	(4)	(6)	(21)
	4	5.25	244	15	42	71
			(16)	(5)	(12)	(22)
	FB		<1	<1	3	42
			(<1)	(2)	(2)	(16)
3-4 Jan 1985	2	6.66	163	5	9	76
	5	6.32	19	<1	9	20
			(na)	(na)	(2)	(15)
	6	6.79	201	7	14	19
	FB		<1	<1	5	27
4-5 Jan 1985	1	6.55	192	9	56	45
			(136)	(12)	(17)	(34)
	2	6.76	124	na	39	ng
	4	5.66	36	5	9	27
			(44)	(4)	(63)	(55)
	6	5.87	37	7	16	57
	8	6.78	3	3	27	65
	FB		<1	5	7	32
			<1	<1	na	(14)

a. FB = field blank; b. () - filtered aliquots (1 m pore size).

APPENDIX C.

SAN JOAQUIN VALLEY FIELD SAMPLING DATA: WINTER 1984-85

2. Aerosol, Ammonia, and Nitric Acid Concentration Data (6 sites)

BUTTONWILLOW (BW) SIte SJV Aerosol/Fog Study 1984-85

nano-equivalent/m3

Date	Start	Min	Na	K	NH4	Ca	Mg	Cl	NO3	SO4	NH3(g)	HNO3(g)	Amm/N+S	ALKa (%)	ALKt (%)
12/28	12: 0	258	5.4	1.9	409.	15.	1.7	16.	287.	107.	31.	8.5	1.039	24. (3)	46.(5)
12/29	0: 0	240	14.8	3.1	496.	40.	5.8	13.	338.	135.	254.	5.0	1.048	74. (7)	323.(25)
12/29	12: 0	240	9.6	3.1	550.	28.	5.8	17.	371.	123.	21.	28.3	1.114	86. (8)	78.(7)
12/29	20: 0	240	10.0	2.9	554.	35.	5.0	17.	435.	138.	188.	8.7	0.967	18. (1)	196.(14)
12/30	0:10	210	9.0	2.6	571.	18.	3.3	26.	417.	121.	419.	6.2	1.062	40. (3)	453.(28)
12/30	8: 0	210	6.7	3.6	410.	16.	3.1	50.	364.	126.	424.	5.2	0.835	-102. (10)	317.(23)
12/30	12:30	228	10.7	2.9	467.	45.	7.0	25.	401.	156.	307.	6.1	0.839	-49. (4)	252.(18)
12/31	0: 0	240	5.8	2.5	440.	15.	3.1	17.	331.	127.	196.	0.0	0.959	-9. (1)	187.(16)
1/ 3	0: 0	138	1.4	4.3	659.	3.	0.7	62.	395.	268.	159.	5.1	0.995	-56. (4)	98.(6)
1/ 3	8: 0	240	2.5	1.9	383.	5.	1.5	4.	296.	113.	242.	0.0	0.939	-18. (2)	223.(21)
1/ 3	12:30	228	5.3	2.6	436.	86.	5.7	15.	316.	149.	250.	9.2	0.939	55. (5)	296.(23)
1/ 3	20:30	114	1.8	3.1	303.	99.	3.1	18.	228.	83.	193.	7.9	0.972	81. (11)	266.(28)
1/ 4	0:20	120	0.8	2.5	183.	106.	4.2	33.	163.	67.	42.	5.0	0.800	35. (6)	71.(12)
1/ 4	4:30	126	4.0	0.8	127.	110.	4.4	79.	139.	83.	32.	5.6	0.572	-55. (10)	-29.(5)
1/ 4	12: 0	246	-1.0	2.8	207.	30.	4.1	77.	175.	118.	276.	5.7	0.708	-126. (20)	145.(16)
1/ 4	19:30	126	9.5	5.6	298.	88.	3.6	20.	198.	139.	79.	-1.0	0.882	47. (6)	126.(15)
1/ 5	2:20	108	6.0	3.2	208.	47.	2.8	32.	134.	97.	102.	0.0	0.900	4. (1)	105.(17)
1/ 5	4:15	234	3.2	2.1	259.	1.	1.7	24.	184.	105.	145.	8.5	0.896	-45. (8)	92.(13)
1/ 5	8:20	258	5.0	2.7	341.	16.	1.9	6.	190.	122.	760.	0.0	1.093	48. (7)	808.(56)
1/ 5	13: 0	246	4.9	7.7	388.	67.	7.7	10.	224.	136.	390.	9.3	1.079	106. (12)	487.(39)
1/ 6	0: 0	240	5.8	3.1	433.	34.	3.5	13.	271.	117.	696.	0.0	1.118	80. (9)	776.(49)
1/ 6	7: 0	246	0.8	3.3	419.	49.	6.1	4.	331.	134.	650.	0.0	0.900	9. (1)	659.(41)
1/ 6	12: 0	246	5.1	3.7	563.	36.	4.3	12.	386.	144.	382.	13.0	1.061	70. (6)	439.(28)
1/ 7	0: 0	240	3.7	2.5	275.	1.	1.5	6.	210.	58.	288.	12.1	1.023	9. (2)	284.(33)

NOTES:

1. All units in nano-equivalents per cubic meter; -1 means not analyzed; 0 meams below detection limit.
2. Detection limits for NH3(g) and HNO3(g): 20 and 5 nano-eq/m3 , respectively.
3. Amm/N+S is NH4/(NO3+SO4)
4. Alka (%) is aerosol alkalinity calculation: aerosol cation - anion equivalents; (%) is as percent of total ions.
5. Alkt (%) is total alkalinity calculation: Alka + NH3(g) - HNO3(g); (%) is as percent of total ions plus gases.

BAKERSFIELD AIRPORT (NW) Site SJV Aerosol/Fog Study 1984-85

nano-equivalent/m3

Date	Start	Min	Na	K	NH4	Ca	Mg	Cl	NO3	SO4	NH3(g)	HNO3(g)	Amm/N+S	ALKa (%)	ALKt (%)
12/28	0: 0	146	15.1	17.5	336.	20.	4.1	38.	158.	260.	363.	-1.0	0.803	-63. (7)	300.(25)
12/28	4:35	130	10.3	4.7	450.	11.	2.8	31.	288.	278.	0.	5.6	0.796	-118. (11)	-124.(11)
12/28	12: 0	243	8.6	3.7	753.	11.	2.9	70.	486.	208.	494.	19.3	1.086	16. (1)	490.(24)
12/29	0: 0	232	14.0	3.7	616.	10.	4.3	20.	442.	123.	78.	6.9	1.092	64. (5)	134.(10)
12/30	0: 0	234	17.3	3.4	735.	8.	2.4	18.	481.	201.	256.	0.0	1.078	67. (5)	323.(19)
12/30	12: 0	223	3.4	1.1	374.	2.	0.9	22.	251.	173.	0.	43.9	0.884	-65. (8)	-108.(12)
12/30	20: 0	236	6.1	2.1	436.	13.	1.9	17.	326.	129.	72.	10.6	0.958	-13. (1)	48.(5)
12/31	2:40	246	5.3	1.6	543.	8.	1.6	18.	376.	148.	508.	6.5	1.035	16. (1)	518.(32)
1/ 2	18: 0	195	6.7	4.7	571.	24.	3.9	17.	369.	221.	107.	8.6	0.967	3. (0)	102.(8)
1/ 2	21:15	166	7.8	5.4	328.	13.	6.0	18.	235.	277.	0.	0.0	0.641	-170. (19)	-170.(19)
1/ 3	0: 0	178	5.1	5.6	371.	8.	1.1	17.	247.	270.	39.	0.0	0.717	-143. (16)	-104.(11)
1/ 3	3: 0	225	10.0	4.7	387.	9.	2.7	11.	147.	358.	262.	0.0	0.767	-102. (11)	160.(13)
1/ 3	7: 0	153	17.6	8.5	494.	6.	2.6	20.	128.	500.	118.	0.0	0.786	-119. (10)	-1.(0)
1/ 3	12: 0	233	6.2	9.2	491.	19.	3.6	15.	343.	180.	811.	11.2	0.939	-10. (1)	790.(42)
1/ 3	20: 0	127	4.7	3.9	217.	15.	3.5	16.	158.	102.	252.	7.1	0.833	-32. (6)	213.(27)
1/ 3	23: 0	176	4.0	8.0	148.	14.	2.8	23.	117.	80.	91.	0.0	0.754	-43. (11)	48.(10)
1/ 4	4: 0	233	6.0	7.3	137.	5.	1.7	11.	90.	60.	64.	0.0	0.914	-4. (1)	61.(16)
1/ 4	12: 0	232	5.2	6.2	338.	40.	3.0	17.	194.	121.	815.	10.8	1.075	61. (8)	865.(56)
1/ 4	20: 0	175	4.0	3.4	303.	74.	2.6	14.	154.	191.	40.	0.0	0.876	27. (4)	67.(9)
1/ 4	23:10	175	5.1	6.0	460.	57.	2.9	26.	140.	431.	0.	0.0	0.805	-66. (6)	-66.(6)
1/ 5	4: 0	247	5.7	3.2	364.	48.	2.0	16.	101.	320.	0.	0.0	0.866	-14. (2)	-14.(2)
1/ 5	12: 0	236	4.0	5.7	496.	11.	3.4	23.	199.	239.	267.	9.3	1.130	58. (6)	316.(25)
1/ 5	20: 0	236	6.8	7.4	547.	37.	7.2	47.	299.	303.	343.	8.9	0.908	-43. (3)	291.(18)
1/ 6	2:20	240	2.1	10.2	494.	21.	3.7	29.	288.	288.	513.	0.0	0.859	-73. (6)	439.(27)
1/ 6	12: 0	237	7.2	4.2	534.	24.	3.6	32.	407.	274.	987.	13.1	0.783	-141. (11)	834.(36)
1/ 7	13: 0	237	-1.0	-1.0	219.	7.	1.3	17.	106.	103.	0.	9.7	1.050	2. (0)	-8.(2)
1/ 8	9: 0	132	7.6	4.2	208.	85.	3.8	68.	163.	57.	265.	6.1	0.948	21. (4)	280.(32)
1/ 8	15:40	246	1.6	1.2	118.	11.	1.0	8.	102.	55.	163.	5.7	0.753	-32. (11)	125.(27)
1/ 9	0: 0	241	6.6	8.7	203.	59.	4.8	17.	141.	112.	257.	0.0	0.803	12. (2)	270.(33)
1/ 9	22: 0	243	2.7	1.4	272.	2.	1.0	19.	226.	66.	486.	7.8	0.930	-32. (5)	446.(41)
1/10	7: 0	96	10.5	4.2	356.	104.	4.7	37.	204.	241.	21.	-1.0	0.800	-3. (0)	18.(2)
1/10	12: 0	253	4.9	2.0	585.	2.	1.8	12.	265.	148.	162.	5.1	1.416	170. (17)	327.(28)
1/11	6:30	111	9.0	3.6	703.	4.	1.8	32.	297.	306.	72.	6.3	1.164	86. (6)	151.(11)
1/14	1:30	181	7.7	3.9	376.	53.	3.3	28.	210.	199.	0.	-1.0	0.919	7. (1)	7.(1)
1/14	4:45	98	7.7	-1.0	852.	3.	3.1	10.	454.	357.	20.	12.2	1.050	45. (3)	53.(3)
1/18	20:15	227	4.6	5.7	535.	51.	1.3	42.	267.	302.	0.	6.2	0.942	-12. (1)	-19.(2)
1/19	0: 0	182	4.9	6.6	346.	83.	2.2	28.	201.	228.	0.	9.3	0.808	-13. (1)	-22.(2)
1/19	3:10	173	2.9	4.0	254.	50.	2.3	12.	121.	110.	0.	8.1	1.100	70. (13)	62.(11)
1/19	6: 5	236	3.6	3.6	345.	39.	1.7	15.	203.	176.	0.	5.9	0.911	-1. (0)	-7.(1)
1/19	12: 0	238	8.8	5.9	639.	14.	2.3	29.	225.	521.	50.	55.9	0.856	-106. (7)	-111.(7)
1/20	0: 0	239	5.9	4.6	661.	44.	2.9	38.	435.	372.	29.	15.9	0.819	-126. (8)	-113.(7)
1/20	7:20	143	6.6	2.8	427.	80.	3.8	35.	255.	262.	0.	23.1	0.825	-32. (3)	-55.(5)
1/20	20: 0	224	5.8	4.9	955.	9.	2.2	34.	511.	549.	0.	44.6	0.901	-116. (6)	-161.(8)

DOWNTOWN BAKERSFIELD (BA) Site — SJV Aerosol/Fog Study 1984-85 — 4/9/85 Jed

nano-equivalent/m3

Date	Start	Min		Na	K	NH4	Ca	Mg	Cl	NO3	SO4	NH3(g)	HNO3(g)	Amm/N+S	ALKa (%)	ALKt (%)
12/28	0: 0	240		7.3	11.2	381.	2.	1.9	50.	213.	213.	333.	0.0	0.897	-72. (8)	262.(22)
12/28	12: 0	240		9.4	4.8	806.	20.	5.2	29.	396.	210.	313.	12.9	1.330	210. (14)	510.(28)
12/29	0: 0	240		20.2	7.1	763.	15.	5.8	35.	525.	148.	217.	5.4	1.133	103. (7)	314.(18)
12/29	12: 0	240		11.7	3.5	510.	17.	4.8	3.	392.	150.	117.	31.2	0.942	3. (0)	88.(7)
12/30	0: 0	0	miss	-1.0	-1.0	-1.	-1.	-1.0	-1.	-1.	-1.	-1.	-1.0	-1.000	0. (0)	0.(0)
12/30	12: 0	240		6.0	2.5	454.	13.	3.3	19.	285.	202.	54.	31.7	0.932	-28. (3)	-5.(0)
12/31	0: 0	240		5.8	2.1	538.	11.	2.5	17.	350.	279.	196.	25.0	0.854	-87. (7)	84.(6)
1/ 3	0: 0	240		5.6	6.0	433.	16.	3.3	17.	229.	292.	142.	0.0	0.832	-73. (7)	68.(6)
1/ 3	12: 0	240		5.0	4.8	400.	52.	7.7	17.	317.	154.	500.	13.7	0.849	-18. (2)	468.(32)
1/ 4	0: 0	240		4.0	3.7	240.	15.	2.5	8.	115.	204.	-1.	0.0	0.752	-63. (11)	-63.(11)
1/ 4	12: 0	246		5.9	6.5	218.	57.	6.3	20.	191.	150.	362.	17.5	0.637	-69. (11)	275.(27)
1/ 5	0: 0	240		3.7	4.6	429.	16.	2.1	13.	146.	438.	175.	0.0	0.736	-140. (13)	35.(3)
1/ 5	12: 0	240		0.8	6.9	581.	52.	7.3	23.	244.	360.	342.	16.2	0.962	22. (2)	347.(21)
1/ 6	0: 0	246		5.3	8.7	498.	20.	4.3	39.	323.	226.	520.	6.5	0.907	-51. (5)	463.(28)
1/ 6	12: 0	240		9.8	5.8	740.	47.	7.3	69.	531.	333.	375.	29.2	0.855	-124. (7)	222.(10)

WASCO (WA) Site — SJV Aerosol/Fog Study 1984-85 — 4/9/85 Jed

nano-equivalent/m3

Date	Start	Min		Na	K	NH4	Ca	Mg	Cl	NO3	SO4	NH3(g)	HNO3(g)	Amm/N+S	ALKa (%)	ALKt (%)
12/28	12: 0	291		10.5	3.6	591.	17.	5.0	22.	423.	136.	69.	5.5	1.059	46. (4)	109.(9)
12/29	0: 0	0	miss	-1.0	-1.0	-1.	-1.	-1.0	-1.	-1.	-1.	-1.	-1.0	-1.000	0. (0)	0.(0)
12/29	12: 0	261		9.2	3.1	568.	6.	2.9	56.	423.	153.	180.	14.9	0.987	-42. (3)	123.(9)
12/30	0: 0	0	miss	-1.0	-1.0	-1.	-1.	-1.0	-1.	-1.	-1.	-1.	-1.0	-1.000	0. (0)	0.(0)
12/30	12: 0	252		6.0	2.0	472.	13.	2.6	36.	306.	131.	135.	16.7	1.082	24. (2)	142.(13)
12/31	0: 0	239		6.3	3.1	485.	8.	2.7	19.	387.	115.	460.	0.0	0.967	-15. (2)	445.(30)
1/ 5	0: 0	238		2.9	3.4	275.	49.	3.6	19.	200.	86.	277.	0.0	0.963	30. (5)	307.(34)
1/ 5	12:30	263		0.8	3.6	350.	22.	2.7	11.	222.	120.	278.	0.0	1.022	25. (3)	303.(30)
1/ 6	0: 0	258		10.7	7.2	380.	47.	3.9	23.	250.	132.	419.	-1.0	0.995	43. (5)	462.(36)
1/ 6	12: 0	251		3.2	5.2	426.	14.	2.0	10.	383.	116.	279.	12.7	0.856	-58. (6)	208.(17)
1/ 7	0: 0	261		4.4	3.3	450.	1.	1.5	12.	308.	92.	88.	6.9	1.124	49. (6)	130.(13)

LOST HILLS (LH) Site SJV Aerosol/Fog Study 1984-85 4/9/85 Jed

nano-equivalent/m3

Date	Start	Min		Na	K	NH4	Ca	Mg	Cl	NO3	SO4	NH3(g)	HNO3(g)	Amm/N+S	ALKa (%)	ALKt (%)
12/28	12: 0	240		10.4	2.3	619.	2.	3.3	19.	388.	138.	71.	13.7	1.179	93. (8)	150.(12)
12/29	0: 0	0	miss	-1.0	-1.0	-1.	-1.	-1.0	-1.	-1.	-1.	-1.	-1.0	-1.000	0. (0)	0.(0)
12/29	12: 0	240		7.7	1.7	385.	8.	2.5	13.	285.	117.	25.	43.8	0.958	-9. (1)	-28.(3)
12/30	0: 0	240		7.9	2.9	452.	13.	3.7	33.	354.	113.	404.	8.7	0.969	-21. (2)	375.(27)
12/30	12: 0	240		6.2	1.7	358.	2.	2.1	13.	321.	127.	0.	28.3	0.800	-90. (11)	-119.(14)
12/31	0: 0	240		5.8	1.7	371.	11.	2.1	26.	319.	115.	46.	0.0	0.856	-68. (8)	-22.(2)
1/ 5	0: 0	246		2.8	1.2	165.	9.	0.4	0.	75.	89.	69.	-1.0	1.000	13. (4)	82.(20)
1/ 5	12: 0	240		3.3	3.3	271.	19.	1.7	13.	163.	108.	154.	10.8	1.000	15. (2)	158.(21)
1/ 6	0: 0	246		5.7	2.0	321.	16.	2.8	12.	183.	83.	118.	0.0	1.206	69. (11)	187.(25)
1/ 6	12: 0	240		4.6	3.5	315.	19.	2.1	8.	221.	83.	250.	15.8	1.035	31. (5)	265.(29)
1/ 7	0: 0	240		3.3	1.5	385.	17.	2.9	19.	258.	100.	96.	7.1	1.076	33. (4)	121.(14)

McKITTRICK (MK) Site SJV Aerosol/Fog Study 1984-85 4/9/85 Jed

nano-equivalent/m3

Date	Start	Min	Na	K	NH4	Ca	Mg	Cl	NO3	SO4	NH3(g)	HNO3(g)	Amm/N+S	ALKa (%)	ALKt (%)
12/28	12: 0	270	12.0	2.8	343.	34.	5.6	20.	183.	204.	-1.	31.5	0.885	-10. (1)	-42.(5)
12/29	0: 0	264	12.5	1.7	208.	13.	4.4	19.	201.	87.	-1.	9.8	0.724	-67. (12)	-77.(14)
12/29	12: 0	258	10.3	2.3	417.	44.	6.0	17.	260.	132.	0.	35.7	1.064	71. (8)	35.(4)
12/30	0: 0	258	7.8	2.5	490.	10.	2.3	23.	256.	128.	-1.	78.7	1.278	106. (12)	27.(3)
12/30	12: 0	258	6.6	1.6	523.	12.	2.7	31.	335.	188.	23.	16.7	1.000	-9. (1)	-2.(0)
12/31	0: 0	258	9.3	1.7	504.	15.	3.9	19.	312.	142.	78.	5.4	1.111	60. (6)	133.(12)
1/ 3	14: 0	282	11.0	4.3	411.	82.	9.6	xx.	xxx.	xxx.	75.	24.5	handling error on anions		
1/ 4	0: 0	258	10.5	2.7	240.	25.	3.7	4.	101.	114.	27.	55.8	1.117	63. (13)	34.(6)
1/ 4	12: 0	288	19.8	5.7	406.	156.	17.5	26.	208.	297.	97.	20.8	0.804	74. (7)	150.(12)
1/ 5	0: 0	252	0.8	2.4	107.	19.	2.8	14.	73.	54.	40.	25.8	0.843	-9. (3)	5.(1)
1/ 5	12: 0	252	9.3	4.4	274.	53.	6.7	12.	163.	157.	48.	50.8	0.857	16. (2)	13.(2)
1/ 6	0: 0	246	13.6	2.8	346.	29.	3.9	4.	177.	181.	134.	13.8	0.966	33. (4)	154.(17)
1/ 6	12: 0	252	17.7	2.6	308.	43.	5.4	20.	202.	222.	99.	26.2	0.724	-69. (8)	4.(0)
1/ 7	0: 0	258	5.6	1.9	93.	16.	3.7	12.	45.	47.	0.	9.7	1.021	18. (8)	8.(3)

APPENDIX C.

SAN JOAQUIN VALLEY FIELD SAMPLING DATA: WINTER 1984-85

3. Deposition Rate Data for Solute Ions (NW & BW sites)

*** SAN JOAQUIN VALLEY DEPOSITION DATA 1984-85 *** Data checked: 6/2/85

Bakersfield Airport (NW) Site: 1984-85

	Date	PICKUP	hr	EXT(mL)	PREC	Collector		DEPOSITION RATE: micro-eq/m2-hr pH	Na	K	NH4	Ca	Mg	Cl	NO3	SO4	-/+
2	12/24	11:30	23.50	20.	0.0	PD-hi -		5.43	0.09	0.07	1.27	0.88	0.11	0.22	0.77	1.60	0.987
3	12/24	8: 0	8.92	20.	0.0	PD-hi -		5.82	0.00	0.04	0.29	0.58	0.10	1.16	0.35	0.42	1.562
4	12/24	23:50	15.83	20.	0.0	PD-hi -		5.48	0.00	0.03	0.74	0.53	0.07	0.41	0.36	1.31	1.269
5	12/25	11:30	11.67	20.	0.0	PD-hi -		5.38	0.00	0.00	0.45	0.23	0.02	0.56	0.28	0.67	1.290
6	12/25	11:30	15.67	140.	0.0	Bucket-		5.44	0.19	0.08	2.41	1.19	0.14	0.16	1.54	1.85	0.772
7	12/26	0: 0	12.50	10.	0.5	PD-hi -Dew		5.03	0.02	0.03	4.20	0.51	0.07	0.33	0.28	5.30	1.108
8	12/26	10: 0	9.00	10.	0.0	PD-hi -		5.81	0.14	0.06	0.29	1.15	0.13	0.65	0.40	0.64	0.898
9	12/26	10: 0	21.25	140.	0.0	Bucket-		5.15	0.08	0.05	2.73	1.28	0.15	0.12	1.15	3.55	0.940
10	12/27	23: 0	37.00	0.	106.7	Funnel-Rain		6.43	0.51	-1.00	12.48	1.18	0.22	0.79	7.62	7.11	1.078
11	12/27	23: 0	37.00	140.	19.0	Bucket-Rain		5.32	0.18	0.05	8.58	1.51	0.14	0.23	3.94	5.95	0.935
12	12/28	2:25	2.42	10.	0.5	PD-hi -Fog		5.31	0.14	0.06	15.50	0.85	0.11	0.85	2.79	11.50	0.839
13	12/28	2:40	2.67	10.	0.5	PD-lo -Fog		6.12	0.66	0.51	15.07	1.15	0.18	1.15	3.75	12.26	0.966
14	12/28	4:35	2.17	10.	0.0	PD-hi -Fog		5.14	0.15	0.06	8.68	0.15	0.03	0.54	3.20	5.42	0.815
15	12/28	4:35	1.92	10.	0.0	PD-lo -Fog		5.37	0.41	0.14	7.78	0.34	0.03	0.98	3.01	5.24	0.911
16	12/28	4:30	4.50	65.	5.0	Bucket-Fog		5.61	0.28	0.11	20.98	1.68	0.20	0.84	4.90	15.95	0.906
17	12/28	7: 0	2.42	10.	0.0	PD-hi -Dew		5.03	0.30	0.05	*2.15	1.88	0.03	0.32	0.54	1.37	0.323
18	12/28	7: 0	2.42	10.	0.0	PD-lo -Dew		5.24	0.21	0.05	1.07	0.40	0.03	0.40	0.54	1.64	0.777
19	12/28	16:40	9.67	10.	0.0	PD-hi -		5.62	0.16	0.09	1.88	0.10	0.05	0.27	0.94	1.85	1.250
20	12/28	16:40	9.67	10.	0.0	PD-lo -		5.22	0.11	0.08	2.95	0.60	0.11	0.32	1.05	3.08	1.039
21	12/29	7:50	16.17	10.	0.0	PD-hi -Dew		5.83	0.11	0.03	1.20	0.30	0.06	0.14	0.96	0.74	1.044
22	12/29	7:50	16.17	10.	0.0	PD-lo -Dew		6.15	0.12	0.03	1.20	0.46	0.07	0.15	0.95	0.84	1.017
23	12/29	7:50	27.25	140.	0.0	Bucket-		5.43	0.10	0.03	2.49	0.55	0.07	0.28	1.39	2.22	1.079
24	12/29	20:20	12.50	10.	0.0	PD-hi -		6.53	0.11	0.04	1.30	0.14	0.10	0.10	0.94	1.19	1.307
25	12/29	20:20	12.50	10.	0.0	PD-lo -		6.30	0.09	0.05	1.04	0.13	0.09	0.05	0.94	1.14	1.496
26	12/30	8:25	12.08	10.	0.0	PD-hi -Dew		6.54	0.22	0.05	*1.29	2.37	0.08	0.22	0.49	2.31	0.750
27	12/30	8:25	12.08	10.	0.0	PD-lo -Dew		6.00	0.13	0.02	3.92	0.95	0.07	0.19	0.46	3.27	0.762
28	12/30	8:25	24.58	140.	0.0	Bucket-		5.44	0.01	0.04	1.13	0.32	0.04	0.41	1.06	0.58	1.073
29	12/30	8:25	24.58	140.	0.0	Bucket-	2nd	5.48	0.00	-1.00	0.00	0.00	0.00	0.10	0.00	0.10	0.604

NOTES:

1. Date & PICKUP is end of exposure period; hr is hours of exposure.
2. EXT & PREC are mL of extraction or precipitation recovered from collector.
3. Collector Area: PD=154; Bucket=556; Funnel=730 cm2. Bucket @ 2.5 m; hi @ 3m; mid @ 1.8m; lo @ 20cm.
4. Fog, Dew & Rain were observations at pickup.
5. Rep means replicate or overlapping sample; 2nd means 2nd extraction of collector.
6. RATE in micro-eq/m2-hour calculated from [Conc. in ueq/l]x(ext+prec in mL)x10/(area in cm2xtime in hr).
7. -1 means not analyzed; *#.## means that NH4+ was thought to be reduced by Ca contamination.

Bakersfield Airport (NW) Site: 1984-85

	Date	PICKUP	hr	EXT(mL)	PREC	Collector	DEPOSITION RATE: micro-eq/m2-hr pH	Na	K	NH4	Ca	Mg	Cl	NO3	SO4	-/+
30	12/30	16:35	8.08	10.	0.0	PD-lo -	5.52	0.04	0.00	0.24	0.48	0.03	0.23	0.23	0.76	1.169
31	12/31	8:55	16.67	10.	0.0	PD-hi -	5.68	0.03	0.02	0.23	0.29	0.04	0.12	0.38	0.21	1.029
32	12/31	8:55	16.67	9.	0.0	PD-lo -	5.70	0.03	0.02	0.25	0.29	0.04	0.12	0.28	0.19	0.868
33	12/31	8:55	24.00	140.	0.0	Bucket-	5.66	0.00	0.00	1.78	0.12	0.01	0.31	0.78	0.63	0.804
34	1/ 2	16: 0	55.08	10.	2.0	PD-hi -Fog	3.83	0.21	0.12	2.94	0.61	0.08	0.57	4.02	3.69	1.366
35	1/ 2	16: 0	55.08	10.	2.0	PD-lo -Fog	5.15	0.13	0.05	2.35	0.74	0.07	0.40	1.29	2.69	1.269
36	1/ 2	16:15	54.50	140.	0.0	Bucket-Fog	4.69	0.15	0.04	3.19	0.83	0.08	0.23	1.50	3.74	1.046
37	1/ 2	21: 0	4.75	10.	0.5	PD-hi -	6.34	1.21	0.85	10.19	1.58	0.22	4.31	2.76	5.68	0.904
38	1/ 2	21: 0	4.75	10.	0.5	PD-lo -	6.00	0.62	0.32	8.61	3.30	0.32	2.15	2.47	4.98	0.722
39	1/ 2	21: 0	4.50	50.	0.0	Bucket-	5.92	0.18	0.12	13.59	2.00	0.18	1.00	2.60	6.08	0.593
40	1/ 3	0: 0	3.00	10.	0.5	PD-hi -Fog	5.65	0.59	0.36	18.18	0.57	0.14	2.50	4.73	17.05	1.193
41	1/ 3	0: 0	3.00	10.	0.5	PD-lo -Fog	5.76	0.93	0.89	22.73	1.02	0.18	1.36	6.55	24.09	1.224
42	1/ 3	3: 0	3.00	10.	0.5	PD-hi -Fog	6.16	2.77	1.45	*7.05	0.80	0.14	2.05	8.73	17.50	2.287
43	1/ 3	3: 0	3.00	10.	0.5	PD-lo -Fog	6.55	2.66	1.39	36.14	0.68	0.14	2.27	9.70	24.55	0.889
44	1/ 3	7: 0	4.00	10.	0.5	PD-hi -Fog	6.65	17.90	-1.00	*6.99	1.02	0.43	12.78	2.98	6.84	0.857
45	1/ 3	7: 0	4.00	10.	0.5	PD-lo -Fog	6.58	4.72	2.40	13.64	0.60	0.14	1.02	3.32	8.37	0.590
46	1/ 3	10: 0	3.00	10.	0.5	PD-hi -Fog	5.90	4.07	1.86	15.00	1.48	0.27	2.73	1.70	17.39	0.950
47	1/ 3	10: 0	3.00	10.	0.5	PD-lo -Fog	6.52	4.16	1.86	18.18	1.14	0.18	1.36	1.61	21.66	0.963
48	1/ 3	10: 0	9.50	0.	2.4	PD-hi -Fog Rep	-1.00	2.03	0.27	16.90	0.66	0.06	0.82	4.76	19.52	1.260
49	1/ 3	10: 0	13.00	70.	13.0	Bucket-Fog	-1.00	0.24	0.08	22.36	0.76	0.08	0.86	4.81	22.62	1.203
50	1/ 3	10: 0	13.00	70.	0.0	Bucket-Fog 2nd	-1.00	0.00	0.00	0.00	0.00	0.00	0.00	0.00	0.00	0.000
51	1/ 3	19:30	9.50	10.	1.0	PD-hi -Dew	5.91	0.20	0.10	2.41	0.68	0.10	0.30	0.52	2.29	0.871
52	1/ 3	19:30	9.50	10.	1.0	PD-lo -Dew	6.14	0.10	0.10	2.48	1.20	0.14	0.60	0.49	2.14	0.794
53	1/ 3	22:50	3.33	10.	0.5	PD-hi -Fog	6.50	4.91	2.60	9.01	1.54	0.29	2.46	1.97	5.18	0.522
54	1/ 3	22:50	3.33	10.	0.5	PD-lo -Fog	6.60	3.60	1.95	8.19	1.84	0.29	1.84	1.68	4.75	0.520
55	1/ 4	10:50	12.00	0.	3.3	PD-hi -Fog	-1.00	0.36	0.08	5.64	0.75	0.09	0.14	0.25	2.52	0.420
56	1/ 4	10:50	12.00	0.	4.3	PD-lo -Fog	6.04	0.23	0.13	6.65	1.23	0.12	0.33	0.35	3.16	0.458
57	1/ 4	10:50	24.83	0.	12.5	Bucket-Fog	5.08	0.13	0.09	3.74	0.74	0.08	0.17	0.84	5.00	1.237

Bakersfield Airport (NW) Site: 1984-85

	Date PICKUP	hr	EXT(mL)	PREC	Collector	DEPOSITION RATE: micro-eq/m2-hr pH	Na	K	NH4	Ca	Mg	Cl	NO3	SO4	-/+
65	1/ 4 10:50	15.33	0.	4.6	PD-hi -Fog Rep	6.38	0.21	0.09	5.79	0.80	0.07	0.58	0.76	6.25	1.090
66	1/ 4 10:50	15.33	10.	0.0	PD-hi -Fog 2nd	6.15	0.18	0.07	0.47	0.23	0.02	0.55	0.07	0.39	1.012
58	1/ 4 20: 5	9.25	10.	0.0	PD-hi -	6.45	0.06	0.06	3.72	0.77	0.08	0.84	0.29	1.37	0.529
59	1/ 4 20: 5	9.25	10.	0.0	PD-mid-	6.70	0.10	0.11	4.00	0.98	0.11	1.76	0.37	1.49	0.680
60	1/ 4 20: 5	9.25	10.	0.0	PD-lo -	6.61	0.15	0.15	3.44	1.26	0.13	2.04	0.24	1.08	0.651
61	1/ 4 23: 0	3.00	10.	0.0	PD-hi -Fog	5.60	0.24	0.09	4.76	0.43	0.09	2.81	0.69	5.43	1.454
62	1/ 4 23: 0	3.00	10.	0.0	PD-mid-Fog	5.50	0.22	0.09	7.14	0.65	0.13	2.66	0.91	8.55	1.360
63	1/ 4 23: 0	3.00	10.	0.0	PD-lo -Fog	5.55	0.17	0.06	9.09	0.54	0.11	2.38	1.00	12.36	1.486
64	1/ 4 23: 0	3.00	10.	0.0	PD-lo -Fog Rep	5.61	0.19	0.04	9.74	0.76	0.13	1.95	1.04	11.34	1.257
67	1/ 5 3:45	4.75	10.	0.0	PD-hi -Fog	5.03	0.26	0.10	10.53	0.48	0.10	0.48	1.60	15.72	1.398
68	1/ 5 3:45	4.75	10.	0.0	PD-mid-Fog	5.02	0.51	0.15	16.40	0.68	0.12	0.85	2.02	19.14	1.148
69	1/ 5 3:45	4.75	10.	0.0	PD-lo -Fog	4.88	0.45	0.07	19.69	0.75	0.14	0.60	2.02	23.24	1.130
70	1/ 5 3:45	4.75	10.	0.0	PD-lo -Fog Rep	4.92	0.55	0. 2	20.51	0.96	0.15	0.70	2.06	23.51	1.098
71	1/ 5 10: 0	6.25	10.	0.0	PD-hi -Fog	4.92	0.15	0.03	7.48	0.21	0.05	0.29	0.92	7.69	0.971
72	1/ 5 10: 0	6.25	10.	0.0	PD-mid-Fog	4.92	0.08	0.03	7.79	0.26	0.05	0.33	1.08	9.45	1.148
73	1/ 5 10: 0	6.25	10.	0.0	PD-lo -Fog	4.86	0.10	0.03	11.22	0.36	0.06	0.35	1.27	12.16	1.042
74	1/ 5 10: 0	6.25	10.	0.0	PD-lo - og Rep	4.92	0.11	0.03	11.43	0.31	0.07	0.39	1.26	12.47	1.069
75	1/ 5 10: 0	22.83	140.	2.0	Bucket-Fog	4.80	1.14	0.53	10.52	1.12	0.11	1.12	1.51	14.21	1.109
76	1/ 5 17:15	7.25	10.	0.0	PD-hi -	5.52	0.19	0.08	0.68	0.58	0.10	0.22	0.07	0.69	0.518
77	1/ 5 17:15	7.25	10.	0.0	PD-mid-	5.80	0.30	0.04	0.64	0.81	0.15	0.12	0.08	0.82	0.490
78	1/ 5 17:15	7.25	10.	0.0	PD-lo -	-1.00	0.25	0.13	0.37	1.03	0.15	0.96	0.13	0.90	1.023
79	1/ 5 17:15	7.25	10.	0.0	PD-up -	-1.00	0.91	0.20	0.27	0.99	0.19	0.81	0.41	0.98	0.860
80	1/ 6 7:30	14.25	10.	0.0	PD-hi -	5.73	0.42	0.11	1.87	1.18	0.11	0.36	0.21	2.51	0.815
81	1/ 6 7:30	14.25	10.	0.0	PD-mid-	5.88	0.12	0.04	2.60	1.05	0.11	0.14	0.23	2.60	0.747
82	1/ 6 7:30	14.25	10.	0.0	PD-lo -	6.09	0.18	0.04	1.96	1.09	0.10	0.18	0.19	1.73	0.616
83	1/ 6 7:30	14.25	10.	0.0	PD-up -	-1.00	0.72	0.30	2.42	1.14	0.13	0.68	0.26	2.42	0.715
84	1/ 6 7:30	21.50	140.	0.0	Bucket-	5.70	0.40	0.19	1.29	0.87	0.11	1.05	0.23	1.76	0.989
85	1/ 6 18:30	11.00	10.	0.0	PD-hi -	5.87	0.03	0.04	0.53	0.71	0.06	0.12	0.43	0.75	0.892
86	1/ 6 18:30	11.00	10.	0.0	PD-lo -	5.86	0.24	0.05	0.47	1.59	0.11	0.12	0.34	1.30	0.689
87	1/ 7 12: 0	15.25	0.	77.0	PD-hi -Rain	4.27	0.36	0.00	11.48	1.64	0.20	0.98	13.11	19.34	1.069
88	1/ 7 12: 0	15.25	0.	77.0	PD-lo -Rain	4.32	0.49	0.20	*4.92	11.15	0.46	0.98	12.95	23.93	1.151
89	1/ 7 12: 0	27.50	0.	294.8	Bucket-Rain	4.38	0.77	0.25	9.26	2.51	0.21	1.16	8.49	11.96	1.027
90	1/ 7 12: 0	11.50	0.	350.2	Funnel-Rain	3.76	0.83	0.17	12.93	4.17	0.58	2.50	15.85	20.44	0.429

Bakersfield Airport (NW) Site: 1984-85

	Date	PICKUP	hr	EXT(mL)	PREC	Collector	DEPOSITION RATE: micro-eq/m2-hr pH	Na	K	NH4	Ca	Mg	Cl	NO3	SO4	-/+
91	1/ 8	0: 0	12.00	0.	47.0	PD-hi -Rain	4.78	1.48	0.05	9.92	0.89	0.38	2.03	4.02	10.68	0.988
92	1/ 8	0: 0	13.00	0.	199.9	Bucket-Rain	4.94	1.36	0.11	8.85	0.97	0.33	2.21	3.87	10.51	1.122
93	1/ 8	9: 0	9.00	0.	6.0	PD-hi -Rain	6.53	1.15	0.04	8.05	0.17	0.25	1.26	2.60	5.15	0.931
94	1/ 8	12: 0	3.00	10.	0.0	PD-hi -	6.20	4.33	0.15	0.87	0.11	0.04	1.08	0.91	0.91	0.515
95	1/ 8	12: 0	3.00	10.	0.0	PD-lo -	5.71	0.17	0.00	0.87	0.32	0.09	1.08	1.06	0.91	1.630
96	1/ 8	12: 0	11.75	0.	21.3	Bucket-Rain	6.60	0.85	0.06	12.72	0.11	0.12	0.72	2.02	6.46	0.663
97	1/ 8	21:50	9.83	10.	2.0	PD-hi -Dew	-1.00	0.03	0.00	2.30	0.24	0.03	0.40	0.17	1.01	0.607
98	1/ 8	21:50	9.83	10.	2.0	PD-lo -Dew	-1.00	0.07	0.02	1.03	0.32	0.05	0.48	0.17	0.52	0.782
99	1/ 9	9: 0	11.17	10.	3.5	PD-hi -Dew	-1.00	0.07	0.02	6.36	0.27	0.05	-1.00	0.45	5.96	0.947
100	1/ 9	9: 0	11.17	10.	3.0	PD-lo -Dew	-1.00	0.09	0.03	3.70	0.30	0.05	0.45	0.82	2.86	0.991
101	1/ 9	9: 0	21.00	140.	0.0	Bucket-	5.35	0.00	0.00	4.92	0.19	0.05	0.36	0.36	4.08	0.843
102	1/10	6: 0	21.00	10.	2.2	PD-hi -Dew	-1.00	0.79	0.68	4.49	0.75	0.10	0.79	1.36	3.24	0.791
103	1/10	6: 0	21.00	10.	3.7	PD-lo -Dew	-1.00	0.14	0.08	4.15	0.85	0.09	0.21	1.36	2.88	0.837
104	1/10	9:30	3.50	10.	0.0	PD-hi -	-1.00	0.59	0.37	2.41	0.19	0.04	0.37	0.80	1.19	0.655
105	1/10	9:30	3.50	10.	0.0	PD-lo -	-1.00	0.85	0.71	4.82	0.28	0.06	0.56	1.35	3.27	0.771
106	1/10	9:30	24.00	140.	0.0	Bucket-	5.47	0.00	0.00	3.25	0.47	0.07	0.42	1.36	2.31	0.985
107	1/11	6:30	21.00	10.	0.5	PD-hi -	-1.00	0.03	0.03	1.46	1.01	0.06	0.32	0.46	1.71	0.960
108	1/11	6:30	21.00	10.	0.5	PD-lo -	-1.00	0.04	0.03	1.66	0.75	0.05	0.23	0.39	1.04	0.657
109	1/11	10: 0	24.50	140.	0.0	Bucket-	5.20	0.00	0.02	1.23	0.32	0.04	0.31	0.52	1.34	0.959
110	1/13	1:15	42.75	10.	3.5	PD-hi -	5.23	0.31	0.07	1.80	1.13	0.11	0.10	0.83	3.73	1.314
111	1/13	1:15	42.75	10.	3.5	PD-lo -	5.62	0.66	0.09	1.19	1.56	0.15	0.21	0.78	3.24	1.143
112	1/14	1:30	24.25	10.	1.8	PD-hi -Dew	6.04	0.31	0.03	2.17	0.63	0.07	0.09	0.72	2.18	0.927
113	1/14	1:30	24.25	10.	2.5	PD-lo -Dew	6.26	0.55	0.05	1.97	1.07	0.11	0.10	0.75	2.25	0.820
114	1/14	4:30	3.00	10.	0.0	PD-hi -Fog	5.56	0.19	0.04	16.02	0.32	0.06	0.43	4.74	15.28	1.186
115	1/14	4:30	3.00	10.	0.0	PD-lo -Fog	5.81	0.48	0.04	22.51	0.65	0.09	0.43	5.71	16.49	0.939
116	1/18	20:40	102.67	20.	2.0	PD-hi -	4.18	0.24	0.12	6.55	2.07	0.22	2.60	3.10	6.85	1.239
117	1/18	20:40	102.67	20.	2.0	PD-hi - Rep	4.88	0.16	0.05	6.33	0.93	0.11	1.75	2.85	5.45	1.296
118	1/18	20:40	102.67	20.	2.0	PD-lo -	4.88	0.22	0.08	4.55	1.78	0.17	0.56	2.69	5.61	1.268

Bakersfield Airport (NW) Site: 1984-85

	Date	PICKUP	hr	EXT(mL)	PREC	Collector	DEPOSITION RATE: micro-eq/m2-hr pH	Na	K	NH4	Ca	Mg	Cl	NO3	SO4	-/+
119	1/19	0: 0	3.33	10.	1.0	PD-hi -Fog	4.75	0.19	0.26	27.89	0.97	0.13	12.23	21.02	20.16	1.607
120	1/19	0: 0	3.33	10.	1.0	PD-lo -Fog	4.72	0.49	0.28	28.31	2.25	0.21	2.57	17.80	18.66	1.095
121	1/19	3:25	3.42	10.	1.0	PD-hi -Fog	-1.00	0.17	0.13	20.26	0.42	0.08	2.30	14.62	9.82	1.270
122	1/19	3:25	3.42	10.	1.0	PD-lo -Fog	-1.00	0.17	0.13	16.50	0.52	0.08	1.67	12.11	8.35	1.273
123	1/19	6: 0	2.58	10.	1.0	PD-hi -Fog	4.68	3.82	1.77	16.06	1.11	0.39	3.88	12.18	8.31	0.842
124	1/19	6: 0	2.58	10.	1.0	PD-lo -Fog	4.89	1.77	1.91	16.06	0.97	0.22	3.60	14.12	9.14	1.096
125	1/19	6: 0	2.58	10.	1.0	PD-grd-Fog	4.61	0.33	0.30	25.47	0.55	0.06	1.11	15.78	10.52	0.818
126	1/19	10: 0	4.00	10.	0.5	PD-hi -Fog	4.75	0.39	0.37	15.51	0.43	0.05	1.19	10.91	9.03	1.068
127	1/19	10: 0	4.00	10.	0.5	PD-lo -Fog	5.21	1.57	1.70	15.17	0.77	0.17	2.90	11.59	9.55	1.176
128	1/19	10: 0	4.00	10.	0.5	PD-grd-Fog	4.72	0.32	0.29	17.39	0.68	0.10	1.36	12.61	10.40	1.106
129	1/19	10: 0	13.33	20.	2.0	PD-hi -Fog Rep	4.72	0.11	0.83	12.97	0.38	0.05	1.61	9.11	8.68	1.185
130	1/19	18:30	8.50	10.	0.0	PD-hi -	-1.00	0.35	0.14	1.22	2.37	0.19	0.38	0.99	2.75	0.966
131	1/19	18:30	8.50	10.	0.0	PD-hi - Rep	-1.00	0.44	0.27	0.69	1.99	0.16	0.23	0.74	1.99	0.836
132	1/19	18:30	8.50	10.	0.0	PD-lo -	5.46	0.14	0.06	0.84	1.07	0.11	0.15	0.57	1.12	0.737
133	1/19	18:30	8.50	10.	0.0	PD-grd-	5.54	0.18	0.10	1.22	0.95	0.14	0.23	0.33	1.76	0.824
134	1/19	18:30	8.50	10.	0.0	PD-hi - 2nd	5.54	0.08	-1.00	0.15	0.11	0.01	0.08	0.02	0.13	0.396
135	1/20	10:30	15.75	10.	1.0	PD-hi -Fog	4.22	0.31	0.19	8.07	1.00	0.13	1.27	7.80	6.26	1.233
136	1/20	10:30	15.75	10.	1.0	PD-lo -Fog	4.20	0.21	0.08	8.07	0.95	0.13	1.72	7.57	5.76	1.224
137	1/20	10:30	15.75	10.	1.0	PD-grd-Fog	4.18	0.81	0.34	11.11	1.54	0.22	1.36	9.66	7.94	1.114
138	1/20	10:30	2.83	10.	0.0	PD-hi -Fog	4.56	0.18	0.14	13.77	0.57	0.05	1.15	10.33	7.57	0.906
139	1/20	10:30	2.83	10.	0.0	PD-lo -Fog	4.65	0.28	0.16	15.14	1.15	0.09	1.61	13.54	9.18	1.108
140	1/20	10:30	16.00	140.	3.0	Bucket-Fog	4.66	0.10	0.10	8.84	0.72	0.10	0.96	7.23	5.95	1.058
141	1/21	10:30	24.00	10.	0.0	PD-hi -	4.80	0.31	0.15	6.14	0.54	0.09	0.43	3.06	4.73	1.074
142	1/21	10:30	24.00	10.	0.5	PD-lo -	5.00	0.28	0.12	5.63	0.57	0.11	0.40	3.44	5.03	1.268
143	1/21	10:30	17.42	10.	0.0	PD-hi - Rep	4.82	0.32	0.09	5.85	0.35	0.09	0.45	3.88	5.74	1.384
144	1/21	10:30	24.00	140.	0.0	Bucket-	4.95	0.14	-1.00	5.25	0.33	0.07	0.60	3.04	3.25	0.991

Buttonwillow (BW) Site: 1984-85 6/2/85 Jed

DEPOSITION RATE: micro-eq/m2-hr

	Date	PICKUP	hr	EXT(mL)	PREC	Collector	pH	Na	K	NH4	Ca	Mg	Cl	NO3	SO4	-/+
1	12/26	8:45	22.50	30.	4.0	PD-hi -Dew	-1.00	0.14	-1.00	2.45	2.75	0.32	1.18	0.54	2.86	0.808
2	12/26	8:45	22.50	140.	0.0	Bucket-	-1.00	0.51	0.07	2.91	2.13	0.29	1.34	0.71	3.02	0.858
3	12/28	9:30	48.75	0.	12.0	PD-hi -Rain	-1.00	0.37	-1.00	3.48	2.57	0.42	0.58	1.53	1.61	0.544
4	12/28	9:30	48.75	70.	10.0	Bucket-Rain	-1.00	0.32	0.22	2.83	1.15	0.23	0.62	1.18	2.74	0.956
5	12/29	8: 0	22.30	30.	0.0	PD-hi -	-1.00	0.24	0.13	0.44	2.18	0.24	1.66	0.91	1.46	1.246
6	12/29	8: 0	22.30	140.	0.0	Bucket-	-1.00	0.00	0.00	0.00	0.00	0.00	0.00	0.00	0.00	0.000
7	12/30	8: 0	12.30	10.	0.0	PD-hi -	-1.00	0.12	0.06	0.05	1.03	0.12	2.22	0.22	0.29	1.958
8	12/30	8: 0	24.00	140.	0.0	Bucket-	-1.00	0.37	0.12	0.52	2.10	0.22	1.99	0.79	0.82	1.082
9	12/30	17:10	9.17	10.	0.0	PD-hi -	-1.00	0.41	0.10	0.21	2.27	0.23	3.75	0.28	0.38	1.371
10	12/31	12:30	19.33	10.	0.0	PD-hi -	-1.00	0.12	0.08	0.03	1.48	0.16	1.48	0.33	0.62	1.296
11	12/31	12:30	28.50	140.	0.0	Bucket-	-1.00	0.35	0.10	0.53	1.77	0.22	1.59	0.77	1.77	1.390
12	1/ 3	2:15	61.75	0.	6.0	PD-hi -Fog	-1.00	0.25	0.14	5.24	2.62	0.30	0.23	2.07	3.15	0.637
13	1/ 3	2:45	62.25	140.	10.0	Bucket-Fog	-1.00	0.31	0.11	4.07	2.60	0.27	0.48	2.25	3.47	0.841
14	1/ 3	7: 0	4.45	10.	1.0	PD-hi -Fog	-1.00	0.00	0.11	28.41	1.65	0.10	1.12	17.82	7.54	0.875
15	1/ 3	14:30	7.50	10.	0.0	PD-hi -	-1.00	0.10	0.10	1.82	2.42	0.26	0.17	2.25	1.73	0.884
16	1/ 4	0: 0	9.30	10.	0.0	PD-hi -Fog	-1.00	0.07	0.03	2.58	0.28	0.03	0.14	1.40	1.40	0.981
17	1/ 4	4:30	4.50	10.	0.0	PD-hi -Fog	-1.00	0.00	0.04	7.94	1.36	0.06	0.14	4.91	3.32	0.891
18	1/ 4	9:30	5.00	10.	0.0	PD-hi -Fog	-1.00	0.00	0.05	2.60	1.53	0.04	0.13	0.75	1.32	0.523
19	1/ 4	9:45	31.00	0.	19.0	Bucket-Fog	-1.00	0.25	0.05	6.61	1.36	0.16	0.24	4.41	3.49	0.967
20	1/ 4	17:30	8.00	10.	0.0	PD-hi -	-1.00	0.28	0.19	2.27	4.71	0.54	0.24	0.44	1.46	0.268
21	1/ 4	17:30	7.50	140.	0.0	Bucket-	-1.00	0.64	0.71	2.35	3.16	0.44	3.36	0.97	2.05	0.876
22	1/ 4	21:40	4.17	10.	0.0	PD-hi -Fog	-1.00	0.17	0.12	9.50	3.89	0.28	0.31	4.05	3.74	0.580
23	1/ 5	2:45	9.25	10.	0.0	PD-hi -Fog	-1.00	0.17	0.13	8.42	0.79	0.07	0.28	2.95	4.49	0.806
24	1/ 5	6:15	3.25	10.	0.7	PD-hi -Fog	-1.00	0.47	0.30	8.12	0.66	0.09	0.86	3.53	5.34	1.009
25	1/ 5	10:30	4.00	10.	0.0	PD-hi -Fog	-1.00	0.00	0.05	4.55	1.83	0.06	0.08	1.75	2.53	0.672
26	1/ 5	10:30	17.00	10.	3.2	PD-hi -Fog Rep	-1.00	0.09	0.06	9.13	0.77	0.06	0.15	2.37	4.39	0.684
27	1/ 5	13:20	19.83	140.	5.0	Bucket-Fog	-1.00	0.03	0.07	6.58	0.79	0.08	1.05	2.37	3.81	0.960
28	1/ 6	7: 0	20.30	10.	0.2	PD-hi -Dew	-1.00	0.25	0.13	0.29	3.16	0.37	0.23	0.22	0.88	0.316
29	1/ 6	7: 0	17.67	140.	0.0	Bucket-	-1.00	0.44	0.50	0.86	2.57	0.29	1.71	0.41	1.24	0.724
30	1/ 7	9:10	26.10	0.	110.0	PD-hi -Rain	-1.00	0.00	0.05	7.94	1.78	0.19	1.09	6.84	6.84	1.484
31	1/ 7	9:10	26.17	0.	399.7	Bucket-Rain	-1.00	0.00	-1.00	11.00	2.03	0.19	2.47	6.05	7.15	1.185
32	1/ 9	13:10	52.00	0.	45.0	PD-hi -Rain	-1.00	0.87	0.21	5.90	1.69	0.35	1.29	1.35	3.03	0.629
33	1/ 9	13: 0	52.00	0.	164.9	Bucket-Rain	-1.00	0.91	-1.00	6.45	1.43	0.31	2.28	1.43	3.60	0.803

NOTES:
1. See NW site notes.

APPENDIX C.

SAN JOAQUIN VALLEY FIELD SAMPLING DATA: WINTER 1984-85

4. Calculated Deposition Velocities for Solute Ions

*** SJV DATA: DEPOSITION VELOCITY CALCULATIONS *** Data checked: 6/2/85

Bakersfield Airport (NW) Site: 1984-85

	Date	PICKUP	hr	Collector	LWC	DEPOSITION VELOCITY FROM AERO (cm/s) Na	K	NH4	+NH3	Ca	Mg	Cl	NO3	SO4	% time
12	12/28	2:25	2.4	PD-hi -Fog	0.237	0.26	0.09	1.28	0.62	1.18	0.76	0.62	0.49	1.23	99.9
13	12/28	2:40	2.7	PD-lo -Fog	0.213	1.22	0.81	1.25	0.60	1.60	1.21	0.85	0.66	1.31	91.1
14	12/28	4:35	2.2	PD-hi -Fog	0.061	0.28	0.10	0.72	0.35	0.21	0.20	0.40	0.56	0.58	0.9
15	12/28	4:35	1.9	PD-lo -Fog	0.061	1.09	0.80	0.48	0.00	0.86	0.34	0.87	0.29	0.52	0.0
16	12/28	4:30	4.5	Bucket-Fog	0.142	0.51	0.18	1.74	0.83	2.34	1.33	0.62	0.86	1.70	54.1
17	12/28	7: 0	2.4	PD-hi -Dew	0.000	0.80	0.32	0.13	0.00	4.79	0.27	0.29	0.05	0.14	89.5
18	12/28	7: 0	2.4	PD-lo -Dew	0.000	0.58	0.32	0.07	0.00	1.03	0.27	0.36	0.05	0.16	89.5
19	12/28	16:40	9.7	PD-hi -	0.164	0.52	0.66	0.07	0.04	0.26	0.51	0.11	0.05	0.25	41.9
20	12/28	16:40	9.7	PD-lo -	0.164	0.37	0.60	0.11	0.07	1.54	1.09	0.13	0.06	0.41	41.9
21	12/29	7:50	16.2	PD-hi -Dew	0.000	0.23	0.21	0.05	0.04	0.85	0.37	0.16	0.06	0.16	26.3
22	12/29	7:50	16.2	PD-lo -Dew	0.000	0.25	0.21	0.05	0.04	1.31	0.45	0.17	0.06	0.18	26.3
23	12/29	7:50	27.3	Bucket-	0.164	0.26	0.20	0.11	0.08	1.48	0.60	0.18	0.09	0.32	37.0
26	12/30	8:25	12.1	PD-hi -Dew	0.000	0.35	0.44	0.05	0.04	8.11	0.93	0.33	0.03	0.32	32.3
27	12/30	8:25	12.1	PD-lo -Dew	0.000	0.22	0.13	0.15	0.11	3.24	0.81	0.29	0.03	0.45	32.3
28	12/30	8:25	24.6	Bucket-	0.000	0.02	0.33	0.04	0.03	1.09	0.47	0.64	0.06	0.08	15.9
30	12/30	16:35	8.1	PD-lo -	0.000	0.33	0.00	0.02	0.02	7.44	0.99	0.29	0.02	0.12	46.0
31	12/31	8:55	16.7	PD-hi -	0.000	0.15	0.23	0.01	0.01	0.79	0.62	0.19	0.03	0.04	48.2
32	12/31	8:55	16.7	PD-lo -	0.000	0.14	0.26	0.01	0.01	0.81	0.56	0.19	0.02	0.04	48.2
33	12/31	8:55	24.0	Bucket-	0.000	0.00	0.00	0.11	0.07	0.43	0.20	0.46	0.07	0.12	49.0
37	1/ 2	21: 0	4.7	PD-hi -	0.400	5.00	5.01	0.50	0.42	1.81	1.53	6.95	0.21	0.71	63.2
38	1/ 2	21: 0	4.7	PD-lo -	0.400	2.56	1.87	0.42	0.35	3.79	2.25	3.48	0.19	0.63	63.2
39	1/ 2	21: 0	4.5	Bucket-	0.400	0.75	0.71	0.66	0.56	2.29	1.28	1.61	0.20	0.76	66.7
40	1/ 3	0: 0	3.0	PD-hi -Fog	0.229	2.13	1.89	1.45	1.37	1.13	0.65	3.85	0.53	1.74	100.0
41	1/ 3	0: 0	3.0	PD-lo -Fog	0.229	3.36	4.61	1.81	1.71	2.04	0.87	2.10	0.74	2.46	100.0

NOTES:

1. Deposition velocity = DEP rate/(Aerosol Concentration).
2. Values for "+NH3" = DEP (NH4)/(NH4+NH3(g)).
3. % time = percent of DEP interval for which filter samples were run.
4. LWC from RAC collection rate.
5. See DEPOSITION RATE notes.

Bakersfield Airport (NW) Site: 1984-85

	Date PICKUP	hr	Collector	LWC	DEPOSITION VELOCITY FROM AERO (cm/s) Na	K	NH4	+NH3	Ca	Mg	Cl	NO3	SO4	% time
42	1/ 3 3: 0	3.0	PD-hi -Fog	0.214	15.06	7.22	0.53	0.48	2.79	3.36	3.36	0.98	1.80	99.4
43	1/ 3 3: 0	3.0	PD-lo -Fog	0.214	14.44	6.88	2.71	2.45	2.39	3.36	3.73	1.09	2.53	99.4
44	1/ 3 7: 0	4.0	PD-hi -Fog	0.205	49.72	-1.00	0.50	0.30	3.05	4.38	31.99	0.56	0.53	93.7
45	1/ 3 7: 0	4.0	PD-lo -Fog	0.205	13.12	14.20	0.98	0.58	1.78	1.40	2.56	0.63	0.65	93.7
46	1/ 3 10: 0	3.0	PD-hi -Fog	0.123	6.42	6.09	0.84	0.68	6.96	2.91	3.87	0.37	0.97	85.0
47	1/ 3 10: 0	3.0	PD-lo -Fog	0.123	6.56	6.09	1.02	0.83	5.35	1.94	1.93	0.35	1.20	85.0
48	1/ 3 10: 0	9.5	PD-hi -Fog Rep	0.180	5.22	1.26	1.14	0.82	2.30	0.72	1.50	0.78	1.45	92.3
49	1/ 3 10: 0	13.0	Bucket-Fog	0.193	0.68	0.38	1.57	1.21	2.25	0.70	1.50	0.70	1.82	94.5
51	1/ 3 19:30	9.5	PD-hi -Dew	0.018	0.88	0.30	0.14	0.05	1.02	0.75	0.56	0.04	0.35	40.9
52	1/ 3 19:30	9.5	PD-lo -Dew	0.018	0.44	0.30	0.14	0.05	1.81	1.04	1.11	0.04	0.33	40.9
53	1/ 3 22:50	3.3	PD-hi -Fog	0.170	29.04	18.52	1.16	0.53	2.84	2.28	4.35	0.35	1.41	63.6
54	1/ 3 22:50	3.3	PD-lo -Fog	0.170	21.30	13.85	1.05	0.49	3.41	2.28	3.26	0.30	1.29	63.6
55	1/ 4 10:50	12.0	PD-hi -Fog	0.179	1.96	0.29	1.11	0.72	2.41	1.14	0.25	0.07	1.02	56.8
56	1/ 4 10:50	12.0	PD-lo -Fog	0.179	1.25	0.49	1.30	0.85	3.96	1.49	0.57	0.10	1.28	56.8
57	1/ 4 10:50	24.8	Bucket-Fog	0.166	0.67	0.34	0.40	0.18	1.63	0.80	0.31	0.13	1.29	51.6
65	1/ 4 10:50	15.3	PD-hi -Fog Rep	0.176	1.18	0.38	1.01	0.58	2.19	0.78	1.03	0.18	2.27	58.3
58	1/ 4 20: 5	9.3	PD-hi -	0.000	0.34	0.25	0.31	0.09	0.52	0.78	1.37	0.04	0.31	42.7
59	1/ 4 20: 5	9.3	PD-mid-	0.000	0.53	0.48	0.33	0.10	0.67	0.98	2.84	0.05	0.34	42.7
60	1/ 4 20: 5	9.3	PD-lo -	0.000	0.79	0.70	0.28	0.08	0.86	1.24	3.30	0.03	0.25	42.7
61	1/ 4 23: 0	3.0	PD-hi -Fog	0.167	1.65	0.71	0.44	0.39	0.16	0.93	5.47	0.12	0.79	97.2
62	1/ 4 23: 0	3.0	PD-mid-Fog	0.167	1.50	0.71	0.66	0.58	0.24	1.39	5.17	0.16	1.24	97.2
63	1/ 4 23: 0	3.0	PD-lo -Fog	0.167	1.20	0.53	0.83	0.74	0.20	1.16	4.63	0.18	1.79	97.2
64	1/ 4 23: 0	3.0	PD-lo -Fog Rep	0.167	1.35	0.35	0.89	0.79	0.28	1.39	3.78	0.19	1.65	97.2
67	1/ 5 3:45	4.7	PD-hi -Fog	0.234	1.41	0.44	0.64	0.00	0.23	0.92	0.52	0.32	1.01	61.4
68	1/ 5 3:45	4.7	PD-mid-Fog	0.234	2.75	0.70	0.99	0.00	0.33	1.18	0.92	0.40	1.23	61.4
69	1/ 5 3:45	4.7	PD-lo -Fog	0.234	2.46	0.32	1.19	0.00	0.36	1.31	0.65	0.40	1.50	61.4
70	1/ 5 3:45	4.7	PD-lo -Fog Rep	0.234	2.98	0.57	1.24	0.00	0.46	1.44	0.75	0.41	1.51	61.4
71	1/ 5 10: 0	6.2	PD-hi -Fog	0.171	0.71	0.27	0.57	0.00	0.12	0.72	0.50	0.25	0.67	65.9
72	1/ 5 10: 0	6.2	PD-mid-Fog	0.171	0.41	0.27	0.59	0.00	0.15	0.72	0.57	0.30	0.82	65.9
73	1/ 5 10: 0	6.2	PD-lo -Fog	0.171	0.51	0.27	0.86	0.00	0.21	0.87	0.61	0.35	1.06	65.9
74	1/ 5 10: 0	6.2	PD-lo -Fog Rep	0.171	0.56	0.27	0.87	0.00	0.18	1.01	0.68	0.35	1.08	65.9
75	1/ 5 10: 0	22.8	Bucket-Fog	0.191	6.25	3.13	0.80	0.49	0.58	1.20	1.72	0.29	1.51	60.5

Bakersfield Airport (NW) Site: 1984-85

6/2/85 Jed

	Date	PICKUP	hr	Collector	LWC	DEPOSITION VELOCITY FROM AERO (cm/s) Na	K	NH4	+NH3	Ca	Mg	Cl	NO3	SO4	% time
76	1/ 5	17:15	7.3	PD-hi -	0.000	1.31	0.39	0.04	0.02	1.47	0.80	0.27	0.01	0.08	54.3
77	1/ 5	17:15	7.3	PD-mid-	0.000	2.11	0.22	0.04	0.02	2.04	1.24	0.14	0.01	0.10	54.3
78	1/ 5	17:15	7.3	PD-lo -	0.000	1.74	0.65	0.02	0.01	2.60	1.24	1.14	0.02	0.10	54.3
79	1/ 5	17:15	7.3	PD-up -	0.000	6.34	0.96	0.02	0.01	2.49	1.54	0.96	0.06	0.11	54.3
80	1/ 6	7:30	14.3	PD-hi -	0.000	2.63	0.36	0.10	0.05	1.13	0.58	0.27	0.02	0.24	55.7
81	1/ 6	7:30	14.3	PD-mid-	0.000	0.74	0.11	0.14	0.08	1.00	0.56	0.10	0.02	0.24	55.7
82	1/ 6	7:30	14.3	PD-lo -	0.000	1.11	0.13	0.10	0.06	1.04	0.51	0.13	0.02	0.16	55.7
83	1/ 6	7:30	14.3	PD-up -	0.000	4.49	0.95	0.13	0.07	1.08	0.65	0.50	0.02	0.23	55.7
84	1/ 6	7:30	21.5	Bucket-	0.000	2.58	0.67	0.07	0.04	1.04	0.62	0.89	0.02	0.18	55.2
85	1/ 6	18:30	11.0	PD-hi -	0.000	0.11	0.27	0.03	0.01	0.83	0.46	0.10	0.03	0.08	35.9
86	1/ 6	18:30	11.0	PD-lo -	0.000	0.91	0.35	0.02	0.01	1.88	0.82	0.10	0.02	0.13	35.9
89	1/ 7	12: 0	27.5	Bucket-Rain	0.000	2.98	1.66	0.48	0.17	2.95	1.64	1.02	0.58	1.21	14.4
91	1/ 8	0: 0	12.0	PD-hi -Rain	0.000	-1.00	-1.00	1.26	1.21	3.64	8.15	3.34	1.06	2.87	32.9
92	1/ 8	0: 0	13.0	Bucket-Rain	0.000	-1.00	-1.00	1.12	1.08	3.96	7.09	3.64	1.02	2.82	30.4
94	1/ 8	12: 0	3.0	PD-hi -	0.070	15.82	1.00	0.12	0.05	0.04	0.32	0.44	0.16	0.44	73.3
95	1/ 8	12: 0	3.0	PD-lo -	0.070	0.63	0.00	0.12	0.05	0.11	0.63	0.44	0.18	0.44	73.3
96	1/ 8	12: 0	11.8	Bucket-Rain	0.070	3.10	0.39	1.70	0.75	0.04	0.88	0.29	0.34	3.16	18.7
97	1/ 8	21:50	9.8	PD-hi -Dew	0.000	0.55	0.00	0.54	0.23	0.62	0.88	1.36	0.05	0.51	41.7
98	1/ 8	21:50	9.8	PD-lo -Dew	0.000	1.24	0.55	0.24	0.10	0.83	1.32	1.63	0.05	0.26	41.7
99	1/ 9	9: 0	11.2	PD-hi -Dew	0.000	0.30	0.08	0.87	0.38	0.13	0.27	-1.00	0.09	1.48	36.0
100	1/ 9	9: 0	11.2	PD-lo -Dew	0.000	0.38	0.10	0.51	0.22	0.14	0.26	0.76	0.16	0.71	36.0
101	1/ 9	9: 0	21.0	Bucket-	0.000	0.00	0.00	0.85	0.37	0.15	0.46	0.81	0.08	1.36	38.7
102	1/10	6: 0	21.0	PD-hi -Dew	0.000	8.15	13.47	0.46	0.16	13.10	2.83	1.19	0.17	1.37	19.3
103	1/10	6: 0	21.0	PD-lo -Dew	0.000	1.44	1.68	0.42	0.15	14.71	2.47	0.32	0.17	1.22	19.3
104	1/10	9:30	3.5	PD-hi -	0.035	1.57	2.45	0.19	0.18	0.05	0.22	0.28	0.11	0.14	45.5
105	1/10	9:30	3.5	PD-lo -	0.035	2.26	4.66	0.38	0.36	0.07	0.33	0.42	0.18	0.38	45.5
106	1/10	9:30	24.0	Bucket-	0.035	0.00	0.00	0.31	0.14	0.43	1.00	0.49	0.17	0.56	23.5
107	1/11	6:30	21.0	PD-hi -	0.000	0.18	0.45	0.07	0.05	17.47	1.00	0.76	0.05	0.32	20.1
108	1/11	6:30	21.0	PD-lo -	0.000	0.22	0.36	0.08	0.06	12.96	0.80	0.54	0.04	0.19	20.1

Bakersfield Airport (NW) Site: 1984-85

6/2/85 Jed

	Date	PICKUP	hr	Collector	LWC	DEPOSITION VELOCITY FROM AERO (cm/s) Na	K	NH4	+NH3	Ca	Mg	Cl	NO3	SO4	% time
109	1/11	10: 0	24.5	Bucket-	0.016	0.00	0.23	0.06	0.05	4.01	0.63	0.48	0.05	0.19	24.8
110	1/13	1:15	42.8	PD-hi -	0.016	0.96	0.55	0.07	0.06	8.70	1.77	0.09	0.08	0.34	4.3
111	1/13	1:15	42.8	PD-lo -	0.016	2.04	0.66	0.05	0.04	12.03	2.28	0.18	0.07	0.29	4.3
114	1/14	4:30	3.0	PD-hi -Fog	0.249	0.70	0.31	1.18	1.13	0.17	0.55	0.44	0.63	2.13	100.0
115	1/14	4:30	3.0	PD-lo -Fog	0.249	1.72	0.31	1.66	1.59	0.34	0.73	0.44	0.76	2.30	100.0
116	1/18	20:40	102.7	PD-hi -	0.250	1.47	0.58	0.34	0.00	1.13	4.76	1.72	0.32	0.63	0.4
117	1/18	20:40	102.7	PD-hi - Rep	0.250	0.94	0.26	0.33	0.00	0.51	2.26	1.16	0.30	0.50	0.4
118	1/18	20:40	102.7	PD-lo -	0.250	1.30	0.40	0.24	0.00	0.97	3.57	0.37	0.28	0.52	0.4
119	1/19	0: 0	3.3	PD-hi -Fog	0.243	1.17	1.25	1.45	0.00	0.52	2.75	8.11	2.19	1.86	100.0
120	1/19	0: 0	3.3	PD-lo -Fog	0.243	2.98	1.36	1.47	0.00	1.22	4.58	1.71	1.86	1.72	100.0
121	1/19	3:25	3.4	PD-hi -Fog	0.159	0.98	0.54	1.65	0.00	0.14	1.06	2.41	2.08	1.24	97.1
122	1/19	3:25	3.4	PD-lo -Fog	0.159	0.98	0.54	1.34	0.00	0.18	1.06	1.75	1.72	1.06	97.1
123	1/19	6: 0	2.6	PD-hi -Fog	0.000	36.60	12.30	1.75	0.00	0.62	4.68	9.28	2.79	2.10	100.0
124	1/19	6: 0	2.6	PD-lo -Fog	0.000	16.97	13.27	1.75	0.00	0.54	2.67	8.62	3.23	2.31	100.0
125	1/19	6: 0	2.6	PD-grd-Fog	0.000	3.18	2.11	2.78	0.00	0.31	0.67	2.65	3.61	2.66	100.0
126	1/19	10: 0	4.0	PD-hi -Fog	0.122	3.03	2.89	1.25	0.00	0.30	0.83	2.25	1.50	1.43	99.2
127	1/19	10: 0	4.0	PD-lo -Fog	0.122	12.13	13.13	1.22	0.00	0.54	2.77	5.45	1.59	1.52	99.2
128	1/19	10: 0	4.0	PD-grd-Fog	0.122	2.51	2.23	1.40	0.00	0.48	1.66	2.57	1.73	1.65	99.2
129	1/19	10: 0	13.3	PD-hi -Fog Rep	0.178	0.74	4.67	0.96	0.00	0.19	0.81	1.87	1.26	1.17	99.0
130	1/19	18:30	8.5	PD-hi -	0.000	1.11	0.65	0.05	0.05	4.77	2.31	0.36	0.12	0.15	46.9
131	1/19	18:30	8.5	PD-hi - Rep	0.000	1.38	1.26	0.03	0.03	4.00	1.94	0.22	0.09	0.11	46.9
132	1/19	18:30	8.5	PD-lo -	0.000	0.44	0.29	0.04	0.03	2.15	1.39	0.14	0.07	0.06	46.9
133	1/19	18:30	8.5	PD-grd-	0.000	0.58	0.47	0.05	0.05	1.92	1.66	0.22	0.04	0.09	46.9
135	1/20	10:30	15.8	PD-hi -Fog	0.040	1.39	1.35	0.39	0.38	0.48	1.09	0.96	0.59	0.52	40.4
136	1/20	10:30	15.8	PD-lo -Fog	0.040	0.96	0.55	0.39	0.38	0.46	1.09	1.30	0.57	0.48	40.4
137	1/20	10:30	15.8	PD-grd-Fog	0.040	3.64	2.41	0.54	0.52	0.74	1.87	1.03	0.73	0.67	40.4
138	1/20	10:30	2.8	PD-hi -Fog	0.037	0.77	1.37	0.90	0.00	0.20	0.34	0.91	1.12	0.80	72.3
139	1/20	10:30	2.8	PD-lo -Fog	0.037	1.16	1.59	0.99	0.00	0.40	0.67	1.27	1.47	0.97	72.3
140	1/20	10:30	16.0	Bucket-Fog	0.040	0.43	0.68	0.43	0.42	0.35	0.83	0.73	0.55	0.50	39.8
141	1/21	10:30	24.0	PD-hi -	0.000	1.46	0.86	0.18	0.18	1.60	1.13	0.36	0.17	0.24	15.6
142	1/21	10:30	24.0	PD-lo -	0.000	1.35	0.68	0.16	0.16	1.68	1.43	0.33	0.19	0.25	15.6
143	1/21	10:30	17.4	PD-hi - Rep	0.000	1.55	0.53	0.17	0.17	1.05	1.08	0.37	0.21	0.29	21.4
144	1/21	10:30	24.0	Bucket-	0.000	0.65	-1.00	0.15	0.15	0.96	0.93	0.50	0.17	0.16	15.6

Buttonwillow (BW) Site: 1984-85 6/2/85 Jed

	Date	PICKUP	hr	Collector	LWC	DEPOSITION VELOCITY FROM AERO (cm/s) Na	K	NH4	+NH3	Ca	Mg	Cl	NO3	SO4	% time
5	12/29	8: 0	22.3	PD-hi -	0.000	0.68	1.47	0.03	0.02	2.27	1.78	3.28	0.08	0.34	37.2
7	12/30	8: 0	12.3	PD-hi -	0.000	0.34	0.64	0.00	0.00	1.06	0.80	2.91	0.01	0.06	61.0
8	12/30	8: 0	24.0	Bucket-	0.000	1.07	1.11	0.03	0.02	2.13	1.29	2.83	0.05	0.18	47.9
9	12/30	17:10	9.2	PD-hi -	0.000	1.30	0.85	0.01	0.01	2.02	1.27	2.82	0.02	0.08	79.6
10	12/31	12:30	19.3	PD-hi -	0.000	0.56	0.86	0.00	0.00	2.67	1.47	2.46	0.03	0.14	20.7
11	12/31	12:30	28.5	Bucket-	0.000	1.27	0.91	0.03	0.02	1.92	1.39	1.48	0.06	0.36	39.6
12	1/ 3	2:15	61.8	PD-hi -Fog	0.206	5.01	0.90	0.22	0.18	25.14	12.02	0.10	0.15	0.33	3.6
13	1/ 3	2:45	62.3	Bucket-Fog	0.204	6.19	0.73	0.17	0.14	24.91	10.66	0.21	0.16	0.36	3.7
15	1/ 3	14:30	7.5	PD-hi -	0.000	0.84	1.24	0.13	0.08	2.12	2.49	0.61	0.21	0.39	80.0
16	1/ 4	0: 0	9.3	PD-hi -Fog	0.234	0.57	0.27	0.20	0.12	0.08	0.18	0.23	0.14	0.34	37.6
17	1/ 4	4:30	4.5	PD-hi -Fog	0.181	0.00	0.48	1.20	0.98	0.35	0.38	0.12	0.84	1.38	44.4
18	1/ 4	9:30	5.0	PD-hi -Fog	0.153	0.00	1.80	0.57	0.45	0.39	0.25	0.05	0.15	0.44	42.0
19	1/ 4	9:45	31.0	Bucket-Fog	0.166	2.18	0.59	0.58	0.37	0.53	1.23	0.27	0.49	0.90	44.5
20	1/ 4	17:30	8.0	PD-hi -	0.074	-1.00	1.93	0.30	0.13	4.34	3.68	0.09	0.07	0.34	51.3
21	1/ 4	17:30	7.5	Bucket-	0.049	-1.00	6.99	0.31	0.13	2.91	2.96	1.21	0.15	0.48	54.7
22	1/ 4	21:40	4.2	PD-hi -Fog	0.171	0.50	0.62	0.89	0.70	1.23	2.16	0.44	0.57	0.75	50.4
23	1/ 5	2:45	9.2	PD-hi -Fog	0.140	0.52	0.67	0.83	0.64	0.27	0.56	0.36	0.44	0.95	27.2
24	1/ 5	6:15	3.2	PD-hi -Fog	0.136	3.10	3.33	0.94	0.61	1.03	1.13	0.89	0.59	1.46	96.4
25	1/ 5	10:30	4.0	PD-hi -Fog	0.105	0.00	0.55	0.41	0.16	5.44	0.99	0.17	0.26	0.61	95.4
26	1/ 5	10:30	17.0	PD-hi -Fog Rep	0.133	0.46	0.53	0.92	0.48	0.69	0.66	0.21	0.37	1.07	58.6
27	1/ 5	13:20	19.8	Bucket-Fog	0.133	0.14	0.57	0.63	0.29	0.75	0.91	1.65	0.36	0.91	62.7
28	1/ 6	7: 0	20.3	PD-hi -Dew	0.000	1.32	0.72	0.02	0.01	2.00	2.09	0.62	0.03	0.19	49.4
29	1/ 6	7: 0	17.7	Bucket-	0.000	2.29	2.60	0.06	0.02	1.42	1.43	4.17	0.05	0.27	44.0
30	1/ 7	9:10	26.1	PD-hi -Rain	0.000	0.00	0.48	0.52	0.26	1.70	1.34	4.02	0.61	1.69	46.5
31	1/ 7	9:10	26.2	Bucket-Rain	0.000	0.00	-1.00	0.73	0.35	1.94	1.34	9.11	0.54	1.76	46.6

APPENDIX C.

SAN JOAQUIN VALLEY FIELD SAMPLING DATA: WINTER 1984-85

5. Calculated Fog Deposition Velocites for Solute Ions

Bakersfield Airport (NW) Site: 1984-85 6/2/85 Jed

DEPOSITION VELOCITY FROM FOG (cm/s)

	Date	PICKUP	hr	Collector	LWC	Na	K	NH4	+NH3	Ca	Mg	Cl	NO3	SO4	% time
12	12/28	2:25	2.4	PD-hi -Fog	0.237	1.15	1.29	0.67	0.67	1.82	1.29	2.57	0.60	0.83	65.4
13	12/28	2:40	2.7	PD-lo -Fog	0.213	5.82	12.73	0.72	0.72	2.76	2.24	4.24	0.84	0.98	68.7
14	12/28	4:35	2.2	PD-hi -Fog	0.061	2.17	4.33	1.65	1.65	1.70	1.24	11.08	1.34	1.79	84.6
15	12/28	4:35	1.9	PD-lo -Fog	0.061	5.79	10.19	1.54	1.54	3.96	1.46	20.90	1.34	1.82	82.6
16	12/28	4:30	4.5	Bucket-Fog	0.142	2.98	4.04	1.54	1.54	6.39	3.66	5.92	1.42	1.98	75.9
19	12/28	16:40	9.7	PD-hi -	0.164	4.67	5.93	0.30	0.30	0.48	1.54	-1.00	0.83	0.42	16.4
20	12/28	16:40	9.7	PD-lo -	0.164	3.31	5.47	0.47	0.47	2.87	3.26	-1.00	0.93	0.70	16.4
23	12/29	7:50	27.3	Bucket-	0.164	2.95	1.88	0.40	0.40	2.64	2.11	-1.00	1.23	0.50	5.8
37	1/ 2	21: 0	4.7	PD-hi -	0.400	41.87	20.28	0.75	0.75	6.45	5.98	-1.00	0.48	0.90	15.8
38	1/ 2	21: 0	4.7	PD-lo -	0.400	21.43	7.56	0.64	0.64	13.49	8.77	-1.00	0.43	0.79	15.8
39	1/ 2	21: 0	4.5	Bucket-	0.400	6.25	2.87	1.00	1.00	8.16	5.00	-1.00	0.45	0.96	16.7
40	1/ 3	0: 0	3.0	PD-hi -Fog	0.229	16.43	19.11	1.60	1.60	2.56	3.96	19.78	1.49	1.79	100.0
41	1/ 3	0: 0	3.0	PD-lo -Fog	0.229	25.91	46.57	2.00	2.00	4.61	5.28	10.79	2.06	2.53	100.0
42	1/ 3	3: 0	3.0	PD-hi -Fog	0.214	64.32	51.39	0.69	0.69	7.64	7.68	23.64	2.81	2.52	100.0
43	1/ 3	3: 0	3.0	PD-lo -Fog	0.214	61.68	48.99	3.55	3.55	6.55	7.68	26.27	3.13	3.53	100.0
44	1/ 3	7: 0	4.0	PD-hi -Fog	0.205	109.33	-1.00	1.10	1.10	10.71	33.18	271.03	1.40	1.36	87.5
45	1/ 3	7: 0	4.0	PD-lo -Fog	0.205	28.84	96.22	2.15	2.15	6.25	10.62	21.68	1.56	1.67	87.5
46	1/ 3	10: 0	3.0	PD-hi -Fog	0.123	121.56	105.39	1.83	1.83	4.97	12.83	44.86	2.46	2.01	100.0
47	1/ 3	10: 0	3.0	PD-lo -Fog	0.123	124.28	105.39	2.22	2.22	3.82	8.56	22.43	2.33	2.50	100.0
48	1/ 3	10: 0	9.5	PD-hi -Fog Rep	0.180	23.54	11.77	2.12	2.12	4.00	3.41	10.84	2.48	2.92	94.7
49	1/ 3	10: 0	13.0	Bucket-Fog	0.193	3.32	3.76	2.51	2.51	4.32	3.66	9.72	2.12	3.04	96.2
51	1/ 3	19:30	9.5	PD-hi -Dew	0.018	3.95	10.05	0.33	0.33	2.87	23.86	-1.00	0.92	0.27	2.6
52	1/ 3	19:30	9.5	PD-lo -Dew	0.018	1.98	10.05	0.34	0.34	5.11	33.04	-1.00	0.87	0.26	2.6
53	1/ 3	22:50	3.3	PD-hi -Fog	0.170	177.88	85.50	1.79	1.79	4.04	5.86	63.23	2.07	1.18	36.5
54	1/ 3	22:50	3.3	PD-lo -Fog	0.170	130.45	63.96	1.63	1.63	4.84	5.86	47.42	1.77	1.08	36.5

NOTES:

1. Deposition velocities in fog = Deposition rate/(LWC x Fogwater concentration)
2. % time is percent of Dep. interval in which fog samples were collected.
3. LWC calculated from RAC collection rates.
4. Index #'s refer to Deposition interval #'s; see DEPOSITION RATE notes.

Bakersfield Airport (NW) Site: 1984-85 6/2/85 Jed

	Date PICKUP	hr	Collector	LWC	DEPOSITION VELOCITY FROM FOG (cm/s) Na	K	NH4	+NH3	Ca	Mg	Cl	NO3	SO4	% time
55	1/ 4 10:50	12.0	PD-hi -Fog	0.179	9.65	4.27	2.24	2.24	0.53	1.06	-1.00	0.57	1.06	21.0
56	1/ 4 10:50	12.0	PD-lo -Fog	0.179	6.13	7.17	2.64	2.64	0.87	1.39	-1.00	0.80	1.34	21.0
57	1/ 4 10:50	24.8	Bucket-Fog	0.166	3.70	4.05	1.04	1.04	0.72	1.19	4.4	1.40	1.49	16.0
65	1/ 4 10:50	15.3	PD-hi -Fog Rep	0.176	6.24	3.82	1.73	1.73	0.74	0.97	15.04	1.26	2.07	24.4
61	1/ 4 23: 0	3.0	PD-hi -Fog	0.167	2.20	3.78	0.65	0.65	1.40	2.07	21.07	0.75	0.92	77.8
62	1/ 4 23: 0	3.0	PD-mid-Fog	0.167	2.00	3.78	0.97	0.97	2.10	3.10	19.93	0.98	1.44	77.8
63	1/ 4 23: 0	3.0	PD-lo -Fog	0.167	1.60	2.83	1.23	1.23	1.75	2.58	17.83	1.08	2.08	77.8
64	1/ 4 23: 0	3.0	PD-lo -Fog Rep	0.167	1.80	1.89	1.32	1.32	2.45	3.10	14.59	1.12	1.91	77.8
67	1/ 5 3:45	4.7	PD-hi -Fog	0.234	0.99	3.36	0.74	0.74	1.46	2.15	3.71	0.83	1.13	80.7
68	1/ 5 3:45	4.7	PD-mid-Fog	0.234	1.93	5.27	1.15	1.15	2.09	2.76	6.57	1.04	1.37	80.7
69	1/ 5 3:45	4.7	PD-lo -Fog	0.234	1.72	2.40	1.38	1.38	2.29	3.07	4.66	1.04	1.66	80.7
70	1/ 5 3:45	4.7	PD-lo -Fog Rep	0.234	2.09	4.31	1.43	1.43	2.92	3.37	5.40	1.07	1.68	80.7
71	1/ 5 10: 0	6.2	PD-hi -Fog	0.171	1.90	1.14	1.15	1.15	1.74	3.42	2.21	0.90	1.04	84.0
72	1/ 5 10: 0	6.2	PD-mid-Fog	0.171	1.09	1.14	1.20	1.20	2.18	3.42	2.52	1.05	1.28	84.0
73	1/ 5 10: 0	6.2	PD-lo -Fog	0.171	1.36	1.14	1.73	1.73	3.05	4.11	2.68	1.23	1.65	84.0
74	1/ 5 10: 0	6.2	PD-lo -Fog Rep	0.171	1.49	1.14	1.76	1.76	2.61	4.79	2.99	1.22	1.69	84.0
75	1/ 5 10: 0	22.8	Bucket-Fog	0.191	7.77	19.39	1.13	1.13	4.85	3.63	8.54	1.15	1.53	50.0
93	1/ 8 9: 0	9.0	PD-hi -Rain	0.070	8.00	1.84	2.32	2.32	0.63	4.16	83.22	1.81	3.84	0.6
94	1/ 8 12: 0	3.0	PD-hi -	0.070	30.21	7.17	0.25	0.25	0.39	0.72	71.74	0.63	0.68	33.3
95	1/ 8 12: 0	3.0	PD-lo -	0.070	1.21	0.00	0.25	0.25	1.18	1.43	71.74	0.74	0.68	33.3
96	1/ 8 12: 0	11.8	Bucket-Rain	0.070	5.91	2.78	3.67	3.67	0.42	2.00	47.55	1.41	4.81	8.9
104	1/10 9:30	3.5	PD-hi -	0.035	18.66	33.96	0.73	0.73	2.71	6.54	7.54	0.75	0.51	45.2
105	1/10 9:30	3.5	PD-lo -	0.035	26.82	64.52	1.45	1.45	4.06	9.80	11.31	1.28	1.40	45.2
106	1/10 9:30	24.0	Bucket-	0.035	0.00	0.00	0.98	0.98	6.89	12.93	8.53	1.29	0.99	6.6
109	1/11 10: 0	24.5	Bucket-	0.016	0.00	1.48	0.43	0.43	2.18	8.21	26.17	0.42	0.78	3.7
110	1/13 1:15	42.8	PD-hi -	0.016	9.12	5.16	0.62	0.62	7.72	22.93	8.70	0.67	2.17	2.1
111	1/13 1:15	42.8	PD-lo -	0.016	19.33	6.19	0.41	0.41	10.67	29.49	17.40	0.62	1.88	2.1

Bakersfield Airport (NW) Site: 1984-85

6/2/85 Jed

	Date	PICKUP	hr	Collector	LWC	DEPOSITION VELOCITY FROM FOG (cm/s) Na	K	NH4	+NH3	Ca	Mg	Cl	NO3	SO4	% time
114	1/14	4:30	3.0	PD-hi -Fog	0.249	0.83	1.85	0.76	0.76	0.97	1.55	-1.00	0.84	1.00	100.0
115	1/14	4:30	3.0	PD-lo -Fog	0.249	2.03	1.85	1.07	1.07	1.94	2.07	-1.00	1.02	1.08	100.0
116	1/18	20:40	102.7	PD-hi -	0.250	2.16	-1.00	0.30	0.30	9.21	3.05	8.50	0.45	0.52	0.6
117	1/18	20:40	102.7	PD-hi - Rep	0.250	1.39	-1.00	0.29	0.29	4.14	1.45	5.73	0.41	0.42	0.6
118	1/18	20:40	102.7	PD-lo -	0.250	1.92	-1.00	0.21	0.21	7.92	2.29	1.82	0.39	0.43	0.6
119	1/19	0: 0	3.3	PD-hi -Fog	0.243	3.52	4.80	1.81	1.81	5.04	3.40	48.38	3.00	3.00	100.0
120	1/19	0: 0	3.3	PD-lo -Fog	0.243	9.01	5.20	1.84	1.84	11.76	5.67	10.19	2.54	2.78	100.0
121	1/19	3:25	3.4	PD-hi -Fog	0.159	5.51	3.50	2.38	2.38	3.53	4.46	9.73	3.39	2.90	87.8
122	1/19	3:25	3.4	PD-lo -Fog	0.159	5.51	3.50	1.94	1.94	4.41	4.46	7.08	2.81	2.47	87.8
126	1/19	10: 0	4.0	PD-hi -Fog	0.122	14.77	9.28	1.81	1.81	5.44	4.09	13.79	2.01	2.31	70.8
127	1/19	10: 0	4.0	PD-lo -Fog	0.122	59.07	42.20	1.77	1.77	9.78	13.64	33.50	2.14	2.44	70.8
128	1/19	10: 0	4.0	PD-grd-Fog	0.122	12.20	7.17	2.02	2.02	8.70	8.19	15.76	2.32	2.66	70.8
129	1/19	10: 0	13.3	PD-hi -Fog Rep	0.178	2.82	20.09	1.17	1.17	2.83	2.26	7.78	1.62	1.82	68.7
135	1/20	10:30	15.8	PD-hi -Fog	0.040	8.24	9.63	1.73	1.73	10.98	8.65	4.87	1.89	2.42	14.3
136	1/20	10:30	15.8	PD-lo -Fog	0.040	5.69	3.90	1.73	1.73	10.48	8.65	6.61	1.83	2.23	14.3
137	1/20	10:30	15.8	PD-grd-Fog	0.040	21.56	17.20	2.38	2.38	16.97	14.83	5.22	2.34	3.07	14.3
138	1/20	10:30	2.8	PD-hi -Fog	0.037	5.46	7.99	3.11	3.11	6.33	3.18	4.55	2.63	3.08	64.7
139	1/20	10:30	2.8	PD-lo -Fog	0.037	8.19	9.32	3.43	3.43	12.66	6.37	6.37	3.45	3.73	64.7
140	1/20	10:30	16.0	Bucket-Fog	0.040	2.58	4.88	1.89	1.89	7.96	6.57	3.70	1.75	2.30	14.1

Buttonwillow (BW) Site: 1984-85 6/2/85 Jed

	Date	PICKUP	hr	Collector	LWC	DEPOSITION VELOCITY FROM FOG (cm/s) Na	K	NH4	+NH3	Ca	Mg	Cl	NO3	SO4	% time
12	1/ 3	2:15	61.8	PD-hi -F g	0.206	3.85	7.18	0.58	0.58	7.29	7.63	1.45	0.47	0.71	9.6
13	1/ 3	2:45	62.3	Bucket-Fog	0.204	4.85	5.91	0.45	0.45	7.39	6.91	3.12	0.51	0.80	9.8
14	1/ 3	7: 0	4.5	PD-hi -Fog	0.127	0.00	9.85	5.36	5.36	26.99	9.78	31.78	5.24	5.38	89.9
16	1/ 4	0: 0	9.3	PD-hi -Fog	0.234	2.08	1.28	0.48	0.48	0.67	0.62	0.28	0.62	0.93	32.3
17	1/ 4	4:30	4.5	PD-hi -Fog	0.181	0.00	6.05	2.21	2.21	23.19	8.88	0.82	2.75	3.45	44.4
18	1/ 4	9:30	5.0	PD-hi -Fog	0.153	0.00	5.74	0.82	0.82	22.05	3.64	0.78	0.81	0.90	96.7
19	1/ 4	9:45	31.0	Bucket-Fog	0.166	8.82	3.80	1.55	1.55	9.58	9.41	1.20	2.20	2.55	44.9
20	1/ 4	17:30	8.0	PD-hi -	0.074	14.11	23.90	1.06	1.06	45.83	41.39	7.64	0.81	1.64	8.3
21	1/ 4	17:30	7.5	Bucket-	0.049	35.68	94.64	1.37	1.37	28.73	58.08	105.38	1.80	2.30	2.2
22	1/ 4	21:40	4.2	PD-hi -Fog	0.171	10.30	11.97	1.69	1.69	16.02	8.88	-1.00	2.99	3.89	50.0
23	1/ 5	2:45	9.2	PD-hi -Fog	0.140	10.89	14.55	2.24	2.24	6.49	4.37	7.63	2.92	2.83	76.9
24	1/ 5	6:15	3.2	PD-hi -Fog	0.136	39.02	49.81	2.99	2.99	14.16	11.76	7.30	4.15	4.52	100.0
25	1/ 5	10:30	4.0	PD-hi -Fog	0.105	0.00	6.11	2.04	2.04	31.73	7.08	1.98	2.72	3.28	62.5
26	1/ 5	10:30	17.0	PD-hi -Fog Rep	0.133	6.36	7.59	2.86	2.86	8.55	4.46	2.30	2.61	3.28	78.6
27	1/ 5	13:20	19.8	Bucket-Fog	0.133	1.84	8.25	2.06	2.06	8.80	6.34	15.99	2.61	2.85	67.4

APPENDIX C.

SAN JOAQUIN VALLEY FIELD SAMPLING DATA: WINTER 1984-85

6. Liquid Water Content Measurements by Various Methods (NW site)

Table

RAC COLLECTION RATE AND OTHER DETERMINATIONS OF LWC AT BAKERFIELD AIRPORT: WINTER 1984-85

Start	Stop[a]	min	LWC ($g\ m^{-3}$) RAC[b]	Hi-Vol[c]	OPC[d]	FSSP[d]
28 December						
0034	0114	40	0.198	-	0.786	-
0130	0215	45	0.116	-	0.068	-
0215	0315	60	0.037	-	0.042	-
0315	0415	60	0.067	-	0.155	-
0700	0800	60	0.111	-	0.443	-
0800	0834	35	0.076	-	0.289	-
2-3 January						
2015	2100	45	0.240	-	1.571	-
2100	2300	120	0.140	-	0.673	-
2300	0000	60	0.131	0.111	0.112	-
0000	0200	120	0.136	0.206	0.430	-
0200	0305	65	0.113	0.099	0.175	-
0305	0500	115	0.122	0.179	0.341	-
0530	0700	90	0.126	0.259	0.684	-
0700	0830	90	0.102	0.197	0.547	-
0830	0930	60	0.064	0.104	0.365	-
0930	1015	45	0.011	-	0.083	-
3-4 January						
1957	2100	63	0.108	0.204	0.461	-
2100	2110	10	0.066	0.160	2.226	-
2300	0000	60	0.059	0.159	0.319	-
0000	0100	60	0.129	0.235	1.230	-
0125	0154	30	0.163	0.246	1.167	-
Discontinued because of icing on RAC and Hi-Vol filters						
4-5 January						
2010	2100	50	0.116	0.180	0.384	-
2100	2130	30	0.064	-	0.646	-
2200	2300	60	0.106	0.125	0.026	-
2300	0000	60	0.139	0.128	-	-
0000	0100	60	0.122	0.234	-	-
0100	0200	60	0.133	0.222	0.759	-
0240	0330	50	0.172	-	0.082	-
0400	0500	60	0.096	0.133	0.053	-
0500	0600	60	0.104	0.163	0.239	-
0600	0700	60	0.113	0.170	0.254	-
0700	0800	60	0.121	0.232	0.555	-
0800	0900	60	0.097	0.246	0.872	-
0900	0915	15	0.025	0.062	-	-

Table (cont.)

Start	Stop[a]	min	LWC ($g\ m^{-3}$) RAC[b]	Hi-Vol[c]	OPC[d]	FSSP[d]
14 January						
0130	0230	60	0.200	0.187	-	0.111
0230	0330	60	0.139	0.115	-	0.063
0330	0430	60	0.110	0.164	-	0.071
18-19 January						
2005	2105	60	0.150	-	0.834	0.320
2105	2200	55	0.137	0.215	0.280	0.106
2200	2300	60	0.140	0.215	0.351	0.137
2300	0000	60	0.157	0.199	0.473	0.218
0000	0100	60	0.103	0.179	0.272	0.115
0100	0200	60	0.100	0.156	0.165	0.071
0200	0300	60	0.083	0.086	0.092	0.076
0610	0700	50	0.087	0.133	0.149	0.128
0700	0800	60	0.068	-	0.153	0.049
0800	0900	60	0.067	0.133	0.265	0.076
19-20 January						
0715	0800	45	0.031	-	0.016	0.023
0800	0845	45	0.029	-	0.032	0.048
0845	0930	45	0.011	-	0.031	0.007

Note:

a. RAC collection intervals; - indicates datum not available.

b. Based on nominal sampling rate: 5.0 cubic meter per min.

c. Based on 3-5 min samples at 2-10 per h.

d. Based on integrated size distributions with activity correction; continuous CSASP 30-s readings at 60 per h; FSSP readings taken 10-s each, generally 3-6 times per h.

Hi-Vol LWC Data: 2-3 January 1985 - Airport (NW) Site

1	22:50	22:54	5 min	0.154 g/m3
2	22:56	23: 2	6 min	0.090 g/m3
3	23:30	23:35	5 min	0.133 g/m3
4	23:35	23:39	5 min	0.070 g/m3
5	0:28	0:33	5 min	0.219 g/m3
6	0:34	0:40	6 min	0.201 g/m3
7	1: 6	1:11	5 min	0.230 g/m3
8	1:12	1:18	6 min	0.195 g/m3
9	1:22	1:28	6 min	0.246 g/m3
10	1:28	1:33	5 min	0.153 g/m3
11	1:49	1:55	6 min	0.238 g/m3
12	1:55	2: 0	5 min	0.165 g/m3
13	2:15	2:20	5 min	0.161 g/m3
14	2:20	2:24	5 min	0.039 g/m3
15	2:25	2:30	5 min	0.078 g/m3
16	2:45	2:50	5 min	0.124 g/m3
17	2:50	2:54	5 min	0.092 g/m3
18	3:14	3:19	5 min	0.149 g/m3
19	3:19	3:24	5 min	0.110 g/m3
20	3:45	3:50	5 min	0.178 g/m3
21	3:50	3:54	5 min	0.133 g/m3
22	4:15	4:20	5 min	0.199 g/m3
23	4:20	4:24	5 min	0.202 g/m3
24	4:46	4:52	5 min	0.236 g/m3
25	4:52	4:56	5 min	0.224 g/m3
26	5:35	5:40	5 min	0.237 g/m3
27	6: 0	6: 6	6 min	0.238 g/m3
28	6: 6	6:11	5 min	0.225 g/m3
29	6:30	6:35	5 min	0.257 g/m3
30	6:35	6:39	4 min	0.194 g/m3
31	6:50	6:52	2 min	0.320 g/m3
32	6:52	6:54	2 min	0.300 g/m3
33	6:54	6:57	3 min	0.300 g/m3
34	7:33	7:38	5 min	0.196 g/m3
35	7:38	7:41	2 min	0.210 g/m3
36	8:15	8:20	5 min	0.186 g/m3
37	8:20	8:24	5 min	0.196 g/m3
38	9:15	9:20	5 min	0.142 g/m3
39	9:20	9:23	3 min	0.067 g/m3

Hi-Vol LWC Data: 3-4 January 1985 - Airport (NW) Site

1	20:24	20:29	5 min	0.210 g/m3
2	20:28	20:33	5 min	0.198 g/m3
3	21: 5	21: 9	5 min	0.160 g/m3
4	21:10	21:12	2 min	0.020 g/m3
5	23: 5	23: 9	4 min	0.225 g/m3
6	23: 9	23:12	3 min	0.134 g/m3
7	23:45	23:49	4 min	0.119 g/m3
8	0: 3	0: 9	7 min	0.235 g/m3
9	1:16	1:21	5 min	0.255 g/m3
10	1:21	1:24	3 min	0.317 g/m3
11	1:55	2: 0	5 min	0.194 g/m3

Hi-Vol LWC Data: 4-5 January 1985 - Airport (NW) Site

1	20:23	20:27	5 min	0.275 g/m3
2	20:29	20:33	4 min	0.175 g/m3
3	20:46	20:50	4 min	0.188 g/m3
4	20:50	20:53	3 min	0.130 g/m3
5	20:53	20:56	3 min	0.132 g/m3
6	22:13	22:17	4 min	0.148 g/m3
7	22:21	22:24	3 min	0.092 g/m3
8	22:48	22:55	7 min	0.146 g/m3
9	22:58	23: 2	4 min	0.113 g/m3
10	23:33	23:39	7 min	0.161 g/m3
11	23:41	23:46	5 min	0.095 g/m3
12	0:25	0:29	4 min	0.230 g/m3
13	0:30	0:34	4 min	0.150 g/m3
14	0:52	0:55	3 min	0.300 g/m3
15	0:55	1: 0	5 min	0.257 g/m3
16	1:30	1:33	3 min	0.262 g/m3
17	1:33	1:40	7 min	0.182 g/m3
18	2: 0	2: 4	4 min	0.238 g/m3
19	2: 4	2: 7	3 min	0.158 g/m3
20	4: 0	4: 4	4 min	0.149 g/m3
21	4: 4	4: 7	3 min	0.115 g/m3
22	4:30	4:34	4 min	0.104 g/m3
23	4:34	4:37	3 min	0.165 g/m3
24	5: 0	5: 4	4 min	0.204 g/m3
25	5: 4	5: 8	4 min	0.128 g/m3
26	5:30	5:34	4 min	0.190 g/m3
27	5:34	5:40	5 min	0.129 g/m3
28	6: 0	6: 5	5 min	0.210 g/m3
29	6: 5	6: 9	5 min	0.116 g/m3
30	6:30	6:35	5 min	0.195 g/m3
31	6:35	6:39	5 min	0.159 g/m3
32	7: 0	7: 4	4 min	0.272 g/m3
33	7: 4	7: 7	3 min	0.192 g/m3
34	8: 0	8: 4	4 min	0.300 g/m3
35	8: 4	8: 9	5 min	0.206 g/m3
36	8:30	8:33	3 min	0.330 g/m3
37	8:33	8:37	4 min	0.146 g/m3
38	9: 0	9: 5	5 min	0.196 g/m3
39	9: 5	9:10	5 min	0.082 g/m3
40	9:30	9:35	5 min	0.074 g/m3
41	9:35	9:43	7 min	0.041 g/m3

Hi-Vol LWC Data: 14 January 1985 - Airport (NW) Site

1	1:51	1:55	4 min	0.213 g/m3
2	1:55	1:58	3 min	0.139 g/m3
3	2: 2	2: 7	5 min	0.195 g/m3
4	2: 7	2:10	3 min	0.200 g/m3
5	3:10	3:15	5 min	0.090 g/m3
6	3:15	3:20	5 min	0.140 g/m3
7	3:45	3:50	5 min	0.191 g/m3
8	3:49	3:52	3 min	0.192 g/m3
9	4:20	4:26	6 min	0.108 g/m3

Hi-Vol LWC Data: 18-19 January 1985 - Airport (NW) Site

1	21:28	21:33	5 min	0.284 g/m3
2	21:33	21:38	5 min	0.146 g/m3
3	22: 0	22: 5	5 min	0.190 g/m3
4	22: 5	22: 9	5 min	0.188 g/m3
5	22:57	23: 0	3 min	0.267 g/m3
6	23: 0	23: 3	3 min	0.186 g/m3
7	23: 3	23: 7	4 min	0.198 g/m3
8	23:35	23:39	5 min	0.227 g/m3
9	23:39	23:44	5 min	0.183 g/m3
10	0:33	0:38	5 min	0.200 g/m3
11	0:38	0:45	7 min	0.158 g/m3
12	1:40	1:46	6 min	0.180 g/m3
13	1:46	1:49	3 min	0.132 g/m3
14	2:35	2:39	5 min	0.102 g/m3
15	2:38	2:43	5 min	0.071 g/m3
16	6:15	6:20	5 min	0.145 g/m3
17	6:20	6:23	3 min	0.122 g/m3
18	8:45	8:49	4 min	0.146 g/m3
19	8:49	8:53	4 min	0.119 g/m3

APPENDIX C.

SAN JOAQUIN VALLEY FIELD SAMPLING DATA: WINTER 1984-85

7. Gas-Phase Concentrations for SO_2 and NO_x at Valley Locations

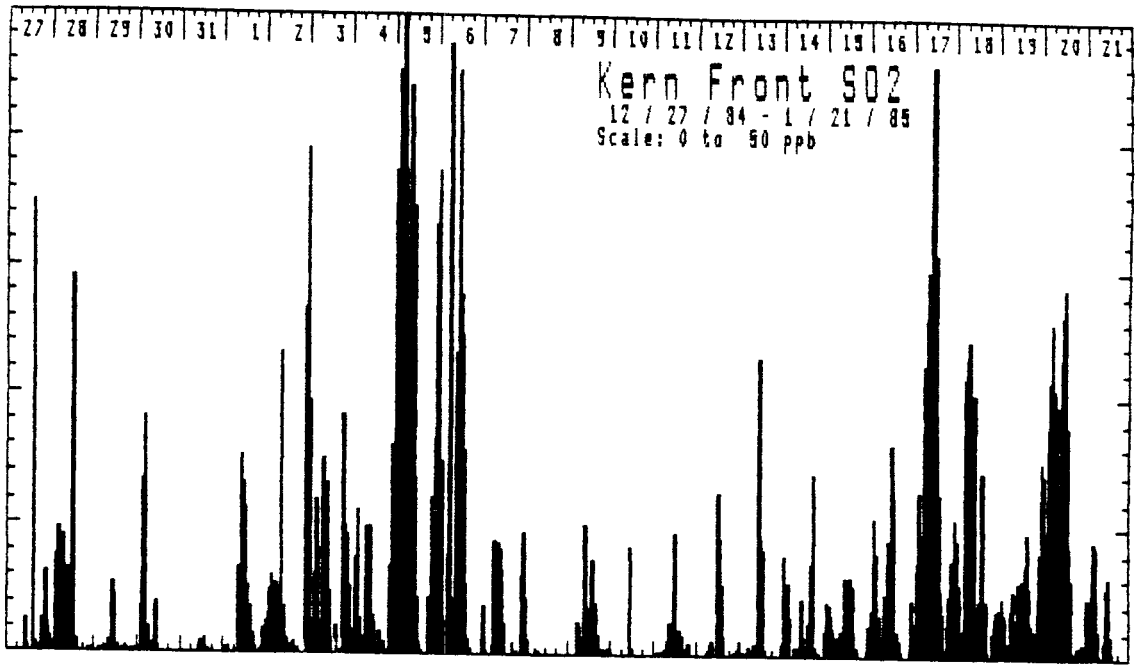
27 28 29 30 31 1 2 3 4 5 6 7 8 9 10 11 12 13 14 15 16 17 18 19 20 21
Kern Front SO2
12 / 27 / 84 - 1 / 21 / 85
Scale: 0 to 50 ppb

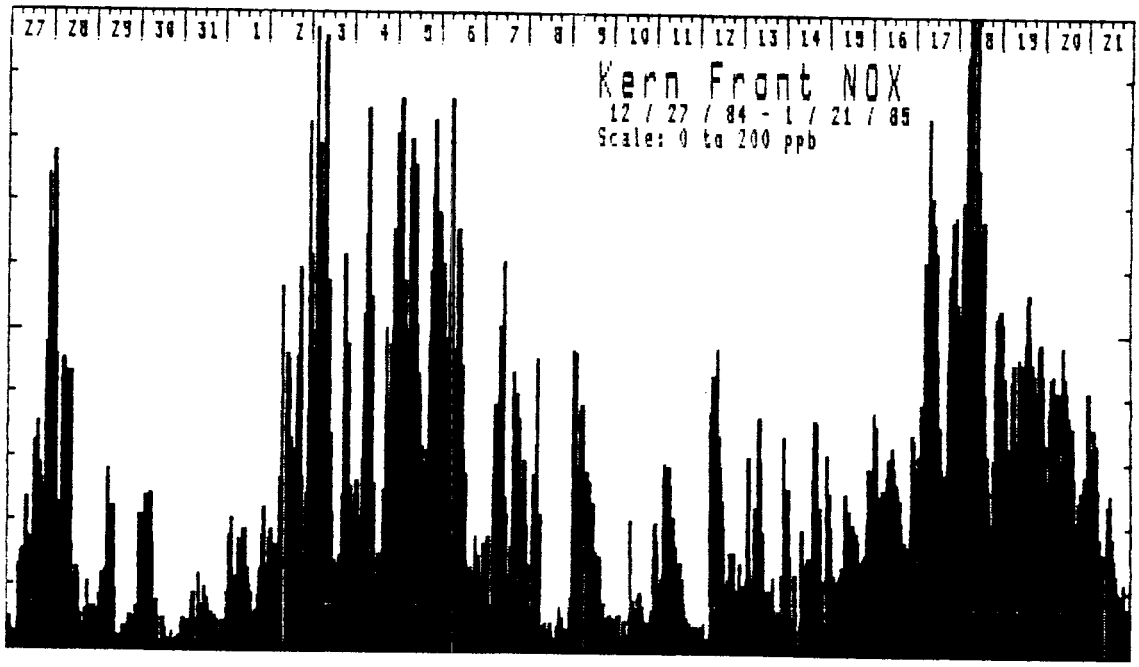
27 28 29 30 31 1 2 3 4 5 6 7 8 9 10 11 12 13 14 15 16 17 18 19 20 21
Kern Front NOX
12 / 27 / 84 - 1 / 21 / 85
Scale: 0 to 200 ppb

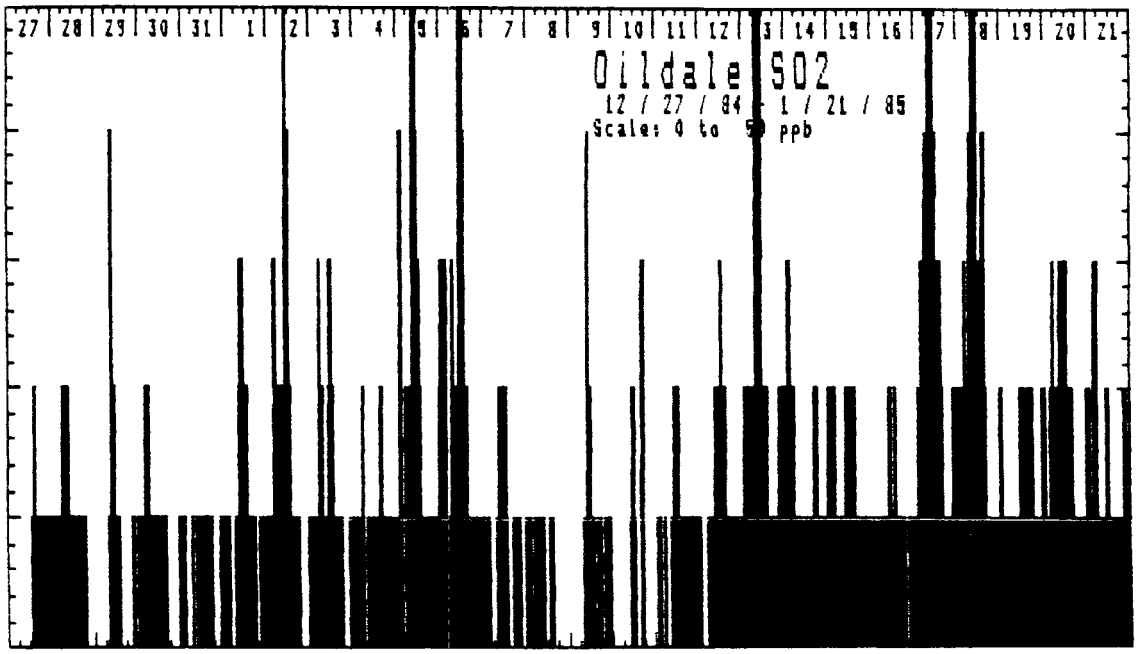
Oildale SO2
12 / 27 / 84 - 1 / 21 / 85
Scale: 0 to

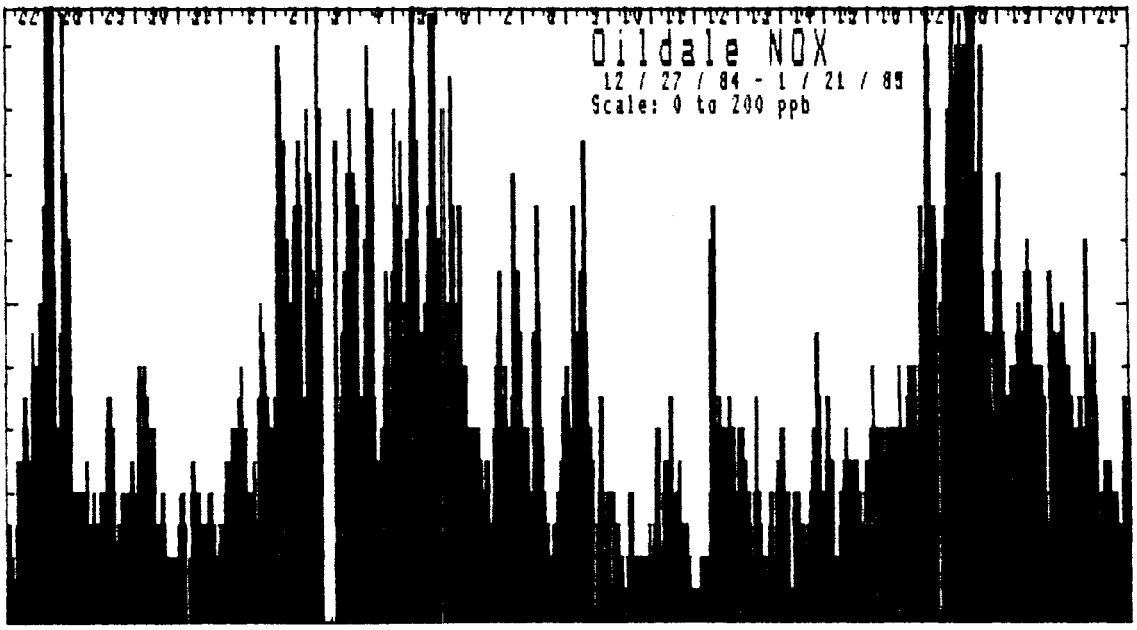
Oildale NOX
12 / 27 / 84 - 1 / 21 / 85
Scale: 0 to 200 ppb

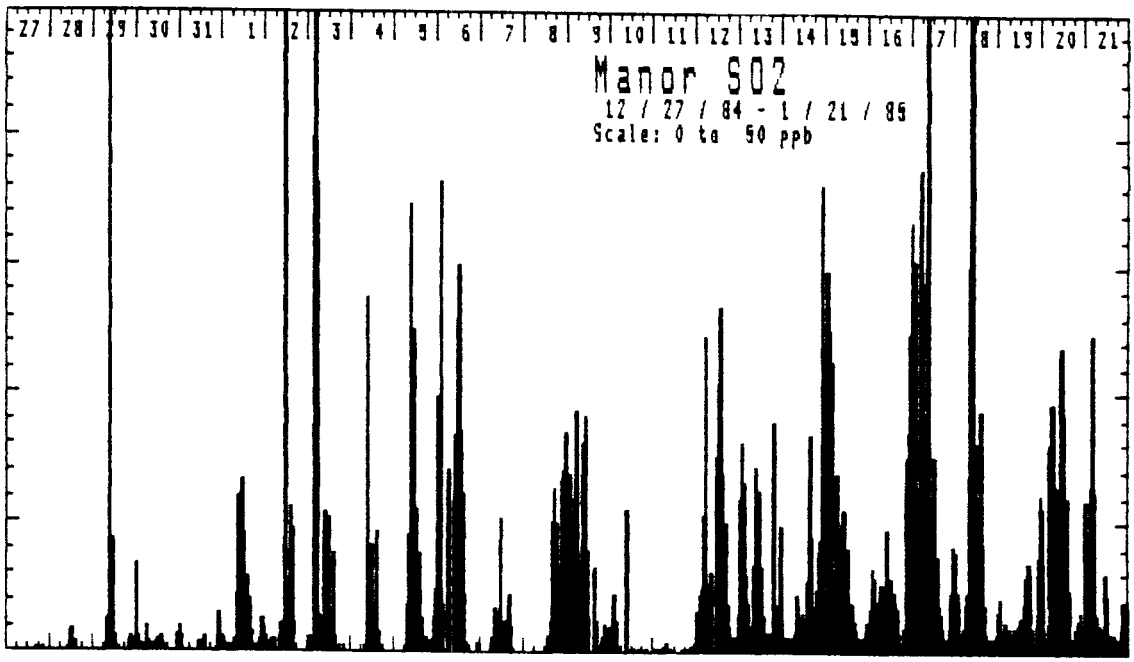
27 28 29 30 31 1 2 3 4 5 6 7 8 9 10 11 12 13 14 15 16 17 18 19 20 21
Manor SO2
12 / 27 / 84 - 1 / 21 / 85
Scale: 0 to 50 ppb

SO_2 uniformly low throughout: 10 ppb or less
90% of the sample hours

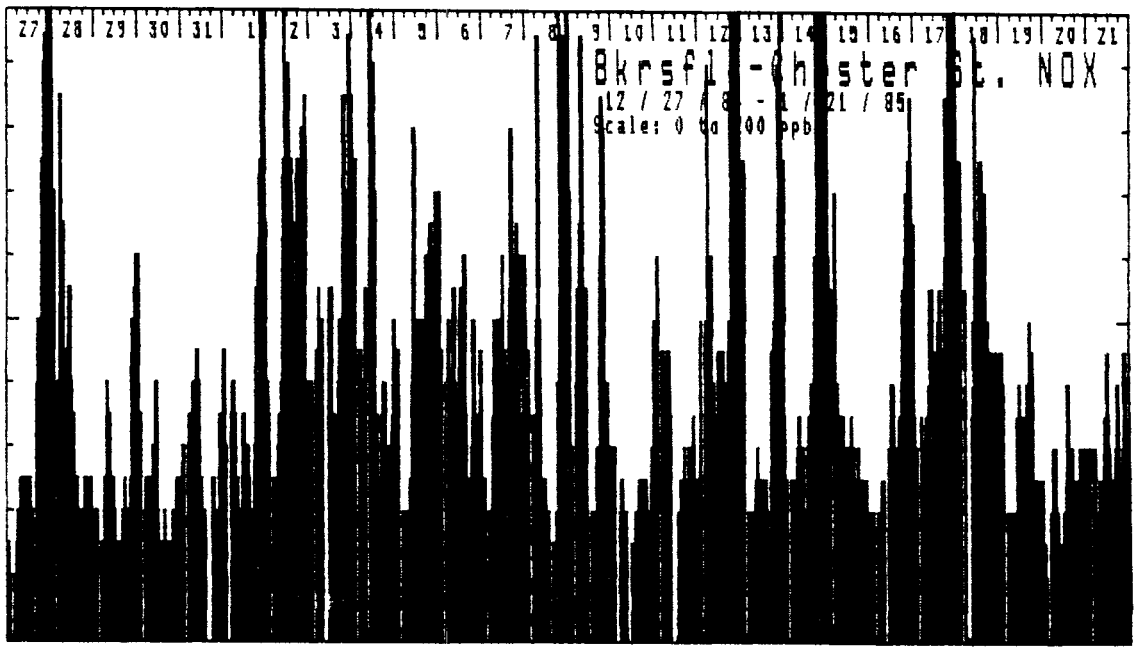

SO_2 uniformly low throughout: 10 ppb or less
90 % of the sampled hours.

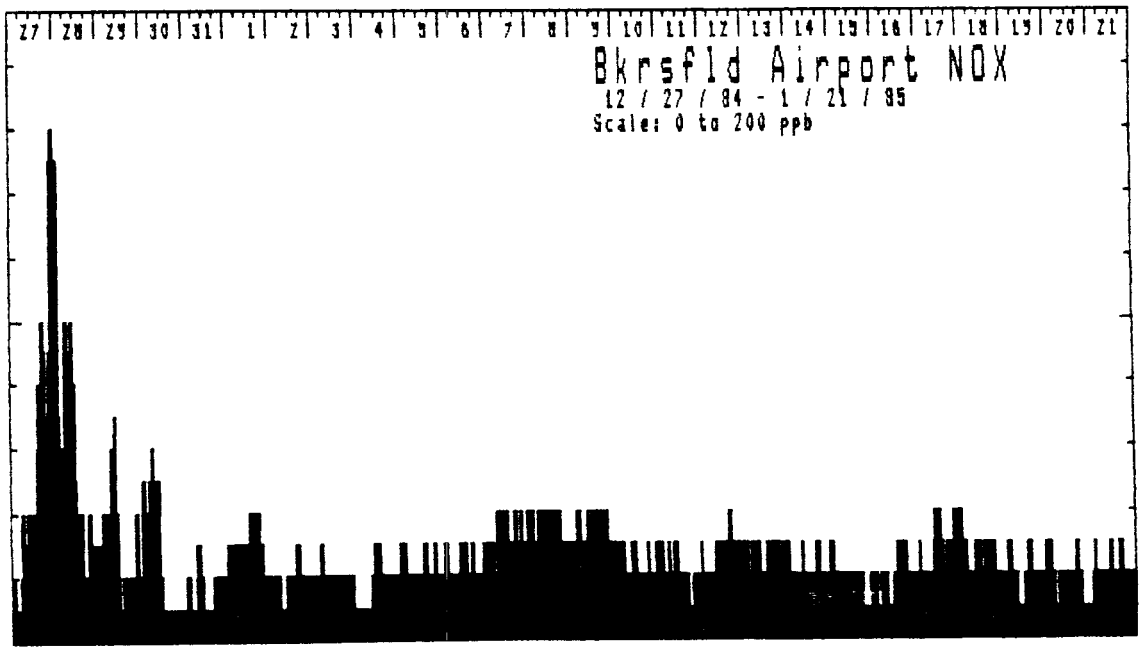

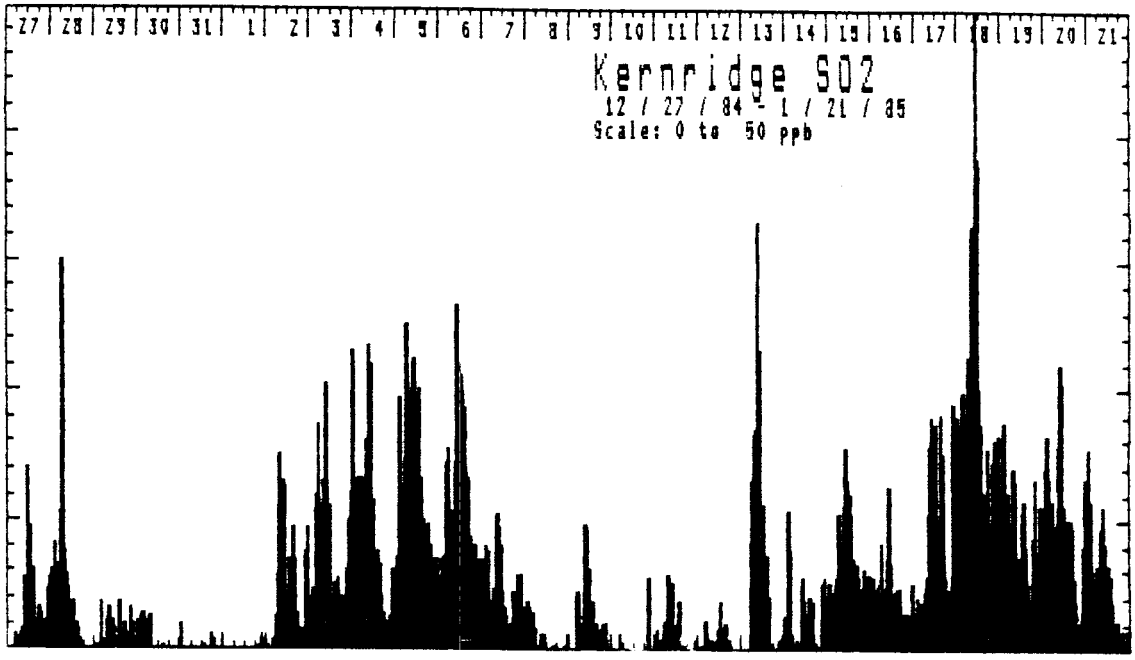
27 28 29 30 31 1 2 3 4 5 6 7 8 9 10 11 12 13 14 15 16 17 18 19 20 21
Kernridge SO2
12 / 27 / 84 - 1 / 21 / 85
Scale: 0 to 50 ppb

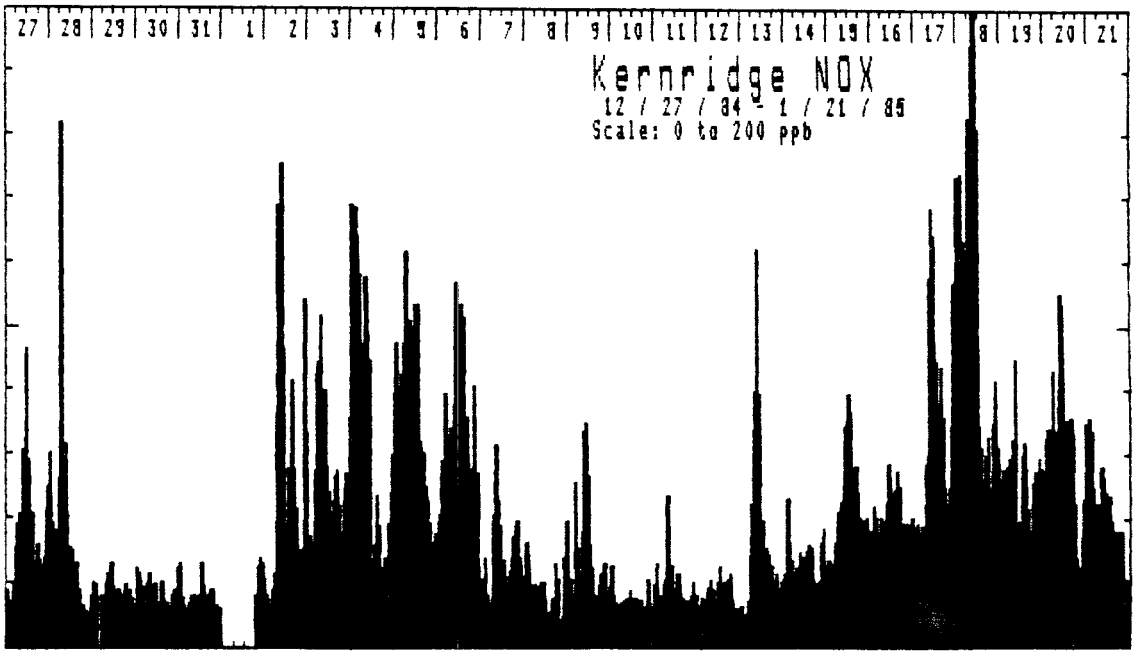
27 28 29 30 31 1 2 3 4 5 6 7 8 9 10 11 12 13 14 15 16 17 18 19 20 21
Kernridge NOX
12 / 27 / 84 - 1 / 21 / 85
Scale: 0 to 200 ppb

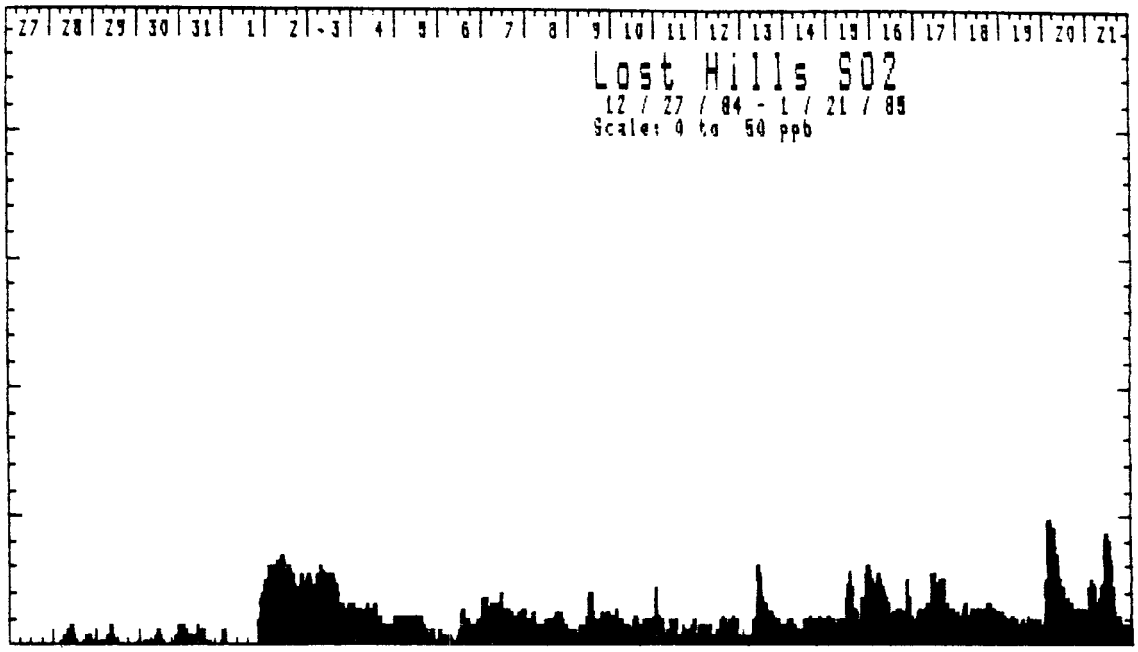
27 28 29 30 31 1 2 3 4 5 6 7 8 9 10 11 12 13 14 15 16 17 18 19 20 21
Lost Hills SO2
12 / 27 / 84 - 1 / 21 / 85
Scale: 0 to 50 ppb

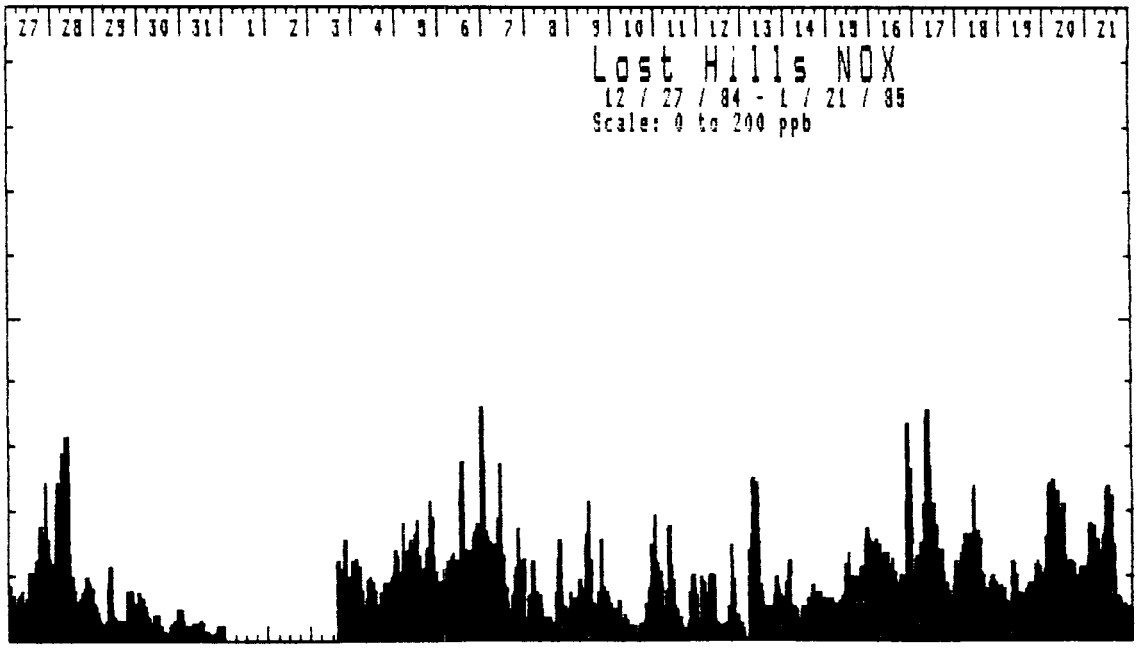
27 28 29 30 31 1 2 3 4 5 6 7 8 9 10 11 12 13 14 15 16 17 18 19 20 21
Lost Hills NOX
12 / 27 / 84 - 1 / 21 / 85
Scale: 0 to 200 ppb